



**HAL**  
open science

# Rôle de l'immunomodulateur P2RX7 dans le cancer et la fibrose pulmonaire

Serena Janho Dit Hreich

► **To cite this version:**

Serena Janho Dit Hreich. Rôle de l'immunomodulateur P2RX7 dans le cancer et la fibrose pulmonaire. Médecine humaine et pathologie. Université Côte d'Azur, 2022. Français. NNT : 2022COAZ6020 . tel-03987715

**HAL Id: tel-03987715**

**<https://theses.hal.science/tel-03987715>**

Submitted on 14 Feb 2023

**HAL** is a multi-disciplinary open access archive for the deposit and dissemination of scientific research documents, whether they are published or not. The documents may come from teaching and research institutions in France or abroad, or from public or private research centers.

L'archive ouverte pluridisciplinaire **HAL**, est destinée au dépôt et à la diffusion de documents scientifiques de niveau recherche, publiés ou non, émanant des établissements d'enseignement et de recherche français ou étrangers, des laboratoires publics ou privés.

# THÈSE DE DOCTORAT

Rôle de l'immunomodulateur P2RX7  
dans le cancer et la fibrose pulmonaire

**Serena JANHO DIT HREICH**

Institut de Recherche sur le Cancer et le Vieillissement de Nice – IRCAN  
UMR 7284 - U1081 – UCA

**Présentée en vue de l'obtention  
du grade de docteur en Sciences de la Vie  
et de la Santé, option Immunologie et  
microbiologie  
de l'Université Côte d'Azur**

**Dirigée par :** Valérie Vouret-Craviari, DR

**Soutenue le :** 10 novembre 2022

**Devant le jury, composé de :**

**Oliver Kepp**, CR, Université Paris-Saclay  
**Sahil Adriouch**, Pr, Université de Rouen  
**Stoyan Ivanov**, CR, Université Côte d'Azur  
**Valérie Lecureur**, MCU, Université de  
Rennes 1  
**Valérie Vouret-Craviari**, DR, Université  
Côte d'Azur  
**Véronique Braud**, DR, Université Côte  
d'Azur



Ecole Doctorale des Sciences de la Vie et de la Santé  
Unité de recherche : IRCAN – CNRS UMR 7284 – INSERM U1081 - UCA

## **Thèse de Doctorat**

Défendue par

**Serena Janho dit Hreich**

En vue de l'obtention du grade de Docteur en Sciences  
de l'Université Côte d'Azur – UFR Sciences

Mention : Immunologie et microbiologie

# **Rôle de l'immunomodulateur P2RX7 dans le cancer et la fibrose pulmonaire**

## **JURY**

### **Présidente :**

**Dr Véronique Braud**, Directrice de Recherche - Université Côte d'Azur

### **Rapporteurs :**

**Dr Oliver Kepp**, Chargé de Recherche – Université Paris-Saclay

**Dr Valérie Lecureur**, Maître de Conférence Universitaire - Université de Rennes 1

### **Examineurs :**

**Pr Sahil Adriouch**, Chargé de Recherche - Université de Rouen

**Dr Stoyan Ivanov**, Chargé de Recherche - Université Côte d'Azur

### **Invité :**

**Pr Paul Hofman**, Professeur des universités - Praticien Hospitalier - Université Côte d'Azur

### **Directrice de thèse :**

**Dr Valérie Vouret-Craviari**, Directrice de Recherche - Université Côte d'Azur



## Résumé

Malgré de nouvelles connaissances biologiques et des avancées thérapeutiques récentes, les cancers du poumon sont encore la première cause de décès liés au cancer alors que la fibrose pulmonaire idiopathique est incurable. Il est donc urgent d'élaborer de nouvelles approches pour aider les patients atteints de ces pathologies.

P2RX7 est un récepteur canal activé par de fortes concentrations d'ATP extracellulaire (ATPe), concentrations retrouvées dans les tissus tumoraux et fibreux. Il joue un rôle majeur dans la modulation du système immunitaire par sa capacité à activer l'inflammasome NLRP3 et à libérer les cytokines IL-1 $\beta$  et IL-18. L'activation de P2RX7 conduit aussi à la formation de macropores à la membrane pouvant induire la mort cellulaire. Ces observations font de P2RX7 un récepteur aux capacités immunomodulatrices et antitumorales qui peuvent être exploitées. Ainsi, une collaboration avec des chimistes a permis de synthétiser une molécule nommée HEI3090 que j'ai utilisé pendant ma thèse.

Durant la première partie de ma thèse, j'ai étudié l'effet de HEI3090 dans le contrôle de la croissance tumorale en utilisant deux modèles murins immunocompétents de cancer du poumon. J'ai d'abord identifié HEI3090 comme un modulateur positif de P2RX7 qui nécessite la présence d'ATPe pour potentialiser ses activités. J'ai ensuite montré que HEI3090 inhibe la croissance des tumeurs en réactivant une réponse immunitaire antitumorale, cet effet repose sur la production d'IL-18 par les cellules dendritiques. L'augmentation d'IL-18 se fait de façon NLRP3-dépendante et favorise le recrutement et la cytotoxicité des lymphocytes T CD4+ et NK ainsi que l'immunogénicité de la tumeur. De ce fait, la combinaison de HEI3090 avec des anti-PD-1 guérit 80% des souris dans le modèle de tumeurs transplantées et réduit de 60% la charge tumorale dans le modèle de carcinogenèse *in situ*. De plus, ces souris sont protégées d'un rechallenge tumoral grâce à la mise en place d'une réponse immunitaire mémoire CD8-dépendante. Ces résultats mettent en évidence que l'activation de P2RX7 constitue une stratégie thérapeutique prometteuse dans les cancers du poumon.

Durant la deuxième partie de ma thèse, j'ai étudié la capacité de HEI3090 à contrôler le développement de fibroses pulmonaires. J'ai d'abord montré que l'expression de la voie P2RX7/IL-18/IFN- $\gamma$  est diminuée chez les patients atteints de fibrose pulmonaire idiopathique (FPI), suggérant le potentiel anti-fibrosant de P2RX7. Ensuite, grâce au modèle murin de fibrose pulmonaire induite par inhalation de bléomycine, j'ai montré que HEI3090 empêche le développement de fibroses pulmonaires. HEI3090 cible la voie P2RX7/NLRP3/IL-18 dans les cellules immunitaires et favorise un profil immunitaire anti-fibrosant caractérisé par une forte production d'IFN- $\gamma$  par les lymphocytes T,

une diminution de production de TGF $\beta$  ainsi qu'une réduction du nombre de cellules inflammatoires. J'ai également montré que les niveaux élevés d'IL-18 plasmatique chez les patients FPI semblent prédire une meilleure survie des patients. L'ensemble de ces résultats suggère que P2RX7 est une nouvelle stratégie thérapeutique dans la FPI et nous permet de proposer que le niveau d'IL-18 plasmatique pourrait constituer un biomarqueur prédictif dans la FPI.

Enfin, j'ai développé un protocole permettant d'étudier l'activation de P2RX7 *in vivo* basé sur la formation de macropores dans des souris sauvages et *p2rx7<sup>-/-</sup>*. Ce protocole permet d'étudier l'effet *in vivo* de molécules ciblant P2RX7, dont HEI3090. Actuellement, ces molécules ne sont étudiées qu'*in vitro* ou de façon indirecte *in vivo*. De plus, ce protocole permet d'identifier la cellule ciblée et de déterminer les doses à administrer pour une meilleure efficacité.

L'ensemble de ce travail a permis de mettre en avant une stratégie thérapeutique dans deux pathologies pulmonaires mais également d'identifier un potentiel biomarqueur prédictif qui est l'IL-18.

**Mots-clés** : P2RX7, immunité, cancer du poumon, fibrose pulmonaire, thérapie, ATP

## Abstract

Despite new findings and recent therapeutic progress, lung cancer is still the leading cause of cancer-related deaths whereas idiopathic pulmonary fibrosis (IPF) is still incurable. It is therefore urgent to find new strategies to help patients affected by these pathologies.

P2RX7 is a canal receptor activated by high levels of extracellular ATP (eATP). Such levels of eATP are found in tumor and fibrotic tissues. P2RX7 plays a major role in modulating the immune response since it induces the activation of the NLRP3 inflammasome and the release of IL-1 $\beta$  and IL-18. Activation of P2RX7 allows the opening of macropores at the plasma membrane that could lead to cell death. Therefore, P2RX7 has immunomodulatory and antitumoral proprieties that could be boosted. Therefore, the team collaborated with chemists to synthesize a molecule named HEI3090 which I used during my PhD.

During the first part of my PhD, I studied the impact of HEI3090 on tumor growth using two immunocompetent mouse models of lung cancer. I first identified HEI3090 as a positive modulator of P2RX7 that requires the presence of eATP to enhance P2RX7's activities. Then, I showed that HEI3090 inhibits lung tumor growth by reactivating an antitumor immune response that relies on IL-18 release by dendritic cells. HEI3090 enhances IL-18 release in a NLRP3-dependant manner and favors the recruitment and cytotoxicity of tumor infiltrating CD4+ T cells and NK cells as well as the enhancement of tumor immunogenicity. Hence, the combination of HEI3090 with anti-PD-1 cures 80% of mice in the subcutaneous mouse model and reduces the tumor burden by 60% in the *in situ* carcinogenesis mouse model. Moreover, cured mice were protected from a tumor rechallenge in a CD8-dependant manner. These results highlight the activation of P2RX7 as a therapeutic strategy in the treatment of lung cancer.

During the second part of my PhD, I studied the ability of HEI3090 to control lung fibrosis progression. I first showed that the P2RX7/IL-18/IFN- $\gamma$  pathway is downregulated in patients with IPF suggesting the antifibrotic potential of P2RX7. Using the bleomycin induced lung fibrosis mouse model, I showed that HEI3090 inhibits lung fibrosis progression by targeting the P2RX7/NLRP3/IL-18 pathway in immune cells. HEI3090 favors an antifibrotic immune profile since it enhances the production of IFN- $\gamma$  by T cells, reduces TGF $\beta$  production as well as reduces the number of proinflammatory cells in the lung. I also showed that high levels of plasmatic IL-18 in IPF patients seem to predict a better survival. These findings suggest that targeting P2RX7 is a new therapeutic strategy in IPF. We also propose that plasmatic IL-18 levels could be a predictive biomarker in this disease.



Lastly, I set up a protocol to evaluate the *in vivo* activation of P2RX7. The protocol is based on studying the macropore opening in wild type mice, which was further validated in *p2rx7<sup>-/-</sup>* mice. The ultimate goal of the protocol is to study the impact of molecules targeting P2RX7, notably HEI3090. Indeed, such molecules are currently studied *in vitro* or indirectly *in vivo*. Moreover, the protocol allows to identify the cell type targeted by such molecules as well as to define a therapeutic dose for better efficacy.

Overall, this work highlights a therapeutic strategy in two lung pathologies and identifies a potential new predictive biomarker that is IL-18.

**Keywords:** P2RX7, immunity, lung cancer, lung fibrosis, therapy, ATP





## Remerciements

*Je souhaite commencer par remercier ma directrice de thèse, le **Dr Valérie Vouret-Craviari**. Valérie, je te remercie de m'avoir permis de faire cette thèse. Merci d'avoir toujours été là quand j'avais besoin d'aide, à n'importe quelle heure, n'importe quel jour. Je te remercie également pour cette autonomie et liberté que tu m'as laissée, j'ai conscience de cette chance incroyable, j'ai énormément appris ! Merci aussi pour ta confiance absolue, même quand il s'agit de manips complètement farfelues! Je te remercie infiniment pour tout ce que tu as fait pour moi tout au long de cette thèse, et de m'avoir donné toutes les opportunités que tu as pu me donner. Merci beaucoup.*

*Je remercie également le **Pr Paul Hofman**, pour m'avoir accueillie dans son équipe, pour sa confiance, ses conseils et son regard précieux de clinicien envers mes projets et leur applicabilité à l'homme.*

*Je souhaite remercier les membres de mon jury d'avoir accepté de juger mon travail. C'est un honneur pour moi de vous compter parmi ce jury. Merci au **Dr Oliver Kepp** et au **Dr Valérie Lecureur** pour avoir pris le temps de lire et commenter mon manuscrit. Merci au **Pr Sahil Adriouch** et au **Dr Stoyan Ivanov** pour leur regard critique et leur aide pendant ma thèse. Je remercie également le **Dr Véronique Braud** d'avoir accepté de présider ce jury.*

*Je souhaite également remercier le **Pr Sylvie Leroy**. Merci pour nos nombreux échanges et discussions qui m'ont permis de mieux comprendre la fibrose pulmonaire idiopathique. Merci de m'avoir donné la chance de voir le côté clinique de cette pathologie et la prise en charge des patients, ce qui m'a permis de rendre mes travaux de recherche beaucoup plus concrets.*

*Je remercie également la team P2RX7! Les présents, les anciens, merci pour tout! **Laetitia**, merci infiniment pour tout ce que tu m'as appris durant mon stage et merci pour tes précieux conseils. Merci aussi pour ta confiance, cela me fait très plaisir d'avoir partagé ce projet avec toi! **Titou**, merci d'être resté jusqu'à la toute fin de ma thèse et pour ton aide précieuse avec les souris tout au long! Je ne sais pas ce que j'aurais fait sans toi !! Merci! **Jonathan**, merci pour tes conseils, ta bonne humeur non-stop, tes blagues et ta gentillesse. Merci également à **Ouafaa** et **Jeanne**, j'ai eu un immense bonheur de vous encadrer durant votre master. Merci énormément pour votre aide! Je suis très fière et très contente de ce que vous avez fait durant votre stage et même aujourd'hui. Je vous souhaite le meilleur pour la suite. Je remercie également **Cindy** pour son aide dans les Western blots, tu m'as souvent sauvée! **Anne-Laure**, je ne sais pas par où commencer. Merci énormément pour ton aide au labo, merci pour cette bouffée d'oxygène avec ta bonne humeur, ton rire, tes blagues et ta gentillesse, ne change jamais. Merci d'avoir partagé mes soirées de manips (voir nuitées) au labo, au FACS, à l'ordi. Merci*

*pour tous ces fous rires qu'on a eus tous les jours, merci d'avoir été là pendant les moments difficiles, je ne sais pas comment j'aurais fait sans toi. Merci aussi d'avoir lu cette thèse. Tu es devenue une de mes meilleures amies, je ne pourrai jamais assez te remercier.*

*Je souhaite remercier tout le reste de l'équipe, le **Dr Patrick Brest**, le **Dr Jérémie Roux**, le **Dr Baharia Mograbi** et le **Pr Marius Ilié** pour leurs conseils. Je remercie également tous les autres copains de labo, **Iris, Barnabé, Marie, Mickael, Ludovic, Benjamin, Simon, Olivia V, Victoria, Asma, Marielle, Karine, Nicolas, Grégoire, Tifenn**, merci pour votre aide, vos conseils et tous ces moments partagés ensemble. **Ludo** et **Simon**, merci énormément pour toutes nos discussions (qui me manquent !!), toujours très enrichissantes. **Iris**, ta petite folie au labo m'a énormément manqué cette dernière année, je suis ravie que tu sois épanouie dans ta nouvelle vie. **Marie** et **Barnabé**, merci d'être toujours à l'écoute, et d'être toujours là pour m'aider quand j'en ai besoin, vous êtes géniaux. **Victoria**, merci d'avoir relu la thèse et pour ton aide avec les abréviations! Et merci pour nos trafics de magnets, la collection s'agrandit !*

*Je remercie aussi tous les membres des deux équipes voisines du CAL, pour leur suivi, leur aide, leurs conseils, leur bonne humeur et leur gentillesse. Une pensée particulière à **Manon C** avec qui j'ai partagé pleins d'étapes clés au cours de ces années et surtout cette dernière étape de thèse, dernière ligne droite, je suis sûre que tu vas tout gérer! A **Olivia R, Saharnaz, Alessandra, Charlotte, Clément, Laurent**, merci d'être les personnes que vous êtes, et merci pour tous ces moments partagés au labo et en dehors du labo, j'espère sincèrement qu'on restera en contact.*

*Je remercie également tous les membres de l'institut que j'ai pu croiser et avec qui j'ai travaillé durant toutes ces années, je les remercie pour leur aide, leur gentillesse et leur bonne humeur. Je remercie toutes les personnes en charge des plateformes, sans qui ce travail n'aurait pas été possible. Je souhaite remercier **Marielle** pour ses conseils pour mes manip souris et pour sa gentillesse. Je souhaite également remercier **Ludo** pour son aide indéniable au FACS, alors, est-ce que je cytomaîtrise?*

***Julien**, je ne pourrai jamais assez te remercier. Merci de m'avoir accompagné et d'avoir toujours été là depuis mon stage avec toi jusqu'à aujourd'hui, à toujours me donner des conseils et à m'aider. Merci pour toutes ces pauses café (pas de café pour moi of course!), merci d'avoir été là pour les moments joyeux et difficiles que j'ai pu affronter durant ces dernières années. Merci pour ta bonne humeur constante et tes blagues (constantes aussi, mais géniales !), ne change jamais.*

*Je remercie également mes amies, doctorantes (en bio et autre !) ou non, pour leur soutien constant. J'ai pu partager avec vous **Julie, Ophélie, Prune** et **Melissa** cette aventure qu'est la thèse, partager ensemble nos difficultés et joies du quotidien a été rassurant et stimulant. Certaines sont déjà*

*docteurs et d'autres le seront très bientôt, je suis fière de vous compter parmi mes amies et je suis sûre que vos thèses seront géniales comme vous l'êtes.*

*Tout ce travail n'aurait pas été le même sans le soutien infaillible de **ma famille**. Merci de m'avoir permis de faire ce que je suis en train de faire aujourd'hui, de m'avoir toujours encouragée, d'avoir toujours cru en moi, d'avoir aussi compris et accepté tout ce temps que je passais au labo. Une pensée à ma petite sœur **Céline** qui s'est embarquée dans la même aventure, je suis sûre que ta thèse sera brillante comme tu l'as toujours été.*

*Je remercie toutes les personnes, citées ci-dessus ou non, qui ont contribué, de près ou de loin, à la réalisation et à l'aboutissement de ce travail.*



## Table des matières

Résumé.....	3
Abstract.....	5
Remerciements.....	9
Abréviations.....	17
Table des figures.....	20
Table des tableaux.....	21
INTRODUCTION.....	23
A. Généralités sur le système immunitaire pulmonaire.....	25
1. Système immunitaire inné.....	25
1.1 Les monocytes.....	25
1.2 Les macrophages.....	26
1.3 Les granulocytes.....	26
1.4 Les cellules innées lymphoïdes et Natural Killer (NK).....	27
1.5 Les cellules dendritiques.....	28
1.6 Détection des dommages/ infections par le système immunitaire inné.....	29
2. Système immunitaire adaptatif.....	30
2.1 Les lymphocytes T.....	31
2.1.1 Activation du lymphocyte T CD4+ et CD8+.....	31
2.1.2 Polarisation des lymphocytes T.....	33
2.1.2.1 Immunité de type 1.....	33
2.1.2.2 Immunité de type 2.....	33
2.1.2.3 Immunité de type 3.....	34
2.1.2.4 Les lymphocytes T régulateurs (Treg).....	34
2.1.3 Autres lymphocytes T.....	35
2.2 Les lymphocytes B.....	35
3. Système immunitaire et développement de pathologies.....	36
B. Rôle de l'immunité dans le cancer du poumon.....	37
1. Rôle du système immunitaire dans la croissance tumorale.....	38
1.1 La réponse immunitaire antitumorale.....	38
1.1.1 Capture des antigènes tumoraux.....	38
1.1.2 Présentation antigénique et activation des lymphocytes.....	40
1.1.3 Elimination des cellules tumorales.....	41
1.1.3.1 Production d'IFN- $\gamma$ .....	41
1.1.3.2 Libération de granules cytotoxiques et des ligands de mort.....	42



1.2 Développement tumoral et échappement .....	43
1.2.1 L'immunoédition.....	43
1.2.2 Composition immunosuppressive du microenvironnement tumoral .....	44
1.2.2.1 Cellules immunosuppressives.....	44
1.2.2.2 Points de contrôle immunitaires .....	46
2. Le cancer du poumon .....	47
2.1 Facteurs de risque.....	47
2.1.1 Facteurs environnementaux.....	47
2.1.2 Facteurs intrinsèques.....	48
2.2 Classification .....	48
2.2.1 Classification histologique .....	48
2.2.2 Classification TNM .....	49
2.2.3 Classification moléculaire .....	49
2.3 Traitements.....	51
2.3.1 Thérapies ciblant la tumeur .....	51
2.3.2 Immunothérapies .....	52
2.3.3 Résistances et marqueurs d'efficacité des immunothérapies .....	53
C. Rôle de l'immunité dans la fibrose pulmonaire idiopathique .....	56
1. La fibrose pulmonaire idiopathique.....	56
1.1 Facteurs de risques .....	56
1.1.1 Facteurs intrinsèques.....	56
1.1.2 Facteurs environnementaux.....	57
1.2 Caractéristiques de la fibrose pulmonaire idiopathique .....	57
1.2.1 Caractéristiques cliniques .....	57
1.2.2 Caractéristiques physiopathologiques.....	58
2. Implication du système immunitaire .....	60
2.1 Système immunitaire inné.....	61
2.1.1 Monocytes et Macrophages .....	61
2.1.2 Granulocytes .....	62
2.1.3 Cellules dendritiques .....	63
2.2 Système immunitaire adaptatif : les lymphocytes T .....	63
2.2.1 La balance des lymphocytes Th1/Th2.....	64
2.2.2 Les lymphocytes Th17.....	65
2.2.3 Les lymphocytes T régulateurs .....	66
2.2.4 Les lymphocytes T CD8+ .....	67

3. Thérapies.....	67
D. P2RX7 : un récepteur immunomodulateur .....	69
1. P2RX7 : un récepteur purinergique unique .....	69
1.1 Les récepteurs P2X.....	70
1.1.1 Structure des récepteurs P2X .....	70
1.1.2 Affinité pour l'ATPe.....	71
1.2 Particularités du récepteur P2RX7 : la queue C-terminale.....	72
1.2.1 Fonction macropore .....	72
1.2.2 L'inflammasome NLRP3 .....	73
1.2.2.1 Mécanisme d'activation.....	74
1.2.2.2 Les interleukines-1 $\beta$ et 18.....	76
1.2.3 Expression de P2RX7 .....	77
2. Rôle de P2RX7 dans le cancer et la fibrose.....	78
2.1 Rôle de P2RX7 dans la croissance tumorale .....	78
2.1.1 Rôle pro-tumoral.....	78
2.1.2 Rôle antitumoral .....	79
2.2 Rôle de P2RX7 dans la fibrose.....	80
2.3 P2RX7 : une cible thérapeutique .....	81
OBJECTIFS DE LA THESE .....	83
RESULTATS .....	87
ARTICLE I .....	91
"A small-molecule P2RX7 activator promotes anti-tumor immune responses and sensitizes lung tumor to immunotherapy" .....	91
ARTICLE II .....	125
"Reshaping the lung immune phenotype by activation P2RX7 .....	125
inhibits lung fibrosis progression" .....	125
ARTICLE III .....	163
"Protocol for evaluating <i>in vivo</i> the activation of the P2RX7 immunomodulator" .....	163
DISCUSSION ET PERSPECTIVES.....	190
A. L'activation de P2RX7 favorise les réponses immunitaires antitumorales et sensibilise les tumeurs aux immunothérapies. ....	192
1. P2RX7 : un récepteur antitumoral .....	192
2. Universalité de la stratégie .....	193
3. L'IL-18 : pivot de l'immunité antitumorale .....	195
B. La modulation de l'infiltrat immunitaire par l'activation de P2RX7 freine le développement d'une fibrose pulmonaire.....	197

1. P2RX7 : un récepteur anti-fibrosant .....	197
2. Rôle des lymphocytes T .....	199
3. Limitations.....	200
C. L'activation de P2RX7 constitue une stratégie thérapeutique prometteuse.....	201
1. P2RX7 : une cible thérapeutique .....	201
2. HEI3090 est un modulateur positif de P2RX7.....	202
ANNEXES .....	207
BIBLIOGRAPHIE .....	285

## Abréviations

**ADCC** : Antibody-dependent cellular cytotoxicity/Cytotoxicité à médiation Cellulaire Dépendante des Anticorps

**ADN** : Acide Désoxyribonucléique

**ADP** : Adénosine Diphosphate

**ALK** : Anaplastic lymphoma kinase/Kinase du lymphome anaplasique

**AMP** : Adénosine Monophosphate

**ANXA1** : Annexine A1

**APC** : Antigen-Presenting cell/Cellules Présentatrice d'Antigènes

**APRIL** : A proliferation-inducing ligand

**AREL1** : Apoptosis Resistant E3 Ubiquitin Protein Ligase 1

**ASC** : Apoptosis-associated speck-like protein containing a CARD

**ATP** : Adénosine Triphosphate

**ATPe** : ATP extracellulaire

**BAFF** : B-cell activating factor

**BCR** : B cell receptor

**BRAF** : B- Rapidly Accelerated Fibrosarcoma

**Breg** : lymphocyte B régulateur

**bzATP** : 2'(3')-O-(4-Benzoylbenzoyl)adenosine-5'-triphosphate

**CAF** : Cancer associated fibroblast/fibroblaste associé aux tumeurs

**CALR** : Calreticuline

**CARD** : Caspase recruitment domain/Domaine de recrutement de la caspase

**CCL** : C-C chemokine Ligand

**CCR** : C-C chemokine Receptor

**CD** : Cluster of Differentiation

**cDC1/2** : cellules dendritiques conventionnelles de type 1/2

**CLR** : C-Lectin receptor

**CMH-I/II** : Complexe Majeur d'Histocompatibilité de classe I/II

**CPNPC** : cancer du poumon non à petites cellules

**CPPC** : cancer du poumon à petites cellules

**CTLA-4** : cytotoxic T-lymphocyte-associated protein 4/antigène 4 du lymphocyte T

**CVF** : Capacité Vitale Forcée

**Da** : Dalton

**DAMPs** : Damage Associated Molecular Patterns

**DC** : Cellules Dendritiques

**DLCO** : Diffusing Lung Capacity for Carbon Monoxide/Capacité de diffusion du monoxyde de carbone

**DNase** : désoxyribonucléase

**EC50** : concentration efficace médiane

**EGFR** : Epidermal Growth Factor Receptor

**ENTPD1** : Ectonucleoside triphosphate diphosphohydrolase 1

**EOMES** : Eomesodermin

**ERK1/2** : Extracellular signal-regulated kinases 1/2

**FDA** : Food Drug Administration

**FGF** : Fibroblast Growth Factor / Facteur de croissance des fibroblastes

**FGFR** : Fibroblast Growth Factor Receptor / Récepteur du facteur de croissance des fibroblastes

**FLT3L** : FMS-like tyrosine kinase 3 ligand

**FOXP3** : forkhead box P3

**FPI** : Fibrose Pulmonaire Idiopathique

**FPR1** : Formyl peptide receptor 1

**GAS** : Gamma interferon activation site

**G-CSF** : Granulocyte colony-stimulating factor/Facteur stimulant les colonies de granulocytes

**GDP** : Guanosine Diphosphate

**Gr** : Granzyme

**GTP** : Guanosine Triphosphate

**HEK** : Human Embryonic Kidney

**HER2** : Human Epidermal Growth Factor Receptor 2

**HMGB1** : High Mobility Group Box 1

**HRAS** : Harvey Rat sarcoma virus

**HSP** : heat shock proteins/protéines de choc thermique

**IASLC** : Association Internationale pour l'étude du cancer du poumon

**iBALT** : induced Bronchus Associated Lymphoid Tissue

**IC** : immune checkpoint

**ICI** : immune checkpoint inhibitor

**IFN- $\gamma$**  : Interféron gamma

**IFNGR1/2**: interferon gamma receptor 1/2

**Ig** : Immunoglobuline

**IGIF** : IFN- $\gamma$  inducing factor

**IHC** : immunohistochimie

**IKK** : I kappa B ( $\text{I}\kappa\text{B}$ ) kinase

**IL-18BP** : IL-18 Binding Protein

**IL-1R1/2** : Interleukin 1 receptor, type I/II

**IL-1Ra** : Interleukin-1 receptor antagonist

**IL-1RacP** : Interleukin-1 receptor accessory protein

**IL-1 $\beta$**  : Interleukine 1 bêta

**ILC** : Cellules Innées Lymphoïdes

**ILT2** : Leukocyte immunoglobulin-like receptor subfamily B member 1

**IRF1**: Interferon regulatory factor 1

**ISG**: interferon-stimulated genes

**ISRE**: interferon-stimulated response element

**JAK1/2**: janus kinase 1/2

**JNK** : c-Jun N-terminal kinases

**KIRs** : Killer-cell immunoglobulin-like receptors

**KRAS** : Kirsten rat sarcoma virus

**LAG-3** : Lymphocyte-activation gene 3

**LB** : Lymphocyte B

**LPS** : Lipopolysaccharide

**LRP1**: Low density lipoprotein receptor-related protein 1

**LRR** : Leucine rich region

**LT** : lymphocytes T

**M1** : Macrophages M1

**M2** : Macrophages M2

**MAPK** : Mitogen-activated protein kinase

**MDSCs** : Myeloid-derived suppressor cells/Cellules myéloïdes suppressives

**MEC** : matrice extracellulaire

**M-MDSCs** : monocyte-MDSCs

**moDCs** : Cellules dendritiques dérivées de monocytes

**mTOR** : mammalian target of rapamycin

**MUC5** : Mucine 5

**MyD88** : Myeloid differentiation primary response 88

**NCRs** : Natural cytotoxicity triggering receptor

**NE** : neutrophile élastase

**NEK7** : NIMA related kinase 7

**NET** : Neutrophil Extracellular Trap

**NFAT** : Nuclear factor of activated T-cells

**NF- $\kappa\text{B}$**  : Nuclear factor kappa-light-chain-enhancer of activated B cells

**NIK**: NF- $\kappa\text{B}$ -induced kinase

**NK** : Natural Killer

**NKT** : Natural Killer T

**NLRP3** : NLR family pyrin domain containing 3

**NLRs** : NOD like-receptor

**NRAS** : Neuroblastoma RAS viral oncogene

**NT5E** : ecto-5'-nucleotidase

**o-ATP** : Oxidized ATP / ATP oxydé

**P2RX7** : Récepteur P2X7

**PAMPs** : Pathogen Associated Molecular Patterns

**PARN** : Poly(A)-specific ribonuclease

**PD-1** : Programmed Cell Death-1

**pDCs** : cellules dendritiques plasmacytoides

**PDGF** : Platelet-derived growth factor

**PDGFR** : Platelet-derived growth factor receptor

**PD-L1/2** : Programmed death-ligand 1/2

**PI3K** : phosphoinositide 3-kinase

**PID** : Pneumopathies interstitielles diffuses

**PKB/C** : Protein Kinase B/C

**PMN-MDSC** : Polymorphonucléaires-MDSC

**Prf1** : Perforine-1

**PRRs** : Pattern Recognition Receptors

**PYD** : pyrin domain

**RAGE** : Receptor for advanced glycation endproducts

**RIP1** : Receptor interacting serine/threonine kinase 1

**RLRs** : RIG-like receptors

**ROR $\gamma$ T** : Rorc RAR-related orphan receptor gamma

**ROS** : Reactive oxygen species/espèces réactives de l'oxygène

**RTEL1** : Regulator of telomere length helicase 1

**SFTPA2** : Surfactant Protein A2

**SFTPC** : Surfactant Protein C

**SNP** : single nucleotide polymorphism

**STAT1** : Signal transducer and activator of transcription 1

**TAMs** : Tumor associated Macrophages/ Macrophages associés aux tumeurs

**t-bet** : T-box expressed in T cells

**Tcm** : lymphocytes T centraux mémoires

**TCR** : T cell receptor

**Tem** : lymphocytes T effecteurs mémoires

**TERC** : Telomerase RNA component

**TERT** : Telomerase Reverse Transcriptase

**TFAM** : Mitochondrial transcription factor A

**TGF $\beta$**  : Transforming Growth Factor beta

**Th1**: T helper 1

**TILs** : lymphocytes infiltrant la tumeur

**TIM-3** : T-cell immunoglobulin and mucin-domain containing-3

**TIR**: Toll-interleukin-1 receptor

**TLR** : Toll-Like Receptor

**TM1/2** : Domaine transmembranaire 1/2

**TMB** : Tumor mutation burden

**TNF $\alpha$**  : Tumor Necrosis Factor

**TNM** : Tumor Node Metastasis

**TRAF6**: TNF receptor-associated factor 6

**TRAIL** : Tumor-necrosis-factor related apoptosis inducing ligand

**TRAIL-R** : Trail-Récepteur

**Treg** : Lymphocytes T régulateurs

**TRIP12** : thyroid hormone receptor interactor 12

**Trm** : lymphocytes T résidents mémoires

**Tscm** : lymphocytes T souches mémoires

**UBE2L3** : Ubiquitin-conjugating enzyme E2 L3

**VEGF** : Vascular endothelial growth factor

**VEGFR** : VEGF-Receptor

**WT** : Wildtype/ sauvage

**$\alpha$ -SMA** :  $\alpha$ -smooth muscle actin /  $\alpha$ -actine du muscle lisse

## Table des figures

Figure 1 : Les différents PRRs et leurs voies de signalisations.....	30
Figure 2 : Les trois principales voies de polarisation des lymphocytes T .....	33
Figure 3 : Hallmarks of cancers .....	37
Figure 4 : Le microenvironnement tumoral.....	38
Figure 5 : L'IFN- $\gamma$ et son récepteur.....	41
Figure 6 : Les effets antitumoraux de l'IFN- $\gamma$ .....	42
Figure 7 : Le cycle cancer-immunité .....	43
Figure 8 : L'immunoédition .....	44
Figure 9 : Cellules immunitaires et croissance tumorale.....	45
Figure 10 : Les différents immune checkpoints et leurs ligands .....	46
Figure 11 : Mutations promotrices du CPNPC dans les stades précoces et métastatiques....	50
Figure 12 : Schéma thérapeutique des patients atteints de CPNPC de stade IV .....	51
Figure 13 : Réactivation des lymphocytes T par les ICIs .....	52
Figure 14 : Vitesses de progression de la FPI.....	58
Figure 15 : Le processus de fibrose.....	59
Figure 16 : Coupes histologiques d'une biopsie de poumons FPI .....	60
Figure 17 : Rôle des populations immunitaires dans la progression de la FPI .....	64
Figure 18 : La balance des lymphocytes Th1 et Th2 .....	65
Figure 19 : Ralentissement de la maladie avec des anti-fibrosants .....	68
Figure 20 : La signalisation purinergique .....	69
Figure 21 : Structure des récepteurs P2RX1-6 et P2RX7 .....	70
Figure 22 : L'inflammasome NLRP3 .....	74
Figure 23 : Mécanisme d'activation de l'inflammasome NLRP3 .....	75
Figure 24 : L'IL-1 $\beta$ , l'IL-18, leurs récepteurs et leurs antagonistes .....	76
Figure 25 : Activation du récepteur de l'IL-18.....	77
Figure 26 : Pourcentage de cellules exprimant P2RX7 dans la rate de souris sauvage.....	77
Figure 27 : Poches de liaison de l'ATP et des modulateurs allostériques de P2RX7 .....	81

## Table des tableaux

Tableau 1 : Les DAMPs majeurs libérés en cas de mort immunogène.....	39
Tableau 2 : Stades des cancers du poumons selon la 8ème classification TNM .....	49
Tableau 3 : Caractéristiques des récepteurs P2X .....	71





## INTRODUCTION



## A. Généralités sur le système immunitaire pulmonaire

Le poumon, siège des échanges gazeux entre l'air et le sang, est un organe vital fortement exposé aux pathogènes et aux particules polluantes. Ainsi, au-delà de capter l'oxygène de l'air et d'évacuer le dioxyde de carbone du sang, le poumon est un organe immunitaire impliqué dans l'élimination de pathogènes, de molécules ou de particules étrangères. La durée et l'intensité de ces agressions, mais aussi l'âge ou certaines pathologies - telle que l'obésité - conduisent à une inflammation qui peut être aiguë ou chronique et qui favorise le développement des pathologies pulmonaires [1] telles que le cancer et la fibrose [2], [3]. Ces observations positionnent la modulation du système immunitaire comme une stratégie thérapeutique prometteuse.

En plus des barrières physiques (épithélium, mucus et surfactant) contre les pathogènes, le poumon possède une panoplie de cellules immunitaires résidentes qui confèrent une protection spécifique au tissu pulmonaire. Ces cellules font partie du système immunitaire inné et adaptatif. Je traiterai ici les caractéristiques et le rôle des cellules immunitaires majeures qui seront mentionnés tout au long de cette thèse.

### 1. Système immunitaire inné

Les cellules immunitaires pulmonaires résidentes appartenant au système immunitaire inné comprennent les macrophages, les cellules lymphoïdes innées mais aussi les cellules dendritiques. D'autres cellules, non résidentes, peuvent être recrutées au niveau du poumon lors d'une infection/blessure comme les monocytes et granulocytes.

#### 1.1 Les monocytes

Les monocytes sont des cellules myéloïdes provenant de la moelle osseuse qui circulent dans le sang et sont recrutés essentiellement via l'axe CCL2/CCR2 [4] vers le tissu en cas de lésion ou d'infection. Ces monocytes sont dits inflammatoires via la production de myéloperoxydase, de cathepsines et de cytokines telles que l'IL-1 $\beta$ , l'IL-6 ou le TGF $\beta$ . Ce sont également des cellules phagocytaires capable de détruire les pathogènes et débris cellulaires, mais ont aussi des fonctions immunorégulatrices grâce à leur fonction de cellules présentatrices d'antigène [5]. Les monocytes constituent également des cellules progénitrices qui peuvent se différencier en macrophage [6] ou en cellule dendritique [7].

## *1.2 Les macrophages*

Les macrophages sont essentiels pour limiter l'inflammation : ils ont la capacité de phagocyter des particules et des débris cellulaires ce qui forme une protection supplémentaire à l'épithélium. Ils constituent la première ligne de défense des voies respiratoires et interagissent essentiellement avec les cellules épithéliales pulmonaires afin de réguler leur phagocytose.

Les macrophages pulmonaires comprennent majoritairement les macrophages alvéolaires qui sont les plus abondants parmi les cellules immunitaires pulmonaires. Comme leur nom l'indique, ils sont situés au niveau des alvéoles et sont de ce fait directement exposés à des stimulants. Ils sont essentiellement d'origine foetale [8]–[10], mais une faible proportion est différenciée à partir de monocytes circulants. Une autre population de macrophages résidents, dits interstitiels, est moins abondante et est d'origine monocyttaire, se différenciant essentiellement à partir de monocytes circulants [8], [11]. Les macrophages ont une longue durée de vie et s'auto-renouvellent en conditions normales [12], [13]. Cependant, en conditions inflammatoires, les monocytes sont recrutés et se différencient en macrophages et acquièrent des caractéristiques similaires aux macrophages résidents [14].

Les macrophages ont des fonctions de défense, de cicatrisation et d'immunorégulation, qui dépendent de l'environnement immunitaire. La notion de polarisation de macrophages a été introduite pour permettre de distinguer les différents états du macrophage. Il est important de noter que cette notion de polarisation ne distingue pas des sous-types de macrophages ontologiquement différents mais permet de simplifier les différents états du macrophage et sa plasticité en fonction des changements dans le microenvironnement tissulaire [15]. Les macrophages sont ainsi classés en M1 et M2, et se distinguent par leurs marqueurs de surfaces, le type de cytokines qu'ils produisent et leur métabolisme. Ainsi, les macrophages M1 (voie classique, activés par l'IFN- $\gamma$  ou le LPS) ont des fonctions antimicrobiennes et antiprolifératives et les macrophages M2 (voie alternative, activés par l'IL-4 ou l'IL-13) sont immunosuppresseurs et sont impliqués dans les processus de cicatrisation et de régénération tissulaire [16].

## *1.3 Les granulocytes*

Les granulocytes font partie de la lignée myéloïde et regroupent les neutrophiles, les éosinophiles et les basophiles. Comme leur nom l'indique, ces cellules contiennent des granules composés d'enzymes, de cytokines/chimiokines ou de peptides antimicrobiens, qui sont libérés une fois les cellules activées. Ces cellules sont historiquement connues pour être uniquement circulantes et recrutées en cas d'infection ou de blessure. Cependant, des études récentes mettent en évidence l'existence de

neutrophiles et d'éosinophiles résidents dans le poumon [17]–[19], ce qui leur permet d'agir encore plus rapidement.

Les neutrophiles sont les cellules les plus abondantes dans le sang circulant [20] et sont les premières cellules à être recrutées en cas d'infection/blessure [21] via la production de cytokines et chimiokines (essentiellement IL-8, CXCL1/2/5/15) par les cellules épithéliales et macrophages alvéolaires [22]. En plus de leur pouvoir de dégranulation, les neutrophiles sont capables d'éliminer les pathogènes grâce à leur pouvoir phagocytaire mais aussi grâce à leur capacité à libérer des filets appelés NET (neutrophil extracellular trap) contenant entre autres des protéases (Myeloperoxidase, neutrophil elastase, DNAase). Les neutrophiles produisent également des cytokines régulant d'autres cellules immunitaires comme les macrophages alvéolaires [23] ou les lymphocytes T [24].

Contrairement aux neutrophiles, la population d'éosinophiles est la moins abondante dans le sang circulant. Leur production par la moelle osseuse est considérablement augmentée en cas d'infection ou d'allergie [25]; ils sont activés et recrutés par des cytokines de type Th2 (IL-3, IL-5). Une fois activés, les éosinophiles relarguent leurs granules qui contiennent entre autres des protéases (éosinophile élastase) et des toxines (neurotoxines dérivées d'éosinophiles) afin d'éliminer le pathogène. Ils produisent également des cytokines [26] et ont de ce fait des fonctions immunorégulatrices. Il a été décrit que les éosinophiles peuvent promouvoir une réponse immunitaire adaptative de type Th2 soit en agissant en tant que cellules présentatrices d'antigène [27] soit en induisant l'activation des cellules dendritiques [28], faisant des éosinophiles des cellules fortement inflammatoires associées aux allergies.

#### *1.4 Les cellules innées lymphoïdes et Natural Killer (NK)*

Les cellules innées lymphoïdes (ILC) sont des cellules du système immunitaire inné de la lignée lymphoïde, divisées en 3 sous-groupes qui dépendent de leurs fonctions : ILC1 ILC2 et ILC3. Ces cellules ne sont pas spécifiques à des antigènes et répondent aux cytokines présentes dans leur microenvironnement. Ce sont des cellules résidentes qui permettent de lutter contre les infections et favorisent l'homéostasie et la réparation tissulaire [29].

Les cellules tueuses naturelles ou Natural Killer (NK) font partie des ILC1. Elles sont fortement cytotoxiques via leur production de perforine et de granzyme B mais également la production d'IFN- $\gamma$ , permettant de tuer les cellules infectées ou tumorales. Les NK possèdent également un rôle immunorégulateur. En effet, les NK produisent des cytokines (IFN- $\gamma$ , IL-10), interagissent avec d'autres cellules immunitaires comme les cellules dendritiques mais également reconnaissent les anticorps liés

à des antigènes ce qui leur permet de déclencher la cytotoxicité à médiation cellulaire dépendante des anticorps (ADCC).

Il a récemment été montré que seulement 20% des NK pulmonaires sont des cellules résidentes du poumon [30]. Même si l'origine des NK résidents n'est pas encore clairement définie, elles sont décrites pour être plus fonctionnelles que les NK circulants d'après leur capacité de dégranulation (expression de CD170a) et de production d'IFN- $\gamma$ . Ceci suggère le rôle protecteur des NK résidents et le contrôle rapide des infections et de la prolifération tumorale [31], [32].

Les NK possèdent des récepteurs activateurs et inhibiteurs leur permettant de dicter leur état actif/inactif. En effet, en conditions physiologiques, les NK sont inactifs grâce à la reconnaissance du CMH-I (exprimé par les cellules du « soi ») via ses récepteurs inhibiteurs (KIRs, ILT2). L'activation des NK repose sur l'absence d'expression du CMH-I et la lyse de la cellule d'intérêt, mais également sur l'augmentation des signaux activateurs par rapport aux signaux inhibiteurs (comme l'expression du CMH-I) via ses récepteurs activateurs (NKG2C/D, NCRs)[33].

### *1.5 Les cellules dendritiques*

Les cellules dendritiques sont des cellules présentatrices d'antigènes (APC) professionnelles. Elles jouent un rôle clé dans la réponse immunitaire puisqu'elles permettent de faire le lien entre l'immunité innée et adaptative, et sont les seules cellules présentatrices d'antigènes capable d'activer efficacement des lymphocytes T naïfs.

Les cellules dendritiques sont présentes sous forme immature au niveau des épithéliums et sont immobiles, à proximité de l'interface avec l'environnement extérieur [34] afin de capturer rapidement les antigènes. En effet, les cellules dendritiques immatures ont une capacité phagocytaire élevée contre les pathogènes, les cellules apoptotiques/nécroptotiques et les débris cellulaires, et un faible pouvoir d'activation des lymphocytes T. Ces particularités font qu'elles sont impliquées dans le processus de tolérance immunitaire qui est essentiel pour limiter les réponses immunitaires contre les tissus sains [35]. En effet, les cellules dendritiques immatures produisent des cytokines anti-inflammatoires (IL-10, TGF $\beta$ ), induisent l'apoptose des lymphocytes T [36] ou leur anergie [37], ou bien la génération de lymphocytes T régulateurs immunosuppresseurs [38], [39] mais expriment également des points de contrôle immunitaires tels que PD-L1 et CTLA-4 empêchant leur pouvoir d'activation. Dans un contexte tumoral par exemple, la présence de cellules dendritiques immatures contribue fortement à l'échappement des cellules tumorales du système immunitaire ; elles représentent ainsi une cible thérapeutique pour réactiver la réponse immunitaire.

Une fois l'antigène reconnu et capturé, les cellules dendritiques s'activent et acquièrent une capacité migratoire grâce à l'expression de CCR7 [40]. Elles migrent ainsi vers les ganglions drainants (dans le cas du poumon, les ganglions médiastinaux) par les vaisseaux lymphatiques afin d'y activer les lymphocytes T [41]. Dans le cadre d'inflammation chronique, des structures lymphoïdes tertiaires appelés iBALT (induced bronchus associated lymphoid tissue) se mettent en place dans le poumon. Ces structures sont maintenues par les cellules dendritiques elles-mêmes et peuvent également y activer les lymphocytes T [42], favorisant ainsi le déclenchement d'une réponse immunitaire locale et plus rapide.

Les cellules dendritiques (DC) pulmonaires résidentes sont les cellules dendritiques conventionnelles de type 1 (cDC1), les cellules dendritiques conventionnelles de type 2 (cDC2) et les cellules dendritiques plasmacytoïdes (pDCs) mais la présence d'inflammation induit aussi la génération de cellules dendritiques dérivées de monocytes (moDCs). Même si les cDC et moDCs sont capables d'activer les lymphocytes T CD4+ et CD8+, il est admis que les cDC1s sont plus efficaces dans la présentation antigénique aux lymphocytes T CD8+ via le CMH-I (dite présentation croisée) [43] tandis que les cDC2s sont plus efficaces dans la présentation antigénique aux lymphocytes T CD4+ via le CMH-II [44].

Les cellules dendritiques peuvent également réguler l'activation des NK de l'immunité innée grâce à des molécules d'adhésion qu'elles expriment (comme CD155 et CD112). Les cellules dendritiques stimulent les NK en libérant des cytokines comme l'IL-12 pour induire la production d'IFN- $\gamma$ , favorisant ainsi leur cytotoxicité, ce qui est particulièrement le cas dans le contexte tumoral [45].

### *1.6 Détection des dommages/ infections par le système immunitaire inné*

Les cellules du système immunitaire et non immunitaire possèdent des récepteurs appelés PRRs (Pattern Recognition Receptors) qui leur permettent de détecter différents types de dommages ou d'infection pour la mise en place de la réponse immunitaire. Ces PRRs reconnaissent des motifs moléculaires associés à des dommages (DAMPs : damage associated molecular pattern) qui sont libérés par les cellules de l'hôte, et des motifs associés à des pathogènes (PAMPs : pathogen associated molecular pattern) qui dérivent de pathogènes.



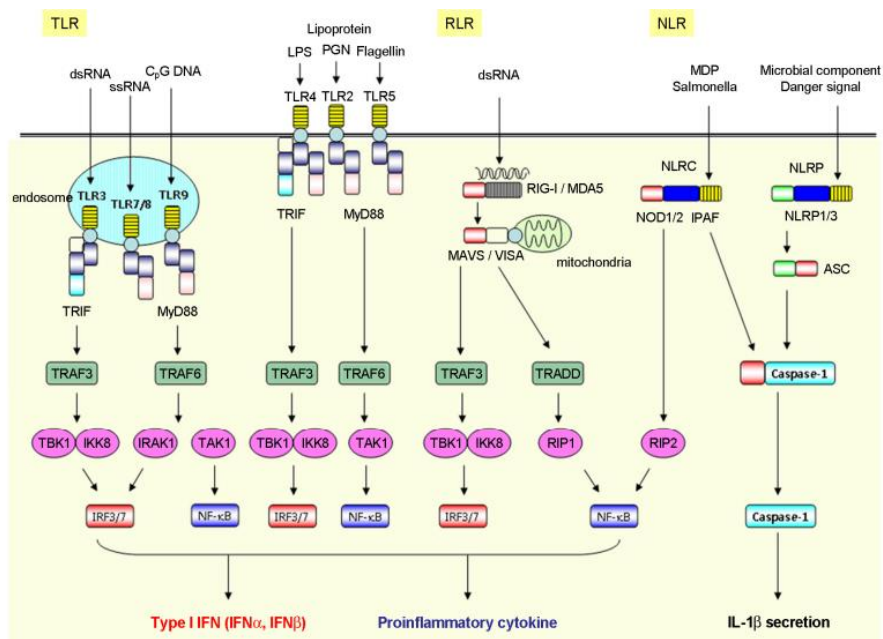


Figure 1 : Les différents PRRs et leurs voies de signalisations [46]

Les PRRs regroupent plusieurs familles de récepteurs : les TLRs, NLRs, RLRs, CLRs et des récepteurs senseurs d'ADN (Figure 1). Etant donné que les DAMPs/PAMPs sont très variés et peuvent être intrinsèque ou extrinsèque à la cellule, ces récepteurs sont spécialisés dans la détection de motifs et sont retrouvés à la membrane plasmique, dans le cytoplasme, les endosomes, ou lysosomes, en fonction du motif qu'ils reconnaissent [47]. En effet, l'expression différentielle des PRRs est liée à deux mécanismes de reconnaissance. La reconnaissance intrinsèque à la cellule se fait par les PRRs intracellulaires exprimés dans des cellules pouvant être infectées, qui émettent par la suite des cytokines, chimiokines pour attirer les cellules immunitaires. De la même manière, les PRRs reconnaissant des motifs extracellulaires sont situés à la membrane plasmique mais également dans le cytosol. Les cellules possédant ce type de PRRs sont spécialisées dans la détection de pathogènes et regroupent les macrophages, cellules dendritiques, ou bien l'épithélium, pouvant directement les éliminer ou initier une réponse immunitaire.

## 2. Système immunitaire adaptatif

La particularité du système adaptatif est de développer une réponse immunitaire spécifique et mémoire pour un antigène donné, permettant la mise en place d'une réponse immunitaire plus rapide et efficace dans le cas d'une deuxième exposition à ce même antigène.

Le système immunitaire adaptatif comprend les lymphocytes T et les lymphocytes B, induisant respectivement une immunité mémoire à médiation cellulaire et humorale. Leur activation et fonction dépendent des cellules du système immunitaire inné, en particulier les cellules dendritiques. Même si

les lymphocytes sont majoritairement circulants ou situés dans les organes lymphoïdes secondaires, il existe des populations de lymphocytes T et B résidentes dans le poumon. Cette partie abordera principalement le rôle des lymphocytes T et la mise en place d'une réponse immunitaire.

### 2.1 Les lymphocytes T

Les lymphocytes T sont des cellules de la lignée lymphoïde, générés à partir de précurseurs dans la moelle osseuse. Ils sont ensuite maturés et sélectionnés dans le thymus avant d'être exportés dans les structures lymphoïdes secondaires sous forme naïve. Leur rôle est d'assurer l'immunité cellulaire spécifique en reconnaissant l'antigène grâce à leur TCR (T cell receptor) afin d'éliminer la cellule infectée/tumorale. Le TCR se met en place pendant la maturation des lymphocytes et subit le phénomène de réarrangement somatique (recombinaison VDJ) ; 90% des lymphocytes T possèdent un TCR qui est composé d'une chaîne  $\alpha$  et d'une chaîne  $\beta$  (les lymphocytes T conventionnels : CD4+ et T CD8+) et une faible proportion de cellules dites  $T\gamma\delta$  (CD4-CD8-, lymphocytes non conventionnels) porte un TCR formé d'une chaîne  $\gamma$  et d'une chaîne  $\delta$ .

Les lymphocytes T sont essentiellement retrouvés dans les structures lymphoïdes secondaires (rate et ganglions lymphatiques), dans le sang circulant mais également au niveau des muqueuses dont celle du poumon.

#### 2.1.1 Activation du lymphocyte T CD4+ et CD8+

Comme évoqué plus haut, l'activation d'un lymphocyte T dépend de la présentation antigénique via le CMH par les cellules présentatrices d'antigène comme les cellules dendritiques. Une fois que les cellules dendritiques ont reconnu un antigène, elles migrent dans le ganglion lymphatique et deviennent matures. Elles expriment alors à leur surface des molécules de costimulation (CD80 CD86 CD40) nécessaires aux processus d'activation des lymphocytes T naïfs. Elles présentent l'antigène sur le CMH-I ou CMH-II et forment une synapse immunologique avec le lymphocyte T naïf qui se déroule en une succession de trois signaux :

1. Reconnaissance du complexe peptide antigénique-CMH grâce au TCR du lymphocyte T et liaison des molécules de costimulation CD80/86 et CD40 aux molécules CD28 et CD40L du lymphocyte T
2. Expansion clonale des lymphocytes T via la sécrétion autocrine d'IL-2 induite à la suite du signal 1.
3. Polarisation du lymphocyte T CD4+ naïf en lymphocyte T auxiliaire (helper) Th1, Th2, Th17 ou Treg en fonction de la production cytokinique de la cellule dendritique et la nature de l'antigène, et activation du lymphocyte T CD8+ en lymphocyte T cytotoxique Tc1, Tc2 ou Tc17.

Une fois activés, les lymphocytes T seront dirigés vers la cellule d'intérêt grâce à un réseau de chimiokines. Une fois l'antigène éliminé, la majorité des lymphocytes T effecteurs rentrent en apoptose mais une petite partie reste maintenue (étape de contraction) et constitue le pool de lymphocytes mémoires. Les lymphocytes T mémoires persistent dans l'organisme pendant des années, et sont capables de détruire directement une cellule présentant le même antigène lors d'une deuxième exposition, sans être réactivés par une APC.

Les lymphocytes T mémoires sont de plusieurs types et diffèrent selon leur localisation et fonctionnalité. Il existe quatre sous-type de lymphocytes T mémoires :

- Lymphocytes T centraux mémoires (T<sub>cm</sub>) : sont localisés dans les structures lymphoïdes secondaires, ils possèdent une forte capacité de prolifération.
- Lymphocytes T effecteurs mémoires (T<sub>em</sub>) : sont localisés dans les structures lymphoïdes secondaires, ils possèdent des capacités migratoires leur permettant de migrer vers des organes non lymphoïdes comme les tumeurs. Les T<sub>em</sub> sont dotés d'une forte cytotoxicité.
- Lymphocytes T résidents mémoires (T<sub>rm</sub>) : sont localisés dans le tissu, au niveau des muqueuses et sont non circulants. Ils constituent ainsi une forte barrière locale.
- Lymphocytes T souches mémoires (T<sub>scm</sub>) : sont circulants et peuvent être retrouvés dans les ganglions ou le tissu. Ces cellules ont des caractéristiques de cellules souches à savoir une forte capacité d'auto-renouvellement et de prolifération.

Cependant, leur répartition n'est pas équitable : ces cellules peuplent majoritairement les muqueuses plutôt que les ganglions lymphatiques ou la rate [48]. Étant donné que les muqueuses pulmonaires sont exposées fréquemment à des pathogènes, la présence de cellules mémoires à proximité constitue un avantage conséquent.

Les lymphocytes T sont ainsi des cellules comprenant de nombreux sous-groupes et sont impliqués dans l'homéostasie tissulaire. La dérégulation de cette réponse peut être fortement délétère et participe au développement de pathologies chroniques dont les pathologies pulmonaires.

La différenciation et fonctions des lymphocytes T dépendent du milieu cytokinique, de signaux co-inhibiteurs et co-stimulateurs mais aussi de facteurs épigénétiques modulant l'expression de facteurs de transcription impliqués dans la production de cytokines. De ce fait, les lymphocytes T possèdent une forte plasticité, ce qui place la modulation de la réponse T comme stratégie thérapeutique intéressante.

## 2.1.2 Polarisation des lymphocytes T

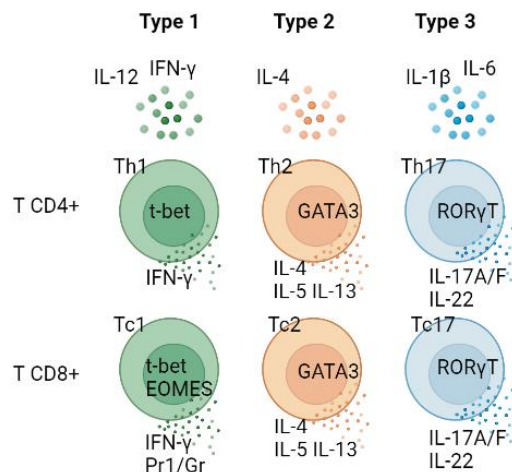


Figure 2 : Les trois principales voies de polarisation des lymphocytes T  
Crée avec biorender.com

Lors de l'activation des lymphocytes T, la cellule dendritique produit différentes cytokines en fonction de l'antigène reconnu et de la présence de particules environnementales dans le cas du poumon. Ces facteurs vont orienter la différenciation des lymphocytes T en induisant l'expression de facteurs de transcription. Trois voies majeures sont induites en fonction des différentes cytokines (Figure 2).

### 2.1.2.1 Immunité de type 1

Les lymphocytes Th1, font partie de l'immunité de type 1 avec les lymphocytes Tc1 et les NK (ILC1). Grâce à leur facteur de transcription t-bet, ils sont capables d'inhiber l'expression des facteurs de transcription GATA3 et RORγT, empêchant ainsi la différenciation des T CD4+ en Th2 et Th17 [49], [50]. Ils stimulent les lymphocytes T CD8+, les macrophages et les lymphocytes B grâce à leur production d'IFN-γ mais sont également stimulés par l'IFN-γ produit par les NK. En plus de leur importance dans l'élimination des bactéries ou de virus, les cellules de l'immunité de type 1 jouent un rôle important dans l'élimination des cellules tumorales via la production d'IFN-γ mais également de granules cytolytiques (perforine et granzyme) dans le cas des Tc1 et NK.

### 2.1.2.2 Immunité de type 2

L'immunité de type 2 comprend les lymphocytes Th2, Tc2 et ILC2. Les lymphocytes Th2 sont fortement retrouvés au niveau des voies respiratoires, particulièrement en cas d'exposition à des allergènes grâce à la production de chimiokine CCL17 par l'épithélium pulmonaire reconnu par le récepteur CCR4 des Th2 [51]. La production de cytokines de type 2 permet le recrutement et l'activation de granulocytes, notamment les éosinophiles. Non seulement la voie Th2 permet de lutter contre les infections, ce type de voie est également associé aux allergies [52], [53] et aux maladies

inflammatoires [54]. De façon similaire à t-bet dans les Th1, GATA3 réprime l'expression de t-bet et ROR $\gamma$ T pour la différenciation des Th2 [55], [56]. De façon intéressante, le récepteur de l'IL-12R est non seulement exprimé par les Th1, mais aussi par les Th2, ce qui contribue à la différenciation du Th2 en Th1 en présence d'IL-12 [57]. De même, les Tc2 peuvent acquérir un phénotype Tc1 en produisant d'IFN- $\gamma$ , mais restent moins cytotoxiques que les Tc1.

### 2.1.2.3 Immunité de type 3

L'immunité de type 3 comprend les Th17, Tc17 et ILC3. Contrairement aux Th1 et Th2, les Th17 sont minoritaires au site inflammatoire. En effet, il existe des mécanismes limitant leur expansion : ils possèdent une faible capacité de production d'IL-2 [58], d'entrer en division [59], mais également possèdent une forte plasticité leur permettant de se différencier en Th1 et produire de l'IFN- $\gamma$  [60] sous l'action de l'IL-12 [61]. De façon similaire, les Tc17 peuvent produire l'IFN- $\gamma$  sous l'action de l'IL-12 tout en maintenant leur production d'IL-17 et leur faible cytotoxicité par rapport aux Tc1 [62]–[64]. La production d'IL-17A/F et d'IL-22 permet l'activation de cellules immunitaires (neutrophiles) et non immunitaires (cellules épithéliales, fibroblastes) pour produire des métalloprotéases, des cytokines ainsi que des peptides antimicrobiens permettant l'élimination des pathogènes. Ces cytokines jouent ainsi un rôle dans la réparation tissulaire [64]–[66] et sont également impliqués dans des pathologies inflammatoires.

### 2.1.2.4 Les lymphocytes T régulateurs (Treg)

La présence des lymphocytes T régulateurs (CD4<sup>+</sup> ou CD8<sup>+</sup>) est favorisée par le TGF $\beta$ , et l'IL-2. Les Tregs contrôlent l'excès d'inflammation pour maintenir une homéostasie tissulaire et jouent ainsi un rôle important dans la tolérance. De ce fait, ils ont une fonction immunorégulatrice modulant l'activité des lymphocytes T CD4<sup>+</sup>, CD8<sup>+</sup>, NK, NKT, lymphocytes B ainsi que les cellules myéloïdes [67]. Cette régulation peut se faire via leur production d'IL-10 et de TGF $\beta$  mais aussi grâce leur forte consommation d'IL-2 [68]. Ils peuvent exprimer des récepteurs de surface aux fonctions inhibitrices tels que les points de contrôle immunitaire (PD-1, CTLA-4) [69] ou des ectonucléotidases (CD73, CD39) générant de l'adénosine aux propriétés immunosuppressives [70]. Les Tregs sont également capables de tuer directement les APC ou les lymphocytes T en relarguant des granzymes et perforines [71] mais aussi en diminuant l'expression des molécules de costimulation CD80/86 des APC par trans-endoctose [72].

Etant donné leur rôle immunosuppresseur, ils ont à la fois un rôle protecteur et délétère en fonction de la pathologie. En effet, la présence des Tregs permet de limiter l'inflammation dans les maladies

inflammatoires mais empêche les fonctions effectrices des autres cellules immunitaires dans un contexte tumoral [73].

### 2.1.3 Autres lymphocytes T

Les lymphocytes non conventionnels regroupent les lymphocytes  $T\gamma\delta$  et NKT du fait de leur système de reconnaissance de l'antigène. En effet, les lymphocytes  $T\gamma\delta$  ne nécessitent pas de présentation antigénique par le CMH mais reconnaissent des phospho-antigènes via leur TCR exprimés par les cellules infectées/tumorales afin de les éliminer. Quant aux lymphocytes NKT (Natural Killer T), ils reconnaissent des glycolipides présentés par un CMH non conventionnel appelé CD1d.

## 2.2 Les lymphocytes B

Les lymphocytes B font partie de la lignée lymphoïde. Leur rôle est d'assurer l'immunité humorale, en produisant des anticorps spécifiques à des antigènes (IgM, IgA, IgG, IgE). Ils possèdent également la capacité de présentation antigénique et amplifient la réponse T.

Les lymphocytes B (B1 et B2) sont générés par la moelle osseuse à partir de précurseurs hématopoïétiques et sont présents dans les organes lymphoïdes secondaires (rate et ganglions lymphatiques). Cependant, une fraction des lymphocytes B1 est d'origine fœtale [74] et est retrouvée au niveau des muqueuses, dont la muqueuse pulmonaire.

La reconnaissance de l'antigène se fait grâce à une panoplie de récepteurs appelés BCR (B cell receptor) qui se mettent en place durant leur différenciation (recombinaison VDJ); chaque cellule B possède un BCR spécifique à un antigène donné. Une fois l'antigène reconnu, le lymphocyte B prolifère et se différencie en plasmocyte ou lymphocyte B mémoire dans des structures appelées centres germinatifs des ganglions lymphatiques ou dans les iBALTs. Les plasmocytes produisent constitutivement un grand nombre d'anticorps avec une très forte affinité contre l'antigène alors que les cellules mémoires ne produisent d'anticorps que lors d'une deuxième rencontre avec l'antigène. L'anticorps lié à l'antigène sera reconnu par les phagocytes ou les NK pour déclencher respectivement l'opsonisation ou l'ADCC (IgG, IgA) mais peuvent aussi empêcher la liaison de pathogènes au niveau des muqueuses (IgA, IgG) ou activer la cascade du complément (IgG, IgM).

L'activation des lymphocytes B1 ne nécessite pas d'interaction avec les lymphocytes T et permet une production rapide d'IgA et d'IgM au niveau des muqueuses. Les lymphocytes B1 produisent spontanément de grandes quantités d'IgA et d'IgM, nécessaires pour la reconnaissance rapide de pathogènes et le maintien de l'homéostasie [75]. De ce fait, elles sont également décrites pour contribuer au développement de maladies auto-immunes [76].

A l'instar des lymphocytes B1, les lymphocytes B2 requièrent une interaction avec les lymphocytes T auxiliaires [77] par l'intermédiaire de cytokines et de la reconnaissance du couple CD40/CD40-L exprimés respectivement par les B et T. Cette interaction permet l'activation des lymphocytes B mais favorise aussi l'activation des lymphocytes T et leur production de cytokines via la présentation antigénique par les B [78]. La survie des lymphocytes B est augmentée par la production de facteurs de croissance APRIL et BAFF par les cellules dendritiques qui peuvent aussi les activer [79]. Leur production d'anticorps dépend du lymphocyte T : les Th1 favorisent la production d'IgG tandis que les Th2 induisent la production d'IgA et d'IgE [80].

Il existe également des lymphocytes B régulateurs (Breg) aux fonctions immunosuppressives via leur production d'IL-10 ou de TGF $\beta$ . Les Bregs sont ainsi impliqués dans le processus de tolérance mais également dans le cadre d'infections ou de cancer.

### 3. Système immunitaire et développement de pathologies

Ainsi, les différentes cellules immunitaires ont des propriétés propres et interagissent entre elles pour éliminer rapidement et efficacement les pathogènes, les cellules infectées ou tumorales, et pour réparer le tissu en cas de blessure. Cependant, la dérégulation de cette réponse, qu'elle soit excessive (chronique ou aigue) ou atténuée contribue au développement de pathologies. Je me suis intéressée au cours de ma thèse à deux pathologies pulmonaires associées à une dérégulation immunitaire : le cancer et la fibrose.

## B. Rôle de l'immunité dans le cancer du poumon

Le cancer est une maladie caractérisée par une transformation maligne des cellules qui prolifèrent de façon incontrôlée formant un amas cellulaire (tumeur) ; elles résistent aux mécanismes cellulaires internes mis en place pour éviter leur prolifération excessive. Au cours de cette croissance, les cellules acquièrent de nouvelles propriétés et exploitent les mécanismes de l'hôte en faveur de leur survie.

Les cellules cancéreuses possèdent ainsi plusieurs propriétés communes proposées par Hanahan et Weinberg pour la première fois en 2000 au nombre de 8, sous le nom « Hallmarks of cancer » [81]. Le nombre et la diversité de propriétés ne fait qu'augmenter depuis ; la dernière actualisation par Hanahan [82] regroupe 14 propriétés (Figure 3). Les cellules cancéreuses sont essentiellement caractérisées par leur instabilité génomique qui favorise l'apparition de mutations et qui contribuent fortement à leur résistance intrinsèque à la mort cellulaire et leur prolifération constante.

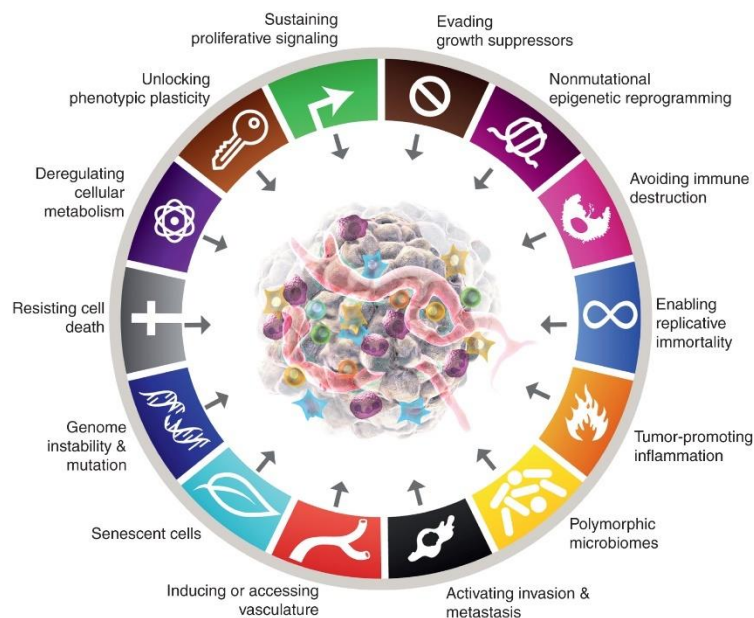


Figure 3 : Hallmarks of cancers [82]

Il est à noter que l'implication du système immunitaire n'a été introduite parmi les « Hallmarks of cancer » qu'en 2011 [83]. En effet, le rôle du système immunitaire dans le contrôle de la croissance tumorale a été décrit depuis le XIX<sup>ème</sup> siècle, mais la communauté scientifique n'a accepté ce concept qu'au début du XX<sup>ème</sup> siècle. Depuis, les recherches en onco-immunologie n'ont fait qu'augmenter et ont révolutionné le traitement des cancers. En effet, la découverte et la compréhension des mécanismes immunitaires antitumoraux ont permis le développement de thérapies, appelées immunothérapies, afin de potentialiser la réponse immunitaire antitumorale.



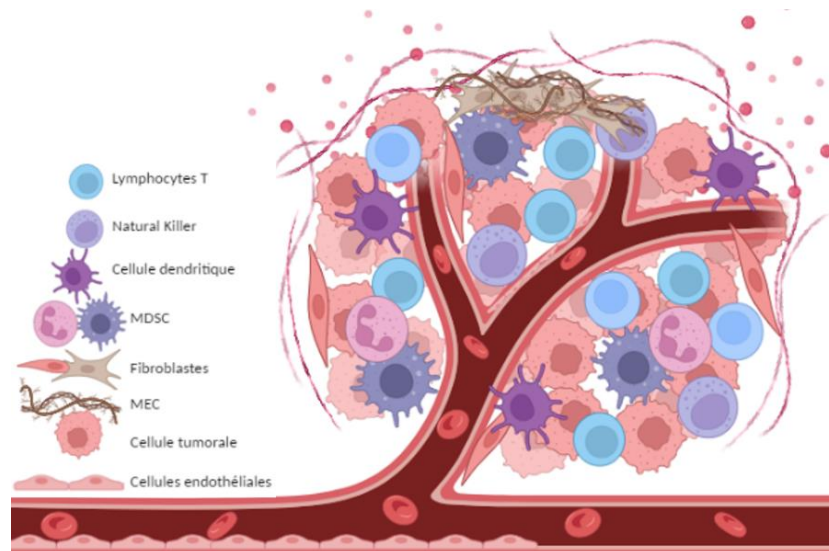


Figure 4 : Le microenvironnement tumoral  
Crée avec biorender.com

La tumeur maligne comprend l'amas de cellules cancéreuses mais également d'autres types cellulaires et forment le microenvironnement tumoral. Le microenvironnement tumoral regroupe, à part les cellules tumorales, les cellules immunitaires, les fibroblastes associés aux tumeurs et les cellules endothéliales. Les différents constituants du microenvironnement tumoral interagissent entre eux et contribuent au développement de la tumeur d'après la figure 4.

## 1. Rôle du système immunitaire dans la croissance tumorale

### 1.1 La réponse immunitaire antitumorale

La réponse immunitaire antitumorale regroupe les cellules du système immunitaire inné et adaptatif. Parmi les cellules du système inné, nous retrouvons principalement les NK et les macrophages M1 capables d'éliminer la cellule tumorale de façon non spécifique. Du côté des lymphocytes T, les lymphocytes T CD8+ cytotoxiques (Tc1) jouent un rôle prépondérant dans l'élimination spécifique des cellules tumorales aux côtés des lymphocytes Th1, ce qui souligne l'implication majeure des cellules présentatrices d'antigène, dont les cellules dendritiques.

Le processus d'oncogenèse favorise la présence d'antigènes tumoraux présentés par le CMH-I à leur surface et qui seront détectés par les cellules immunitaires [84].

#### 1.1.1 Capture des antigènes tumoraux

La capture des antigènes tumoraux se fait essentiellement par les cellules dendritiques (mais aussi par les autres APC) au niveau du site tumoral. La libération d'antigènes, et des DAMPs, par les cellules

tumorales permet le recrutement des cellules dendritiques au site tumoral ainsi que leur maturation (expression des molécules de costimulation) pour une présentation antigénique optimale. Cette dernière est fortement favorisée lors d'une mort cellulaire immunogène : ce type de mort est capable de déclencher une réponse immunitaire [85] grâce à la libération de DAMPs par les cellules tumorales. Ce type de mort peut être déclenché par les lymphocytes T/NK mais également par des inducteurs de mort immunogène (certaines chimiothérapies, radiothérapie, photothérapies) qui induisent des stress cellulaires conduisant à la mort cellulaire. En effet, les DAMPs regroupent une variété de protéines intracellulaires, d'acides nucléiques et de nucléotides qui possèdent des fonctions non immunogènes lorsqu'ils sont contenus dans une cellule vivante (Tableau 1). Cependant, leur présence dans le milieu extracellulaire ou bien leur exposition membranaire permet la stimulation et le recrutement de cellules immunitaires du système adaptatif et inné. Les DAMPs, leurs récepteurs respectifs ainsi que leur impact sur les cellules immunitaires sont regroupés dans le tableau 2. L'attraction des cellules dendritiques cDC1 est également favorisée par la production de chimiokines CCL5/XCL1 par les NK sur le site tumoral [86].

<b>DAMP</b>	<b>Nature</b>	<b>Effet</b>	<b>Récepteurs principaux</b>
ANXA1	Protéine de surface	Dirige les APCs vers les cellules mourantes	FPR1
ATP	Nucléotide	Recrutement, maturation et présentation croisée des APCs	P2RX7 P2RY2
CALR	Protéine chaperonne du RE	Favorise la capture des cellules mourantes des APCs	LRP1
CCL2 CXCL1 CXCL10	Cytokines	Recrutement des T et des neutrophiles	CCR2 CXCR2 CXCR3
HMGB1	Histone	Favorise la maturation et la présentation croisée des APCs	AGER TLR2 TLR4
HSP70 HSP90	Protéines chaperonnes du RE	Favorise la capture des cellules mourantes par les APCs	LRP1
TFAM	Facteur de transcription	Favorise la maturation et le recrutement des APCs	RAGE

*Tableau 1 : Les DAMPs majeurs libérés en cas de mort immunogène.  
Adapté de [87]*

### 1.1.2 Présentation antigénique et activation des lymphocytes

Une fois les antigènes tumoraux capturés et les DAMPs reconnus, les cellules dendritiques migrent vers les ganglions lymphatiques drainants le site tumoral afin d'y activer les lymphocytes T. Les cellules dendritiques peuvent également migrer vers les structures lymphoïdes tertiaires qui se mettent en place dans le microenvironnement tumoral. En effet, ces structures se développent en cas d'inflammation chronique dans des tissus non lymphoïdes, comme dans le microenvironnement tumoral et sont constitutivement similaires aux structures lymphoïdes secondaires (ganglions lymphatiques). La présence des ganglions lymphatiques et des structures lymphoïdes tertiaires assurent une proximité avec le site tumoral qui permet une réponse immunitaire antitumorale plus rapide et plus robuste [88], [89].

L'antigène tumoral capturé est dégradé par des protéases lysosomales ou par le protéasome pour ensuite être présenté sur le CMH-I ou II et permettre l'activation des lymphocytes T [90]–[92]. La production d'IL-12 par les cellules dendritiques, la reconnaissance du complexe CMH-TCR et des molécules de costimulation par les lymphocytes T va permettre l'activation des lymphocytes T CD4+ en Th1 et CD8+ en Tc1 ainsi que leur expansion clonale par la suite. Les lymphocytes T CD4+ favorisent également l'activation et la prolifération des T CD8+ via la production de cytokines [93]. La présence des lymphocytes B en tant qu'APC favorise l'activation des lymphocytes T. En effet, non seulement les lymphocytes B peuvent présenter l'antigène aux T, ils sont capables de le transférer aux cellules dendritiques [94] pour une activation des lymphocytes T plus robuste. De plus, l'interaction avec les lymphocytes T permet également l'activation des lymphocytes B et la production d'anticorps antitumoraux [95], [96].

Les cellules NK ne nécessitent pas de présentation antigénique pour reconnaître et éliminer les cellules tumorales. Cependant, elles interagissent avec les cellules dendritiques via CD40-CD40L [97]. En effet, la production d'IL-2/IL-12/IL-15/IL-18 par les cDC1s favorise l'activation des NK, leur prolifération et leur production d'IFN- $\gamma$  [98], [99] qui favorise la différenciation des T CD4+ naïfs en Th1 [100] et une meilleure réponse CD8+ antitumorale. De même, les NK stimulent la maturation [101] et la survie des cellules dendritiques cDC1 en produisant FLT3L [102], dans le but de favoriser l'activation des T.

Une fois les cellules T activées, elles sont dirigées vers le site tumoral via les vaisseaux sanguins [103] grâce à un réseau de chimiokines sécrétées par les cellules tumorales et stromales. En effet, l'activation des lymphocytes T permet l'expression de CXCR3 à leur surface, qui reconnaît les chimiokines CXCL9/10/11 [104], permettant l'attraction des lymphocytes vers le site tumoral et

améliorant ainsi la réponse antitumorale [105], [106]. D'autres chimiokines CXCR3-independantes ont également été décrites pour favoriser l'infiltrat lymphocytaire dans les tumeurs comme CCXL16 ou CCL21 [107], [108].

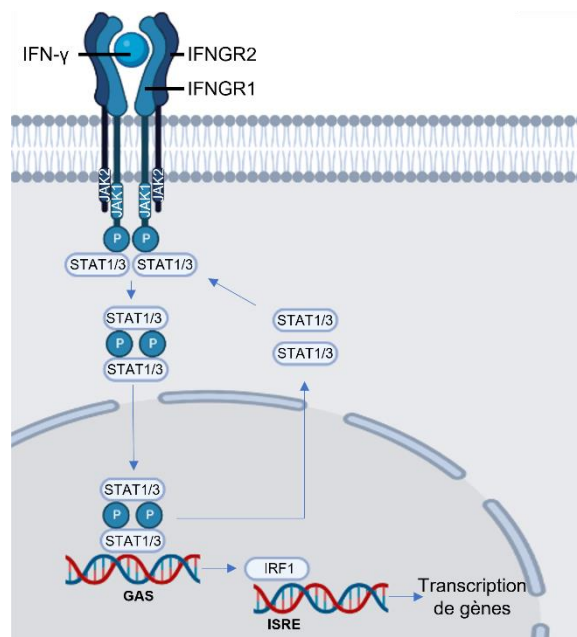
### 1.1.3 Elimination des cellules tumorales

La cellule tumorale est éliminée par les lymphocytes Th1 et CD8+ Tc1 activés infiltrant la tumeur, mais également par les cellules NK et les macrophages M1. L'élimination des cellules tumorales se faisant essentiellement par production de cytokines et granules de cytotoxiques par ces cellules.

#### 1.1.3.1 Production d'IFN- $\gamma$

L'IFN- $\gamma$  est une cytokine produite par les Th1, Tc1, NK ou M1, se lie sur son récepteur, l'IFNGR, exprimé de façon constitutive non seulement par les cellules tumorales, mais par les cellules endothéliales et immunitaires.

L'IFNGR est un tétramère composé de deux sous unités : l'IFNGR1 et IFNGR2. L'IFNGR1 est composé



de deux chaînes qui reconnaissent l'IFN- $\gamma$ . L'IFNGR2 est également formé de deux chaînes, s'associe à l'IFNGR1 pour l'activation optimale du récepteur. La reconnaissance de l'IFN- $\gamma$  par l'IFNGR1 induit l'activation de JAK1 et JAK2 liés respectivement à l'IFNGR1 et IFNGR2 en intracellulaire, afin de phosphoryler les deux chaînes de l'IFNGR1 permettant la liaison du facteur de transcription STAT1 (activation canonique) ou STAT3 (activation non canonique) au récepteur, leur dimérisation et leur migration dans le noyau (Figure 5) [109]. STAT1/3 se lie sur des éléments GAS (gamma-activated sites) régions promotrices de gènes stimulés

Figure 5 : L'IFN- $\gamma$  et son récepteur.

par l'interféron (ISGs : interferon stimulated genes) induisant la transcription d'IRF1 (interferon-regulatory factor 1) [110]. IRF1 est un facteur de transcription permettant la transcription d'une grande variété de gènes en se liant à des régions géniques contenant des éléments de réponses stimulés par l'interféron (ISRE), pouvant être liés à la mort cellulaire [110], [111] ou au cycle cellulaire [112], [113] (Figure 6).

L'IFN- $\gamma$  possède plusieurs propriétés antitumorales. En effet, il est décrit pour être antiprolifératif en induisant dans les cellules tumorales l'expression de p21, une protéine kinase essentielle dans l'arrêt du cycle cellulaire [114] et en induisant la mort des cellules tumorales par apoptose via les caspases -1-3 et -8 [115]–[117] et par nécroptose via RIP1 [118]. De plus, l'IFN- $\gamma$  a des effets anti-angiogéniques [119], [120].

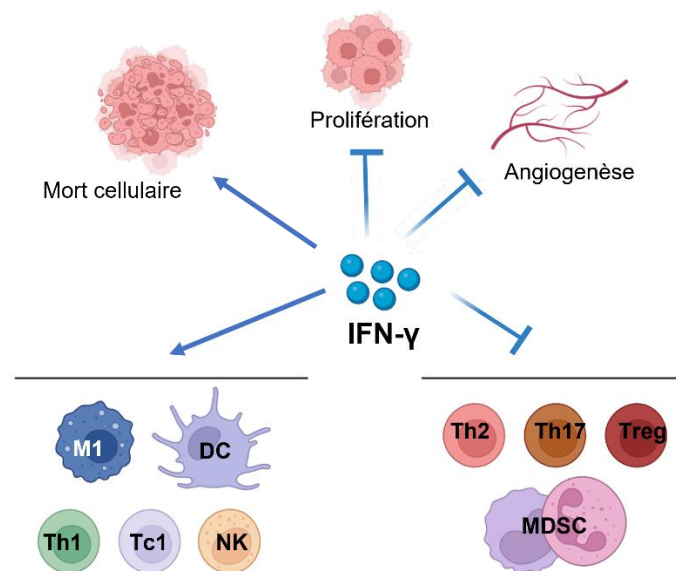


Figure 6 : Les effets antitumoraux de l'IFN- $\gamma$ .  
Crée avec biorender.com

L'IFN- $\gamma$  régule également les cellules immunitaires pour maintenir le contrôle de la croissance tumorale. Il permet le maintien de l'immunité de type 1 en : favorisant l'expression de la voie STAT1/tbet des lymphocytes CD4+ intra tumoraux [121]–[123], en favorisant le profil M1 des macrophages, en inhibant les MDSCs (cellules myéloïdes suppressives) et en favorisant la cytotoxicité des NK et des Tc1 (Figure 6).

### 1.1.3.2 Libération de granules cytotoxiques et des ligands de mort

Les lymphocytes Tc1 et NK reconnaissent la cellule tumorale via respectivement leur TCR et les ligands activateurs pour former une synapse immunologique avec la tumeur. Ceci déclenche les mécanismes effecteurs de ces cellules : la libération de granules cytotoxiques ainsi que la libération de ligands de mort (Fas Ligand et TRAIL).

Les granzymes et perforines sont les protéases majoritaires dans les granules cytotoxiques. Elles sont libérées et concentrées au niveau de la synapse. La perforine permet la formation de pores à la membrane plasmique de la cellule tumorale, facilitant l'entrée des granzymes. Les granzymes A et B sont les plus décrites, elles activent l'apoptose des cellules tumorales [124]. Il existe d'autres

granzymes libérés par dégranulation mais dont le mécanisme d'action n'est pas encore clairement défini [125].

Quant aux ligands de morts, ils sont reconnus par leur récepteurs respectifs Fas et TRAIL-R et induisent la mort des cellules tumorales. Ces ligands peuvent être contenus dans les granules des NK et Tc1 ou sont exprimés à leur membrane plasmique.

La mort des cellules tumorales redéclenche le recrutement des cellules dendritiques. La réponse immunitaire antitumorale constitue ainsi un cycle suivant la figure 7.

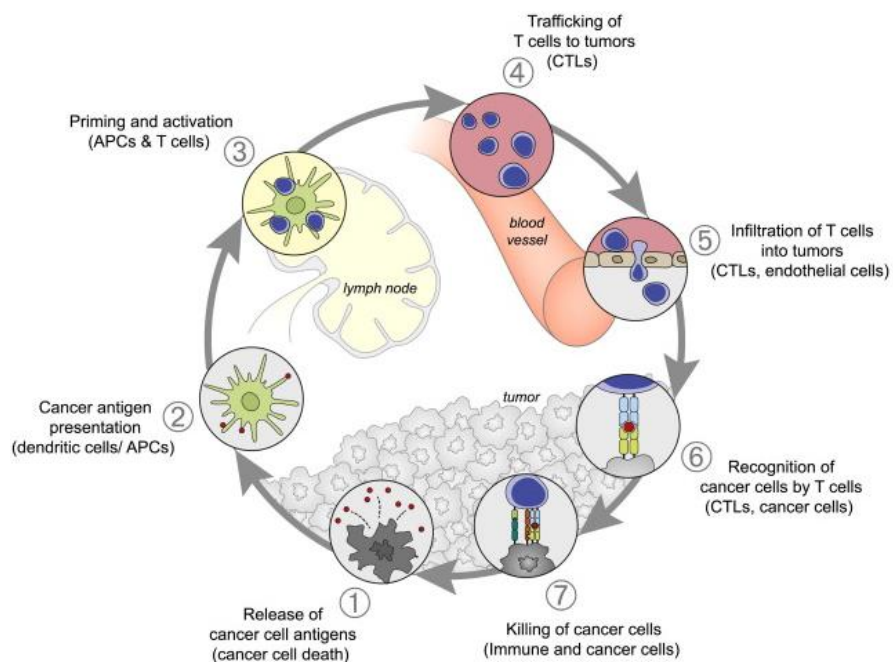


Figure 7 : Le cycle cancer-immunité [126]

## 1.2 Développement tumoral et échappement

Malgré les capacités du système immunitaire à induire une réponse antitumorale efficace, les cellules immunitaires mettent en place des mécanismes de rétrocontrôles négatifs fortement favorisés par la nature du microenvironnement tumoral, pour freiner une réponse immunitaire excessive. Ceci induit l'échappement des tumeurs à l'immunosurveillance et favorise ainsi une croissance tumorale.

### 1.2.1 L'immunoédition

L'immunoédition est un concept regroupant trois étapes clés du contrôle tumoral par le système immunitaire : l'élimination, l'équilibre et l'échappement (Figure 8).

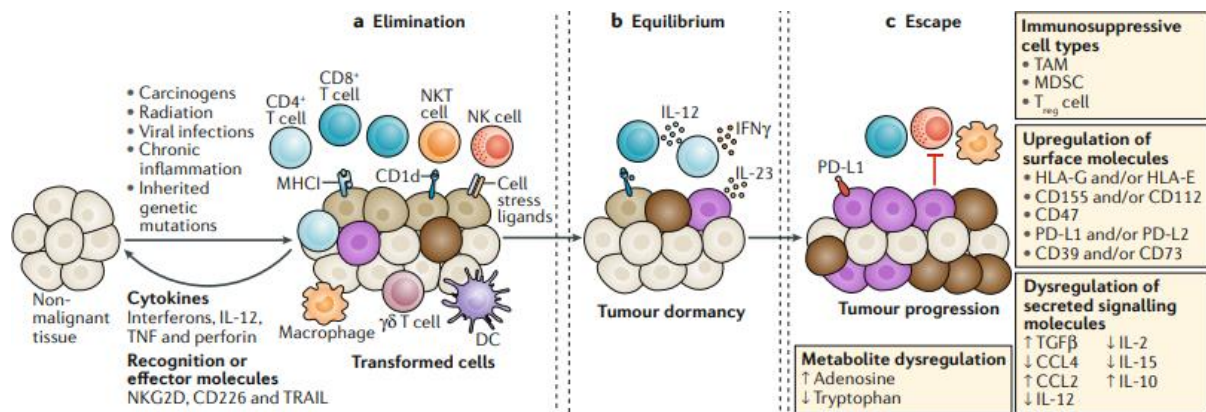


Figure 8 : L'immunoédition [127]

La phase d'élimination correspond à la phase durant laquelle les cellules tumorales sont complètement éliminées par le système immunitaire, suivant une réponse immunitaire antitumorale efficace (décrite dans la partie précédente) regroupant le système adaptatif et inné. Cependant quelques rares cellules tumorales survivent à la phase d'élimination, et sont maintenues en dormance par les cellules du système adaptatif, en particulier l'IL-12, l'IFN- $\gamma$ , les lymphocytes T CD4+ et CD8+. Cette phase d'équilibre empêche ainsi la prolifération des cellules tumorales tout en exerçant une pression de sélection, pouvant modifier leur immunogénicité (capacité à être reconnues par le système immunitaire). La reprise de la prolifération tumorale correspond à la phase d'échappement. Plusieurs mécanismes sont à l'origine de cette reprise : les cellules tumorales peuvent (i) développer des mécanismes de résistance à la mort induite par les cellules immunitaires effectrices, et (ii) peuvent ne plus exprimer d'antigènes, de CMH-I ou des ligands activateurs des NK pour ne plus être détectées. De plus, les cellules tumorales peuvent promouvoir un environnement immunitaire immunosuppresseur, inhibant les fonctions effectrices antitumorales des cellules immunitaires [128].

### 1.2.2 Composition immunosuppresseur du microenvironnement tumoral

Le microenvironnement tumoral contribue à la croissance tumorale par plusieurs mécanismes intrinsèques et extrinsèques à la cellule tumorale, impliquant le système immunitaire. Ces mécanismes regroupent la production de cytokines, de facteurs de croissance ainsi que des cellules et molécules immunosuppresseur.

#### 1.2.2.1 Cellules immunosuppresseur

La production de chimiokines et de facteurs de croissance contribue fortement au phénotype immunosuppresseur du microenvironnement tumoral, en recrutant ou générant des cellules

immunosuppressives. Ces dernières sont les Tregs, les MDSCs et les macrophages associés aux tumeurs de type 2 (TAM2).

L'activité des lymphocytes effecteurs est inhibée non seulement par les Tregs mais aussi par les MDSCs. Les MDSCs sont des cellules myéloïdes immatures regroupant deux types de cellules : les monocytes-MDSC (M-MDSC) et les polymorphonucléaires-MDSC (PMN-MDSC). Ces cellules produisent des enzymes (Arginase-1, nitrite oxide synthase) et des espèces réactives de l'oxygène (ROS) qui affectent l'activité des lymphocytes en diminuant les concentrations d'acides aminés nécessaires à leur survie et cytotoxicité [129]. Elles produisent également des cytokines immunosuppressives (TGFβ, IL-10) pour inhiber les fonctions des lymphocytes T et NK effecteurs [130], [131] et des cellules dendritiques. Ces mécanismes immunosuppressifs sont également employés par les TAM2 [132]. De plus, les MDSCs et TAM2 cellules favorisent l'angiogénèse en produisant des facteurs de croissances et la migration des cellules tumorales en produisant des métalloprotéases. En plus de favoriser l'angiogénèse, le VEGF, (produit par les TAM2, MDSCs et cellules tumorales) favorise également l'infiltration des Tregs et des MDSCs dans la tumeur et empêche la maturation des cellules dendritiques [133].

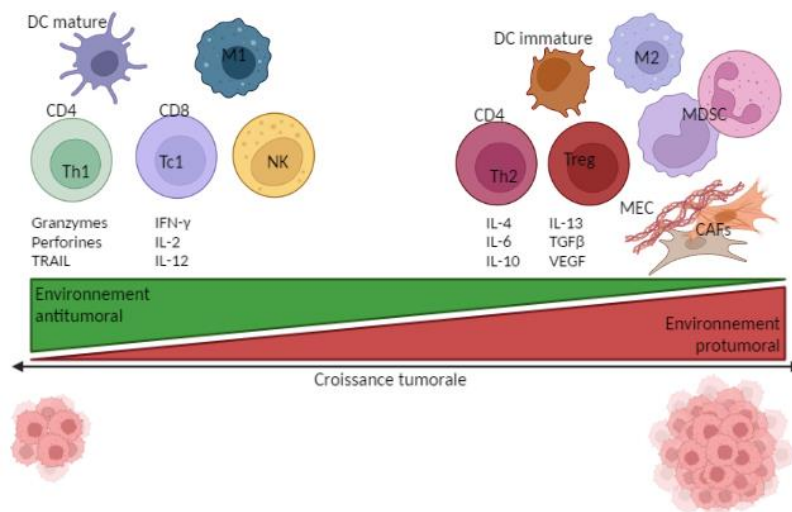


Figure 9 : Cellules immunitaires et croissance tumorale  
Crée avec biorender.com

Les fibroblastes associés aux tumeurs (CAFs) interagissent également avec les cellules immunitaires et contribuent à la prolifération et à l'invasion des cellules tumorales. Ils produisent des cytokines favorisant la présence des TAM2 et induisent la mort des T CD8+ [134]. Les CAFs produisent et sont maintenus par le TGFβ, facteur de croissance favorisant le dépôt de protéines de la matrice extracellulaire (MEC) comme le collagène. Il est décrit que le collagène empêche l'infiltration des lymphocytes dans la tumeur [135], [136], l'interaction des lymphocytes T CD8+ avec la cellule tumorale [137] et par conséquent la marginalisation des lymphocytes T des cellules tumorales,



notamment dans les tumeurs pulmonaires [138], [139]. Les cellules tumorales échappent également à la reconnaissance et cytotoxicité des NK en augmentant l'expression de récepteurs inhibiteurs et en diminuant celle des récepteurs activateurs [140], [141].

Ainsi, les différents composants du microenvironnement tumoral interagissent entre eux via des chimiokines, cytokines ou facteurs de croissance, afin de promouvoir la croissance tumorale et favoriser un environnement immunitaire immunosuppresseur.

### 1.2.2.2 Points de contrôle immunitaires

En conditions physiologiques, le système immunitaire possède des mécanismes permettant de limiter sa stimulation et son action. L'expression de molécules nommées points de contrôle immunitaires (immune checkpoints, IC) évite l'emballement de la réponse immunitaire. La liaison des ICs avec leur ligand induit la perte de fonctionnalité ainsi que la survie de la cellule immunitaire et limite par conséquent l'élimination de la cellule portant l'antigène. Dans le contexte tumoral, l'environnement immunosuppresseur ainsi que l'exposition chronique et forte à l'antigène favorisent l'expression des ICs.

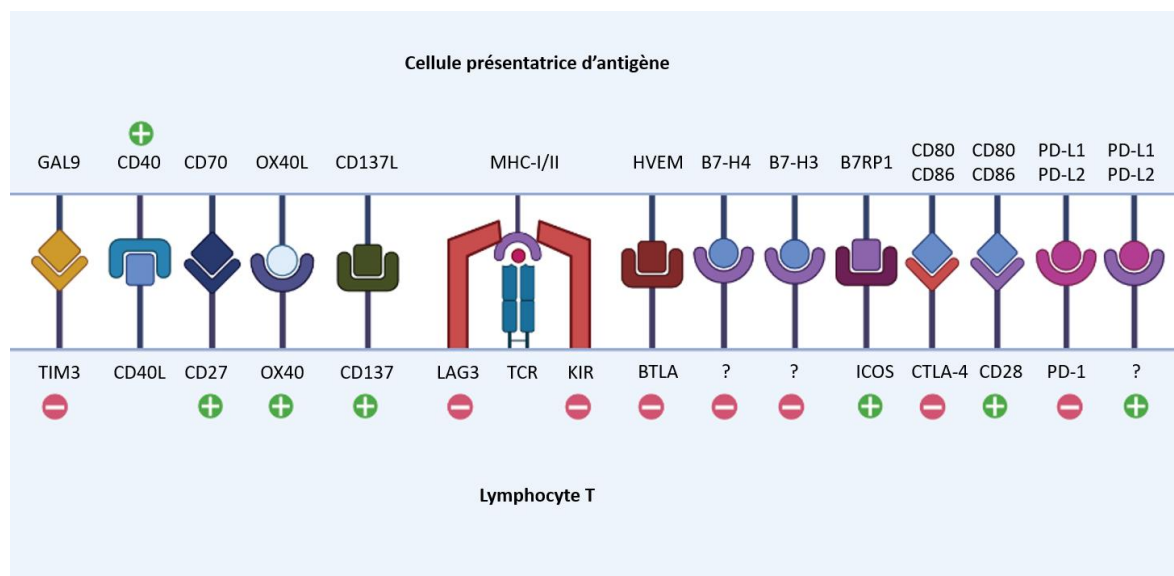


Figure 10 : Les différents immune checkpoints et leurs ligands  
Crée avec biorender.com

Il existe de nombreux ICs (Figure 10) : nous nous attarderons sur les deux ICs les plus étudiés : PD-1 et CTLA-4. PD-1 (CD279) est un récepteur IC possédant deux ligands : PD-L1 (CD274) et PD-L2 (CD273). PD-1 est retrouvé à la surface des lymphocytes T activés, des NK [142] et des APCs alors que PD-L1 et PD-L2 sont exprimés par les cellules tumorales, les CAFs et les MDSCs. La reconnaissance ligand/récepteur empêche l'activation des lymphocytes [143], [144] en inhibant la signalisation TCR et CD28 [145]. De plus, la prolifération des lymphocytes T, la sécrétion de cytokines et la cytotoxicité

sont réduites [146]–[148]. CTLA-4 est un autre récepteur IC se liant aux molécules de costimulation CD80 et CD86, de façon compétitive avec CD28 [149]. CTLA-4 est exprimé par les lymphocytes T et NK activés [150] alors qu’il est aussi constitutivement exprimé par les Tregs [151]. Étant donné le rôle de CD28-CD80/86 dans l’activation des lymphocytes T, la liaison CTLA-4-CD80/86 empêche l’activation [72] et la prolifération des lymphocytes [152]. Le microenvironnement immunosuppresseur favorise davantage l’expression des ICs et regroupe entre autres la présence d’IL-10, de TGFβ, de ROS, des MDSCs et des Tregs [151]. De plus, l’IFN-γ contribue à l’augmentation d’expression de PD-L1 à la surface des cellules tumorales et constitue un des mécanismes permettant de limiter une réponse immunitaire excessive [153].

## 2. Le cancer du poumon

Le cancer du poumon est la première cause de décès par cancer dans le monde et fait partie des trois cancers les plus fréquents avec le cancer colorectal et le cancer du sein [154] et ce, malgré la panoplie d’options thérapeutiques actuelles. Le fort taux de décès et de la faible survie des patients sont dus au diagnostic tardif de la maladie. En effet, les stades précoces sont souvent asymptomatiques, les symptômes apparaissent à des stades tardifs. Ceci implique la nécessité de détecter précocement la présence de cancer mais également de trouver de nouvelles stratégies thérapeutiques plus efficaces pour les cancers de stades avancés.

### 2.1 Facteurs de risque

#### 2.1.1 Facteurs environnementaux

Étant donné l’exposition directe du poumon avec l’environnement extérieur, la majorité des facteurs favorisant le cancer pulmonaire sont non génétiques et/ou environnementaux.

Le tabagisme constitue le facteur de risque le plus important de développer un cancer pulmonaire. En effet, 80-90% des cancers pulmonaires y sont liés [155]. Le tabac contient plus de 9500 éléments chimiques et plus de 80 carcinogènes [156]. Ainsi, la consommation ou l’exposition au tabac favorise l’incidence de ce cancer de façon dose-dépendante, et est de ce fait le facteur de risque le plus facilement évitable. La fumée des combustibles non transformés comme le bois ou le charbon contient de fortes concentrations de carcinogènes et est également associée à une augmentation d’incidence de cancer pulmonaire [157], [158]. De plus, l’exposition professionnelle liée à l’inhalation de particules toxiques et irritantes favorise fortement l’apparition du cancer. Parmi les particules toxiques ou irritantes on peut compter l’amiante [159], la silice [160] ou le radon [155]. La présence

de particules fines due à la pollution favorise aussi l'incidence du cancer du poumon [161], [162] et corrèle fortement avec le taux de mortalité [163].

### 2.1.2 Facteurs intrinsèques

Il existe des facteurs intrinsèques à l'individu qui favorisent le développement de cancers pulmonaires. Les maladies chroniques pulmonaires comme la bronchopneumopathie chronique obstructive [164], [165], la tuberculose [166], [167] ou bien la fibrose pulmonaire [168], [169] constituent un terrain favorable au développement de cancer. En effet, ces pathologies sont accompagnées d'une inflammation chronique (environnement immunosuppresseur) facilitant le développement tumoral [82].

De plus, il existe des facteurs de risques génétiques. Il a été décrit que la présence d'un cas de cancer de poumon dans la famille, en particulier les proches du premier degré, peut augmenter le risque de développer la maladie [170], [171]. Des régions chromosomiques ont été montrées pour contenir des gènes associés à un risque de développer un cancer pulmonaire [172], [173]. Parmi ces gènes, on note la présence de gènes associés à l'addiction au tabac, au gène de la télomérase (TERT, réactivée dans 90% des cancers) et des gènes associés à l'inflammation.

## 2.2 Classification

### 2.2.1 Classification histologique

Le cancer du poumon à petites cellules (CPPC) et le cancer du poumon non à petites cellules (CPNPC) sont les deux grands sous types du cancer du poumon. Ils sont différenciés en fonction de la morphologie cellulaire et du ratio taille du noyau/taille du cytoplasme.

Le CPPC représente 15% des cancers du poumon et constitue la forme la plus agressive de ce cancer. Plus de 70% des patients CPPC ont déjà des métastases au moment du diagnostic. En effet, ce type de cancer a la capacité de métastaser tôt dans le processus d'oncogenèse. Il est fortement associé à la consommation de tabac étant donné que plus de 95% de ces patients sont ou étaient fumeurs [174].

Le CPNPC est le cancer du poumon le plus courant et représente 85% des cancers pulmonaires. C'est un groupe très hétérogène qui a été classifié en plusieurs sous types dont les adénocarcinomes qui sont majoritaires. Même si le tabagisme augmente fortement le risque de développer un adénocarcinome, c'est la forme de cancer de poumon la plus fréquente dans la population générale et chez les non-fumeurs : il constitue 60% des CPNPC et 40% de tous les cancers pulmonaires. Ce type de CPNPC se développe en périphérie du poumon et a une forme glandulaire. Le carcinome

épidermoïde, un autre type de CPNPC, correspond à 20% des cancers pulmonaires et se développe dans la région centrale du poumon, vers les bronches [175]. Cette forme de CPNPC est fortement associée au tabagisme ; sa fréquence a baissé depuis le siècle dernier avec la baisse de consommation de tabac [176], [177].

Etant donné le taux d'incidence du CPNPC, nous nous intéresserons dans ce manuscrit à ce type de cancer en particulier.

### 2.2.2 Classification TNM

La classification TNM (Tumor, Node, Metastasis) est établie par l'association internationale pour l'étude du cancer du poumon (IASLC) et est régulièrement mise à jour. La dernière et la 8ème actualisation date de 2017 (Tableau 2) [178]. Elle permet de classer les différents stades des cancers du poumons dont le CPNPC. C'est aujourd'hui la technique la plus fiable permettant d'indiquer le pronostic afin de pouvoir mettre en place la meilleure stratégie thérapeutique, prenant en compte également la charge mutationnelle correspondante (discutée dans la partie suivante). Cette classification est basée sur la taille et localisation de la tumeur primaire, le nombre et localisations de tumeurs (T), la présence de cellules tumorales dans les ganglions lymphatiques (N) et la présence de métastases (M). Ainsi, plus le stade est avancé, plus le taux de survie est diminué.

T/M	Sous-catégorie	N0	N1	N2	N3
<b>T1</b>	T1a	IA1	IIB	IIIA	IIIB
	T1b	IA2	IIB	IIIA	IIIB
	T1c	IA3	IIB	IIIA	IIIB
<b>T2</b>	T2a	IB	IIB	IIIA	IIIB
	T2b	IIA	IIB	IIIA	IIIB
<b>T3</b>	T3	IIB	IIIA	IIIB	IIIC
<b>T4</b>	T4	IIIA	IIIA	IIIB	IIIC
<b>M1</b>	M1a	IVA	IVA	IVA	IVA
	M1b	IVA	IVA	IVA	IVA
	M1c	IVB	IVB	IVB	IVB

Tableau 2 : Stades des cancers du poumons selon la 8ème classification TNM

*T : tumeur primaire, sous-catégorie en fonction de sa taille (T1 petite <3cm – T4 grande >7cm), N : ganglion lymphatique, sous-catégorie en fonction de la présence et la distance d'invasion par rapport à la tumeur (N0 pas d'invasion, N3 invasion éloignée), M : métastase, sous-catégorie en fonction du nombre et de la distance. Pour plus de précisions, voir [178]*

### 2.2.3 Classification moléculaire

En plus de classer les cancers pulmonaires par histologie et en fonction de l'avancement de la pathologie, les cancers sont également classés en fonction de la mutation somatique ou

réarrangement chromosomique qu'ils présentent. Les différents changements moléculaires sont regroupés dans la figure 11, et affectent des gènes suppresseurs de tumeurs ou des gènes favorisant le développement tumoral. Il est à noter que leur proportion varie entre les stades précoces et métastatiques, due à la progression tumorale. La présence de ces mutations est fortement associée aux différents facteurs de risque, en particulier le tabagisme. En effet, les carcinogènes contenus dans le tabac induisent des dommages à l'ADN favorisant fortement l'apparition de mutations [179]. Les mutations les plus fréquentes dans le CPNPC sont les mutations touchant les gènes de l'EGFR et de KRAS.

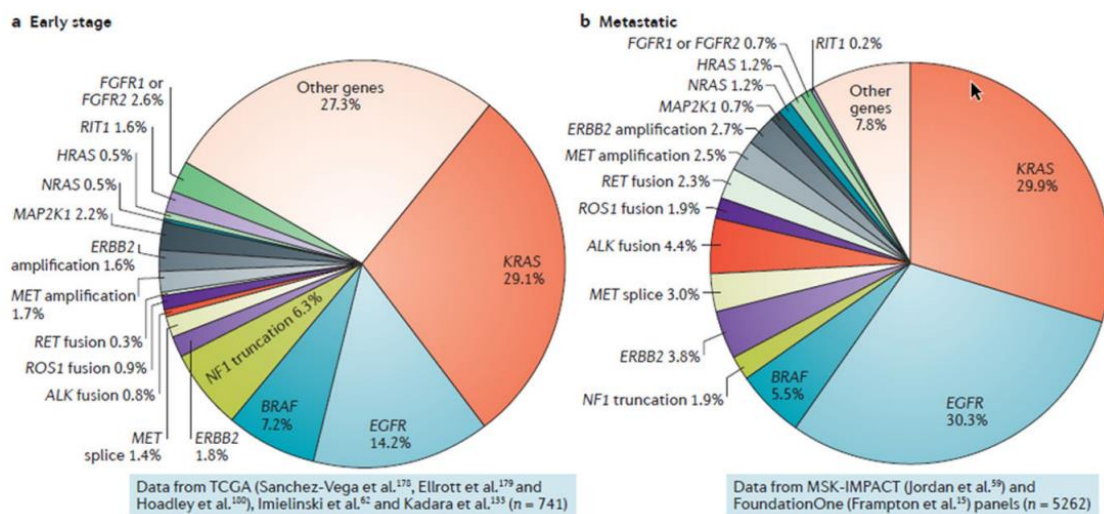


Figure 11 : Mutations promotrices du CPNPC dans les stades précoces et métastatiques [180]

L'EGFR (Epidermal Growth Factor Receptor) est un récepteur tyrosine kinase impliqué dans la prolifération, la migration et la survie cellulaire via l'activation des voies RAS/RAF/MAPK et PI3K/AKT/mTOR. Les mutations de l'EGFR affectent le domaine catalytique tyrosine kinase du récepteur induisant son activation constitutive et l'amplification des voies de signalisation en aval [181]. KRAS est une petite GTPase de la famille des protéines RAS avec NRAS et HRAS, activée en aval des récepteurs tyrosines kinases dont l'EGFR. L'activation de KRAS par hydrolyse du GTP (Guanosine Triphosphate) en GDP (Guanosine Diphosphate) induit les voies de signalisations impliquées dans la prolifération, la régulation du cycle cellulaire, la différenciation et la survie cellulaire. KRAS est la forme la plus mutée des RAS (85%) [182] dans les cancers dont le CPNPC, et plus particulièrement dans les adénocarcinomes. La mutation rend KRAS hyperactive (KRAS-GTP) avec une forte affinité avec les protéines en aval notamment RAF. Les mutations les plus répandues dans le CPNPC sont des substitutions de la glycine du codon 12 (G12X) en Cystéine, Valine ou Asparagine et sont respectivement les mutations KRAS<sup>G12C</sup>, KRAS<sup>G12V</sup> et KRAS<sup>G12D</sup>. La présence de ces mutations est associée au statut fumeur/non-fumeur du patient : la mutation KRAS<sup>G12C</sup> est observée chez les

fumeurs ou anciens fumeurs alors que la mutation KRAS<sup>G12D</sup> est observée chez les non-fumeurs et correspond à la mutation la plus courante chez ces patients [183].

### 2.3 Traitements

Le schéma thérapeutique des patients dépend du type et sous-type des cancers du poumon, du stade de la maladie et de la présence d'altérations moléculaires.

#### 2.3.1 Thérapies ciblant la tumeur

La résection totale de la tumeur ou même du lobe entier (lobectomie) par chirurgie chez les patients atteints d'un CPNPC de stade précoce (stades I-IIIa) est la meilleure thérapie curative. Elle peut être couplée à une thérapie néoadjuvante (avant chirurgie) ou adjuvante (après chirurgie) dans le but d'augmenter le taux de résection, réduire les métastases à distance ou limiter les récives tumorales en éliminant les micrométastases. Les thérapies néoadjuvantes peuvent être des chimiothérapies, radiothérapies, thérapies ciblées ou plus récemment, des immunothérapies.

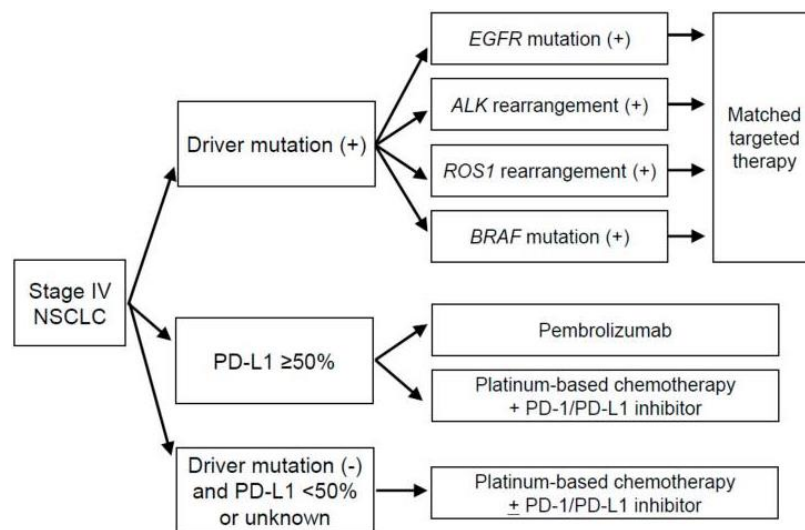


Figure 12 : Schéma thérapeutique des patients atteints de CPNPC de stade IV [184]

La chimiothérapie était le seul traitement disponible pour traiter les CPNPC de stades avancés (stades IIIb-IV). Cette thérapie consiste à tuer les cellules en forte prolifération en induisant des dommages excessifs à l'ADN induisant leur mort. L'introduction de thérapies ciblées contre les mutations promotrices dans le CPNPC au début des années 2000 a augmenté la survie des patients avec et sans progression (Figure 12). Il existe actuellement des thérapies ciblant l'EGFR, ALK, RET, BRAF, ROS1, NTRK, MET et KRAS<sup>G12C</sup>. Par exemple, le traitement ciblant une mutation EGFR augmente la survie du patient de 3 à 5 ans par rapport à la chimiothérapie [185]. Cependant, moins de 25% des patients

peuvent bénéficier des thérapies ciblées. De plus, la majorité de ces patients développent des résistances à ces thérapies pendant le traitement [186].

### 2.3.2 Immunothérapies

L'immunothérapie a révolutionné le traitement des cancers depuis son introduction cette dernière décennie. En effet, ce traitement a montré une augmentation de survie considérable des patients, qui n'avait jamais été atteinte auparavant [187]–[189]. Contrairement aux autres thérapies ciblant la cellule tumorale, l'immunothérapie consiste à exploiter les fonctions effectrices antitumorales des cellules immunitaires.

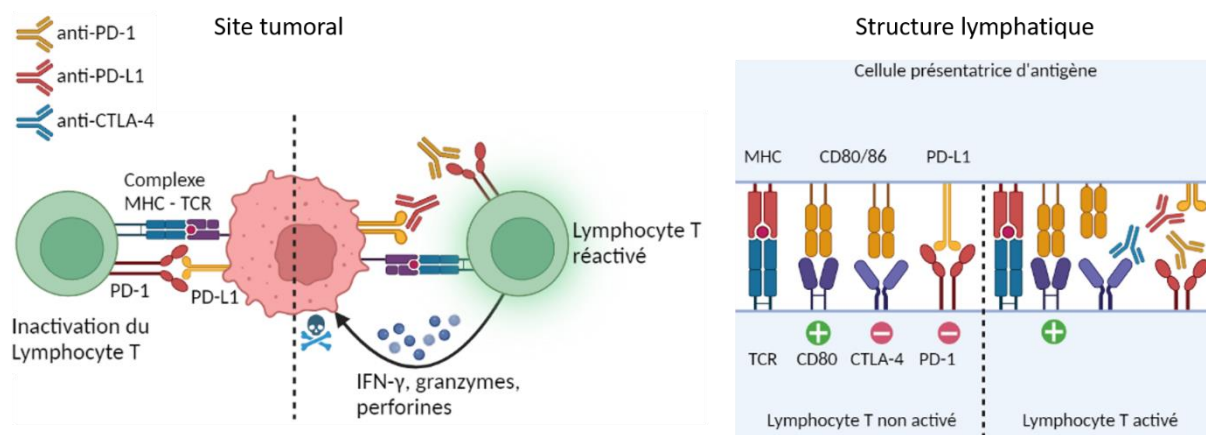


Figure 13 : Réactivation des lymphocytes T par les ICI anti-PD-1/PD-L1 dans le site tumoral et anti-CTLA-4 au niveau des structures lymphatiques. Créé avec biorender.com

Les immunothérapies actuellement utilisées dans le CPNPC sont des anticorps bloquants les points de contrôles immunitaires ou Immune Checkpoint (IC). Ces anticorps sont appelés inhibiteurs des points de contrôles immunitaires ou immune checkpoint inhibitors (ICIs). Ils sont dirigés contre PD-1 (prembrolizumab, nivolumab et cemiplimab), PD-L1 (atezolizumab et durvalumab) et CTLA-4 (ipilimumab) [190]. Ces anticorps consistent à lever l'inhibition causée par ces ICs qu'elle soit au niveau de l'interaction cellule dendritique-lymphocyte T ou au niveau de l'interaction lymphocyte T-cellule tumorale (Figure 13) afin de réactiver les fonctions antitumorales de ces cellules.

L'immunothérapie présente des avantages par rapport à la chimiothérapie : elle est mieux tolérée, permet de mettre en place une réponse immunitaire mémoire, protectrice et durable dans le temps. L'immunothérapie augmente la survie du patient par rapport à la chimiothérapie. Par exemple, la prise de nivolumab réduit le risque de mort de 28% par rapport au docetaxel, augmente le taux de survie de 8% jusqu'à 23% dans les CPNPC épidermoïdes et de 16% à 29% dans les CPNPC non épidermoïdes, et ce avec moins d'effets secondaires [191].

L'administration d'ICIs repose sur le niveau d'expression de PD-L1 (Figure 12) déterminé par immunohistochimie (IHC) : un fort niveau impliquerait la présence de lymphocytes infiltrant la tumeur (TILs) et signerait une meilleure réponse au traitement. Plus récemment, les patients sont traités avec des combinaisons d'immunothérapies et de chimiothérapies. Cette combinaison favoriserait la mort des cellules tumorales, la génération d'antigènes tumoraux, l'augmentation d'expression de PD-L1 mais également la libération de DAMPs dans le cas d'une mort immunogène (utilisation d'inducteurs de mort immunogène) dans le but de favoriser davantage une réponse immunitaire antitumorale. Cette combinaison a augmenté la survie des patients, en particulier ceux ayant un niveau d'expression de PD-L1 inférieur à 50% [188], [189], [192].

### 2.3.3 Résistances et marqueurs d'efficacité des immunothérapies

Malgré l'efficacité des immunothérapies, uniquement 15 à 20% des patients [193] répondent à ce traitement : la majorité des patients présentent des résistances primaires ou développent des résistances pendant le traitement. Etant donné que le mécanisme d'action des ICIs repose sur une la réactivation d'une réponse immunitaire antitumorale, toute altération au niveau des différentes étapes peut induire une résistance aux immunothérapies.

Les résistances sont ainsi liées au microenvironnement tumoral. Le concept de tumeurs « froides » et « chaudes » a été introduit [194] pour distinguer les types de tumeurs pouvant répondre ou non aux ICIs. Les tumeurs « froides » n'expriment pas ou peu PD-L1 ainsi que le CMH-I. Les tumeurs « froides » ont également une faible charge mutationnelle (TMB : tumor mutation burden) qui correspond à l'accumulation de mutations somatiques acquises durant le processus d'oncogenèse à l'origine d'antigènes tumoraux. De plus, ces tumeurs sont soit faiblement infiltrées par des TILs soit ces TILs sont marginalisés dans le stroma, loin du tissu tumoral. Ce type de tumeurs étant faiblement immunogène (peu de PD-L1, peu d'infiltration de TILs, faible TMB) ne répondrait pas aux ICIs. Au contraire, les tumeurs « chaudes » expriment de forts niveaux de PD-L1, sont fortement infiltrées par les TILs avec une expression de la signalisation liée à l'IFN- $\gamma$  [195], mais également un fort TMB [196]. De ce fait, les tumeurs chaudes répondraient mieux aux immunothérapies [197]. Cependant, ce concept est très simplifié alors que la réalité est beaucoup plus complexe avec plusieurs autres acteurs, cellules immunitaires, stromales, tumorales et cytokines, qui rentrent en jeu [127]. La représentation et la répartition des différents acteurs au sein de la tumeur permettrait ainsi de prédire l'efficacité des ICIs, et constitue un concept appelé Immunoscore [198]. Ce score est fortement prédictif et est actuellement utilisé en clinique pour le cancer colorectal [199]. Il a été récemment testé sur une cohorte de 133 patients atteints de CPNPC et a également montré une efficacité de



prédiction des réponses aux ICIs [200]. De plus, la faible infiltration de cellules effectrices antitumorales (CD8, NK) ou la forte présence de cellules et cytokines immunosuppressives (Tregs, MDSCs, TGF $\beta$ , IL-10) constituent un mécanisme de résistance et représentent également des biomarqueurs prédictifs de réponse aux ICIs [201]–[204].

Certains patients ne répondent pas à l'immunothérapie malgré les niveaux élevés de PD-L1 tandis que d'autres y répondent alors qu'ils présentent de faibles niveaux de PD-L1. Ceci montre davantage que l'expression unique de PD-L1 ne constitue pas un marqueur robuste d'efficacité. Cependant, ce résultat peut être dû à des facteurs techniques. La biopsie étudiée ne représente pas forcément l'hétérogénéité de la tumeur et de ce fait la distribution d'expression de PD-L1 est inégale au sein de la tumeur [205], [206]. De plus, la détermination du niveau d'expression de PD-L1 dépend du clone utilisé en IHC étant donné que les différents clones d'anticorps anti-PD-L1 disponibles montrent des résultats variables [207].

Un autre mécanisme de résistance pourrait être dû à une faible génération de lymphocytes T mémoires. En effet, non seulement le mécanisme des ICIs repose sur la réactivation des fonctions effectrices antitumorales, il est aussi basé sur la mise en place d'une réponse mémoire à l'origine de la perdurance d'efficacité même après arrêt du traitement. Ce mécanisme décrit dans le mélanome n'a pas pour l'instant été décrit dans le CPNPC [208].

Les mécanismes de résistances sont aussi intrinsèques à la cellule tumorale. Comme décrit précédemment, les antigènes spécifiques à la tumeur et le CMH-I sont essentiels pour activer les lymphocytes T et leur permettre de reconnaître la tumeur. Le faible taux de TMB [209]–[211], la faible expression ou une déficience du CMH-I ou de ses composants ( $\beta$ 2-microglobuline) [212]–[214] ont montré une faible réponse aux ICIs anti-PD-1/PD-L1 dans le CPNPC. La faible présentation d'antigènes tumoraux ou l'expression de PD-L1 peuvent être dues aux fortes modifications épigénétiques qui caractérisent la cellule tumorale [82], [215], [216]. D'un autre côté, il a été montré chez les patients atteints de CPNPC comme dans des modèles murins, que la résistance aux anti-PD-1/PD-L1 est due à l'expression d'autres ICs [217] telles que TIM-3 [218], [219] ou LAG-3 [220]. Ces derniers inhibent davantage les fonctions effectrices antitumorales, suggérant que la combinaison anti-PD-1/PD-L1 avec des anti-TIM-3 et anti-LAG3 serait efficace. Des études précliniques ont en effet montré l'efficacité de ces combinaisons [221], [222] et sont actuellement en essai clinique [223]–[225].

De plus, les différentes mutations et altérations génomiques promotrices dans le CPNPC peuvent être à l'origine de la résistance aux immunothérapies. En effet, l'expression d'oncogènes et la répression de gènes suppresseurs de tumeurs peuvent modifier le profil cytokinique et la composition

immunitaire du microenvironnement tumoral. Les ICI sont en effet inefficaces dans la majorité de ces tumeurs bien que certaines expriment de hauts niveaux de PD-L1 (EGFR, ALK, ROS1, MET) et d'autres de faibles niveaux (RET, HER2) [226]–[230].

Il existe ainsi une variété de résistances aux immunothérapies, il est alors crucial d'essayer de les contourner par exemple en exploitant davantage les fonctions antitumorales du système immunitaire.

## C. Rôle de l'immunité dans la fibrose pulmonaire idiopathique

La fibrose pulmonaire correspond au stade final de l'évolution d'un groupe très hétérogène de pneumopathies interstitielles diffuses (PID) associées à une inflammation. Les PID sont des maladies respiratoires chroniques et ont des causes, des pronostics et des traitements différents mais possèdent comme points communs la localisation du processus pathologique au niveau de l'interstitium pulmonaire (tissu conjonctif de soutien des alvéoles et capillaires sanguins) ainsi que le déclin progressif des fonctions respiratoires. La fibrose pulmonaire idiopathique (FPI) fait partie des PID à laquelle je m'intéressai dans cette thèse.

### 1. La fibrose pulmonaire idiopathique

La FPI est une maladie rare mais correspond à la PID la plus fréquente et la plus agressive [231]. Le taux d'incidence de la FPI dépend des régions et varie entre 0.09 à 1.30 pour 10 000 personnes par an [232]. Elle touche plutôt les hommes que les femmes [231], pour des raisons encore inconnues. De plus, les hommes ont un risque de mortalité plus élevé que les femmes [233].

C'est une pathologie progressive, chronique et irréversible. La FPI est limitée au poumon et elle est associée à un fort déclin des fonctions respiratoires et à une détérioration de vie du patient. Le diagnostic est souvent tardif puisqu'il se fait par exclusion des autres PID, ce qui est compliqué étant donné les similitudes cliniques entre les différentes PID et que son origine est inconnue. De plus, l'apparition de symptômes peut se faire plusieurs années après le déclenchement de la maladie, ce qui peut expliquer que la médiane de survie est en moyenne de 3 ans [234], une fois le diagnostic posé.

#### 1.1 Facteurs de risques

##### 1.1.1 Facteurs intrinsèques

La FPI est décrite pour être une maladie liée à l'âge. En effet, le taux d'incidence de la maladie augmente avec l'âge et elle est diagnostiquée chez les patients de plus de 60 ans [235]. Les mécanismes liés au développement de la FPI dus à l'âge sont de plus en plus mis en évidence et impliquent des caractéristiques liées au vieillissement comme le raccourcissement des télomères [236] ou l'instabilité génomique [237]. De plus, diverses prédispositions génétiques favorisent l'apparition de la FPI. En effet, entre 15 et 25% des patients FPI ont déjà eu un cas de FPI dans la famille. Le polymorphisme nucléotidique (SNP) (rs35705950) dans la région promotrice du gène de la mucine 5B (MUC5B), présent dans 10% de la population européenne, augmente le risque de

développer la FPI et représente le facteur de risque le plus robuste [238]. De plus, la présence de SNP de gènes liés à l'inflammation comme TLR3 ou IL-1RA (récepteur antagoniste de l'IL-1) a également été montrée chez des patients FPI [239]–[241]. Plusieurs mutations ont été liées au développement de la FPI dans des cas de FPI familiales ou non. Par exemple, on note les mutations qui touchent des gènes de la télomérase (*TERT*, *TERC*, *RTEL1*, *PARN*) [242], [243], enzyme qui maintient la longueur des télomères au cours de la division cellulaire, mais également de protéines du surfactant (*SFTPC*, *SFTPA2*), indispensables pour une respiration normale [244], [245]. Des modifications épigénétiques ont également été montrées chez des patients atteints de FPI par rapport à des sujets sains, par exemple au niveau du gène de MBD2 dans les macrophages, affectant ainsi la production de TGFβ et favorisant le développement de fibroses [246].

### 1.1.2 Facteurs environnementaux

Différents stimuli environnementaux ont aussi été décrits pour favoriser l'apparition de la FPI : ils peuvent agir en synergie ou être à l'origine des variations génétiques des patients.

Le tabagisme constitue un facteur de risque majeur de cette pathologie mais également le facteur de risque le plus fréquent, puisqu'il corrèle fortement avec l'apparition de la FPI de façon dose-dépendante [247], [248]. En effet, les patients fumeurs ont une faible espérance de vie par rapport aux patients non-fumeurs et développent la maladie plus tôt que les non-fumeurs [249]. L'exposition à des poussières ou fumées de métaux ou de bois [250] mais également à des poussières organiques [251] a montré une corrélation avec l'apparition de la maladie chez les patients. Récemment une étude clinique a montré que l'exposition à l'amiante favorise l'apparition de la FPI chez les patients ayant de prédispositions génétiques pour *MUC5* [252] (NCT03211507). Les particules de l'air [253] ainsi que la pollution [254], [255] mais également des infections virales [256] ont également été montrées comme facteurs de risque ou d'exacerbation de la maladie.

## 1.2 Caractéristiques de la fibrose pulmonaire idiopathique

### 1.2.1 Caractéristiques cliniques

Les symptômes des patients atteints de FPI correspondent à une toux sèche, une dyspnée d'effort qui apparait progressivement mais également de râles crépitants secs et diffus. Au cours de la progression de la maladie, ces symptômes s'amplifient et induisent de fortes gênes respiratoires.

La progression de la maladie peut être suivie en étudiant la variation des fonctions respiratoires grâce aux valeurs de la capacité vitale forcée (CVF) et de la capacité de transfert du monoxyde de carbone

(DLco). Ces valeurs, ainsi que l'âge et le sexe du patient, permettent de calculer un score GAP permettant d'identifier le stade de progression de la maladie [257].

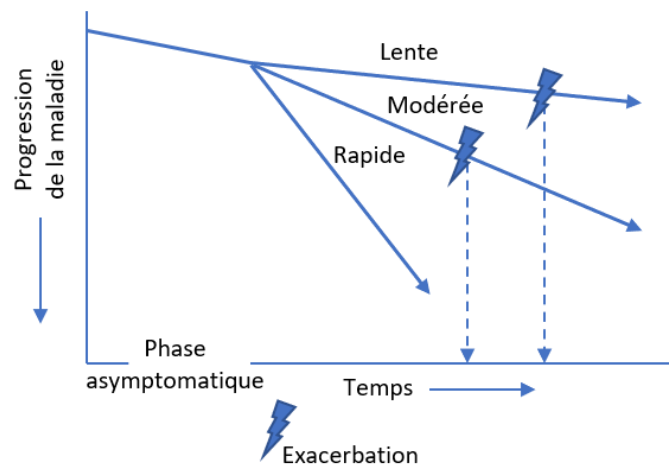


Figure 14 : Vitesses de progression de la FPI

Il existe plusieurs états cliniques de la FPI en fonction de la vitesse de progression de la maladie (Figure 14). La FPI à progression lente est caractérisée par une faible détérioration des fonctions respiratoires, entraînant la mort plusieurs années après le diagnostic alors que la FPI à progression rapide correspond à une faible survie des patients [258]. Ces patients possèdent un profil d'expression génique différents que ceux ayant une progression lente bien que leurs fonctions respiratoires, histologies et radiographies soient similaires au moment du diagnostic [259]. Les patients atteints de FPI sont également sujets à des périodes d'exacerbations aiguës de la maladie qualifiées par le déclin rapide des fonctions respiratoires (diminution de plus de 10% de la CVF ou de 15% de la DLco en moins d'un mois) et l'amplification des symptômes et de l'aspect des poumons par radiographie. Les patients ayant des exacerbations ont une espérance de vie très courte, de 3-4 mois. Ces exacerbations peuvent être dues à des infections, des inhalations de particules, à des médicaments ou peuvent être d'origine inconnue [260].

### 1.2.2 Caractéristiques physiopathologiques

Bien que l'étiologie de la FPI soit inconnue, il est aujourd'hui admis qu'une agression répétée de l'épithélium alvéolaire est le facteur déclenchant de la maladie [261], [262]. Le processus de fibrose, dans la FPI comme dans tout autre pathologie fibrosante, est le résultat d'une réparation tissulaire excessive due à cette agression, qui peut être induite par des facteurs environnementaux comme la fumée de cigarette. La FPI est également associée à une inflammation, qui sera discutée dans la partie suivante.

Le TGF $\beta$  joue un rôle central dans la physiopathologie de la fibrose. En effet, cette cytokine favorise la prolifération des fibroblastes, leur différenciation en myofibroblastes, la production de protéines de

la MEC ainsi que la transition épithelio-mésenchymateuse (TEM) [263], [264]. Le TGF $\beta$  est produit par plusieurs types cellulaires, notamment les fibroblastes, myofibroblastes, les cellules épithéliales, les macrophages et les Tregs.

L'origine des fibroblastes dans la FPI n'est pas clairement définie et pourrait être due à plusieurs mécanismes : la prolifération des fibroblastes résidents, l'activation de fibrocytes en fibroblastes [265] mais également TEM des cellules alvéolaires en fibroblastes [266].

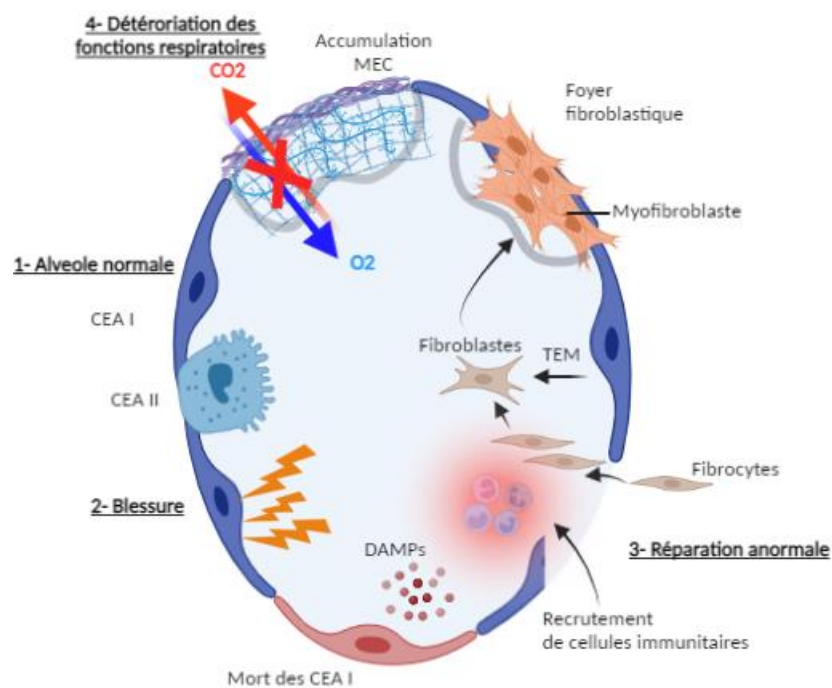


Figure 15 : Le processus de fibrose  
Créé avec biorender.com

Les myofibroblastes sont des fibroblastes activés ayant les propriétés d'une cellule musculaire lisse, et se différencient du fibroblaste par l'expression, entre autres, de l' $\alpha$ -actine du muscle lisse ( $\alpha$ -SMA). Les myofibroblastes sont activés par le TGF $\beta$ , et sont producteurs de facteurs de croissance qui agissent de façon autocrine et paracrine pour favoriser la prolifération, la survie et la différenciation des fibroblastes et myofibroblastes, selon une boucle de rétrocontrôle positif [263]. Contrairement au processus de réparation tissulaire normal, la fibrose se caractérise par une résistance des myofibroblastes à la mort cellulaire, qui contribue fortement à leur accumulation [267]. Ces cellules produisent également des quantités importantes de protéines de la MEC, comme le collagène ou la fibronectine. L'accumulation de ces cellules ainsi que le dépôt excessif de protéines de la MEC rigidifient l'épithélium alvéolaire et diminuent la contractilité du poumon, à l'origine de la diminution du volume pulmonaire et des difficultés respiratoires [268] (Figure 15).

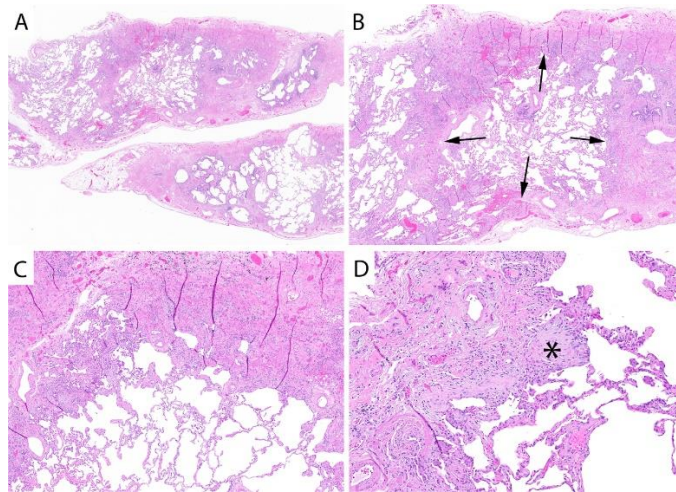


Figure 16 : Coupes histologiques d'une biopsie de poumons FPI

A. Vue générale de la destruction de l'architecture du poumon B. Zones de fibrose à la périphérie (flèches) C. Démarcation entre des régions de fibrose (haut) et une région normale (bas) C. Foyer fibroblastique (\*) : zone active de fibrose. Tiré de [269]

L'accumulation de fibroblastes induit l'épaississement progressif des alvéoles, ce qui diminue la capacité des échanges gazeux, sans modifier le volume total du poumon. D'un point de vue histologique (Figure 16), la surface libre des voies aériennes est ainsi réduite, alors que l'architecture du poumon est détruite [268], [270]. Les régions actives de fibrose sont appelées foyers fibroblastiques siège de la prolifération des fibroblastes et myofibroblastes ainsi que du dépôt de collagène. La FPI se caractérise également par des régions en rayon de miel qui correspondent à des kystes entourés d'un tissu fibreux et bordées par un épithélium [271].

## 2. Implication du système immunitaire

Le rôle du système immunitaire dans la pathogenèse de la FPI est controversé, malgré la présence d'inflammation chronique chez les patients. Cette controverse est due à l'essai clinique PANTHER basé sur l'administration d'anti-inflammatoires (prednisone, azathioprine, et la N-acétylcystéine) qui n'a pas montré d'effets bénéfiques, voire a augmenté la fréquence d'hospitalisation et de décès des patients [272]. Cependant, ceci ne suggère pas forcément l'absence d'implication du système immunitaire, mais plutôt l'utilisation d'une thérapie immunomodulatrice non adaptée. En effet, malgré le manque de connaissances sur l'origine et le mécanisme inflammatoire associée à la FPI, la description des différentes cellules immunitaires et cytokines impliquées, met en avant l'existence de cellules immunitaires ayant des propriétés pro-fibrosantes et anti-fibrosantes aussi bien chez les patients que dans les modèles précliniques.

Même si le mécanisme immunitaire n'est pas clairement défini, il est admis que les agressions de l'épithélium alvéolaire entraînent le relargage de DAMPs, de cytokines/chimiokines et de facteurs de croissance, qui favorisent le recrutement des différentes cellules immunitaires et l'accumulation de

fibroblastes [262], [273], [274]. Dans la partie qui suit, je vais présenter les cellules immunitaires majeures décrites pour être impliquées dans le processus de fibrose (Figure 17).

## 2.1 Système immunitaire inné

### 2.1.1 Monocytes et Macrophages

Les macrophages jouent un rôle prépondérant dans cette maladie. Ils sont différenciés à partir de monocytes recrutés dans le poumon par l'axe CCL2/CCR2 [4] et constituent les cellules immunitaires les plus étudiées dans la fibrose pulmonaire.

Les modèles précliniques ont montré que les monocytes contribuent au développement de la fibrose d'après des déplétions cellulaires et l'inhibition de leur recrutement en utilisant des souris *ccr2*<sup>-/-</sup> [275], [276]. Leur importance dans la progression de la FPI a également été montrée chez les patients : l'augmentation de CCL2 [277]–[279] et du nombre de monocytes circulants est associée à une faible survie et à une augmentation de la fréquence d'hospitalisation [280]–[282]. Ces monocytes recrutés se différencient en macrophages alvéolaires qui sont essentiels pour le développement de la fibrose pulmonaire [283]–[285]. Les macrophages alvéolaires dérivés de monocytes sont plutôt de type M2, exprimant des gènes pro-fibrosants [283]. En effet, les cytokines de type 2 (IL-4, IL-13) et d'IL-10 présentes dans les poumons fibrosés, polarisent les macrophages en type M2 [15], [16] exprimant l'arginine-1, produisant des facteurs de croissance (TGFβ, FGF, PDGF, VEGF) et des chimiokines (CCL18, CCL22). Ceci favorise la prolifération des fibroblastes, leur activation et le dépôt de collagène [286]–[290]. Chez les patients FPI, on retrouve également une augmentation d'expression des gènes pro-fibrosants dans les macrophages alvéolaires, décrits pour être d'origine monocyttaire [291]. La production des cytokines de type 2, dont CCL18, laisse penser que les macrophages pulmonaires de patients FPI sont de type 2 [292]. La présence de ces macrophages ainsi que la production de CCL18 est liée avec une mortalité élevée et une baisse de DLco [293].

La contribution des macrophages M1 dans le développement de la maladie n'est pas très bien définie. Contrairement aux macrophages M2, les macrophages M1 sont pro-inflammatoires (production d'IL-1β, TNFα, IL-12) : ils sont activés par l'IFN-γ et reconnaissent grâce à leurs PRR des DAMPs (dont l'ATP, HMGB1) libérés par les cellules épithéliales. L'inhibition pharmacologique du TLR2/TLR4 ou de HMGB1 ou bien l'utilisation de souris *tlr2*<sup>-/-</sup>/*tlr4*<sup>-/-</sup> dans un modèle préclinique de fibrose pulmonaire a montré des résultats contradictoires [294]–[297]. Quant aux cytokines caractéristiques du macrophage M1, elles ont également des effets contradictoires : l'IL-1β est une cytokine pro-inflammatoire décrite pour



favoriser l'inflammation et l'apparition d'une fibrose pulmonaire [298], [299] alors que l'IL-12 l'inhibe [300].

Etant donné la plasticité des macrophages [15] et la co-expression de marqueurs M1/M2 dans les macrophages alvéolaires dérivés de monocytes *in vivo* [283], il semble difficile de distinguer deux types distincts de macrophages dans cette pathologie. En effet, une étude récente a identifié deux types de macrophages (pro-fibrosants et anti-fibrosants) en fonction des cytokines qu'ils produisent. Cette étude a aussi montré qu'une activation du TLR7 permet de modifier le profil cytokinique de ces macrophages pour les rendre anti-fibrosants [301]. L'ensemble de ces observations démontre la nécessité d'étudier davantage les différents types de macrophages ainsi que leur rôle dans la fibrose pulmonaire.

### 2.1.2 Granulocytes

Comme décrit dans le premier chapitre, les neutrophiles et éosinophiles sont des cellules impliquées dans l'inflammation.

Le rôle des neutrophiles dans la fibrose pulmonaire n'est pas clair : l'étude de leur rôle dans les modèles précliniques a donné des résultats différents. En effet, des études ont montré que la déplétion des neutrophiles n'a pas d'effet sur le développement de la fibrose [302], [303] alors que dans d'autres études les souris déficientes pour la neutrophile élastase (NE) étaient protégées [304], [305]. Ce dernier résultat suggère le rôle pro-fibrosant des neutrophiles est en cohérence avec une étude indépendante qui démontre que les NET favorisent l'activation et la prolifération des fibroblastes [306]. Ceci explique les études faites chez les patients FPI où les niveaux élevés de neutrophiles corrélaient avec un taux de mortalité plus élevé et avec un déclin de la CVF [307]–[309]. Etant donné l'implication de la NE dans le renouvellement de la MEC et la différenciation des fibroblastes [305], [306], et étant donné les niveaux élevés de NE chez les patients [310] et de cytokines/chimiokines impliquées dans le recrutement des neutrophiles (IL-8/G-CSF) [311], [312], il est possible d'envisager une contribution des neutrophiles dans le développement de la pathologie.

L'étude des éosinophiles dans un modèle murin de fibrose induite par la bléomycine a montré que ces cellules ne sont pas impliquées dans la mise en place de la fibrose [313]. De même, les niveaux d'éosinophiles chez les patients FPI ne sont pas associés à la progression de la maladie ni à la mortalité [309], suggérant que les éosinophiles ne jouent pas de rôle majeur dans le développement de la FPI. Cependant, les éosinophiles sont des cellules clés dans les maladies inflammatoires pulmonaires : leur activation et leur survie dépend de l'IL-5. Cette cytokine est produite par les Th2 [18], [314], fortement

abondantes dans les tissus fibrosés (discuté dans la partie 2.2.1 de ce chapitre). Peu d'études sont disponibles sur le rôle des éosinophiles dans la fibrose mais d'après leurs propriétés et les études faites sur les cytokines de type 2 [315]–[317], ces cellules pourraient jouer un rôle dans le développement ou le maintien de la fibrose pulmonaire.

### 2.1.3 Cellules dendritiques

Les cellules dendritiques sont essentielles pour une mise en place d'une réponse immunitaire. Le rôle de ces cellules n'est pas clairement défini mais plusieurs observations faites chez l'homme et la souris permettent de suggérer leur contribution dans la progression de la maladie.

Il a été montré que le sang périphérique de patients FPI présentait moins de cellules dendritiques (cDC1, cDC2 et pDC) et plus d'IL-6, cytokine inflammatoire, que le sang de sujets sains [318]. D'un autre côté, l'analyse d'extraits pulmonaires de patients FPI montre que les foyers fibroblastiques contiennent des cellules dendritiques immatures, recrutées par un réseau de chimiokines (CCL19, CXCL12, CCL21) secrétées par les fibroblastes et les cellules épithéliales [319], [320]. Les cellules dendritiques matures sont retrouvées dans les iBALT à proximité de lymphocytes T activés [321]. Cependant, les fibroblastes dérivés de patients FPI empêchent l'activation des cellules dendritiques d'après des expériences de co-culture [322]. Les fibroblastes favorisent ainsi un environnement immunosuppresseur. L'ensemble de ces observations suggère un rôle immunorégulateur des cellules dendritiques dans la FPI. En effet, un modèle murin de fibrose pulmonaire induite par le TGFβ a permis de montrer que les cellules dendritiques pulmonaires étaient essentielles pour ralentir la progression de la maladie [323]. De même, les cellules dendritiques cDC1 ont été montrées pour limiter l'inflammation (notamment la diminution d'IL-6, augmentation d'IL-12) dans un modèle murin induit par la bléomycine [324]. Ceci est cohérent avec les hauts niveaux de FLT3L présents dans les poumons de patients FPI [323]. L'ensemble de ces résultats suggère un rôle anti-fibrosant des cellules dendritiques, rôle inhibé par l'environnement immunosuppresseur pulmonaire, qui reste à être démontré.

## 2.2 *Système immunitaire adaptatif : les lymphocytes T*

Le rôle des lymphocytes T dans la progression de la FPI est grandement controversé. Ceci est dû à l'échec des thérapies basées sur l'administration d'anti-inflammatoires dans la FPI. Cet échec est probablement dû au manque de caractérisation des sous-types de lymphocytes dans cette pathologie. En effet, déterminer plus précisément le rôle des différents sous-types lymphocytaires permettrait d'identifier des stratégies thérapeutiques plus adaptées. Cette partie traitera des connaissances

obtenues sur cette population immunitaire très hétérogène, dans les modèles précliniques et chez les patients FPI.

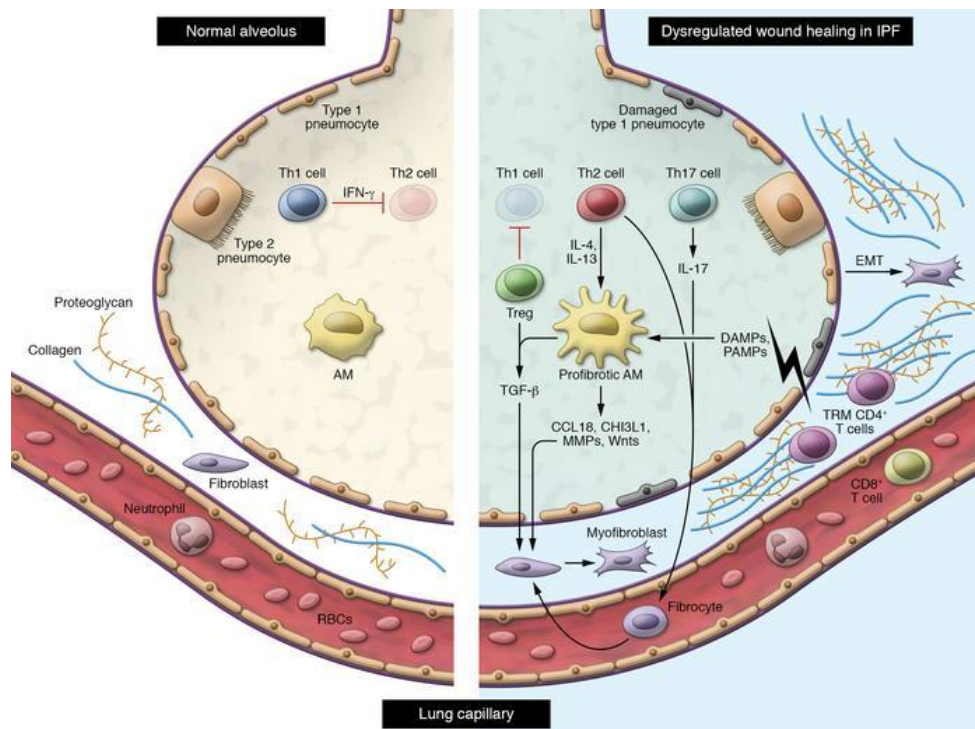


Figure 17 : Rôle des populations immunitaires dans la progression de la FPI  
 Gauche : structure et composition immunitaire d'une alvéole saine. Droite : Structure et composition immunitaire d'une alvéole d'un poumon fibrosé. Tiré de [325]

### 2.2.1 La balance des lymphocytes Th1/Th2

La balance des lymphocytes Th1/Th2 a longtemps été considérée importante dans le développement de la fibrose pulmonaire, du fait des propriétés anti-fibrosantes des Th1 et pro-fibrosantes des Th2 [326].

Le rôle anti-fibrosant des Th1 repose sur leur capacité de production d'IFN- $\gamma$ . La polarisation des lymphocytes *in vivo* en Th1 grâce à l'administration d'IL-12 a réduit l'intensité de la fibrose pulmonaire, et ce d'une façon dépendante de l'IFN- $\gamma$  [300]. En effet, l'IFN- $\gamma$  possède plusieurs propriétés anti-fibrosantes : il a des capacités antiprolifératives [114], [116]–[118], [327], inhibe l'activité du TGF $\beta$  [328], [329] et empêche l'accumulation de protéines de la MEC dont le collagène [330]–[333]. De plus, l'IFN- $\gamma$  permet de maintenir une immunité de type 1 comprenant la polarisation des macrophages en M1.

Le rôle protecteur des lymphocytes T mémoires résidents (Trm) producteurs d'IFN- $\gamma$  dans un modèle murin de fibrose pulmonaire a été montré [334], suggérant une protection à long terme contre la progression de la maladie. De façon similaire, une diminution de lymphocytes T CD4+ mémoires a été

décrite dans le sang circulants de patients atteints de FPI et corrèle avec une meilleure survie et une meilleure fonction respiratoire [282]. Les analyses de sang ou de liquide de lavage bronchoalvéolaire patients FPI ont montré une baisse d'IFN- $\gamma$  et une dominance des cytokines de type Th2 et Th17 [335]–[338], ceci peut être dû à l'expression de PD-1 sur les lymphocytes T CD4+ favorisant un profil Th17 plutôt que Th1 [339]. De plus, les cytokines de type Th2 corrélient avec le déclin des fonctions respiratoires et de la sévérité de la maladie [340]. En effet, le rôle pro-fibrosant de ces cytokines a été montré dans les modèles précliniques [341], [342]. La progression de la fibrose est liée à la production d'IL-5 qui favorise le recrutement d'éosinophiles, la production de TGF $\beta$ , d'IL-13 et de PDGF [315]–[317], [343]. De plus, l'IL-4 et l'IL-13 favorisent directement la prolifération des fibroblastes pulmonaires et leur différenciation en myofibroblastes, en induisant l'expression du TGF $\beta$  [344]–[346]. Enfin, ces cytokines polarisent les macrophages en M2, favorisant ainsi un environnement propice au développement de la fibrose.

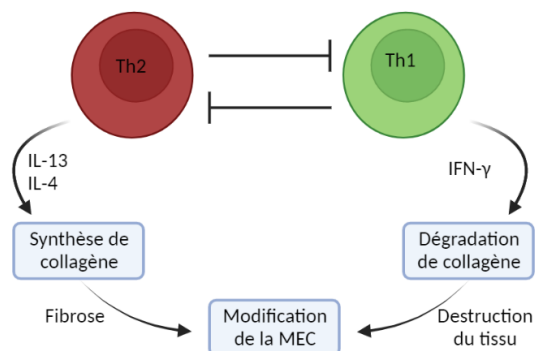


Figure 18 : La balance des lymphocytes Th1 et Th2  
inspiré de [326] Créé avec biorender.com

Étant donné que les cellules/cytokines de type 1 et 2 peuvent s'inhiber mutuellement [326], la balance Th1/Th2 a été introduite (Figure 18). Dans le but de favoriser un profil de type Th1, des essais cliniques basés sur l'administration d'IFN- $\gamma$  ou d'anticorps neutralisants anti-IL-13 ont été menés mais n'ont pas eu de succès. Plusieurs explications sont possibles : leur administration se faisant en systémique, il est probable que les concentrations d'IFN- $\gamma$  [347] ou d'anti-IL-13 [348] soient insuffisantes dans le poumon et nécessite alors une administration locale. En effet, plusieurs cas d'administration d'IFN- $\gamma$  par inhalation ont montré des effets bénéfiques [349]–[352]. D'un autre côté, il est fortement probable que l'administration unique d'IFN- $\gamma$  ne soit pas suffisante pour modifier le profil immunitaire pulmonaire, mais plutôt qu'une modification complète de la réponse immunitaire vers un profil Th1 soit nécessaire.

### 2.2.2 Les lymphocytes Th17

Les lymphocytes Th17, cellules productrices majeures d'IL-17A, sont décrits pour être pro-fibrosants, dans les modèles murins mais également chez l'homme. En effet, l'utilisation de souris *il17a*<sup>-/-</sup> ou la

neutralisation d'IL-17A a montré une réduction de fibrose (notamment une réduction de collagène) [353]–[355]. De plus, il a été montré que la balance Th1/Th17 est importante dans la progression de la maladie [297]. L'effet pro-fibrosant de la production d'IL-17A est décrit pour être dépendant de la production d'IL-1 $\beta$  dans le modèle murin induit par la bléomycine et induit des niveaux élevés de neutrophiles [355] et contribue ainsi à un environnement immunitaire pro-inflammatoire et immunosuppresseur [354]. Au niveau cellulaire, il a été montré que l'IL-17A favorise la TEM des cellules épithéliales, l'expression du TGF $\beta$  et de  $\alpha$ -SMA [354], [356] ainsi que la production de collagène [339], [354], [357]. Il a été montré que la production de collagène favorisée par l'IL-17A est dépendante de l'inhibition de l'autophagie, elle-même responsable de la dégradation du collagène [354]. Même si l'IL-17A est majoritairement produite par les Th17, il est important de noter que l'IL-17A peut également être produite par les lymphocytes T  $\gamma\delta$ , les lymphocytes T CD8, les NK, les neutrophiles et les macrophages.

De façon cohérente, il a été observé chez l'homme que les concentrations d'IL-17A ainsi que d'IL-1 $\beta$  sont élevées dans le liquide de lavage bronchoalvéolaire de patients FPI [355] et dans les foyers fibroblastiques [358], ainsi que l'expression du récepteur de l'IL-17A est augmentée dans les fibroblastes humains pulmonaires [357]. De même, les lymphocytes T CD4+ de patients FPI expriment des niveaux élevés de PD-1 et produisent l'IL-17A et le TGF $\beta$  de façon importante [339]. L'inhibition de PD-1 *ex vivo* diminue la production de ces deux cytokines et le dépôt de collagène. Les auteurs de cette étude ont également montré que l'utilisation d'ICIs anti-PD-L1 réduit l'intensité de la fibrose pulmonaire induite par la bléomycine et proposent cette thérapie pour limiter la progression de la fibrose en diminuant la production d'IL-17A et de TGF $\beta$  [339].

### 2.2.3 Les lymphocytes T régulateurs

Le rôle des lymphocytes T régulateurs dans la FPI est controversé. Il a été montré que les Tregs favorisent le développement de la fibrose [359] en changeant la balance Th1/Th2/Th17 vers un profil Th2. De façon cohérente, la déplétion des Tregs dans deux modèles murins améliore l'état fibrosé des souris [360], [361]. D'un autre côté, d'autres études démontrent le rôle anti-fibrosant des Tregs [362]. Dans ces études, la présence des Tregs en milieu inflammatoire, après l'induction de la fibrose, aggrave le développement de la maladie. Or, leur présence avant l'induction de la fibrose par la bléomycine protégeait les souris. Cette dernière étude pourrait permettre d'expliquer les résultats obtenus chez l'homme. En effet, des études ont montré une réduction du nombre de Treg et une diminution des fonctions immunosuppressives de ces cellules issues de patients FPI qui corrèlent avec une progression de la maladie (CVF, DLco) [363]. Au contraire, une autre étude montre une

augmentation des Tregs activés et la préservation de leur fonction immunosuppressive, qui est associée à la sévérité de la maladie (CVF, DLco, score GAP) [364].

#### 2.2.4 Les lymphocytes T CD8+

La présence de lymphocytes T CD8+ est décrite pour être délétère, faisant d'eux des cellules pro-fibrosantes. En effet, le nombre de lymphocytes T CD8+ dans les liquides de lavages broncho-alvéolaires et dans les tissus fibrosés patients FPI est décrit pour être élevé et corrèle avec la progression et la sévérité de la maladie [358], [365], [366]. Ainsi, un ratio CD4/CD8 est utilisé pour prédire la progression de la maladie [366]–[369] : un ratio bas correspondrait à une maladie plus avancée. Nous savons d'après une étude préclinique que les lymphocytes T CD8+ sont du type Tc2 [370]. La présence de cytokines de type 2 (IL-4, IL-21) favorise leur polarisation en Tc2 d'où leur production d'IL-13 [370]. Ceci est en cohérence avec une étude récente montrant une augmentation de lymphocytes T CD8+ activés dans les tissus FPI ayant un profil pro-fibrosant [371]. Le profil cytokinique des lymphocytes T CD8+ dans la FPI étant très peu exploré, il est important de l'étudier davantage afin de voir si un changement de polarisation des lymphocytes T CD8+, notamment en Tc1, pourrait être bénéfique.

### 3. Thérapies

Il n'existe pour le moment aucun traitement curatif de la FPI. Ceci est lié à la complexité de cette pathologie associé au manque de connaissances sur son étiologie.

La seule thérapie curative actuelle est la transplantation de poumon (mono ou bilatérale) : elle augmente le taux de survie et allège les symptômes [235]. Cependant, peu de patients peuvent en bénéficier, la disponibilité des transplants compatibles étant souvent très limitée. De plus, il existe plusieurs contre-indications tels que l'âge avancé du patient et la présence de comorbidités, qui peuvent augmenter le risque de complications liées à l'intervention.

Il existe cependant deux traitements anti-fibrosants utilisés en routine dans le monde, approuvés par la FDA (Food Drug Administration) en 2014 qui ralentissent uniquement la progression de la maladie (Figure 19).

La pirfénidone a des effets anti-fibrosants, anti-inflammatoires et anti-oxydants. Même si le mécanisme d'action de cette molécule n'est pas encore clairement défini, il est clair que la pirfénidone permet de diminuer les effets du TGF $\beta$ . En effet, des études *in vitro* ont montré qu'elle diminue la prolifération et la différenciation des fibroblastes, avec notamment une diminution de production de

protéines de la MEC dont le collagène [372]–[375]. Des modèles précliniques ont également montré les effets anti-fibrosants de la pirfénidone avec des réductions des niveaux de TGFβ et de l'accumulation de myofibroblastes, mais également de l'inflammation [376]–[378].

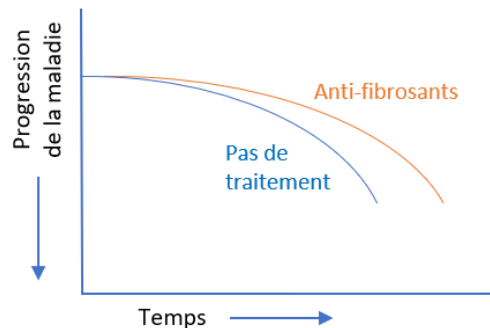


Figure 19 : Ralentissement de la maladie avec des anti-fibrosants

Le mécanisme d'action du nintedanib est quant à lui connu : cette molécule était initialement synthétisée pour le traitement des cancers [379]. C'est un inhibiteur de plusieurs récepteurs tyrosines kinases notamment des récepteurs PDGFR, FGFR et VEGFR qui sont impliqués dans l'activation, la prolifération et l'invasion des fibroblastes. Son efficacité a été montrée sur des fibroblastes dérivés de patients atteints de FPI [380] avec une baisse de prolifération, d'invasion, d'activation (moins de TGFβ, α-SMA, collagène). De même, les modèles précliniques ont montré moins de fibrose et d'inflammation [381] et une réduction de la quantité de macrophages M2 [382], [383].

L'administration de ces molécules chez les patients a montré un ralentissement du déclin de la CVF, une meilleure survie sans progression, un retard d'apparition des épisodes d'exacerbations et une mortalité réduite [384]–[387]. Cependant, ces anti-fibrosants ont de forts effets secondaires comme des diarrhées, nausées, vomissements, une baisse d'appétit mais également une phototoxicité dans le cas de la pirfénidone. Le choix d'une molécule par rapport à l'autre n'est pour le moment pas défini : il se fait en fonction du patient et des effets indésirables [388], [389].

## D. P2RX7 : un récepteur immunomodulateur

Il est intéressant de noter que le cancer du poumon et la fibrose pulmonaire possèdent plusieurs propriétés similaires comme la prolifération cellulaire, les mutations somatiques, le dépôt de protéines de la MEC, mais également une dérégulation immunitaire favorisant un environnement immunosuppresseur.

En plus de ces similitudes cellulaires et moléculaires, la présence d'un stress cellulaire induisant la mort des cellules (tumoraux/épithéliales) ainsi que le relargage de DAMPs les unis. Parmi ces DAMPs, nous notons la présence d'ATP extracellulaire (ATPe), retrouvé plus concentré que dans un tissu sain [390], [391], l'ATP étant normalement présent dans la cellule où il constitue un substrat énergétique majeur pour son fonctionnement.

La présence extracellulaire de l'ATP est d'origines diverses : elle est essentiellement due à la mort des cellules (tumoraux/épithéliales). Cependant, son relargage peut également se faire de façon passive à travers des pores ou de façon active par exocytose. L'ATPe peut également provenir des cellules immunitaires ou stromales retrouvées dans le microenvironnement tumoral et fibrosé [392].

### 1. P2RX7 : un récepteur purinergique unique

L'ATPe est à la tête d'une chaîne de signalisation extracellulaire, issue d'une dégradation en série de ce nucléotide appartenant à la famille des purines. Les enzymes impliquées dans le processus de dégradation de l'ATP sont des ectonucléotidases, CD39 (ou ENTPD1) et CD73 (ou NT5E), exprimées à la membrane plasmique de plusieurs types cellulaires (Tregs, CAFs, TILs, macrophages, cellules épithéliales...) [392]. En effet, CD39 dégrade l'ATP en ADP, et l'ADP en AMP. L'AMP est ensuite dégradé en adénosine par CD73. L'ATP ainsi que chacun de ses produits de dégradation sont reconnus par des récepteurs distincts, et forment dans l'ensemble la signalisation purinergique (Figure 20).

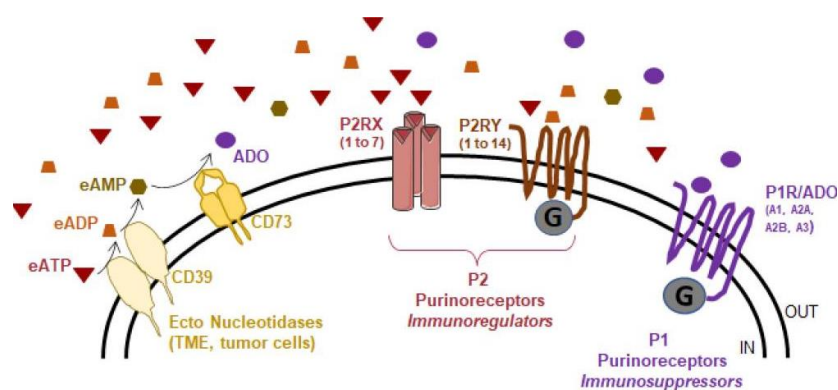


Figure 20 : La signalisation purinergique



Chacun des constituants de cette signalisation est impliqué dans la régulation de la réponse immunitaire, qui dépend des (i) concentrations extracellulaires de ces différentes purines, (ii) de l'expression et l'activité de leurs récepteurs ainsi que (iii) l'expression et l'activité des ectonucléotidases. Les acteurs de la signalisation purinergique peuvent ainsi jouer le rôle de points de contrôle immunitaire, notion que nous avons discuté dans la revue suivante [392] (Annexe, **Revue II**).

### 1.1 Les récepteurs P2X

L'ATPe est reconnu par deux familles de récepteurs purinergiques, les récepteurs P2X et P2Y. Les P2X sont des récepteurs ionotropiques à action rapide (10 millisecondes), alors que les P2Y sont des récepteurs métabotropiques, à action lente (100 millisecondes) [393]. Cette partie s'intéressera aux récepteurs de la famille P2X, qui comprend le récepteur P2RX7. Ce récepteur est le seul récepteur de la famille purinergique pouvant être activé par les fortes concentrations d'ATPe du microenvironnement tumoral et du tissu fibrosé.

#### 1.1.1 Structure des récepteurs P2X

La famille des récepteurs P2X comprend 7 membres : P2RX1 à P2RX7. Ces récepteurs sont assemblés en trimère, chaque monomère étant constitué de deux domaines transmembranaires (TM1 et TM2), une grande boucle extracellulaire, et deux domaines N-terminal et C-terminal en intracellulaire [394], selon la Figure 21. Contrairement aux récepteurs P2X1-6, le récepteur P2RX7 possède une longue queue C-terminale en intracellulaire (Figure 21, Tableau 3), qui lui confère des propriétés biologiques distinctes des autres P2X comme discuté ci-dessous.

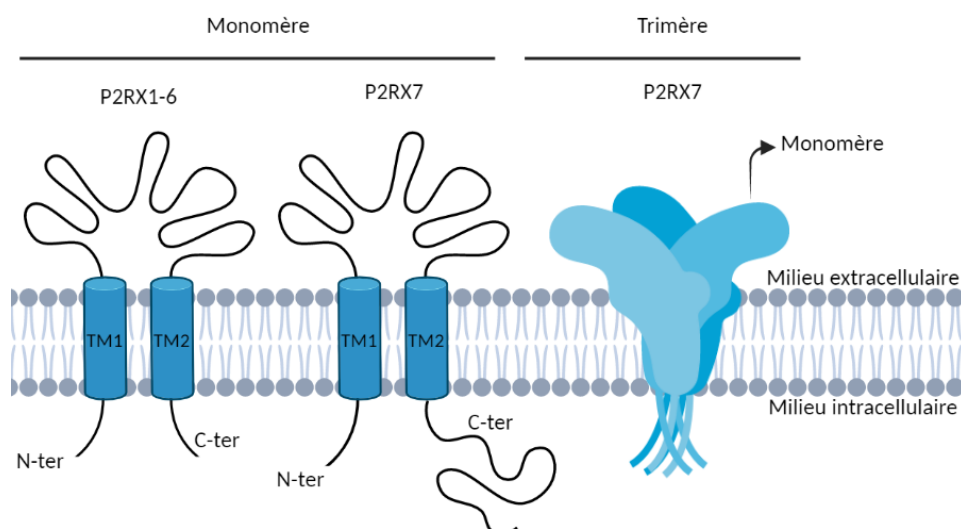


Figure 21 : Structure des récepteurs P2RX1-6 et P2RX7  
 Droite : structure en 2D des récepteurs P2X sous forme monomérique. Gauche : structure en 3D du récepteur P2RX7 sous forme trimérique. Créé avec biorender.com

L'activation des récepteurs P2X se fait uniquement sous forme trimérique. En effet, la poche de liaison de l'ATP se situe du côté de la boucle extracellulaire, au niveau de la juxtaposition de deux monomères. Ainsi, un récepteur P2X trimérique possède 3 poches de liaison à l'ATP, et nécessite 3 molécules d'ATP pour être activé [394]. Les récepteurs P2X peuvent s'assembler en homotrimères (par exemple 3 monomères de P2RX7) ou en hétérotrimères (par exemple 1 monomère de P2RX1 et 2 monomères de P2RX2) [395].

Il a été longtemps décrit que P2RX7 ne peut s'assembler qu'en homotrimère [396]. Une étude a montré la capacité de P2RX7 à former un hétérotrimère avec P2RX4 [397] : elle se base sur le fait que P2RX4 et P2RX7 ont la plus forte homologie de séquence parmi tous les P2X, ils sont souvent coexprimés, du fait de leur localisation proche au niveau du chromosome 12 (24 kpb d'écart) [398] (Tableau 3). Cependant, d'autres études consécutives ne confirment pas ce résultat [399], [400]. Ainsi, la capacité de P2RX7 à former un hétérotrimère avec P2RX4 n'est pas formellement admise dans la communauté scientifique [398].

### 1.1.2 Affinité pour l'ATPe

Les récepteurs P2X ont des affinités différentes pour l'ATPe et nécessitent par conséquent des concentrations différentes d'ATPe pour être activés (Tableau 3). La différence d'affinité semble être due à la variation d'acides aminés entre les différents P2X au niveau de la poche de liaison de l'ATP, malgré la forte conservation de séquence de la boucle extracellulaire parmi les P2X [393], [401].

	<b>P2RX1</b>	<b>P2RX2</b>	<b>P2RX3</b>	<b>P2RX4</b>	<b>P2RX5</b>	<b>P2RX6</b>	<b>P2RX7</b>
<b>Location chromosomique (humain)</b>	17p13.3	12q24.33	11q12.1	12q24.32	17p13.3	22q11.21	12q24.31
<b>Taille (acides aminés)</b>	399	471	397	388	444	441	595
<b>Longueur de la queue C-ter (acides aminés)</b>	41	113	56	29	82	87	240
<b>Désensibilisation</b>	lente	rapide	lente	rapide	rapide	rapide	non
<b>Valeurs d'EC50 ATP (µM)</b>	0.56–0.70	2–8	0.5–1	1–10	0.44–10	12	>100
<b>Expression majeure</b>	Muscle lisse	Neurones	Neurones	Neurones, microglies	Muscle squelettique	Ubiquitaire	Cellules immunitaires

Tableau 3 : Caractéristiques des récepteurs P2X  
EC50 : concentration efficace médiane. Adapté de [402]

Les P2X sont des récepteurs-canaux cationiques non sélectifs, ayant comme activité commune l'entrée de calcium ( $\text{Ca}^{2+}$ ) et de sodium ( $\text{Na}^+$ ) dans la cellule et la sortie de potassium ( $\text{K}^+$ ). Etant donné que le calcium intracellulaire est un second messenger, l'activation des P2X induit l'activation de plusieurs voies de signalisations liées à leurs fonctions, allant de la perception douloureuse pour P2RX2-4 [403] à la régulation de la réponse immunitaire pour P2RX7 [401], [404]–[406]. Par exemple, l'influx de calcium après la stimulation des cellules avec l'ATP, permet la translocation dans le noyau de facteurs de transcriptions impliqués dans la réponse immunitaire, comme NFAT et NF- $\kappa$ B et ce, de façon dépendante de P2RX7 [405]–[409].

Les P2X sont aussi caractérisés par des vitesses de désensibilisation différentes (Tableau 4). La désensibilisation est décrite pour être dépendante des domaines N-terminal et C-terminal des différents P2X, mais elle est également liée aux concentrations d'ATPe : une plus forte concentration d'ATPe induirait une désensibilisation plus rapide [410]. Les récepteurs P2RX1 et P2RX3 se désensibilisent rapidement (de l'ordre de 10 millisecondes) alors que les récepteurs P2RX2, P2RX4, P2RX5, P2RX6 se désensibilisent beaucoup plus lentement (de l'ordre de plusieurs secondes ou minutes) [411]. P2RX7, quant à lui, est décrit pour ne pas se désensibiliser : son activation est maintenue en présence d'ATPe [412].

### *1.2 Particularités du récepteur P2RX7 : la queue C-terminale*

La queue C-terminale de P2RX7 permet de le distinguer structurellement des autres récepteurs P2X. Les fonctions biologiques de P2RX7 sont également très distinctes des autres récepteurs et parmi les plus significatives d'un point de vue pathologique. Son activation induit une grande variété de voies de signalisation, comme la prolifération cellulaire, l'autophagie ou la mort cellulaire [413]. Ces fonctions biologiques nécessitent l'activité canal du récepteur, mais aussi la présence de la queue C-terminale. En effet, la queue C-terminale est constituée de plusieurs domaines d'interactions avec des protéines intracellulaires [413]. L'attribution de l'origine de l'activation de la voie signalisation (ionique ou C-terminale) est de façon générale peu définie. Nous nous intéresserons dans cette partie aux deux fonctions discriminantes du récepteur P2RX7, à savoir sa fonction macropore et sa capacité à activer l'inflammasome NLRP3.

#### *1.2.1 Fonction macropore*

Le récepteur P2RX7 était initialement appelé P2Z : sa découverte a été faite à cause d'une forte perméabilisation et mort cellulaire (Z : distinction des autres P2X) en présence de fortes concentrations d'ATPe (récepteur P2) dans des macrophages [414]–[416]. Le clonage du récepteur en

1996 a mis en évidence sa forte homologie de séquence et de structure avec les récepteurs P2X et devient ainsi le 7ème membre de cette famille [417]. Nous savons aujourd'hui que P2RX7 peut induire la mort cellulaire, contrairement aux autres P2X, grâce à sa longue queue C-terminale [417].

La capacité de P2RX7 à perméabiliser la cellule dépend de sa fonction macropore (ou large pore). En effet, l'activation de P2RX7 induit la formation de pores membranaires (8.5 Å) faisant passer des macromolécules, dont l'ATP, d'une taille inférieure à 900 Da. Le flux de molécules se fait de façon non sélective et bidirectionnelle [418], perturbant ainsi l'homéostasie cellulaire. La particularité de ce pore réside dans sa réversibilité. En effet, le retrait d'ATP 15 à 30 minutes après le début de la stimulation, permet la rétraction du pore et le retour à la normale des fonctions cellulaires malgré les perturbations dues aux flux de molécules [418]. L'ouverture de ce pore peut être détectée en utilisant des sondes fluorescentes d'une taille inférieure à 900 Da, comme le bromure d'éthidium, le YO-PRO-1 ou le TO-PRO-3.

Encore aujourd'hui, la nature de ce pore est débattue. Néanmoins, parmi la multitude d'études contradictoires, deux hypothèses sont retenues : (i) l'activation de P2RX7 permettrait le recrutement à la membrane de protéines formant des pores comme la pannexine-1 ou la connexine-43 [419]–[421] et/ou (ii) la formation du large pore serait une propriété intrinsèque à P2RX7, due à une dilatation du canal [422]–[425]. Une chose est sûre : la présence de la queue C-terminale contenant une séquence de 177 acides aminés est indispensable pour cet effet [417].

### 1.2.2 L'inflammasome NLRP3

P2RX7 active l'inflammasome NLRP3 (nucleotide-binding domain leucine-rich repeat [LRR] and pyrin-containing receptor 3) qui constitue la fonction la plus étudiée parmi les fonctions de P2RX7. La protéine NLRP3 est un PRR faisant partie de la famille des NLRs (NOD-Like Receptor), NLRP3 est ainsi impliqué dans la reconnaissance de signaux de danger [426]. La protéine NLRP3 n'est pas un récepteur en tant que tel, mais plutôt un senseur de stress cytosolique qui interagit avec d'autres protéines pour former un complexe multiprotéique appelé inflammasome NLRP3. Cet inflammasome est composé des protéines NLRP3, pro-caspase-1 et ASC (Apoptosis-associated speck-like protein containing a CARD). Cette dernière agit comme une plateforme d'ancrage (composée des domaines PYD et CARD) des deux autres protéines, en se liant au domaine PYD de NLRP3 et au domaine CARD de la pro-caspase-1. La protéine NEK7 (NIMA Related Kinase 7) a été récemment identifiée comme faisant partie du complexe, permettant l'oligomérisation des différentes sous-unités NLRP3 [427].

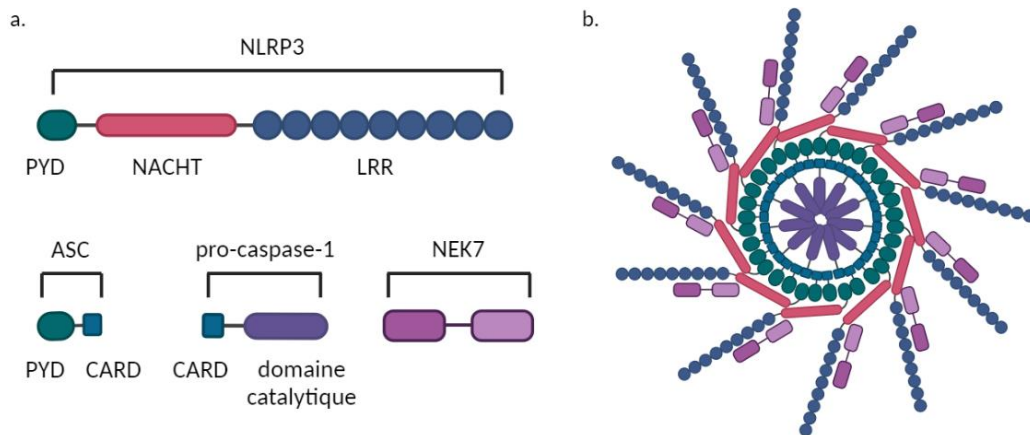


Figure 22 : L'inflammasome NLRP3

a. Les constituants de inflammasome NLRP3 (NLRP3, ASC, pro-caspase-1, NEK7) et leurs domaines, b. l'inflammasome NLRP3 assemblé. NLRP3 : NOD-, LRR- and pyrin domain-containing protein 3 PYD : pyrin domain, containing a caspase recruitment domain, NEK7: NIMA-related kinase 7. Créée avec biorender.com

Plusieurs familles d'inflammasomes sont décrites. Elles sont caractérisées par des senseurs de stress différents, et ont comme finalité commune l'activation de la caspase-1, protéase inflammatoire qui assure le clivage intracellulaire de précurseurs inactifs de deux cytokines, l'IL-1 $\beta$  et l'IL-18 et leur libération de la cellule. L'inflammasome NLRP3 est ainsi important pour les réponses immunitaires contre les infections mais aussi pour les réponses immunitaires antitumorales. Ainsi, il est majoritairement activé et étudié dans les cellules immunitaires innées de la lignée myéloïde (cellules dendritiques, macrophages, monocytes), qui font partie des premières cellules à reconnaître un signal de danger. De ce fait, et de façon cohérente avec la fonction de P2RX7, ce sont ces cellules, parmi l'ensemble des populations de cellules immunitaires, qui expriment les plus hauts niveaux de P2RX7 (Figure 25) [413], [428].

L'inflammasome NLRP3 peut être activé par une variété de signaux de stress, comme par des toxines formant des pores, des ionophores, des cristaux d'acides uriques ou bien par l'ATP [429]. Cependant, nous nous intéresserons uniquement au rôle de P2RX7 dans l'activation de l'inflammasome NLRP3.

#### 1.2.2.1 Mécanisme d'activation

L'assemblage de l'inflammasome NLRP3 se fait en deux étapes : une étape d'amorçage (priming, étape 1) suivie d'une étape d'activation (étape 2) (Figure 23).

L'étape de priming repose sur l'activation de la voie NF- $\kappa$ B par la reconnaissance de PAMPs/DAMPs par le TLR4, comme le LPS (Lipopolysaccharide) ou HMGB1 et l'activation de la voie MyD88. Cette étape est nécessaire pour l'assemblage de l'inflammasome. En effet, elle permet l'expression de NLRP3 mais aussi de la pro-IL-1 $\beta$  (précurseur inactif de l'IL-1 $\beta$ ) qui, contrairement à la pro-IL-18, n'est pas présent constitutivement dans la cellule [430], [431]. L'étape de priming permet d'induire des

modifications post-traductionnelles (déubiquitination, phosphorylation/déphosphorylation) de la protéine NLRP3 qui assurent un assemblage optimal de l'inflammasome [432]. Cependant, la voie NF- $\kappa$ B n'impacte pas les niveaux d'ASC, de la pro-caspase-1 ou de la pro-IL-18 [431].

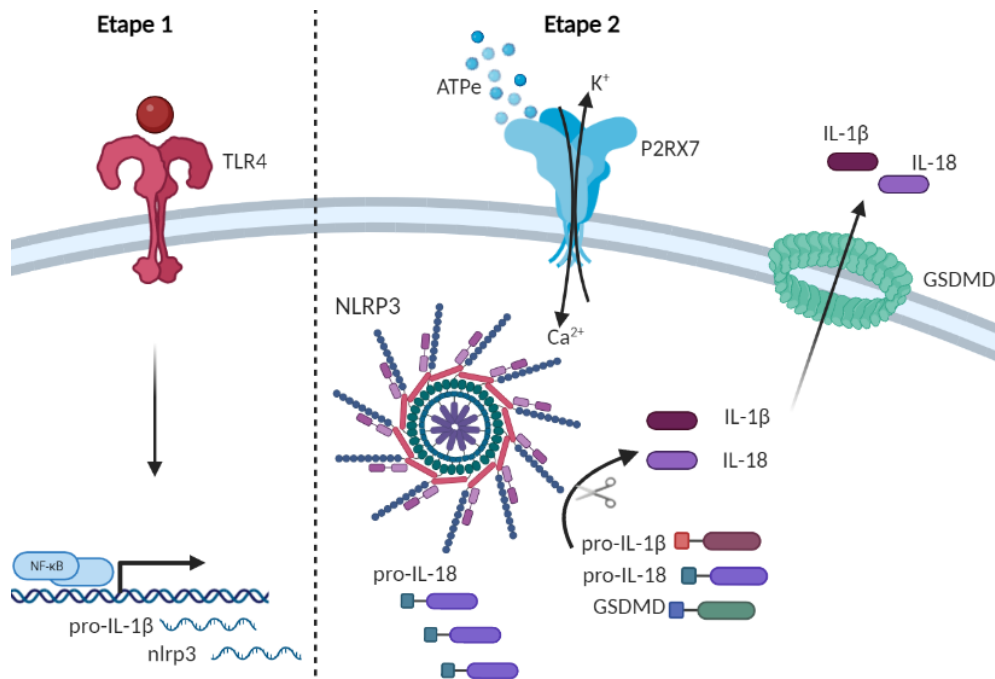


Figure 23 : Mécanisme d'activation de l'inflammasome NLRP3  
Crée avec biorender.com

L'activation de P2RX7 par l'ATP signe le début de l'étape d'activation (ou d'assemblage) de l'inflammasome NLRP3. Il est admis que ce signal d'activation repose sur l'efflux de potassium, qui est un mécanisme commun de tous les activateurs connus de NLRP3 [429], [433], qui a longtemps été associé à l'activation de la fonction canal de P2RX7 mais dont on sait aujourd'hui qu'il requiert la protéine TWIK2, un canal potassique qui agit de concert avec P2RX7 [434]. Il est également décrit que P2RX7 et NLRP3 peuvent interagir et être colocalisés à la membrane plasmique, en particulier au niveau de la queue C-terminale de P2RX7 [435], [436]. En effet, la présence de la queue C-terminale est nécessaire pour l'assemblage de l'inflammasome et la libération d'IL-1 $\beta$  en réponse à l'ATPe [437]. Ainsi, l'efflux de potassium permet le recrutement de NEK7 et sa liaison à NLRP3, permettant l'oligomérisation des constituants (NEK7, NLRP3, ASC, pro-caspase-1) du complexe. Cet assemblage permet l'auto-clivage de la pro-caspase-1 en caspase-1 active, qui clivera les précurseurs pro-IL-1 $\beta$  et pro-IL-18 en cytokines matures IL-1 $\beta$  et IL-18. La caspase-1 induit également le clivage d'une protéine cytosolique appelée Gasdermine-D : son domaine N-terminal libéré s'oligomériser pour former des pores à la membrane plasmique par lesquels sont libérées l'IL-1 $\beta$  et l'IL-18 ; ces pores participent également à la perméabilité cellulaire en induisant une mort immunogène appelée pyroptose [438].

### 1.2.2.2 Les interleukines-1 $\beta$ et 18

Comme mentionné précédemment, la régulation de l'expression de ces deux cytokines est différente : la pro-IL-18 est constitutivement exprimée, par les cellules immunitaires [430] comme par les cellules épithéliales et fibroblastes pulmonaires [439], [440] alors que l'expression de la pro-IL-1 $\beta$  nécessite l'activation de la voie NF- $\kappa$ B.

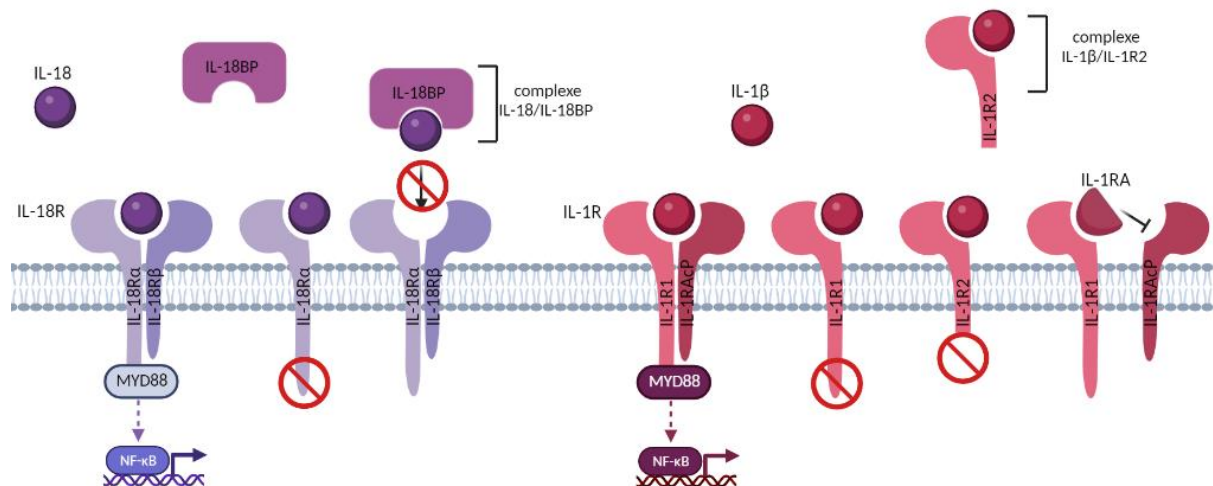


Figure 24 : L'IL-1 $\beta$ , l'IL-18, leurs récepteurs et leurs antagonistes  
Crée avec biorender.com

L'IL-1 $\beta$  est reconnue par deux récepteurs : l'IL-1R1 et l'IL-1R2. L'expression de ces récepteurs varie en fonction du type cellulaire : l'IL-1R1 est exprimé par les lymphocytes T, les fibroblastes, les cellules épithéliales et endothéliales alors que l'IL-1R2 est exprimé par une multitude de cellules immunitaires dont les granulocytes [441]. La reconnaissance d'IL-1 $\beta$  par l'IL-1R1 induit le recrutement d'une protéine adaptatrice IL-1RAcP nécessaire à la signalisation IL-1R. L'IL-1R2 est un récepteur leurre (decoy), pouvant être membranaire ou soluble, qui empêche la mise en place de la signalisation par son incapacité à recruter l'IL-1RAcP. L'IL-1 $\beta$  possède également un antagoniste, l'IL-1Ra, qui se fixe sur l'IL-1R1 empêchant le recrutement de l'IL-1RAcP [442], [443] (Figure 24).

L'IL-18 a été initialement appelée IGIF pour « IFN- $\gamma$  inducing factor » [444] par sa capacité à induire l'expression de l'IFN- $\gamma$  par les lymphocytes T et NK [444] et à favoriser un profil Th1 et Tc1. Avec les cellules dendritiques, ces cellules sont les seules à exprimer la sous unité IL-18R $\beta$  (gène *IL18RAP*) nécessaire à l'activation du récepteur IL-18R [445]. En effet, la reconnaissance de l'IL-18 se fait par l'IL-18R $\alpha$  (gène *IL18R1*) permettant le recrutement de l'IL-18R $\beta$  un complexe hétérodimérique à forte affinité pour l'IL-18. Ceci induit le recrutement de la protéine MyD88 au domaine TIR intracellulaire des deux chaînes (IL-18R $\alpha$  et IL-18R $\beta$ ) afin d'induire une succession de phosphorylations. Ceci permet

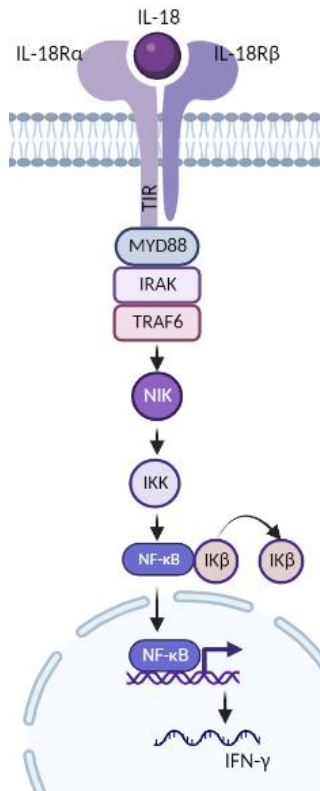


Figure 25 : Activation du récepteur de l'IL-18

la liaison et la phosphorylation de la protéine IRAK. IRAK phosphorylée se détache du complexe pour se lier à TRAF6 qui phosphoryle à son tour NIK (NF-κB-induced kinase). Ceci permet l'activation d'IKK (IκB kinase) pour dégrader IκB et permettre la migration de NF-κB au noyau et induire la transcription d'IFN-γ (Figure 25). L'IL-18 possède un antagoniste naturel secrété constitutivement appelé IL-18BP (IL-18 Binding Protein). IL-18BP possède une grande affinité pour l'IL-18 et est présente en excès dans la circulation (Figure 24), et empêche ainsi la liaison de l'IL-18 sur son récepteur. Son expression est augmentée lors d'une forte production d'IFN-γ. Ainsi, le contrôle de l'activité d'IL-18 par l'IL-18BP se fait par un mécanisme de rétrocontrôle négatif [445].

Ainsi, chacune de ces cytokines possède plusieurs niveaux de régulation, pour d'une part freiner une libération excessive d'IL-1β et éviter les pathologies inflammatoires [446] mais aussi pour contrôler les niveaux d'IL-18 en amont des réponses antitumorales ou anti-fibrosantes comme discuté dans cette thèse.

### 1.2.3 Expression de P2RX7

A l'origine, P2RX7 était décrit pour être exprimé uniquement par les cellules immunitaires. Or, nous savons aujourd'hui que ce récepteur est exprimé de façon ubiquitaire sur toutes les cellules de l'organisme. Cependant, son rôle et son activation sont majoritaires dans les cellules immunitaires. En effet, P2RX7 est le plus fortement exprimé dans ces cellules, en cohérence avec sa capacité de reconnaissance de l'ATPe en tant que PRR et la modulation de la réponse immunitaire [428].

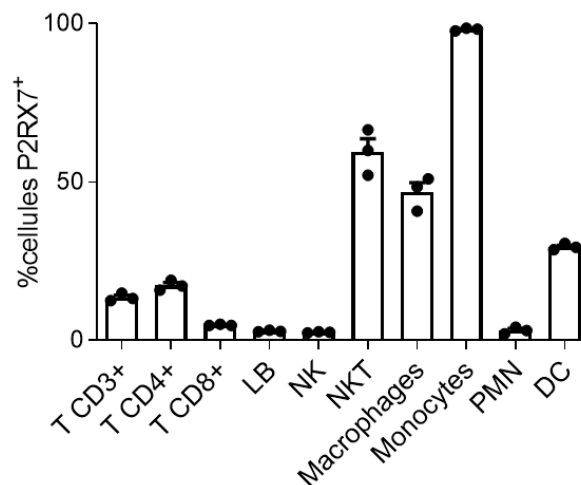


Figure 26 : Pourcentage de cellules exprimant P2RX7 dans la rate de souris sauvages N=3 souris. LB : lymphocyte B, NK : Natural Killer, NKT : Natural Killer T, PMN : polymorphonucléaires, DC : cellules dendritiques



Parmi les cellules immunitaires, les monocytes, macrophages et cellules dendritiques expriment le plus fortement P2RX7. Ces cellules sont aussi les principales cellules productrices d'IL-1 $\beta$  et d'IL-18 [413], [428] (Figure 26). Au-delà des cellules immunitaires, les cellules épithéliales du poumon, les fibroblastes et les cellules endothéliales l'expriment aussi [447], [448].

Il existe plusieurs variants de P2RX7 issus d'épissages alternatifs. Douze variants ont été décrits chez l'homme, quatre chez la souris [447] (Annexe, **Revue III**). Il est intéressant de noter que le variant humain P2RX7-B ne possède pas de queue C-terminale, de ce fait il est incapable de former des macropores [449], [450] (Annexe, **Article IV**). Il n'existe pas d'équivalent naturel chez la souris. Cependant, les souris *p2rx7<sup>-/-</sup>* générées par la délétion de l'exon 13 s'en rapprochent fonctionnellement [451]. Le gène codant pour P2RX7 présente aussi des polymorphismes ayant pour conséquence un défaut ou une suractivation de la protéine, comme sont détaillé dans les revues [447], [452]. Par exemple, le SNP rs3751143 empêche la libération d'IL-1 $\beta$  et favorise la croissance tumorale et métastatique chez des patientes atteintes de cancer du sein [453], [454].

## 2. Rôle de P2RX7 dans le cancer et la fibrose

L'activation de P2RX7 permet de moduler une panoplie de voies de signalisation entraînant des répercussions sur la progression du cancer et de la fibrose.

### 2.1 Rôle de P2RX7 dans la croissance tumorale

Le rôle de P2RX7 dans la croissance tumorale est aujourd'hui encore sujet à discussion. Cette partie mettra en avant ses rôles pro-tumoraux et antitumoraux.

#### 2.1.1 Rôle pro-tumoral

Même si l'expression de P2RX7 sur les MDSCs et les TAMs a été montrée pour favoriser la croissance tumorale [455], [456], le rôle pro-tumoral du récepteur est essentiellement dû à son expression sur la cellule tumorale, où il est décrit pour être surexprimé et ce, dans plusieurs lignées de cellules tumorales ou sur des biopsies de patients [457]–[461].

Plusieurs études ont montré que P2RX7 favorise la prolifération cellulaire *in vitro* et la croissance tumorale *in vivo* [457], [458], [462], [463]. Il a été aussi montré que l'activation de P2RX7 promeut l'invasion et les métastases *in vitro* et *in vivo* [459], [460], [463]–[468]. En effet, P2RX7 peut activer des kinases impliquées dans la prolifération comme les MAP kinases (ERK1/2, p38, JNK), les protéines kinases B (PKB/Akt), et PKC [413]. L'angiogenèse est également favorisée par P2RX7 : la sécrétion du

VEGF a été montrée par des cellules de glioblastomes et de neuroblastomes après l'activation de ce récepteur [469], [470]. De plus, les tumeurs formées par des cellules HEK293 exprimant P2RX7 étaient plus angiogéniques que les tumeurs ne l'exprimant pas une fois injectées dans des souris immunodéficientes [457].

Cependant, une des particularités de P2RX7 est la formation de macropores et l'induction de la mort cellulaire. Ainsi on peut se demander comment un récepteur induisant la mort peut aussi favoriser la croissance tumorale. La réponse pourrait être liée à l'expression du variant P2RX7-B. En effet, nous savons que de dernier est surexprimé dans les adénocarcinomes pulmonaires [449], la leucémie aigüe myéloïde [471], l'ostéosarcome [472], le neuroblastome [473] et le glioblastome [474]. Dans les cancers pulmonaires, P2RX7-B est associé à une faible infiltration de cellules immunitaires et une perte de sa fonction macropore [449]. e plus, l'existence d'un P2RX7 non fonctionnel, impacté dans la fonction de macropore, a été mise en évidence dans différents types de cancers [475], [476]. La nature exacte de ce récepteur non fonctionnel n'est pas connue. De même, il n'est pas encore démontré que l'expression de la forme non fonctionnelle soit liée avec l'expression de P2RX7-B. Néanmoins, l'existence de ces isoformes non fonctionnelles, tronquées ou non pourrait expliquer le paradoxe entre l'induction de la mort, induite par un récepteur pleinement fonctionnel, et de la prolifération cellulaire, induite par l'activité canal de P2RX7.

### 2.1.2 Rôle antitumoral

L'activation de P2RX7 dans des cellules tumorales a permis de réduire la prolifération cellulaire et d'induire la mort dans plusieurs modèles cellulaires et précliniques [477]–[481]. Dans ces études, l'effet antitumoral est essentiellement dû aux propriétés immunomodulatrices de ce récepteur qui participe à la mise en place des différentes étapes clés de la réponse immunitaire antitumorale.

Il a été montré que l'utilisation de souris invalidées pour l'expression de P2RX7, ainsi que l'utilisation d'un inhibiteur pharmacologique, favorisent un développement tumoral plus rapide et agressif. Ces résultats suggèrent que l'expression de P2RX7 par les cellules de l'hôte, dont les cellules immunitaires, est nécessaire pour contrôler la croissance des tumeurs [482]–[484]. De plus, ces souris présentent un environnement immunosuppresseur avec une augmentation de TGF $\beta$ , de Tregs et de neutrophiles [482], [484], mais également moins de cellules effectrices antitumorales [484]. D'un autre côté, l'injection en intraveineuse de cellules B16 de mélanome (exprimant P2RX7) dans des souris *p2rx7<sup>-/-</sup>* a montré une augmentation du nombre de tumeurs pulmonaires [483], ce qui souligne la capacité de P2RX7 à contrôler le développement de métastases.

Nous avons précédemment mentionné que l'ATPe fait partie des DAMPs favorisant une réponse immunitaire antitumorale dans le cadre d'une mort immunogène [87] : la libération d'ATP par les cellules tumorales ainsi que l'expression de P2RX7 par les cellules dendritiques sont essentielles pour la mise en place d'une réponse immunitaire antitumorale [454], [485]. En effet, la voie ATPe/P2RX7 (avec une implication de P2Y2) attire les cellules dendritiques au site tumoral [454], [486], [487], favorise leurs capacités migratoires [488] et leur maturation [489].

De plus, l'expression de P2RX7 est impliquée dans le processus d'activation et de migration des lymphocytes T [490], [491]. En effet, l'axe ATP/P2RX7 favorise la prolifération des lymphocytes T de façon autocrine au moment de leur activation, ce qui contribue à leur expansion clonale [404]. D'un autre côté, P2RX7 participe à la sortie des lymphocytes T du ganglion lymphatique après leur activation en induisant le clivage membranaire de CD62L [492], [493]. De plus, parmi les lymphocytes T, P2RX7 est le plus fortement exprimé par les Tregs et favorise la mort de ces cellules [494] : P2RX7 participe ainsi dans la diminution d'un microenvironnement tumoral immunosuppresseur.

## *2.2 Rôle de P2RX7 dans la fibrose*

Le rôle de P2RX7 dans le développement de la fibrose pulmonaire a été adressé uniquement dans deux études précliniques. La première a été faite dans le modèle de fibrose induite par la bléomycine, avec moins de fibrose observée dans les souris *p2rx7<sup>-/-</sup>* versus WT, d'où la conclusion que l'activation de P2RX7 favorise le développement de fibrose. Dans cette étude, les auteurs démontrent que l'ATP est libéré par les cellules épithéliales sous l'action de la bléomycine, une action qui nécessite la présence de P2RX7 [391]. De façon complémentaire, il a été montré que la bléomycine augmente l'expression de P2RX7 sur des cellules épithéliales pulmonaires [495]. La stimulation de ces cellules avec du bzATP (analogue stable de l'ATP) induit leur mort [496]. Le rôle de P2RX7 a aussi été étudié dans un modèle murin induit par l'inhalation de silice, où les auteurs montrent une fibrose moins intense dans les souris *p2rx7<sup>-/-</sup>*, de façon cohérente avec la première étude [497]. Ces deux études précliniques démontrent que l'axe ATPe/P2RX7 augmente la production d'IL-1 $\beta$ , l'une dans le liquide de lavage bronchoalvéolaire [391], et l'autre par les macrophages et fibroblastes [497], mais également une infiltration plus importante de cellules immunitaires dans les poumons de souris sauvages par rapport aux souris *p2rx7<sup>-/-</sup>*.

Cependant, ces deux études précliniques n'ont pas adressé la contribution du compartiment immunitaire dans le développement de la maladie. En d'autres termes, le rôle de P2RX7 exprimé par les différentes cellules immunitaires n'a pas encore été démontré. De plus, il est important de noter que dans ces modèles murins, l'apparition de la fibrose est favorisée par l'induction de l'inflammation.

Etant donné le rôle de P2RX7/NLRP3/IL-1 $\beta$  dans l'inflammation [394], le rôle de P2RX7 dans le développement de la fibrose, et non dans la mise en place d'une inflammation, n'a pas encore été adressée pour le moment.

### 2.3 P2RX7 : une cible thérapeutique

Etant donné le rôle de l'axe P2RX7/IL-1 $\beta$  dans l'inflammation [394] mais également le rôle pro-tumoral du récepteur, de nombreuses approches sont menées pour l'inhiber. Des inhibiteurs compétitifs de l'ATP ont d'abord été générés, comme l'o-ATP ou la suramine, qui se lient de façon compétitive au site de liaison de l'ATP pour empêcher l'activation de P2RX7 [498]. Cependant, ces inhibiteurs ne sont pas spécifiques de P2RX7, d'où la nécessité de développer des approches plus spécifiques [498].

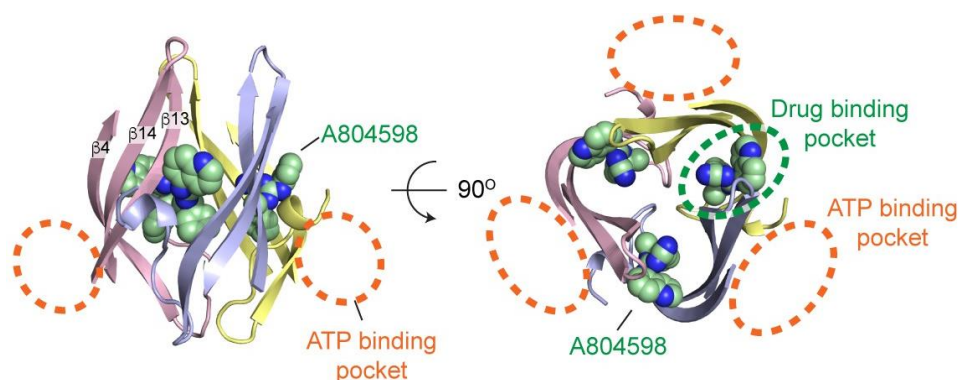


Figure 27 : Poches de liaison de l'ATP et des modulateurs allostériques de P2RX7 [499]

En plus du site de liaison à l'ATP, P2RX7 possède une poche de liaison entre les sous-unités adjacentes du récepteur. Cette poche est située à proximité de celle de l'ATP, et elle est identifiée comme liant des modulateurs allostériques (Figure 27) [499]. La liaison de ces molécules sur P2RX7 empêche la rotation des différentes sous-unités une fois l'ATP lié sur son site. Il existe aujourd'hui plus de 16 modulateurs allostériques négatifs de P2RX7. Par exemple, les molécules AZD9056 (AstraZeneca), CE-224,535 (Pfizer), EVT-401 (Evotec), et GSK1482160 (GlaxoSmithKline plc) sont en essai clinique. Cependant, aucun effet bénéfique n'a été observé à ce jour [498]. Des analyses de cristallographie ont permis d'expliquer cette absence d'effet : la liaison de l'ATP sur son site induit un changement de conformation du récepteur rendant la poche allostérique inaccessible aux inhibiteurs [499]. Etant donné les concentrations d'ATP élevées dans les tissus inflammatoires [390], [391], il est difficile d'envisager une efficacité de liaison de ces inhibiteurs sur P2RX7 et d'autres approches doivent être envisagées pour moduler l'activité de ce récepteur canal. Parmi ces approches, le développement de nouveaux outils biologiques tels que les anticorps conventionnels et les anticorps dépourvus de chaînes légères (nanobodies) est en cours. Par exemple, il a été montré que le nanobody 13A7 qui inhibe P2RX7 chez la souris (inhibition du clivage de CD27 dans les lymphocytes T et de l'activité

macropore dans les macrophages) améliore l'inflammation dans des modèles murins de glomérulonéphrite et d'allergie de contact [500].

## OBJECTIFS DE LA THESE



Le laboratoire d'accueil est l'un des premiers à avoir montré que l'absence ou l'inactivation de P2RX7 favorise le développement tumoral [482]. Etant donné la capacité de P2RX7 à induire la mort cellulaire et à moduler la réponse immunitaire et étant donné les fortes concentrations d'ATPe dans le microenvironnement tumoral, le laboratoire a proposé d'augmenter l'activation du récepteur dans le but de freiner la croissance tumorale. A mon arrivée au laboratoire, une collaboration avec une équipe de chimistes avait permis d'identifier une molécule qui potentialise l'effet de l'ATP, cette molécule est nommée HEI3090.

La première partie de ma thèse a consisté à étudier le potentiel antitumoral d'un activateur de P2RX7, ici HEI3090, et à décortiquer son mécanisme d'action, dans deux modèles murins immunocompétents de cancers pulmonaires. Ce travail a permis de mettre en avant le rôle de l'axe ATPe/P2RX7/IL-18/IFN- $\gamma$  dans la réponse antitumorale (**Article I**).

Etant donné le fort potentiel anti-fibrosant de l'IFN- $\gamma$ , les fortes concentrations d'ATPe dans les tissus fibrosés et les résultats des travaux de l'article I, la deuxième partie de ma thèse avait pour but de démontrer le potentiel de l'axe ATPe/P2RX7/IL-18/IFN- $\gamma$  dans le développement de fibroses pulmonaires, dans un modèle murin immunocompétent induit par la bléomycine (**Article II**).

Le but de la troisième partie de ma thèse consistait à développer un protocole permettant d'étudier l'activation de P2RX7 *in vivo* dans les poumons de souris (**Article III**). En effet, l'étude directe de l'activation de P2RX7 (influx de calcium, formation de macropores) ainsi que l'étude des effets de molécules modulatrices ne se faisant qu'*in vitro*, ou *in vivo* de façon indirecte (IL-1 $\beta$ /IL-18), il était important de démontrer l'augmentation de l'activité de P2RX7 *in vivo* par HEI3090, en développant un protocole d'activation *in vivo*.





## RESULTATS



## ARTICLE I

“A small-molecule P2RX7 activator promotes anti-tumor immune responses and sensitizes lung tumor to immunotherapy”

## ARTICLE II

“Reshaping the lung immune phenotype by activating P2RX7 inhibits lung fibrosis progression”

## ARTICLE III

“Protocol for evaluating *in vivo* the activation the P2RX7 immunomodulator”



## ARTICLE I

“A small-molecule P2RX7 activator promotes anti-tumor immune responses and sensitizes lung tumor to immunotherapy”

Publié dans ***Nature Communications***, janvier 2021, co-première auteure



# Une molécule activatrice de P2RX7 favorise une réponse immunitaire antitumorale et sensibilise les tumeurs pulmonaires aux immunothérapies

## Contexte

P2RX7 est un récepteur exprimé par la majorité des cellules du microenvironnement tumoral, notamment par les cellules immunitaires. Etant donné que P2RX7 possède des propriétés antitumorales et sachant que le microenvironnement tumoral contient des concentrations d'ATP extracellulaire permettant son activation, le laboratoire a proposé d'amplifier ses fonctions antitumorales en utilisant un modulateur positif. La collaboration avec des chimistes a permis de synthétiser une série de molécules et d'identifier la molécule HEI2328 comme molécule potentialisatrice de P2RX7. Après des améliorations chimiques visant à augmenter la solubilité de HEI2328, une nouvelle molécule nommée HEI3090 a été produite. Le but de cet article est de tester l'hypothèse selon laquelle HEI3090 peut contrôler la croissance tumorale et caractériser son mécanisme d'action.

## Méthodes

L'impact de HEI3090 sur l'activité du récepteur a été étudié via l'augmentation de la concentration cellulaire en calcium (sonde Fluo-4-AM) et de la formation de macropores (sonde TO-PRO™ -3) sur des cellules HEK 293 exprimant la forme murine de P2RX7 (C57BL6J) et sur des splénocytes isolés à partir de souris WT et *p2rx7<sup>-/-</sup>*.

L'activation de P2RX7 par HEI3090 a ensuite été étudiée *in vivo* dans deux modèles murins immunocompétents : la transplantation en sous cutanée de cellules tumorales pulmonaires de la lignée LLC (Lewis Lung Carcinoma) et un modèle de tumorigénèse *in situ* initiée par l'oncogène KRAS<sup>G12D</sup>.

Le mécanisme d'action de la molécule a été mis en évidence grâce à des expériences de transferts adoptifs, de déplétions cellulaires et l'utilisation de souris transgéniques ainsi que l'étude de l'infiltrat immunitaire.

Enfin, nous avons étudié l'expression du récepteur humain dans les cancers du poumon non à petites cellules grâce à la base de données « The Cancer Genome Atlas » et son impact sur la survie des patients.

## Résultats

Nous avons montré que HEI3090 augmente la concentration cellulaire en calcium et la formation de macropores uniquement en présence d'ATP extracellulaire et nécessite l'expression de P2RX7 pour induire cet effet.













L'activation de P2RX7 par HEI3090 inhibe la croissance des tumeurs pulmonaires en ciblant les cellules immunitaires, et plus particulièrement les cellules dendritiques, afin de réactiver une réponse immunitaire antitumorale qui repose sur la production d'IL-18. De plus, HEI3090 sensibilise les tumeurs à l'immunothérapie dans les deux modèles murins, en éradiquant 80% des tumeurs dans le modèle transplanté et en diminuant de 60% la charge tumorale dans le modèle *in situ*. Les souris guéries sont également protégées d'un rechallenge tumoral grâce à une réponse immunitaire mémoire.


Nous avons également mis en avant la validité de cette stratégie chez l'homme. En effet, l'expression de P2RX7 dans les adénocarcinomes humains est fortement liée à une réponse immunitaire antitumorale. De plus l'expression de P2RX7 est également corrélée à l'expression des points de contrôle immunitaire PD-1 et PD-L1, suggérant que la combinaison d'un activateur du récepteur avec les immunothérapies serait plus efficace, en cohérence avec les résultats que l'on a obtenus dans les modèles murins.

L'ensemble de ces résultats mettent en avant l'axe ATP/P2RX7/IL-18 comme nouvelle stratégie thérapeutique dans le cancer du poumon et mettent en évidence l'IL-18 comme pivot de l'immunité antitumorale.

# A small-molecule P2RX7 activator promotes anti-tumor immune responses and sensitizes lung tumor to immunotherapy

Laetitia Douguet<sup>1,15</sup>, Serena Janho dit Hreich<sup>1,2,3,15</sup>, Jonathan Benzaquen<sup>1,2,3</sup>, Laetitia Seguin<sup>1,2</sup>, Thierry Juhel<sup>1</sup>, Xavier Dezitter<sup>4,5</sup>, Christophe Duranton<sup>6</sup>, Bernhard Ryffel<sup>7</sup>, Jean Kanellopoulos<sup>8</sup>, Cecile Delarasse<sup>9</sup>, Nicolas Renault<sup>4,5</sup>, Christophe Furman<sup>4,5</sup>, Germain Homerin<sup>4,10</sup>, Chloé Féral<sup>1,2</sup>, Julien Cherfils-Vicini<sup>1</sup>, Régis Millet<sup>4,5</sup>, Sahil Adriouch<sup>11</sup>, Alina Ghinet<sup>4,10,12</sup>, Paul Hofman<sup>1,2,13,14</sup> & Valérie Vouret-Craviari<sup>1,2,3</sup>

Only a subpopulation of non-small cell lung cancer (NSCLC) patients responds to immunotherapies, highlighting the urgent need to develop therapeutic strategies to improve patient outcome. We develop a chemical positive modulator (HEI3090) of the purinergic P2RX7 receptor that potentiates  $\alpha$ PD-1 treatment to effectively control the growth of lung tumors in transplantable and oncogene-induced mouse models and triggers long lasting antitumor immune responses. Mechanistically, the molecule stimulates dendritic P2RX7-expressing cells to generate IL-18 which leads to the production of IFN- $\gamma$  by Natural Killer and CD4<sup>+</sup> T cells within tumors. Combined with immune checkpoint inhibitor, the molecule induces a complete tumor regression in 80% of LLC tumor-bearing mice. Cured mice are also protected against tumor re-challenge due to a CD8-dependent protective response. Hence, combination treatment of small-molecule P2RX7 activator followed by immune checkpoint inhibitor represents a strategy that may be active against NSCLC.

<sup>1</sup> Université Côte d'Azur, CNRS, INSERM, IRCAN, Nice, France. <sup>2</sup> FHU OncoAge, Nice, France. <sup>3</sup> Centre Antoine Lacassagne, Nice, France. <sup>4</sup> Inserm, CHU Lille, U1286—Infinite—Institute for Translational Research in Inflammation, University of Lille, Lille, France. <sup>5</sup> Institut de Chimie Pharmaceutique Albert Lespagnol, IFR114, Lille, France. <sup>6</sup> Université Côte d'Azur, CNRS, INSERM, LP2M, Nice, France. <sup>7</sup> INEM—UMR7355, Institute of Molecular Immunology and Neurogenetic, University and CNRS, Orleans, France. <sup>8</sup> Institute for Integrative Biology of the Cell (I2BC), CEA, CNRS, Université Paris-Saclay, Gif-sur-Yvette Cedex, France. <sup>9</sup> INSERM, CNRS, Institut de la Vision, Sorbonne Université, Paris, France. <sup>10</sup> Hautes Etudes d'Ingénieur (HEI), JUNIA, UC Lille, Laboratoire de Chimie Durable et Santé, Lille, France. <sup>11</sup> Institute for Research and Innovation in Biomedicine, Normandie University, Rouen, France. <sup>12</sup> Faculty of Chemistry, 'Al. I. Cuza' University of Iasi, Iasi, Romania. <sup>13</sup> Hospital-Related Biobank (BB-0033-00025), Pasteur Hospital, Nice, France. <sup>14</sup> Laboratory of Clinical and Experimental Pathology and Biobank, Pasteur Hospital, Nice, France. <sup>15</sup> These authors contributed equally: Laetitia Douguet, Serena Janho dit Hreich.  
email: [ldouguet@gmail.com](mailto:ldouguet@gmail.com); [valerie.vouret@univ-cotedazur.fr](mailto:valerie.vouret@univ-cotedazur.fr)

Despite new biological insights and recent therapeutic advances, many tumors remain resistant to treatments, leading to premature death of the patient. This is particularly true for lung cancer, which is the leading cause of cancer death for men and women worldwide. The 5-year survival rate for patients with any type of lung cancer is around 20%, which dramatically drops to 6% for metastatic lung cancers. Recent advances in effective therapies such as targeted therapies and immunotherapies have revolutionized lung cancer treatments<sup>1</sup>. However, it is limited to a small percentage of patients and alternative approaches are urgently needed to improve patient outcome.

The P2RX7 receptor (also called P2X7R) is an ATP-gated ion channel composed of three protein subunits (encoded by the *P2RX7* gene), which is expressed predominantly in immune cells and in some tumor cells<sup>2</sup>. Activation of P2RX7 by high doses of extracellular ATP (eATP) leads to Na<sup>+</sup> and Ca<sup>2+</sup> influx, and, after prolonged activation, to the opening of a larger conductance membrane pore. One consequence of this large pore opening, a unique characteristic of P2RX7, is to induce cell death in eATP rich microenvironments. Noteworthy, such high doses of eATP are present in the inflammatory and tumor microenvironments (TMEs)<sup>3</sup>. P2RX7 functions are largely described in immune cells, where it is involved in NLRP3 activation to induce the maturation and secretion of IL-1 $\beta$  and IL-18 pro-inflammatory cytokines by macrophages and dendritic cells (DCs)<sup>4</sup>. In line, several P2RX7 inhibitors have been developed with the aim to treat inflammatory diseases. In addition to its ability to finely tune the amplitude of the inflammatory response<sup>5</sup>, P2RX7 has been shown to orchestrate immunogenic cell death (ICD) and to potentiate DC activation and ability to present tumor antigens to T cells<sup>6</sup>. Among immune cells, regulatory T cells (Treg) are highly sensitive to P2RX7-induced cell death and, in the presence of eATP, P2RX7 negatively regulates their number and their suppressive function<sup>7</sup>. Such response can participate in P2RX7-dependent immune surveillance by unleashing the effector functions of adaptive immune T cells<sup>8</sup>. Therefore, P2RX7 has been proposed to represent a positive modulator of antitumor immune response. This is in agreement with data from our group showing that P2RX7-deficient mice are more sensitive to colitis-associated cancer<sup>9</sup>. Also, in this model, we noticed that transplanted Lewis lung carcinoma (LLC) tumors grew faster in line with the findings of Adinolfi et al. using transplanted B16 melanoma and CT26 colon carcinoma tumors<sup>10</sup>. Collectively, these results support the notion that P2RX7 expression by host immune cells coordinates antitumor immune response.

Capture of tumor antigens by antigen-presenting DC is a key step in immune surveillance. Activated DCs present tumor antigens to naïve T cells leading to their activation and differentiation in effector T cells. Tumor infiltrated effector T cells and NK cells can recognize and kill tumor cells resulting in the release of additional tumor antigens and amplification of the immune response. However, this response is often inhibited by immunosuppressive mechanisms present within the TME. Different mechanisms sustain tumor escape as the reduced immune recognition of tumors due to the absence of tumor antigens, or the loss of MHC-I and related molecules, the increased resistance of tumor cells edited by the immune responses, and the development of a favorable TME associated with the presence of immunosuppressive cytokines and growth factors (such as VEGF, TGF- $\beta$ ) or the expression of checkpoint inhibitors such as PD-1/PD-L1<sup>11</sup>. Inhibitory checkpoint inhibitors ( $\alpha$ PD-1/PD-L1 and anti-CTLA-4) are used in daily practice for the treatment of advanced malignancies, including melanoma and non-small cell lung cancer (NSCLC)<sup>12</sup>. These antibodies reduce

immunosuppression and reactivate cytotoxic effector cell functions to elicit robust antitumor responses<sup>13,14</sup>. High response rate to  $\alpha$ PD-1/PD-L1 therapy is often associated with immune inflamed cancer phenotype characterized by the presence in the TME of both CD4<sup>+</sup> and CD8<sup>+</sup> T cells, PD-L1 expression on infiltrating immune and tumor cells and many pro-inflammatory and effector cytokines, such as IFN- $\gamma$ <sup>15</sup>. Noteworthy, only few cancer patients achieve a response with anti-immune checkpoint administered as single-agent<sup>16</sup>, suggesting that strategies based on combined therapies would likely enhance antitumor efficacy and immunity.

Despite the role of P2RX7 in stimulating antitumor immunity and the observation that tumor development is more aggressive in *p2rx7*-deficient animals<sup>9</sup>, it is currently not known whether P2RX7 activation can modulate tumor progression in vivo. The purpose of this study is to investigate the effect of a positive modulator (PM) of P2RX7 on lung tumor fate. To do so, we use syngeneic immunocompetent tumor mice models and show that activation of P2RX7 improves mice survival. Mechanistically, activation of P2RX7 leads to increased production of IL-18 in a NLRP3-dependent manner, which in turn activates NK and CD4<sup>+</sup> T cells to produce IFN- $\gamma$  and consequently increases tumor immunogenicity. Finally, activation of P2RX7 combined with  $\alpha$ PD-1 immune checkpoint inhibitor allows tumor regression, followed by the establishment of a robust immunological memory response.

## Results

**HEI3090 is a positive modulator of P2RX7.** In order to identify positive modulator of P2RX7, 120 compounds from the HEI's proprietary chemical library were screened for their ability to increase P2RX7-mediated intracellular calcium concentration during external ATP exposure. We first produced an HEK cell line expressing the cDNA encoding for P2RX7 from C57BL/6 origin (HEK mP2RX7) and determined the minimal dose of ATP (333  $\mu$ M) that should be used to initiate an increase in Ca<sup>2+</sup> concentration. We tested five promising compounds and identified HEI3090 as a hit (patent WO2019185868A1). HEI3090 corresponds to a pyrrolidin-2-one derivative decorated with a 6-chloropyridin-3-yl-amide in position 1 and with a 2,4-dichlorobenzylamide moiety in position 5 (Fig. 1a and Supplementary Fig. 1). HEI3090 alone showed no toxic activity, was unable to induce intracellular Ca<sup>2+</sup> variation, and required the presence of eATP to rapidly and dose dependently enhance the P2RX7-mediated intracellular calcium concentration (Fig. 1b, c). The maximum effect of HEI3090 was observed at 250 nM, which is in the range of doses identified in pharmacokinetic analysis (Fig. 1g). HEI3090 action required the expression of P2RX7, since HEK cells transfected with empty plasmid (pcDNA6) showed no increase in intracellular calcium concentration (Fig. 1c). P2RX7 has the unique capacity to form a large pore under eATP stimulation. Large pore opening of P2RX7 was assayed with the quantification of the uptake of the fluorescent TO-PRO-3 dye. As expected, HEI3090 alone had no effect and required eATP stimulation to enhance TO-PRO-3 entry within the cells. HEI3090 increased by 2.5-fold the large pore opening (Fig. 1d). The rapid uptake of TO-PRO-3 was consistent with direct P2RX7 activation rather than ATP/P2RX7-induced cell death (Fig. 1e). We also tested HEI3090's effect on splenocytes expressing physiologic levels of P2RX7 (Fig. 1f). In these immune cells, HEI3090 alone did not affect Fluo-4-AM nor TO-PRO-3 uptake. However, in the presence of eATP, HEI3090 enhanced Ca<sup>2+</sup> influx and TO-PRO-3 uptake. We also showed that HEI3090 required the expression of P2RX7, since its effect was lost in splenocytes isolated from *p2rx7*<sup>-/-</sup> mice.

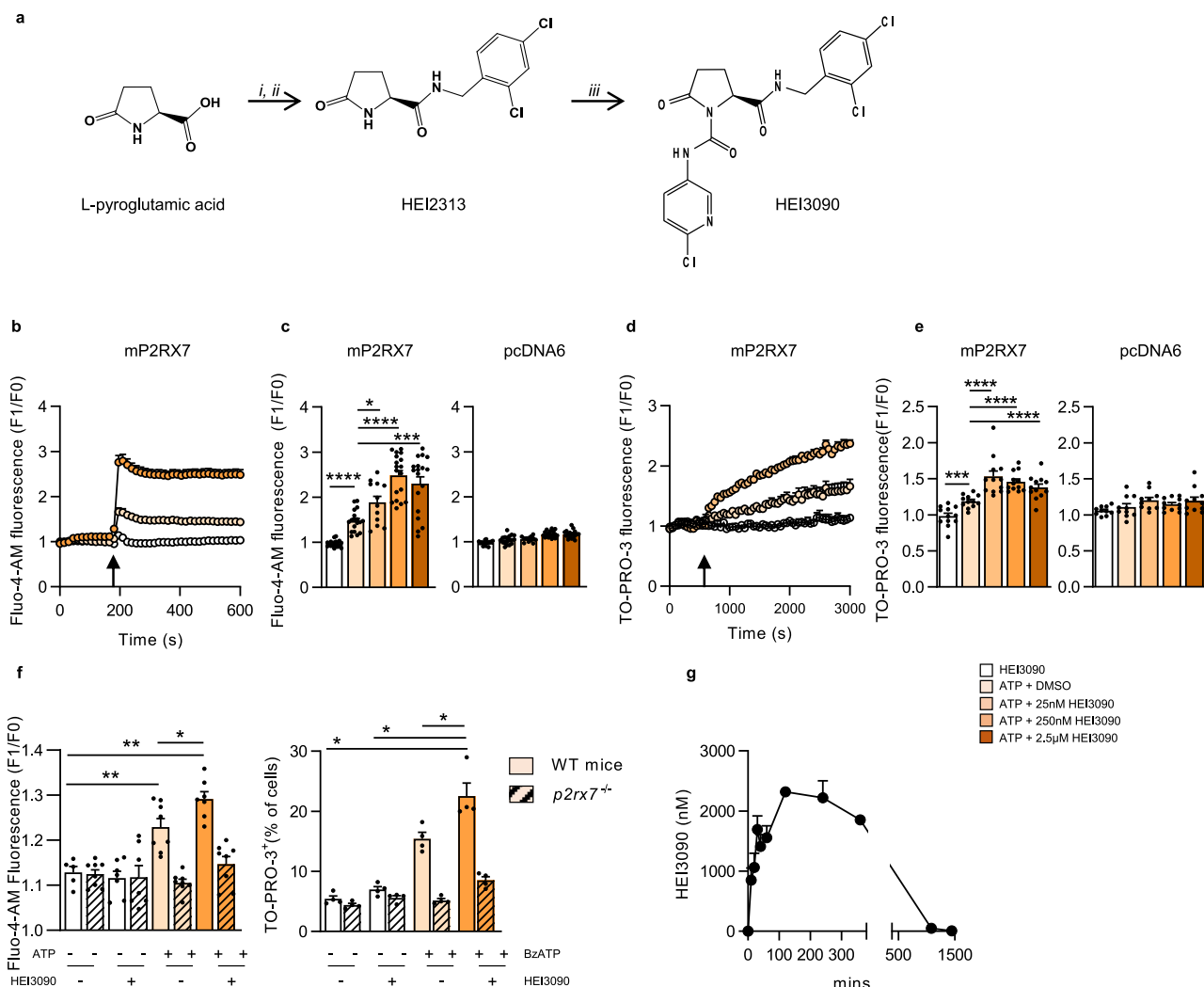


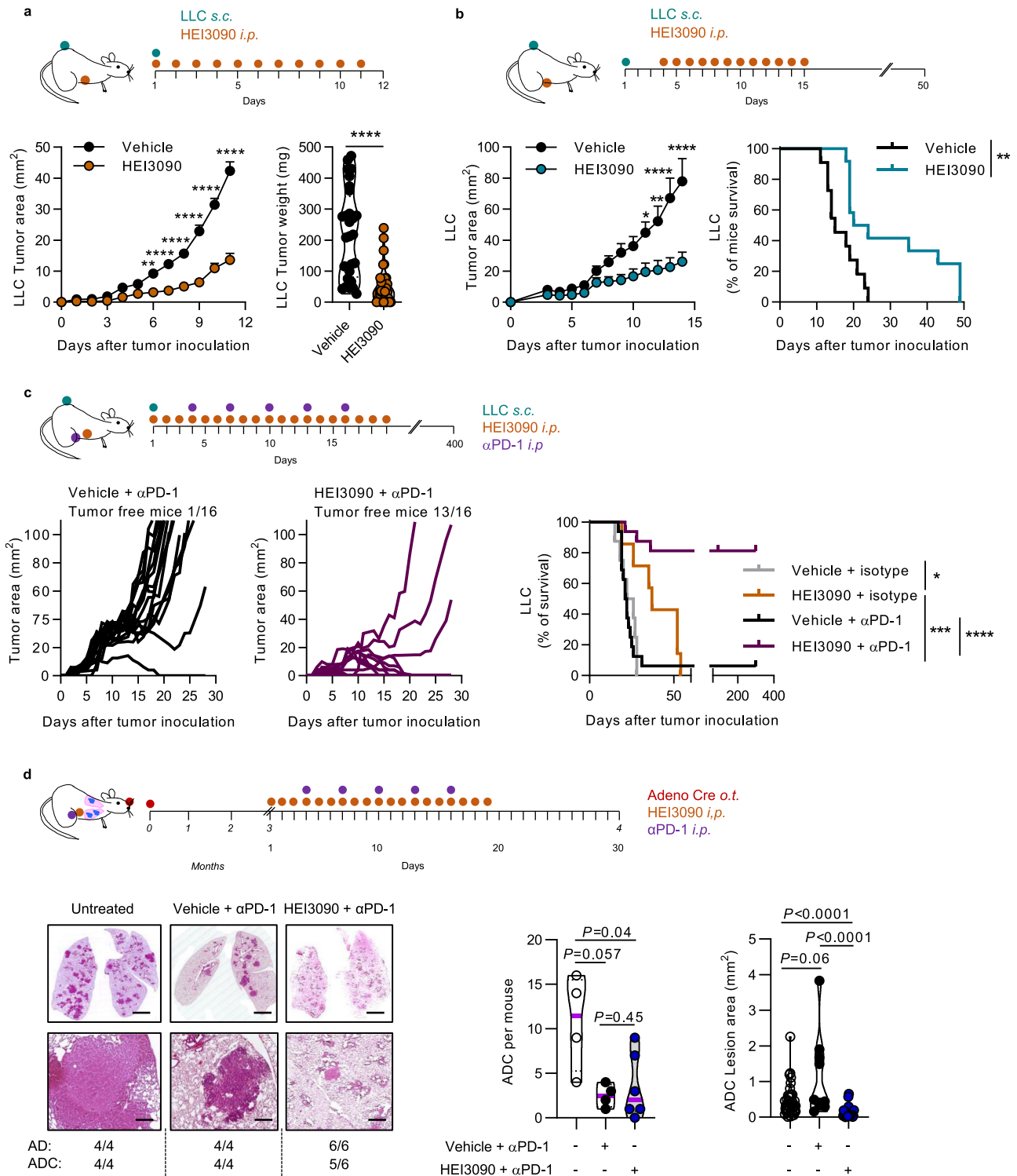
**Fig. 1 HEI3090 enhances ATP-induced receptor channel activity.** **a** Representation of HEI3090's synthesis steps. **b** Modulation of ATP-induced intracellular  $Ca^{2+}$  variation (F1/F0) in HEK293T-mP2RX7 cells (C57Bl/6 origin). After ten baseline cycles, ATP (333  $\mu$ M) and HEI3090 (250 nM) were injected. Error bars are mean  $\pm$  SEM ( $n = 3$  independent experiments, 6 replicates). **c** Average Fluo-4-AM fluorescence intensities in HEK293T mP2RX7 or control HEK pcDNA6 measured 315 s after stimulation with ATP (333  $\mu$ M) and HEI3090 at concentrations of 25, 250, and 2.5  $\mu$ M, as indicated in the color code. Data are presented as scatter dot plots  $\pm$  SEM ( $n = 3$  independent experiments and 6 replicates, two-tailed Mann-Whitney test). **d** Modulation of ATP-induced TO-PRO-3 uptake in HEK293T mP2RX7 cells (F1/F0) in cells treated with ATP and HEI3090 (25 nM). Error bars are mean  $\pm$  SEM ( $n = 3$  independent experiments, 4 replicates, two-tailed Mann-Whitney test). **e** Average fluorescence intensities in HEK293T mP2RX7 or control HEK pcDNA6 measured 10 min after stimulation with ATP and HEI3090 at concentrations of 25, 250, and 2.5  $\mu$ M, as indicated in the color code. Data are presented as scatter dot plots  $\pm$  SEM ( $n = 3$  independent experiments and 4 replicates, two-tailed Mann-Whitney test). **f** Left: average Fluo-4-AM fluorescence intensities in WT or  $p2rx7^{-/-}$  splenocytes stimulated with 50  $\mu$ M ATP measured at the plateau i.e., 10 min after stimulation. Data are presented as scatter dot plots  $\pm$  SEM ( $n = 2$  independent experiments and 4 replicates). Right: graph represents the percentage of TO-PRO-3 positive cells in splenocytes isolated from naïve WT or  $p2rx7^{-/-}$  mice. Data are presented as scatter dot plots  $\pm$  SEM ( $n = 3$  independent experiments in duplicate, two-tailed Man-Whitney test). **g** Pharmacokinetic analysis of HEI3090 intraperitoneally injected in WT mice. Error bars are means  $\pm$  SEM ( $n = 3$  independent experiments in duplicate). Bars are mean  $\pm$  SEM.  $p$  values: \* $p < 0.05$ , \*\* $p < 0.01$ , \*\*\* $p < 0.001$ , \*\*\*\* $p < 0.0001$ . Source data are provided as a Source Data file.

Collectively these results demonstrate that HEI3090 requires P2RX7 expression to be active and enhances eATP-induced P2RX7 activation.

**HEI3090 inhibits tumor growth and enhances antitumor efficacy of  $\alpha$ PD-1 treatment.** We previously suggested that P2RX7 expression might favor the activation of immune responses<sup>9</sup>. We therefore evaluated the immuno-stimulatory effect and antitumor efficacy of HEI3090 in vivo, hypothesizing that the high level of eATP contained within the TME<sup>17</sup> would be sufficient to stimulate P2RX7. To do so, we used syngeneic LLC and B16-F10 melanoma cell lines expressing P2RX7 (Supplementary Fig. 2). Vehicle or

HEI3090 (1.5 mg/kg) was administered concomitantly to LLC tumor cell injection and mice were treated daily for 11 days. Mice treated with HEI3090 displayed significantly reduced tumor growth and more than fourfold decrease in tumor weight (Fig. 2a and Supplementary Fig. 3). We next tested the efficacy of HEI3090 to inhibit tumor growth in a therapeutic model, in which treatment started when tumor reached 10–15 mm<sup>2</sup> in size. HEI3090 (3 mg/kg) inhibited tumor growth and increased by twofold the median survival (Fig. 2b). We also tested the effect of HEI3090 in the melanoma B16-F10 tumor mouse model and observed the same efficacy (Supplementary Fig. 4a, b).

Given the efficacy of HEI3090 to inhibit tumor growth, we next evaluated the combination of HEI3090 and  $\alpha$ PD-1 antibody.



After tumor inoculations, mice were treated daily with HEI3090 or vehicle and αPD-1 was administered at days 4, 7, 10, 13, and 16. While only 1 mouse out of the 16 mice treated with the αPD-1 alone showed a tumor regression, 13 out of the 16 mice treated with HEI3090 + αPD-1 were tumor-free, suggesting that this molecule increased the efficacy of immune checkpoint inhibitor to induce effective antitumor immune responses and tumor regression (Fig. 2c). Importantly, only the combo treatment allows a long-lasting improved survival of at least 340 days (Fig. 2c, right panel). The combo treatment also increased the survival of mice grafted with B16-F10 tumors (Supplementary

Fig. 4c). As illustrated in Fig. 2d, we tested the combo treatment on the KRAS-driven lung cancer (LSL *Kras*<sup>G12D</sup>) model, which leads to adenocarcinomas 4 months after instillation of adenoviruses expressing the Cre recombinase<sup>18</sup>. Whereas αPD-1 treatment tends to reduce the number of ADC (Fig. 2d), HEI3090 was able to enhance αPD-1's effects in this mouse model. Indeed, tumor burden in mice treated with the combo treatment is reduced by 60% compared to mice treated with αPD-1 alone. Accordingly, the cell number per mm<sup>2</sup> and the number of cells positively stained for the proliferation marker Ki67 were decreased by 50% in lesion areas (Supplementary Fig. 4d). One

**Fig. 2 HEI3090 inhibits tumor growth and combined with immunotherapy ameliorates mice survival. a** Prophylactic administration. Average tumor area and weight of LLC allograft after daily treatment with HEI3090. Curves showed mean tumor area in  $\text{mm}^2 \pm \text{SEM}$  (vehicle  $n = 28$ , HEI3090  $n = 32$ , two-way Anova test, left panel) and graph showed tumor weight the day of sacrifice. Data are presented by violin plots showing all points with hatched bar corresponding to median tumor weight (vehicle  $n = 28$ , HEI3090  $n = 32$ . Two-tailed Mann-Whitney test, right panel). **b** Therapeutic administration. Average tumor area and survival curves of LLC allograft. HEI3090 started when tumors reached 10–15  $\text{mm}^2$  of size. Curves showed mean tumor area in  $\text{mm}^2 \pm \text{SEM}$  ( $n = 12$ , two-way Anova test, left panel) and Mantel Cox test, right panel). **c** Combo treatment. Average tumor area of LLC allograft after HEI3090 and  $\alpha\text{PD-1}$  treatment. Spaghetti plots and survival curves of animals are shown ( $n = 16$ , Mantel Cox test). **d** Schematic illustration of treatment given to LSL-*Kras*<sup>G12D</sup> mice. Representative images showing lung tumor burden (Bar = 2 mm upper panel and 500  $\mu\text{m}$  lower panel) with tumor histopathology ( $n = 4$ ). Average tumor burden of LSL-*Kras*<sup>G12D</sup> mice in response to treatments were studied as the number of ADC per mouse (untreated,  $n = 4$ , vehicle +  $\alpha\text{PD-1}$ ,  $n = 4$ , HEI3090 +  $\alpha\text{PD-1}$ ,  $n = 6$ ; two-tailed Mann-Whitney test) and the surface of ADC lesions per lung. Each point represents one lesion, all lesions are shown to illustrate the heterogeneity (untreated and vehicle +  $\alpha\text{PD-1}$ ,  $n = 4$  mice, HEI3090 +  $\alpha\text{PD-1}$ ,  $n = 6$ , Two-tailed Mann-Whitney test).  $p$  values: \* $p < 0.05$ , \*\* $p < 0.01$ , \*\*\* $p < 0.001$ , \*\*\*\* $p < 0.0001$ . Source data are provided as a Source Data file. AD adenoma, ADC adenocarcinoma.

mouse out of the six treated with HEI3090 and  $\alpha\text{PD-1}$  was protected against adenocarcinoma formation.

**DCs mediate the antitumor effect of HEI3090.** LLC tumor cells express an active P2RX7, since the presence of high doses of eATP leads to an increase in intracellular  $\text{Ca}^{2+}$  concentration, which is blocked by the GSK1370319A P2RX7 inhibitor<sup>19</sup> (Supplementary Fig. 2a). To functionally investigate which cells are targeted by HEI3090, we inoculated LLC in *p2rx7*<sup>-/-</sup> mice and treated them with HEI3090. Whereas HEI3090 efficiently blocked LLC tumor growth in WT mice (Fig. 2a), the same treatment was inefficient in *p2rx7*<sup>-/-</sup> mice, as tumor growth was indistinguishable in treated or untreated groups (Fig. 3a). This result suggests that HEI3090 requires P2RX7 expression by mouse host cells to inhibit tumor growth. The importance of immune cells was further confirmed by the demonstration that the antitumor efficacy of HEI3090 was restored after adoptive transfer of WT splenocytes into *p2rx7*<sup>-/-</sup> mice. DCs express P2RX7 and orchestrate antitumor immunity. Purified DC from WT spleens transferred into *p2rx7*<sup>-/-</sup> mice were able to restore the antitumor effect of HEI3090 (Fig. 3b). This experiment was further supported by the fact that phagocytic cells (macrophages and DC) were required for HEI3090's antitumor effect (Supplementary Fig. 5a) and that macrophages are less implicated in HEI3090's effect in vivo since HEI3090 is still able to inhibit tumor growth in *p2rx7*<sup>fl/fl</sup> LysM mice (Supplementary Fig. 5b).

Flow cytometry analyses revealed that the TME of mice treated with HEI3090 were more infiltrated by immune cells than control mice (Fig. 3d). An increased infiltration of CD8<sup>+</sup> T cells was also observed in the LSL-*Kras*<sup>G12D</sup> lung tumor mouse model (Fig. 3e). Furthermore, we showed that HEI3090-treated mice showed higher levels of P2RX7 on DC (Supplementary Fig. 5c). Deeper characterization of immune cell infiltrate in the LLC tumor model revealed that anti-CD3 staining of tumors from HEI3090-treated mice contained four times more CD3<sup>+</sup> T cells than tumors from vehicle-treated mice (Fig. 3f). Whereas the proportion of CD4<sup>+</sup>FOXP3<sup>+</sup> Treg cells was comparable between treated or untreated mice (Fig. 3g), we found fewer myeloid derived suppressor cells (PMN-MDSCs) after HEI3090 therapy (Fig. 3h) and higher NK/PMN-MDSC and CD4/PMN-MDSC ratios (Fig. 3i) but the treatment failed to consistently increase the CD8/PMN-MDSC ratio. We also showed that HEI3090 targets immune cells in the low immunogenic B16-F10 melanoma syngeneic mouse model, where it was able to increase antitumor effector cells and decrease M-MDSCs infiltration (Supplementary Fig. 6).

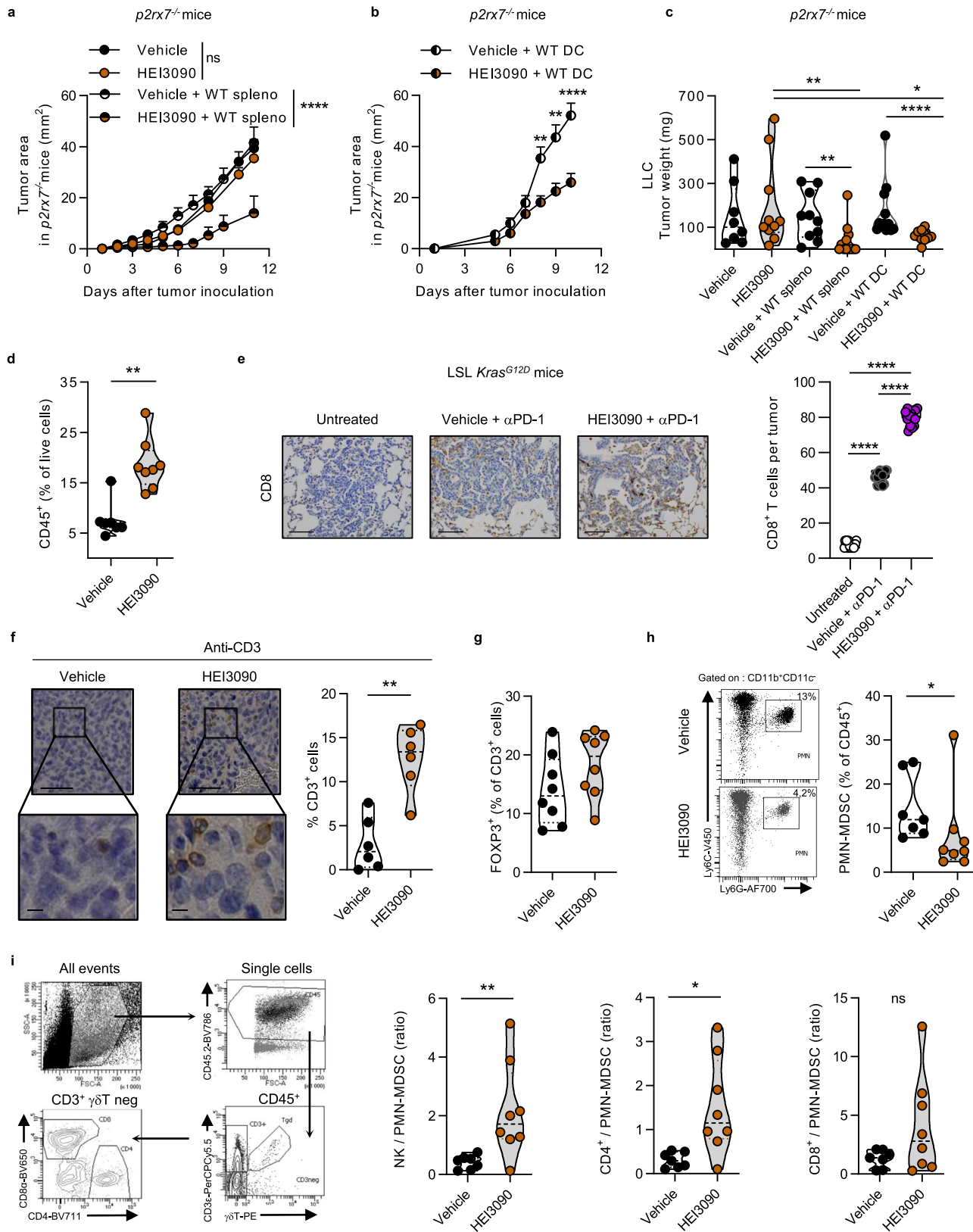
P2RX7 expressed by DC has been shown to link innate and adaptive immune responses against dying tumor cells upon chemotherapy-induced ICD and facilitate tumor antigens presentation to T cells<sup>6</sup>. We evaluated the capacity of HEI3090

treatment to kill tumor cells and concomitant stimulation of DC maturation. Our results showed that HEI3090 is not an ICD inducer (Supplementary Fig. 7).

The two tumor cell lines used in this study express different levels of P2RX7 (Supplementary Fig. 2), yet HEI3090 required P2RX7's expressing immune cells to inhibit tumor growth in both tumor mouse models. These results demonstrate that HEI3090 controls tumor growth by recruiting and activating P2RX7-expressing immune cells, especially DC, within the TME to initiate an effective antitumor immune response.

**IL-18 is produced in response to HEI3090 treatment and is required to mediate its antitumor activity.** We then investigated how the activation of P2RX7 enhanced antitumor immune responses.

In addition to increasing intracellular  $\text{Ca}^{2+}$  concentration and stimulating the formation of a large membrane pore (see Fig. 1), P2RX7's activation is also known to activate the NLRP3 inflammasome that leads to the activation of caspase-1 and consequently to the maturation and release of the pro-inflammatory cytokines IL-1 $\beta$  and IL-18. We showed that HEI3090 enhanced caspase-1 cleavage (Supplementary Fig. 8). Whereas neutralization of IL-1 $\beta$  did not impact HEI3090's antitumor activity, neutralization of IL-18 suppressed the antitumor effect of HEI3090 (Fig. 4a). This result was confirmed using *il18*<sup>-/-</sup> mice in which HEI3090 had no impact on tumor growth (Fig. 4b). IHC staining of LLC tumors from HEI3090-treated mice showed a significant intratumor amount of IL-18 compared to mice treated with the vehicle (Fig. 4c), whereas staining of tumors from *il18*<sup>-/-</sup> mice revealed no staining (Supplementary Fig. 9a). Concordantly, serum levels of IL-18 were statistically more abundant in mice treated with HEI3090 than in vehicle mice (Fig. 4d), and no IL-18 was detected in the serum of mice that received IL-18 neutralizing antibody. In addition, HEI3090 was unable to modulate the levels of IL-18 in *p2rx7*<sup>-/-</sup> mice. Moreover, HEI3090-treated WT and *p2rx7*<sup>-/-</sup> mice show indeed a significant difference in the release of IL-18. Finally, primary peritoneal macrophages and bone-marrow-derived dendritic cells (BMDC) from WT mice-cultured ex vivo with ATP and HEI3090 produce more IL-18 than cells cultured with ATP and vehicle (Fig. 4e and Supplementary Fig. 10c). IL-18 release by HEI3090 required the NLRP3 inflammasome, since its production is inhibited by the NLRP3 inflammasome-specific inhibitor (MCC950) (Fig. 4e). Moreover, we showed that HEI3090 enhanced caspase-1 cleavage (Supplementary Fig. 8) meaning that HEI3090 was able to increase IL-18 production by enhancing the activation of the NLRP3 inflammasome. Activation of P2RX7 by HEI3090 in macrophages from *p2rx7*<sup>-/-</sup> mice failed to increase IL-18 secretion (Supplementary Fig. 9a) and no staining was observed in LLC tumors from HEI3090-treated *p2rx7*<sup>-/-</sup> mice (Supplementary Fig. 9b). In agreement with the observation



that HEI3090 retained its antitumor activity in mice treated with IL-1 $\beta$  neutralizing antibody, HEI3090 did not modify IL-1 $\beta$  protein levels in serum (Fig. 4d) and did not modulate IL-1 $\beta$  secretion in macrophages cultured ex vivo (Supplementary Fig. 9c, d).

Increased production of IL-18 was also observed in the LSL-*Kras<sup>G12D</sup>* lung tumor mouse model. Indeed, cells within lesions of mice treated with HEI3090 combined with  $\alpha$ PD-1 expressed more IL-18 than mice treated with  $\alpha$ PD-1 alone (Fig. 4f). IL-18 protein levels in serum of mice that received the combo treatment were

**Fig. 3 Immune cells mediate the antitumor activity induced by HEI3090.** **a** Average tumor area of LLC allograft in  $p2rx7^{-/-}$  mice after daily treatment with HEI3090 or after adoptive transfer of WT splenocytes and daily treatment with HEI3090. Curves showed mean tumor area in  $\text{mm}^2 \pm \text{SEM}$  (vehicle  $n = 13$ , HEI3090  $n = 16$  mice, vehicle + WT spleno  $n = 11$ , HEI3090 + WT spleno:  $n = 12$ , two-way Anova test). **b** Average tumor area of LLC allograft in  $p2rx7^{-/-}$  mice after adoptive transfer of WT DCs and daily treatment with HEI3090. Curves showed mean tumor area in  $\text{mm}^2 \pm \text{SEM}$  ( $n = 8$ , two-way Anova test). **c** Tumor weight of animals from the study shown in **a** and **b**. Data are presented by violin plots showing all points with hatched bar corresponding to median tumor weight (vehicle  $n = 8$ , HEI3090  $n = 10$  mice, vehicle + WT spleno  $n = 10$ , HEI3090 + WT spleno  $n = 12$ , vehicle + WT DC  $n = 13$ , HEI3090 + WT DC  $n = 12$  mice, two-tailed Mann-Whitney test). **d** Characterization of immune infiltrate at day 12. Percentage of  $\text{CD45}^+$  analyzed by flow cytometry among living cells within TME. Data are presented by violin plots showing all points with hatched bar corresponding to median tumor weight (vehicle  $n = 7$ , HEI3090  $n = 8$ , two-tailed Mann-Whitney test). **e** Representative picture of  $\text{CD8}^+$  cells recruitment in LSL-*Kras*<sup>G12D</sup> mice over six mice studied (bar = 100  $\mu\text{m}$ ) and quantification. Data are presented by violin plots showing all points with hatched bar corresponding to median  $\text{CD8}^+$  T cells (four tumors per mouse,  $n = 4$  mice per group, two-tailed Mann-Whitney test). **f** Representative images of CD3 staining in LLC tumors over six mice studied (bar = 100- $\mu\text{m}$  upper panel and 50- $\mu\text{m}$  lower panel) and quantification data are presented by violin plots showing all points with hatched bar corresponding to median  $\text{CD8}^+$  T cells ( $n = 6$  per group, two-tailed Mann-Whitney test). **g** Percentage of regulatory T cells determined by flow cytometry as  $\text{FOXP3}^+ \text{CD4}^+$  among  $\text{CD3}^+$  within LLC tumors. Data are presented by violin plots showing all points with hatched bar corresponding to median  $\text{FOXP3}^+$  cells of  $\text{CD3}^+$  cells ( $n = 8$  per group, two-tailed Mann-Whitney test). Gating strategy is presented in Supplementary Fig. 12. **h** Proportion of PMN-MDSC among  $\text{CD45}^+$  within LLC tumors. Data are presented by violin plots showing all points with hatched bar corresponding to median PMN-MDSC cells among  $\text{CD45}^+$  cells ( $n = 7$ , per group. Two-tailed Mann-Whitney test). Full gating strategy is presented in Supplementary Fig. 12. **i** Gating strategy (left panel) and ratio of NK,  $\text{CD4}^+$ , or  $\text{CD8}^+$  T cells on PMN-MDSC within LLC tumors (right panel). Data are presented by violin plots showing all points with hatched bar corresponding to median of indicated cells ( $n = 8$  per group, Two-tailed Mann-Whitney test).  $p$  values: \* $p < 0.05$ , \*\* $p < 0.01$ , \*\*\* $p < 0.0001$ . Source data are provided as a Source Data file. Spleno Splenocytes, DC dendritic cells, PMN-MDSC poly morpho nuclear-myeloid-derived suppressor cells.

also increased by sixfold (Fig. 4f and Supplementary Fig. 9e). As described with the LLC tumor model, HEI3090 did not impact the levels of IL-1 $\beta$  in this in situ genetic tumor mouse model (Supplementary Fig. 9f).

Collectively, these results demonstrate that the antitumor effect of HEI3090 is highly dependent on P2RX7 expression and on its capacity to induce the production of mature IL-18 in the presence of eATP.

**IL-18 is required to increase antitumor functions of NK and  $\text{CD4}^+$  T cells.** To identify which immune cells were involved in the HEI3090-induced antitumor response, we performed antibody-specific cell depletion experiments. While NK and  $\text{CD4}^+$  T cells depletions prevented HEI3090 treatment from inhibiting tumor growth (Fig. 5a, b),  $\text{CD8}^+$  T cells depletion had no impact on HEI3090 treatment efficacy (Fig. 5a). To further study the effect of HEI3090 treatment on these subsets, we assessed their cytokine production within the TME. Analyses of tumor infiltrating immune cells first revealed that HEI3090 treatment significantly increased their capacity to produce IFN- $\gamma$  (Fig. 5c). To precisely evaluate which cells in the TME produce IFN- $\gamma$ , we studied the TIL subpopulation and determined the ratios of IFN- $\gamma$  to IL-10 production in each subset (Fig. 5d). NK and  $\text{CD4}^+$  T cells were more biased to produce IFN- $\gamma$  than the IL-10 immunosuppressive cytokine.  $\text{CD8}^+$  T cells were relatively less prone to modification in this cytokine ratio profile upon HEI3090 treatment. In addition, twofold more NK cells from mice treated with HEI3090 degranulate after ex vivo restimulation with LLC compared to NK from control mice (Fig. 5e), confirming their activation state, while no effect was noticeable on  $\text{CD8}^+$  T cells. These phenotypic and functional analyses of intratumor immune infiltration suggested furthermore that treatment with HEI3090 stimulates  $\text{CD4}^+$  T cells and NK cells' activation in the TME. Importantly, IL-18 neutralization abrogated the increase of the IFN- $\gamma$ /IL-10 ratio by  $\text{CD4}^+$  T cells and NK cells (Fig. 5f), suggesting that its production is a direct consequence of IL-18 release and signaling. We showed that DC and IL-18 were necessary for HEI3090's activity (Figs. 3b and 4a, b). In vitro stimulation of splenocytes treated with BzATP and HEI3090 did not increase IFN- $\gamma$  production by T cells and NK cells indicating that its higher production in the tumor of treated mice is rather an indirect consequence of the therapy

(Supplementary Fig. 10a). Concordantly,  $\text{CD45}^+$  cells,  $\text{CD8}^+$  T cells, and NK cells in the TME of  $p2rx7^{-/-}$  mice supplemented with WT DC showed an increase in the IFN- $\gamma$ /IL-10 ratio in the HEI3090-treated mice (Supplementary Fig. 10b). This result indicates that WT DC were able to produce IL-18 after the adoptive transfer, since antitumor effector cells were more prone to produce IFN- $\gamma$  than the IL-10 immunosuppressive cytokine.

Finally, we uncovered that HEI3090 treatment of LLC tumor bearing mice in vivo increased the expression of MHC-I and PD-L1 by 2.2-fold (Fig. 5g). However, when LLC cells were treated in vitro with HEI3090, neither MHC-I nor PD-L1 expression were increased. By contrast, IFN- $\gamma$  induced the expression of these two proteins (Supplementary Fig. 10d). Taken together, our results suggest that the in vivo increase of MHC-I and PD-L1 expression is a consequence of IFN- $\gamma$  upregulation driven by IL-18. Finally, using the LSL-*Kras*<sup>G12D</sup> tumor mouse model, we showed that tumor cells from mice that received both HEI3090 and  $\alpha\text{PD-1}$  expressed more PD-L1 than tumor cells from mice treated with  $\alpha\text{PD-1}$  only (Fig. 5h). Altogether, our results indicate that HEI3090 increases IL-18 production allowing the recruitment and activation of NK and  $\text{CD4}^+$  T cells and the production of IFN- $\gamma$ . In turn, IFN- $\gamma$  stimulates expression of MHC-I and PD-L1 on cancer cells, leading to an increased-tumor immunogenicity and an increased sensitivity to anti-immune checkpoint inhibitors.

### Combined with $\alpha\text{PD-1}$ antibody, HEI3090 cures mice carrying LLC tumors and allows memory immune response.

Combined with an  $\alpha\text{PD-1}$  antibody, HEI3090 cured 80% of LLC-tumor-bearing mice (Fig. 2d). To determine whether cured mice developed an antitumor immune memory response, they were rechallenged with LLC tumor cells 90 days after the first inoculation and were maintained without any therapy as illustrated in Fig. 6a. All long-term-recovered mice were protected from LLC rechallenge, whereas all age-matched control mice developed tumors (Fig. 6b). The rechallenged mice were still alive 150 days after the initial challenge (Fig. 6c), sustaining the hypothesis that combo treatment effectively promoted an efficient antitumor memory immune response. Our results suggested that  $\text{CD8}^+$  T cells are not directly involved in the primary antitumor effect of HEI3090 (see Fig. 5a). Nevertheless, it is well-characterized that these cells play a pivotal role in the host's ability to mount an



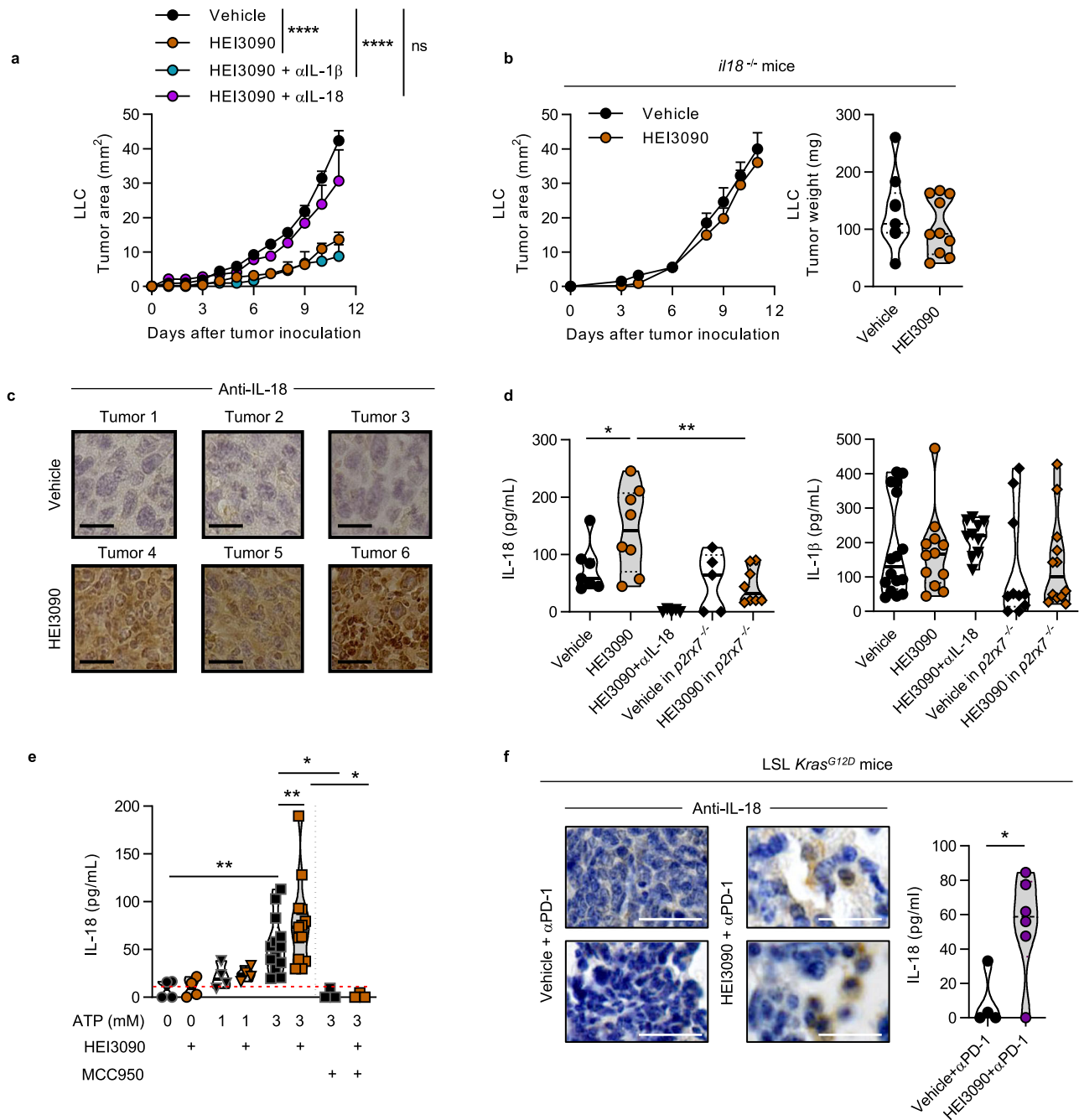
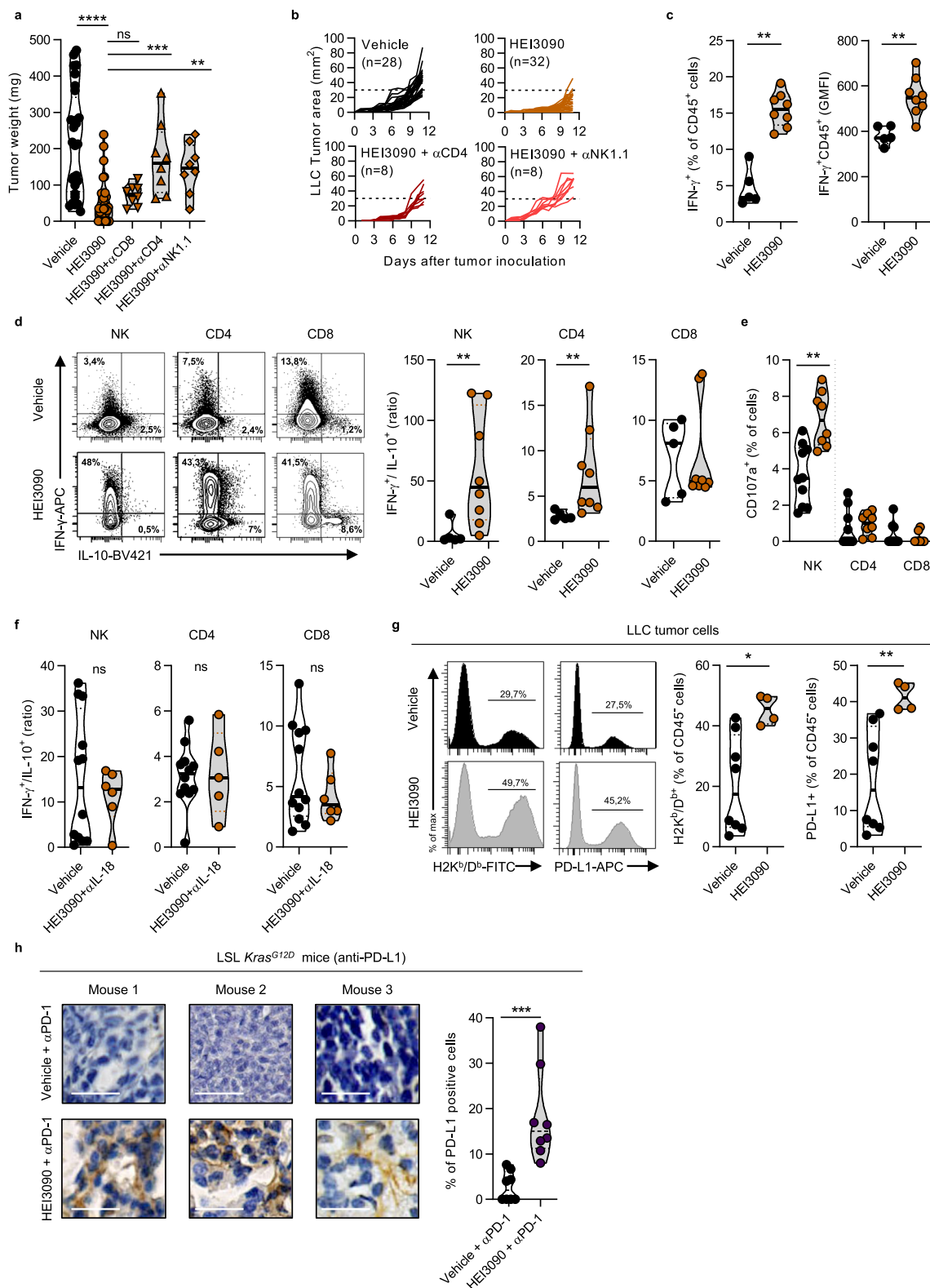


**Fig. 4** HEI3090-induced IL-18 production is required to inhibit tumor growth. **a** Average tumor area of LLC allograft in WT mice injected with IL-1 $\beta$  and IL-18 neutralizing antibodies and daily treatment with HEI3090. Curves showed mean tumor area in mm<sup>2</sup>  $\pm$  SEM (vehicle  $n = 28$ , HEI3090  $n = 32$ , HEI3090 + IL-1 $\beta$  treated  $n = 6$ , HEI3090 + IL-18  $n = 8$ . Two-way Anova test). **b** Average tumor area and tumor weight of LLC allograft in *il-18*<sup>-/-</sup> mice and daily treatment with HEI3090. Curves showed mean tumor area in mm<sup>2</sup>  $\pm$  SEM (vehicle  $n = 9$ , HEI3090  $n = 10$ . Two-way Anova test, left panel) and graph showed tumor weight the day of sacrifice. Data are presented by violin plots showing all points with hatched bar corresponding to median tumor weight (vehicle  $n = 9$ , HEI3090  $n = 10$ . Two-tailed Mann-Whitney test, right panel). **c** Representative images of IL-18 staining in LLC tumors of six mice studied. Bar = 50  $\mu$ m. **d** Production of IL-18 and IL-1 $\beta$  in serum of treated mice determined by ELISA. Data are presented by violin plots showing all points with plain bar corresponding to median cytokine concentration (IL-18 production: vehicle  $n = 7$ , HEI3090  $n = 8$ , HEI3090 +  $\alpha$ IL-18  $n = 6$ , vehicle *p2rx7*<sup>-/-</sup>  $n = 5$ , HEI3090 *p2rx7*<sup>-/-</sup>  $n = 8$ , (IL-1 $\beta$  production: vehicle  $n = 13$ , HEI3090  $n = 12$ , HEI3090 +  $\alpha$ IL-18  $n = 10$ , vehicle *p2rx7*<sup>-/-</sup>  $n = 10$ , HEI3090 *p2rx7*<sup>-/-</sup>  $n = 12$ . Two-tailed Mann-Whitney test). **e** Ex vivo production of IL-18 in primary peritoneal macrophages. Data are presented by violin plots showing all points with hatched bar corresponding to median cytokine concentration (no treatment  $n = 4$ , HEI3090  $n = 4$ , ATP 1 mM  $n = 4$ , ATP 1 mM + HEI3090  $n = 4$ , ATP 3 mM  $n = 13$ , ATP 3 mM + HEI3090  $n = 13$ , ATP 3 mM + MCC950  $n = 3$ , ATP 3 mM + HEI3090 + MCC950  $n = 3$ . Two-tailed Mann-Whitney test). **f** Representative images of IL-18 staining in lung tumor lesions from LSL-*Kras*<sup>G12D</sup> mice over four mice studied (bar = 100  $\mu$ m) and production of IL-18 in serum of LSL-*Kras*<sup>G12D</sup> mice. Data are presented by violin plots showing all points with hatched bar corresponding to median IL-18 concentration (vehicle +  $\alpha$ PD-1,  $n = 4$ , HEI3090 +  $\alpha$ PD-1,  $n = 6$ . Two-tailed Mann-Whitney test).  $p$  values: \* $p < 0.05$ , \*\* $p < 0.01$ , \*\*\*\* $p < 0.0001$ . Source data are provided as a Source Data file.



antitumoral adaptive immune response<sup>20</sup>. To evaluate the involvement of secondary memory CD8<sup>+</sup> T cells response in these mice, we sorted CD8<sup>+</sup> cells from age-matched naïve mice or 5 months (day 150) surviving rechallenged mice (see Fig. 6a) and injected them to naïve mice prior to inoculation of LLC tumor cell in a 1/1 ratio. No treatment was given to mice. In this experimental condition, tumor growth was reduced by twofold in mice that received CD8<sup>+</sup> T cells isolated from cured mice

(Fig. 6d), indicating that the combo therapy promoted a functional immune memory response that partly depends on CD8<sup>+</sup> T cells.

We next characterized the mice that were cured for a very long period (300 days), as illustrated in Fig. 6e. First, to discriminate between dormancy and eradication of tumor cells, we depleted CD8<sup>+</sup> T cells from 300-day-old cured mice and followed mice welfare in the absence of treatment (Fig. 6f). In this condition, no

**Fig. 5 HEI3090 triggers antitumor responses mediated by IL-18-induced NK and CD4<sup>+</sup> T cells.** **a** Average tumor weight of LLC allograft in WT mice injected with depleting antibody and daily treated with HEI3090. Data are presented by violin plots showing all points with plain bar corresponding to median tumor weight (vehicle  $n = 28$ , HEI3090  $n = 32$ , HEI3090 +  $\alpha$ CD8  $n = 8$ , HEI3090 +  $\alpha$ CD4  $n = 8$ , HEI3090 +  $\alpha$ NK1.1  $n = 8$ . Two-tailed Mann-Whitney test). **b** Spaghetti plots of LLC allograft in WT mice injected with depleting antibody and daily treated with HEI3090. vehicle  $n = 28$ , HEI3090  $n = 32$ , HEI3090 +  $\alpha$ CD4  $n = 8$ , HEI3090 +  $\alpha$ NK1.1  $n = 8$ . **c** Average of IFN- $\gamma$ <sup>+</sup> cells among CD45<sup>+</sup> cells in LLC tumors. Data are presented by violin plots showing all points with plain bar corresponding to median of IFN- $\gamma$ <sup>+</sup> cells among CD45<sup>+</sup> cells (vehicle  $n = 5$ , HEI3090  $n = 8$ . Two-tailed Mann-Whitney test). **d** Representative dot plots of IFN- $\gamma$  and IL-10 staining on TILs (left panel) and ratios of IFN- $\gamma$  on IL-10 in the same positive cells of each TILs (right panel). Data are presented by violin plots showing all points with plain bar corresponding to median of the cytokine ratio vehicle  $n = 5$ , HEI3090  $n = 8$ . Two-tailed Mann-Whitney test). **e** Ex vivo degranulation assay of splenocytes from LLC tumor bearing mice. CD107a<sup>+</sup> cells in NK, CD4<sup>+</sup>, and CD8<sup>+</sup> T cells are shown. Data are presented by violin plots showing all points with plain bar corresponding to median % of CD107a<sup>+</sup> cells (vehicle  $n = 10$  vehicle and HEI3090  $n = 8$ . Two-tailed Mann-Whitney test). **f** Ratios of IFN- $\gamma$  on IL-10 in the same positive cells of each TILs of IL-18 neutralized mice. Data are presented by violin plots showing all points with plain bar corresponding to median of the cytokine ratio (vehicle  $n = 12$ , HEI3090  $n = 6$ . Two-tailed Mann-Whitney test). **g** Flow cytometry analyses of MHC-I and PD-L1 expression on CD45<sup>-</sup> cells in LLC tumors. Data are presented by violin plots showing all points with plain bar corresponding to median of positive cells over CD45 cells (vehicle  $n = 8$ , HEI3090  $n = 4$ . Two-tailed Mann-Whitney test). **h** Representative images of PD-L1 staining in cancer lesion of LSL-KRas<sup>G12D</sup> mice representative of six mice studied. (Bar = 100  $\mu$ m) and quantification. Data are presented by violin plots showing all points with hatched bar corresponding to median of positive cells over total cells (vehicle  $n = 7$ , HEI3090  $n = 8$ . Two-tailed Mann-Whitney test).  $p$  values: \* $p < 0.05$ , \*\* $p < 0.01$  \*\*\* $p < 0.001$ , \*\*\*\* $p < 0.0001$ . Source data are provided as a Source Data file.

tumor relapse was observed during the 40 days of the experiment and the weight of the mice remained constant, revealing that the combo treatment efficiently eliminated tumor cells. Second, since circulating CD8<sup>+</sup> T cells are actively involved in the immune memory response<sup>20</sup> and participated in the HEI3090-induced antitumor response (see Fig. 6d), we investigated their involvement in the long-term memory immune response. To do so, 340-day-old cured or age-matched naïve mice were inoculated with LLC tumor cells in the absence of CD8<sup>+</sup> T cells. Both naïve- and cured-age-matched mice developed tumors (Figs. 6g, h). However, the tumor growth was significantly reduced in cured mice and three out of the six mice did not have tumors (Fig. 6g, right panel). Cured mice survival was also significantly increased in comparison to naïve mice (Fig. 6i). Collectively, these results suggest that circulating CD8<sup>+</sup> T cells participate in the antitumor immune response induced by HEI3090.

**P2RX7 is positively correlated with high infiltration of anti-tumor immune cells in NSCLC patients.** Using the lung adenocarcinomas (LUAD) TCGA dataset, we analyzed the effect of *P2RX7* expression levels on the recruitment of cytotoxic immune cells. We clustered tumors of 80 patients with all stage (I-IV) of lung adenocarcinoma according to *P2RX7* expression and showed that high levels of *P2RX7* expression correlated with an increased immune response in LUAD patients, characterized by a high mRNA expression of *CD274* (*PD-L1*), *IL1B*, *IL18*, a signature of primed cytotoxic T cells (defined by *CD8A*, *CD8B*, *IFN-G*, *GZMA*, *GZMB*, *PRF1*) (Fig. 7a). Accordingly, Gene set enrichment analysis (GSEA) demonstrated a positive correlation between high *P2RX7* expression and the well-characterized established signatures of “adaptive immune response,” “T-cell-mediated immunity,” “cytokine production” (Fig. 7b). Furthermore, high *P2RX7* expression is correlated with high levels of *CD274* (*PD-L1*), independently of the stage of the disease (Fig. 7c). Consistently, a significant reduced overall survival is observed for *P2RX7* hi, *CD274* hi, and *P2RX7* hi + *CD274* hi LUAD patients (Fig. 7d), suggesting that high expression levels of *P2RX7* is sufficient to bypass immune responses in the presence of high levels of *CD274*. Such a situation is considered to benefit from anti-checkpoint blockade and/or strategies aiming to reactivate immune responses, e.g., with an activator of *P2RX7*. Indeed, only few cancer patients achieve a response with anti-immune checkpoint administered as single-agent and combined therapies to enhance antitumor immunity and bring a clinical benefit for patients are actively tested. We showed in this study

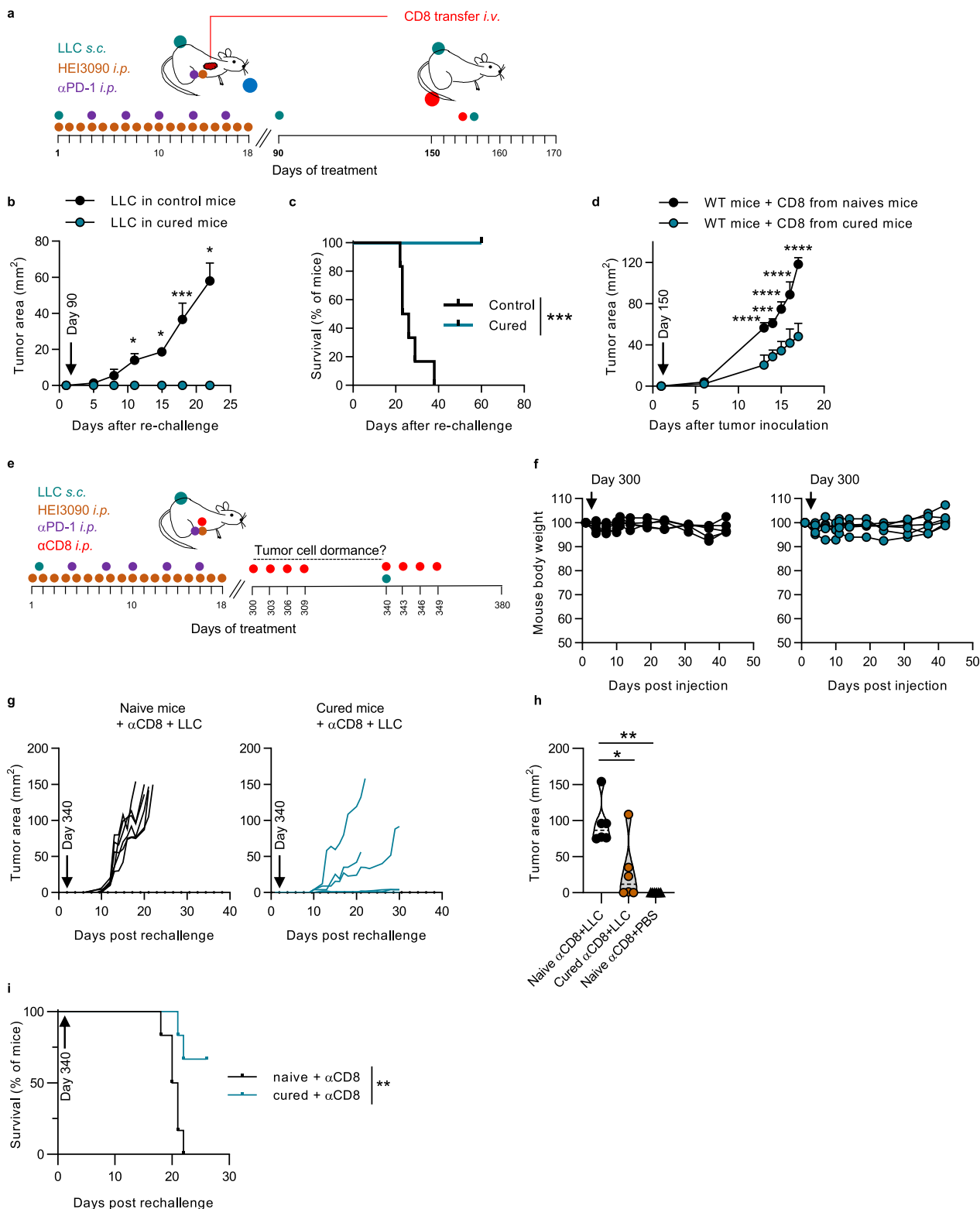
that the combination of HEI3090 and  $\alpha$ PD-1 is more efficient to inhibit lung tumor growth than  $\alpha$ PD-1 alone (see Fig. 2c).

## Discussion

We demonstrated in this study that activation of the purinergic P2RX7 receptor represents a promising strategy to control tumor growth. We developed a positive modulator of P2RX7, called HEI3090, that stimulates antitumor immunity. HEI3090 induces production of IL-18 by P2RX7-expressing immune cells, by mainly targeting DC. IL-18 drives IFN- $\gamma$  production to increase tumor immunogenicity and reinforces NK and CD4<sup>+</sup> T cells immune responses and generates protective CD8<sup>+</sup> T cells responses from recidivism. Noteworthy, therapeutic association of HEI3090 with  $\alpha$ PD-1 antibody synergizes to cure mice in the LLC syngeneic model of lung cancer and elicits an antitumor immunity. We also observed that the combo treatment is more efficient than  $\alpha$ PD-1 alone to inhibit tumor growth in the LSL-KRas<sup>G12D</sup> lung tumor genetic mouse model. Lung tumor regression correlates with an increased immune cell infiltration, more secretion of IL-18 within the TME and higher expression of PD-L1 by tumor cells. Furthermore, this mode of action was confirmed using the B16-F10 melanoma tumor model (Supplementary Fig. 6). Collectively these results demonstrate that the antitumor activity of HEI3090 follows the same rules in all tumor models tested and highlight the strength of HEI3090 to reactivate antitumor immunity.

The design of P2RX7’s modulators was based on a ligand-based approach allowing the generation of a pharmacophore model. One hundred and twenty compounds were generated and were tested for their ability to enhance P2RX7’s activities; five of them were able to do so. HEI3090 was the most promising and effective compound of the five and was therefore chosen for our study. Other natural or synthetic molecules have been described to facilitate P2RX7 response to ATP<sup>21–23</sup>. P2RX4 is another member of the P2X family that is described to regulate P2RX7’s activities in macrophages. Recently Kawano et al. have shown that a positive modulator of P2RX4, the ginsenoside CK compound<sup>24</sup>, calibrates P2RX7-dependent cell death in macrophages<sup>25</sup>. Therefore, we checked whether HEI3090 modulates P2RX4’s activities, which is not the case (Supplementary Fig. 11).

Until now, neither of these molecules has been tested in cancer models. Moreover, attempt to facilitate P2RX7 activation in the field of oncology has been limited by the finding that P2RX7 variants expressed by some tumor cells may sustain their proliferation and metabolic activity<sup>2</sup>. To explore this question, we analyzed P2RX7’s functional features in ex vivo lung cancer



samples<sup>26</sup> and showed that P2RX7 is functional in leukocytes whereas it is nonfunctional in tumor cells. Considering that P2RX7 is a pro-apoptotic receptor, it makes sense that tumor cells express a nonfunctional receptor. Whether this nonfunctional receptor corresponds to the non-conformational P2RX7 (nfP2RX7), described to be expressed by tumor cells<sup>27</sup>, remains to be determined as well as the effect of HEI3090 on nfP2RX7.

Despite the finding that P2RX7 expression by immune cells restrains tumor growth<sup>9,10</sup>, the use of specific P2RX7 antagonists

has been promoted to treat cancers on the basis that inhibition of tumor cell proliferation would be more efficient<sup>28,29</sup>. Considerable effort has been made to engineer-specific P2RX7 antagonists<sup>30</sup> and two of them (A74003 and AZ10606120) inhibited B16 tumor growth in immunocompetent mice<sup>10</sup>. However, to our knowledge, these compounds have not been tested to treat cancer and have failed in the first clinical trials to treat inflammatory and pain-related diseases<sup>30</sup>. In addition, in the preclinical mouse model, we were unable to inhibit LLC and B16-F10 tumor growth

**Fig. 6 HEI3090 combined with  $\alpha$ PD-1 induces antitumor memory immune response.** **a** Schematic illustration of treatments with transfer of CD8 cells. **b** Average tumor area of LLC allograft in 90-day-old WT and 90-day-old cured mice in absence of treatment. Curves showed mean tumor area in  $\text{mm}^2 \pm \text{SEM}$  ( $n = 7$  per group, two-way Anova test). **c** Survival curves of animals from the study shown in **b**. Curves showed survival ( $n = 7$  per group, Mantel Cox test). **d** Average tumor area of LLC allograft in WT mice injected with CD8<sup>+</sup> T cells isolated from rechallenged cured mice as shown in **a**. Curves showed mean tumor area in  $\text{mm}^2 \pm \text{SEM}$  ( $n = 4$  per group, two-way Anova test). **e** Long-lasting antitumor immune response: schematic illustration of treatments. **f** Mouse body weight follow up of 300-day-old cured mice injected with anti-isotype (black circle) or depleting  $\alpha$ CD8 antibodies (blue circle). Each curve represents one mouse ( $n = 6$  per group). **g** Individual survival curves of 340-day-old WT and cured animals injected with anti-CD8 antibody and rechallenge with LLC in absence of treatment. ( $n = 6$  per group). **h** Average tumor area from animals shown in **g**. Data are presented by violin plots showing all points with hatched bar corresponding to median of tumor area ( $n = 6$  per group. Two-tailed Mann-Whitney test). **i** Survival curves from animals shown in **g**. ( $n = 6$  per group, Mantel Cox test). *p* values: \* $p < 0.05$ , \*\* $p < 0.01$ , \*\*\* $p < 0.001$ , \*\*\*\* $p < 0.0001$ . Source data are provided as a Source Data file.

when we tested the GSK1370319A compound, a well-characterized P2RX7 antagonist<sup>19</sup>. In line with this finding, our present results suggest that facilitation of P2RX7 is associated with efficient antitumor immunity in two different models of transplantable tumor (expressing moderate or higher level of P2RX7) as well as in the LSL-*KRas*<sup>G12D</sup> genetic lung cancer mouse model. These results illustrate the view that P2RX7 activation, rather than inhibition, represents a promising strategy in cancer immunotherapy to unleash the immune responses, notably in conjunction with anti-checkpoint blockade. Therapeutic antibody represents another promising field of investigation to treat cancer. In particular, Gilbert et al. described an antibody against a nonfunctional P2RX7 variant that is promising to treat basal cell carcinoma<sup>31</sup>. It would be interesting to combine HEI3090 with the therapeutic P2RX7 antibody and assay the efficacy of this combo treatment.

Antineoplastic action of eATP was previously explored using ATP administration in cancer patients and abandoned for lack of convincing results<sup>32,33</sup>. Extracellular ATP is naturally degraded to adenosine by ectoenzymes, and adenosine is an immunosuppressive molecule<sup>34</sup>. To inhibit the production of adenosine, blocking antibodies against CD39 and CD73 ectoenzymes were produced and tested in mouse cancer models but also in ongoing clinical trials (NCT03454451). This strategy seems to be promising, at least, in mice tumor models. In a first study, Perrot et al. showed that antibodies targeting human CD39 and CD73 promoted antitumor immunity by stimulating DC and macrophages which, in turn, restored the activation of effector T cells<sup>35</sup>. The authors also reported that the combination of anti-CD39 monoclonal antibody with oxaliplatin increased the survival of tumor bearing mice, at least for 50 days. In a second study, an independent anti-CD39 antibody was generated and tested on different mouse tumor models. This antibody alone dampened tumor growth and when combined with  $\alpha$ PD-1, it further slowed tumor progression and 50% of the mice showed a complete rejection<sup>36</sup>. Mechanistically, the anti-CD39 antibody treatment led to an increased eATP levels via the P2RX7/NLRP3/IL-18 to stimulate myeloid cells. Next, the authors demonstrated that anti-CD39 antibody sensitized  $\alpha$ PD-1 resistant tumors by increasing CD8<sup>+</sup> T cells infiltration. Our results confirm these findings but also bring additional highlights. First, we showed that activation of the eATP/P2RX7/NLRP3/IL-18 pathway by HEI3090 increased long-lasting immune responses when combined with  $\alpha$ PD-1 antibody. Second, we demonstrated that the endogenous eATP levels present in the TME were sufficient to enhance P2RX7's activation in the presence of HEI3090. These conditions are ideal to allow P2RX7 activation where it is needed and avoid the possible adverse effects associated with a systemic increase of ATP levels, such as the one observed in response to anti-CD39 and -CD73 antibodies.

It was shown that eATP attracts DC precursors toward the TME and promotes their activation state and their capacity to present antigen<sup>37,38</sup>. During this study, we showed that HEI3090

targets P2RX7-expressing immune cells, especially phagocytic cells, such as macrophages and DCs (Supplementary Fig. 6a). Between macrophages and DCs, DCs were the most promising candidate; they express high levels of P2RX7, they are able to release IL-18, and they are professional antigen-presenting cells able to induce a potent antitumor immune response. We therefore tested their involvement by doing an adoptive transfer of WT DC in *p2rx7*<sup>-/-</sup> mice. Doing so, we restored responsiveness to HEI3090 (Fig. 3b). We also observed that cDC CD4<sup>+</sup> from mice treated with HEI3090 expressed higher levels of P2RX7 (Supplementary Fig. 4c). Collectively, these results demonstrated that DCs mediate HEI3090's antitumor activity, but macrophages may have a secondary role in this effect.

Intriguingly, we did not observe an enhanced production of mature IL-1 $\beta$  in mice treated with HEI3090 (Fig. 4d). This was unexpected as secretion of mature IL-1 $\beta$  depends on the ATP/P2RX7-induced NLRP3 inflammasome activation as well<sup>39</sup>. However, unlike IL-1 $\beta$ , the inactive precursor form of IL-18 is constitutively expressed in most human and animal cells. Whether this explanation is sufficient to account for this differential IL-1 $\beta$ /IL-18 production is currently not known.

Whereas IL-1 $\beta$  is described to induce immune escape<sup>40</sup>, IL-18 is involved in Th1 polarization and NK cell activation. We showed here that IL-18 produced in response to HEI3090 treatment orchestrated the antitumor immune response by driving IFN- $\gamma$  production by NK and CD4<sup>+</sup> T cells. This is in line with the well-known IFN- $\gamma$  stimulating activity of IL-18 (originally designated as IFN- $\gamma$ -inducing factor), and with its Th1 and NK cells stimulating activity<sup>41,42</sup>. Protective effect of IL-18, but also the activation of NLRP3, have been previously reported in various mouse cancer models<sup>43,44</sup>. NLRP3 activation in DCs as well as IL-18 have been linked to better prognosis, to drive antitumor immunity and to enhance the efficacy of immunotherapies in different tumor models<sup>45,46</sup>. In fact, when we combined HEI3090 with an  $\alpha$ PD-1 antibody, we observed that the combo therapy efficiently controlled tumor burden in the three cancer models studied. Notably, the combo treatment cured 80% of LLC tumor bearing mice and very interestingly, cured mice developed an antitumor memory response.

CD8 memory T cells, comprising the circulating memory pool—composed of effector memory (T<sub>EM</sub>) and central memory (T<sub>CM</sub>) cells—and the tissue resident (T<sub>RM</sub>) pool, play crucial roles in antitumor memory responses<sup>47</sup>. We showed that circulating CD8<sup>+</sup> T cells participated in cancer immunosurveillance after HEI3090 treatment (Fig. 6d). However, this CD8<sup>+</sup> T cells pool cannot be responsible for the entire response, since antitumor responses were still effective when CD8<sup>+</sup> T cells were depleted (Fig. 6g). These results suggest that other immune cells participate in local cancer surveillance. Possible candidates are the non-circulating CD8<sup>+</sup> T<sub>RM</sub> cells. The persistence of T<sub>RM</sub> cells in tissues has been shown to depend on signaling programs driven by TGF $\beta$  and Notch-dependent signaling signature. Whether HEI3090 directly stimulates those programs remains to be

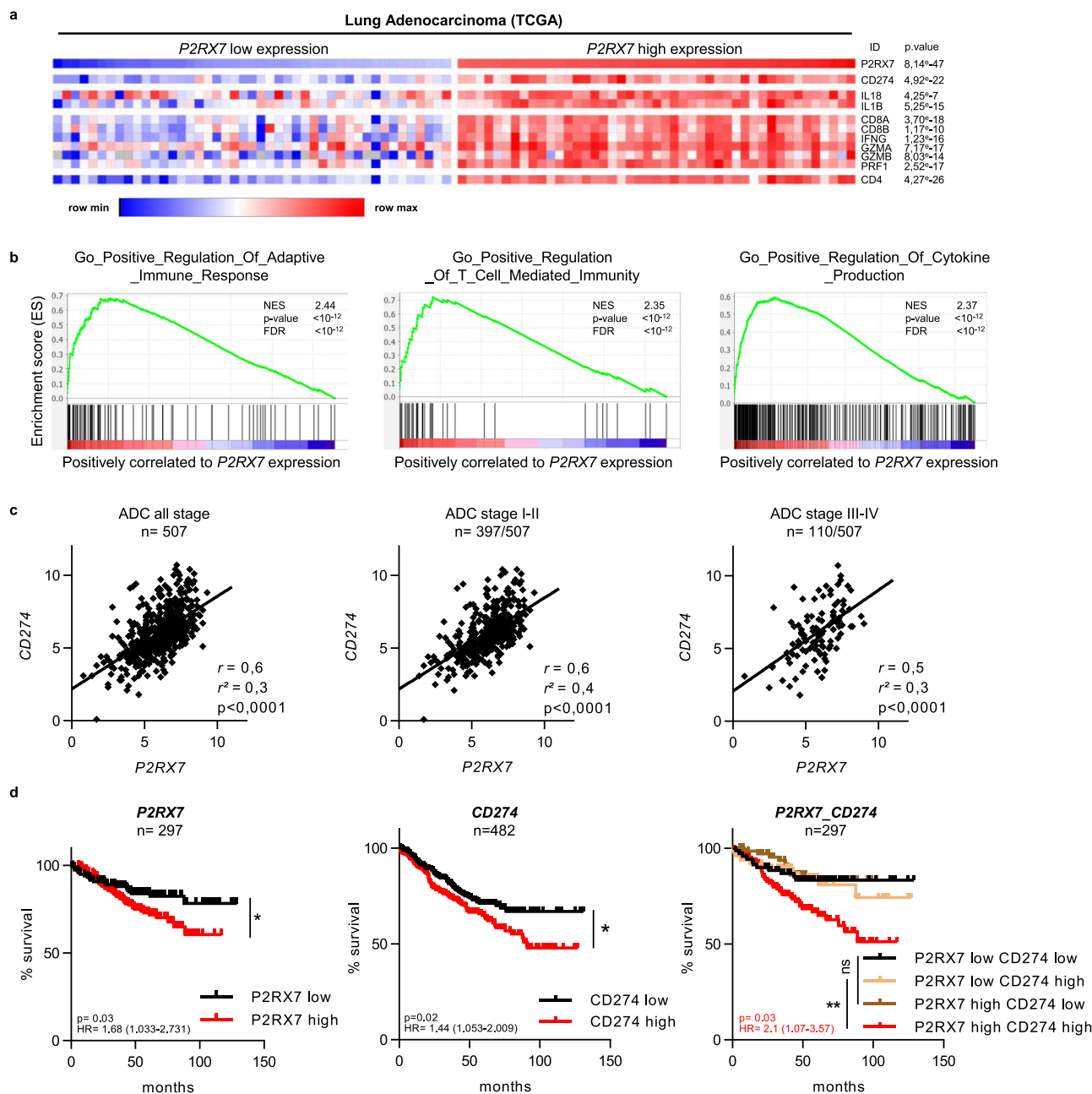


**Fig. 7 P2RX7 expression in LUAD is associated with “hot” immunophenotype signature.** **a** Association of *P2RX7* mRNA expression with a cluster of inflammatory genes (heatmap). Expression values are represented as colors, where the range of colors (red, pink, light blue, dark blue) shows the range of expression values (high, moderate, low, lowest). Raw *p* values (Linear models for microarray analysis, Limma) are shown. **b** Gene set enrichment analysis (GSEA) plot associating *P2RX7* high mRNA levels from LUAD patients (TCGA) with three inflammatory signatures. The enrichment score is shown as a green line, and the vertical black bars below the plot indicate the positions of specific inflammatory signature-associated genes, which are mostly grouped in the fraction of upregulated genes. For each signature, normalized enriched score (NES), *p* values (bilateral Kolmogorov-Smirnov), and false discovery rate (FDR) are shown. **c** Correlation curves of *P2RX7* and *CD274* expression from LUAD patients (TCGA) of all stage (left panel), low stage (middle panel), and high stage (right panel). *r*, *r*<sup>2</sup>, and *p* values are shown in each panel, (Person correlation and *t* test). **d** Kaplan-Meier plot (<http://kmplot.com>) showing survival curves of *P2RX7* high vs. *P2RX7* low patients (left panel), *CD274* high vs. *CD274* low (middle panel), and *P2RX7* high or low vs. *CD274* high or low (right panel). For all panels, the optimal cutoff is determined on KMplot. The *p* value (log-rank, Mantel Cox test), the hazard ratio, and number of patients are indicated. Source data are provided as a Source Data file. ADC adenocarcinoma, HR hazard ratio.

determined but we observed, using HEK mP2RX7 cells, that HEI3090 enhanced ATP-stimulated ERK pathways. Our results are also compatible with a role for CD4<sup>+</sup> T memory cells and the setup of a humoral response, in which B lymphocytes produce antibody against tumor cells.

Therapy with different αPD-1/PD-L1 antibodies was approved in NSCLC in the first- and second-line settings. However, a

significant fraction of patients does not benefit from the treatment (primary resistance), and some responders relapse after a period of response (acquired resistance)<sup>48</sup>. Expression of PD-L1 per se is not a robust biomarker with a predictive value since the αPD-L1 response has also been observed in some patients with PD-L1-negative tumors. Improvement of patient management for immunotherapy undoubtedly relies on the identification of such

predictive markers. Using TCGA dataset, we uncovered that *P2RX7* expression is correlated to *CD274* (PD-L1) expression and “hot” immunophenotype signatures in NSCLC patients. In addition, patients with high *P2RX7* and low *CD274* or high *CD274* and low *P2RX7* have a better overall survival than patients with high *CD274* and high *P2RX7*. This result suggests that immunotherapies may be efficient in double positive patients and questions the ability of *P2RX7* to represent a valuable biomarker for  $\alpha$ PD-1/PD-L1 therapies. In this context, we showed in another study<sup>26</sup> that the expression of *P2RX7B* splice variant in tumor immune cells is associated with less infiltrated tumors in lung adenocarcinoma. Mechanistically, we observed that the differential expression of the *P2RX7B* splice variant in immune cells within tumor area correlates with the expression of a less functional *P2RX7* and lower leukocytes recruitment into LUAD.

We demonstrated that a small-molecule activator of *P2RX7* boosts immune surveillance by unleashing the effector functions of adaptive immune T cells and improving the efficacy of  $\alpha$ PD-1 treatment. This therapeutic strategy holds new hopes for cancer patients; by increasing tumor immunogenicity, it could first increase the number of patients eligible to immunotherapies and second, it could also be used as a neoadjuvant or adjuvant therapies of locally advanced lung tumors.

## Methods

**Mice.** Mice were housed under standardized light–dark cycles in a temperature-controlled air-conditioned environment under specific pathogen-free conditions at IRCAN, Nice, France, with free access to food and water. All mouse studies were approved by the committee for Research and Ethics of the local authorities (CIEPAL #28, protocol numbers MESRI 23707, 13656) and followed the European directive 2010/63/UE, in agreement with the ARRIVE guidelines. Experiments were performed in accord with animal protection representative at IRCAN. *P2rx7<sup>-/-</sup>* (B6.129P2-*P2rx7<sup>tm1</sup>Gab1/J*) and *il18<sup>-/-</sup>* mice were from the Jackson Laboratory. *LSL-KRas<sup>G12D</sup>* are from the Jackson Laboratories (ref 008179). *P2rx7-flox* mice were engineered as follow: ES clones (C57/BL/6) containing a construct for the conditional elimination or re-expression of *P2RX7* (purchased from The European Conditional Mouse Mutagenesis Program) were injected into blastocysts of C57Bl6/N, chimeric mice were selected and crossed with deleter mice that are transgenic for the Flip-recombinase under the control of the ubiquitous *Actin* promoter to produce *p2rx7<sup>loxP/loxP</sup>* mice. Our *p2rx7<sup>loxP/loxP</sup>* mice, with loxP sequence floxing the second exon of *p2rx7*, were crossed with (C57BL/6NTacGt (ROSA)26Sor<tm1(ACTB-Cre,-EGFP)) transgenic mice which express the Cre recombinase under the control of the b-actin promoter to produce *p2rx7<sup>exon2-/-</sup>* mice or with *LysM-Cre* mice (B6.129P2-*Lys2tm1*(cre)lfo from the Jackson Laboratories (obtained from Dr B. Chazaud, France) to generate myeloid cell conditional *p2rx7* knockout and WT control (*p2rx7<sup>loxP/loxP</sup>*) mice. Control C57BL/6J OlaHsd female (WT mouse) was supplied from Envigo (Gannat, France).

**In vivo treatments.** Five  $10^5$  tumor cells were injected s.c. into the left flank of WT mice. Pharmacokinetic analysis (Fig. 1g), to characterize the clearance of HEI3090 showed that after a period of 18-h HEI3090 concentration is <10 nM. Therefore, we have decided to inject HEI3090 daily. Mice were treated i.p. with vehicle (PBS, 10% DMSO) or with HEI3090 (1.5 mg/kg in PBS, 10% DMSO), which corresponds to the highest soluble dose. For therapeutic settings, treatment started at day 3, when tumor reached ~10–15 mm<sup>2</sup>, for a maximum of 20 days and mice received vehicle or HEI3090 (3 mg/kg in PBS, 10% DMSO) daily. Depleting and neutralizing antibodies from BioXCell were given i.p. in the right flank at days -1, 3, 7, and 10.  $\alpha$ PD-1 antibody was given i.p. at days 4, 7, 10, and 13 (or as stated in the legend of the figure) post-tumor cell inoculation. Antibodies are listed in Supplementary Table 1.  $\alpha$ PD-1 and HEI3090 were injected separately, with at least 30 min delay between the two injections. Two hundred microliters liposome clonate (Liposoma) were injected i.p. 3 days before LLC tumor cell inoculation in WT mice and then every 3 days, at least 1 h before HEI3090 treatment after the treatment started.  $CD8^+$  T cells were sorted from peripheral lymph nodes of cured or naïve WT mice with Dynabeads® Untouched™ Mouse CD8 Cells (Invitrogen) according to the supplier’s instructions.  $5.10^5$   $CD8^+$  T cells were adoptively transferred into 8-week-old naïve WT mice (i.v.) 1 day before tumor inoculation.  $5.10^5$  LLC cells were injected s.c. into the left flank of these mice and given no further treatment.

Intratracheal delivery of adenoCre induces oncogenic KRAS in lung airway cells, leading to multifocal adenocarcinomas and a median survival of about 6 months<sup>49</sup>. Starting with tumors established for 3 months in adult *LSL-Kras<sup>G12D</sup>* mice of either gender, treatment with vehicle or 1.5 mg/kg HEI3090 daily by i.p. injection was performed for 21 additional days.

**Adoptive transfer in *p2rx7*-deficient mice.** Spleens from WT C57BL/6J female mice were collected and digested in RPMI 1640 medium containing 5% FCS, 1-mg/ml collagenase IV (Sigma-Aldrich), and 50 U/ml DNase I (Roche) for 7 min at 37 °C. Single-cell suspensions of spleens were prepared by passage through 100  $\mu$ m cell strainers (BD Biosciences) and counted. For WT DCs isolation, spleens were digested with the spleen dissociation kit (Miltenyi Biotech) and isolated with the CD11c Microbeads UltraPure (Miltenyi biotech) according to the supplier’s instructions.  $5.10^6$  splenocytes or  $1.2.10^6$  DCs were injected i.v. in *p2rx7<sup>-/-</sup>* mice 1 day before subcutaneous injection of  $5.10^5$  LLC cells into the left flank. Mice were treated i.p. every day for 12 days with vehicle (PBS, 10% DMSO) or with HEI3090 (1.5 mg/kg in PBS, 10% DMSO). At day 12, tumors were collected, weighted, and digested, when flow cytometry analyses were done.

**Flow cytometry and antibodies.** Tumors were mechanically dissociated and digested with 1-mg mL<sup>-1</sup> collagenase A and 0.1-mg mL<sup>-1</sup> DNase I for 20 min at 37 °C. Then single-cell suspensions of tumors were prepared by passage through 100  $\mu$ m cell strainers (BD Biosciences). Surface staining was performed by incubating cells on ice, for 20 min, with saturating concentrations of labeled Abs in PBS, 5% FCS, and 0.5% EDTA. After blocking Fc receptors using anti-CD16/32 antibodies, cells were stained with the appropriate combination of antibodies (see Supplementary Table 1). The transcription factor staining Buffer Set (eBioscience) was used for the FoxP3 staining. For intracellular cytokines, staining was performed after stimulation of single-cell suspensions with Phorbol 12-myristate 13-acetate (PMA at 50 ng mL<sup>-1</sup>, Sigma), ionomycin (0.5  $\mu$ g mL<sup>-1</sup>, Sigma) and 1  $\mu$ L mL<sup>-1</sup> Golgi Plug™ (BD Biosciences) for 4 h at 37 °C 5% CO<sub>2</sub>. Cells were incubated with Live/Dead Near-IR stain (Invitrogen), according to the manufacturer’s protocol prior to Ab surface staining. Then, intracellular staining was performed using Cytofix/Cytoperm™ kit (BD biosciences) following the manufacturer’s instructions. The production of IFN- $\gamma$  and IL-10 was simultaneously analyzed in CD45<sup>+</sup>, NK, CD4<sup>+</sup> T, or CD8<sup>+</sup> T cells. Data files were acquired and analyzed on Aria III using Diva software (BD Biosciences) or on the CytoFlex LX (Beckman Coulter) and analyzed using FlowJo software (LLC). Gating strategies are shown in Supplementary Fig. 12.

**Immunohistological analysis of tumors.** Collected tumors or lungs were fixed in 3% formalin for 16 h prior inclusion in paraffin. We used the following antibodies: anti-CD3, anti-CD8, anti-IL-18,  $\alpha$ PD-L1, and anti-Ki67 (see Supplementary Table 1). After staining, slides were captured and analyzed using NDP view2 software. For the analyses, five zones per tumor were randomly selected and cells were counted using ImageJ software. Results are expressed as number of positive cells per total cell number.

**Characterization of lung lesions in the *LSL-KRas<sup>G12D</sup>* mouse model.** At the end of the treatment mice were sacrificed, exsanguinated and lungs processed for histologic and immunological analyses. After deparaffinization, HE stains were performed and slides were captured and analyzed using NDP view2 software. Tumor burden was calculated by determining the mean of total tumor area per lung using the NDP view2 software. To count the cells and determine the percentage of Ki67-positive cells within lesions, ten lesions per lung, from grade 2 to 5 according to the Sutherland scoring<sup>50</sup>, were randomly selected, their perimeter was determined, and positive and negative nuclei were counted using ImageJ software. Results are expressed as number of cells per mm<sup>2</sup> and the percentage of Ki67-positive cells.

**Ex vivo macrophages and BMDC stimulation.** Peritoneal lavage was done with RPMI 1640 medium on WT or *p2rx7<sup>-/-</sup>* mice.  $4.10^5$  macrophages were seeded in a 96-well plate overnight in RPMI 1640 containing 10% FBS, 2% sodium pyruvate, 1% penicillin/streptomycin, and 50- $\mu$ M  $\beta$ -mercaptoethanol. After two washes with the complete medium, cells were primed for 4 h with 100 ng/ml LPS (Sigma-Aldrich) at 37 °C and then stimulated for 30 min at 37 °C with ATP (Sigma-Aldrich) with or without 50  $\mu$ M of HEI3090 or with 10  $\mu$ M nigericin. When indicated, NLRP3 inflammasome was inhibited with 1  $\mu$ M of MCC950 (Invivogen) for 1 h at 37 °C before cell stimulation. To prepare BMDC, leg bones were removed from C57Bl6/J mice, cut with scissors, and flushed with sterile PBS pH 7.4 via syringe. Bone-marrow-derived dendritic cells (BMDCs) were obtained from bone-marrow cells seeded in Petri dishes and cultured in RPMI medium containing 10% fetal calf serum, 2 mM L-Glutamine, 50-U/mL Penicillin, 50  $\mu$ g/mL Streptomycin and 20% conditioned medium from GM-CSF-producing J558L cells. Medium was refreshed every 3 days. On the 7th day of the differentiation protocol, semi-adherent BMDCs were collected using PBS containing 10 mM EDTA and re-plated in new Petri dishes with fresh medium. Mature and semi-adherent BMDCs were used for experiments on the 14th day of culture. Supernatants were collected and stored at -80 °C before cytokine detection by ELISA using mouse IL-1 beta/IL-1F2 (R&D) and IL-18 (MBL) according to the supplier’s instructions.

Cells were lysed with Laemmli buffer (10% glycerol, 3% SDS, 10 mM Na<sub>2</sub>HPO<sub>4</sub>) with protease inhibitor cocktail (Roche). Proteins were separated on a 12% SDS-PAGE gel and electro transferred onto PVDF membranes, which were blocked for 30 min at RT with 3% bovine serum albumin. Membranes were incubated with primary antibodies diluted 1/1000 at 4 °C overnight. The following antibodies were

used: anti-NLRP3, anti-ASC, anti-caspase-1, and anti- $\beta$ -actin (see Supplementary Table 1). Secondary antibodies (Sigma-Aldrich) were incubated for 1 h at RT. Immunoblot detection was achieved by exposure with a chemiluminescence imaging system (PXI Syngene, Ozyme) after membrane incubation with ECL (Immobilon Western, Millipore). The bands intensity values were normalized to that of  $\beta$ -actin using ImageJ software. Full scan blots are presented in the Source Data file.

**Cell lines.** The LLC cell line (ATCC CRL-1642), the melanoma B16-F10 (ATCC CRL-6475) cell line, and HEK293T cells (ATCC CRL-3216) were used in this study. Cells were cultured in DMEM medium supplemented with 10% FBS and 100 U/mL penicillin and 100 mg/mL streptomycin at 37 °C in a humid atmosphere containing 5% CO<sub>2</sub> and routinely checked for mycoplasma contamination. Cells were used between passages 5 and 15.

**Calcium uptake assay.** 20.10<sup>3</sup> HEK293T-mP2RX7<sup>C57BL/6J</sup> or HEK293T-pcDNA6 cells were seeded per well on a poly-L-Lysine (Sigma-Aldrich) 96 well-coated plate in complete medium. Twenty-four hours later, cells were washed in sucrose buffer (300 mM sucrose, 5 mM KCl, 1 mM MgCl<sub>2</sub>, 1 mM CaCl<sub>2</sub>, 10 mM Glucose, 20 mM HEPES, pH 7-7.4) and incubated for 1 h at 37 °C with 1  $\mu$ M of Fluo-4 AM (Life Technologies). Cells were washed once with PBS + 5% FBS then twice with the sucrose buffer. Fluo-4 AM fluorescence was read on a Xenius, microplate reader (SAFAS) at 485/528 nm at 37 °C. After 3 min of baseline readings, 333  $\mu$ M of ATP (Sigma-Aldrich) were added with or without various concentrations of HEI3090. For the assay on splenocytes, spleens were digested with the spleen dissociation kit (Miltenyi Biotec). 5.10<sup>5</sup> splenocytes were seeded per well on a 96-well plate in sucrose buffer and incubated for 30 min at RT with 1  $\mu$ M of Fluo-4-AM.

**TO-PRO-3 uptake assay.** 30.10<sup>3</sup> HEK293T-mP2RX7<sup>C57BL/6J</sup> or HEK293T-pcDNA6 cells were seeded per well on a poly-L-Lysine (Sigma-Aldrich) black clear bottom 96 well-coated plate (Perkin Elmer) in complete medium. Twenty-four hours later, cells were washed twice in sucrose buffer (300 mM sucrose, 5 mM KCl, 1 mM MgCl<sub>2</sub>, 1 mM CaCl<sub>2</sub>, 10 mM Glucose, 20 mM HEPES, pH 7-7.4). One microliter of TO-PRO-3 (Life Technologies) was added in the sucrose buffer. TO-PRO-3 fluorescence was read on a Xenius, microplate reader (SAFAS) at 550/660 nm at 37 °C. After 10 min of baseline readings, 250  $\mu$ M of ATP (Sigma-Aldrich) were added with or without various concentrations of HEI3090. Alternatively, percentage of TO-PRO-3<sup>+</sup> cells was analyzed on non-adherent cells by flow cytometry.

**Cell viability.** Colorimetric assay based on XTT (Roche) was used to quantify the viability of tumor cells treated with 1 mM of BzATP and 50  $\mu$ M of HEI3090. LLC cells were treated for 16 h and B16-F10 for 3 h. Cellular viability was determined as described in the supplier's protocol.

**In vivo assay for ICD.** B16-F10 was exposed to 3 mM ATP and 50  $\mu$ M HEI3090 for 3 h at 37 °C. Cells were then washed and resuspended in PBS, and cell death was determined with trypan blue. Dying B16-F10 cells reached 97% in this assay. 1.10<sup>5</sup> dying cells were injected s.c. into the right flank of WT mice (in 200- $\mu$ L PBS). Control mice received 200  $\mu$ L PBS into the right flank. Seven days later, mice were challenged with live 5.10<sup>5</sup> B16-F10 cells into the left flank. Tumor growth was routinely monitored at both injection sites.

**Synthesis of HEI3090.** Starting materials are commercially available and were used without further purification (suppliers: Carlo Erba Reagents S.A.S., Thermo Fisher Scientific Inc., and Sigma-Aldrich Co.). Intermediates were synthesized<sup>28</sup> and melting points were measured on the MPA 100 OptiMelt<sup>®</sup> apparatus and are uncorrected. Nuclear magnetic resonance (NMR) spectra were acquired at 400 MHz for <sup>1</sup>H NMR and at 100 MHz for <sup>13</sup>C NMR, on a Varian 400-MR spectrometer with tetramethylsilane (TMS) as internal standard, at 25 °C. Chemical shifts ( $\delta$ ) are expressed in ppm relative to TMS. Splitting patterns are designed: s, singlet; d, doublet; dd, doublet of doublet; t, triplet; m, multiplet; sym m, symmetric multiplet; br s, broaden singlet; br t, broaden triplet. Coupling constants (*J*) are reported in Hertz (Hz). Thin layer chromatography (TLC) was realized on Macherey Nagel silica gel plates with fluorescent indicator and were visualized under a UV lamp at 254 and 365 nm. Column chromatography was performed with a CombiFlash Rf Companion (Teledyne-Isco System) using RediSep packed columns. IR spectra were recorded on a Varian 640-IR FT-IR Spectrometer. Elemental analyses (C, H, N) of new compounds were determined on a Thermo Electron apparatus by "Pôle Chimie Moléculaire-Welience," Faculté de Sciences Mirande, Université de Bourgogne, Dijon, France. LC-MS was accomplished using an HPLC combined with a Surveyor MSQ (Thermo Electron) equipped with APCI source.

The synthesis of the title compound was accomplished starting from L-pyroglytamic acid also known as the "forgotten amino acid," bio-sourced affordable raw material (Fig. 1a). After simple esterification of the L-pyroglytamic acid, the resulting methyl pyroglytamate was reacted with 2,4-dichlorobenzylamine in presence of catalytic amount of zirconium (IV) chloride in solvent-less

conditions to provide pyroglytamide (HEI2313) in 90% yield. To obtain (S)-N<sup>1</sup>-(6-chloropyridin-3-yl)-N<sup>2</sup>-(2,4-dichlorobenzyl)-5-oxopyrrolidine-1,2-dicarboxamide (HEI3090), a mixture of pyroglytamide (HEI2313) (1.86 g, 6.48 mmol) and 2-chloro-5-isocyanatopyridine (1.00 g, 6.48 mmol) in toluene was refluxed for 24 h under nitrogen atmosphere and magnetic stirring. After cooling to room temperature, the mixture has been concentrated in vacuo and the resulting crude has been purified by column chromatography (CH<sub>2</sub>Cl<sub>2</sub>/MeOH: 1/0 to 9/1) to afford pure HEI3090 as a white powder in 54% yield (1.62 g, 3.51 mmol). mp 187–190 °C (MeOH); TLC Rf (CH<sub>2</sub>Cl<sub>2</sub>/MeOH: 95/5) 0.8; <sup>1</sup>H NMR (CDCl<sub>3</sub>, 400 MHz)  $\delta$  ppm 2.21–2.37 (m, 2H, CH<sub>2</sub>CH<sub>2</sub>CH), 2.59–2.68 (m, 1H, CH<sub>2</sub>CH<sub>2</sub>CH), 2.99–3.10 (m, 1H, CH<sub>2</sub>CH<sub>2</sub>CH), 4.49 (dd, *J* = 15.2, 6.2 Hz, 1H NHCH<sub>2</sub>), 4.55 (dd, *J* = 15.2, 6.2 Hz, 1H, NHCH<sub>2</sub>), 4.77 (dd, *J* = 7.2, 2.8 Hz, 1H, CH<sub>2</sub>CH<sub>2</sub>CH), 6.65 (br t, *J* = 6.2 Hz, 1H, NHCH<sub>2</sub>), 7.22 (dd, *J* = 8.1, 2.0 Hz, 1H, ArH), 7.29 (d, *J* = 8.6 Hz, 1H, ArH), 7.33 (d, *J* = 8.1 Hz, 1H, ArH), 7.38 (d, *J* = 2.0 Hz, 1H, ArH), 7.92 (dd, *J* = 8.6, 2.5 Hz, 1H, ArH), 8.49 (d, *J* = 2.5 Hz, 1H, ArH), 10.66 (br s, 1H, NHAr); <sup>13</sup>C NMR (CDCl<sub>3</sub>, 100 MHz)  $\delta$  ppm 21.4 (CH<sub>2</sub>), 32.4 (CH<sub>2</sub>), 41.4 (CH<sub>2</sub>), 59.2 (CH), 124.3 (CH), 127.5 (CH), 129.5 (CH), 130.2 (CH), 130.9 (CH), 133.1 (C), 133.6 (2C), 134.2 (C), 141.3 (CH), 146.2 (C), 150.3 (C), 170.0 (C), 177.7 (C); IR (neat):  $\nu$  cm<sup>-1</sup> 3271, 3095, 1720, 1655, 1594, 1542, 1464, 1217, 1104, 829.

**Statistical analyses.** All analyses were carried out using Prism software (Graph-Pad). Mouse experiments were performed on at least *n* = 5 individuals, as indicated in Fig legends. Mice were equally divided for treatments and controls. Data were represented as mean values and error bars represent SD or SEM. Mann-Whitney, *t*-test, and Mantel Cox were used to evaluate the statistical significance between groups. The corresponding two-way Anova tests and *p* values were mentioned in the legend of each figure. For survival analysis, patients were separated based on optimal cutoff of the expression value of the marker determined using KMplot.

## Data availability

In silico data used in this study are available in the Tumor Comprehensive Genome Atlas (TCGA) project database, at <https://software.broadinstitute.org/morpheus/>. We used the TCGA Lung Adenocarcinoma (LUAD) cohort. The Gene Set Enrichment Analysis (GSEA) signatures sets are available at <https://www.gsea-msigdb.org/gsea/msigdb/index.jsp> and into the folder named « GSEA\_SIGNATURE\_SET » as source data files named: « GO\_POSITIVE\_REGULATION\_OF\_ADAPTIVE\_IMMUNE\_RESPONSE » « GO\_POSITIVE\_REGULATION\_OF\_CYTOKINE\_PRODUCTION » « GO\_POSITIVE\_REGULATION\_OF\_T\_CELL\_MEDIATED\_IMMUNITY » « GO\_RESPONSE\_TO\_TUMOR\_CELL » The GSEA analyses results are available into the folder named « GSEA\_ANALYSES » as Excel Data Sheets named: « ANALYSIS\_GO\_POSITIVE\_REGULATION\_OF\_ADAPTIVE\_IMMUNE\_RESPONSE » « ANALYSIS\_GO\_POSITIVE\_REGULATION\_OF\_CYTOKINE\_PRODUCTION » « ANALYSIS\_GO\_POSITIVE\_REGULATION\_OF\_T\_CELL\_MEDIATED\_IMMUNITY » « ANALYSIS\_GO\_RESPONSE\_TO\_TUMOR\_CELL » Source data are available as a Source Data file. The remaining data are available within the Article, Supplementary Information or available from the authors upon request. Source data are provided with this paper.

Received: 20 December 2019; Accepted: 23 December 2020;  
Published online: 28 January 2021

## References

- Schrank, Z. et al. Current molecular-targeted therapies in NSCLC and their mechanism of resistance. *Cancers* **10**, E224 (2018).
- Benzaquen, J. et al. Alternative splicing of P2RX7 pre-messenger RNA in health and diseases: myth or reality? *Biomed. J.* **42**, 141–154 (2019).
- Pellegatti, P. et al. Increased level of extracellular ATP at tumor sites: in vivo imaging with plasma membrane luciferase. *PLoS ONE* **3**, e2599 (2008).
- Perregaix, D. G., McNiff, P., Laliberte, R., Conklyn, M. & Gabel, C. A. ATP acts as an agonist to promote stimulus-induced secretion of IL-1 $\beta$  and IL-18 in human blood. *J. Immunol.* **165**, 4615–4623 (2000).
- Cesaro, A. et al. Amplification loop of the inflammatory process is induced by P2X<sub>7</sub> R activation in intestinal epithelial cells in response to neutrophil transepithelial migration. *Am. J. Physiol. - Gastrointest. Liver Physiol.* **299**, G32–G42 (2010).
- Ghiringhelli, F. et al. Activation of the NLRP3 inflammasome in dendritic cells induces IL-1 $\beta$ -dependent adaptive immunity against tumors. *Nat. Med.* **15**, 1170–1178 (2009).
- Rissiek, B., Haag, F., Boyer, O., Koch-Nolte, F. & Adriouch, S. ADP-ribosylation of P2X<sub>7</sub>: a matter of life and death for regulatory T cells and natural killer T cells. *Curr. Top. Microbiol. Immunol.* **384**, 107–126 (2014).
- Hubert, S. et al. Extracellular NAD<sup>+</sup> shapes the Foxp3<sup>+</sup> regulatory T cell compartment through the ART2-P2X<sub>7</sub> pathway. *J. Exp. Med.* **207**, 2561–2568 (2010).



9. Hofman, P. et al. Genetic and pharmacological inactivation of the purinergic P2RX7 receptor dampens inflammation but increases tumor incidence in a mouse model of colitis-associated cancer. *Cancer Res.* **75**, 835–845 (2015).
10. Adinolfi, E. et al. Accelerated tumor progression in mice lacking the ATP receptor P2X7. *Cancer Res.* **75**, 635–644 (2015).
11. Vesely, M. D., Kershaw, M. H., Schreiber, R. D. & Smyth, M. J. Natural innate and adaptive immunity to cancer. *Annu. Rev. Immunol.* **29**, 235–271 (2011).
12. Hughes, P. E., Caenepeel, S. & Wu, L. C. Targeted therapy and checkpoint immunotherapy combinations for the treatment of cancer. *Trends Immunol.* **37**, 462–476 (2016).
13. Postow, M. A. et al. Peripheral T cell receptor diversity is associated with clinical outcomes following ipilimumab treatment in metastatic melanoma. *J. Immunother. Cancer* **3**, 23 (2015).
14. Topalian, S. L. et al. Immunotherapy: the path to win the war on cancer? *Cell* **161**, 185–186 (2015).
15. Chen, D. S. & Mellman, I. Elements of cancer immunity and the cancer-immune set point. *Nature* **541**, 321–330 (2017).
16. Eggermont, A. M. M., Maio, M. & Robert, C. Immune checkpoint inhibitors in melanoma provide the cornerstones for curative therapies. *Semin. Oncol.* **42**, 429–435 (2015).
17. Di Virgilio, F., Sarti, A. C., Falzoni, S., De Marchi, E. & Adinolfi, E. Extracellular ATP and P2 purinergic signalling in the tumour microenvironment. *Nat. Rev. Cancer* **18**, 601–618 (2018).
18. DuPage, M., Dooley, A. L. & Jacks, T. Conditional mouse lung cancer models using adenoviral or lentiviral delivery of Cre recombinase. *Nat. Protoc.* **4**, 1064–1072 (2009).
19. Homerin, G. et al. Pyroglutamide-based P2X7 receptor antagonists targeting inflammatory bowel disease. *J. Med. Chem.* **63**, 2074–2094 (2020).
20. Mittal, D., Gubin, M. M., Schreiber, R. D. & Smyth, M. J. New insights into cancer immunoediting and its three component phases—elimination, equilibrium and escape. *Curr. Opin. Immunol.* **27**, 16–25 (2014).
21. Fischer, W., Urban, N., Immig, K., Franke, H. & Schaefer, M. Natural compounds with P2X7 receptor-modulating properties. *Purinergic Signal.* **10**, 313–326 (2014).
22. Di Virgilio, F., Giuliani, A. L., Vultaggio-Poma, V., Falzoni, S. & Sarti, A. C. Non-nucleotide agonists triggering P2X7 receptor activation and pore formation. *Front. Pharmacol.* **9**, 39 (2018).
23. Bidula, S. M., Cromer, B. A., Walpole, S., Angulo, J. & Stokes, L. Mapping a novel positive allosteric modulator binding site in the central vestibule region of human P2X7. *Sci. Rep.* **9**, 1–11 (2019).
24. Dhuna, K. et al. Ginsenosides act as positive modulators of P2X4 receptors. *Mol. Pharmacol.* **95**, 210–221 (2019).
25. Kawano, A. et al. Regulation of P2X7-dependent inflammatory functions by P2X4 receptor in mouse macrophages. *Biochem. Biophys. Res. Commun.* **420**, 102–107 (2012).
26. Benzaquen, J. et al. P2RX7B is a new theranostic marker for lung adenocarcinoma patients. *Theranostics* **10**, 10849–10860 (2020).
27. Gilbert, S. et al. ATP in the tumour microenvironment drives expression of nfp2X7, a key mediator of cancer cell survival. *Oncogene* **38**, 194–208 (2019).
28. Di Virgilio, F. P2RX7: a receptor with a split personality in inflammation and cancer. *Mol. Cell. Oncol.* **3**, e1010937-1 (2016).
29. Young, C. N. J. & Görecki, D. C. P2RX7 purinoceptor as a therapeutic target—the second coming? *Front. Chem.* **6**, 248 (2018).
30. Park, J. H. & Kim, Y. C. P2X7 receptor antagonists: a patent review (2010–2015). *Expert Opin. Ther. Pat.* **27**, 257–267 (2017).
31. Gilbert, S. M. et al. A phase I clinical trial demonstrates that nfp2X7-targeted antibodies provide a novel, safe and tolerable topical therapy for basal cell carcinoma. *Br. J. Dermatol.* **177**, 117–124 (2017).
32. Agteresch, H. J., Burgers, S. A., Van Der Gaast, A., Wilson, J. H. P. & Dagnelie, P. C. Randomized clinical trial of adenosine 5'-triphosphate on tumor growth and survival in advanced lung cancer patients. *Anticancer. Drugs* **14**, 639–644 (2003).
33. Beijer, S. et al. Effect of adenosine 5'-triphosphate infusions on the nutritional status and survival of preterminal cancer patients. *Anticancer. Drugs* **20**, 625–633 (2009).
34. Vijayan, D., Young, A., Teng, M. W. L. & Smyth, M. J. Targeting immunosuppressive adenosine in cancer. *Nat. Rev. Cancer* **17**, 709–724 (2017).
35. Perrot, I. et al. Blocking antibodies targeting the CD39/CD73 immunosuppressive pathway unleash immune responses in combination cancer therapies. *Cell Rep.* **27**, 2411–2425.e9 (2019).
36. Li, X. Y. et al. Targeting CD39 in cancer reveals an extracellular ATP-and inflammasome-driven tumor immunity. *Cancer Discov.* **9**, 1754–1773 (2019).
37. Mutini, C. et al. Mouse dendritic cells express the P2X7 purinergic receptor: characterization and possible participation in antigen presentation. *J. Immunol.* **163**, 1958–1965 (1999).
38. Ma, Y. et al. ATP-dependent recruitment, survival and differentiation of dendritic cell precursors in the tumor bed after anticancer chemotherapy. *Oncimmunology* **2**, 5–7 (2013).
39. Bours, M. J. L., Swennen, E. L. R., Di Virgilio, F., Cronstein, B. N. & Dagnelie, P. C. Adenosine 5'-triphosphate and adenosine as endogenous signaling molecules in immunity and inflammation. *Pharmacol. Ther.* **112**, 358–404 (2006).
40. Kaplanov, I. et al. Blocking IL-1 $\beta$  reverses the immunosuppression in mouse breast cancer and synergizes with anti-PD-1 for tumor abrogation. *Proc. Natl Acad. Sci. U. S. A.* **116**, 1361–1369 (2019).
41. Okamura, H. et al. A novel costimulatory factor for gamma interferon induction found in the livers of mice causes endotoxemic shock. *Infect. Immun.* **63**, 3966–3972 (1995).
42. Ushio, S. et al. Cloning of the cDNA for human IFN-gamma-inducing factor, expression in *Escherichia coli*, and studies on the biologic activities of the protein. *J. Immunol.* **156**, 4274–4279 (1996).
43. Fabbì, M., Carbotti, G. & Ferrini, S. Context-dependent role of IL-18 in cancer biology and counter-regulation by IL-18BP. *J. Leukoc. Biol.* **97**, 665–675 (2015).
44. Segovia, M. et al. Targeting TMEM176B enhances antitumor immunity and augments the efficacy of immune checkpoint blockers by unleashing inflammasome activation. *Cancer Cell* **35**, 767–781.e6 (2019).
45. Zhou, T. et al. IL-18BP is a secreted immune checkpoint and barrier to IL-18 immunotherapy. *Nature* **583**, 609–614 (2020).
46. Zhivaki, D. et al. Inflammasomes within hyperactive murine dendritic cells stimulate long-lived T cell-mediated anti-tumor immunity. *Cell Rep.* **33**, 108381 (2020).
47. Park, S. L., Gebhardt, T. & Mackay, L. K. Tissue-resident memory T cells in cancer immunosurveillance. *Trends Immunol.* **40**, 735–747 (2019).
48. Sharma, P., Hu-Lieskovan, S., Wargo, J. A. & Ribas, A. Primary, adaptive, and acquired resistance to cancer immunotherapy. *Cell* **168**, 707–723 (2017).
49. Regala, R. P. et al. Atypical protein kinase C is required for bronchioalveolar stem cell expansion and lung tumorigenesis. *Cancer Res.* **69**, 7603–7611 (2009).
50. Sutherland, K. D. et al. Multiple cells-of-origin of mutant K-Ras-induced mouse lung adenocarcinoma. *Proc. Natl Acad. Sci. U. S. A.* **111**, 4952–4957 (2014).

## Acknowledgements

The authors wish to thank Prof L. Counillon for valuable discussions, Anne Laure Rossi for technical expertise and graphical art, and Alexandre Gallerand for BMDC preparation. The authors greatly acknowledge the IRCAN's Animal core facility and IRCAN's Flow Cytometry Facility that is supported by FEDER, Ministère de l'Enseignement Supérieur, Région Provence Alpes-Côte d'Azur, Conseil Départemental 06, ITMO Cancer Aviesan (plan cancer), Canceropole PACA, CNRS, and Inserm. The funding sources for this work were Institut National du Cancer (INCa, plan Cancer), Canceropole PACA, Bristol-Myers Squibb Foundation for Research in Immuno-Oncology, the Ligue Nationale Contre le Cancer, the French Government (National Research Agency, ANR) through the "Investments for the Future" programs LABEX SIGNALIFE ANR-11-LABX-0028 and IDEX UCAJedi ANR-15-IDEX-01 and the Centre National de la Recherche Scientifique (CNRS), the Institut National de la Santé et Recherche Médicale (INSERM) and the University of Orleans, The Region Centre Val de Loire (2003-00085470), the Conseil General du Loiret and European Regional Development Fund (FEDER No. 2016-00110366 and EX005756).

## Author contributions

L.D., S.J.H., J.B., L.S., X.D., and V.V.-C. conceived and design the study. L.D., S.J.H., X.D., C.Du., J.K., C.D., N.R., C.F., G.H., A.G., and V.V.-C. developed the methodology. L.D., S.J.H., J.B., L.S., T.J., X.D., B.R., J.K., C.Du., A.G., and J.C.-V. acquired the data (provided animals, provided facilities, and so on). L.D., S.J.H., J.B., L.S., X.D., N.R., C.F., G.H., J.C.-V., R.M., S.A., A.G., P.H., and V.V.-C. analyzed and interpreted the data. S.J.H. and V.V.-C. wrote the manuscript. All authors reviewed the manuscript.

## Competing interests

The authors declare no competing interests.

## Additional information

**Supplementary information** The online version contains supplementary material available at <https://doi.org/10.1038/s41467-021-20912-2>.

**Correspondence** and requests for materials should be addressed to L.D. or V.V.-C.

**Peer review information** *Nature Communications* thanks Raphael Nemenoff, Robert Zeiser, and the other, anonymous reviewer(s) for their contribution to the peer review of this work. Peer review reports are available.

**Reprints and permission information** is available at <http://www.nature.com/reprints>

**Publisher's note** Springer Nature remains neutral with regard to jurisdictional claims in published maps and institutional affiliations.

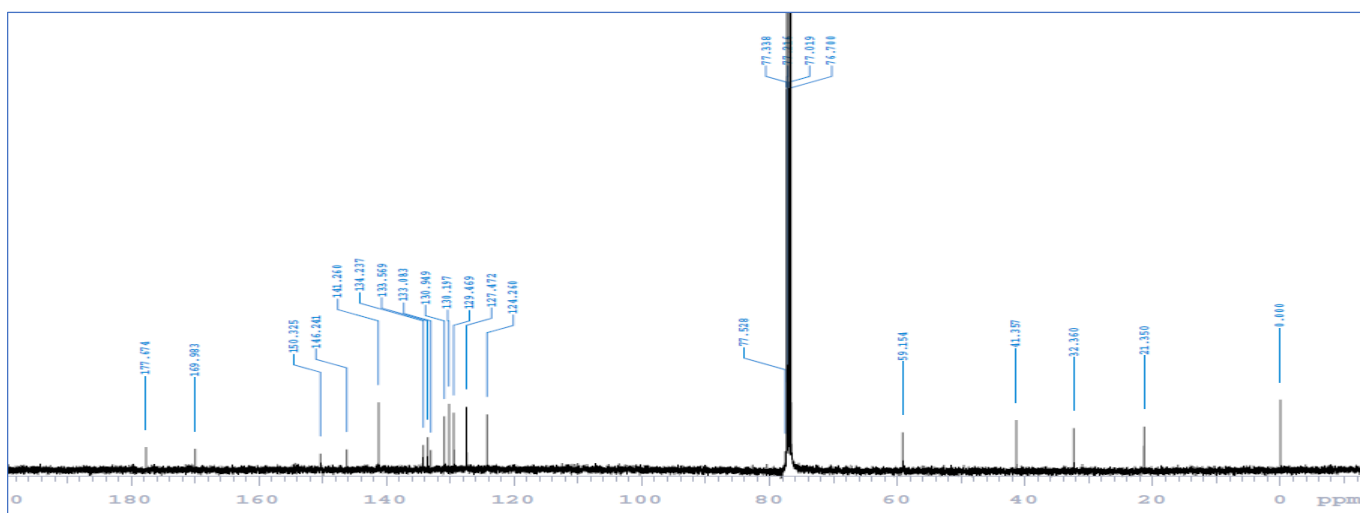
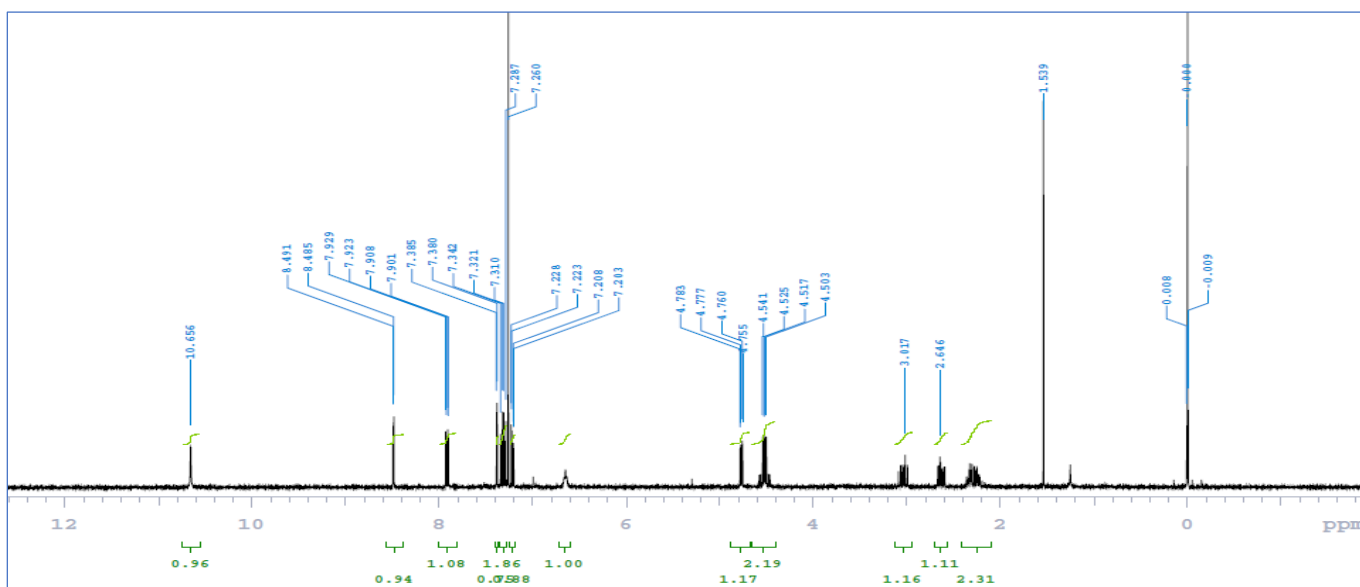
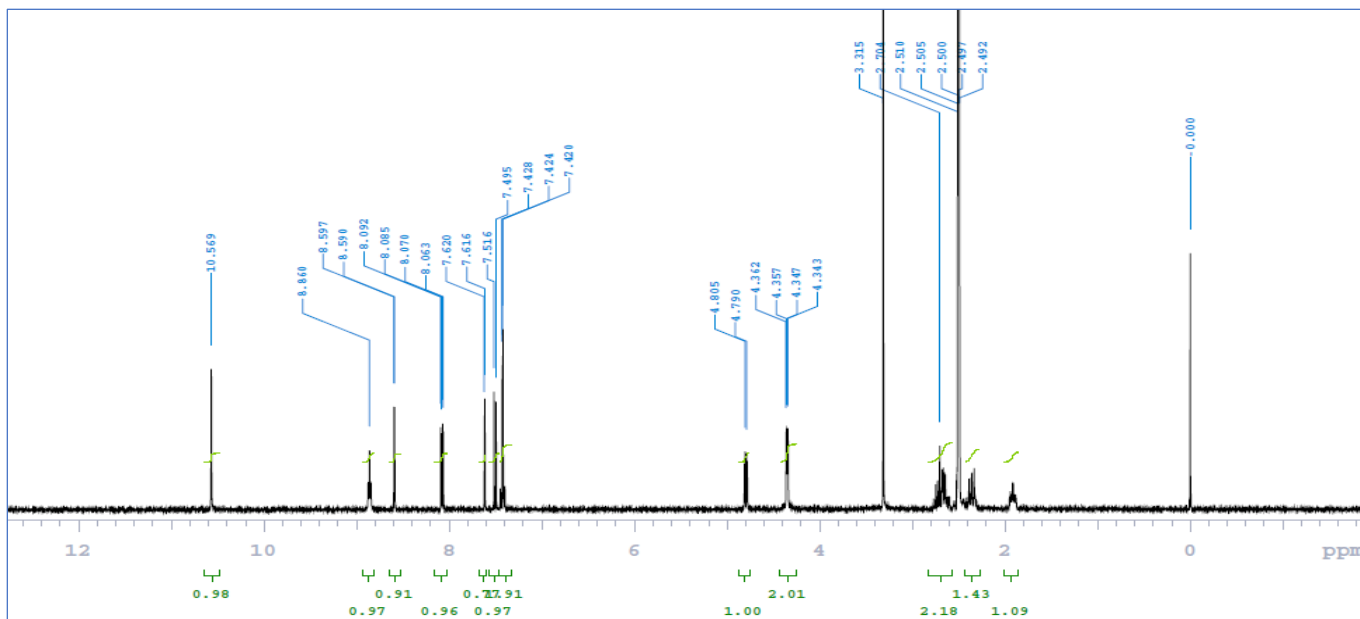


**Open Access** This article is licensed under a Creative Commons Attribution 4.0 International License, which permits use, sharing, adaptation, distribution and reproduction in any medium or format, as long as you give appropriate credit to the original author(s) and the source, provide a link to the Creative Commons license, and indicate if changes were made. The images or other third party material in this article are included in the article's Creative Commons license, unless indicated otherwise in a credit line to the material. If material is not included in the article's Creative Commons license and your intended use is not permitted by statutory regulation or exceeds the permitted use, you will need to obtain permission directly from the copyright holder. To view a copy of this license, visit <http://creativecommons.org/licenses/by/4.0/>.

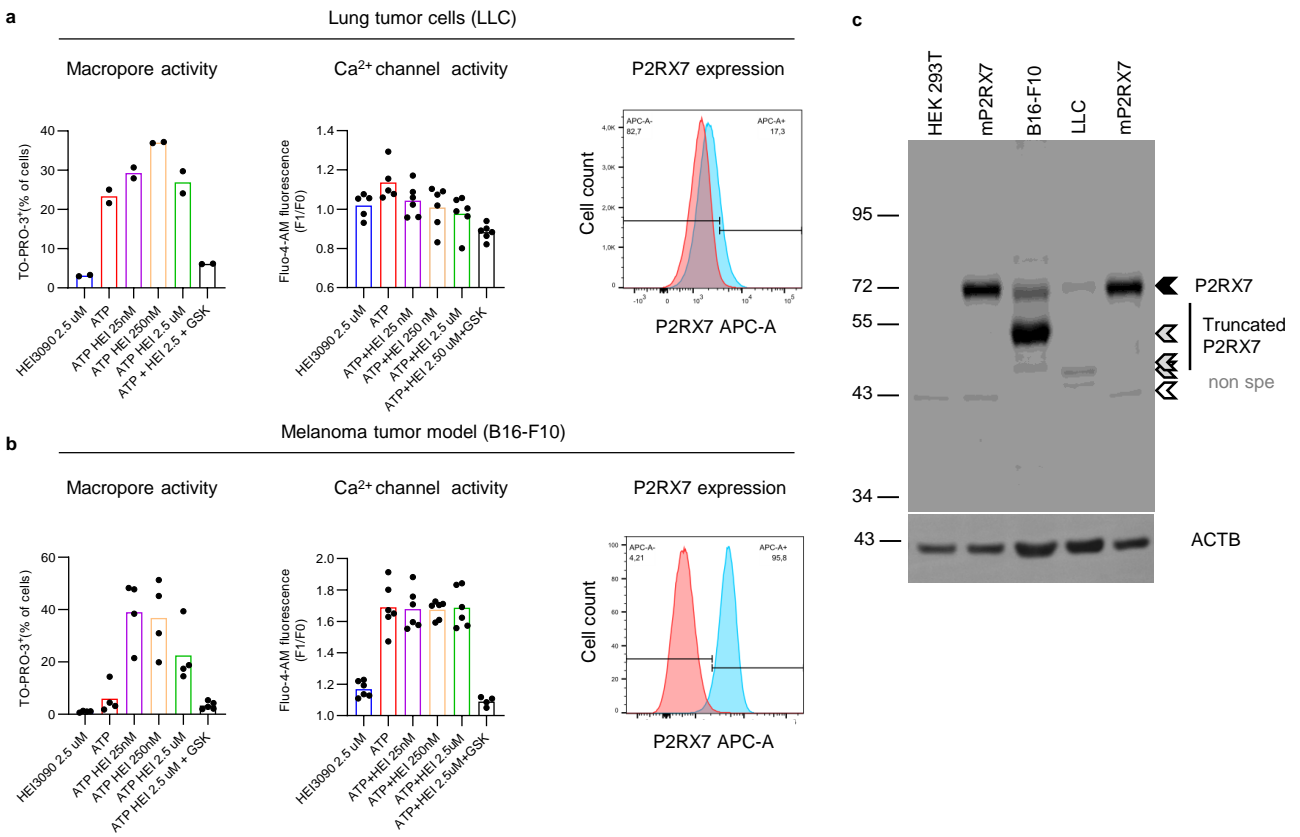
© The Author(s) 2021

**Supplementary Table 1: Antibodies used in this study**

Antibody	Compagny	Clone	Species	Isotype	Fluorochrome	Stock Conc.	Dilution
CD16/CD32 Fc Block	BD Biosciences	2.4G2	Rat SD (outbred)	IgG2B. κ	Uncoupled	0.5mg/ml	1/100
CD3ε	BD Biosciences	145-2611	Armenian Hamster	IgG1. κ	PerCP-Cy5.5	0.2mg/ml	1/100
CD4	Biolegend	GK1.5	Rat	IgG2b. κ	AF647	0.5 mg/ml	1/100
CD4	BD Biosciences	GK1.5	Rat LEW	IgG2b. κ	PE	0.2mg/ml	1/100
CD4	BD Biosciences	RM4-5	Rat DA	IgG2a. κ	BV711	0.2mg/ml	1/100
CD8α	Biolegend	53-6.7	Rat	IgG2a. κ	BV650	50μg/ml	1/100
CD8α	BD Biosciences	53-6.7	Rat LOU	IgG2a. κ	BV650	0.2mg/ml	1/100
γδ TCR	BD Biosciences	GL3	Armenian Hamster	IgG2. κ	PE	0.2mg/ml	1/100
CD25	BD Biosciences	PC61	Rat OFA	IgG1. λ	V450	0.2mg/ml	1/100
CD44	BD Biosciences	IM7	Rat	IgG2. κ	APC	0.2mg/ml	1/100
CD44	BD Biosciences	IM7	Rat	IgG2. κ	PE-Cy7	0.2mg/ml	1/100
CCR7	BD Biosciences	4B12	Rat LOU	IgG2a.	P2-CF594	0.2mg/ml	1/100
CD107a	BD Biosciences	1D4B	Rat SD (outbred)	IgG2a. κ	PE-Cy7	0.2mg/ml	1/100
NK1.1	BD Biosciences	PK136	Mouse C3H x BALB/c	IgG2a. κ	PE-CF594	0.2mg/ml	1/100
B220	eBiosciences	RA3-6B2	Rat	IgG2a. κ	FITC	0.5 mg/ml	1/200
CD19	BD Biosciences	ID3	Rat LEW	IgG2a. κ	FITC	0.5 mg/ml	1/100
CD45.2	BD Biosciences	104	Mouse SJL	IgG2a. κ	BV786	0.2mg/ml	1/100
CD11b	eBiosciences	M1/70	Rat	IgG2b. κ	APC	0.2mg/ml	1/400
CD11c	BD Biosciences	HL3	Armenian Hamster	IgG1. λ2	PE-Cy7	0.2mg/ml	1/100
Ly6C	BD Biosciences	AL-21	Rat	IgM. κ	V450	0.2mg/ml	1/100
Ly6G	BD Biosciences	1A8	Rat LEW	IgG2a. κ	AF700	0.2mg/ml	1/100
Ly6G	BD Biosciences	1A8	Rat LEW	IgG2a. κ	FITC	0.5mg/ml	1/100
CD80	Biolegend	16-10A1	Armenian Hamster	IgG	PE	0.2mg/ml	1/100
CD86	BD Biosciences	GL1	Rat LOU	IgG2a. κ	AF700	0.2mg/ml	1/100
CD86	BD Biosciences	GL1	Rat LOU	IgG2a. κ	APC	0.2mg/ml	1/100
I-A/I-E	Biolegend	M5/114.15.2	Rat	IgG2b. κ	APCfire750	0.2mg/ml	1/100
H-2Kb/H-2Db	Biolegend	28//8//6	Mouse (C3H)	IgG2a. κ	FITC	0.5mg/ml	1/100
IL-10	BD Biosciences	JESS-16E3	Rat	IgG2b	BV421	0.2mg/ml	1/100
Foxp3	eBiosciences	FJK16S	Rat	IgG2a. κ	PE	0.2mg/ml	1/100
CD103	Biolegend	2E/7	Armenian Hamster	IgG	PerCP-Cy5.5	0.2mg/ml	1/100
IFNγ	BD Biosciences	XMG1.2	Rat	IgG1. κ	APC	0.2mg/ml	1/100
IL-17A	BD Biosciences	TC11-18H10	Armenian Hamster	IgG1. κ	AF700	0.2mg/ml	1/100
IL-4	BD Biosciences	11B11	Rat	IgG1	BV711	0.2mg/ml	1/100
IL-13	eBiosciences	eBio13A	Rat	IgG1. κ	AF488	0.5 mg/ml	1/100
GATA3	BD Biosciences	L50-823	Mouse BALB/c	IgG1. κ	BV421	0.2mg/ml	1/100
CD279 (PD1)	BD Biosciences	J43	Rat	IgG2a. κ	APC	0.2mg/ml	1/100
CD274 (PD-L1)	Biolegend	10F.9G2	Rat	IgG2b. κ	APC	0.2mg/ml	1/100
CD274 (PD-L1)	Biolegend	10F.9G2	Rat	IgG2b. κ	BV421	100μg/ml	1/100
CD273 (PD-L2)	Biolegend	TY25	Rat	IgG2a. κ	PEdazzle594	0.2mg/ml	1/100
CTLA4	BD Biosciences	UC10-4F10-11	Armenian Hamster	IgG1. κ	PE	0.2mg/ml	1/100
TIM-3	BD Biosciences	5D12/TIM-3	Mouse	IgG1. κ	PE	0.2mg/ml	1/100
P2RX7	Biolegend	1F11	Rat	IgG2b. κ	PE	0.2mg/ml	1/8
IL-1β	BioXCell	B122	Armenian Hamster	IgG	na	na	200μg
IL-18	BioXCell	YIGIF74-1G7	Rat	IgG2b. κ	na	na	200μg
CD-8	BioXCell	53-6.7	Rat	IgG2a. κ	na	na	200μg
CD-4	BioXCell	GK1.5	Rat	IgG2b. κ	na	na	200μg
NK1.1	BioXCell	PK136	Mouse	IgG2a. κ	na	na	300μg
αPD-1	BioXCell	RPM1-4	Rat	IgG2a. κ	na	na	200μg
CD3	Roche	2GV6	Rabbit	IgG	na	Ready to use	na
CD8	Roche	SP57	Rabbit	IgG	na	Ready to use	na
IL-18	BioVision	na	Rabbit	IgG	na	0.5mg/ml	1/200
αPD-1	Dako	22C3	Mouse	IgG1	na	150mg/L	1/50
Ki67	Abcam	SP6	Rabbit	IgG	na	1mg/ml	1/100
NLRP3	Adipogen	Cryo-2	Mouse	IgG2b	na	1mg/ml	1/1000
ASC	Adipogen	AL177	Rabbit	IgG	na	1mg/ml	1/1000
Caspase 1	Adipogen	Casper-1	Mouse	IgG1	na	1mg/ml	1/1000
ACTB	Biorad	VMA00048	Mouse	IgG1	na	1mg/ml	1/60000
P2RX7	Alomone Labs	APR-008	Rabbit	IgG	na	1mg/ml	1/1000

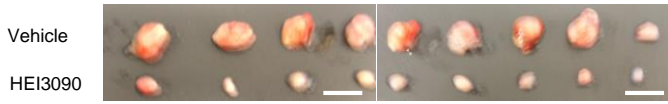


**Supplementary Fig. 1. Spectra <sup>1</sup>H and <sup>13</sup>C NMR of synthesized acylurea HEI3090.** Representative image of Spectra <sup>1</sup>H in DMSO-d<sub>6</sub> and CDCl<sub>3</sub> and <sup>13</sup>C in CDCl<sub>3</sub> of (S)-N<sup>1</sup>-(6-chloropyridin-3-yl)-N<sup>2</sup>-(2,4-dichlorobenzyl)-5-oxopyrrolidine-1,2-dicarboxamide (HEI3090)



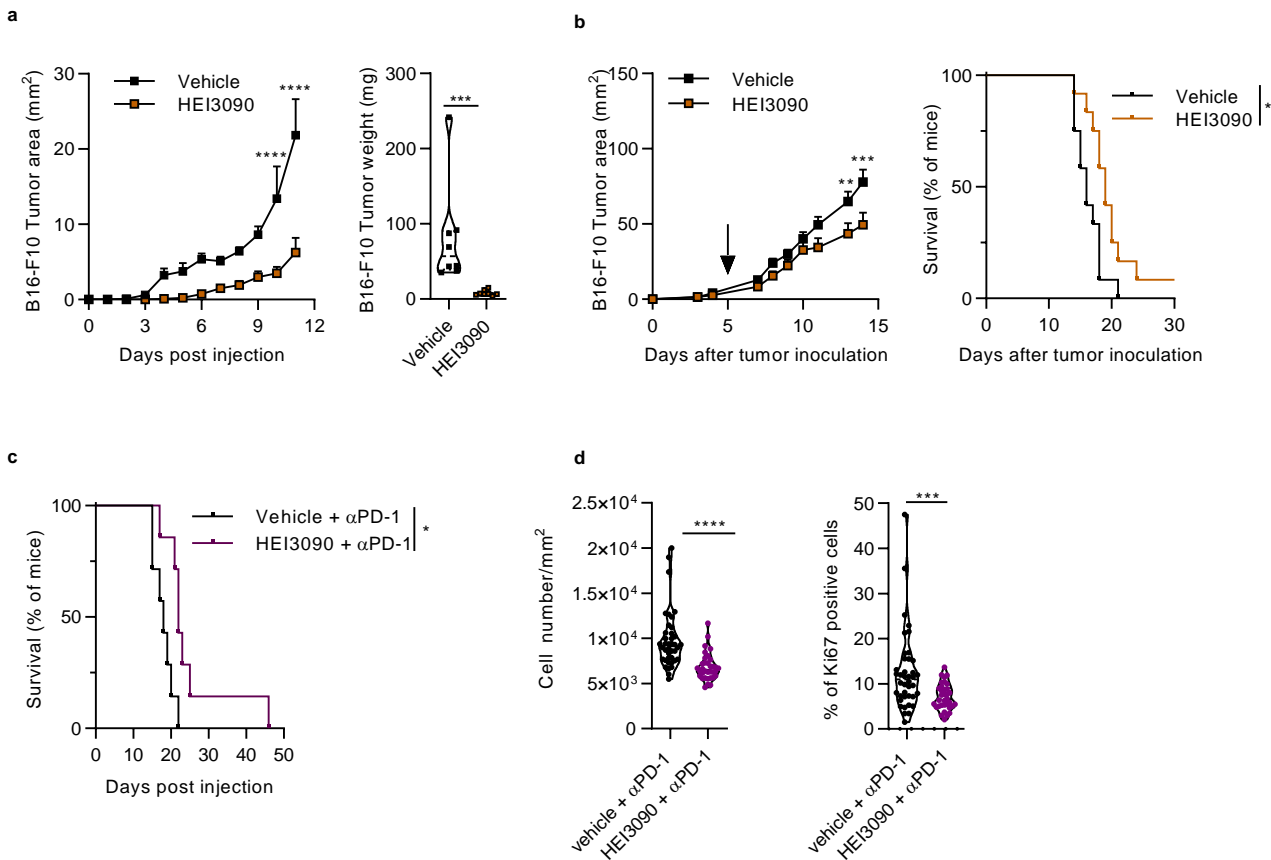
**Supplementary Fig. 2. P2RX7 is expressed on LLC and B16-F10 tumor cells**

P2RX7 characterization in Lewis Lung carcinoma (LLC) (a) and melanoma (B16-F10) cell lines (b) showing that tumor cell lines express a functional P2RX7 (macropore and channel activity). Macropore activity: Tumor cells were loaded with TO-PRO-3 and stimulated with 500  $\mu$ M ATP alone or in the presence of HEI3090 or GSK 1370319A, a P2RX7 antagonist. At 15min post stimulation an image was taken and TO-PRO-3<sup>+</sup> cells were counted. Data are presented as scatter dot plots (n = >1000 cells examined over 2 independent experiments). The P2RX7's Ca<sup>2+</sup> channel activity we measured the ATP-induced increase of intracellular Ca<sup>2+</sup> concentration (Fluo-4-AM uptake) in the presence of the P2RX7's inhibitor (GSK1370319A), using a plate reader. Data are presented as scatter dot plots (n=2 independent experiments, in triplicate). P2RX7 expression was assayed by flow cytometry (n= 100000 cells examined over 2 independent experiments) using the anti P2RX7 antibody (clone 1F11, right panel a and b) or by western blotting using an anti-extracellular loop of P2RX7 antibody (APR-008, Alomone Labs) that recognizes a band of 70kDa, the expected size for P2RX7 (1 experiment performed) (c). These results demonstrated that both cell lines expressed an active P2RX7, with B16-F10 cells expressing higher P2RX7 levels than LLC cells. Further we showed that tumor cell lines express truncated P2RX7's isoforms and that HEI3090 only impacts the macropore activity on these P2RX7 isoforms. Source data are provided as a Source Data file.



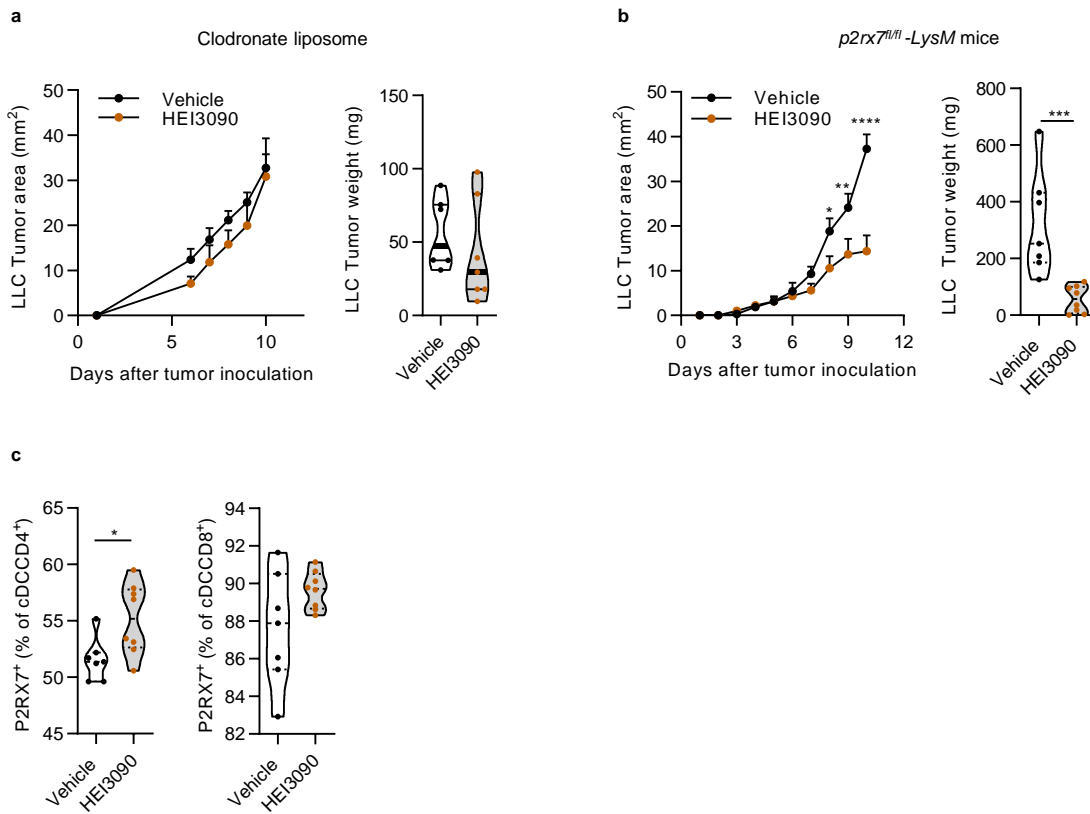
**Supplementary Fig. 3: HEI3090 effect on LLC tumor size**

$5 \times 10^5$  LLC were injected s.c. into the flank of C57BL6/J mice. Mice were injected i.p every day with vehicle or HEI3090 (1.5 mg/kg) from day 1 to day 12. Representative picture of tumors from Fig 2a showing tumor size the day of the sacrifice. Bar = 10 mm



**Supplementary Fig. 4: HEI3090 inhibits the growth of melanoma B16-F10 tumor cells and increased mice survival when combined with anti-PD-1 antibody**

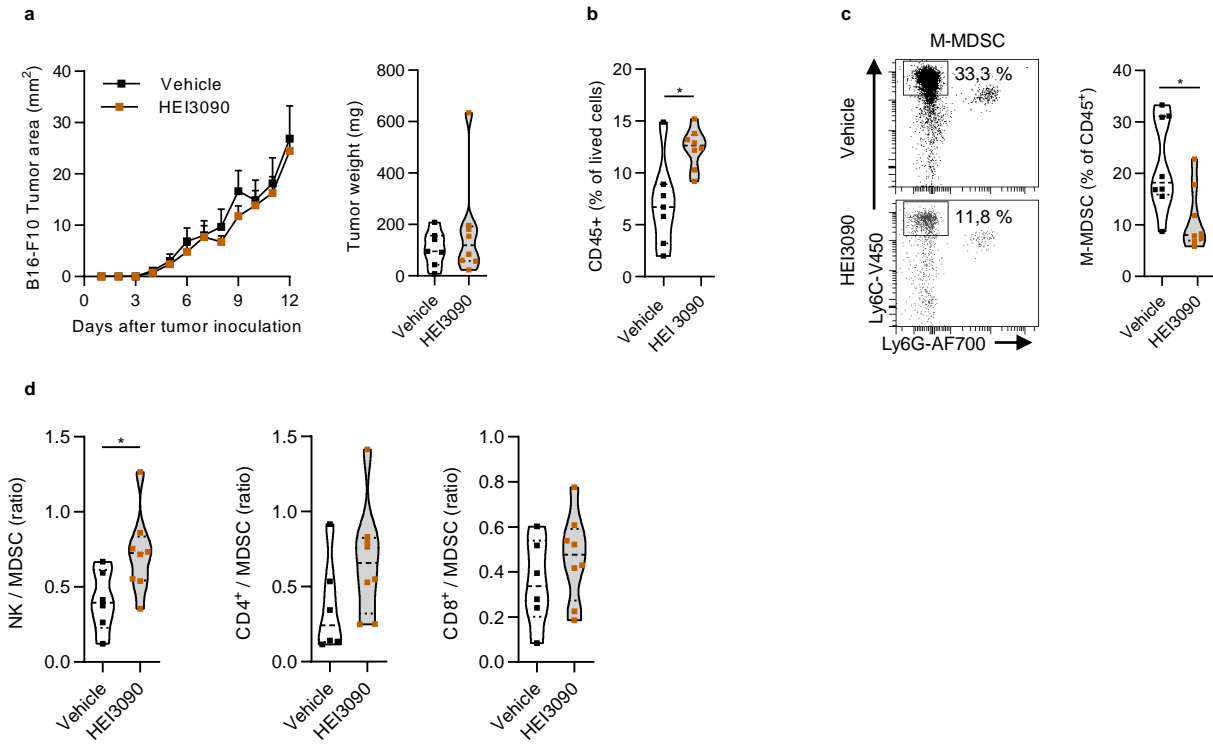
**a.**  $5 \times 10^5$  B16-F10 were injected s.c. into the flank of C57BL6/J mice. Mice were injected i.p. every day with vehicle or HEI3090 (1.5 mg/kg) from day 1 to day 12. Curves showed mean tumor area in mm<sup>2</sup>  $\pm$  SEM (n= 8 mice, Two-way Anova test, left panel) and graph showed tumor weight the day of sacrifice. Data are presented by violin plots showing all points with hatched bar corresponding to median tumor weight (n= 8 mice, Two-tailed Mann Whitney test, right panel). **b.** Effect of HEI3090 in therapeutic administration. Mice were treated i.p. with vehicle or HEI3090 (3 mg/kg) from days 5 (when tumors reached a volume of approximately 5-10 mm<sup>2</sup>) to 15. Curves showed mean tumor area in mm<sup>2</sup>  $\pm$  SEM (n= 12 mice, Two-way Anova test, left panel) and survival of B16-F10 tumor bearing mice (n= 8 mice, Mantel Cox test, right panel). **c.** Effect of HEI3090 and  $\alpha$ PD-1 checkpoint inhibitor on survival of B16-F10 tumor-bearing mice.  $5 \times 10^5$  B16-F10 were injected s.c. into the flank of WT mice. Mice were treated i.p. with vehicle or with HEI3090 (3 mg/kg) from day 1 to day 18. Each mouse received 200  $\mu$ g of  $\alpha$ PD-1 i.p. at day 4, 7, 10, 12 and 16. Mice were sacrificed when tumor reached 100 mm<sup>2</sup>. (n= 7 mice, Mantel Cox test). **d.** Efficacy of the combo treatment in the *in situ* (LSL *KRas*<sup>G12D</sup>) genetic lung tumor mouse model. Ten lung lesions per mouse (5 large, 5 small) were selected. Average cell number/mm<sup>2</sup> and Ki67<sup>+</sup> cells are shown. Data are presented by violin plots showing all individual lesion to overcome the individual heterogeneity of each lesion, with plain bar corresponding to the median (n= 5 mice, Two-tailed Mann Whitney test). p-values: \*p<0.05, \*\*p<0.01, \*\*\*p<0.001, \*\*\*\*p<0.0001. Source data are provided as a Source Data file.



**Supplementary Fig. 5: HEI3090 targets P2RX7-expressing dendritic cells.**

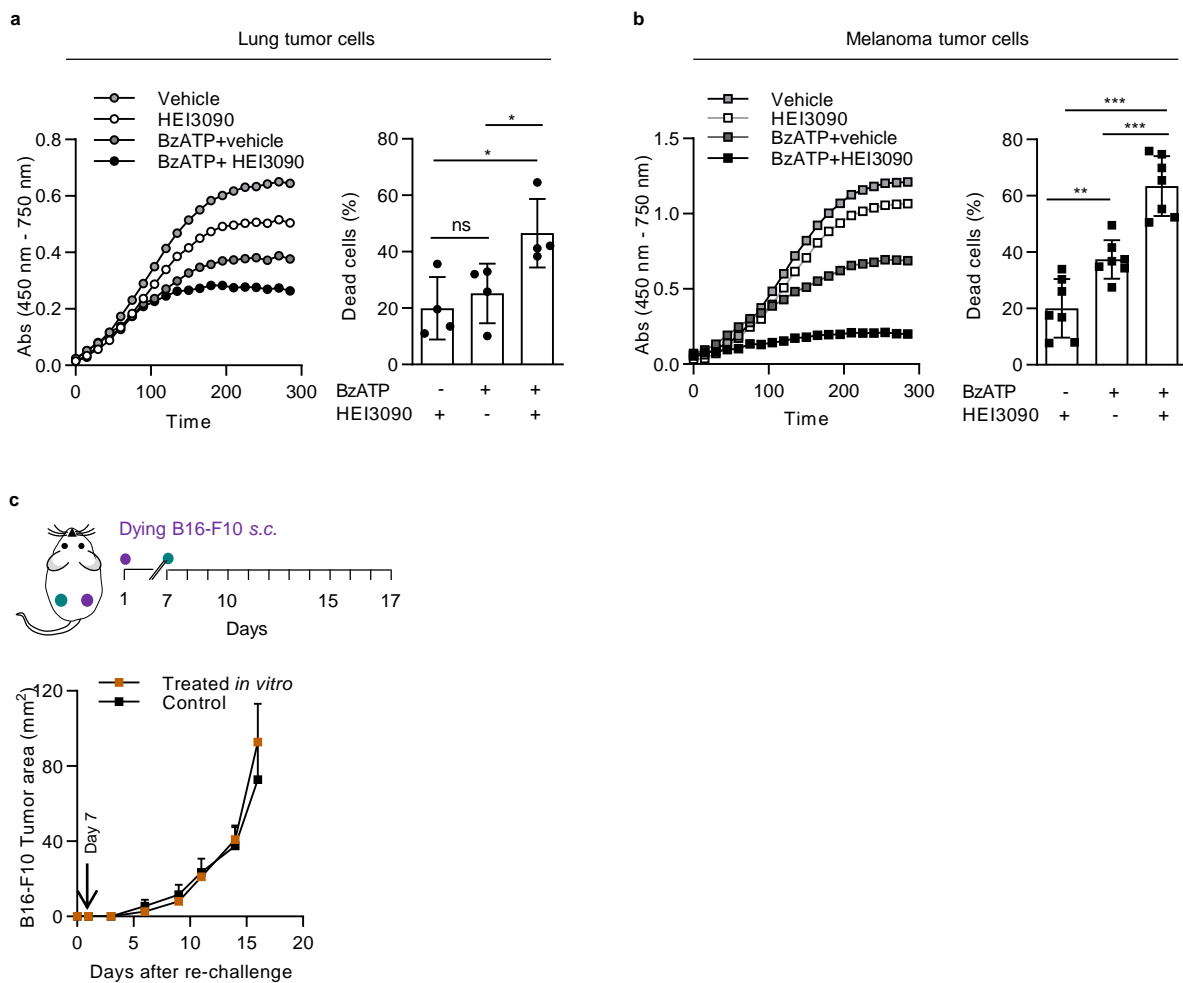
**a.** Cells from the myeloid lineage do not support HEI3090-induced antitumor response.  $5 \times 10^5$  LLC cells were injected s.c. to *p2rx7<sup>fl/fl</sup>*-LysM mice and mice were daily treated with HEI3090 or vehicle, as detailed in the method section. Curves showed mean tumor area in mm<sup>2</sup>  $\pm$  SEM (n= 7 mice, Two-way Anova test, left panel) and graph showed tumor weight the day of sacrifice. Data are presented by violin plots showing all points with hatched bar corresponding to the median of tumor weight (n= 7 mice, Two-tailed Mann Whitney test, right panel). **b.** Three days prior to tumor cell inoculation, liposome clodronate (200  $\mu$ l) was injected i.p. to mice. Mice were then injected every 3 days with liposome clodronate 1h before HEI3090 treatment.  $5 \cdot 10^5$  LLC cells were inoculated s.c. and mice were treated daily with 1.5 mg/kg of HEI3090 or vehicle. Tumor area was measured with a caliper. At the end of the experiment, tumors were weighted. Curves showed mean tumor area in mm<sup>2</sup>  $\pm$  SEM (n= 7 mice, Two-way Anova test, left panel) and graph showed tumor weight the day of sacrifice. Data are presented by violin plots showing all points with hatched bar corresponding to the median of tumor weight (n= 7 mice, Two-tailed Mann Whitney test, right panel). **c.** P2RX7 expression by DC CD4<sup>+</sup> cells is increased in response to HEI3090. Data are presented by violin plots showing the percentage of P2RX7<sup>+</sup> cells of indicated cells, with hatched bar corresponding to the median of positive cells (n= 6 mice, Two-tailed Mann Whitney test). p-values: \*p<0.05, \*\*p<0.01 \*\*\*p<0.001, \*\*\*\*p<0.0001. Source data are provided as a Source Data file.





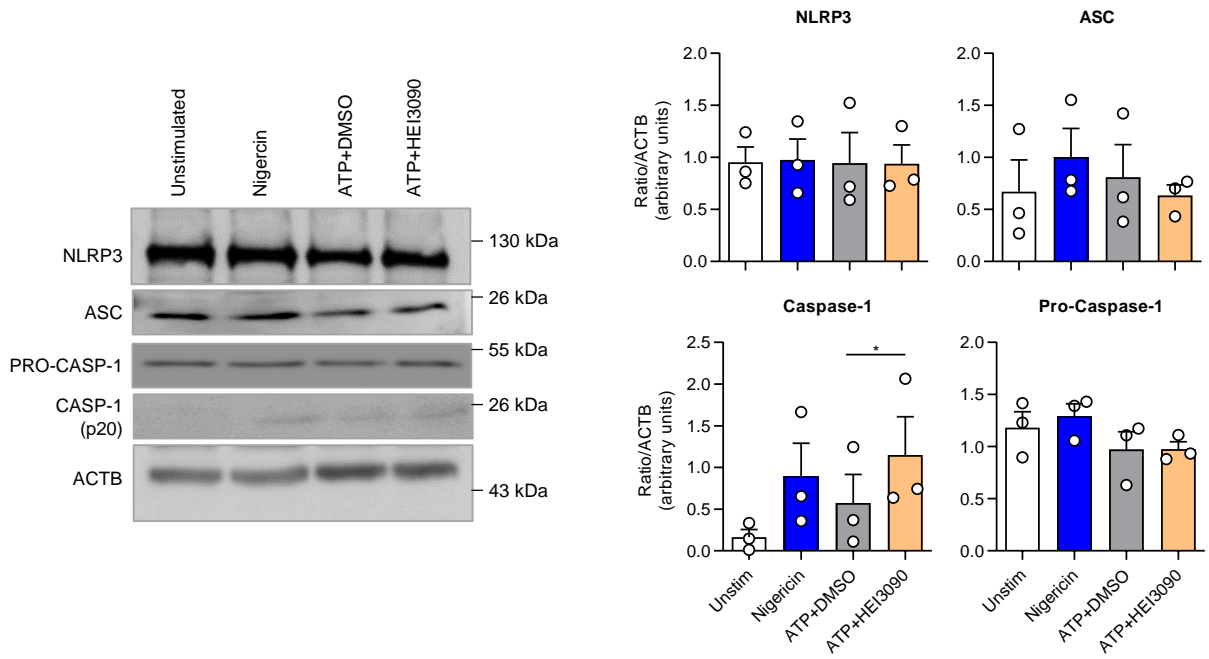
**Supplementary Fig. 6: Immune cells mediate the antitumor activity induced by HEI3090 in the B16-F10 tumor mouse model**

**a.** Effect of HEI3090 on B16-F10 tumor growth in *p2rx7<sup>-/-</sup>* mice.  $5 \times 10^5$  cells were injected s.c. into the flank of *p2rx7<sup>-/-</sup>* mice. Mice were treated i.p. with vehicle or with HEI3090 (1.5 mg/kg). Curves showed mean tumor area in  $\text{mm}^2 \pm \text{SEM}$  ( $n = 7$  mice, Two-way Anova test, left panel) and graph showed tumor weight the day of sacrifice. Data are presented by violin plots showing all points with hatched bar corresponding to the median of tumor weight ( $n = 7$  mice, Two-tailed Mann Whitney test, right panel). **b.** Effect of HEI3090 on the recruitment of immune cells within the TME.  $5 \times 10^5$  B16-F10 cells were injected s.c. into the flank of WT mice. Mice were injected i.p. every day with vehicle or HEI3090. At day 12, tumors were collected for flow cytometry analyses. Data are presented by violin plots showing all points with hatched bar corresponding to the median of CD45<sup>+</sup> cells of total lived cells ( $n = 7$  mice, Two-tailed Mann Whitney test). **c.** Proportion of M-MDSC within the TME among CD45<sup>+</sup> within B16-F10 tumors from mice treated with vehicle or HEI3090. Gating strategy is shown in left panel. Data are presented by violin plots showing all points with hatched bar corresponding to the median of M-MDSC cells over CD45<sup>+</sup> cells ( $n = 7$  mice, Two-tailed Mann Whitney test). **d.** Ratio of NK, CD4<sup>+</sup> or CD8<sup>+</sup> T cells over M-MDSC within the TME. Data are presented by violin plots showing all points with hatched bar corresponding to the median of indicated cells of MDSC cells ( $n = 7$  mice, Two-tailed Mann Whitney test).  $p$ -values: \* $p < 0.05$ . Source data are provided as a Source Data file.



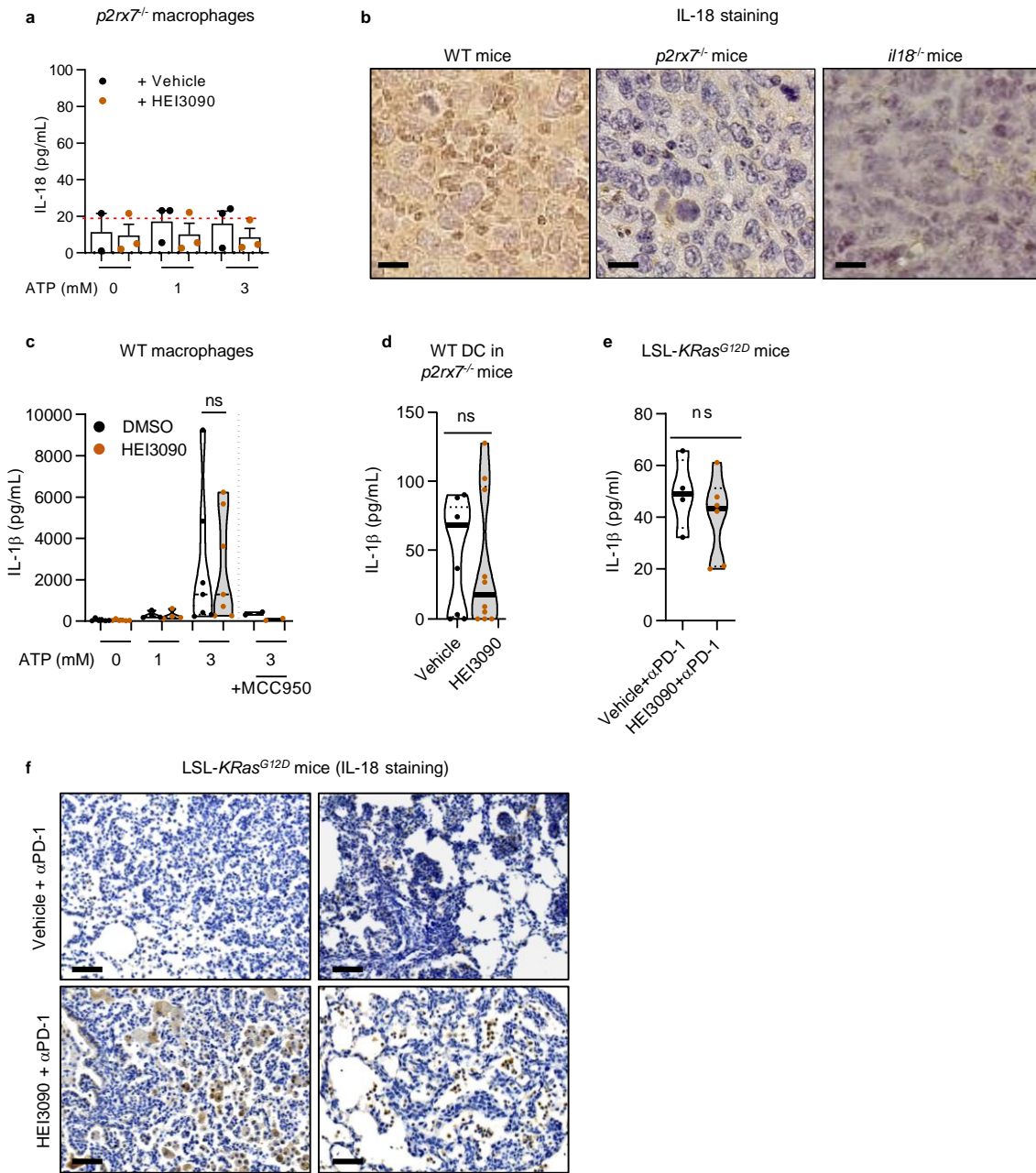
**Supplementary Fig. 7: HEI3090 does not promote immunogenic cell death (ICD)**

HEI3090-induced LLC (**a**) and B16-F10 (**b**) tumor cell toxicity. Curves showed mean of absorbance ( $n=4$  independent experiments in **a** and  $n=7$  in **b**, left panel) and graph showed the percentage of dead cells. Data are presented by scatter dot plots showing all points with hatched bar corresponding to the median of dead cells (Two-tailed Mann Whitney test, right panel). **c**. *In vivo* assay for the evaluation of HEI3090 as an inducer of immunogenic cell death. B16-F10 were exposed to 3mM ATP and 50 $\mu$ M HEI3090. WT mice were inoculated s.c. with  $1.10^5$  dying B16-F10 cells in the right flank ( $n=6$ ) or PBS as control ( $n=4$ ). 7 days later,  $5.10^5$  live B16-F10 cells were injected s.c. in the contralateral and tumor growth in the left flank was measured daily. Curves showed mean tumor area in  $\text{mm}^2 \pm \text{SEM}$  ( $n=5$  mice, Mantel Cox test). The details of the ICD experiment are provided in the methods section.  $p$ -values: \* $p<0.05$ , \*\* $p<0.01$  \*\*\* $p<0.001$ . Source data are provided as a Source Data file.



**Supplementary Fig. 8: HEI3090 increased eATP-induced caspase-1 cleavage in macrophages**

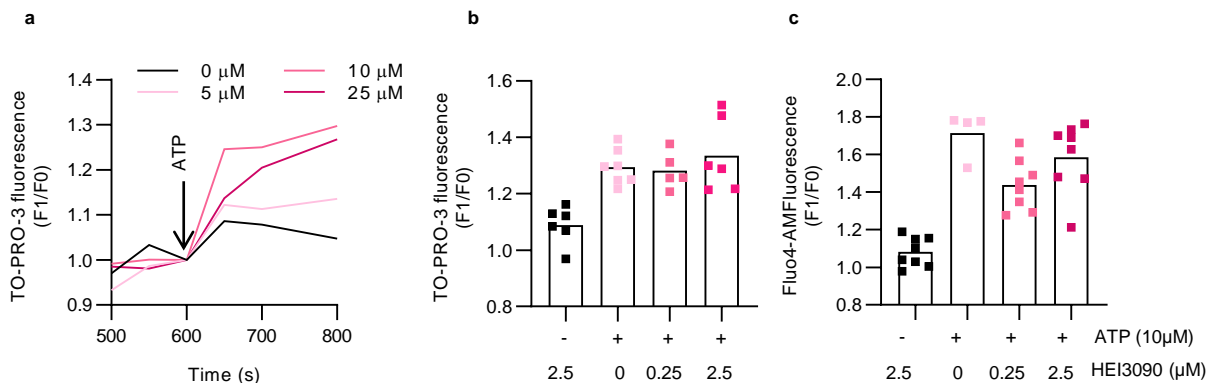
4.10<sup>5</sup> peritoneal macrophages from WT mice were primed for 4h at 37°C with 100 ng/ml LPS and then stimulated for 30 minutes with 10 μM nigericin or 3 mM ATP with 50 μM HEI3090 or DMSO. **Left panel.** Whole cell protein extracts were analyzed by western blotting by using antibodies recognizing NLRP3, ASC, pro-caspase-1 and active form caspase-1, and β-actin as a loading control. Samples derived from the same experiment and gels/blots were processed in parallel. **Right panel.** Relative band intensities of each protein were assessed to that of β-actin. Data are presented by scatter dot plots, mean ± SEM (n=3, Two-tailed paired t-test). p-values: \*<0.05. Source data are provided as a Source Data file.



**Supplementary Fig. 9: HEI3090-induced IL-18 production required P2RX7 expression**

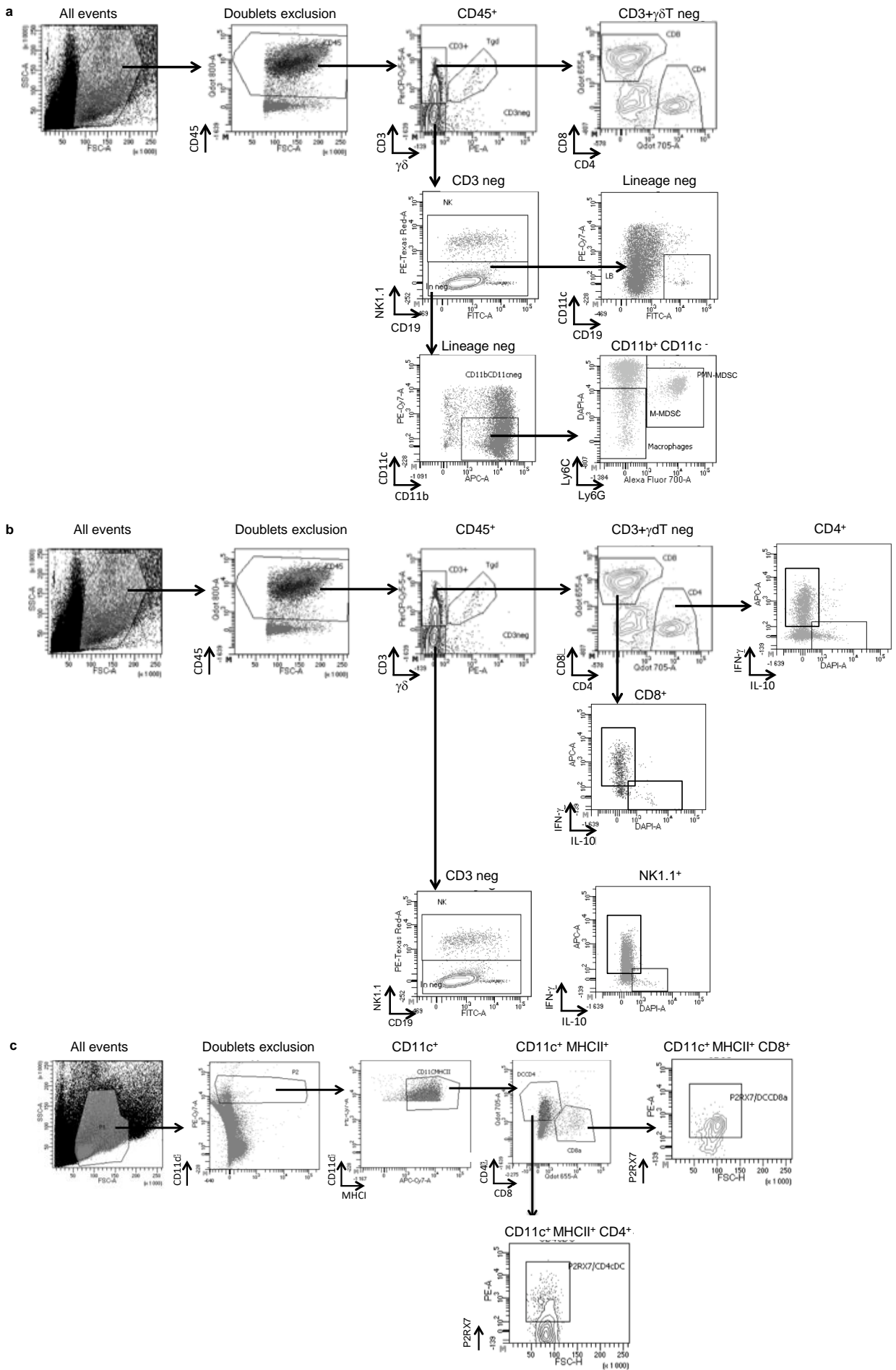
**a.** Production of IL-18 (ELISA) by peritoneal macrophages isolated from *p2rx7<sup>-/-</sup>* mice, demonstrating that without P2RX7 expression, HEI3090 is unable to increase IL-18 levels. Data are presented by scatter dot plots ( $n=3$  mice, Two-tailed Mann Whitney test) **b.** IL-18 staining of LLC tumors collected from WT, *p2rx7<sup>-/-</sup>* or *il18<sup>-/-</sup>* mice, demonstrating the specificity of IL-18 antibody. Images are representative of staining of 5 independent mice. Bar= 250nm **c.** Production of IL-1 $\beta$  (ELISA) by peritoneal macrophages isolated from WT mice, demonstrated that HEI3090 was unable to increase IL-1 $\beta$  levels. The specific inhibitor of NLRP3 (MCC950 compound) efficiently inhibits IL-1 $\beta$  production. Vehicle  $n=6$ , HEI3090  $n=6$ , ATP 1mM,  $n=4$ , ATP 1mM + HEI3090,  $n=4$ , ATP 3mM,  $n=7$ , ATP 3mM + HEI3090,  $n=7$ , ATP 3mM + MCC950,  $n=2$ , ATP 3mM + HEI3090 + MCC950,  $n=2$ , **d.** Quantification of IL-1 $\beta$  levels from serum of indicated mice confirming that HEI3090 does not modulate the production of IL-1 $\beta$  in *p2rx7<sup>-/-</sup>* complemented with WT DC. Vehicle  $n=9$ , HEI3090  $n=10$  **e.** Quantification of IL-1 $\beta$  levels from serum of LSL *KRas<sup>G12D</sup>* mice treated with HEI3090 and  $\alpha$ PD-1 antibody. Vehicle +  $\alpha$ PD-1,  $n=4$ , HEI3090 +  $\alpha$ PD-1,  $n=6$ . Data are presented by violin plots showing all points with hatched bar corresponding to the median for **c**, **d** and **e** (Two-tailed unpaired t-test) **f.** IL-18 staining from lung of LSL *KRas<sup>G12D</sup>*, illustrating that IL-18 expression was increased in lung macrophages of HEI3090 +  $\alpha$ PD-1 treated mice. Images are representative of staining of 5 independent mice. Bar= 100 $\mu$ m. Source data are provided as a Source Data file.





**Supplementary Fig. 11: HEI3090 is not a positive modulator for ATP-induced mP2RX4-mediated TOPRO-3 uptake and Ca<sup>2+</sup> influx in HEK cells**

**a.** HEK293T cells were stably transfected with mouse P2RX7 coding vector and cells were stimulated with various concentrations of ATP. TOPRO-3 uptake over 200 sec was measured. Curve show mean of TO-PRO-3 fluorescence acquired with a spectrophotometer from 2 independent experiments **b.** TOPRO-3 uptake in response to ATP (10  $\mu\text{M}$ ) and the indicated doses of HEI3090 150 sec post stimulation. Data are presented by scatter dot plots showing all points from 2 independent experiments with 4 replicates. All points are shown to overcome the high heterogeneity observed between replicates. **c.** Intracellular Ca<sup>2+</sup> response was measured in Fluo4-AM loaded mP2RX4 HEK cells 50 sec post stimulation. Data are presented by scatter dot plots showing all points. Mean from 2 independent experiments with 4 replicates are shown to overcome the high heterogeneity observed between replicates. Source data are provided as a Source Data file.



**Supplementary Fig.12: Gating strategies**

**a.** Gating strategy for tumor immunophenotyping. **b.** Gating strategy for cytokine production within tumor. **c.** Gating strategy for P2RX7 expression by DC in spleen







## ARTICLE II

“Reshaping the lung immune phenotype by activation P2RX7  
inhibits lung fibrosis progression”

Soumis dans *American Journal of Respiratory and Critical Care Medicine*, première auteure



# L'activation de P2RX7 favorise un profil immunitaire anti-fibrosant et inhibe le développement de fibrose pulmonaire

## Contexte

La fibrose pulmonaire idiopathique (FPI) est la maladie la plus fréquente et agressive des maladies interstitielles du poumon. Elle ne possède pas de traitement curatif ; les deux traitements utilisés en clinique ne font que ralentir la progression de cette maladie tout en induisant de nombreux effets secondaires. Ces éléments mettent en avant la nécessité de trouver de nouvelles stratégies thérapeutiques.

La FPI est caractérisée par une accumulation de fibroblastes et un dépôt important de protéines de la matrice extracellulaire mais également par un dérèglement du système immunitaire, où l'expression et l'activité de l'IFN- $\gamma$ , cytokine aux fortes propriétés anti-fibrosantes, est considérablement inhibée. Etant donné (i) les fortes concentrations d'ATP extracellulaire dans les poumons fibrosés, (ii) la capacité de la voie ATP/P2RX7/IL-18 à augmenter la production d'IFN- $\gamma$  pour inhiber la croissance des tumeurs pulmonaires (**Article I**) et (iii) l'environnement immunosuppresseur dans le tissu fibrosé, nous avons proposé d'augmenter l'activation de la voie ATP/P2RX7/IL-18 en utilisant un modulateur positif de P2RX7 (HEI3090) pour traiter la FPI.

## Méthodes

Grâce à la base de données publique Gene Expression Omnibus (GEO), nous avons tout d'abord étudié les niveaux d'expression des transcrits codant pour la voie P2RX7/IL-18/IFN- $\gamma$  dans des tissus fibrosants et sains. Pour évaluer la capacité de cette voie à inhiber le développement de la fibrose pulmonaire, nous avons utilisé la molécule HEI3090 dans un modèle murin de fibrose pulmonaire induit par la bléomycine. La mise en place de ce modèle est basée sur la mort des cellules épithéliales alvéolaires en réponse à la bléomycine qui induit le relargage de DAMPs, dont l'ATP, et le recrutement de cellules immunitaires. Nous avons analysé la progression de la fibrose dans ce modèle par histologie ainsi que le profil immunitaire par cytométrie. Les acteurs cellulaires et moléculaires ont été mis en évidence grâce des transferts adoptifs de rates issues de souris transgéniques (*p2rx7<sup>-/-</sup>*, *nlrp3<sup>-/-</sup>*, *il-18<sup>-/-</sup>* et *il-1 $\beta$ <sup>-/-</sup>*) vers des souris *p2rx7<sup>-/-</sup>*. De plus, nous avons dosé l'IL-18 plasmatique de patients atteints de FPI et de sujets sains afin de corrélérer sa valeur à la progression de la maladie, aux fonctions respiratoires du patient et à sa survie.

## Résultats

Nous avons montré que la voie P2RX7/IL-18/IFN- $\gamma$  est sous exprimée chez les patients FPI comparé à des sujets sains et que l'expression de P2RX7 corrèle négativement avec des marqueurs de fibrose. Nous avons montré que l'activation de cette voie avec HEI3090 freine le développement de la fibrose

pulmonaire, quel que soit le mode d'administration prophylactique ou thérapeutique. HEI3090 augmente la production d'IL-18, diminue l'inflammation et favorise un profil immunitaire pulmonaire anti-fibrosant, via notamment l'augmentation de production d'IFN- $\gamma$  par les lymphocytes T et la diminution de production de TGF- $\beta$ . De plus, nous avons mis en évidence que la voie P2RX7/NLRP3/IL-18 dans les cellules immunitaires est nécessaire pour l'effet anti-fibrosant de la molécule, mettant en avant le rôle du système immunitaire dans la progression de la maladie mais aussi le rôle clé de l'IL-18. Nous avons montré sur un faible nombre de patients FPI que l'état actif/inactif de l'IL-18 plasmatique semble prédire la survie de ces patients.

Ce travail a permis 1/ de proposer une nouvelle stratégie thérapeutique basée sur l'activation de P2RX7 et 2/ de souligner le rôle anti-fibrosant de l'IL-18 ainsi que sa capacité à constituer un biomarqueur de survie pour les patient FPI.

# **Reshaping the lung immune phenotype**

## **by activating P2RX7 inhibits lung fibrosis progression**

Serena Janho dit Hreich<sup>1,2</sup>, Thierry Juhel<sup>1</sup>, Sylvie Leroy<sup>2,3,4</sup>, Alina Ghinet<sup>5,6,7</sup>, Frederic Brau<sup>3</sup>,  
Véronique Hofman<sup>1,2,8,9</sup>, Paul Hofman<sup>1,2,8,9</sup>, Valérie Vouret-Craviari<sup>1,2</sup>

1. Université Côte d'Azur, CNRS, INSERM, IRCAN, 06108 Nice, France
2. FHU OncoAge, Nice, France
3. Université Côte d'Azur, CNRS, Institut Pharmacologie Moléculaire et Cellulaire, Sophia-Antipolis, France.
4. Université Côte d'Azur, Centre Hospitalier Universitaire de Nice, Pneumology Department, Nice, France
5. Inserm U995, LIRIC, Université de Lille, CHRU de Lille, Faculté de médecine – Pôle recherche, Place Verdun, F-59045 Lille Cedex, France
6. Hautes Etudes d'Ingénieur (HEI), JUNIA Hauts-de-France, UCLille, Laboratoire de chimie durable et santé, 13 rue de Toul, F-59046 Lille, France
7. 'Al. I. Cuza' University of Iasi, Faculty of Chemistry, Bd. Carol I, nr. 11, 700506 Iasi, Romania
8. Laboratory of Clinical and Experimental Pathology and Biobank, Pasteur Hospital, Nice, France
9. Hospital-Related Biobank (BB-0033-00025), Pasteur Hospital, Nice, France

## **ABSTRACT**

**Rationale:** Idiopathic pulmonary fibrosis (IPF) is an aggressive interstitial lung disease accompanied by progressive decline of respiratory functions that are ultimately fatal. It is linked to lung inflammation and characterized by the destruction of the pulmonary architecture due to the accumulation of fibroblasts and extracellular matrix proteins as well as a dysregulated immune response. P2RX7 is an immunomodulator expressed in fibrotic tissue, is active in IPF and important for fibrosis progression.

**Objective:** We sought to investigate the role of the P2RX7/NLRP3/IL18 axis in pulmonary fibrosis and demonstrate the therapeutic potential of a positive modulator of P2RX7.

**Methods:** Publicly available dataset of whole lung homogenate and homemade cohort of plasma from control and IPF patients were used in this study. We used pharmacologic activation and adoptive transfer approaches in the well-characterized bleomycin mouse model.

**Measurements and Main Results:** P2RX7 expression and IL-18 activity are dampened in IPF patients. Pharmacologic activation of P2RX7 inhibits bleomycin-induced lung fibrosis, and reshapes immune cell infiltration in the lung, downstream of P2RX7/NLRP3/IL-18 axis. IL-18 bioavailability increases in IPF patients and high levels of free IL-18 could predict better outcome of IPF patients.

**Conclusions:** This study identifies active IL-18 as an important regulator of lung fibrosis and provides a proof of principle for P2RX7 activation as a potential novel therapeutic strategy for IPF.

## Introduction

Idiopathic pulmonary fibrosis (IPF) is an aggressive interstitial lung disease accompanied by progressive decline of respiratory functions that are ultimately fatal. It is characterized by the destruction of the pulmonary architecture due to the accumulation of fibroblasts and extracellular matrix proteins, increasing therefore the stiffness of the lungs and impairing normal respiration.

Pirfenidone and nintedanib are FDA-approved since 2014 for treatment of IPF. They target respectively the key fibrotic cytokine TGF $\beta$  and multiple receptor tyrosine kinases, targeting therefore fibroblast activation and extracellular matrix proteins production(1). However, they only slow down disease progression, hence the need for new therapeutic strategies and targets.

Fibrosis is also linked to inflammation. Indeed, fibrosis is an excessive wound healing and tissue remodeling process due to repetitive epithelial injuries that release damage associated molecular patterns (DAMPs) that trigger both the adaptive and innate immune system. Even though inflammation was not considered worth targeting in IPF due to unsuccessful initial clinical trials with anti-inflammatory drugs(2) or cyclophosphamide during exacerbations(3) increasing evidence suggest that altering specific immune populations that promote or attenuate disease progression could be beneficial(4).

Extracellular adenosine triphosphate (eATP) is a DAMP released from injured cells at high levels in IPF patients. High levels of eATP are recognized by the P2X7 receptor (P2RX7) and are both required for the establishment of the bleomycin lung fibrosis mouse model(5). Activation of P2RX7 induces macropore opening, that leads to cell death(6) but also leads to the assembly of the NLRP3 inflammasome and the release of mature IL-1 $\beta$  and IL-18(7). Consequently, P2RX7 has the ability to trigger an immune response.

IL-1 $\beta$  is a pro-inflammatory cytokine with high profibrotic properties since it favors collagen deposition through IL-17A and TGF $\beta$  production(8–10) but also favors activation and recruitment of inflammatory cells such as eosinophils and neutrophils. Indeed, IL-1 $\beta$ R deficiency or blocking ameliorates



experimental fibrosis(11–13). The role of IL-18, on the other hand, is not clear. Indeed, conflicting experimental studies show that IL-18 could either favor fibrosis(14) or attenuate it(15). However, high levels of IL-18BP, a natural antagonist of IL-18, are linked to a reduced overall survival of IPF patients(16), hinting that IL-18 activity could be required for better survival.

IL-18 was originally described as IFN- $\gamma$  inducing factor (IGIF) and therefore has the ability to boost IFN- $\gamma$  production by T cells and NK cells(17). Besides having anti-proliferative properties (18), IFN- $\gamma$  inhibits TGF $\beta$  activity(19, 20) and therefore inhibits fibroblasts activation and differentiation into myofibroblasts, relieves TGF $\beta$ -mediated immunosuppression, inhibits extracellular matrix accumulation and collagen production(21–24) and favors therefore an anti-fibrotic immune microenvironment, making IFN- $\gamma$  a cytokine with anti-fibrotic properties. However, parenteral systemic administration of IFN- $\gamma$  failed in clinical trials (INSPIRE; NCT 00075998)(25) whereas local administration by inhalation showed promising results(26–29).

One way to enhance IFN- $\gamma$  production locally and selectively in the lung would be by shaping the phenotype of lung T cells that have been shown to be immunosuppressive (4, 30–32). Indeed, activated T cells(33, 34), and more precisely CD4<sup>+</sup> producing IFN- $\gamma$  T cells, have been shown to correlate with a better prognosis in IPF patients(31) and ameliorate bleomycin-induced lung fibrosis mouse model(35, 36).

Given the ability of IL-18 to induce IFN- $\gamma$  production by T cells and the ability of IFN- $\gamma$  to inhibit TGF $\beta$ , we proposed to boost locally IFN- $\gamma$  production through the P2RX7/IL-18 axis as a therapeutic strategy in pulmonary fibrosis. We opted to use a P2RX7-specific positive modulator that we synthesized that enhances P2RX7's activities, particularly IL-18, only in presence of high eATP(37).

## Results

### Expression of P2RX7 and IL-18 activity are dampened in IPF patients

The canonical release of IL-18 is due to the activation of the P2RX7/NLRP3 pathway(7). Since high levels of eATP are found in IPF patients(5) and that P2RX7 is activated by such levels, it was of particular interest to study the involvement of P2RX7 in this disease. We used publicly available dataset of whole lung homogenate of control and IPF patients (GSE47460). We found that expression of P2RX7 is downregulated in IPF patients (Fig 1a, supp Fig 1a) as well as the components of the NLRP3 inflammasome (supp Fig 1). P2RX7 expression is negatively correlated with fibrosis markers  $\alpha$ SMA and TGF $\beta$  (fig 1b) indirectly suggesting its potency to ameliorate fibrosis. Since IL-18 is constitutively expressed(38) explaining in part the absence of difference between control and IPF patients (Fig 1c), we investigated the pathway downstream of IL-18. IL-18 binds to its receptor IL-18R1 coupled to its adaptor protein IL-18RAP, that leads to the expression of IFN- $\gamma$ . We show that IL-18R1, IL-18RAP (Fig 1d) and IFN- $\gamma$  (Fig 1e) are downregulated in IPF patients and that the expression of IFNG and IL-18RAP as well as P2RX7 are indeed correlated in IPF (Fig 1f). Moreover, the expression of P2RX7 is correlated with the expression of PTPRC (Fig 1g), the marker of immune cells, suggesting the ability of a P2RX7-dependant immune response (Fig 1). These results highlight that the P2RX7/IL-18 pathway and activity is dampened in IPF patients.

### Activation of P2RX7 inhibits onset of pulmonary fibrosis in experimental bleomycin mouse model

In order to boost the P2RX7/IL-18 pathway, we chose to use a positive modulator of P2RX7, named HEI3090, that enhances its activity only in presence of high extracellular ATP levels(37) i.e. only in fibrotic lungs. Using the bleomycin (BLM) mouse model of lung fibrosis, we tested the ability of HEI3090 to reduce fibrosis. Prophylactic treatment (Fig 2a) with HEI3090 reduced lung fibrosis development as per reduced thickening of alveolar walls and free airspace (Fig 2b) evaluated by the fibrosis score (Fig 2c). Accumulation of extracellular matrix proteins is a hallmark of fibrosis. Therefore, collagen content was assessed by polarized-light microscopy on Sirius Red stained lung sections. We

show that collagen content was reduced in HEI3090-treated lungs (Fig 2b,d). We also weighted lungs of mice at the end of the experiment and show a decreased lung weight of HEI3090-treated mice in comparison with control mice (Fig 2e) indicative of less fibrosis and inflammation. Moreover, activation of P2RX7 with HEI3090 enhanced IL-18 release in sera of mice (Fig 2f). Of note, HEI3090 administered after the first signs of fibrosis, i.e. in a therapeutic setting, also inhibits lung fibrosis (sup Fig 2). Overall, these results show that boosting the activation of P2RX7 with a positive modulator reduces lung fibrosis and enhances IL-18 release.

### **HEI3090 reshapes immune cell infiltration in the lungs**

Since IL-18 is boosted by HEI3090, we tested IL-18 activity by checking IFN- $\gamma$  production by lung immune cells. We show that CD3<sup>+</sup> T cells preferentially produce IFN- $\gamma$  rather than the profibrotic IL-17A in HEI3090-treated mice (Fig 3a). Increase of IFN- $\gamma$  production is only seen in CD3<sup>+</sup> T cells and not in overall immune cells (Fig 3b) or other subsets of lymphocytes (supp Fig 3a,b). Even though levels of CD3<sup>+</sup> T cells and T cell subsets remained unchanged (supp Fig 3c,d) including profibrotic Th17 cells (Fig 3c), IL-17A production by Th17 cells is significantly dampened after HEI3090 treatment (Fig 3c), consistent with the ability of IFN- $\gamma$  to inhibit IL-17A production(39).

Lung fibrosis is also associated and driven by the recruitment of inflammatory cells, mainly from the myeloid lineage. Monocytes are highly inflammatory cells that are recruited to the lungs and differentiate into alveolar macrophages, both having high profibrotic properties (40–42). We show that in HEI3090-treated mice, levels of inflammatory monocytes are considerably decreased (Fig 3d) whereas levels of alveolar macrophages remained unchanged (Fig 3e) in line with the prognostic ability of monocytes count in IPF progression(43, 44). We also looked at other inflammatory cells with profibrotic properties such as eosinophils(45) that are less present in HEI3090-treated lungs (Fig 3f) or PMN levels that are unchanged by HEI3090 treatment (supp Fig 3c).

Given the high profibrotic properties of TGF $\beta$  and the mutual antagonism with IFN- $\gamma$ (46, 47), we checked if HEI3090 had any impact on TGF $\beta$  levels. Indeed, HEI3090 treatment reduced TGF $\beta$ -

producing overall lung immune cells as well as its production (Fig 3g). Particularly, HEI3090 treatment decreased the production of TGF $\beta$  in NK cells but not in T cell subsets (supp Fig 4g).

Of note, activation of P2RX7 with HEI3090 had mainly an impact on immune populations in the lung since no major change in cell populations was observed in spleens of mice (supp Fig3c). However, HEI3090 reactivates an immune response with higher levels of dendritic cells and lymphocytes in spleens of mice treated in a therapeutic setting (supp Fig3).

These results indicate that activation of P2RX7 with HEI3090 favors an antifibrotic cytokinic profile in lung immune cells that is associated with dampened lung inflammation.

### **HEI3090 requires the P2RX7/NLRP3/IL-18 pathway in immune cells to inhibit lung fibrosis**

We showed this far the ability of HEI3090 to inhibit lung fibrosis and remodel immune infiltration, we wanted to investigate furthermore its mechanism of action by identifying the cellular compartment and the pathway required for its activity. Expression of P2RX7 (Fig 1g) and P2RX7-dependant IL-18 release is mostly associated with immune cells(48) and given the HEI3090 impact on immune infiltration (Fig 3), we studied the requirement of immune cells.

In order to do so, we performed an adoptive transfer experiment of WT-P2RX7 expressing splenocytes (Fig 4a, supp Fig 4i) into *p2rx7*<sup>-/-</sup> mice one day prior to BLM administration. We show that the restriction of the expression of P2RX7 on immune cell was able to restore HEI3090 antifibrotic activity given the architecture of the lungs: HEI3090-treated lungs show more free airspace and thinner alveolar walls (Fig 4b) and overall reduced fibrosis score (Fig 4c) than control lungs. Moreover, HEI3090 activity requires the expression of P2RX7 since this effect was lost in *p2rx7*<sup>-/-</sup> mice (supp Fig 4d,e,f)(37). We validated furthermore the importance of P2RX7-expressing immune cells by reducing its expression and activity by repeated i.v. of *p2rx7*<sup>-/-</sup> splenocytes into WT mice (Supp Fig 4a,b,c). This highlights the major role of immune cells for HEI3090's effect.

Accordingly, to test the importance of the NLRP3/IL-18 pathway downstream of P2RX7, we did the same experiment but with *nlrp3*<sup>-/-</sup> and *il18*<sup>-/-</sup> splenocytes instead, that express similar levels of P2RX7

as WT splenocytes (supp Fig 4i), but also same levels of IL-18 and NLRP3 respectively (supp Fig 4j). Lack of NLRP3 and IL-18 in P2RX7-expressing immune cells abrogated the ability of HEI3090 to inhibit lung fibrosis since lung architecture was similar to control mice (Fig 4d,e,f,g). Activation of the P2RX7/NLRP3 pathway is generally associated with pro-inflammatory and pro-fibrotic IL-1 $\beta$  release. However, IL-1 $\beta$  was not implicated in HEI3090's antifibrotic effect (supp Fig 4g,h) nor were its levels affected by HEI3090 in WT mice (supp Fig 4k).

Overall, we show that the P2RX7/NLRP3/IL-18 axis in immune cell is required for HEI3090 antifibrotic effect.

### **Evaluation of IL-18 bioavailability is a promising tool to predict outcome in IPF patients**

Given the requirement of IL-18 for the anti-fibrotic effect of HEI3090, we wondered if IL-18 could predict outcome of IPF patients. To that extend, we analyzed IL-18 levels of 9 healthy controls and 18 IPF patients in plasma samples collected before the start of their treatment (Table 1). Since IL-18 has higher affinity with IL-18BP than with its receptor and that human commercial ELISAs do not solely detect free IL-18, we were particularly interested in studying free active IL-18 levels as well as neutralized, non-active, IL-18 (IL-18/IL-18BP complex).

We show that IL-18 bioavailability (i.e. levels of IL-18 free and complexed IL-18) as well as levels of total IL-18 are increased in patients versus healthy subjects (Fig 5a, Supp Fig 5a) whereas levels of its antagonist IL-18BP are unchanged (Fig Supp 5a). When looking at the overall survival of these patients, we show that high levels of free IL-18 seem to predict better outcome of IPF patients (Fig 5b) whereas levels of complexed IL-18 do not. However, due to the low number of patients in our cohort, this result should be confirmed on a bigger scale.

These results suggest the possible benefit of an active IL-18 in the pathophysiology of pulmonary fibrosis and warrant analysis of free IL-18 as a promising biomarker for predicting outcome in IPF patients.

## Discussion

Using a positive modulator of the purinergic receptor P2RX7, we highlight the ability of the P2RX7/IL-18 pathway in immune cells to boost local IFN- $\gamma$  production by lung T cells and consequently inhibit lung fibrosis in the bleomycin mouse model. We also show that the expression of the P2RX7/IL-18/IFN- $\gamma$  pathway is dampened in IPF patients and that plasmatic IL-18 state predicts their outcome.

Indeed, we show that the expression of P2RX7 is decreased in IPF patients and is associated with immune cells and IFN- $\gamma$  expression (Fig 1), consistent with its capacity to modulate the immune response. Moreover, the IL-18 pathway is also downregulated in IPF patients where TGF $\beta$  levels are high (supp Fig 1)(49), in line with the ability of TGF $\beta$  to downregulate IL-18R expression and IL-18-mediated IFN- $\gamma$  production(50). These results suggest the beneficial effects of boosting the activation of the P2RX7/IL-18/IFN- $\gamma$  pathway. Accordingly, using HEI3090, a positive modulator of P2RX7 previously characterized in our lab (37), we have shown an inhibition of lung fibrosis development in a prophylactic setting, with notably decreased levels of collagen content (Fig 2). Moreover, HEI3090 efficiently inhibits lung fibrosis when administered at the fibrotic stage (supp Fig 2). The inhibition of fibrosis development by activation of P2RX7 was also linked to a reshaping of the immune populations (Fig 3, supp Fig 2e) in line with the immunomodulatory properties of the receptor. Consistently, the activation of the P2RX7/NLRP3/IL-18 pathway in immune cells is required for HEI3090's antifibrotic effect (Fig 4). Moreover, increased IL-18 release by HEI3090 (Fig 2f) is accompanied by increased production of IFN- $\gamma$  by T cells only (Fig 3a,b). P2RX7 is expressed by various immune and non-immune cells, but its expression is the highest in dendritic cells (DCs) and macrophages(51), by which IL-18 is mainly released to shape the T cell response(52) and enhance T cell-IFN- $\gamma$  production(53). Altogether, these observations allow us to speculate that HEI3090 could target P2RX7-expressing antigen-presenting cells to shape the T cell response, which could explain the selective T-cell increase of IFN- $\gamma$  in HEI3090-treated mice. Of note, we have previously shown that HEI3090 targets the P2RX7/IL-18 axis in DCs in a lung tumor mouse model(37) to shape the immune response.

Not only did the treatment with HEI3090 increase IFN- $\gamma$  by T cells, it also reshaped the immune and cytokinic composition of the lung (Fig 3). Indeed, HEI3090-treated mice exhibit a decrease of IL-17A production by Th17 cells (Fig 3c) and TGF $\beta$  production by immune cells (Fig 3g). Moreover, dampened lung inflammation after HEI3090 treatment is noted given the decrease in levels of inflammatory monocytes and eosinophils (Fig 3d,f). It is not known whether this cytokinic and inflammatory switch is due to the IL-17 and TGF $\beta$ -suppressive property of IFN- $\gamma$  alone that consequently act on immune cells(54–56) or if it is a combination with the cell death-inducing property of P2RX7(6).

The novelty of this approach relies on targeting and modifying the lung immune environment. The use of a P2RX7-specific modulator that works only in an ATP-rich environment was indeed effective in favoring anti-inflammatory and anti-fibrotic phenotype by altering several important mediators of the disease. Unlike current therapies(57), treatment of mice with HEI3090 resulted in no noted side effects, supporting furthermore this targeted approach. Moreover, since current therapies and HEI3090 have distinct mechanisms, combining these therapies could have additive or synergistic effects.

It is also important to note that our strategy is unconventional since P2RX7 is known to be pro-inflammatory through IL-1 $\beta$  release. However, HEI3090 was unable to enhance IL-1 $\beta$  release *in vivo* in this model (Supp Fig 4k), even though it efficiently increased the release of IL-18, consistent with our previous *in vivo* and *in vitro* studies(37), allowing us to rule out the pro-inflammatory and pro-fibrotic effects of a P2RX7-dependant IL-1 $\beta$  release. In line with this finding, it has been reported that ATP stimulation of alveolar macrophages derived from IPF as well as lung cancer patients resulted in an increase of IL-18 only(58, 59) that was explained by an impaired NLRP3 inflammasome and a defective autophagy which is described in IPF patients(60). Of interest, autophagy can be regulated by P2RX7(61) and is one of the pathways that allows IL-1 $\beta$  release from the cell(62). Moreover, unlike IL-1 $\beta$ , IL-18 is constitutively expressed in human and mouse immune cells(38) but also in non-immune cells such as fibroblasts(63) and lung epithelium(64) and are both matured and released following NLRP3 activation. It is therefore currently not known if absence of IL-1 $\beta$  release is due to the different expression pattern

of the cytokines or if there is an IL-1 $\beta$ -specific regulation following an enhanced-P2RX7 activation or a defective NLRP3 inflammasome.

We highlight in this study the importance of IL-18 for an antifibrotic effect. However, several studies have pointed out that the P2RX7/NLRP3/IL-18 favor disease progression using knock out mice or inhibitors(5, 14, 63). However, experimental mouse models rely on lung epithelial cell injury that have been shown to activate the NLRP3 inflammasome in the lung epithelium as an initial step(5, 12) and release danger signals, that activate the immune system as a second step. Therefore, initial lung injury on epithelial cells, in *p2rx7*<sup>-/-</sup> and *nlrp3*<sup>-/-</sup> mice namely, is reduced or nonexistent, showing the requirement of P2RX7/NLRP3 for the establishment of the bleomycin mouse model rather than their impact on an already-established fibrosis, which has not been investigated yet. Moreover, NLRP3 as well as the release of IL-1 $\beta$  and IL-18 from fibroblasts have been shown to promote myofibroblast differentiation and extracellular matrix production(63, 65, 66). These observations suggest that fibrosis mouse models rely first on NLRP3 activation by nonimmune cells and encourage further studies on the contribution of the inflammasome in immune cells on fibrosis progression *in vivo*. Furthermore, we have shown that the NLRP3 pathway is downregulated in IPF patients (supp Fig1b) but plasmatic IL-18 is increased (Fig 2f). It is important to note that these two results cannot be compared since NLRP3 and IL-18 levels are assessed in bulk regardless of the cell source, in lung tissue versus plasma respectively. Moreover, NLRP3 activity cannot be assessed on a mRNA level since its activation is based on an assembly of proteins and sequential cleavages. Since we have highlighted the importance of this pathway in immune cells for delaying fibrosis progression, we propose that IL-18 could have distinct effects depending on the cell type source.

There is a lack of biomarkers for IPF, whether they would be prognostic biomarkers, disease activity markers and especially drug efficacy markers. Since IL-18 is important for the anti-fibrotic effect of HEI3090 and can be easily detected in plasma of patients, we wondered if IL-18 could constitute a biomarker for IPF. We show that plasmatic free IL-18 has the potential to be indicative of survival of patients (Fig 5), by evaluating for the first time in IPF the levels of free and complexed IL-18. Indeed,



most human studies assess total IL-18 without considering its binding to IL-18BP and free active levels of the cytokine. Our preliminary results show that IL-18 state in plasma of patients is promising in predicting their outcome. However, it is imperative to further validate its predictive value to the broader IPF population with a bigger cohort of patients to accurately adopt IL-18 for clinical use. Moreover, determining IL-18 levels in bronchoalveolar lavage fluid of patients could more precisely represent lung IL-18 state. Furthermore, given the potential impact of pirfenidone and nintedanib on IL-18 levels (67, 68) (69), determining IL-18 shifts during the treatment would be highly interesting to evaluate potential changes in patients' outcome and study IL-18 levels as a companion test for treatment efficacy.

Overall, we highlight in this study the ability of the P2RX7/NLRP3/IL-18 pathway in immune cells to inhibit lung fibrosis onset by using a positive modulator of P2RX7 that selectively works in eATP-rich environment such as fibrotic lungs. The particularity of this strategy, unlike current therapies targeting the immune system, enhances and attenuates the anti-fibrotic and pro-fibrotic properties of the immune system, respectively, with no reported side effects. Moreover, we show that active IL-18 may predict a better patient outcome that could help in the long run in the patients' care strategy and thereafter implement drugs pipeline (70).

## **Methods**

Detailed methods are included in the online supplement.

Plasmas used in this study were collected from IPF patients enrolled at the Nice University Hospital (see table 1) in compliance with consent procedures accepted by the French Data Protection Authority (CNIL authorization number #DR-2018-094) and the French ethical research committee (CPP reference number #2017 AO266251).

Mice were handled in accordance with the committee for Research and Ethics of the local authorities (CIEPAL #598, protocol number APAFIS 21052-2019060610506376) and followed the European directive 2010/63/UE.

### **Statistical analyses**

All analyses were carried out using Prism software (GraphPad). Mouse experiments were performed on at least  $n = 5$  individuals, as indicated. Mice were equally divided for treatments and controls. Data is represented as mean values and error bars represent SEM. Two-tailed Mann–Whitney and unpaired t-test were used to evaluate the statistical significance between groups. For correlation analyses, two-tailed spearman test was used. For survival analyses, the log-rank Mantel-Cox test was used.

## **Acknowledgements**

The authors wish to thank Dr George Birchenough, Dr Laurent Boyer and Dr Bernhard Ryffel for sharing *il18<sup>-/-</sup>*, *nlrp3<sup>-/-</sup>* and *il1b<sup>-/-</sup>* spleens respectively. We thank Jennifer Griffonet and Lorenne Philibert for patient management.

## **Authors contribution**

S.J.H. and VV-C, conception and design; S.J.H., TJ and VV-C, performed research; S.J.H., SL, PH and VV-C, analysis and interpretation; AG, contributed reagents; SL, VH and PH, contributed tissue specimens; S.J.H. and VV-C, wrote the paper

## **Funding**

This research was funded by Cancéropôle PACA, the French Government (National Research Agency, ANR through the “Investments for the Future”: program reference #ANR-11-LABX-0028-01), SJH is funded by the “Ligue Nationale Contre le Cancer” and the “Fondation pour la recherche medicale” grant number #FDT202106013099 and ARC (grant number ARCTHEM2021020003478). The authors also acknowledge the financial support received from the Executive Unit for Financing Higher Education, Research, Development and Innovation (UEFISCDI), Bucharest, Romania (grant number PN-III-P4-ID-PCE-2020-0818, acronym REPAIR).

## Methods

### Patients

We conducted a retrospective study on patients harboring idiopathic pulmonary fibrosis(71) enrolled at the Nice University Hospital since 2014. Before analysis, all samples were stored in the biobank of the Nice University Hospital, France (BB-0033-00025) approved by French Government. Written informed consent was obtained from each participant. The clinical database COLIBRI linked to the biobank was authorized by the French Data Protection Authority (CNIL authorization number #DR-2018-094) and the French ethical research committee (CPP reference number #2017 AO266251). Clinical characteristics are listed in table 1. Progressive IPF was defined as at least two of three criteria (Worsened respiratory symptoms, increased extent of fibrotic changes on chest imaging, and absolute decline in FVC  $\geq 10\%$  predicted or in DLCO  $\geq 10\%$ ) occurring within one year of biobanking with no alternative diagnosis.

### Free IL-18 measurement in plasma of patients

Levels of total IL-18, IL-18BP and IL-18/IL-18BP complex were determined by human DuoSet ELISA kits from R&D systems according to manufacturer's instructions. The law of mass action was used to calculate the level of free IL-18. Single IL-18BP molecule binds a single molecule of IL-18, with a dissociation constant (Kd) of 400 pM. Therefore, the level of free IL-18 was calculated from the equation(72)  $x = \frac{-b + \sqrt{b^2 - 4c}}{2}$  where:  $x = [\text{IL-18free}]$ ,  $b = [\text{IL-18BP}] - [\text{IL-18}] + \text{Kd}$ , and  $c = -\text{Kd} \times [\text{IL-18}]$

### Microarray

mRNA expression profile was obtained from Gene Expression Omnibus (GEO) database (GSE47460) using the GPL14550. Microarray was done on whole lung homogenate from subjects undergoing thoracic surgery from healthy subjects with no lung-related pathology or from subjects diagnosed as having interstitial lung disease as determined by clinical history, CT scan, and surgical pathology. Expression profile belong to the Lung Tissue Research Consortium (LTRC). 122 patients with UIP/IPF and 91 healthy controls were analyzed in this study.

### Mice

Mice were housed under standardized light–dark cycles in a temperature-controlled air-conditioned environment under specific pathogen-free conditions at IRCAN, Nice, France, with free access to food and water. All mouse studies were approved by the committee for Research and Ethics of the local authorities (CIEPAL #598, protocol number APAFIS 21052-2019060610506376) and followed the European directive 2010/63/UE, in agreement with the ARRIVE guidelines. Experiments were performed in accord with animal protection representative at IRCAN. *p2rx7<sup>-/-</sup>* (B6.129P2-

P2rx7tm1Gab/J) are from the Jackson Laboratory. C57BL/6J OlaHsD male mice (WT) were supplied from Envigo (Gannat, France).

### **Induction of lung fibrosis**

WT or *p2rx7*<sup>-/-</sup> male mice (8 weeks) were anesthetized with ketamine (25mg/kg) and xylazine (2.5 mg/kg) under light isoflurane and were given 2.5 U/kg of bleomycin sulfate (Sigma-Aldrich) by intranasal route. Mice were treated i.p. every day with vehicle (PBS, 10% DMSO) or with HEI3090 (1.5 mg/kg in PBS, 10% DMSO) (37) starting D1 or D7 post bleomycin delivery, as mentioned in the figures.

After 14 days of treatment, lungs were either fixed for paraffin embedding or weighted and analyzed by flow cytometry.

### **Adoptive transfer in *p2rx7* deficient mice**

Spleens from C57BL/6J male mice (8-10 weeks) were collected and digested with the spleen dissociation kit (Miltenyi Biotech) according to the supplier's instructions. 3.10<sup>6</sup> splenocytes were injected i.v. in *p2rx7*<sup>-/-</sup> mice 1 day before intranasal delivery of bleomycin. Mice were treated i.p. every day for 14 days with vehicle (PBS, 10% DMSO) or with HEI3090 (1.5 mg/kg in PBS, 10% DMSO). *Nlrp3*<sup>-/-</sup> spleens were a kind gift from Dr Laurent Boyer, *il18*<sup>-/-</sup> spleens from Dr George Birchenough and *il1b*<sup>-/-</sup> spleens from Dr Bernhard.Ryffel, all on a C57BL/6J background.

### **Histology**

Lungs were collected and fixed in 3% formamide for 16 h prior inclusion in paraffin. Lungs sections (3 µm) were stained with hematoxylin & eosin or with Sirius red (Abcam) according to the supplier's instructions. Fibrosis was assessed on whole lungs using the Ashcroft modified method (73).

Levels of collagen on whole lungs were assessed on Sirius Red polarized light images taken with HD - Axio Observer Z1 Microscope ZEISS microscope using ImageJ. The collagen amount given by the polarization intensity of the Sirius red staining of the lung slices was quantified with a homemade ImageJ/Fiji (74) macro program. The mean gray value of the collagen staining was measured in the fibrotic regions excluding the signal coming from vessels and lung epithelia using dedicated masks. The binary masks were obtained after median filtering and manual thresholding, from the transmission images for the fibrotic one and the polarization images for the vessels. The intersection of these masks is then applied on the polarization image to get specifically the mean gray value of fibrotic collagen.

### **Flow cytometry and antibodies**

Lungs or spleens were collected and digested with the lung or spleen dissociation kit (Miltenyi Biotech) according to the supplier's instructions. Red blood cells were lysed using ACK lysis buffer (Gibco). Fc receptors were blocked using anti-CD16/32 (2.4G2) antibodies followed by surface staining by

incubating cells on ice, for 20 min, with saturating concentrations of labeled Abs (see Table 2) in PBS, 5% FBS and 0.5% EDTA. Tregs were identified using the transcription factor staining Buffer Set (eBioscience) for FoxP3 staining. Intracellular staining was performed after stimulation of single-cell suspensions with Phorbol 12-myristate 13-acetate (PMA at 50 ng mL<sup>-1</sup>, Sigma), ionomycin (0.5 µg mL<sup>-1</sup>, Sigma) and 1 µL mL<sup>-1</sup> Golgi Plug™ (BD Biosciences) for 4 h at 37°C 5% CO<sub>2</sub>. Cells were incubated with Live/Dead stain (Invitrogen), according to the manufacturer protocol prior to surface staining. Intracellular staining was performed using Cytofix/Cytoperm™ kit (BD biosciences) following the manufacturer's instructions. Samples were acquired on CytoFLEX LX (Beckman Coulter) and analyzed using FlowJo (LLC).

### **ELISA**

Sera of mice were collected at the end of the experiment and stored at -80 °C before cytokine detection by ELISA using mouse IL-1 beta/IL-1F2 (R&D) and IL-18 (MBL) according to the supplier's instructions.

### **Western Blot**

Single cell suspensions of whole lungs were lysed with Laemmli buffer (10% glycerol, 3% SDS, 10 mM Na<sub>2</sub>HPO<sub>4</sub>) with protease inhibitor cocktail (Roche). Proteins were separated on a 12% SDS-PAGE gel and electro transferred onto PVDF membranes, which were blocked for 30 min at RT with 3% bovine serum albumin or 5% milk. Membranes were incubated with primary antibodies (see Table 2) diluted at 4 °C overnight. Secondary antibodies (Promega) were incubated for 1 h at RT. Immunoblot detection was achieved by exposure with a chemiluminescence imaging system (PXI Syngene, Ozyme) after membrane incubation with ECL (Immobilon Western, Millipore). The bands intensity values were normalized to that of β-actin using ImageJ software.

### **Statistical analyses**

All analyses were carried out using Prism software (GraphPad). Mouse experiments were performed on at least n = 5 individuals, as indicated. Mice were equally divided for treatments and controls. Data is represented as mean values and error bars represent SEM. Two-tailed Mann–Whitney and unpaired t-test were used to evaluate the statistical significance between groups. For correlation analyses, two-tailed spearman test was used. For survival analyses, the log-rank Mantel-Cox test was used.

**Table1. Clinical characteristics of IPF patients**

Clinical characteristics	IPF Patients	Progressive disease	Non Progressive disease	Control
Number n=	18	4	14	9
Age (years, mean $\pm$ SD)	73.3 $\pm$ 5.54	70.75 $\pm$ 6.18	74.07 $\pm$ 5.35	41.29 $\pm$ 16.54
Gender				
Male n=	15	3	12	4
Female n=	3	1	2	5
Smoking history				
Non smoker n=	6	1	5	
Active smoker n=	2	2	8	
Past smoker n=	10	1	1	
Pack-years (mean $\pm$ SD)	22.33 $\pm$ 17.65	25.33 $\pm$ 4.04	21.33 $\pm$ 20.49	
Antifibrotic treatment				
Pirfenidone n=	5	1	4	
Nintedanib n=	9	3	6	
Other n=	1	0	1	
None n=	3	0	3	
Pulmonary function test				
FVC (% mean $\pm$ SD)	78.89 $\pm$ 18.8	59.25 $\pm$ 12.45	84.5 $\pm$ 16.55	
DLCO (% mean $\pm$ SD)	60.28 $\pm$ 18.59	41.75 $\pm$ 13.25	65.57 $\pm$ 16.6	
GAP stage				
Stage 1 n=	10	0	10	
Stage 2 n=	6	3	3	
Stage 3 n=	2	1	1	

**Table2. Antibodies used in this study**

Antibody	Dilution	Fluorochrome	Clone	Reference	Supplier
<b>CD16/CD32</b>	1/100		2.4G2	553142	BD Biosciences
<b>CD3ε</b>	1/100	PerCP-Cy5.5	145-2611	551163	
<b>NK1.1</b>	1/100	PE-CF594	PK136	562864	
<b>CD11c</b>	1/100	PE-Cy7	HL3	558079	
<b>Ly6G</b>	1/100	AF700	1A8	561236	
<b>Ly6C</b>	1/100	V450	AL-21	560594	
<b>SiglecF</b>	1/50	BV605	E50-2440	740388	
<b>CD4</b>	1/100	BV711	RM4-5	563726	
<b>CD8α</b>	1/100	BV650	53-6.7	100741	
<b>CD45.2</b>	1/100	BV786	104	563686	
<b>CD45</b>	1/100	BUV395	30-F11	564279	
<b>γδ TCR</b>	1/100	PE	GL3	553178	
<b>IFNγ</b>	1/100	APC	XMG1.2	554413	
<b>IL-17A</b>	1/100	AF700	TC11-18H10	561718	
<b>I-A/I-E</b>	1/100	APCfire750	M5/114.15.2	107651	Biolegend
<b>CD64</b>	1/20	PE	X54-5/7.1	139303	
<b>P2RX7</b>	1/8	PE	1F11	148706	
<b>CD11b</b>	1/400	APC	M1/70	17-0112-82	eBiosciences
<b>Foxp3</b>	1/100	PE	FJK16S	12-5773-82	
<b>NLRP3</b>	1/1000		Cryo-2	AG-20B-0014	Adipogen
<b>ACTIN BETA</b>	1/60000		monoclonal	VMA00048	Biorad
<b>IL-18</b>	1/250		polyclonal	5180R-100	Biovision



## Legends of figures

### **Figure 1 : The P2RX7/IL-18/IFN- $\gamma$ pathway is downregulated in IPF and negatively correlates with fibrosis markers**

- a. mRNA expression of *P2RX7* between control and IPF patients
- b. Correlation of *P2RX7*'s expression with *ACTA2* and *TGFB3* in IPF patients
- c. mRNA expression levels of *IL-18* d. *IL18r1*, *IL18rap* and e. *IFNG* between control and IPF patients
- f. Correlation of *P2RX7* and *IFNG/PTPRC* in IPF patients
- g. Correlation of *P2RX7* and *PTPRC* in IPF patients

Each point represents one patient. Two-tailed unpaired t-test with Welch's correction, \*\*\*p < 0.001, \*\*\*\*p < 0.0001. Two-tailed Pearson correlation test.

### **Figure 2 : Activation of P2RX7 with a positive modulator inhibits lung fibrosis progression**

- a. Prophylactic treatment. WT mice were given 2.5 U/kg of bleomycin by i.n. route and treated daily i.p. with 1.5 mg/kg of HEI3090 or Vehicle.
- b. Images of lung sections at day 14 after treatment stained with H&E and Sirius Red, bar= 100  $\mu$ m.
- c. Fibrosis score assessed by the Ashcroft method
- d. Collagen levels of whole lung of mice assessed on Sirius Red-polarized images
- e. Lung weight of age-matched naïve and BLM-induced mice treated or not with HEI3090
- f. IL-18 levels in sera of mice 14 days after treatment by ELISA

Each point represents one mouse, two-tailed Mann-Whitney test, p values: \*p < 0.05, \*\*p < 0.01, \*\*\*\*p < 0.0001. WT: Wildtype, BLM: bleomycin, i.p.: intraperitoneal, i.n.: intranasal, H&E: hematoxylin&eosin

### **Figure 3 : HEI3090 dampens inflammation and favors an anti-fibrotic immune signature in the lungs**

Prophylactic treatment. WT mice were given 2.5 U/kg of bleomycin by i.n. route and treated daily i.p. with 1.5 mg/kg of HEI3090 or Vehicle. Lungs were analyzed by flow cytometry at day 14.

- a. Contour plot of IFN- $\gamma$  and IL-17A producing T cells (CD3<sup>+</sup>NK1.1<sup>-</sup>) (left) and ratio of IFN- $\gamma$  over IL-17A in T cells (CD3<sup>+</sup>NK1.1<sup>-</sup>) (right)
- b. Ratio of IFN- $\gamma$  over IL-17A in CD45<sup>+</sup> cells
- c. Percentage and GMFI of IL-17A<sup>+</sup> cells of CD4<sup>+</sup> T cells (CD3<sup>+</sup>CD4<sup>+</sup>NK1.1<sup>-</sup>)
- d. Dotplot showing lung inflammatory monocytes, gated on lineage<sup>-</sup>CD11c<sup>-</sup>CD11b<sup>+</sup> cells (left) and percentage of lung inflammatory monocytes (Ly6C<sup>high</sup>Ly6G<sup>-</sup>) (right)
- e. Percentage of alveolar macrophages (CD11c<sup>+</sup>SiglecF<sup>+</sup>)
- f. Percentage of lung eosinophils (CD11b<sup>+</sup>SiglecF<sup>+</sup>CD11c<sup>-</sup>)
- g. Percentage and GMFI of TGF $\beta$  in CD45<sup>+</sup> cells

Each point represents one mouse, data represented as box&whiskers or mean $\pm$ SEM, two-tailed Mann-Whitney test, \*p < 0.05, \*\*p < 0.01. GMFI: geometric mean fluorescence intensity. i.n.: intranasal, i.p.: intraperitoneal

**Figure 4: The P2RX7/NLRP3/IL-18 pathway in immune cells is required for HEI3090's antifibrotic effect**

- a. *p2rx7*<sup>-/-</sup> mice were given 3.10<sup>6</sup> WT, *nlrp3*<sup>-/-</sup> or *il18*<sup>-/-</sup> splenocytes i.v. one day prior to BLM delivery (i.n. 2.5 U/kg). Mice were treated daily i.p. with 1.5 mg/kg HEI3090 or vehicle for 14 days.
- b. d. f. Images of lung sections at day 14 after treatment stained with H&E and Sirius Red, bar= 100  $\mu$ m.
- c. Fibrosis score assessed by the Ashcroft method of adoptive transfer of WT splenocytes, e. *nlrp3*<sup>-/-</sup> splenocytes and g. *il18*<sup>-/-</sup> splenocytes

Each point represents one mouse, two-tailed Mann-Whitney test, \*p < 0.05. WT: Wildtype, BLM: bleomycin, i.p.: intraperitoneal, i.n.: intranasal, i.v.: intravenous, H&E: hematoxylin&eosin

**Figure 5: IL-18 bioavailability is a predictive biomarker for IPF progression and patient survival**

- a. Levels of free IL-18 and the IL-18/IL-18BP complex in plasma of healthy persons and IPF patients.
- b. Survival curve of IPF patients according to their levels of plasmatic free IL-18 or complexed IL-18.

Cut-off for IL-18/IL-18BP complex and free IL-18 was the median of values of each. Each point represents one patient, mean  $\pm$  SEM. Two-tailed unpaired t-test with Welch's correction and Log-rank Mantel Cox test for survival analyses. \*\*p < 0.01, \*\*\*p < 0.001. IL-18BP: IL-18Binding Protein, IPF: idiopathic pulmonary fibrosis

**Supp Fig 1 : The components of the NLRP3 inflammasome are dampened in IPF and negatively correlate with fibrosis markers**

- a. Heat map of P2RX7 mRNA expression with a cluster of fibrotic genes according to range of colors. Raw p values (Linear models for microarray analysis, Limma) are shown.
- b. mRNA expression levels of *NLRP3*, *PYCARD*, *CASP1* and *GSDMD* between control and IPF patients

Each point represents one patient, mean  $\pm$  SEM. Two-tailed unpaired t-test with Welch's correction, \*\*\*p < 0.001, \*\*\*\*p < 0.0001. IPF: Idiopathic pulmonary fibrosis

**Supp Fig 2 : HEI3090 inhibits lung fibrosis in a therapeutic setting and reactivates an immune response**

- a. Therapeutic treatment. WT mice were given 2.5 U/kg of bleomycin by i.n. route. 1.5 mg/kg of HEI3090 or vehicle were given daily 7 days after BLM administration until day 21.
- b. Images of lung sections at day 14 after treatment stained with H&E and Sirius Red, bar= 100  $\mu$ m.
- c. Fibrosis score assessed by the Ashcroft method
- d. Collagen levels of whole lung of mice assessed on Sirius Red-polarized images
- e. Percentage of immune cells of CD45+ in spleen assessed by flow cytometry

Each point represents one mouse, data represented as mean $\pm$ SEM, two-tailed Mann-Whitney test, \*p < 0.05, \*\*p < 0.01. WT: Wildtype, BLM: bleomycin, i.p.: intraperitoneal, i.n.: intranasal, H&E: hematoxylin&eosin, NK: Natural Killer, NKT: Natural Killer T cells, DC: Dendritic cells, PMN: polymorphonuclear cells.

**Supp Fig 3: Activation of P2RX7 with HEI3090 reshapes immune infiltration in the lungs**

Prophylactic setting. Mice were given 2.5 U/kg at day 1 i.n. and treated for 14 days with 1.5 mg/kg of HEI3090 or Vehicle. At day 14, sera, spleens and lungs were analyzed.

- a. IFN- $\gamma$  over IL-17A ratio in CD4<sup>+</sup> T cells (CD3<sup>+</sup>CD4<sup>+</sup>CD8<sup>-</sup>NK1.1<sup>-</sup>)
- b. Percentage of IFN- $\gamma$ <sup>+</sup> CD8<sup>+</sup> T cells (CD3<sup>+</sup>CD8<sup>+</sup>CD4<sup>-</sup>NK1.1<sup>-</sup>) and IFN- $\gamma$ <sup>+</sup> NK cells (NK1.1<sup>+</sup>CD3<sup>-</sup>)
- c. Percentage of cells in lungs of mice
- d. Percentage of Tregs (CD3<sup>+</sup>CD4<sup>+</sup>Foxp3<sup>+</sup>NK1.1<sup>-</sup>) of CD4<sup>+</sup>T cells
- e. GMFI of TGF $\beta$ <sup>+</sup> NK cells (NK1.1<sup>+</sup>CD3<sup>-</sup>), T cells (CD3<sup>+</sup>NK1.1<sup>-</sup>), CD4<sup>+</sup>Foxp3<sup>-</sup> T cells, Tregs and CD8<sup>+</sup> T cells
- f. Percentage of cells in spleens of mice

Each point represents one mouse, data represented as box&whiskers or mean $\pm$ SEM, two-tailed Mann-Whitney test, \*p < 0.05, \*\*p < 0.01. GMFI: geometric mean fluorescence intensity, Tregs: regulatory T cells, NK: Natural Killer, NKT: Natural Killer T cells, DC: Dendritic cells, PMN: polymorphonuclear cells.

**Supp Fig 4 : HEI3090 activity requires P2RX7's expressing immune cells.**

- a. Prophylactic treatment. WT mice were given 2.5 U/kg of bleomycin by i.n. route and treated daily i.p. with 1.5 mg/kg of HEI3090 or Vehicle. Mice were given i.v. 3.10<sup>6</sup> *p2rx7*<sup>-/-</sup> splenocytes from male age-matched mice at day 1,4,7,9 and 11.
- b. Images of lung sections at day 14 after treatment stained with H&E and Sirius Red, bar= 100  $\mu$ m.
- c. Fibrosis score assessed by the Ashcroft method
- d. *p2rx7*<sup>-/-</sup> mice were given 3.10<sup>6</sup> *p2rx7*<sup>-/-</sup> or *il18*<sup>-/-</sup> splenocytes i.v. one day prior to BLM delivery (i.n. 2.5 U/kg). Mice were treated daily i.p. with 1.5 mg/kg HEI3090 or vehicle for 14 days.
- e. Images of lung sections at day 14 after treatment stained with H&E and Sirius Red with *p2rx7*<sup>-/-</sup> and **g.** *il18*<sup>-/-</sup> splenocytes. Bar= 100  $\mu$ m.
- f. **h.** Fibrosis score assessed by the Ashcroft method
- i. Percentage of P2RX7<sup>+</sup> cells in various KO spleens assessed by flow cytometry
- j. NLRP3 and IL-18 expression in various KO spleens assessed by Western Blot

**k.** IL-1 $\beta$  levels in sera of WT mice at day 14 after treatment in the prophylactic setting

Each point represents one mouse, data represented as box&whiskers or mean $\pm$ SEM, two-tailed Mann-Whitney test, \*p < 0.05. WT: Wildtype, BLM: bleomycin, i.p.: intraperitoneal, i.n.: intranasal, i.v.: intravenous, H&E: hematoxylin&eosin, KO: knock-out

**Supp Figure 5: Bioavailability of IL-18 in IPF patients**

**a.** Levels of total IL-18 and IL-18BP in plasma of IPF patients versus healthy controls.

**b.** Survival curve of IPF patients according to their levels of plasmatic total IL-18 and IL-18BP.

Cut-off for IL-18/IL-18BP complex and free IL-18 was the median of values of each treatment. Each point represents one patient, mean  $\pm$  SEM. Two-tailed unpaired t-test with Welch's correction and Log-rank Mantel Cox test for survival analyses. \*\*p < 0.01. IL-18BP: IL-18Binding Protein.

## References

1. Heukels P, Moor CC, von der Thüsen JH, Wijsenbeek MS, Kool M. Inflammation and immunity in IPF pathogenesis and treatment. *Respir Med* 2019;147:79–91.
2. Idiopathic Pulmonary Fibrosis Clinical Research Network, Raghu G, Anstrom KJ, King TE, Lasky JA, Martinez FJ. Prednisone, azathioprine, and N-acetylcysteine for pulmonary fibrosis. *N Engl J Med* 2012;366:1968–77.
3. Naccache J-M, Jouneau S, Didier M, Borie R, Cachanado M, Bourdin A, Reynaud-Gaubert M, Bonniaud P, Israël-Biet D, Prévot G, Hirschi S, Lebargy F, Marchand-Adam S, Bautin N, Traclet J, Gomez E, Leroy S, Gagnadoux F, Rivière F, Bergot E, Gondouin A, Blanchard E, Parrot A, Blanc F-X, Chabrol A, Dominique S, Gibelin A, Tazi A, Berard L, *et al.* Cyclophosphamide added to glucocorticoids in acute exacerbation of idiopathic pulmonary fibrosis (EXAFIP): a randomised, double-blind, placebo-controlled, phase 3 trial. *Lancet Respir Med* 2022;10:26–34.
4. Shenderov K, Collins SL, Powell JD, Horton MR. Immune dysregulation as a driver of idiopathic pulmonary fibrosis. *J Clin Invest* 2021;131:.
5. Riteau N, Gasse P, Fauconnier L, Gombault A, Couegnat M, Fick L, Kanellopoulos J, Quesniaux VFJ, Marchand-Adam S, Crestani B, Ryffel B, Couillin I. Extracellular ATP is a danger signal activating P2X7 receptor in lung inflammation and fibrosis. *Am J Respir Crit Care Med* 2010;182:774–83.
6. Surprenant A, Rassendren F, Kawashima E, North RA, Buell G. The cytolytic P2Z receptor for extracellular ATP identified as a P2X receptor (P2X7). *Science* 1996;272:735–8.
7. Perregaux DG, McNiff P, Laliberte R, Conklyn M, Gabel CA. ATP acts as an agonist to promote stimulus-induced secretion of IL-1 beta and IL-18 in human blood. *J Immunol* 2000;165:4615–23.
8. Wilson MS, Madala SK, Ramalingam TR, Gochuico BR, Rosas IO, Cheever AW, Wynn TA. Bleomycin and IL-1beta-mediated pulmonary fibrosis is IL-17A dependent. *J Exp Med* 2010;207:535–52.
9. Sutton CE, Lalor SJ, Sweeney CM, Brereton CF, Lavelle EC, Mills KHG. Interleukin-1 and IL-23 induce innate IL-17 production from gammadelta T cells, amplifying Th17 responses and autoimmunity. *Immunity* 2009;31:331–41.
10. Doerner AM, Zuraw BL. TGF-beta1 induced epithelial to mesenchymal transition (EMT) in human bronchial epithelial cells is enhanced by IL-1beta but not abrogated by corticosteroids. *Respir Res* 2009;10:100.
11. Gasse P, Mary C, Guenon I, Noulain N, Charron S, Schnyder-Candrian S, Schnyder B, Akira S, Quesniaux VFJ, Lagente V, Ryffel B, Couillin I. IL-1R1/MyD88 signaling and the inflammasome are essential in pulmonary inflammation and fibrosis in mice. *J Clin Invest* 2007;117:3786–99.
12. Gasse P, Riteau N, Charron S, Girre S, Fick L, Pétrilli V, Tschopp J, Lagente V, Quesniaux VFJ, Ryffel B, Couillin I. Uric acid is a danger signal activating NALP3 inflammasome in lung injury inflammation and fibrosis. *Am J Respir Crit Care Med* 2009;179:903–13.

13. Couillin I, Vasseur V, Charron S, Gasse P, Tavernier M, Guillet J, Lagente V, Fick L, Jacobs M, Coelho FR, Moser R, Ryffel B. IL-1R1/MyD88 signaling is critical for elastase-induced lung inflammation and emphysema. *J Immunol* 2009;183:8195–202.
14. Zhang L-M, Zhang Y, Fei C, Zhang J, Wang L, Yi Z-W, Gao G. Neutralization of IL-18 by IL-18 binding protein ameliorates bleomycin-induced pulmonary fibrosis via inhibition of epithelial-mesenchymal transition. *Biochem Biophys Res Commun* 2019;508:660–666.
15. Nakatani-Okuda A, Ueda H, Kashiwamura S-I, Sekiyama A, Kubota A, Fujita Y, Adachi S, Tsuji Y, Tanizawa T, Okamura H. Protection against bleomycin-induced lung injury by IL-18 in mice. *Am J Physiol Lung Cell Mol Physiol* 2005;289:L280-7.
16. Nakanishi Y, Horimasu Y, Yamaguchi K, Sakamoto S, Masuda T, Nakashima T, Miyamoto S, Iwamoto H, Ohshimo S, Fujitaka K, Hamada H, Hattori N. IL-18 binding protein can be a prognostic biomarker for idiopathic pulmonary fibrosis. *PLoS One* 2021;16:e0252594.
17. Okamura H, Tsutsi H, Komatsu T, Yutsudo M, Hakura A, Tanimoto T, Torigoe K, Okura T, Nukada Y, Hattori K. Cloning of a new cytokine that induces IFN-gamma production by T cells. *Nature* 1995;378:88–91.
18. Elias JA, Jimenez SA, Freundlich B. Recombinant gamma, alpha, and beta interferon regulation of human lung fibroblast proliferation. *Am Rev Respir Dis* 1987;135:62–5.
19. Ulloa L, Doody J, Massagué J. Inhibition of transforming growth factor-beta/SMAD signalling by the interferon-gamma/STAT pathway. *Nature* 1999;397:710–3.
20. Varga J, Olsen A, Herhal J, Constantine G, Rosenbloom J, Jimenez SA. Interferon-gamma reverses the stimulation of collagen but not fibronectin gene expression by transforming growth factor-beta in normal human fibroblasts. *Eur J Clin Invest* 1990;20:487–93.
21. Gurujeyalakshmi G, Giri SN. Molecular mechanisms of antifibrotic effect of interferon gamma in bleomycin-mouse model of lung fibrosis: downregulation of TGF-beta and procollagen I and III gene expression. *Exp Lung Res* 21:791–808.
22. Gillery P, Serpier H, Polette M, Bellon G, Clavel C, Wegrowski Y, Birembaut P, Kalis B, Cariou R, Maquart FX. Gamma-interferon inhibits extracellular matrix synthesis and remodeling in collagen lattice cultures of normal and scleroderma skin fibroblasts. *Eur J Cell Biol* 1992;57:244–53.
23. Duncan MR, Berman B. Gamma interferon is the lymphokine and beta interferon the monokine responsible for inhibition of fibroblast collagen production and late but not early fibroblast proliferation. *J Exp Med* 1985;162:516–27.
24. Yuan W, Yufit T, Li L, Mori Y, Chen SJ, Varga J. Negative modulation of alpha1(I) procollagen gene expression in human skin fibroblasts: transcriptional inhibition by interferon-gamma. *J Cell Physiol* 1999;179:97–108.
25. King TE, Albera C, Bradford WZ, Costabel U, Hormel P, Lancaster L, Noble PW, Sahn SA, Swarcberg J, Thomeer M, Valeyre D, du Bois RM, INSPIRE Study Group. Effect of interferon gamma-1b on survival in patients with idiopathic pulmonary fibrosis (INSPIRE): a multicentre, randomised, placebo-controlled trial. *Lancet* 2009;374:222–8.



26. Diaz KT, Skaria S, Harris K, Solomita M, Lau S, Bauer K, Smaldone GC, Condos R. Delivery and safety of inhaled interferon- $\gamma$  in idiopathic pulmonary fibrosis. *J Aerosol Med Pulm Drug Deliv* 2012;25:79–87.
27. Smaldone GC. Repurposing of gamma interferon via inhalation delivery. *Adv Drug Deliv Rev* 2018;133:87–92.
28. Skaria SD, Yang J, Condos R, Smaldone GC. Inhaled Interferon and Diffusion Capacity in Idiopathic Pulmonary Fibrosis (IPF). *Sarcoidosis Vasc Diffuse Lung Dis* 2015;32:37–42.
29. Fusiak T, Smaldone GC, Condos R. Pulmonary Fibrosis Treated with Inhaled Interferon-gamma (IFN- $\gamma$ ). *J Aerosol Med Pulm Drug Deliv* 2015;28:406–10.
30. Prior C, Haslam PL. In vivo levels and in vitro production of interferon-gamma in fibrosing interstitial lung diseases. *Clin Exp Immunol* 1992;88:280–7.
31. Luzina IG, Todd NW, Iacono AT, Atamas SP. Roles of T lymphocytes in pulmonary fibrosis. *J Leukoc Biol* 2008;83:237–44.
32. Celada LJ, Kropski JA, Herazo-Maya JD, Luo W, Creecy A, Abad AT, Chioma OS, Lee G, Hassell NE, Shaginurova GI, Wang Y, Johnson JE, Kerrigan A, Mason WR, Baughman RP, Ayers GD, Bernard GR, Culver DA, Montgomery CG, Maher TM, Molyneaux PL, Noth I, Mutsaers SE, Prele CM, Stokes Peebles R, Newcomb DC, Kaminski N, Blackwell TS, van Kaer L, *et al.* PD-1 up-regulation on CD4<sup>+</sup> T cells promotes pulmonary fibrosis through STAT3-mediated IL-17A and TGF- $\beta$ 1 production. *Sci Transl Med* 2018;10:.
33. Herazo-Maya JD, Noth I, Duncan SR, Kim S, Ma S-F, Tseng GC, Feingold E, Juan-Guardela BM, Richards TJ, Lussier Y, Huang Y, Vij R, Lindell KO, Xue J, Gibson KF, Shapiro SD, Garcia JGN, Kaminski N. Peripheral blood mononuclear cell gene expression profiles predict poor outcome in idiopathic pulmonary fibrosis. *Sci Transl Med* 2013;5:205ra136.
34. Gilani SR, Vuga LJ, Lindell KO, Gibson KF, Xue J, Kaminski N, Valentine VG, Lindsay EK, George MP, Steele C, Duncan SR. CD28 down-regulation on circulating CD4 T-cells is associated with poor prognoses of patients with idiopathic pulmonary fibrosis. *PLoS One* 2010;5:e8959.
35. Xu J, Mora AL, LaVoy J, Brigham KL, Rojas M. Increased bleomycin-induced lung injury in mice deficient in the transcription factor T-bet. *Am J Physiol Lung Cell Mol Physiol* 2006;291:L658-67.
36. Giri SN, Hyde DM, Marafino BJ. Ameliorating effect of murine interferon gamma on bleomycin-induced lung collagen fibrosis in mice. *Biochem Med Metab Biol* 1986;36:194–7.
37. Douguet L, Janho Dit Hreich S, Benzaquen J, Seguin L, Juhel T, Dezitter X, Durantont C, Ryffel B, Kanellopoulos J, Delarasse C, Renault N, Furman C, Homerin G, Féral C, Cherfils-Vicini J, Millet R, Adriouch S, Ghinet A, Hofman P, Vouret-Craviari V. A small-molecule P2RX7 activator promotes anti-tumor immune responses and sensitizes lung tumor to immunotherapy. *Nat Commun* 2021;12:653.
38. Puren AJ, Fantuzzi G, Dinarello CA. Gene expression, synthesis, and secretion of interleukin 18 and interleukin 1beta are differentially regulated in human blood mononuclear cells and mouse spleen cells. *Proc Natl Acad Sci U S A* 1999;96:2256–61.

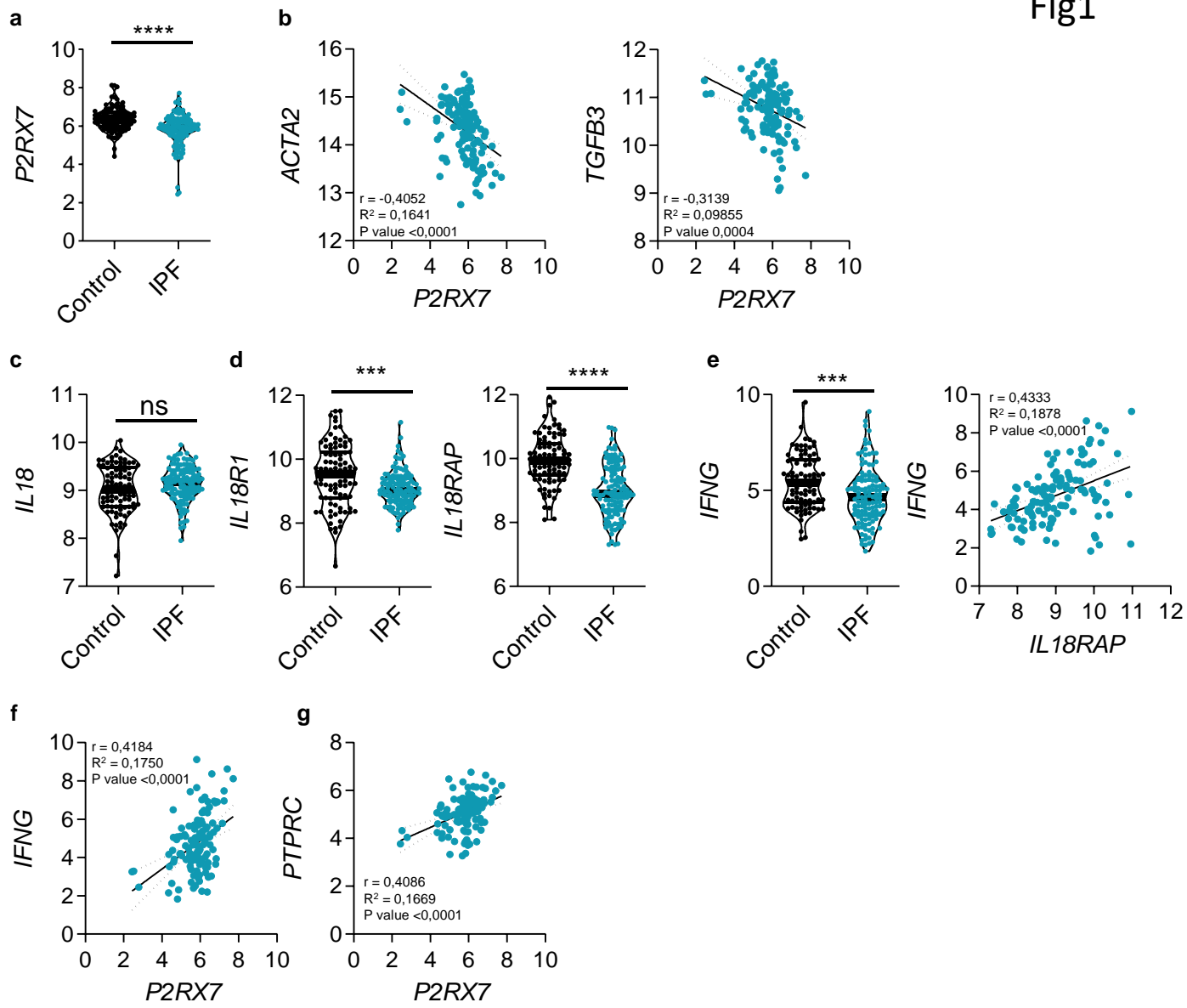
39. Laurence A, Tato CM, Davidson TS, Kanno Y, Chen Z, Yao Z, Blank RB, Meylan F, Siegel R, Hennighausen L, Shevach EM, O'shea JJ. Interleukin-2 signaling via STAT5 constrains T helper 17 cell generation. *Immunity* 2007;26:371–81.
40. Misharin A v, Morales-Nebreda L, Reyfman PA, Cuda CM, Walter JM, McQuattie-Pimentel AC, Chen C-I, Anekalla KR, Joshi N, Williams KJN, Abdala-Valencia H, Yacoub TJ, Chi M, Chiu S, Gonzalez-Gonzalez FJ, Gates K, Lam AP, Nicholson TT, Homan PJ, Soberanes S, Dominguez S, Morgan VK, Saber R, Shaffer A, Hinchcliff M, Marshall SA, Bharat A, Berdnikovs S, Bhorade SM, *et al.* Monocyte-derived alveolar macrophages drive lung fibrosis and persist in the lung over the life span. *J Exp Med* 2017;214:2387–2404.
41. McCubbrey AL, Barthel L, Mohning MP, Redente EF, Mould KJ, Thomas SM, Leach SM, Danhorn T, Gibbings SL, Jakubzick C v, Henson PM, Janssen WJ. Deletion of c-FLIP from CD11bhi Macrophages Prevents Development of Bleomycin-induced Lung Fibrosis. *Am J Respir Cell Mol Biol* 2018;58:66–78.
42. Gibbons MA, MacKinnon AC, Ramachandran P, Dhaliwal K, Duffin R, Phythian-Adams AT, van Rooijen N, Haslett C, Howie SE, Simpson AJ, Hirani N, Gauldie J, Iredale JP, Sethi T, Forbes SJ. Ly6Chi monocytes direct alternatively activated profibrotic macrophage regulation of lung fibrosis. *Am J Respir Crit Care Med* 2011;184:569–81.
43. Kreuter M, Lee JS, Tzouveleakis A, Oldham JM, Molyneaux PL, Weycker D, Atwood M, Kirchgaessler K-U, Maher TM. Monocyte Count as a Prognostic Biomarker in Patients with Idiopathic Pulmonary Fibrosis. *Am J Respir Crit Care Med* 2021;204:74–81.
44. Scott MKD, Quinn K, Li Q, Carroll R, Warsinske H, Vallania F, Chen S, Carns MA, Aren K, Sun J, Koloms K, Lee J, Baral J, Kropski J, Zhao H, Herzog E, Martinez FJ, Moore BB, Hinchcliff M, Denny J, Kaminski N, Herazo-Maya JD, Shah NH, Khatri P. Increased monocyte count as a cellular biomarker for poor outcomes in fibrotic diseases: a retrospective, multicentre cohort study. *Lancet Respir Med* 2019;7:497–508.
45. Morimoto Y, Hirahara K, Kiuchi M, Wada T, Ichikawa T, Kanno T, Okano M, Kokubo K, Onodera A, Sakurai D, Okamoto Y, Nakayama T. Amphiregulin-Producing Pathogenic Memory T Helper 2 Cells Instruct Eosinophils to Secrete Osteopontin and Facilitate Airway Fibrosis. *Immunity* 2018;49:134-150.e6.
46. Ishida Y, Kondo T, Takayasu T, Iwakura Y, Mukaida N. The essential involvement of cross-talk between IFN-gamma and TGF-beta in the skin wound-healing process. *J Immunol* 2004;172:1848–55.
47. Park I-K, Letterio JJ, Gorham JD. TGF-beta 1 inhibition of IFN-gamma-induced signaling and Th1 gene expression in CD4+ T cells is Smad3 independent but MAP kinase dependent. *Mol Immunol* 2007;44:3283–90.
48. Ferrari D, Pizzirani C, Adinolfi E, Lemoli RM, Curti A, Idzko M, Panther E, di Virgilio F. The P2X<sub>7</sub> Receptor: A Key Player in IL-1 Processing and Release. *The Journal of Immunology* 2006;176:3877–3883.
49. Khalil N, O'Connor RN, Unruh HW, Warren PW, Flanders KC, Kemp A, Bereznay OH, Greenberg AH. Increased production and immunohistochemical localization of transforming growth factor-beta in idiopathic pulmonary fibrosis. *Am J Respir Cell Mol Biol* 1991;5:155–62.

50. Koutoulaki A, Langley M, Sloan AJ, Aeschlimann D, Wei X-Q. TNF $\alpha$  and TGF- $\beta$ 1 influence IL-18-induced IFN $\gamma$  production through regulation of IL-18 receptor and T-bet expression. *Cytokine* 2010;49:177–84.
51. di Virgilio F, Vuerich M. Purinergic signaling in the immune system. *Auton Neurosci* 2015;191:117–23.
52. Sáez PJ, Vargas P, Shoji KF, Harcha PA, Lennon-Duménil A-M, Sáez JC. ATP promotes the fast migration of dendritic cells through the activity of pannexin 1 channels and P2X7 receptors. *Sci Signal* 2017;10:.
53. Iwai Y, Hemmi H, Mizenina O, Kuroda S, Suda K, Steinman RM. An IFN- $\gamma$ -IL-18 signaling loop accelerates memory CD8 $^+$  T cell proliferation. *PLoS One* 2008;3:e2404.
54. Penton-Rol G, Polentarutti N, Luini W, Borsatti A, Mancinelli R, Sica A, Sozzani S, Mantovani A. Selective inhibition of expression of the chemokine receptor CCR2 in human monocytes by IFN- $\gamma$ . *J Immunol* 1998;160:3869–73.
55. de Bruin AM, Buitenhuis M, van der Sluijs KF, van Gisbergen KPJM, Boon L, Nolte MA. Eosinophil differentiation in the bone marrow is inhibited by T cell-derived IFN- $\gamma$ . *Blood* 2010;116:2559–69.
56. Iwamoto I, Nakajima H, Endo H, Yoshida S. Interferon gamma regulates antigen-induced eosinophil recruitment into the mouse airways by inhibiting the infiltration of CD4 $^+$  T cells. *J Exp Med* 1993;177:573–6.
57. Raghu G, Rochweg B, Zhang Y, Garcia CAC, Azuma A, Behr J, Brozek JL, Collard HR, Cunningham W, Homma S, Johkoh T, Martinez FJ, Myers J, Protzko SL, Richeldi L, Rind D, Selman M, Theodore A, Wells AU, Hoogsteden H, Schünemann HJ, American Thoracic Society, European Respiratory society, Japanese Respiratory Society, Latin American Thoracic Association. An Official ATS/ERS/JRS/ALAT Clinical Practice Guideline: Treatment of Idiopathic Pulmonary Fibrosis. An Update of the 2011 Clinical Practice Guideline. *Am J Respir Crit Care Med* 2015;192:e3-19.
58. Lasithiotaki I, Tsitoura E, Samara KD, Trachalaki A, Charalambous I, Tzanakis N, Antoniou KM. NLRP3/Caspase-1 inflammasome activation is decreased in alveolar macrophages in patients with lung cancer. *PLoS One* 2018;13:e0205242.
59. Lasithiotaki I, Giannarakis I, Tsitoura E, Samara KD, Margaritopoulos GA, Choulaki C, Vasarmidi E, Tzanakis N, Voloudaki A, Sidiropoulos P, Siafakas NM, Antoniou KM. NLRP3 inflammasome expression in idiopathic pulmonary fibrosis and rheumatoid lung. *Eur Respir J* 2016;47:910–8.
60. Patel AS, Lin L, Geyer A, Haspel JA, An CH, Cao J, Rosas IO, Morse D. Autophagy in idiopathic pulmonary fibrosis. *PLoS One* 2012;7:e41394.
61. Young CNJ, Sinadinos A, Lefebvre A, Chan P, Arkle S, Vaudry D, Gorecki DC. A novel mechanism of autophagic cell death in dystrophic muscle regulated by P2RX7 receptor large-pore formation and HSP90. *Autophagy* 2015;11:113–30.
62. Dupont N, Jiang S, Pilli M, Ornatowski W, Bhattacharya D, Deretic V. Autophagy-based unconventional secretory pathway for extracellular delivery of IL-1 $\beta$ . *EMBO J* 2011;30:4701–11.

63. Artlett CM, Sassi-Gaha S, Rieger JL, Boesteanu AC, Feghali-Bostwick CA, Katsikis PD. The inflammasome activating caspase 1 mediates fibrosis and myofibroblast differentiation in systemic sclerosis. *Arthritis Rheum* 2011;63:3563–74.
64. Cameron LA, Taha RA, Tscopoulos A, Kurimoto M, Olivenstein R, Wallaert B, Minshall EM, Hamid QA. Airway epithelium expresses interleukin-18. *Eur Respir J* 1999;14:553–9.
65. Watanabe A, Sohail MA, Gomes DA, Hashmi A, Nagata J, Sutterwala FS, Mahmood S, Jhandier MN, Shi Y, Flavell RA, Mehal WZ. Inflammasome-mediated regulation of hepatic stellate cells. *Am J Physiol Gastrointest Liver Physiol* 2009;296:G1248-57.
66. Pinar AA, Yuferov A, Gaspari TA, Samuel CS. Relaxin Can Mediate Its Anti-Fibrotic Effects by Targeting the Myofibroblast NLRP3 Inflammasome at the Level of Caspase-1. *Front Pharmacol* 2020;11:1201.
67. Sharawy MH, Serrya MS. Pirfenidone attenuates gentamicin-induced acute kidney injury by inhibiting inflammasome-dependent NLRP3 pathway in rats. *Life Sci* 2020;260:118454.
68. Oku H, Shimizu T, Kawabata T, Nagira M, Hikita I, Ueyama A, Matsushima S, Torii M, Arimura A. Antifibrotic action of pirfenidone and prednisolone: different effects on pulmonary cytokines and growth factors in bleomycin-induced murine pulmonary fibrosis. *Eur J Pharmacol* 2008;590:400–8.
69. Mavrogiannis E, Hagdorn QAJ, Bazioti V, Douwes JM, van der Feen DE, Oberdorf-Maass SU, Westerterp M, Berger RMF. Pirfenidone ameliorates pulmonary arterial pressure and neointimal remodeling in experimental pulmonary arterial hypertension by suppressing NLRP3 inflammasome activation. *Pulm Circ* 2022;12:e12101.
70. Spagnolo P, Kropski JA, Jones MG, Lee JS, Rossi G, Karampitsakos T, Maher TM, Tzouveleakis A, Ryerson CJ. Idiopathic pulmonary fibrosis: Disease mechanisms and drug development. *Pharmacol Ther* 2021;222:107798.
71. Raghu G, Remy-Jardin M, Myers JL, Richeldi L, Ryerson CJ, Lederer DJ, Behr J, Cottin V, Danoff SK, Morell F, Flaherty KR, Wells A, Martinez FJ, Azuma A, Bice TJ, Bouros D, Brown KK, Collard HR, Duggal A, Galvin L, Inoue Y, Jenkins RG, Johkoh T, Kazerooni EA, Kitaichi M, Knight SL, Mansour G, Nicholson AG, Pipavath SNJ, *et al.* Diagnosis of Idiopathic Pulmonary Fibrosis. An Official ATS/ERS/JRS/ALAT Clinical Practice Guideline. *Am J Respir Crit Care Med* 2018;198:e44–e68.
72. Migliorini P, Anzilotti C, Pratesi F, Quattroni P, Bargagna M, Dinarello CA, Boraschi D. Serum and urinary levels of IL-18 and its inhibitor IL-18BP in systemic lupus erythematosus. *Eur Cytokine Netw* 2010;21:264–71.
73. Hübner R-H, Gitter W, Eddine El Mokhtari N, Mathiak M, Both M, Bolte H, Freitag-Wolf S, Bewig B. Standardized quantification of pulmonary fibrosis in histological samples. *Biotechniques* 2008;44:507–517.
74. Schindelin J, Arganda-Carreras I, Frise E, Kaynig V, Longair M, Pietzsch T, Preibisch S, Rueden C, Saalfeld S, Schmid B, Tinevez J-Y, White DJ, Hartenstein V, Eliceiri K, Tomancak P, Cardona A. Fiji: an open-source platform for biological-image analysis. *Nat Methods* 2012;9:676–682.



Fig1



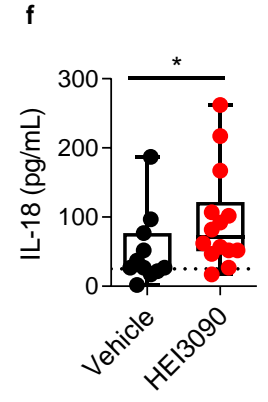
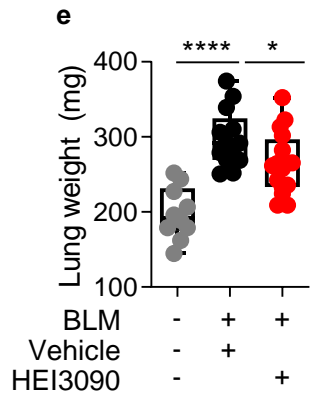
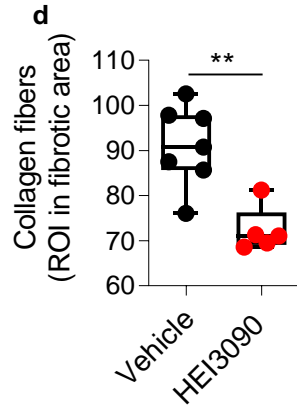
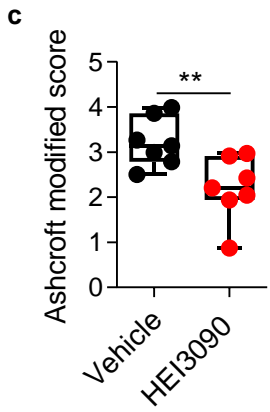
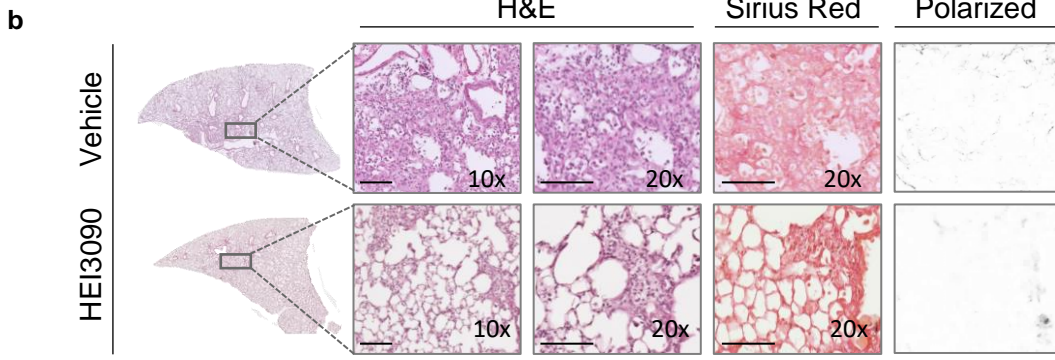
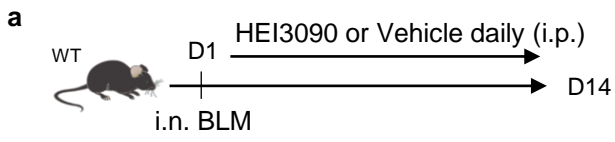


Fig3

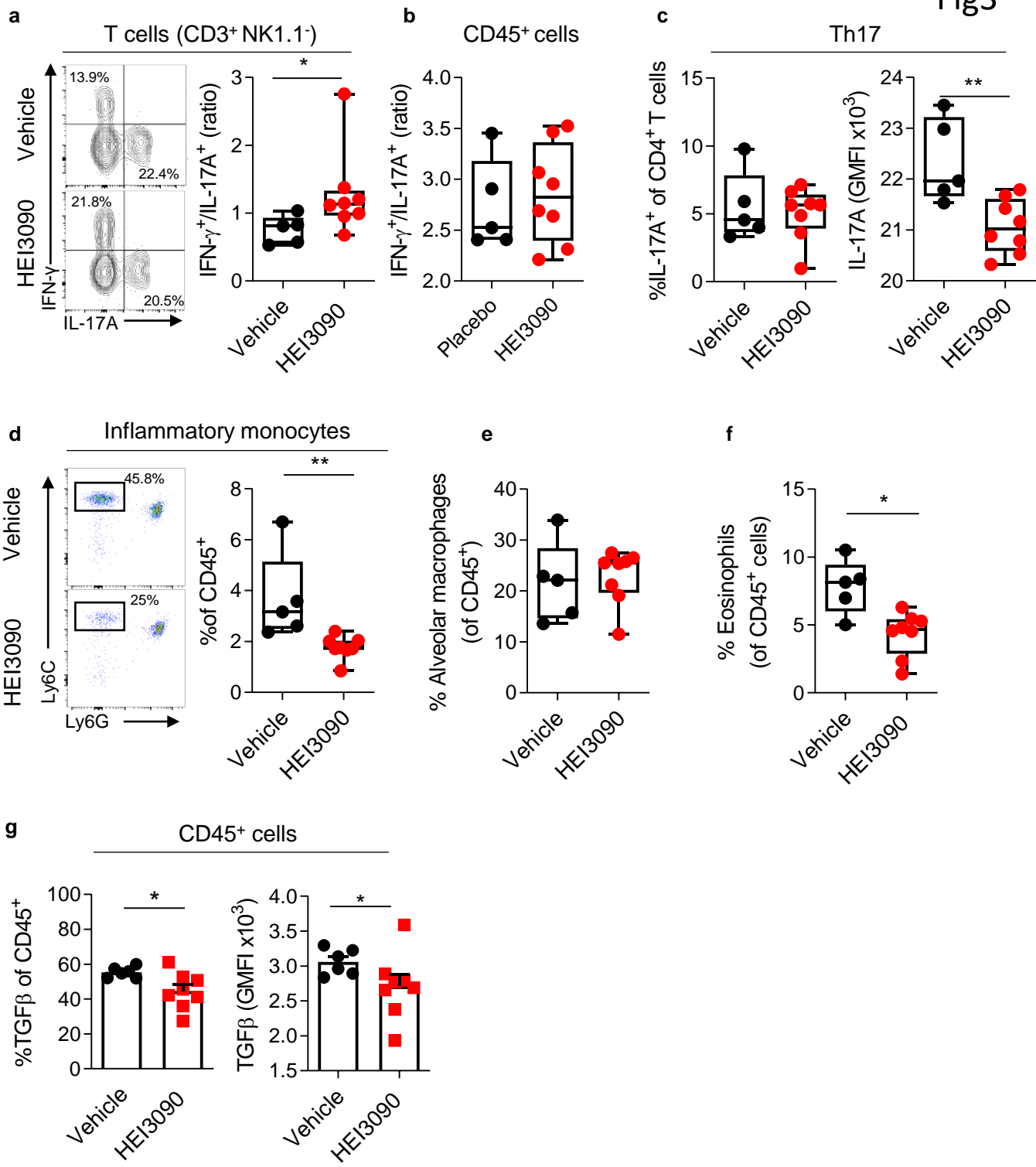




Fig4

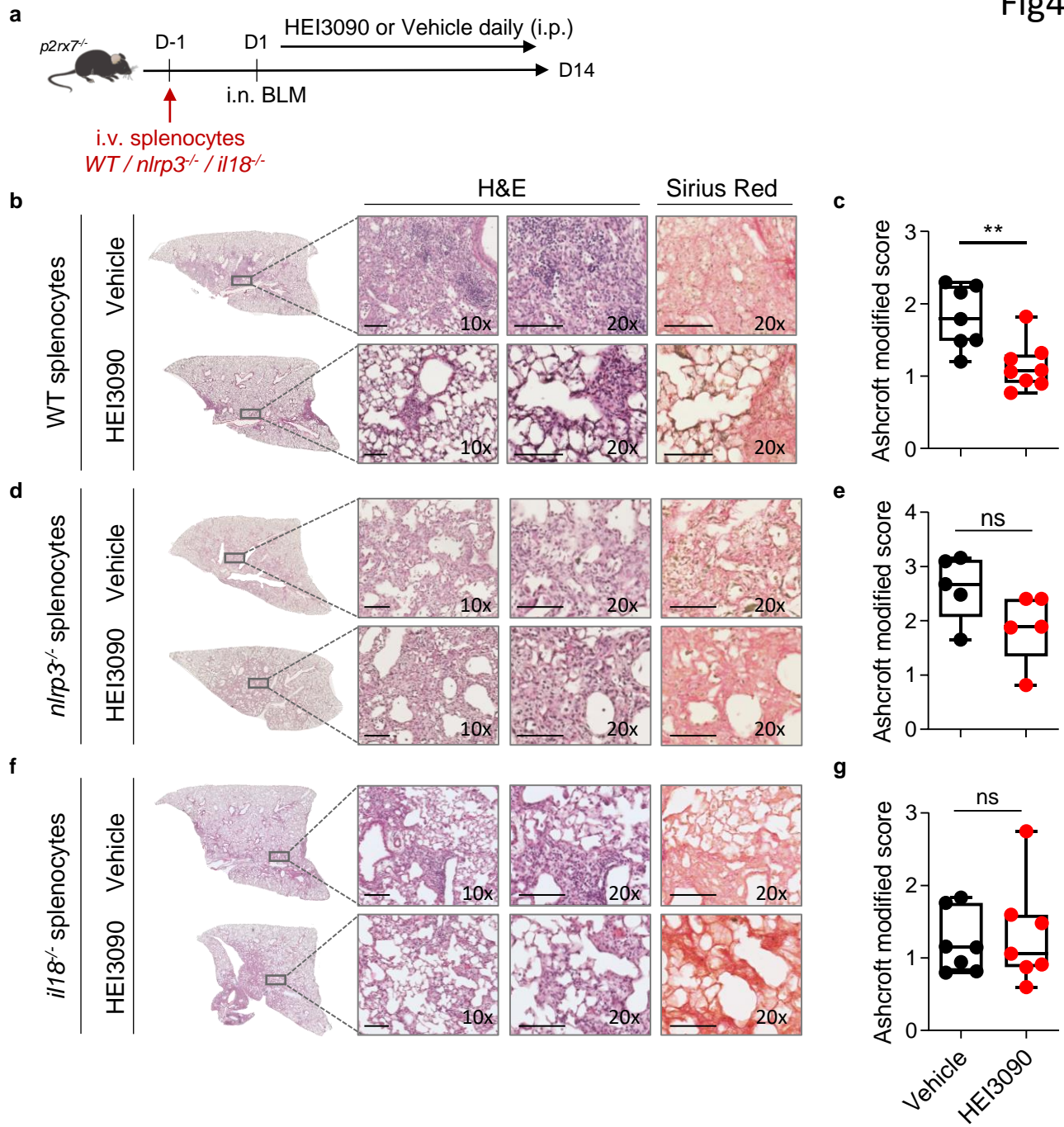
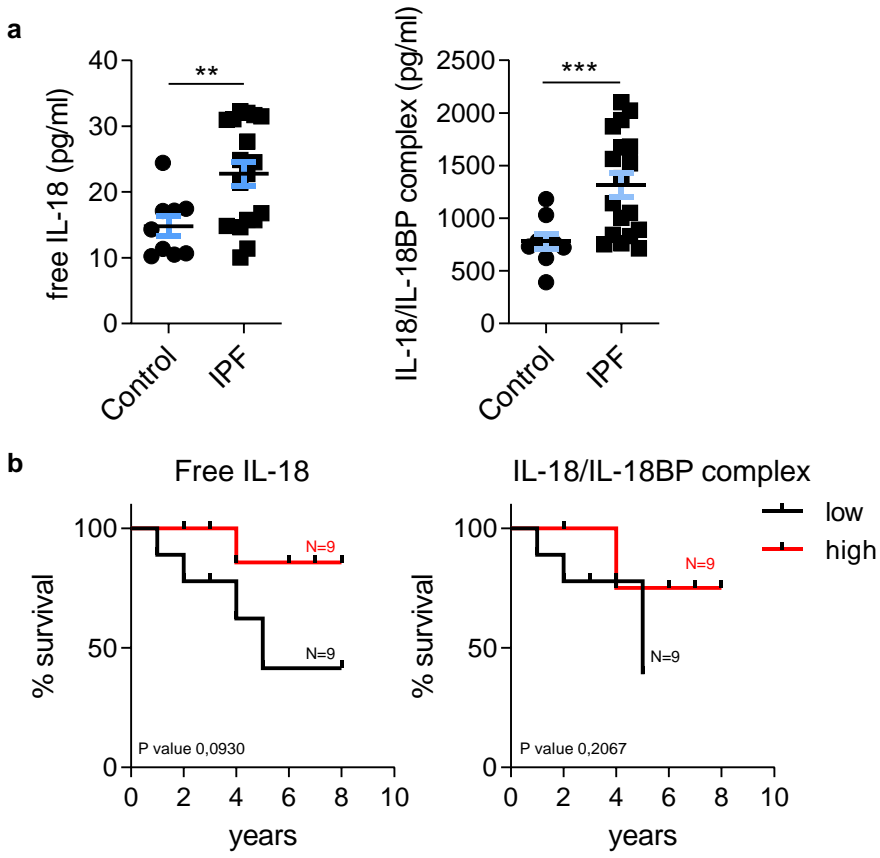
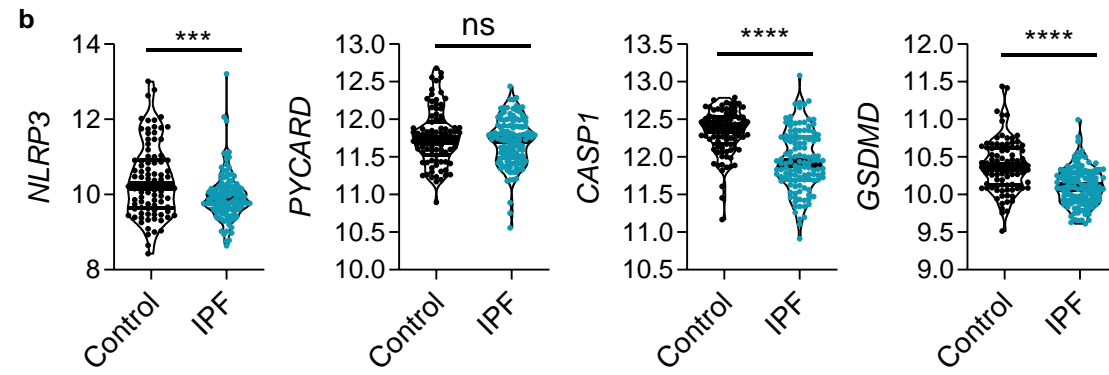
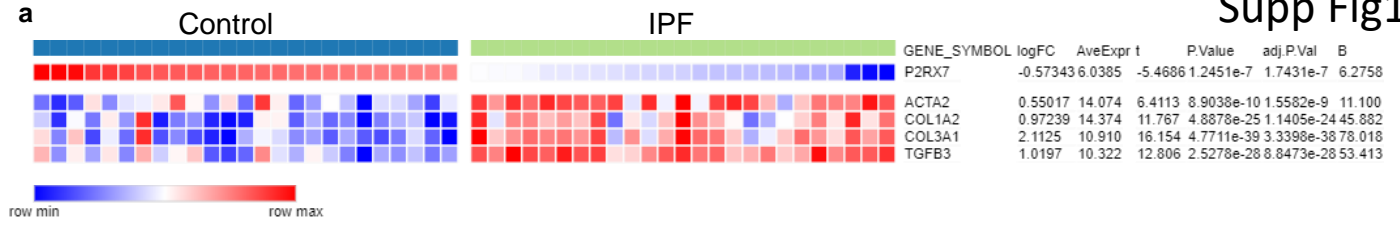
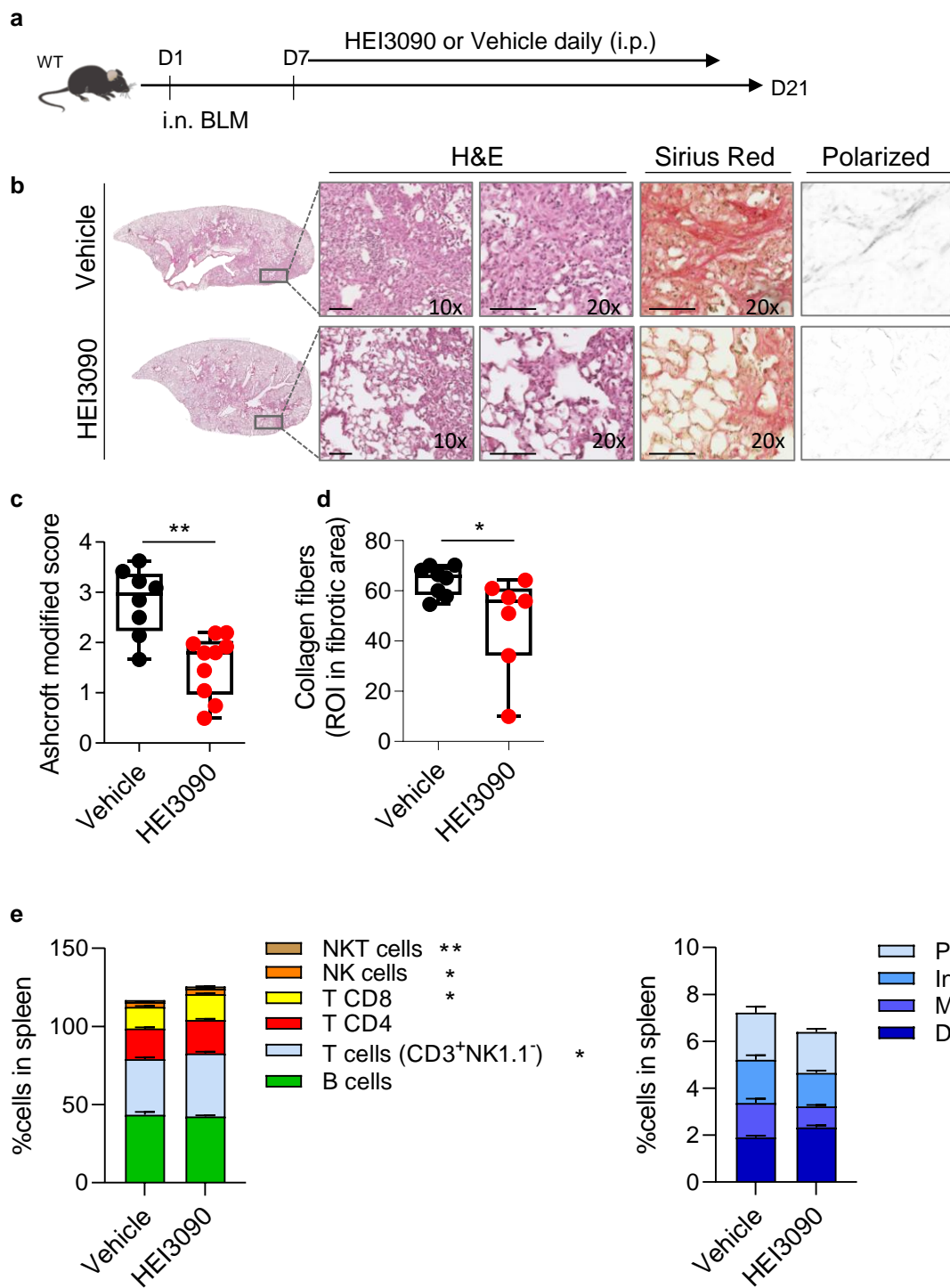


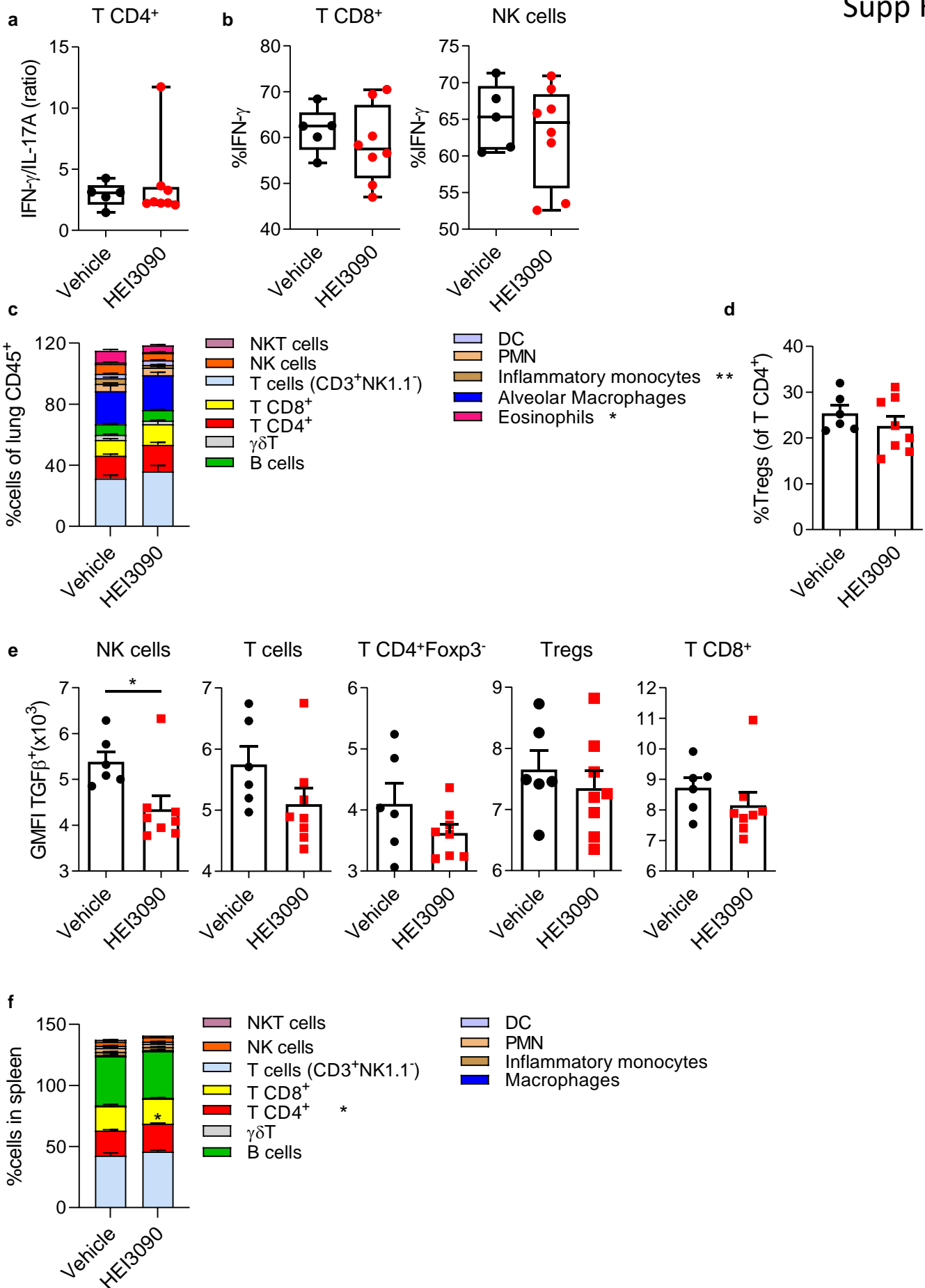
Fig5

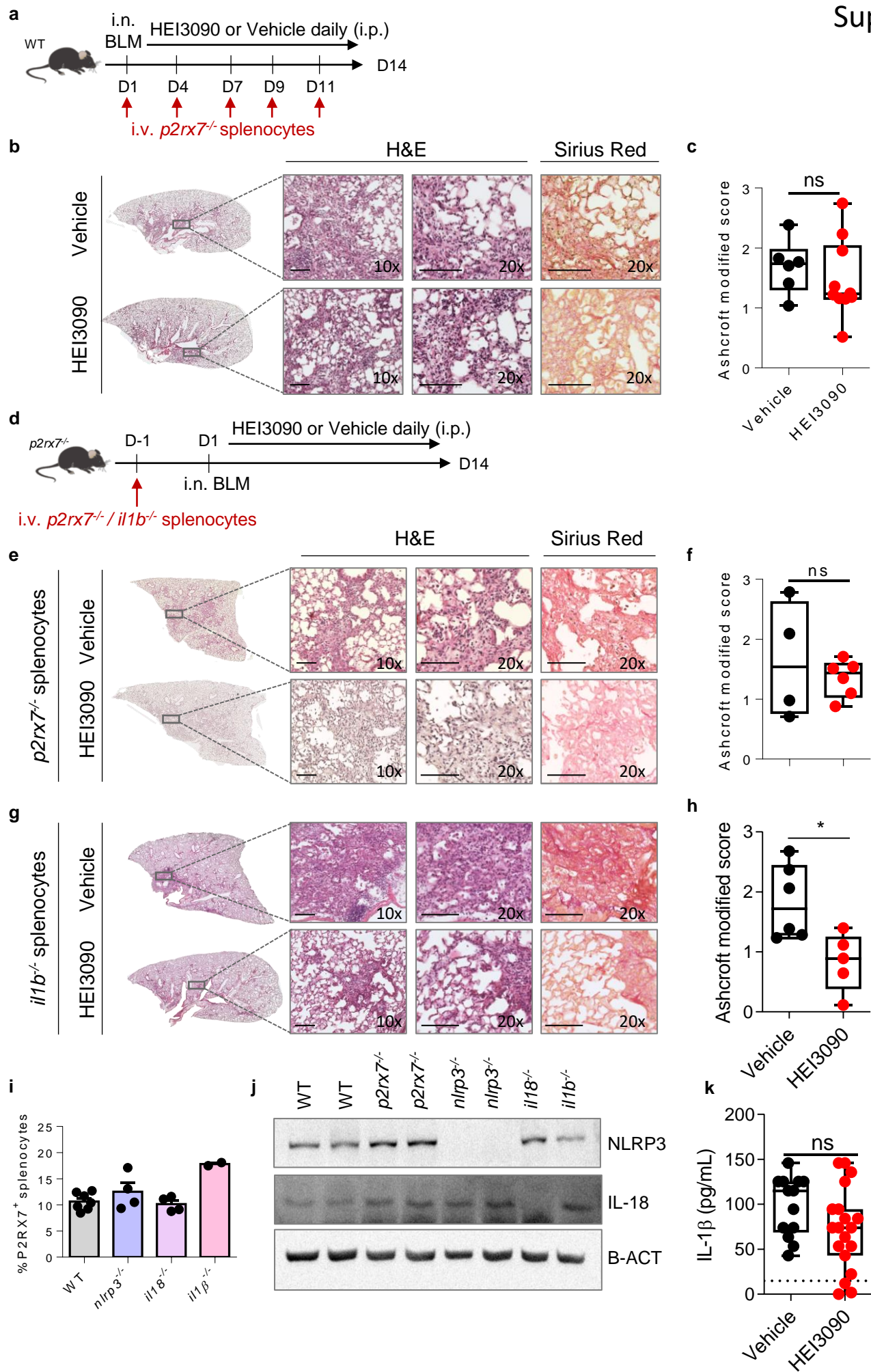


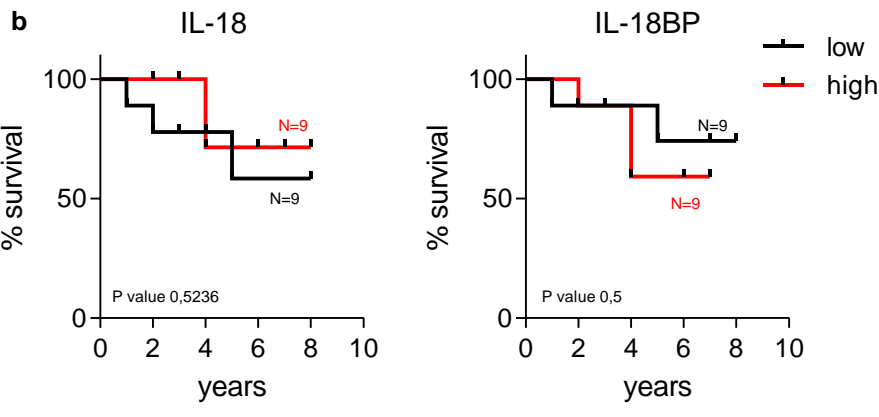
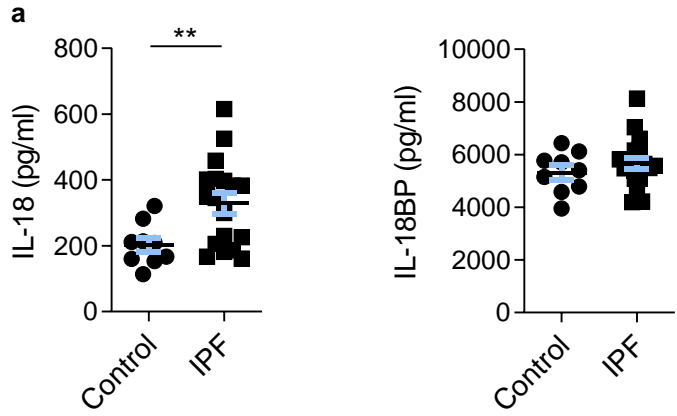
# Supplementary Figures















## ARTICLE III

“Protocol for evaluating *in vivo* the activation of the P2RX7 immunomodulator”

En révision dans ***Biological Procedures Online***, première auteure



## Mise en place d'un protocole pour mesurer l'activation de l'immunomodulateur P2RX7 *in vivo*

### Contexte

L'activation du récepteur purinergique P2RX7 par son ligand l'ATP extracellulaire (ATPe) se traduit par un influx de calcium et une sortie de potassium, la formation de macropores à la membrane plasmique mais aussi l'assemblage de l'inflammasome NLRP3 et la libération des cytokines IL-1 $\beta$  et IL-18.

L'étude de l'activité de P2RX7 se fait *in vitro* ou *ex vivo*, en déterminant l'influx de calcium, la formation de macropores ou bien la libération d'IL-1 $\beta$ /IL-18. Cependant, la mise en œuvre de ces expériences nécessite l'utilisation de milieux et des conditions non physiologiques qui d'une part peuvent affecter l'activation du récepteur et d'autre part peuvent biaiser l'effet de ses agonistes ou antagonistes.

Ayant démontré qu'un modulateur positif de P2RX7 freine la croissance des tumeurs (**Article I**) et le développement de fibroses pulmonaires (**Article II**) via la voie P2RX7/NLRP3/IL-18, nous avons proposé d'étudier *in vivo* l'activation du récepteur dans le poumon.

### Méthodes

Pour évaluer l'activation *in vivo* de P2RX7, nous avons utilisé le modèle murin et en particulier des souris WT ou *p2rx7*<sup>-/-</sup>. Nous avons choisi de regarder l'activité macropore du récepteur, qui est une particularité propre de P2RX7. Nous avons utilisé la sonde TO-PRO<sup>TM</sup>-3, qui ne rentre dans la cellule qu'une fois les macropores formés, pour s'intercaler à l'ADN, rendant ainsi la cellule fluorescente.

Les souris reçoivent par voie intranasale du TO-PRO<sup>TM</sup>-3 dans une narine, et de l'ATP ou du PBS dans l'autre. Trente minutes après, temps nécessaire pour l'entrée des réactifs dans le poumon et pour l'activation de P2RX7, les souris sont mises à mort et les poumons prélevés, dissociés et marqués avec des anticorps couplés à des fluorochromes. Les cellules TO-PRO<sup>TM</sup>-3 positives sont ensuite analysées par cytométrie de flux.

### Résultats

Nous avons montré que l'intensité de fluorescence du TO-PRO<sup>TM</sup>-3 est augmentée dans les souris WT ayant reçu de l'ATP. Cette augmentation n'est pas observée dans les souris *p2rx7*<sup>-/-</sup>, montrant une spécificité de la fluorescence pour P2RX7. Cette augmentation est également observée uniquement dans les cellules immunitaires.

Ainsi, le protocole développé est fonctionnel et permet de mesurer efficacement l'activation de P2RX7. Ce protocole pourrait être utilisé afin d'étudier l'efficacité de molécules modulant l'activité de P2RX7, notamment HEI3090, mais aussi afin de déterminer quel type cellulaire exprimant P2RX7 est ciblé par ces molécules grâce à l'utilisation d'un panel de marqueurs spécifiques.



1 **Protocol for evaluating *in vivo* the activation of**  
2 **the P2RX7 immunomodulator**

3

4 Serena Janho dit Hreich<sup>1,2</sup>, Thierry Juhel<sup>1</sup>, Paul Hofman<sup>1,2,3,4</sup>, Valérie Vouret-  
5 Craviari<sup>1,2</sup>

6 1. Université Côte d'Azur, CNRS, INSERM, IRCAN, 06108 Nice, France

7 2. FHU OncoAge, Nice, France

8 3. Laboratory of Clinical and Experimental Pathology and Biobank, Pasteur Hospital,  
9 Nice, France

10 4. Hospital-Related Biobank (BB-0033-00025), Pasteur Hospital, Nice, France

11

12

13 Corresponding authors: [serena.janho-dit-hreich@etu.univ-cotedazur.fr](mailto:serena.janho-dit-hreich@etu.univ-cotedazur.fr), [valerie.vouret@univ-](mailto:valerie.vouret@univ-)  
14 [cotedazur.fr](http://cotedazur.fr)

15

16

1 **Abstract**

2 **Background:** P2RX7 is a purinergic receptor with pleiotropic activities that is activated by  
3 high levels of extracellular ATP that are found in inflamed tissues. P2RX7 has  
4 immunomodulatory and anti-tumor properties and is therefore a therapeutic target for various  
5 diseases. Several compounds are developed to either inhibit or enhance its activation.  
6 However, studying their effect on P2RX7's activities is limited to *in vitro* and *ex vivo* studies  
7 that require the use of unphysiological media that could affect its activation. Up to now, the  
8 only way to assess the activity of P2RX7 modulators on the receptor *in vivo* was in an indirect  
9 manner.

10 **Results:** We successfully developed a protocol allowing the detection of P2RX7 activation *in*  
11 *vivo* in lungs of mice, by taking advantage of its unique macropore formation ability. The  
12 protocol is based on intranasal delivery of TO-PRO<sup>TM</sup>-3, a non-permeant DNA intercalating  
13 dye, and fluorescence measurement by flow cytometry. We show that ATP enhances TO-  
14 PRO<sup>TM</sup>-3 fluorescence mainly in lung immune cells of mice in a P2RX7-dependant manner.

15 **Conclusions:** The described approach has allowed the successful analysis of P2RX7 activity  
16 directly in the lungs of WT and transgenic C57BL6 mice. The provided detailed guidelines and  
17 recommendations will support the use of this protocol to study the potency of pharmacologic  
18 or biologic compounds targeting P2RX7.

19

20 **Keywords:** P2RX7, P2X7 receptor, purinergic receptors, ATP, macropore, TOPRO-3, activity

21

## 1 **Background**

2 The purinergic P2X family of receptors is a family of 7 receptors that are all activated by  
3 extracellular ATP (eATP) with various affinities. Unlike the other 6 receptors, P2RX7 requires  
4 high levels of eATP (in the range of hundreds of micromolar) to be activated. Such levels of  
5 eATP are found in inflamed tissues such as the tumor microenvironment or fibrotic sites <sup>1</sup>.

6 P2RX7 is a receptor with pleiotropic activities. Its activation leads to calcium influx and  
7 potassium efflux, a feature it shares with all members of the P2X family and that has been  
8 shown to trigger activation of various signaling pathways <sup>2</sup>. However, P2RX7 has its own  
9 particularities: its activation also leads to a macropore opening at the plasma membrane that  
10 allows the non-selective entry of macromolecules (up to 900 Da) to the cell. Compromising  
11 membrane integrity through macropore opening by a prolonged or sustained activation (over  
12 1 hour) of P2RX7 could also lead to cell death<sup>3</sup>. Moreover, activation of P2RX7 leads  
13 subsequently to the assembly of the NLRP3 inflammasome and the release of mature IL-1 $\beta$   
14 and IL-18 from the cell <sup>4</sup>.

15 Due to its ability to induce cell proliferation and death but also to modulate the immune  
16 response, several approaches are undertaken to either inhibit or enhance its activation, by  
17 engineering chemical molecules <sup>5,6</sup> or nanobodies <sup>7</sup> targeting the receptor. Three assays are  
18 classically and routinely used to evaluate their ability to modulate P2RX7's activation, based  
19 on the 3 hallmarks of P2RX7:

- 20 • Calcium influx: the goal is to measure intracellular calcium concentrations using cell  
21 permeant fluorescent calcium indicators such as Fluo-4 AM or Fura 2. Calcium  
22 concentration could be assessed by spectrophotometry, microscopy or flow cytometry.  
23 Calcium influx could also be detected by measuring ion fluxes by electrophysiology  
24 techniques such as patch-clamp.



- 1 • Macropore opening: To evaluate the opening of the macropores, non-permeant DNA  
2 intercalating fluorescent dyes of high molecular weight (up to 900 Da) are used, such  
3 as TO-PRO™-3 or Ethidium bromide. Fluorescence is assessed by  
4 spectrophotometry, microscopy or flow cytometry.
- 5 • NLRP3 inflammasome activation is determined by checking adaptor protein ASC  
6 oligomerization, caspase-1 cleavage or IL-1 $\beta$ /IL-18 release. It is assessed by  
7 immunofluorescence, western blot, flow cytometry or ELISA.

8 However, these assays are *in vitro* or *ex vivo*-based and rely on using unphysiological medias  
9 that could interfere with P2RX7 activation. Indeed, the ionic composition of media is crucial.  
10 ATP-induced cell death has been shown to be delayed in low-salt medias<sup>8</sup>. Moreover,  
11 macropore formation is impacted by Na<sup>+</sup>, iodide, thiocyanate and chloride-enriched medias,  
12 since increasing concentration of these ions inhibited ethidium uptake by cells<sup>9</sup>. Channel  
13 opening is also affected by external anions such as glutamate that potentiates human P2RX7  
14 activation whereas chloride and iodide decreased it <sup>10</sup>. Since P2RX7 activation hangs in the  
15 balance of ions concentrations in media, measurement of its activation *in vitro* and its  
16 translation *in vivo* can be not accurate. For example, under pathological conditions, glutamate  
17 levels increase in the extracellular space during nerve injury, that could affect P2RX7  
18 activation <sup>11</sup>.

19 Since compounds targeting P2RX7 are tested *in vitro*, little is known on their impact on P2RX7  
20 activities *in vivo*, i.e. in complete physiological conditions. Up to now, *in vivo* P2RX7 activation  
21 state is only seen indirectly through eATP levels or IL-1 $\beta$ /IL-18 production. Therefore, we  
22 aimed at setting up a way to measure its activation *in vivo* and developed a protocol based on  
23 intranasal delivery of TO-PRO™-3 and fluorescence measurement by flow cytometry.

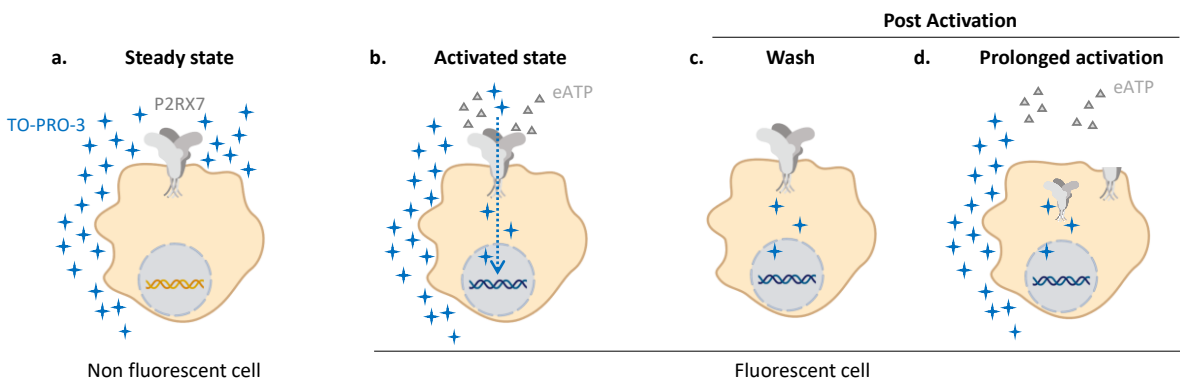
24

25

# 1 Results

## 2 **General strategy to measure P2RX7 activity *in vivo***

3 Since calcium influx is a common feature of P2X receptors and that NLRP3 assembly is a step  
4 downstream of P2RX7 but also not specific to P2RX7, we opted to use macropore opening,  
5 which directly represent the activation state of the receptor, as a readout for P2RX7 activity  
6 (Fig 1). Several dyes are available for measuring macropore opening. We opted to use the  
7 TO-PRO™-3 dye (Invitrogen) since it is the most sensitive non-permeant DNA intercalating  
8 dye and was shown to work best in flow cytometry <sup>12</sup>.



9 **Fig 1.** Activation of P2RX7 and macropore opening using TO-PRO™-3 dye. *Created using*  
10 *biorender.com*

11 When the cell is in steady state (absence of eATP, membrane integrity) TO-PRO™-3 does not  
12 enter the cell and the cell remains non fluorescent (Fig 1a). In the presence of eATP, P2RX7  
13 is activated and macropores are open, permitting the entry of TO-PRO™-3 into the cell. TO-  
14 PRO™-3 binds to DNA and renders the cell fluorescent (Fig 1b). Macropore formation is a  
15 reversible mechanism. However, once P2RX7 is activated, the cell remains fluorescent since  
16 TO-PRO™-3 has already bound to DNA, even if no eATP remains or if P2RX7 is internalized  
17 <sup>13,14</sup> or cleaved <sup>15</sup> during a prolonged activation (Fig 1c,d), allowing the detection of P2RX7  
18 activation at any point in time.

19 Channel opening and P2RX7-dependent calcium influx are detected few seconds after ATP  
20 stimulation. However, detection of macropore formation is much slower due to the

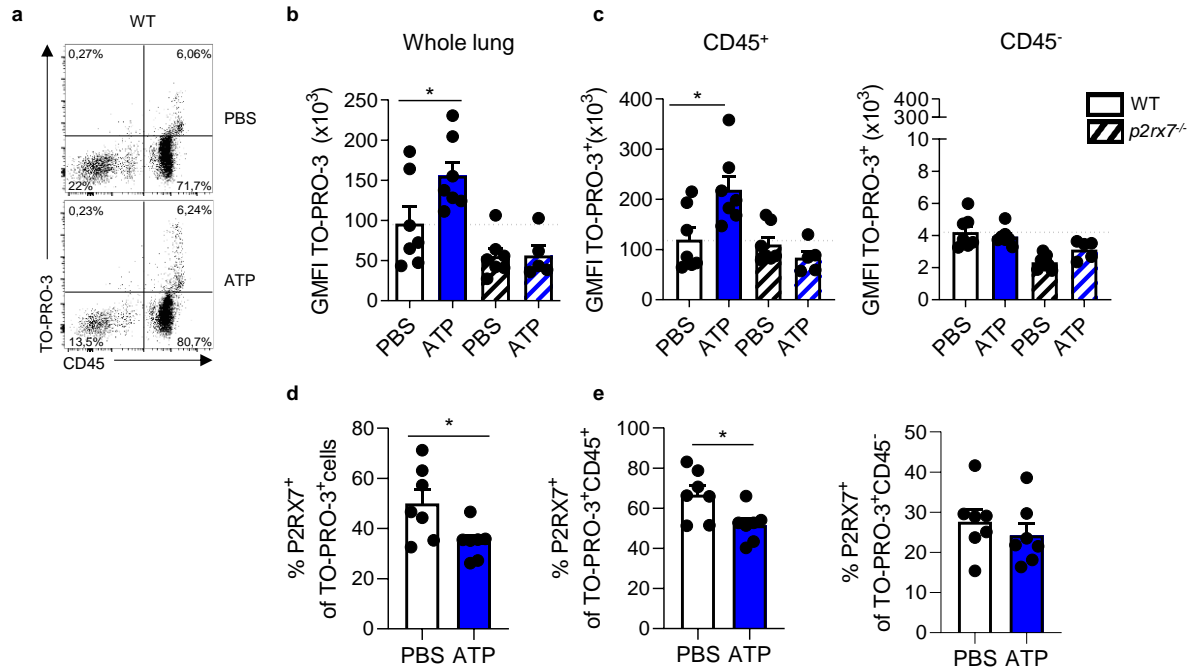
1 incorporation of fluorescent dyes in DNA and can take up to 1 hour to detect all activated  
2 receptors<sup>12</sup>. Moreover, since prolonged activation of P2RX7 (over 1 hour) can also lead to  
3 cell death in a macropore-dependent manner and since TO-PRO<sup>TM</sup>-3 can also detect dead  
4 cells, it is crucial to add a Live/Dead marker. Indeed, excluding dead cells to reduce  
5 background noise and macropore-unrelated TO-PRO<sup>TM</sup>-3 staining is important for accurate  
6 P2RX7-activation measurement. Moreover, in order to detect P2RX7-related TO-PRO<sup>TM</sup>-3  
7 fluorescence and to rule out detection of ATP-induced cell death, we chose to activate P2RX7  
8 for 30 minutes *in vivo*.

### 9 **ATP activates P2RX7 in the lung and increases *in vivo* TO-PRO<sup>TM</sup>-3 fluorescence.**

10 We first analyzed TO-PRO<sup>TM</sup>-3 fluorescence in the whole lung. We observed an increase of  
11 fluorescence in WT mice receiving ATP compared to PBS (Fig 2a,b), indicative of macropore  
12 opening and therefore activation of P2RX7. In order to know if this increase is specific of  
13 P2RX7, the experiment was also done on *p2rx7<sup>-/-</sup>* mice, where the increase of TO-PRO<sup>TM</sup>-3  
14 fluorescence in the ATP group was not observed and was similar to WT-PBS mice (Fig 2b).  
15 No difference was observed in the percentage of TO-PRO<sup>TM</sup>-3 positive cells (supp Fig 1a-c).  
16 These results suggest that TO-PRO<sup>TM</sup>-3 fluorescence after ATP administration was specific  
17 to P2RX7 and indicative of its activation state.

18 To go further, we analyzed TO-PRO<sup>TM</sup>-3 fluorescence in immune and non-immune cells. We  
19 show that WT-ATP mice exhibit an enhanced fluorescence compared to WT-PBS mice only  
20 in immune cells (Fig 2c), and that was only observed in WT mice, demonstrating furthermore  
21 the requirement of P2RX7 for the TO-PRO<sup>TM</sup>-3 signal observed.

22 We also show that TO-PRO<sup>TM</sup>-3<sup>+</sup> cells express P2RX7. However, percentage of P2RX7<sup>+</sup> cells  
23 among TO-PRO<sup>TM</sup>-3<sup>+</sup> cells was decreased in ATP-mice (Fig 2d,e), but not in TO-PRO<sup>TM</sup>-  
24 3<sup>+</sup>CD45<sup>-</sup> cells (Fig 2e). This is not surprising since it has been shown that sustained activation  
25 of P2RX7 leads to the internalization of the receptor<sup>14</sup> or its cleavage<sup>15</sup> after its activation,  
26 explaining the possibility of TO-PRO<sup>TM</sup>-3<sup>+</sup>P2RX7<sup>-</sup> cells.



1 **Fig 2. P2RX7 is activated *in vivo***

- 2 a. Dotplot gated on live single cells of WT mice whole lungs  
 3 b. GMFI of TO-PRO<sup>TM</sup>-3<sup>+</sup> cells in whole lung of WT and *p2rx7*<sup>-/-</sup> mice.  
 4 c. GMFI of TO-PRO<sup>TM</sup>-3<sup>+</sup> cells in CD45<sup>+</sup> cells (left) and CD45<sup>-</sup> cells (right) in WT and *p2rx7*<sup>-/-</sup> mice  
 5 d. Percentage of P2RX7<sup>+</sup> cells among TO-PRO<sup>TM</sup>-3<sup>+</sup> cells, e. among TO-PR<sup>TM</sup>-O3+CD45<sup>+</sup> cells  
 6 (left) and TO-PRO<sup>TM</sup>-3+CD45<sup>-</sup> cells (right)

7 One point represents one mouse, data is represented as mean±SEM. Two-tailed unpaired t-test.  
 8 \*p < 0.05. WT: Wildtype, GMFI: geomean fluorescence intensity

9

10 **P2RX7 is mainly expressed and activated in lung immune cells**

11 Since we observed a decrease of P2RX7 expression, we investigated furthermore its  
 12 expression in whole lungs of mice. We show that the expression of P2RX7 was decreased in  
 13 all cells (Fig 3a) but also in immune cells (Fig 3b), supporting furthermore the idea of an  
 14 internalization of P2RX7 after its activation. Moreover, we show that P2RX7 is more expressed  
 15 by immune cells than non-immune cells (Fig 3c). Even though WT-ATP mice show a decrease  
 16 of P2RX7 expression, P2RX7<sup>+</sup> cells show a higher TO-PRO<sup>TM</sup>-3 fluorescence in all cells (Fig  
 17 3d) and in immune cells (Fig 3e), meaning that P2RX7<sup>+</sup> cells are indeed activated by ATP.



**Fig 3.** TO-PRO™-3 fluorescence is increased in P2RX7<sup>+</sup> cells in WT mice

**a.** Percentage of P2RX7<sup>+</sup> cells in the whole lung of WT mice

**b.** Percentage of P2RX7<sup>+</sup> cells in CD45<sup>+</sup> and CD45<sup>-</sup> cells

**c.** GMFI of TO-PRO™-3 in P2RX7<sup>+</sup> cells

**d.** GMFI of TO-PRO™-3 in P2RX7<sup>+</sup>CD45<sup>+</sup> and P2RX7<sup>+</sup>CD45<sup>-</sup> cells

One point represents one mouse, data is represented as mean±SEM. Two-tailed unpaired t-test. \*p < 0.05, \*\*p < 0.01. WT: Wildtype, GMFI: geomean fluorescence intensity

15 Since TO-PRO™-3 fluorescence (Fig 2c) and P2RX7 expression (Fig 2e, Fig 3b) were  
 16 unchanged after ATP delivery in CD45<sup>-</sup> cells, we can speculate that P2RX7-expressing  
 17 immune cells are the main cells activated by ATP in the lung. However, we observed a  
 18 decrease of TO-PRO™-3 fluorescence in CD45<sup>-</sup> P2RX7<sup>+</sup> cells (fig 3d).

19

## 1 **Discussion**

2 This protocol was set up to assess P2RX7 activation *in vivo*, by taking advantage of its  
3 property of macropore formation. Among P2X receptors, a permeability for large cations was  
4 also described for P2RX2 and P2RX4. However, P2RX7 is activated by high concentrations  
5 of eATP (0.5 to 1 mM), whereas P2RX2 and P2RX4 are activated by much lower  
6 concentrations (3 to 10  $\mu$ M). Unlike P2RX7, P2RX2 and P2RX4 receptors desensitize after  
7 ATP stimulation. Even though P2RX4 is broadly expressed in most tissues of the body, it is  
8 preferentially localized in lysosomes where the acidity prevents its activation <sup>16</sup>. Based on  
9 these properties, we hypothesized that the macropore activity of P2RX2 and P2RX4 will not  
10 interfere with our assay. This is indeed the case since no increase in TO-PRO<sup>TM</sup>-3 signal was  
11 observed in *p2rx7*<sup>-/-</sup> mice (Fig 2b).

12 Our protocol allows the measurement of P2RX7 activation in lungs and is based on TO-  
13 PRO<sup>TM</sup>-3 uptake by cells and detection by flow cytometry. Flow cytometry was previously  
14 shown as a sensitive tool to study P2RX7 activation *in vitro* <sup>12</sup> and is also efficient for analysis  
15 of an *in vivo* activation of the receptor as shown in this study. Moreover, flow cytometry allows  
16 the reduction of background noise by excluding non P2RX7-dependent TO-PRO<sup>TM</sup>-3 staining  
17 of dead cells. The other advantage of using flow cytometry is coupling TO-PRO<sup>TM</sup>-3 with other  
18 surface markers to distinguish P2RX7 activation at the single cell level. We only studied its  
19 activation in immune versus non-immune cells, however, one can easily increase the number  
20 of markers during the surface staining step to precisely identify the subtypes of immune and  
21 non-immune cells activated by ATP.

22 To our knowledge, we show for the first time in a direct manner that P2RX7 is mainly activated  
23 in lung immune cells of mice, as per an increase of TO-PRO<sup>TM</sup>-3 fluorescence. P2RX7 has a  
24 pro-inflammatory role since it releases IL-1 $\beta$  and is at the etiology of inflammatory diseases.  
25 Nonetheless, direct activation of the receptor i.e. calcium influx or macropore formation was  
26 never assessed *in vivo*. However, expression of P2RX7 on hematopoietic cells <sup>17,18</sup>, ATP

1 levels<sup>19,20</sup> and IL-1 $\beta$  release<sup>21,22</sup> were shown *in vivo* to be important for airway inflammation  
2 in mouse models. Even so, these experiments require the use of transgenic and chimeric mice  
3 and do not evaluate the receptor activation status. This protocol could be used instead for  
4 accurate and easier assessment of the activation of P2RX7.

5 We also show that ATP did not enhance TO-PRO<sup>TM</sup>-3 fluorescence in non-immune cells. Lung  
6 CD45<sup>-</sup> cells comprise endothelial cells, fibroblasts, and alveolar epithelial cells of type I (AEC  
7 I) and type II (AEC II). They all express P2RX7 except for AEC II. It has been shown *in vitro*  
8 and *ex vivo* studies that they express a functional receptor (macropore opening, calcium influx,  
9 IL-1 $\beta$  release)<sup>23,24</sup> but we do not seem to detect an activation *in vivo* with our protocol by  
10 measuring TOPRO-3 fluorescence in CD45<sup>-</sup> cells. This could be due to the lower levels of  
11 expression of P2RX7 in CD45<sup>-</sup> cells than in CD45<sup>+</sup> cells (Fig 3b, supp Fig 2b) and the  
12 heterogeneity of the amplitude of its activation in these cells that is lost when looking at overall  
13 CD45<sup>-</sup> cells. One possible way to overcome this is to analyze TO-PRO<sup>TM</sup>-3 fluorescence in  
14 each CD45<sup>-</sup> cell type by including specific markers. Surprisingly, we observed that TO-PRO<sup>TM</sup>-  
15 3 fluorescence was decreased in P2RX7<sup>+</sup>CD45<sup>-</sup> cells in ATP-mice (Fig 3d). It should be noted  
16 that the intensity of TOPRO<sup>TM</sup>-3 fluorescence in P2RX7-expressing CD45<sup>-</sup> cells (Fig 3d) is  
17 identical to the background value observed in *p2rx7*<sup>-/-</sup> mice (Fig 2c) accompanied by  
18 unchanged P2RX7 expression (Fig 3b, supp Fig2b). Thus, these observations support the  
19 background signal of TO-PRO-3 fluorescence rather than an ATP-related effect.

20 We have also shown that the expression of P2RX7 was decreased in WT-ATP mice. P2RX7  
21 activation by ATP stimulates membrane internalization<sup>25</sup> that results to the loss of expression  
22 of many surface proteins<sup>26,27</sup> including P2RX7<sup>13,14</sup>. Indeed, prolonged stimulation with high  
23 levels of ATP results in decreased surface expression and internalization of the receptor in  
24 RAW cells<sup>14</sup>, Caski cells and HEK 293 transfected with the human P2RX7<sup>13</sup>, at least 15 to  
25 30 minutes after its activation depending on the cell type. Decreased expression of the  
26 receptor was also reported on human and mouse monocytes after sustained stimulation with

1 bzATP <sup>28</sup>. Moreover, it has been shown that sustained activation of P2RX7 induces its  
2 cleavage at the plasma membrane by MMP-2, starting 15 minutes after its activation <sup>15</sup>.  
3 Altogether, these observations support the decrease of P2RX7 surface expression in lungs of  
4 mice due to high levels of ATP administration and duration of P2RX7 activation in this study.

5 Even though this protocol successfully detects P2RX7 activation in the lungs, it can be  
6 adapted for studying its activation in other organs by giving TO-PRO<sup>TM</sup>-3 to the mice by  
7 intravenous (i.v.) route. YO-PRO-1 (an analog of TO-PRO<sup>TM</sup>-3) and propidium iodide (PI) are  
8 also used to study macropore formation. They have been given i.v. in mice and rats to study  
9 *in vivo* cell death in lungs <sup>29,30</sup>, brain <sup>31,32</sup> and liver <sup>33</sup>. However, TO-PRO<sup>TM</sup>-3's time to access  
10 and penetrate the organ of interest should be carefully assessed in order to study the  
11 activation of P2RX7.

12 To go further, this protocol could also be helpful to determine the *in vivo* efficacy of compounds  
13 targeting P2RX7, to potentially adapt their administration route or their dosage or even to  
14 identify the targeted cell type of the compounds. HEI3090 is a novel positive modulator of  
15 P2RX7 that enhances calcium influx, macropore opening and IL-18 release, as determined by  
16 *in vitro* and *ex vivo* experiments. Although we showed that HEI3090 enhances IL-18 release  
17 *in vivo* <sup>5</sup>, it is of interest to study its impact on P2RX7 activation *in vivo*, especially since  
18 HEI3090 is a promising molecule for treatment of lung cancer <sup>5</sup>.

19

20

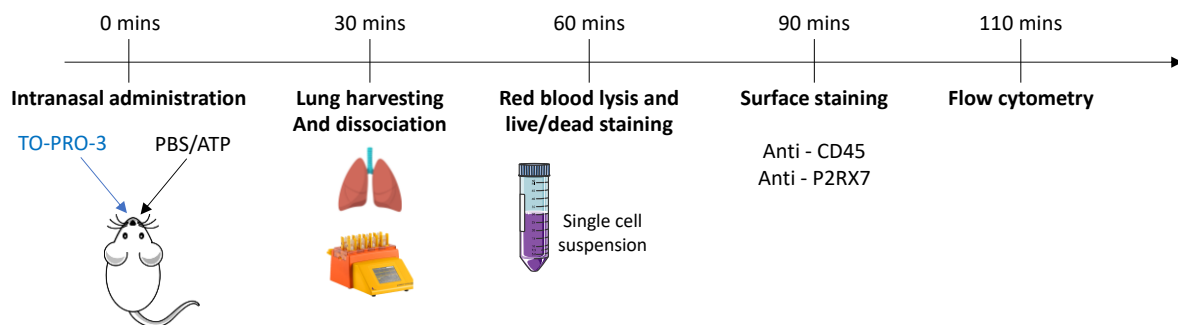


## 1 **Methods**

2 The described methods include the description of the work, along with general guidelines that  
3 can be used for implementing the strategy with various compounds described to modulate  
4 P2RX7 activity.

5 **Animals:** 8 weeks old WT C57BL/6J Olahsd mice are from Envigo, (Gannat, France), and 8  
6 weeks old *p2rx7<sup>-/-</sup>* (B6.129P2-P2rx7tm1Gab/J) are from the Jackson Laboratory. Mice were  
7 housed under standardized light–dark cycles in a temperature-controlled air-conditioned  
8 environment under specific pathogen-free conditions at IRCAN, Nice, France, with free access  
9 to food and water. All experiments were approved by the committee for Research and Ethics  
10 of the local authorities (CIEPAL #772, protocol number MESRI APAFIS #33150-  
11 2021091413316813) and followed the European directive 2010/63/UE, in agreement with the  
12 ARRIVE guidelines. Experiments were performed in accord with animal protection  
13 representative at IRCAN.

14 **Protocol description:** the schematic protocol is presented in fig 4. Measuring P2RX7 activity  
15 *in vivo* requires 5 main steps:



16

### 17 **Time 0 - Intranasal administration**

- 18 1. Anesthetize mouse i.p. with a mixture of 25 mg/kg ketamine and 2.5 mg/kg xylazine  
19 using 1 ml syringe with a 26G needle.
- 20 2. Place mouse in a box with 5% isoflurane for 1 minute.

- 1 3. When asleep, mouse is held upright and was given 25  $\mu$ l of TO-PRO<sup>TM</sup>-3 (1  $\mu$ M/kg) in  
2 one nostril then 25  $\mu$ l of ATP (100 mM) or 1X PBS in another using a micropipette.  
3 *!\ Intranasal administration should be slow and follow the respiration rate of the mouse.*  
4 *!\ Mice should be anesthetized and processed for intranasal delivery one by one.*  
5 *!\ As soon as the 25  $\mu$ l+25  $\mu$ l are completely taken up by the mouse, start the 30*  
6 *minutes timer.*

### 7 **Time 30 minutes – Mouse sacrifice and lung harvesting**

- 8 1. Sacrifice mouse by cervical elongation  
9 2. Spray mouse thorax with 70% ethanol. Harvest lungs using fine and sharp scissors  
10 and pliers.  
11 3. Separate the lobes. Transfer the lobes into a GentleMACS<sup>TM</sup> C-tube (Miltenyi Biotech)  
12 containing the enzymatic buffer for dissociation (Lung dissociation kit, Miltenyi Biotech)  
13 4. Dissociate lungs using the 37\_m\_LDK1 program on a GentleMACS<sup>TM</sup> Octo dissociator  
14 with heaters (Miltenyi Biotech)  
15 5. At the end of the program, resuspend cells and pass them through a 100  $\mu$ m cell  
16 strainer on top of a 50 ml tube for single cell suspensions. Wash the GentleMACS<sup>TM</sup>  
17 C-tube with 1X Buffer S (Lung dissociation kit, Miltenyi Biotech) for maximum retrieval  
18 of cells and pass them through the 100  $\mu$ m cell strainer.  
19 6. Discard the cell strainer and centrifuge the tube at 1200 rpm 4°C for 5 minutes.  
20 *!\ Keep cells in the dark at all times, and on ice except during the dissociation program.*

### 21 **Time 60 minutes – Red blood lysis and live/dead staining**

- 22 1. Aspirate completely the supernatant and resuspend pellet gently with 1 ml of ice-cold  
23 ACK lysis buffer (Gibco) for 30 seconds to lyse red blood cells.  
24 2. Add 30 ml of 1X PBS for stopping the reaction.  
25 3. Centrifuge at 1200 rpm 4°C for 5 minutes  
26 4. Count cells

- 1 5. Add 1 million of lung single cells in 150  $\mu$ l 1X PBS in a 5 ml polypropylene tube
- 2 6. Add 150  $\mu$ l of Green Live/Dead stain (2X) (Invitrogen) or 1X PBS (unstained control)
- 3 into the 5 ml polypropylene tube
- 4 *!\ Prepare appropriate number of samples without Live/Dead staining for single-*
- 5 *stained controls*
- 6 7. Vortex and incubate in the dark at room temperature for 30 minutes
- 7 8. Add 3 ml of FACS buffer (PBS 5% FBS 0.5% EDTA) into the 5 ml polypropylene tube
- 8 9. Centrifuge at 1200 rpm 4°C for 5 minutes
- 9 10. Aspirate supernatant completely and resuspend cells in 100  $\mu$ l FACS Buffer
- 10 *!\ Keep cells in the dark at all times, and on ice unless otherwise stated.*

#### 11 **Time 90 minutes – Surface staining**

- 12 1. Transfer cell suspension to a 96 well V plate
- 13 2. Centrifuge plate at 1300 rpm 4°C for 3 minutes
- 14 3. Flick the plate
- 15 4. Block Fc receptor using anti-CD16/32 (dil 1/100, BD Biosciences) diluted in FACS
- 16 Buffer (1X PBS, 5% FBS, 0.5% EDTA) in the dark under agitation for 10 minutes
- 17 5. Centrifuge plate at 1300 rpm 4°C for 3 minutes
- 18 6. Flick plate
- 19 7. Add antibody mix diluted in FACS buffer and homogenize immediately using a
- 20 multichannel pipette.
- 21 Antibodies: CD45 BUV395 (dil 1/100, BD Biosciences), P2RX7 PE (dil 1/8, Biolegend)
- 22 or isotype control rat IgG2b  $\kappa$  PE (dil 1/8, Biolegend)
- 23 *!\ Prepare appropriate single-stained controls*
- 24 8. Incubate at 4°C in the dark under agitation for 20 minutes
- 25 9. Add 100  $\mu$ l of FACS buffer per well using a multichannel pipette
- 26 10. Centrifuge plate at 1300 rpm 4°C for 3 minutes
- 27 11. Flick the plate

1 12. Resuspend cell in 100 µl of FACS buffer

2 *!\\ Keep cells in the dark at all times, and on ice.*

3 **Time 110 minutes – Flow cytometry analysis**

4 1. Cells were acquired using the CytoFLEX LX (Beckman Coulter)

5 2. Samples were analyzed using FlowJo (LLC)

6

7 **Materials**

8 1. 1 ml syringe omnifix-F (Braun, catalog number 9161406V)

9 2. 26G needle (BD Microlance 3, catalog number 304300)

10 3. Pipette

11 4. Pipette tips

12 5. Fine scissors

13 6. Sharp scissors

14 7. Pliers

15 8. GentleMACS™ C-tube (Miltenyi Biotech, catalog number 130-093-237)

16 9. 100 µm cell strainer (Falcon, catalog number 352360)

17 10. Polypropylene 50 ml tube (Falcon, catalog number 352070)

18 11. Polypropylene 5 ml tube (Falcon, catalog number 352096)

19 12. 96-well clear V bottom plates (Greiner, catalog number 651101)

20 13. Serological pipette (Falcon, catalog number 357543)

21 14. Serological pipette gun

22 15. Multi-channel pipette (Starlab, catalog number 57112-330)

23 **Reagents**

24 1. Ketamine (Virbac, catalog number 03597132111010)

- 1 2. Xylazine (Sedaxylan, Dechra, catalog number 08714225151523)
- 2 1. isoflurane / Aerrane (Baxter, catalog number DAGG9223)
- 3 2. TO-PRO™-3 (Life Technologies, catalog number T3605)
- 4 3. ATP (Sigma-Aldrich, catalog number A6419)
- 5 4. 1X Dulbecco's PBS (Gibco, catalog number 14190144)
- 6 5. 70% ethanol
- 7 6. Double distilled water
- 8 7. 20X Buffer S, enzyme D and enzyme A from the mouse lung dissociation kit (Miltenyi
- 9 Biotech, catalog number 130-095-927)
- 10 8. ACK lysis buffer (Gibco, catalog number A1049201)
- 11 9. LIVE/DEAD™ fixable green dead cell staining kit (Invitrogen, catalog number L23101)
- 12 10. Fetal bovine serum (FBS)
- 13 11. Ethylenediaminetetraacetic acid (EDTA) (Invitrogen, catalog number 15575020)
- 14 12. CD16/32 (BD Biosciences, catalog number 553141)
- 15 13. CD45 BUV395 (BD Biosciences, catalog number 564279)
- 16 14. P2RX7 PE (Biolegend, catalog number 148703)
- 17 15. Rat IgG2b κ PE (Biolegend, catalog number 400607)

## 18 **Equipment**

- 19 1. Anesthesia machine and box (Anesteo)
- 20 2. GentleMACS™ Octo dissociator with heaters (Miltenyi Biotech, catalog number 130-
- 21 096-427)
- 22 3. Tube and plate centrifuge (Thermofischer scientific, catalog number 75009527)
- 23 4. Plate agitator
- 24 5. CytoFLEX LX (Beckman Coulter)

## 25 **Reagent preparation**

26 *!\\ Prepare all reagents in sterile conditions using a PSM II tissue culture hood*

- 1        1. Anesthetics
- 2            Prepare 25 mg/kg of ketamine and 2.5 mg/kg of xylazine in 1X Dulbecco's PBS as per
- 3            250 µl of mix per 25 g of mouse.
- 4        2. Lung dissociation buffer
- 5            Dilute 20X Buffer S in double distilled water and store at 4°C. Resuspend enzyme A
- 6            and enzyme D with 1X Buffer S according to manufacturer's instructions. Add 2.4 ml
- 7            of 1X Buffer S, 15 µl of enzyme A and 100 µl of enzyme D per GentleMACS™ C-tube
- 8            (Miltenyi Biotech)
- 9        3. ATP
- 10           Prepare 100 mM stock of ATP in sterile 1X PBS, pH 6.8, aliquot and store at -80°C
- 11           *! \ Avoid freeze/thaw cycles*
- 12        4. TO-PRO™-3
- 13           Dilute TO-PRO™-3 in 1X PBS to 1 µM/kg
- 14           *! \ Manipulate TO-PRO™-3 in the dark*
- 15           *! \ Aliquot TO-PRO™-3 stock and avoid freeze/thaw cycles*
- 16        5. LIVE/DEAD™ fixable green dead cell staining kit
- 17           Dilute LIVE/DEAD™ in 1X PBS to 2X working concentration per tube. Add 0.4 µL
- 18           LIVE/DEAD™ in 150µL per tube.
- 19           *! \ Manipulate LIVE/DEAD™ green in the dark*
- 20        6. *! \ Prepare mix of appropriate volume*
- 21        7. FACS Buffer
- 22           Prepare 500 ml of FACS Buffer containing 1X Dulbecco's PBS, 5% FBS, 0.5% EDTA
- 23           and store at 4°C
- 24           *! \ Keep on ice at all times*
- 25        8. Antibody mix cocktail
- 26           Dilute CD45 BUV395 (dil 1/100) and P2RX7 PE (dil 1/8) or isotype control rat IgG2b κ
- 27           PE (dil 1/8) in FACS Buffer
- 28           *! \ Keep on ice at all times and manipulate in the dark*

1 **Software**

- 2 1. CytExpert (Beckman Coulter)
- 3 2. FlowJo (LLC) or any other flow cytometry software
- 4 3. Graphpad prism

5 **Statistical analyses:**

6 All analyses were carried out using Prism software (GraphPad). Mouse experiments were  
7 performed on at least  $n = 5$  individuals, as indicated. Mice were equally divided for treatments  
8 and controls. Data is represented as mean values and error bars represent SEM. Two-tailed  
9 Mann–Whitney and unpaired t-test were used to evaluate the statistical significance between  
10 groups.

11

# 1 **Declarations**

## 2 **Author's contribution:**

3 S.J.H. and V.V.-C. conceived and designed the study. S.J.H. developed the methodology.  
4 S.J.H, T.J. and V.V.-C. acquired the data (provided animals, provided facilities, and so on).  
5 S.J.H, P.H. and V.V.-C. analyzed and interpreted the data. S.J.H. and V.V.-C. wrote the  
6 manuscript. All authors reviewed the manuscript.

7 **Funding:** This research was funded by the association for the research on cancer, france  
8 (ARC), the French Government (National Research Agency, ANR through the "Investments  
9 for the Future": program reference #ANR-11-LABX-0028-01), S.J.H. is funded by the "Ligue  
10 Nationale Contre le Cancer" and the "Fondation pour la recherche medicale" grant number  
11 #FDT202106013099 and ARC (grant number ARCTHEM2021020003478).

12 **Availability of data and materials:** All data generated and analyzed during this study are  
13 included in this article and its supplementary files

14 **Ethics Approval:** All experiments were approved by the committee for Research and Ethics  
15 of the local authorities (CIEPAL #772, protocol number MESRI APAFIS #33150-  
16 2021091413316813) and followed the European directive 2010/63/UE, in agreement with  
17 the ARRIVE guidelines.

18 **Consent to participate:** not applicable

19 **Consent for publication:** not applicable

20 **Competing interests:** the authors declare that they have no competing interests

21

22



## 1 **References**

- 2 1. Pellegatti, P. *et al.* Increased level of extracellular ATP at tumor sites: in vivo imaging  
3 with plasma membrane luciferase. *PLoS One* **3**, e2599 (2008).
- 4 2. Kopp, R., Krautloher, A., Ramírez-Fernández, A. & Nicke, A. P2X7 Interactions and  
5 Signaling – Making Head or Tail of It. *Frontiers in Molecular Neuroscience* **12**, (2019).
- 6 3. Surprenant, A., Rassendren, F., Kawashima, E., North, R. A. & Buell, G. The cytolytic  
7 P2Z receptor for extracellular ATP identified as a P2X receptor (P2X7). *Science* **272**, 735–8  
8 (1996).
- 9 4. Perregaux, D. G., McNiff, P., Laliberte, R., Conklyn, M. & Gabel, C. A. ATP acts as  
10 an agonist to promote stimulus-induced secretion of IL-1 beta and IL-18 in human blood. *J*  
11 *Immunol* **165**, 4615–23 (2000).
- 12 5. Douguet, L. *et al.* A small-molecule P2RX7 activator promotes anti-tumor immune  
13 responses and sensitizes lung tumor to immunotherapy. *Nat Commun* **12**, 653 (2021).
- 14 6. Homerin, G. *et al.* Pyroglutamide-Based P2X7 Receptor Antagonists Targeting  
15 Inflammatory Bowel Disease. *J Med Chem* **63**, 2074–2094 (2020).
- 16 7. Gondé, H. *et al.* A Methodological Approach Using rAAV Vectors Encoding  
17 Nanobody-Based Biologics to Evaluate ARTC2.2 and P2X7 In Vivo. *Front Immunol* **12**,  
18 704408 (2021).
- 19 8. di Virgilio, F., Schmalzing, G. & Markwardt, F. The Elusive P2X7 Macropore. *Trends*  
20 *Cell Biol* **28**, 392–404 (2018).
- 21 9. Ou, A., Gu, B. J. & Wiley, J. S. The scavenger activity of the human P2X7 receptor  
22 differs from P2X7 pore function by insensitivity to antagonists, genetic variation and sodium  
23 concentration: Relevance to inflammatory brain diseases. *Biochim Biophys Acta Mol Basis*  
24 *Dis* **1864**, 1051–1059 (2018).
- 25 10. Kubick, C., Schmalzing, G. & Markwardt, F. The effect of anions on the human P2X7  
26 receptor. *Biochim Biophys Acta* **1808**, 2913–22 (2011).

- 1 11. Inquimbert, P. *et al.* Peripheral nerve injury produces a sustained shift in the balance  
2 between glutamate release and uptake in the dorsal horn of the spinal cord. *Pain* **153**, 2422–  
3 2431 (2012).
- 4 12. Barczyk, A. *et al.* Flow cytometry: An accurate tool for screening <sc>P2RX7</sc>  
5 modulators. *Cytometry Part A* **99**, 793–806 (2021).
- 6 13. Feng, Y.-H. *et al.* ATP stimulates GRK-3 phosphorylation and beta-arrestin-2-  
7 dependent internalization of P2X7 receptor. *Am J Physiol Cell Physiol* **288**, C1342-56  
8 (2005).
- 9 14. Hiken, J. F. & Steinberg, T. H. ATP downregulates P2X7 and inhibits osteoclast  
10 formation in RAW cells. *Am J Physiol Cell Physiol* **287**, C403-12 (2004).
- 11 15. Young, C. N. J. *et al.* Sustained activation of P2X7 induces MMP-2-evoked cleavage  
12 and functional purinoceptor inhibition. *J Mol Cell Biol* **10**, 229–242 (2018).
- 13 16. Müller, T. *et al.* A potential role for P2X7R in allergic airway inflammation in mice and  
14 humans. *Am J Respir Cell Mol Biol* **44**, 456–64 (2011).
- 15 17. Lucattelli, M. *et al.* P2X7 receptor signaling in the pathogenesis of smoke-induced  
16 lung inflammation and emphysema. *Am J Respir Cell Mol Biol* **44**, 423–9 (2011).
- 17 18. Riteau, N. *et al.* Extracellular ATP is a danger signal activating P2X7 receptor in lung  
18 inflammation and fibrosis. *Am J Respir Crit Care Med* **182**, 774–83 (2010).
- 19 19. Baxter, M. *et al.* Role of transient receptor potential and pannexin channels in  
20 cigarette smoke-triggered ATP release in the lung. *Thorax* **69**, 1080–9 (2014).
- 21 20. Monção-Ribeiro, L. C. *et al.* P2X7 receptor modulates inflammatory and functional  
22 pulmonary changes induced by silica. *PLoS One* **9**, e110185 (2014).
- 23 21. Eltom, S. *et al.* P2X7 receptor and caspase 1 activation are central to airway  
24 inflammation observed after exposure to tobacco smoke. *PLoS One* **6**, e24097 (2011).
- 25 22. Mishra, A. *et al.* Purinergic P2X7 receptor regulates lung surfactant secretion in a  
26 paracrine manner. *J Cell Sci* **124**, 657–68 (2011).
- 27 23. Benzaquen, J. *et al.* Alternative splicing of P2RX7 pre-messenger RNA in health and  
28 diseases: Myth or reality? *Biomed J* **42**, 141–154 (2019).

- 1 24. Kochukov, M. Y. & Ritchie, A. K. P2X7 receptor stimulation of membrane  
2 internalization in a thyrocyte cell line. *J Membr Biol* **204**, 11–21 (2005).
- 3 25. Qu, Y. & Dubyak, G. R. P2X7 receptors regulate multiple types of membrane  
4 trafficking responses and non-classical secretion pathways. *Purinergic Signal* **5**, 163–73  
5 (2009).
- 6 26. Arguin, G. *et al.* The loss of P2X7 receptor expression leads to increase intestinal  
7 glucose transit and hepatic steatosis. *Sci Rep* **7**, 12917 (2017).
- 8 27. Amadio, S. *et al.* Modulation of P2X7 Receptor during Inflammation in Multiple  
9 Sclerosis. *Front Immunol* **8**, 1529 (2017).
- 10 28. Chagnon, F. *et al.* In vivo intravital endoscopic confocal fluorescence microscopy of  
11 normal and acutely injured rat lungs. *Lab Invest* **90**, 824–34 (2010).
- 12 29. Kanou, T. *et al.* Inhibition of regulated necrosis attenuates receptor-interacting protein  
13 kinase 1-mediated ischemia-reperfusion injury after lung transplantation. *J Heart Lung*  
14 *Transplant* **37**, 1261–1270 (2018).
- 15 30. Unal Cevik, I. & Dalkara, T. Intravenously administered propidium iodide labels  
16 necrotic cells in the intact mouse brain after injury. *Cell Death Differ* **10**, 928–9 (2003).
- 17 31. Whalen, M. J. *et al.* Acute plasmalemma permeability and protracted clearance of  
18 injured cells after controlled cortical impact in mice. *J Cereb Blood Flow Metab* **28**, 490–505  
19 (2008).
- 20 32. Tsurusaki, S., Kanegae, K. & Tanaka, M. In Vivo Analysis of Necrosis and  
21 Ferroptosis in Nonalcoholic Steatohepatitis (NASH). *Methods Mol Biol* **2455**, 267–278  
22 (2022).

23

24





## DISCUSSION ET PERSPECTIVES



Beaucoup de patients atteints de cancer du poumon sont ou deviennent résistants aux immunothérapies alors que les patients atteints de FPI n'ont aucun traitement curatif, d'où l'importance de contourner ces résistances et trouver de nouvelles cibles thérapeutiques.

Mes travaux de thèse ont permis de mettre en avant une stratégie thérapeutique prometteuse qui consiste en l'activation du récepteur purinergique P2RX7 et de la voie NLRP3/IL-18 dans le cancer du poumon (**Article I**) et dans la fibrose pulmonaire (**Article II**). Cette stratégie repose sur la modulation de P2RX7 avec un modulateur positif nouvellement synthétisé par nos collaborateurs chimistes, appelé HEI3090. Cette molécule nécessite la présence de fortes concentrations d'ATPe pour augmenter l'activation de P2RX7 : de telles concentrations sont présentes dans le site tumoral et dans les tissus inflammatoires, dont les tissus fibrosés. Ainsi, l'activation de P2RX7 par HEI3090 se limiterait aux tissus inflammés. Dans le but d'analyser l'activation de P2RX7 en conditions physiologiques, notamment par HEI3090, j'ai développé durant ma thèse un protocole permettant de le faire *in vivo* dans les poumons de souris (**Article III**).

## A. L'activation de P2RX7 favorise les réponses immunitaires antitumorales et sensibilise les tumeurs aux immunothérapies.

### 1. P2RX7 : un récepteur antitumoral

Grâce à HEI3090, nous avons mis en avant les propriétés antitumorales de P2RX7 dans des modèles murins immunocompétents de cancer du poumon. En effet, HEI3090 module la réponse immunitaire via l'activation de la voie ATPe/P2RX7/NLRP3/IL-18 dans les cellules immunitaires, en particulier dans les cellules dendritiques (Figure supplémentaire 1). Ces propriétés ont également été mises en avant par d'autres études concomitantes où l'inhibition de l'ectonucléotidase CD39 dans des modèles précliniques freine la croissance de plusieurs types de tumeurs (mélanome, colon, fibrosarcome, prostate) en activant cette même voie [501]–[503]. En effet, la stratégie sous-jacente dans ces études est de diminuer la production d'adénosine, métabolite de dégradation de l'ATPe par les CD73 et CD39, aux fortes propriétés immunosuppressives. L'ensemble de ces études souligne l'importance des fortes concentrations d'ATPe et de l'activation de P2RX7 pour une meilleure réponse immunitaire antitumorale. Combiner HEI3090 avec des anti-CD39/CD73 serait intéressant pour exploiter davantage les propriétés antitumorales de P2RX7, stratégie que nous avons discuté dans la **Revue II** [392] (Annexe).

Nous avons également montré *in vitro* que HEI3090 augmente la mort cellulaire induite par l'ATPe, cependant, cette mort n'est pas une mort immunogène étant donné que les souris ayant reçu des



cellules tumorales mourantes n'ont pas été protégées lors d'un challenge avec des cellules tumorales vivantes. De plus, le traitement des souris *p2rx7<sup>-/-</sup>* transplantées avec des cellules tumorales (exprimant P2RX7) n'avait aucun effet. Ces observations pourraient être expliquées par (i) un développement rapide de résistance à la mort induite par HEI3090 et/ou par (ii) l'insuffisance de la mort cellulaire induite par HEI3090 pour limiter la croissance tumorale. En effet, nous avons montré que les cellules immunitaires exprimant P2RX7, en particulier les cellules dendritiques, étaient nécessaires pour l'effet antitumoral de la molécule. Nous savons que HEI3090 augmente la production d'IL-18 par les cellules dendritiques; il aurait également été intéressant de voir si HEI3090 participait à la maturation de ces cellules (expression de molécules de costimulation), ainsi qu'à l'activation et prolifération des lymphocytes et à leur prolifération, ces fonctions étant affectées par P2RX7 [404], [489]–[491].

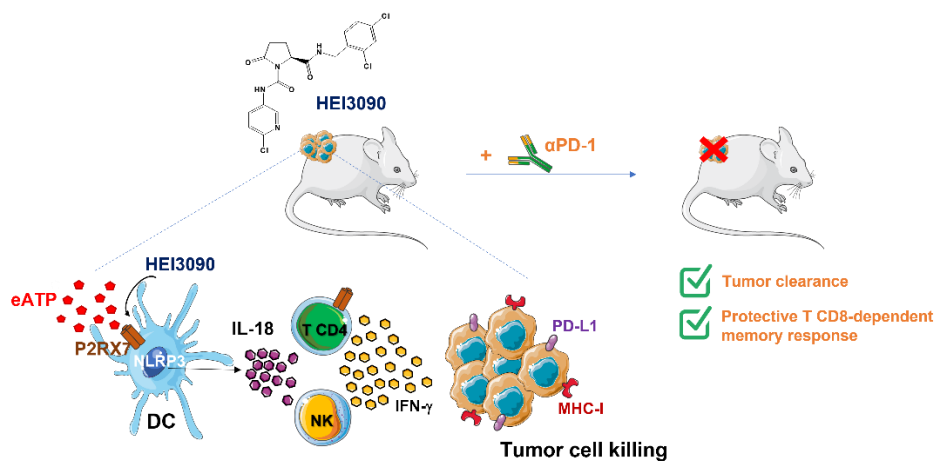


Figure supplémentaire 1. Le mécanisme d'action antitumoral de HEI3090. Publié dans *Nature Cancer Community* [504]

De plus, la réactivation de la réponse immunitaire par HEI3090 augmente l'immunogénicité des tumeurs (augmentation d'expression de PD-L1 et de CMH-I à la surface des cellules tumorales). De ce fait, la combinaison de HEI3090 avec des anti-PD-1 a guéri 80% des souris transplantées et a diminué de 60% la charge tumorale des souris avec un cancer de poumon induit par une mutation inducible *KRAS<sup>G12D</sup>*. De façon très intéressante, les souris guéries sont complètement protégées d'un re-challenge tumoral grâce à une réponse immunitaire mémoire par les lymphocytes T CD8+ (Figure supplémentaire 1). Ceci est en cohérence avec des études récentes montrant que P2RX7 est nécessaire à la survie et aux fonctions effectrices de ces cellules [505], [506], mais aussi pour le contrôle tumoral par les lymphocytes T CD8+ [507].

## 2. Universalité de la stratégie

Nous avons montré l'inhibition de la croissance tumorale pulmonaire dans deux modèles murins différents : un modèle transplanté et un modèle induit par l'oncogène *KRAS<sup>G12D</sup>* [508]. Ces deux

modèles ne sont pas métastatiques : ce choix nous a permis d'étudier spécifiquement la capacité de HEI3090 à contrôler la croissance tumorale. Il serait cependant intéressant de voir si HEI3090, seul ou en combinaison avec des immunothérapies, pourrait contrôler le développement de métastases, en utilisant par exemple un modèle murin avec deux mutations promotrices KRAS<sup>G12D</sup> p53 capable de métastaser [509]. Nous avons également montré l'efficacité de HEI3090 à inhiber la croissance des tumeurs transplantées avec des cellules de mélanomes murines et à les sensibiliser aux anti-PD-1, montrant que cette stratégie ne se limiterait pas aux tumeurs pulmonaires.

Les cellules tumorales murines LLC (Lewis Lung Carcinoma) utilisées dans cette étude sont décrites pour former un environnement tumoral immunosuppresseur, ne répondant pas aux immunothérapies [510]–[512], de même que le modèle KRAS<sup>G12D</sup> ayant une faible charge mutationnelle [513] ou les cellules murines de mélanome B16F10 insensibles aux anti-PD-1 [512], [514]. Or, HEI3090 a permis de sensibiliser ces tumeurs aux anti-PD-1, laissant penser que cette stratégie serait efficace même dans les tumeurs faiblement immunogènes résistantes aux immunothérapies.

D'un autre côté, les trois modèles utilisés ont des mutations promotrices différentes. Les LLC sont mutées KRAS<sup>G12C</sup> [515], les souris génétiquement modifiées sont mutées KRAS<sup>G12D</sup>, alors que les B16F10 n'ont aucune mutation [515]. Étant donné que le type de mutation peut affecter la réponse aux immunothérapies [516], l'activation de P2RX7 par HEI3090 pourrait être efficace quel que soit le statut mutationnel de la tumeur. Ceci pourrait être expliqué par le fait que HEI3090 ne cible pas les cellules tumorales mais les cellules immunitaires.

De plus, nos résultats semblent indiquer que la stratégie serait efficace dans plusieurs types de cancers. En effet, l'activation de la voie ATPe/P2RX7/NLRP3/IL-18 par des anti-CD39 est efficace dans 5 types de cancers différents, sensibles ou non aux anti-PD-1 [501]. Ainsi, ce résultat nous laisse penser que la stratégie d'activation de P2RX7 par HEI3090 pourrait également sensibiliser les tumeurs immunogènes aux immunothérapies, étant donné que certains patients ayant des tumeurs de ce type restent résistants aux traitements.

Cependant, au-delà du statut mutationnel et de l'immunogénicité de la tumeur, il pourrait être important de prendre en compte le niveau d'expression et la fonctionnalité de P2RX7 sur la cellule tumorale dans l'adoption de cette stratégie. En effet, cette stratégie repose sur le ciblage du récepteur exprimé par les cellules immunitaires, plutôt que de cibler le P2RX7 exprimé par la tumeur. Néanmoins, les cellules tumorales dans certains cancers pourraient surexprimer le récepteur P2RX7 [517]. Dans ce cas, il serait peut-être envisageable de cibler la cellule tumorale plutôt que le système immunitaire, en utilisant des inhibiteurs de P2RX7. Ceci est en cohérence avec une étude montrant

que l'inhibition du récepteur P2RX7 exprimé par la cellule tumorale ainsi que son activation par les cellules immunitaires sont bénéfiques [484]. Il existerait une balance entre l'expression et la fonctionnalité du récepteur par les cellules tumorales/immunitaires, qui permettrait de définir la stratégie d'activation/d'inhibition du récepteur.

Dans tous les cas, les résultats de cette étude concernant le mécanisme d'action de HEI3090 nous permettent de considérer cette molécule comme une immunothérapie visant à activer un nouveau point de contrôle immunitaire qui est P2RX7 (Annexe, **Revue II**).

### 3. L'IL-18 : pivot de l'immunité antitumorale

Cette étude a également fait ressortir l'IL-18 comme cytokine clé de la réponse antitumorale. En effet, la neutralisation de la cytokine ou l'utilisation de souris *il18<sup>-/-</sup>* a complètement aboli l'effet antitumoral de HEI3090 ainsi que la cytotoxicité des TILs. L'utilisation de souris *il18<sup>-/-</sup>* ou à l'administration d'IL-18 recombinante aux souris a permis de montrer les effets antitumoraux de l'IL-18 dans plusieurs modèles précliniques de cancer, comme dans le colon [518]–[520] ou le mélanome [520]–[523]. L'effet antitumoral de l'IL-18 dans ces études repose sur une meilleure activation et production d'IFN- $\gamma$  par les lymphocytes T CD4+ et NK, de façon cohérente avec nos résultats. Ainsi, l'IL-18 constitue une cytokine aux fortes propriétés antitumorales.

Cependant, l'administration d'IL-18 recombinante chez les patients, bien que tolérée, n'a pas montré d'effets bénéfiques [524]. En effet, ceci est dû à l'augmentation d'IL-18BP qui empêche l'activité de l'IL-18 [520]. Bien que nous n'ayons pas déterminé les niveaux d'IL-18BP dans notre étude, nous savons que HEI3090 augmente la production d'une IL-18 fonctionnelle vu la perte de l'effet antitumoral de la molécule dans les souris *il18<sup>-/-</sup>* mais également la perte de production d'IFN- $\gamma$  par les TILs lors de la neutralisation d'IL-18. Ainsi, la présence d'IL-18 libre active (non liée à l'IL-18BP, capable de produire de l'IFN- $\gamma$ ) est importante pour permettre les effets antitumoraux. De façon cohérente, il a été montré chez des patients atteints de CPNPC que le récepteur de l'IL-18 est exprimé par les lymphocytes T CD8+ fonctionnels (T-bet+EOMES+) infiltrant la tumeur qui sont par conséquent plus cytotoxiques (production d'IFN- $\gamma$ ) [525]. Il a également été montré que l'expression d'IL-18 et d'IFN- $\gamma$  était diminué dans les cancers du côlon [526], [527] et du mélanome [528] et que cette diminution d'expression était liée à une mauvaise survie, illustrant davantage le potentiel antitumoral de cette cytokine.

Étant donné que l'IL-18 est nécessaire pour l'effet antitumoral de HEI3090 et que HEI3090 sensibilise les tumeurs aux immunothérapies, nous pouvons présumer, bien que pas formellement démontré,

que l'IL-18 sensibilise les tumeurs pulmonaires aux anti-PD-1. Ceci pourrait être dû à l'augmentation d'expression de PD-1, montré pour être lié à la présence d'IL-18 [529]. Plusieurs études précliniques ont montré que l'IL-18 agit en synergie avec les immunothérapies [501], [502], [520], [523]. De façon cohérente, deux études concomitantes à la nôtre, ont montré que l'IL-18 constitue un biomarqueur prédictif de la réponse aux immunothérapies dans les cancers du poumon [530], [531]. Bien que ces études soient encourageantes, elles présentent des limitations. La première étude est basée sur une analyse transcriptomique de biopsies solides de patients CPNPC [531]. Cependant, l'accès à des biopsies n'est pas systématique dans la prise en charge du patient, et devient moins courante, depuis la mise en place des biopsies liquides, surtout pour les cancers de stades avancés. De plus, le niveau des transcrits IL-18 ne reflète pas l'activité de cette cytokine puisqu'elle est constitutivement exprimée et nécessite un clivage protéique pour être libérée. La deuxième étude est basée sur le niveau plasmatique d'IL-18 tout cancer du poumon confondu [530]. Ce dosage plasmatique a été fait dans une faible cohorte de patients atteints de CPNPC et de CPPC, ayant reçu ou non une chimiothérapie, cette dernière pouvant modifier les niveaux de PD-L1 et d'IL-18. De plus, les auteurs de cette étude n'ont pas pris en compte les niveaux d'IL-18BP pouvant impacter l'activité de l'IL-18.

Afin de savoir si l'IL-18 libre active pourrait constituer un biomarqueur prédictif des réponses aux immunothérapies dans le CPNPC, j'ai dosé l'IL-18, l'IL-18BP et le complexe IL-18/IL-18BP dans le plasma de patients atteints de CPNPC de stades IIIb/IV avant le début du traitement, mais également après 1 ou 2 cycles d'immunothérapies. L'étude est rétrospective, les plasmas collectés entre 2018 et 2019, fournis par les biobanques du Centre Antoine Lacassagne et du CHU de Nice. Les analyses des dosages sont en cours, les biostatisticiens cherchent à discriminer les patients répondeurs et non répondeurs aux immunothérapies en fonction de leurs niveaux d'IL-18. J'ai également procédé à des analyses *in silico* grâce à la base de données « The Cancer Genome Atlas ». J'ai pu montrer que l'expression de la voie P2RX7/NLRP3/IL-18 est sous-exprimée chez les patients atteints de CPNPC, en accord avec une étude montrant une diminution des niveaux plasmatiques d'IL-18 et d'IFN- $\gamma$  chez ces patients [525]. J'ai également montré que le récepteur de l'IL-18 corrèle avec l'expression de PD-1 et PD-L1. Ceci suggère une meilleure réponse aux anti-PD-1/PD-L1 en présence d'une activité IL-18.

D'un autre côté, il a été montré que les résistances secondaires aux anti-PD-1/PD-L1 sont dues à l'expression de TIM-3 [218], [219]. Une étude récente a montré que l'expression de TIM-3 inhibe l'activation de l'inflammasome et la production d'IL-18 par les cellules dendritiques, et que l'absence de TIM-3 restaure les propriétés antitumorales de l'IL-18 [532]. Ces résultats appuient la notion que l'IL-18 a d'une part un fort potentiel antitumoral et d'autre part sensibilise les tumeurs aux immunothérapies.

## B. La modulation de l'infiltrat immunitaire par l'activation de P2RX7 freine le développement d'une fibrose pulmonaire

### 1. P2RX7 : un récepteur anti-fibrosant

La deuxième étude effectuée durant ma thèse a confirmé le rôle immunomodulateur de P2RX7. En effet, nous avons montré que HEI3090 inhibe le développement d'une fibrose pulmonaire chez la souris. Cet effet passe par l'activation de la voie P2RX7/NLRP3/IL18 des cellules immunitaires et se traduit par une modification du profil immunitaire pulmonaire. Cependant, nous n'avons pas identifié la cellule ciblée par HEI3090. Étant donné la forte production d'IL-18, la modification du profil cytokinique des lymphocytes T et le niveau d'expression du récepteur sur les différentes populations immunitaires, nous pouvons envisager que HEI3090 cible les cellules dendritiques, comme dans le modèle tumoral. Ceci devrait être cependant démontré, en faisant par exemple des transferts adoptifs de cellules dendritiques WT dans des souris *p2rx7<sup>-/-</sup>*. Ces résultats valident des études montrant l'importance du système immunitaire pour freiner le développement de la maladie [533], [534].

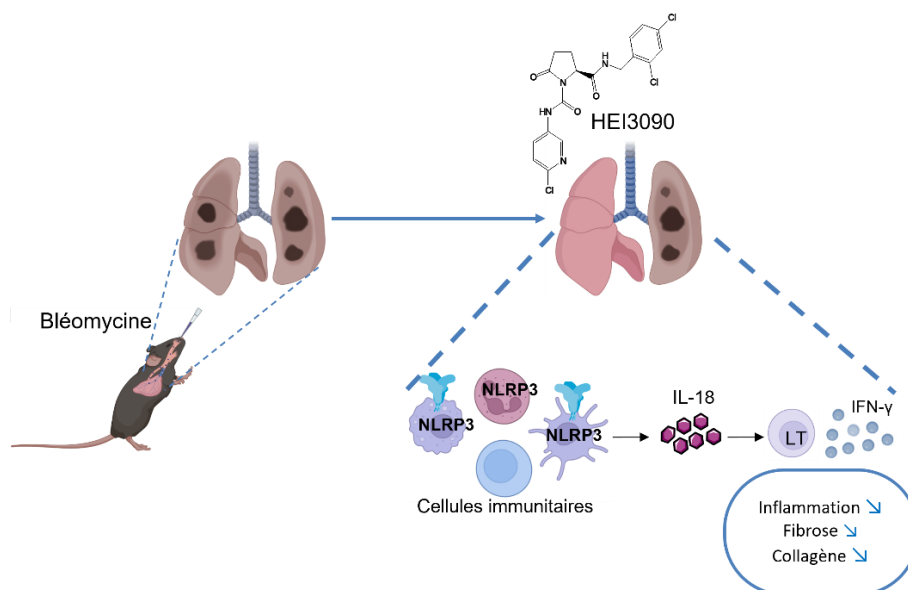


Figure supplémentaire 2. Le mécanisme d'action anti-fibrosant de HEI3090.

La fibrose pulmonaire est essentiellement caractérisée par une accumulation excessive de myofibroblastes conduisant à une accumulation de collagène dans le poumon et les stratégies thérapeutiques actuelles visent à diminuer ces accumulations. Il était donc important d'étudier la contribution du compartiment non immunitaire dans l'effet anti-fibrosant de HEI390. Nous avons pour cela diminué l'expression et l'activité du récepteur P2RX7 exprimé par les cellules immunitaires en faisant des transferts adoptifs répétés de splénocytes *p2rx7<sup>-/-</sup>* dans des souris WT; dans ces conditions, l'effet anti-fibrosant de HEI3090 est perdu. Cette expérience nous a permis de confirmer l'importance du rôle joué par les cellules immunitaires exprimant P2RX7 dans la résolution de la fibrose pulmonaire.

Cependant, nous ne pouvons pas exclure un rôle secondaire ou minoritaire du récepteur exprimé par les fibroblastes ou myofibroblastes. Étant donné la forte prolifération de ces cellules, leur résistance à la mort et le fait que P2RX7 soit un récepteur de mort, il serait intéressant de tester la capacité de HEI3090 à induire la mort de ces cellules : *ex vivo* sur des fibroblastes isolés de poumons fibrosés, ou en IHC sur des coupes histologiques de poumons de souris traités ou non avec HEI3090. D'un autre côté, il serait intéressant de tester la combinaison de HEI3090 avec la pirféridone ou le nintedanib, ces molécules ayant des mécanismes d'action distincts.

L'activation de P2RX7 est connue pour être pro-inflammatoire via l'activation de l'inflammasome NLRP3 et la libération d'IL-1 $\beta$ , notamment dans le modèle de fibrose induite par la bléomycine [299], [391], [394], [401], [535]. Cependant et de façon surprenante, l'activation de P2RX7 par HEI3090 n'a pas d'effet sur les niveaux plasmatiques d'IL-1 $\beta$ , elle augmente uniquement la production d'IL-18, ce qui pourrait expliquer les effets bénéfiques de cette activation. Nous avons en effet montré que HEI3090 diminue l'inflammation dans le poumon, avec notamment moins de monocytes inflammatoires et d'éosinophiles. Le pourcentage de macrophages alvéolaires restant inchangé par le traitement HEI3090, il serait très intéressant d'étudier la production de cytokines par ces cellules, afin de voir si l'activation de P2RX7 pourrait modifier le profil des macrophages en un profil anti-inflammatoire et anti-fibrosant.

Alors que le rôle de l'IL-18 dans la fibrose pulmonaire n'est pas clair [536]–[538]; l'IL-18 ainsi que NLRP3 ont un rôle protecteur contre l'inflammation dans des modèles précliniques de colites [539]–[541], ce qui est cohérent avec nos résultats. D'un autre côté, certaines études démontrent le rôle délétère de la signalisation IL-18/IL-18R, qui conduit à l'accumulation de fibroblastes pulmonaires sénescents ou à la différenciation des myofibroblastes [542], [543]. Dans notre étude, l'IL-18 est produite par les cellules immunitaires et s'est avérée protectrice et nécessaire pour l'effet anti-fibrosant et anti-inflammatoire de HEI3090. Même si l'augmentation d'IL-18 par HEI3090 est bénéfique, il serait important de vérifier que l'IL-18 produite ne favorise pas l'accumulation de cellules sénescents ou de myofibroblastes dans notre modèle. De plus, et malgré le faible nombre de patients, cette étude a mis en évidence le potentiel de l'IL-18 libre plasmatique comme biomarqueur prédictif dans la FPI. Nous cherchons aussi à corrélérer chez les patients FPI la présence d'un infiltrat immunitaire dans les foyers fibroblastiques avec les niveaux d'IL-18 libre plasmatique, l'analyse est en cours.

## 2. Rôle des lymphocytes T

Nous avons montré que HEI3090 favorise la production d'IL-18 ainsi que la production d'IFN- $\gamma$  par les lymphocytes T. Il serait toutefois important de montrer que l'IL-18 produite est active, soit en déterminant les niveaux d'IL-18 libre (IL-18 non liée à l'IL-18BP) soit en montrant que la production d'IFN- $\gamma$  dépend de la production d'IL-18, en neutralisant l'IL-18 *in vivo* par exemple.

De plus, il serait intéressant de montrer l'impact de la production d'IFN- $\gamma$  par HEI3090 sur le devenir de la fibrose, en neutralisant l'IFN- $\gamma$  *in vivo*. Ceci pourrait également être montré par des expériences de co-culture de lymphocytes T pulmonaires avec des fibroblastes et myofibroblastes, afin d'étudier la capacité des lymphocytes T à détruire la MEC, à limiter la TEM mais aussi à freiner la prolifération des fibroblastes et myofibroblastes. En effet, une étude a montré que les lymphocytes T humains inhibent la TEM de fibroblastes issus de patients FPI [544]. De plus, d'autres études ont montré que les myofibroblastes sont résistants à la mort induite par les lymphocytes T, dans les modèles précliniques mais également chez les patients FPI [533], [534], [545], [546]. Enfin, une étude récente a montré que les myofibroblastes limitent les capacités migratoires des lymphocytes T et les marginalisent hors du foyer fibroblastique [545]. Il serait alors également intéressant d'étudier la capacité d'infiltration des lymphocytes T au niveau des foyers fibroblastiques, par des expériences d'invasions cellulaires ou en IHC anti-CD3 et anti- $\alpha$ -SMA sur les poumons traités avec HEI3090.

Nous avons également montré que le traitement HEI3090 augmente la production d'IFN- $\gamma$  par rapport à l'IL-17A dans les lymphocytes T CD3+NK1.1- et pas dans les différents sous-types de lymphocytes T. L'IL-17A a été montrée pour favoriser les réponses Th2 [547]. Comme HEI3090 diminue la production d'IL-17A, il est envisageable que les niveaux des cytokines de type 2 soient également diminuées en réponse à HEI3090. L'étude de la production de cytokines de type 2 (IL-4, IL-5, IL-13) serait intéressante afin de valider davantage la capacité de HEI3090 à augmenter la production d'IFN- $\gamma$ . Il est important de noter que l'analyse de la production de cytokines a été faite sur les poumons entiers de souris, et comprend par conséquent les lymphocytes dans les zones saines, fibrosés et dans les iBALTs. Il serait ainsi intéressant de comparer le profil cytokinique des lymphocytes en fonction de leur localisation dans le poumon. D'un autre côté, il serait aussi possible que les lymphocytes T expriment des ICs, inhibant ainsi leur fonctionnalité et production de cytokine, en particulier l'IFN- $\gamma$ . En effet, des études récentes chez l'homme ont montré que les lymphocytes T CD4+ expriment des niveaux élevés de PD-1 alors que les myofibroblastes expriment des niveaux élevés PD-L1 [339], [548]. L'utilisation d'ICIs a permis de ralentir la progression de la maladie dans plusieurs modèles précliniques [339], [549], [550]. Toutefois, la capacité des lymphocytes à produire l'IFN- $\gamma$  après l'administration d'ICIs n'a pas été étudiée. Étant donné que HEI3090 agit en synergie avec les

immunothérapies dans le modèle tumoral, il serait intéressant de caractériser l'effet de HEI3090 sur le niveau d'expression des ICs dans le modèle bléomycine et de combiner la molécule avec des ICIs.

### 3. Limitations

Le manque de connaissance sur l'étiologie de la FPI fait qu'il est difficile d'avoir un modèle préclinique récapitulant parfaitement cette maladie. Le modèle de fibrose pulmonaire induit par la bléomycine est le modèle le plus couramment utilisé en recherche et a été nommé comme meilleur modèle pour les recherches précliniques [551]. Ce modèle est souvent critiqué à cause (i) de la rapidité de la mise en place d'une fibrose, (ii) d'une inflammation aiguë précédant la phase de fibrose et (iii) de la réversibilité de la fibrose, alors que la FPI chez l'homme est irréversible [552]. Cependant, ce modèle a permis de comprendre certains mécanismes qui ont conduit à l'élaboration des thérapies anti-fibrosantes actuelles (Pirféridone et nintedanib).

Le modèle induit par la bléomycine repose sur l'induction de dommages à l'ADN menant à la mort des cellules épithéliales (Jours 1-3) et à un recrutement de cellules inflammatoires (jours 3-9). Ceci induit une activation des fibroblastes et le dépôt de MEC à partir du jour 7. La fibrose se développe ainsi entre les jours 10 et 21. Nous avons montré que HEI3090 inhibe le développement de la fibrose et démontré son mécanisme d'action lors d'une administration prophylactique de la molécule. Vu que les premiers jours après l'administration de bléomycine sont associés à une forte inflammation, il est admis que cette phase correspondrait aux phases d'exacerbations des patients [553]. Ceci est d'autant plus intéressant étant donné la rapide détérioration des fonctions respiratoires et l'absence de traitements efficaces pour les épisodes d'exacerbations. Il était cependant important de tester l'effet de HEI3090 sur une fibrose établie. Nous avons donc administré la molécule 7 jours après l'induction de la fibrose et confirmé l'efficacité de notre molécule à réduire la fibrose pulmonaire dans ces conditions.

Dans le modèle de fibrose induite par la bléomycine, l'apparition de la fibrose repose sur la libération d'ATP par les cellules épithéliales et nécessite l'expression de P2RX7. [391]. Ainsi, l'expression de P2RX7 est nécessaire pour la mise en place du modèle alors que le rôle de P2RX7 dans la progression d'une fibrose établie n'est pas étudié, de même que la contribution des cellules hématopoïétiques exprimant ce récepteur. Il est alors important de caractériser le rôle de P2RX7 exprimé par les cellules immunitaires et non immunitaires dans un modèle de fibrose établie. Il serait aussi intéressant de tester la capacité de HEI3090 à inhiber la fibrose pulmonaire dans un autre modèle, comme le modèle induit par une surexpression de TGF $\beta$ .



Malgré ces limitations nous avons réussi à démontrer l'importance de l'axe P2RX7/NLRP3/IL-18 dans les cellules immunitaires pour inhiber le développement de la fibrose pulmonaire. Ce résultat nous a aussi permis de suggérer l'IL-18 libre comme potentiel biomarqueur de survie dans la FPI. Il reste cependant important d'augmenter le nombre de patients dans la cohorte afin de valider ce résultat, avant de tester son efficacité sur une plus large cohorte de patients. De plus, notre cohorte comporte majoritairement des patients caractérisés comme non-progresseurs. Un nombre équivalent de patients progresseurs/non progresseurs indiquerait d'une façon plus précise la capacité de l'IL-18 à prédire la survie des patients. De la même façon, il serait très intéressant de voir si les niveaux d'IL-18 libre permettraient de discriminer les patients avec une maladie progressive des patients ayant une fibrose stable. Il serait encore plus intéressant de voir si l'IL-18 libre peut servir comme biomarqueur pour personnaliser le choix du traitement anti-fibrosant, étant donné qu'aucune recommandation pour le choix de l'un ou l'autre n'est pour le moment disponible.

## C. L'activation de P2RX7 constitue une stratégie thérapeutique prometteuse

### 1. P2RX7 : une cible thérapeutique

Les deux axes principaux de ma thèse ont permis de mettre en avant P2RX7 comme cible thérapeutique dans le cancer et la fibrose pulmonaire. En plus de partager des facteurs de risques, ces deux pathologies ont des caractéristiques biologiques similaires : une prolifération cellulaire excessive, une résistance à la mort, la présence de myofibroblastes, l'accumulation de MEC, des mutations et modifications épigénétiques mais également une forte immunosuppression [554]. Ainsi, l'activation de P2RX7 constitue une stratégie thérapeutique commune dans deux pathologies similaires.

En effet, dans les modèles précliniques que nous avons utilisés, HEI3090 a permis de modifier le profil immunitaire immunosuppresseur vers un profil antitumoral et anti-fibrosant. Dans le modèle de fibrose induite par la bléomycine, le traitement par HEI3090 a permis de réduire le dépôt de collagène. Sachant que l'accumulation de la MEC, dont le collagène, constitue un frein à l'efficacité des immunothérapies, en inhibant l'accès et les fonctions des cellules effectrices antitumorales [137]–[139], on peut imaginer que l'efficacité antitumorale de HEI3090 passe aussi par ce mécanisme. Afin de le savoir, il suffirait d'analyser le dépôt de collagène dans les tumeurs traitées ou non avec HEI3090.

D'un autre côté, les deux pathologies, bien que distinctes, sont liées. Effectivement, la FPI est un facteur de risque connu de développer un cancer pulmonaire et constitue la comorbidité la plus sévère dans la FPI. Les patients atteints de ces deux maladies ont une mauvaise survie, une diminution de la

qualité de vie, et aucun traitement adapté [555]. Nous pouvons imaginer que l'activation de P2RX7 serait bénéfique pour ces patients, cette stratégie étant efficace dans les deux pathologies. Il serait important de tester cette hypothèse en induisant par exemple la fibrose pulmonaire dans le modèle de cancer du poumon induit par l'oncogène KRAS<sup>G12D</sup>.

## 2. HEI3090 est un modulateur positif de P2RX7

Alors que de nombreuses études visent à inhiber P2RX7, nous avons choisi de l'activer, avec pour but initial d'augmenter ses propriétés antitumorales dans un microenvironnement riche en ATPe. Cette stratégie disruptive nous a semblé particulièrement intéressante connaissant le manque d'efficacité des approches basées sur l'utilisation d'antagonistes chez les patients.

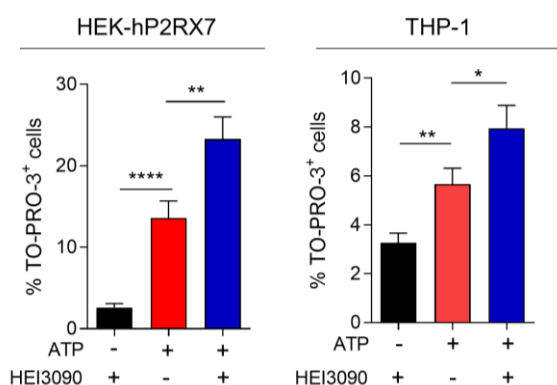


**Figure supplémentaire 3. HEI3090 augmente l'activation du récepteur P2RX7 humain.** Les cellules HEK293 exprimant le P2RX7 humain (HEK-hP2RX7) et la lignée de monocytes humains THP-1 exprimant P2RX7 ont été stimulées pendant 20 minutes avec 250  $\mu$ M d'ATP avec ou sans HEI3090. Le pourcentage de cellules TO-PRO-3+ a été déterminé avec un microscope à fluorescence. Résultats montrant la moyenne  $\pm$  SEM, n=3 expériences indépendantes. Test de Mann-Whitney \* $p < 0.05$ , \*\* $p < 0.01$ , \*\*\*\* $p < 0.0001$

HEI3090 est un nouveau modulateur positif de P2RX7 : il nécessite la présence d'ATPe pour augmenter les activités de P2RX7 à savoir l'influx de calcium, la formation de macropores et la production d'IL-18. Bien que nous n'ayons pas montré la spécificité de cette molécule pour P2RX7, nous avons montré que HEI3090 nécessite l'expression de P2RX7 pour augmenter ces trois activités, que ce soit *in vivo* grâce à l'utilisation de souris *p2rx7<sup>-/-</sup>* dans le modèle tumoral ou de fibrose, ou *ex vivo* en utilisant des splénocytes et macrophages issus de souris *p2rx7<sup>-/-</sup>*. De plus nous avons montré que HEI3090 n'augmente pas l'activation de P2RX4, le récepteur purinergique le plus proche structurellement de P2RX7.

Nous n'avons pas identifié à ce jour le site de liaison de HEI3090 sur P2RX7. Nous savons cependant que la molécule se lie sur des sites distincts du site de liaison à l'ATP et de la poche de liaison des antagonistes, grâce aux expériences faites par nos collaborateurs chimistes. Néanmoins, des modélisations en 3D ont permis d'identifier 3 sites potentiels de liaison, qui sont conservés entre le récepteur murin et humain et sont localisés dans le canal formé par les trois monomères. Nous avons également testé l'efficacité de la molécule sur le récepteur humain transfecté dans des cellules HEK293 (surexpression) mais également sur la lignée de monocytes humains THP-1 (expression

endogène), dans lesquelles HEI3090 augmente l'incorporation de TO-PRO-3 uniquement en présence d'ATPe, et augmente de ce fait la formation de macropores (Figure supplémentaire 3). HEI3090 est ainsi actif sur le récepteur humain. Dans le but de vérifier son efficacité sur les cancers d'origine humaine, nous travaillons sur la mise au point d'une culture d'organoïdes à partir de biopsies CPNPC.

Deux conséquences inattendues de l'activation de P2RX7 par HEI3090 ont été observées dans les modèles tumoraux et le modèle de fibrose. La première étant la cible préférentielle des cellules immunitaires par HEI3090, qui peut être expliquée par une plus forte expression du récepteur sur ces cellules. La deuxième, et la plus surprenante, est l'augmentation de production d'IL-18, et pas celle d'IL-1 $\beta$ . Ces deux cytokines étant produites par la même voie ATP/P2RX7/NLRP3, il était difficile d'envisager que la production de ces cytokines soit différente. Grâce à des expériences réalisées *in vivo* et *ex vivo*, nous avons montré que la production d'IL-18 est dépendante de NLRP3, ce qui suggère l'existence d'un mécanisme de régulation de l'IL-1 $\beta$  en aval de NLRP3 ou indépendant de NLRP3.

De nombreux mécanismes ont été décrits pour éviter une libération excessive d'IL-1 $\beta$  et prévenir les pathologies inflammatoires, parmi lesquels la régulation de son expression, de son activité de sa stabilité et enfin de sa sécrétion. Certains de ces mécanismes comme l'autophagie et le système ubiquitine/protéasome semblent particulièrement pertinents pour expliquer le défaut de sécrétion d'IL-1 $\beta$  puisqu'ils sont également liés à l'activation de P2RX7 [413]. En effet, des enzymes ubiquitines ligase (UBE2L3, TRIP12, AREL1) diminuent la stabilité et favorisent la dégradation de la pro-IL-1 $\beta$  par le protéasome une fois la caspase-1 activée [556]–[558]. Quant à l'autophagie, elle régule la production d'IL-1 $\beta$ , en favorisant l'accumulation de la pro-1 $\beta$  dans les autophagosomes et sa dégradation par les lysosomes [559], [560]. Nos résultats suggèrent qu'en plus d'activer l'inflammasome NLRP3, l'activation de P2RX7 par HEI3090 induit aussi des voies de signalisation qui limitent la production d'IL-1 $\beta$ . Il est cependant important de noter que les études portant sur l'activation de P2RX7 et/ou de l'inflammasome NLRP3 se limitent à étudier la production d'IL-1 $\beta$ . Par conséquent, les mécanismes de régulation de la production d'IL-1 $\beta$  ne sont pas démontrés pour l'IL-18, il est donc important de savoir dans un premier temps si ces mécanismes affectent la production d'IL-18, afin de déterminer dans un deuxième temps les mécanismes à l'origine de cette régulation différentielle.

Quoiqu'il en soit, l'existence de cette production différentielle participe au succès de la stratégie thérapeutique. En effet, l'absence de production excessive d'IL-1 $\beta$  en réponse à HEI3090 a évité les effets pro-inflammatoires et pro-fibrosants de cette cytokine [299], [355], [394], [561]–[563] et permis de mettre en avant le rôle antitumoral et anti-fibrosant de l'IL-18 [519], [520], [536], [538], [564].

Le rôle antitumoral et anti-fibrosant de P2RX7 ainsi que le mécanisme d'action de HEI3090 m'a conduit à développer un protocole permettant de mesurer l'activation de P2RX7 dans les poumons de souris. En effet, les conditions qui existaient pour mesurer l'activation de P2RX7 *in vitro* comme *ex vivo* étant peu physiologiques, il était important de déterminer le niveau d'activation du récepteur *in vivo*. Le protocole développé, basé sur l'incorporation de TO-PRO-3 étant fonctionnel, il serait intéressant de l'adapter pour mesurer l'activation de P2RX7 par l'ATPe libéré dans le modèle tumoral et de fibrose, avant de tester l'effet de HEI3090.

En conclusion, l'ensemble de mes travaux de thèse a mis en avant le rôle immunomodulateur du récepteur P2RX7 qui pourra être exploité dans les futures thérapies pour traiter les cancers du poumon et la fibrose pulmonaire. En effet, nous avons identifié HEI3090, modulateur positif de P2RX7, comme immunothérapie. Ces travaux ont également souligné le rôle clé de l'IL-18 dans cet effet, et permettent de proposer sa capacité à constituer un biomarqueur prédictif dans la réponse aux immunothérapies dans le CPNPC ainsi que dans la survie des patients FPI.



## ANNEXES



## **Revue en première auteure**

### Revue I

“To inhibit or to boost the ATP/P2RX7 pathway: that is the question”

### Revue II

“The Purinergic Landscape of Non-Small Cell Lung cancer”

## **Revue en co-auteure**

### Revue III

“Alternative splicing of *P2RX7* pre-messenger RNA in health and diseases:  
Myth or reality?”

## **Articles en co-auteure**

### Article IV

“P2RX7B is a new theranostic marker for lung adenocarcinoma patients”

### Article V

“A Novel Screen for Expression Regulators of the Telomeric Protein TRF2  
Identified Small Molecules That Impair TRF2 Dependent Immunosuppression  
and Tumor Growth”







# To inhibit or to boost the ATP/P2RX7 pathway to fight cancer—that is the question

Serena Janho dit Hreich<sup>1,2,3</sup> · Jonathan Benzaquen<sup>1,2,3</sup> · Paul Hofman<sup>1,2,3,4,5</sup> · Valérie Vouret-Craviari<sup>1,2,3</sup>

Received: 1 June 2021 / Accepted: 9 July 2021 / Published online: 4 August 2021  
© The Author(s), under exclusive licence to Springer Nature B.V. 2021

## Abstract

Despite new biological insights and recent therapeutic advances, many tumors remain at baseline during treatments. Therefore, there is an urgent need to find new therapeutic strategies to improve the care of patients with solid tumors. P2RX7 receptor (P2XR7), an ATP-gated ion channel characterized by its ability to form large pore within the cell membrane, is described by most of the investigators as a “chef d’orchestre” of the antitumor immune response. The purpose of this review is to detail the recent information concerning different cellular mechanisms linking P2RX7 to hallmarks of cancer and to discuss different progresses in elucidating how activation of the ATP/P2RX7/NLRP3/IL-18 pathway is a very promising approach to fight cancer progression by increasing antitumor immune responses.

**Keywords** Purinergic signaling · P2X7 · Immunotherapies · Tumors · Antitumor immunity · Ectonucleases

## Introduction

According to the International Agency for Research on Cancer (IARC), the global burden of cancer reached 19.3 million new cases and 9.6 million deaths in 2020 ([gco.iarc.fr](http://gco.iarc.fr)). One in five men and one in six women worldwide will develop cancer in their lifetime, and one in eight men and one in 11 women will die from the disease ([gco.iarc.fr](http://gco.iarc.fr)). Nowadays, the 5-year prevalence, corresponding to the total number of people living with cancer within 5 years of diagnosis, is estimated at 50.55 million.

At the beginning of cancer therapy, tumors were surgically removed, then came the time of chemotherapies—with molecules killing dividing cells—in association or not with radiation therapies. During the last 25 years, new approaches

revolutionized clinical cancer care in daily practice. The first one relies on the understanding of oncogene-dependent cell autonomous proliferation, leading to clinically relevant targeted therapies based on molecular targets. The second one relies on immune-oncology and led to the development of immunotherapeutic strategies designed to turn on/off specific immune checkpoints to promote antitumor immunity. Other orientations for fighting cancer progression are continuously in progress and may open new doors for some therapeutic opportunities [1]. However, despite this new arsenal of therapeutics, many patients still do not recover and/or relapse after a variable period of time, therefore testifying for the need for new drug development to fight cancer. In this review, we focus our attention on the P2X7 purinoreceptor (P2RX7), the only receptor being activated by high levels of extracellular adenosine triphosphate (eATP), and discuss recent progress in elucidating how activation of the ATP/P2RX7/NLRP3/IL-18 pathway can be a promising approach to fight cancer diseases by increasing antitumor immunity.

## Exploring the tumor microenvironment to find new therapeutic strategies

It is now well documented that vascular networks and supporting cells are required to ensure the expansion of healthy tissues as well as the growth of tumors [2]. Thus, in addition

✉ Valérie Vouret-Craviari  
Valerie.Vouret@univ-cotedazur.fr

<sup>1</sup> Université Côte D’Azur, CNRS, INSERM, IRCAN, 06108 Nice, France

<sup>2</sup> FHU OncoAge, Nice, France

<sup>3</sup> Centre Antoine Lacassagne, 06107 Nice, France

<sup>4</sup> Laboratory of Clinical and Experimental Pathology and Biobank, Pasteur Hospital, Nice, France

<sup>5</sup> Hospital-Related Biobank (BB-0033-00025), Pasteur Hospital, Nice, France

to directly target tumor cells, the non-cancerous cells present in the tumor microenvironment (TME) can also be viewed as relevant targets, even if this domain is now more and more complex [3]. These cells are mesenchymal supporting cells (epithelial, myoepithelial, fibroblasts, adipocytes), cells of the vascular system (endothelial, perivascular cells), and cells of the immune system (lymphoid and myeloid lineages). Altogether, they participate in the development of tumors as nicely illustrated by Egeblad and coauthors [4]. Furthermore, the continuous interplay between tumor cells and normal surrounding cells influences tumor growth. Indeed, it is well established that fibroblasts, the most abundant population within connective tissue cells, fuel tumor growth [5]. Transforming growth factor beta (TGF- $\beta$ ), a growth hormone secreted by tumor and immune cells, favors the conversion of normal fibroblasts to carcinoma-associated fibroblasts by feeding an autocrine loop involving TGF- $\beta$  and SDF-1 cytokines, which further lead to the production of tumor-promoting chemokines [6, 7] and modulate the composition of immune cells within the TME where they can promote or inhibit tumor growth [8–10]. Is there a common intermediate between all these cells, and if so, what could it be?

An important step to answer this question was taken by Geoff Burnstock decades ago when he postulated that ATP is released by most cells and can be considered an extracellular signaling molecule [11]. This discovery was further sustained by the demonstration that eATP promotes calcium influx in macrophages [12], via the seventh member of P2X purinoreceptor family, formerly identified as the cytolytic P2Z receptor [13], which is described below. Finally, the importance of the ATP/P2RX7 pathway in the field of oncology was buried by the discovery that ATP is present at high levels (millimolar order) in the tumor site [14]. Of interest, all mammalian cells express *P2RX7* mRNA and most of the cells express a functional receptor, i.e., a receptor expressed at the cell membrane, with a channel and a macropore opening activities [15]. In particular, functional P2RX7 was described in cells that composed the TME, such as fibroblasts [16], endothelial cells [17], dendritic cells [18–20], monocytes/macrophages [21, 22], lymphocytes [23], M- and G-MDSC [24], and neutrophils [25] as illustrated in Fig. 1. In addition, expression of a functional P2RX7 was found in both solid [26–29] and liquid cancers [30–32].

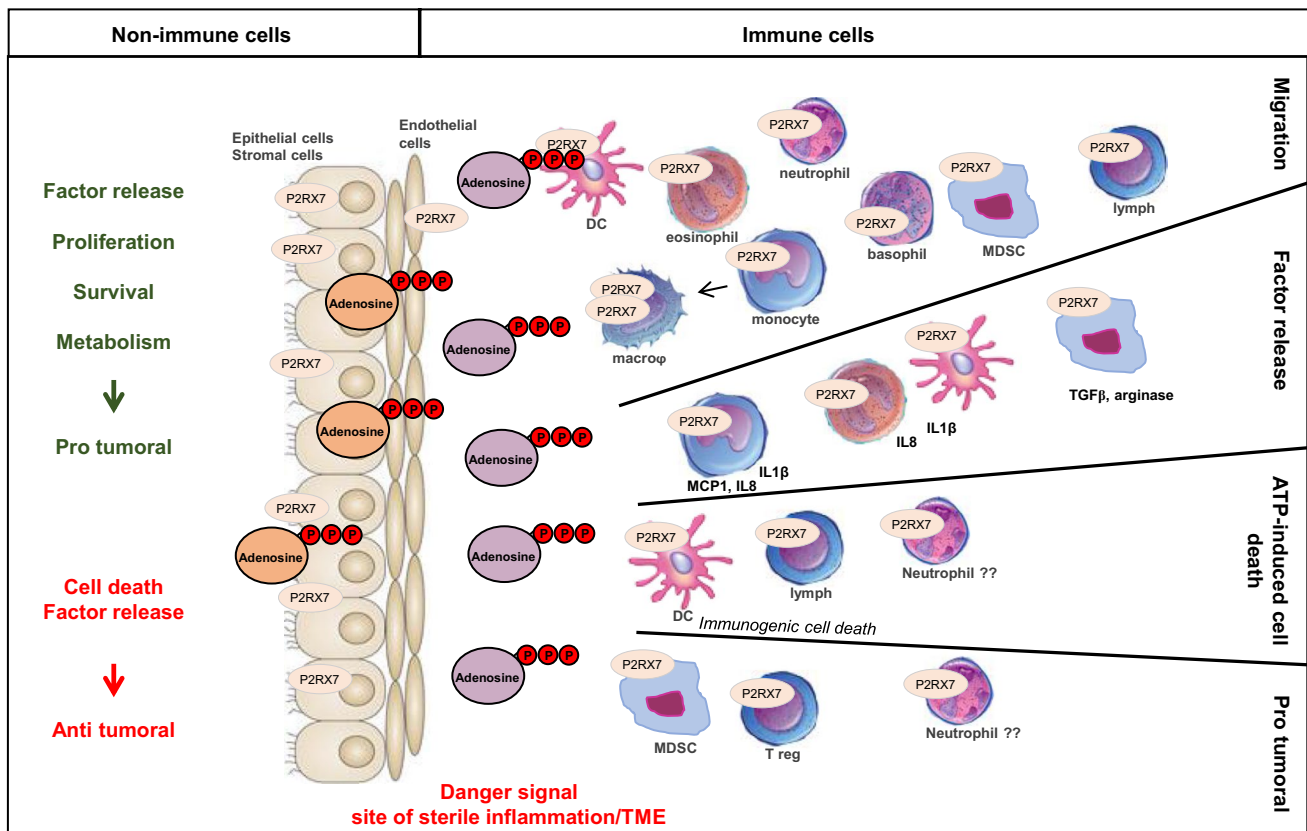


**Fig. 1** P2RX7 expression in eukaryotic cells. Representation of non-immune and immune cells expressing P2RX7 and the main ATP/P2RX7-induced cellular responses

## The P2X7 purinoreceptor: a signaling hub underpinning tumor onset

The P2X7 purinoreceptor (also called P2X7R or P2RX7) belongs to the purinergic receptor family, which is divided into two major families: P2X and P2Y [33]. These receptors have attracted growing interest since the discovery that inflammatory and cancer tissues contain high levels of eATP and adenosine, its immunosuppressive degradation product [14, 34]. Depending on the receptor involved, extracellular purines orchestrate either immune stimulation or immune suppression of host cells, as well as proliferation or cytotoxicity of tumor cells [35].

P2RX7 is an ATP-gated ion channel composed of three protein subunits (encoded by the *P2RX7* gene). Each monomer is composed of two transmembrane domains that are linked by a large extracellular domain made of 285 amino acids; the N and C termini are intracellular, with a very long C-terminus, comprising various moieties such as trafficking and lipid interaction domains and death domain, as nicely illustrated in [36]. This particular feature makes P2RX7 unique, as well as the fact that it is activated by high concentrations of eATP, implicating that it remains active where and when the other P2X receptors showed no current upon agonist application [37].

Activated P2RX7 stimulates not only the entry of  $\text{Ca}^{2+}$  and  $\text{Na}^+$  but also the efflux of  $\text{K}^+$ . Intracellular  $\text{Ca}^{2+}$  is an ubiquitous second messenger known to control various cellular functions such as cell homeostasis, gene expression, cell survival/death, exo- and endocytosis, and contraction [38]. The ATP/P2RX7-induced increase of intracellular  $\text{Ca}^{2+}$  levels is highly relevant in multiple cell responses. In macrophages, P2RX7-dependant calcium entry and subsequent activation of the PKC/c-Src/Pyk2/ERK1/2 pathway have been shown to produce reactive oxygen species (ROS) [39], and also lipase activation and blebbing [36]. In the nervous system, P2RX7 activation has been demonstrated to modulate sodium currents and intrinsic neuron excitability [40]. Ion channel function is independent of the long C-terminus, as its deletion or truncation does not alter it [41]. Accordingly, the truncated P2RX7B isoform retains some ATP-induced channel activity and expression of P2RX7B in HEK293 cells increases stimulates growth [42]. However, it has been shown that domains lying outside of the pore also participate in the regulation of  $\text{Ca}^{2+}$  flux [43].

In addition to increase intracellular  $\text{Ca}^{2+}$  concentrations, P2RX7 activation leads to a decrease in intracellular  $\text{K}^+$  which has been recognized as one of the main activators of NLRP3 inflammasome [44]. Activation of NLRP3 inflammasome is intimately linked to innate immunity being involved in the production of two key potent

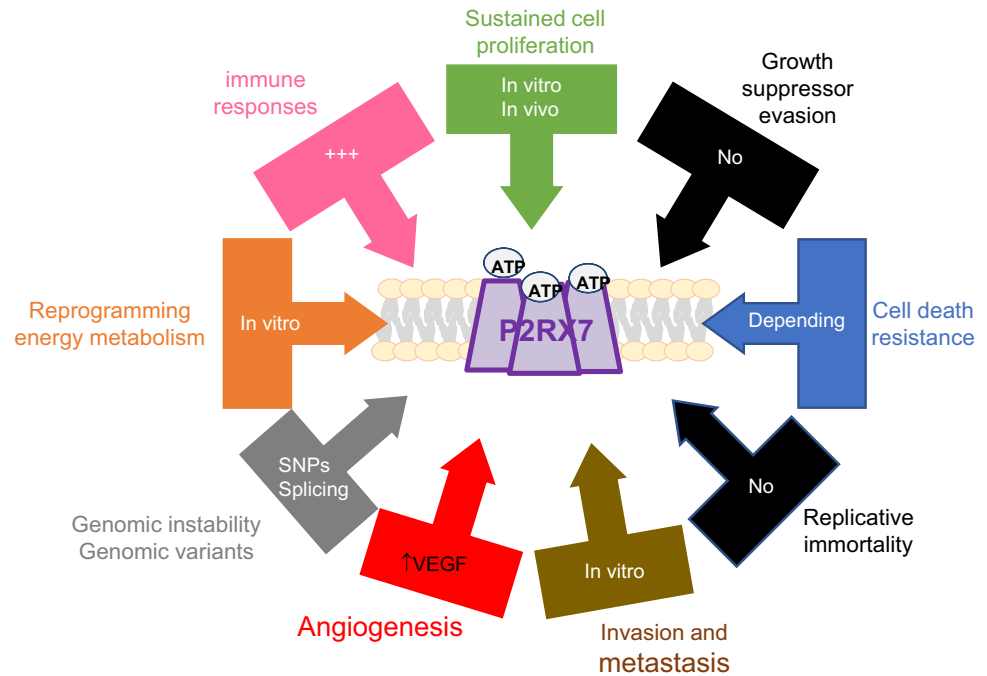
proinflammatory cytokines, IL-1 $\beta$  and IL-18, which have also been described to be important in tumor onset as they stimulate the production of interferon gamma (IFN- $\gamma$ ) by immune effector cells (T lymphocytes, Natural Killer) [45, 46]. In addition, activation of NLRP3 inflammasome leads to the formation of pores in the plasma membrane, via Gasdermin D [47], which results ultimately in pyroptotic cell death. Yet, P2RX7 activation by itself is also associated with the formation of a large pore. After decades of research and various hypothesis (mainly pore dilatation and accessory proteins), it is now well admitted that the pore formation is intrinsic of the channel activity [48, 49] and can be regulated by the C-terminus which interacts with phosphatidylglycerols and sphingomyelins of the cell membrane to facilitate cell permeability [50]. Karasawa and co-authors also elucidated why the truncated P2RX7 was devoid of pore formation by demonstrating that the C-terminal Cys-rich region, which is deleted in the truncated isoform, counteracts the inhibitory effect of cholesterol, as previously discussed [15, 51].

As already mentioned, the long intracellular C-terminus of P2RX7 is required for most of the signaling pathways induced by the ATP/P2RX7 axis. We will focus here on P2RX7-induced cell responses that are related to hallmarks of cancer (Fig. 2) as described by Hanahan et al.

### P2RX7 and sustained cell proliferation

Sustained proliferation is a characteristic of tumor cells and is under the control of growth factors that bind receptors with intracellular tyrosine kinase domains which further stimulate intracellular signaling pathways leading to cell proliferation. ATP, the natural ligand of P2RX7, does not belong to the growth factor family and no tyrosine kinase domains have been described in the C-terminus of P2RX7. However, several reports support the notion that P2RX7 activation by low concentration of ATP, as compared to concentrations inducing cell death, leads to cell proliferation [52–56]. Even in the absence of tyrosine kinase domains, stimulation of the ATP/P2RX7 axis can trigger kinase activation. For instance, cellular sarcoma tyrosine kinase (c-Src), mitogen-activated protein kinases (ERK1/2, p38, JNK), phosphoinositide 3-kinase (PI3Ks)/Protein kinase B (PKB/Akt), and protein kinases C (PKC) have been shown to be activated by P2RX7 [36]. However, no proof of direct interactions exists, and it is likely that kinase activation is mediated via  $\text{Ca}^{2+}$  and/or colocalization of P2RX7 and these kinases in lipid rafts. Accordingly, a lipid interaction motif has been described in the C-terminus of P2RX7 (amino acid 574–589) and P2RX7 moves toward lipid rafts in response to ATP [57–60]. In addition, the proteomic characterization of P2RX7 protein complex in HEK293 cells expressing the rat P2RX7 isoform identified 11 proteins, some of them being

**Fig. 2** P2RX7-induced cell responses related to hallmarks of cancer. Summary of the relationship between P2RX7 and cancer's hallmarks. Both general functions and the mode of action of P2RX7 on these general functions (text in the box) are shown



involved in cytoskeletal rearrangement [61], a cell response directly linked to cell proliferation. However, the effect of P2RX7 on sustained cell proliferation is controversial. For instance, in glioma tissue, inhibition of P2RX7 by ShRNA increased the expression of EGF and phosphor-EGF protein [62] and it was reported that reduced expression of P2RX7 may be related to the development of several cancers [15, 63–65].

### P2RX7 and growth suppressor evasion

To hijack programs that negatively regulate cell proliferation is as important as promoting cell proliferation. To our knowledge, P2RX7 does not inhibit tumor suppressors such as TP53 or retinoblastoma-associated (RB) proteins. On the contrary, it was reported that the ATP/P2RX7 axis supports apoptosis and necrosis by increasing p53 protein levels in mesangial [66] and human cervical cancer cells [67]. Whether the death domain localized in the C-terminus of P2RX7 [57] is involved in this effect has not been studied. Yet, activation of P2RX7 is associated with mechanisms and/or cellular responses leading to growth suppressor evasion since tumors grew faster in *p2rx7*<sup>-/-</sup> mice [68, 69], an effect depending on host immune cells, as discussed below.

### P2RX7 and cell death resistance

Resisting to apoptosis, a programmed cell death viewed as a natural barrier to cancer, is one of the characteristics of tumor cells. Depending on the cellular origin, the ATP/P2RX7 axis induces or inhibits apoptosis. In

colorectal cancer cells, a pharmacological inhibitor of P2RX7 induced apoptosis [56]. In the MCF7 breast cancer model, a decrease of P2RX7 expression with ShRNA induced cell apoptosis [70]. By contrast, in acute myeloid leukemia, the ATP/P2RX7 axis induced apoptosis [71]. Whether some evidence highlights a relationship between P2RX7-induced signaling and apoptosis, it does not seem that these interactions act as a barrier to cancer. The same conclusion can be drawn for autophagy—an ancestral pathway which maintains cellular homeostasis by degrading long-lived proteins and removing unwanted or unnecessary intracellular components—which represents another cellular response that needs to be circumvented for tumor development. P2RX7-induced signaling pathway has been shown to negatively regulate the autophagic flux through the impairment of lysosomal functions in microglial cells [72]. This pathway, in association with HSP90, was also linked to autophagic cell death in myoblasts and was triggered by large pore formation [73]. In contrast, P2RX7-induced necrosis may be of particular relevance since it allows not only the release of growth factors which foster proliferation and invasiveness of cancer cells [54] but also immunomodulatory cytokines as discussed below. Finally, it has been shown that tumor cells express a non-conformal receptor (nfP2RX7) which is unable to induce cell death but retains calcium channel activity and therefore could promote tumor growth [74, 75]. The exact nature of this nfP2RX7 still remains an enigma but it may be linked to P2RX7B expression, as discussed in the “P2RX7 and genomic instability” section.

## P2RX7 and replicative immortality

The unlimited replicative property of cancer cells is required to generate macroscopic tumor. P2RX7 could favor cell proliferation (see above), but whether P2RX7 could be linked to replicative immortality is currently unknown.

## P2RX7 and angiogenesis

The formation of new vessels from pre-existing ones, called neoangiogenesis, is required to fuel tumors with oxygen and nutrients. The architecture of the tumor vasculature is abnormal, i.e., leaky, tortuous, fragile, and blind-ended with few or no perivascular cells. Such defectiveness leads to hypoxia and acidity in the TME, further reinvigorating tumor aggression. Therefore, normalization of abnormal tumor vasculature, resulting in enhanced drug delivery, is as important as inhibiting neovascularization. Angiogenesis is under the control of a growth factor called vascular endothelial growth factor (VEGF) which binds to the VEGF receptor (VEGFR2) to increase endothelial cell proliferation. P2RX7 has been reported to promote VEGF release from human monocytes and rat glioma cells [76, 77]. Tumors obtained after engraftment of human embryonic kidney cells expressing P2RX7 are more angiogenic than tumors obtained with control cells [52]. Mechanistically, it was proposed that the ATP/P2RX7 axis activates the PI3K/AKT and NF $\kappa$ B pathways which further lead to increased production of VEGF and increased vessel density [52, 78, 79]. Therefore, in tumor mice models, P2RX7 activation likely stimulates angiogenesis. However, to our knowledge, no study in human cancer demonstrates a link between P2RX7 expression and neoangiogenesis.

## P2RX7 and invasion and metastasis

Malignant cells possess the ability to invade surrounding tissues and metastasize. Importantly, the metastatic spread of the primary tumor accounts for over 90% of patient mortality associated with solid cancers [80]. Metastasis is closely associated with the epithelial-mesenchymal transition (EMT), a cellular response being under the control of transcription factors belonging to the Twist and Snail families, which in turn inhibit the expression of epithelial marker (E-cadherin) and increase the expression of mesenchymal markers (vimentin, N-cadherin) [81]. P2RX7 is highly expressed and fully functional in the highly invasive human breast cancer cells MDA-MB-435s; its activation leads to the acquisition of a pro-migratory phenotype and enhanced cancer cell invasiveness in vitro and in vivo [82, 83] thanks to the release of extracellular matrix-degrading proteases. In lung cancer cells, the ATP/P2RX7 axis induced an autocrine regulation of TGF- $\beta$ -induced cell migration [84].

Furthermore, the P2RX7 effect on cell migration and invasion was observed not only in response to ATP in pancreatic ductal adenocarcinoma cells [54] but also in the human T47D breast cancer cells and colon cancer cells, where activation of the PI3K/AKT/GSK3 pathway in response to ATP regulates E-cadherin expression and EMT [56, 85]. Whereas many reports highlight the ability of P2RX7 to induce cell invasion and migration in cultured tumor cells, only one study demonstrates its implication in metastasis, considering that metastases correspond to secondary tumors growing at a distance from the primary tumor. Using the mammary 4T1 cancer mouse model, it was shown that P2RX7 expression promotes tumor growth and metastasis development, both of them being reduced when mice were treated with specific P2RX7 antagonists [86]. Mechanistically, P2RX7 expression enhances the ECM-degradative activity of invadopodia and triggers the acquisition of a more aggressive phenotype, characterized by activation of Cdc42Rho-GTPase, remodeling of F-actin, elongation of cells, and formation of filopodia. Furthermore, a higher expression of P2RX7 has been documented in bronchoalveolar lavage cells of tumors with distant metastasis [87] and in B16 melanoma-induced lung metastasis in mice. However, and in contradiction with the above findings, more lung tumors were observed with B16 melanoma cells injected in *p2rx7<sup>-/-</sup>* mice, suggesting that endogenous P2RX7 activity held by host cells restrains B16 migration and invasion [69]. Undoubtedly, additional experiments are required to fully appreciate the role of P2RX7 in invasion and metastasis depending on the cancer origin.

## P2RX7 and genomic instability

Genomic instability of cancer cells favors the selection of subclones demonstrating growth advantage and nowadays study of tumor mutational load is proposed as a sensitive and quantitative clinical marker that can help predict responses to cancer treatment. To our knowledge, P2RX7 was not reported to directly induce DNA mutations. However, several numbers of missense mutations are present in human *P2RX7*, and until now, 16 single nucleotide polymorphisms (SNPs) have been characterized in the coding region of the human *P2RX7* gene [88]. These mutations affect P2RX7 activity. For instance, the polymorphism in exon 13 at the + 1513 position (Glu496Ala substitution, corresponding to SNP rs3751143) has been shown to eradicate the function of this receptor and to be associated with papillary thyroid cancer, hepatocarcinoma, and chronic lymphocytic leukemia [89–92]. However, a recent meta-analysis studying the link between rs3751143 and cancer risk minored these results [93]. Nevertheless, in the field of hematological malignancies, P2RX7 and its genetic variants are now considered biomarkers and potential therapeutic tools [94].

In non-small cell lung cancer, P2RX7 expression and the SNP rs3751143 do not impact tumor onset [95], whereas this SNP was associated with reduced metastatic free survival in anthracycline-treated breast cancer [45]. On the contrary, a genetic statistical interaction between P2RX7 (rs3751143, rs208294) and VEGFR-2 (rs2071559, rs11133360) genotypes may identify a population of prostate cancer patients with a better prognosis [96]. In addition to SNPs, the pre-messenger RNA of *P2RX7* is subjected to alternative splicing leading to the formation of 12 *P2RX7* mRNA variants [15, 97, 98]. The function of only four of them, *P2RX7B* with a deletion in the C-terminal domain ( $\Delta$ Ct) leading to a loss of large pore-forming function, *P2RX7H* with a deletion in the first transmembrane domain ( $\Delta$ TM1) leading to a loss of ion channel function, *P2RX7J* with a deletion in the second transmembrane domain leading to a negative dominant isoform, and the recently described *P2RX7L*, characterized by skipping of exons 7 and 8 leading to deletion of amino acids in the ATP binding site, have been studied in more details [42, 64, 98–100]. The truncated *P2RX7J* was first described to antagonize P2RX7A function in cancer cervical cells, this effect was associated with apoptosis-inhibitory actions [64]. More recently, the *P2RX7B* splice variant has been shown to be differentially upregulated in immune cells of human non-small cell lung cancer. This overexpression correlates with a defect in the activity of P2RX7 in immune cells and lung tumors expressing *P2RX7B* are less inflamed. Therefore, considering that expression of *P2RX7B* in lung tumors correlated with both an alteration in the P2RX7 function and the lesser infiltrated tumor phenotype (also called “cold” tumor), it was proposed that P2RX7B participates in lung tumor development [101]. A similar conclusion was drawn in patients with AML. In those patients, expression levels of both *P2RX7A* and *B* mRNA are increased and daunorubicin, the main chemotherapeutic for AML, only reduced the expression levels of P2RX7A, whereas P2RX7B levels remained high, which correlate with cells more prone to survive [102]. One may hypothesize that the heterotrimers composed of P2RX7A and P2RX7B isoforms may correspond to the nfP2RX7, since they shared the same biological activities, e.g., no large pore formation and low Ca<sup>2+</sup> channel activity [75].

### P2RX7 and reprogramming energy metabolism

Otto Warburg was the first to describe that cancer cells can reprogram their glucose metabolism, thanks to glycolysis, even in the presence of oxygen [103]. In the heterotopic HEK293 cell system, the expression of P2RX7 leads to the regulation of numerous glycolytic markers conferring to this receptor the power to control cellular energy metabolism [104]. In a human cohort which includes more refined measures of glucose homeostasis, P2RX7 has been linked

to glucose regulation [105]. Accordingly, it was shown that P2RX7 loss of function in mice produces defective energy homeostasis [106]. To our knowledge, no study demonstrated that P2RX7 directly regulates the energy metabolism of cancer cells. Yet numerous important studies link P2RX7 to immunometabolism as discussed below.

### P2RX7 and immune responses related to tumor onset

Besides efficiently fighting infections, the immune system is also programmed to eliminate cancer cells that ultimately evade immune surveillance via checkpoint inhibitor expression and secretion of immunosuppressive factors but also survival and migration factors. [107, 108]. As discussed above, P2RX7's functions have been extensively studied in immune cells. We will focus here on P2RX7's immune populations known to be involved in tumor onset [109].

An efficient anticancer immune response is normally sufficient to kill cancer cells. On the one hand, soluble neoantigens expressed by cancer cells are recognized by circulating antigen-presenting cells (APC) such as dendritic cells (DCs) and macrophages. Then, APC present the tumor antigens on MHC-I and MHC-II molecules to T cells (CD8+, CD4+) leading to priming and activation of effector T cell responses which traffic to tumor bed, recognize tumor antigen, and kill tumor cells. On the other hand, the natural killer (NK) cells can directly kill tumor cells by using cytolytic granules and death receptors and by potentiating adaptive immunity through the production of cytokines such as interferon gamma (IFN- $\gamma$ ) [110]. These antitumor immune responses are blunted by immunosuppressive cells such as regulatory T cells (Treg) and myeloid-derived suppressor cells (MDSC) [111].

Both macrophages and DCs from human origin express P2RX7 which is able to modulate cytokine production in response to eATP and LPS [112–115]. The potential of the ATP/P2RX7 axis to enhance antitumor immune responses was suggested by Kroemer's team after the demonstration that eATP attracts DC precursors into the tumor bed, facilitates their permanence in the proximity of dying cells, and promotes their differentiation into mature DCs endowed with the capacity of presenting tumor-associated antigens [116]. In addition, P2RX7 activation in macrophages and DCs induces NLRP3, leading to increased production of IL-1 $\beta$  and IL-18. Both pro-tumorigenic and anti-tumorigenic roles of NLRP3 inflammasome have been described in cancers [117]. This double-edged sword effect may depend on the quantity of cytokine produced. For instance, more IL-18 will trigger a more efficient antitumor immune response [118]. Recent studies involving patients with acute myeloid leukemia revealed that *P2RX7* mRNAs (A and B) are upregulated in immune cancer versus immune non-cancer cells and AML

patients with higher levels of *P2RX7* mRNA show a lower survival rate [102, 119]. Furthermore, engraftment of human myeloid cell lines in immunodeficient mice leads to tumor growth and treatment with specific antagonists of P2RX7 decreases the size of the tumors and increases mice survival rate. The importance of the ATP/P2RX7 axis in leukemic models was further improved by the discovery that P2RX7 is highly expressed in leukemia-initiating cells where it promotes AML development by sustaining Ca<sup>2+</sup>-dependent cell signaling [120].

Human lymphocytes also express P2RX7 and demonstrated a growth-promoting activity [121, 122]. Of note, at least in mice, P2RX7 expression levels are heterogeneous across immune cells. Indeed, it is highly expressed by macrophages, DCs, and monocytes while NK cells, CD8<sup>+</sup> and CD4<sup>+</sup>foxp3<sup>-</sup> T cells, neutrophils, and eosinophils express very low levels [123]. Yet it was shown that P2RX7 is required for the establishment, maintenance, and functionality of long-lived memory CD8<sup>+</sup>T cells (T<sub>RM</sub>), an effect that depends on P2RX7-dependent metabolic fitness [124]. Interestingly, in a melanoma mice model, T<sub>RM</sub> can actively suppress cancer progression [125]. P2RX7 is also expressed by human Tregs. It was shown that esophageal carcinoma from patients expressing the loss-of-function allele of *P2RX7* is more infiltrated with Tregs than tumors from patients bearing the WT allele of *P2RX7* [126]. The same tendency was observed in the colitis-associated cancer mice model and melanoma models, where *p2rx7*<sup>-/-</sup> mice developed more tumors and tumors were more infiltrated with Tregs than tumors grown in WT mice [68, 127]. Such results could be explained by the fact that P2RX7 controls Treg homeostasis, and in the absence of P2RX7, Treg death is decreased [128, 129]. Finally, whereas the level of P2RX7 expression in human MDSCs has not yet been reported, it was shown in the neuroblastoma mice model that the ATP/P2RX7 axis increases immunosuppressive functions of MDSCs [24]. In conclusion, while it is indisputable that P2RX7 modulates immune cell functions, the contradicting results found in the literature make it difficult to predict whether P2RX7, by itself, impinges or enhances antitumor immune responses.

### Should we target P2RX7 in cancer biology?

This is indeed *the question*, and as evidenced in previous sections, this is a puzzling question (Fig. 3). Should we inhibit P2RX7 in order to blunt its proliferative effect on cancer cells? However, this scenario may be dangerous since it may also inhibit antitumor immune responses sustained by P2RX7! Should we activate P2RX7 in order to boost its cytotoxic effect on tumor cells? But is P2RX7 really cytotoxic on tumor cells, since we know that many tumors express a nfP2RX7? If we activate P2RX7, would it really

enhance antitumor immune responses or would it boost the function of immunosuppressive cells that are recruited in the TME?

Since the notion of immunosurveillance emerges only recently in the field of cancer biology [130] and because Big Pharma were more prone to develop inhibitors, especially P2RX7 antagonists that may treat inflammatory disorders, numerous small pharmacological inhibitors and biologics were tested in preclinical and clinical studies as reviewed in [65]. In brief, most of the preclinical studies were based on transplantation in immunodeficient or syngeneic immunocompetent mice of various tumor cell lines (e.g., HEK293, neuroblastoma, colon carcinoma, melanoma, glioma, osteosarcoma, and myeloid leukemia) endowed with endogenous or exogenous expression of P2RX7, where tumor growth was significantly reduced by treatment with AZ10606120, A438079, or A740003, three well-described antagonists of P2RX7 [52, 54, 55, 69, 127, 131]. However, an acceleration of tumor growth was also described when tumor cell lines were transplanted in *p2rx7* KO mice or with chemically induced in situ colon tumors [68, 69]. These results highlight the importance of P2RX7 expressing host cells in tumor onset and suggest that the levels of expression and functionality of P2RX7 in tumor cells are a critical issue that has to be considered before the use of antagonists to treat tumor. As far as we know, no clear benefits to patients have been reported so far and this lack of effect may be related to the fact that inflammatory tissues contain high levels of ATP, a condition that does not favor the binding of antagonists to the allosteric binding site [132]. The use of biologics may be an alternative. In particular, the application of an antibody that specifically recognizes the E200 epitope of nfP2RX7 appears to be promising for the local treatment of the primary basal cell carcinoma lesion [133].

We hypothesized that increasing P2RX7's dependent antitumor immune response by enhancing its activation would inhibit tumor growth. We developed positive allosteric modulators (PAMs) of P2RX7, i.e., molecules that enhance P2RX7 activity in the presence of ATP. HEI3090 was selected as the most potent PAM that enhances P2RX7's activities only in the presence of ATP and showed that it efficiently inhibits tumor growth. HEI3090 enhances antitumor immune responses by boosting the ATP/P2RX7/NLRP3/IL-18 pathway in DCs, sensitizes tumor to anti-PD-1 immunotherapy, and triggers long-lasting antitumor immune responses [134]. Our bet looks like a successful story, which is not so surprising considering that anti CD39 antibody was recently shown to promote the eATP/P2RX7/NLRP3/IL18-driven antitumor responses [123]. In addition, the activation of this pathway with anti CD39 monoclonal antibody in myeloid cells activates the effector function of NK cells and suppresses experimental and spontaneous metastases in a tumor of different origins [135], therefore



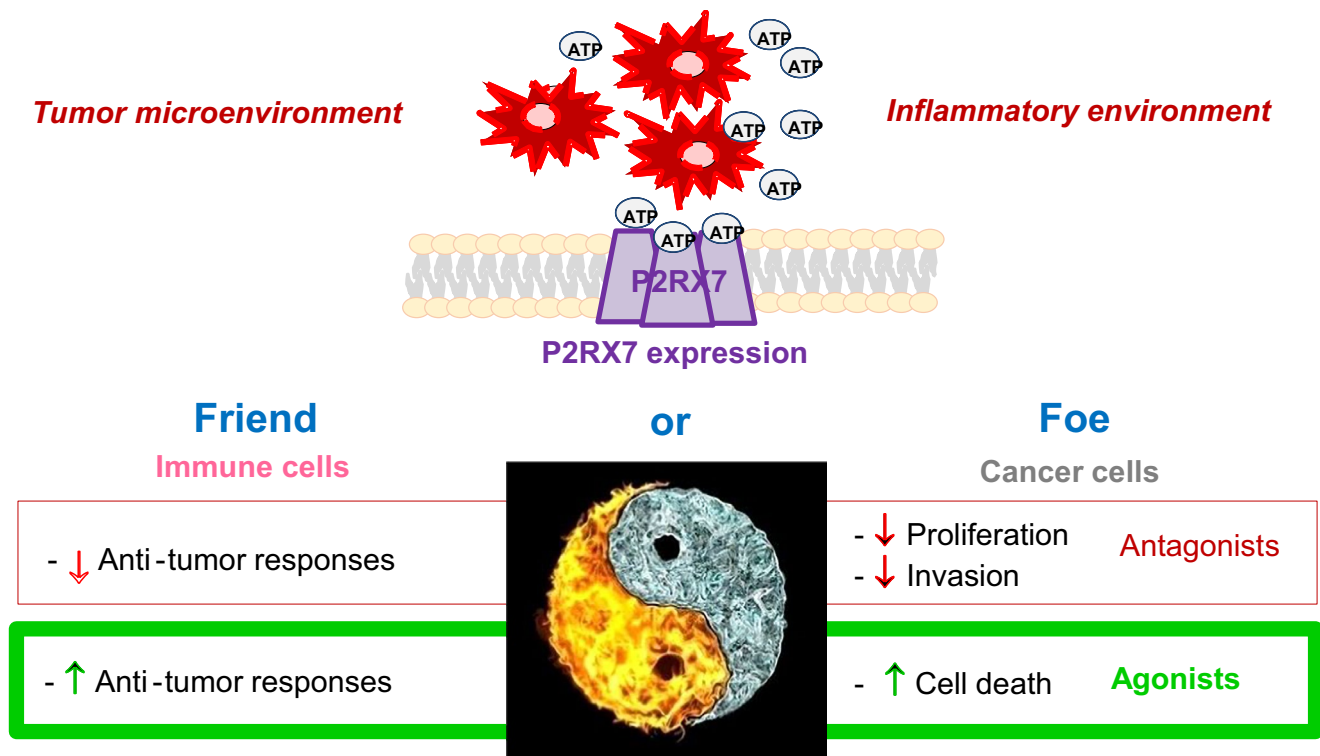


**Fig. 3** The yin and yang of P2RX7's modulators. Dying damaged cells and activated immune cells (in red) produce micromolar concentrations of ATP leading to P2RX7 activation in TME and inflammatory tissues. Whereas cancer cells are always considered as foes, immune cells can be either friends or foes depending on their ability to modulate anti- or pro-tumor responses. P2RX7 being expressed

by both cancer cells and immune cells, two treatment scenarios are possible: the use of antagonists in order to blunt cancer cell proliferation and invasion with the risk of blocking antitumor responses (red square) or the use of agonists aiming at increasing P2RX7-induced cell death and boosting antitumor immune responses (green square)

bringing new hopes for the treatment of cancers. However, more work is needed to understand which immune cells should be targeted to kill tumor cells in order to reconcile data showing a benefit to activate the ATP/P2RX7 axis in specific immune cells (macrophages, DCs) and data showing that the lack of P2RX7 in tumor-specific T cells reduced tumor growth [136]. Furthermore, we need to understand why tumor fate is different in *p2rx7* null mice and mice treated with an antagonist of P2RX7 [127].

## Perspectives

Undoubtedly, targeting P2RX7 to treat cancer is a promising strategy and recent data from several laboratories highlighted the capacity of the ATP/P2RX7/NLRP3/IL-18 axis to activate antitumor immune responses. However, pivotal questions remain to be answered. Among them, how do the new pharmacological positive modulator of P2RX7 (HEI3090) enhance the receptor activity? Does it bind to the receptor itself, and if so, where? Is HEI3090 active on the *nfP2RX7*? And if so, which and

how P2RX7-dependent biological responses are going to be regulated? Would it be interesting to combine HEI3090 with the new anti CD39 antibody in order to maximize the activation of the ATP/P2RX7/NLRP3/IL-18 axis and the consecutive antitumor immune response? Would the other non-nucleotide agonists of P2RX7 (i.e., ginsenoside, LL37 [137, 138]) will also boost the antitumor immune responses supported by the ATP/P2RX7 axis? and if so, could we combine them with HEI3090 and immunotherapies? What would be the effect of an agonist of P2RX7 on inflammatory pain and IL-1 $\beta$ -induced cachexia, knowing that P2RX7 antagonists not only efficiently inhibit the production of IL-1 $\beta$  but also reduced cancer-induced bone pain [139, 140]? In this perspective, the use of HEI3090 may be of particular interest, since we showed in transplantable and oncogene-driven tumor models that it increases seric IL-18 levels with no effect on IL-1 $\beta$ . We believe that these points will be resolved in a near future, and in addition, we are strongly convinced that their resolution will bring new innovative strategies to fight cancers.

**Funding** VV-C was supported by grants from Institut National du Cancer (INCa # 2015–137), Canceropole PACA, Bristol-Myers Squibb Foundation for Research in Immuno-Oncology, the French Government (National Research Agency, ANR through the “Investments for the Future”: program reference #ANR-11-LABX-0028–01) and the Centre National de la Recherche Scientifique (CNRS). SJH was supported by the “Ligue Nationale Contre le Cancer” and the “Fondation pour la recherche médicale # FDT202106013099” JB was supported by the “Plan Cancer: Formation à la recherche Translationnelle en cancérologie.”

**Data availability** Not applicable, review.

## Declarations

**Ethical approval** This review does not contain any studies with participants or animals performed by any of the authors.

**Informed consent** Not applicable, no studies with humans.

**Conflicts of interest** Serena Janho dit Hreich declares that she has no conflict of interest.

Jonathan Benzaquen declares that he has no conflict of interest.

Paul Hofman declares that he has no conflict of interest.

Valérie Vouret-Craviari declares that she has no conflict of interest.

## References

- Hofman P (2020) New insights into the interaction of the immune system with non-small cell lung carcinomas. *Transl Lung Cancer Res* 9:2199–2213. <https://doi.org/10.21037/tlcr-20-178>
- Farc O, Cristea V (2020) An overview of the tumor microenvironment, from cells to complex networks (Review). *Exp Ther Med* 21:96. <https://doi.org/10.3892/etm.2020.9528>
- Bagaev A, Kotlov N, Nomie K et al (2021) Conserved pan-cancer microenvironment subtypes predict response to immunotherapy. *Cancer Cell*. <https://doi.org/10.1016/j.ccell.2021.04.014>
- Egeblad M, Nakasne ES, ZW, (2010) Tumors as organs: complex tissues that interface with the entire organism. *Dev Cell* 18:884. <https://doi.org/10.1016/j.devcel.2010.05.012>
- Kuzet S-E, Gaggioli C (2016) Fibroblast activation in cancer: when seed fertilizes soil. *Cell Tissue Res* 365:607–619. <https://doi.org/10.1007/s00441-016-2467-x>
- Orimo A, Gupta PB, Sgroi DC et al (2005) Stromal fibroblasts present in invasive human breast carcinomas promote tumor growth and angiogenesis through elevated SDF-1/CXCL12 Secretion. *Cell* 121:335–348. <https://doi.org/10.1016/j.cell.2005.02.034>
- Kojima Y, Acar A, Eaton EN et al (2010) Autocrine TGF- and stromal cell-derived factor-1 (SDF-1) signaling drives the evolution of tumor-promoting mammary stromal myofibroblasts. *Proc Natl Acad Sci* 107:20009–20014. <https://doi.org/10.1073/pnas.1013805107>
- Gajewski TF, Schreiber H, Fu Y-X (2013) Innate and adaptive immune cells in the tumor microenvironment. *Nat Immunol* 14:1014–1022. <https://doi.org/10.1038/ni.2703>
- Hanahan D, Coussens LM (2012) Accessories to the crime: functions of cells recruited to the tumor microenvironment. *Cancer Cell* 21:309–322. <https://doi.org/10.1016/j.ccr.2012.02.022>
- Marvel D, Gabrilovich DI (2015) Myeloid-derived suppressor cells in the tumor microenvironment: expect the unexpected. *J Clin Invest* 125:3356–3364. <https://doi.org/10.1172/JCI80005>
- Burnstock G, Campbell G, Satchell D, Smythe A (1970) Evidence that adenosine triphosphate or a related nucleotide is the transmitter substance released by non-adrenergic inhibitory nerves in the gut. *Br J Pharmacol* 40:668–688. <https://doi.org/10.1111/j.1476-5381.1970.tb10646.x>
- Steinberg TH, Silverstein SC (1987) Extracellular ATP<sub>4</sub>- promotes cation fluxes in the J774 mouse macrophage cell line. *J Biol Chem* 262:3118–3122
- Surprenant A, Rassendren F, Kawashima E, et al (1996) The cytolytic P2Z receptor for extracellular ATP identified as a P2X receptor (P2X<sub>7</sub>). *Science* (80- ) 272:735–738. <https://doi.org/10.1126/science.272.5262.735>
- Pellegatti P, Raffaghello L, Bianchi G et al (2008) Increased level of extracellular ATP at tumor sites: in vivo imaging with plasma membrane luciferase. *PLoS ONE* 3:e2599. <https://doi.org/10.1371/journal.pone.0002599>
- Benzaquen J, Heeke S, Janho dit Hreich S, et al (2019) Alternative splicing of P2RX<sub>7</sub> pre-messenger RNA in health and diseases: myth or reality? *Biomed J* 42:141–154. <https://doi.org/10.1016/j.bj.2019.05.007>
- Solini A, Chiozzi P, Morelli A et al (1999) Human primary fibroblasts in vitro express a purinergic P2X<sub>7</sub> receptor coupled to ion fluxes, microvesicle formation and IL-6 release. *J Cell Sci* 305:297–305
- dos Oliveira SD, S, Coutinho-Silva R, Silva CLM, (2013) Endothelial P2X<sub>7</sub> receptors' expression is reduced by schistosomiasis. *Purinergic Signal* 9:81–89. <https://doi.org/10.1007/s11302-012-9332-5>
- Georgiou JG, Skarratt ÅKK, Fuller ÅSJ et al (2005) Human epidermal and monocyte-derived langerhans cells express functional P2X<sub>7</sub> receptors. *J Invest Dermatol* 125:482–490. <https://doi.org/10.1111/j.0022-202X.2005.23835.x>
- Baroni M, Pizzirani C, Pinotti M et al (2007) Stimulation of P2 ( P2X<sub>7</sub> ) receptors in human dendritic cells induces the release of tissue factor-bearing microparticles. *FASEB J* 21:1926–1933. <https://doi.org/10.1096/fj.06-7238com>
- Idzko M, Dichmann S, Ferrari D et al (2002) Nucleotides induce chemotaxis and actin polymerization in immature but not mature human dendritic cells via activation of pertussis toxin-sensitive P2<sub>y</sub> receptors. *Blood* 100:925–932. <https://doi.org/10.1182/blood.V100.3.925>
- Gu BJ, Zhang WY, Bendall LJ et al (2000) Expression of P2X<sub>7</sub> purinoceptors on human lymphocytes and monocytes: evidence for nonfunctional P2X<sub>7</sub> receptors. *Am J Physiol Cell Physiol* 279:1189–1197. <https://doi.org/10.1155/2014/164309>
- Chiozzi P, Sanz JM, Ferrari D et al (1997) Spontaneous cell fusion in macrophage cultures expressing high levels of the P2Z/ P2X<sub>7</sub> receptor. *J Cell Biol* 138:697–707
- Borges H, Beura LK, Wang H et al (2018) The purinergic receptor P2RX<sub>7</sub> directs fitness of long-lived memory CD8 + T cells. *Nature* 559:264–268. <https://doi.org/10.1038/s41586-018-0282-0>
- Bianchi G, Vuerich M, Pellegatti P et al (2014) ATP/P2X<sub>7</sub> axis modulates myeloid-derived suppressor cell functions in neuroblastoma microenvironment. *Cell Death Dis* 5:e1135–e1212. <https://doi.org/10.1038/cddis.2014.109>
- Christenson K, Bjo L, Ta C, Bylund J (2008) Serum amyloid A inhibits apoptosis of human neutrophils via a P2X<sub>7</sub>-sensitive pathway independent of formyl peptide Abstract: neutrophil apoptosis is important for the termination of inflammatory reactions, in that. *J Leukoc Biolo* 83:139–148. <https://doi.org/10.1189/jlb.0507276>
- Deli T, Varga N, Adam A et al (2007) Functional genomics of calcium channels in human melanoma cells. *Int J Cancer* 121:55–65. <https://doi.org/10.1002/ijc.22621>
- Solini A, Cuccato S, Ferrari D et al (2008) Increased P2X<sub>7</sub> receptor expression and function in thyroid papillary cancer : a

- new potential marker of the disease? *Endocrinology* 149:389–396. <https://doi.org/10.1210/en.2007-1223>
28. Vázquez-cuevas FG, Martínez-ramírez AS, Robles-martínez L et al (2014) Paracrine stimulation of P2X7 receptor by ATP activates a. *J Cell Biochem* 115:1955–1966. <https://doi.org/10.1002/jcb.24867>
  29. Santos AAJ, Cappellari AR, De MFO et al (2017) Potential role of P2X7R in esophageal squamous cell carcinoma proliferation. *Purine Pyrimidine Recept Pharmacol* (Jacobson KA, Linden J, eds) 13:279–292. <https://doi.org/10.1007/s11302-017-9559-2>
  30. Adinolfi E, Melchiorri L, Falzoni S et al (2002) Brief report P2X7 receptor expression in evolutive and indolent forms of chronic B lymphocytic leukemia. *Blood* 99:706–709
  31. Zhang X, Zheng G, Ma X et al (2004) Expression of P2X7 in human hematopoietic cell lines and leukemia patients. *Leuk Res* 28:1313–1322. <https://doi.org/10.1016/j.leukres.2004.04.001>
  32. Chong J, Zheng G, Zhu X et al (2010) Abnormal expression of P2X family receptors in Chinese pediatric acute leukemias. *Biochem Biophys Res Commun* 391:498–504. <https://doi.org/10.1016/j.bbrc.2009.11.087>
  33. Jacob F, Novo CP, Bachert C, Van Crombruggen K (2013) Purinergic signaling in inflammatory cells: P2 receptor expression, functional effects, and modulation of inflammatory responses. *Purinergic Signal* 9:285–306
  34. Allard B, Beavis PA, Darcy PK, Stagg J (2016) Immunosuppressive activities of adenosine in cancer. *Curr Opin Pharmacol* 29:7–16. <https://doi.org/10.1016/j.coph.2016.04.001>
  35. White N, Burnstock G (2006) P2 receptors and cancer. *Trends Pharmacol Sci* 27:211–217. <https://doi.org/10.1016/j.tips.2006.02.004>
  36. Kopp R, Krautloher A, Ramírez-Fernández A, Nicke A (2019) P2X7 Interactions and signaling – making head or tail of it. *Front MolNeurosci* 12:<https://doi.org/10.3389/fnmol.2019.00183>
  37. North RA, Surprenant A (2000) Pharmacology of Cloned P2X Receptors. *Annu Rev Pharmacol Toxicol* 40:563–580. <https://doi.org/10.1146/annurev.pharmtox.40.1.563>
  38. Bagur R, Hajnóczky G (2017) Intracellular Ca<sup>2+</sup> sensing: its role in calcium homeostasis and signaling. *Mol Cell* 66:780–788. <https://doi.org/10.1016/j.molcel.2017.05.028>
  39. Martel-Gallegos G, Casas-Pruneda G, Ortega-Ortega F et al (2013) Oxidative stress induced by P2X7 receptor stimulation in murine macrophages is mediated by c-Src/Pyk2 and ERK1/2. *Biochim Biophys Acta - Gen Subj* 1830:4650–4659. <https://doi.org/10.1016/j.bbagen.2013.05.023>
  40. del Puerto A, Fronzaroli-Molinieres L, Perez-Alvarez MJ et al (2015) ATP-P2X7 receptor modulates axon initial segment composition and function in physiological conditions and brain injury. *Cereb Cortex* 25:2282–2294. <https://doi.org/10.1093/cercor/bhu035>
  41. Smart ML, Gu B, Panchal RG et al (2003) P2X7 receptor cell surface expression and cytolitic pore formation are regulated by a distal C-terminal region. *J Biol Chem* 278:8853–8860. <https://doi.org/10.1074/jbc.M211094200>
  42. Adinolfi E, Cirillo M, Woltersdorf R et al (2010) Trophic activity of a naturally occurring truncated isoform of the P2X7 receptor. *FASEB J* 24:3393–3404. <https://doi.org/10.1096/fj.09-153601>
  43. Liang X, Samways DSK, Wolf K et al (2015) Quantifying Ca<sup>2+</sup> current and permeability in ATP-gated P2X7 receptors. *J Biol Chem* 290:7930–7942. <https://doi.org/10.1074/jbc.M114.627810>
  44. Pétrilli V, Papin S, Dostert C et al (2007) Activation of the NALP3 inflammasome is triggered by low intracellular potassium concentration. *Cell Death Differ* 14:1583–1589. <https://doi.org/10.1038/sj.cdd.4402195>
  45. Ghiringhelli F, Apetoh L, Tesniere A et al (2009) Activation of the NLRP3 inflammasome in dendritic cells induces IL-1B-dependent adaptive immunity against tumors. *Nat Med* 15:1170–1178. <https://doi.org/10.1038/nm.2028>
  46. Ma Y, Adjemian S, Yang H et al (2013) ATP-dependent recruitment, survival and differentiation of dendritic cell precursors in the tumor bed after anticancer chemotherapy. *Oncoimmunology* 2:e24568. <https://doi.org/10.4161/onci.24568>
  47. Pelegrin P (2021) P2X7 receptor and the NLRP3 inflammasome: partners in crime. *Biochem Pharmacol* 187:114385. <https://doi.org/10.1016/j.bcp.2020.114385>
  48. Harkat M, Peverini L, Cerdan AH et al (2017) On the permeation of large organic cations through the pore of ATP-gated P2X receptors. *Proc Natl Acad Sci U S A* 114:E3786–E3795. <https://doi.org/10.1073/pnas.1701379114>
  49. Pippel A, Stolz M, Woltersdorf R et al (2017) Localization of the gate and selectivity filter of the full-length P2X7 receptor. *Proc Natl Acad Sci U S A* 114:E2156–E2165. <https://doi.org/10.1073/pnas.1610414114>
  50. Karasawa A, Michalski K, Mikhelzon P, Kawate T (2017) The P2X7 receptor forms a dye-permeable pore independent of its intracellular domain but dependent on membrane lipid composition. *Elife* 6:<https://doi.org/10.7554/eLife.31186>
  51. Di Virgilio F, Schmalzing G, Markwardt F (2018) The elusive P2X7 macropore. *Trends Cell Biol* 28:392–404. <https://doi.org/10.1016/j.tcb.2018.01.005>
  52. Adinolfi E, Raffaghello L, Giuliani AL et al (2012) Expression of P2X7 receptor increases in vivo tumor growth. *Cancer Res* 72:2957–2969. <https://doi.org/10.1158/0008-5472.CAN-11-1947>
  53. Haanes KA, Schwab A, Novak I (2012) The P2X7 receptor supports both life and death in fibrogenic pancreatic stellate cells. *PLoS One* 7:<https://doi.org/10.1371/journal.pone.0051164>
  54. Giannuzzo A, Pedersen SF, Novak I (2015) The P2X7 receptor regulates cell survival, migration and invasion of pancreatic ductal adenocarcinoma cells. *Mol Cancer* 14:203. <https://doi.org/10.1186/s12943-015-0472-4>
  55. Zhang Y, Cheng H, Li W et al (2019) Highly-expressed P2X7 receptor promotes growth and metastasis of human HOS/MNNG osteosarcoma cells via PI3K/Akt/GSK3β/β-catenin and mTOR/HIF1α/VEGF signaling. *Int J Cancer* 145:1068–1082. <https://doi.org/10.1002/ijc.32207>
  56. Zhang W, Luo C, Huang C et al (2021) PI3K/Akt/GSK-3β signal pathway is involved in P2X7 receptor-induced proliferation and EMT of colorectal cancer cells. *Eur J Pharmacol* 899:174041. <https://doi.org/10.1016/j.ejphar.2021.174041>
  57. Denlinger LC, Fisetle PL, Sommer JA et al (2001) Cutting edge: the nucleotide receptor P2X7 contains multiple protein- and lipid-interaction motifs including a potential binding site for bacterial lipopolysaccharide. *J Immunol* 167:1871–1876. <https://doi.org/10.4049/jimmunol.167.4.1871>
  58. Gonnord P, Delarasse C, Auger R et al (2009) Palmitoylation of the P2X7 receptor, an ATP-gated channel, controls its expression and association with lipid rafts. *FASEB J* 23:795–805. <https://doi.org/10.1096/fj.08-114637>
  59. Robinson LE, Shridar M, Smith P, Murrell-Lagnado RD (2014) Plasma membrane cholesterol as a regulator of human and rodent P2X7 receptor activation and sensitization. *J Biol Chem* 289:31983–31994. <https://doi.org/10.1074/jbc.M114.574699>
  60. Murrell-Lagnado RD (2017) Regulation of P2X purinergic receptor signaling by cholesterol. pp 211–232
  61. Kim M, Jiang LH, Wilson HL et al (2001) Proteomic and functional evidence for a P2X7 receptor signalling complex. *EMBO J* 20:6347–6358. <https://doi.org/10.1093/emboj/20.22.6347>
  62. Fang J, Chen X, Zhang L et al (2013) P2X7R suppression promotes glioma growth through epidermal growth factor receptor signal pathway. *Int J Biochem Cell Biol* 45:1109–1120. <https://doi.org/10.1016/j.biocel.2013.03.005>

63. Feng L, Sun X, Csizmadia E, et al (2011) Vascular CD39/ENTPD1 directly promotes tumor cell growth by scavenging extracellular adenosine triphosphate. *Neoplasia* 13:206–IN2. <https://doi.org/10.1593/neo.101332>
64. Feng YH, Li X, Wang L et al (2006) A truncated P2X7 receptor variant (P2X7-j) endogenously expressed in cervical cancer cells antagonizes the full-length P2X7 receptor through hetero-oligomerization. *J Biol Chem* 281:17228–17237. <https://doi.org/10.1074/jbc.M602999200>
65. Lara R, Adinolfi E, Harwood CA, et al (2020) P2X7 in cancer: from molecular mechanisms to therapeutics. *Front Pharmacol* 11:<https://doi.org/10.3389/fphar.2020.00793>
66. Schulze-Lohoff E, Hugo C, Rost S et al (1998) Extracellular ATP causes apoptosis and necrosis of cultured mesangial cells via P2Z/P2X 7 receptors. *Am J Physiol Physiol* 275:F962–F971. <https://doi.org/10.1152/ajprenal.1998.275.6.F962>
67. de Mello P, A, Filippi-Chiela EC, Nascimento J, et al (2014) Adenosine uptake is the major effector of extracellular ATP toxicity in human cervical cancer cells. *Mol Biol Cell* 25:2905–2918. <https://doi.org/10.1091/mbc.e14-01-0042>
68. Hofman P, Cherfils-Vicini J, Bazin M et al (2015) Genetic and pharmacological inactivation of the purinergic P2RX7 receptor dampens inflammation but increases tumor incidence in a mouse model of colitis-associated cancer. *Cancer Res* 75:835–845. <https://doi.org/10.1158/0008-5472.CAN-14-1778>
69. Adinolfi E, Capece M, Franceschini A et al (2015) Accelerated tumor progression in mice lacking the ATP receptor P2X7. *Cancer Res* 75:635–644. <https://doi.org/10.1158/0008-5472.CAN-14-1259>
70. Tan C, Han L, Zou L et al (2015) Expression of P2X7R in breast cancer tissue and the induction of apoptosis by the gene-specific shRNA in MCF-7 cells. *Exp Ther Med* 10:1472–1478. <https://doi.org/10.3892/etm.2015.2705>
71. Salvestrini V, Orecchioni S, Talarico G, et al (2017) Extracellular ATP induces apoptosis through P2X7R activation in acute myeloid leukemia cells but not in normal hematopoietic stem cells. *Oncotarget* 8:5895–5908. <https://doi.org/10.18632/oncotarget.13927>
72. Takenouchi T, Nakai M, Iwamaru Y et al (2009) The activation of P2X7 receptor impairs lysosomal functions and stimulates the release of autophagolysosomes in microglial cells. *J Immunol* 182:2051–2062. <https://doi.org/10.4049/jimmunol.0802577>
73. Young CN, Sinadinos A, Lefebvre A et al (2015) A novel mechanism of autophagic cell death in dystrophic muscle regulated by P2RX7 receptor large-pore formation and HSP90. *Autophagy* 11:113–130. <https://doi.org/10.4161/15548627.2014.994402>
74. Barden AJ (2014) Non-functional P2X7: a novel and ubiquitous target in human cancer. *J Clin Cell Immunol* 05:<https://doi.org/10.4172/2155-9899.1000237>
75. Gilbert S, Oliphant C, Hassan S et al (2019) ATP in the tumour microenvironment drives expression of nP2X7, a key mediator of cancer cell survival. *Oncogene* 38:194–208. <https://doi.org/10.1038/s41388-018-0426-6>
76. Hill LM, Gavala ML, Lenertz LY, Bertics PJ (2010) Extracellular ATP may contribute to tissue repair by rapidly stimulating purinergic receptor X7-dependent vascular endothelial growth factor release from primary human monocytes. *J Immunol* 185:3028–3034. <https://doi.org/10.4049/jimmunol.1001298>
77. Wei W, Ryu JK, Choi HB, McLarnon JG (2008) Expression and function of the P2X7 receptor in rat C6 glioma cells. *Cancer Lett* 260:79–87. <https://doi.org/10.1016/j.canlet.2007.10.025>
78. Amoroso F, Capece M, Rotondo A et al (2015) The P2X7 receptor is a key modulator of the PI3K/GSK3 $\beta$ /VEGF signaling network: evidence in experimental neuroblastoma. *Oncogene* 34:5240–5251. <https://doi.org/10.1038/onc.2014.444>
79. Yang C, Shi S, Su Y et al (2020) P2X7R promotes angiogenesis and tumour-associated macrophage recruitment by regulating the NF- $\kappa$ B signalling pathway in colorectal cancer cells. *J Cell Mol Med* 24:10830–10841. <https://doi.org/10.1111/jcmm.15708>
80. Hanahan D, Weinberg RA (2011) Hallmarks of cancer: the next generation. *Cell* 144:646–674. <https://doi.org/10.1016/j.cell.2011.02.013>
81. Lambert AW, Weinberg RA (2021) Linking EMT programmes to normal and neoplastic epithelial stem cells. *Nat Rev Cancer* 21:325–338. <https://doi.org/10.1038/s41568-021-00332-6>
82. Jelassi B, Chantôme A, Alcaraz-Pérez F et al (2011) P2X7 receptor activation enhances SK3 channels- and cystein cathepsin-dependent cancer cells invasiveness. *Oncogene* 30:2108–2122. <https://doi.org/10.1038/onc.2010.593>
83. Jelassi B, Anachelin M, Chamouton J et al (2013) Anthraquinone emodin inhibits human cancer cell invasiveness by antagonizing P2X7 receptors. *Carcinogenesis* 34:1487–1496. <https://doi.org/10.1093/carcin/bgt099>
84. Takai E, Tsukimoto M, Harada H et al (2012) Autocrine regulation of TGF- $\beta$ 1-induced cell migration by exocytosis of ATP and activation of P2 receptors in human lung cancer cells. *J Cell Sci* 125:5051–5060. <https://doi.org/10.1242/jcs.104976>
85. Xia J, Yu X, Tang L et al (2015) P2X7 receptor stimulates breast cancer cell invasion and migration via the AKT pathway. *Oncol Rep* 34:103–110. <https://doi.org/10.3892/or.2015.3979>
86. Brisson L, Chadet S, Lopez-Charcas O et al (2020) P2X7 receptor promotes mouse mammary cancer cell invasiveness and tumour progression, and is a target for anticancer treatment. *Cancers (Basel)* 12:2342. <https://doi.org/10.3390/cancers12092342>
87. Schmid S, Kübler M, Korcan Ayata C et al (2015) Altered purinergic signaling in the tumor associated immunologic micro-environment in metastasized non-small-cell lung cancer. *Lung Cancer* 90:516–521. <https://doi.org/10.1016/j.lungcan.2015.10.005>
88. Sluyter R, Stokes L (2011) Significance of p2x7 receptor variants to human health and disease. *Recent Patents DNA Gene Seq* 5:41–54. <https://doi.org/10.2174/187221511794839219>
89. Cabrini G, Falzoni S, Forchap SL et al (2005) A His-155 to Tyr polymorphism confers gain-of-function to the human P2X 7 receptor of human leukemic lymphocytes. *J Immunol* 175:82–89. <https://doi.org/10.4049/jimmunol.175.1.82>
90. Dardano A, Falzoni S, Caraccio N et al (2009) 1513A>C polymorphism in the P2X7 receptor gene in patients with papillary thyroid cancer: correlation with histological variants and clinical parameters. *J Clin Endocrinol Metab* 94:695–698. <https://doi.org/10.1210/jc.2008-1322>
91. Duan S, Yu J, Han Z, et al (2016) Association between P2RX7 gene and hepatocellular carcinoma susceptibility: a case-control study in a Chinese han population. *Med Sci Monit* 22:1916–1923. <https://doi.org/10.12659/MSM.895763>
92. Di Virgilio F, Wiley JS (2002) The P2X7 receptor of CLL lymphocytes—a molecule with a split personality. *Lancet* 360:1898–1899. [https://doi.org/10.1016/S0140-6736\(02\)11933-7](https://doi.org/10.1016/S0140-6736(02)11933-7)
93. Wang B, Chen J, Guan Y, et al (2021) Predicted the P2RX7 rs3751143 polymorphism is associated with cancer risk: a meta-analysis and systematic review. *Biosci Rep* 41:<https://doi.org/10.1042/BSR2019387>
94. De Marchi E, Pegoraro A, Adinolfi E (2021) P2X7 receptor in hematological malignancies. *Front Cell Dev Biol* 9:<https://doi.org/10.3389/fcell.2021.645605>
95. Boldrini L, Giordano M, Ali G et al (2014) P2X7 protein expression and polymorphism in non-small cell lung cancer (NSCLC). *J Negat Results Biomed* 13:16. <https://doi.org/10.1186/1477-5751-13-16>
96. Solini A, Simeon V, Derosa L, et al (2015) Genetic interaction of P2X7 receptor and VEGFR-2 polymorphisms identifies a

- favorable prognostic profile in prostate cancer patients. *Oncotarget* 6:28743–28754. <https://doi.org/10.18632/oncotarget.4926>
97. Cheewatrakoolpong B, Gilchrist H, Anthes JC, Greenfeder S (2005) Identification and characterization of splice variants of the human P2X7 ATP channel. *Biochem Biophys Res Commun* 332:17–27. <https://doi.org/10.1016/j.bbrc.2005.04.087>
  98. Skarratt KK, Gu BJ, Lovelace MD et al (2020) A P2RX7 single nucleotide polymorphism haplotype promotes exon 7 and 8 skipping and disrupts receptor function. *FASEB J* 34:3884–3901. <https://doi.org/10.1096/fj.201901198RR>
  99. Giuliani AL, Colognesi D, Ricco T, et al (2014) Trophic activity of human P2X7 receptor isoforms A and B in osteosarcoma. *PLoS One* 9:<https://doi.org/10.1371/journal.pone.0107224>
  100. Ulrich H, Ratajczak MZ, Schneider G, et al (2018) Kinin and purine signaling contributes to neuroblastoma metastasis. *Front Pharmacol* 9:<https://doi.org/10.3389/fphar.2018.00500>
  101. Benzaquen J, Dit Hreich SJ, Heeke S et al (2020) P2RX7B is a new theranostic marker for lung adenocarcinoma patients. *Theranostics* 10:10849–10860. <https://doi.org/10.7150/thno.48229>
  102. Pegoraro A, Orioli E, De Marchi E et al (2020) Differential sensitivity of acute myeloid leukemia cells to daunorubicin depends on P2X7A versus P2X7B receptor expression. *Cell Death Dis* 11:876. <https://doi.org/10.1038/s41419-020-03058-9>
  103. Warburg O, Wind F, Negelein E (1927) The metabolism of tumors in the body. *J Gen Physiol* 8:519–530. <https://doi.org/10.1085/jgp.8.6.519>
  104. Amoroso F, Falzoni S, Adinolfi E et al (2012) The P2X7 receptor is a key modulator of aerobic glycolysis. *Cell Death Dis* 3:e370–e370. <https://doi.org/10.1038/cddis.2012.105>
  105. Todd JN, Poon W, Lyssenko V et al (2015) Variation in glucose homeostasis traits associated with P2RX7 polymorphisms in mice and humans. *J Clin Endocrinol Metab* 100:E688–E696. <https://doi.org/10.1210/jc.2014-4160>
  106. Giacobozzo G, Apolloni S, Coccorello R (2018) Loss of P2X7 receptor function dampens whole body energy expenditure and fatty acid oxidation. *Purinergic Signal* 14:299–305. <https://doi.org/10.1007/s11302-018-9610-y>
  107. Zhang Q, Zhu B, Li Y (2017) Resolution of cancer-promoting inflammation: a new approach for anticancer therapy. *Front Immunol* 8:<https://doi.org/10.3389/fimmu.2017.00071>
  108. Shalpour S, Karin M (2019) Pas de Deux: control of anti-tumor immunity by cancer-associated inflammation. *Immunity* 51:15–26. <https://doi.org/10.1016/j.immuni.2019.06.021>
  109. Chen DS, Mellman I (2013) Oncology meets immunology: the cancer-immunity cycle. *Immunity* 39:1–10. <https://doi.org/10.1016/j.immuni.2013.07.012>
  110. Miller JS, Lanier LL (2019) Natural killer cells in cancer immunotherapy. *Annu Rev Cancer Biol* 3:77–103. <https://doi.org/10.1146/annurev-cancerbio-030518-055653>
  111. Gabrilovich DI, Nagaraj S (2009) Myeloid-derived suppressor cells as regulators of the immune system. *Nat Rev Immunol* 9:162–174. <https://doi.org/10.1038/nri2506>
  112. Hickman S, el Khoury J, Greenberg S et al (1994) P2Z adenosine triphosphate receptor activity in cultured human monocyte-derived macrophages. *Blood* 84:2452–2456. <https://doi.org/10.1182/blood.V84.8.2452.2452>
  113. Ferrari D, Chiozzi P, Falzoni S et al (1997) Extracellular ATP triggers IL-1 beta release by activating the purinergic P2Z receptor of human macrophages. *J Immunol* 159:1451–1458
  114. Berchtold S, Ogilvie ALJ, Bogdan C et al (1999) Human monocyte derived dendritic cells express functional P2X and P2Y receptors as well as ecto-nucleotidases. *FEBS Lett* 458:424–428. [https://doi.org/10.1016/S0014-5793\(99\)01197-7](https://doi.org/10.1016/S0014-5793(99)01197-7)
  115. Ferrari D, La Sala A, Chiozzi P et al (2000) The P2 purinergic receptors of human dendritic cells: identification and coupling to cytokine release. *FASEB J* 14:2466–2476. <https://doi.org/10.1096/fj.00-0031com>
  116. Ma Y, Adjemian S, Mattarollo SR et al (2013) Anticancer chemotherapy-induced intratumoral recruitment and differentiation of antigen-presenting cells. *Immunity* 38:729–741. <https://doi.org/10.1016/j.immuni.2013.03.003>
  117. Hamarshah S, Zeiser R (2020) NLRP3 inflammasome activation in cancer: a double-edged sword. *Front Immunol* 11:<https://doi.org/10.3389/fimmu.2020.01444>
  118. Dinarello CA, Kaplanski G (2018) Indeed, IL-18 is more than an inducer of IFN- $\gamma$ . *J Leukoc Biol* 104:237–238. <https://doi.org/10.1002/JLB.CE0118-025RR>
  119. Feng W, Yang X, Wang L et al (2021) P2X7 promotes the progression of MLL-AF9 induced acute myeloid leukemia by upregulation of Pbx3. *Haematologica* 106:1278–1289. <https://doi.org/10.3324/haematol.2019.243360>
  120. He X, Wan J, Yang X, et al (2021) Bone marrow niche ATP levels determine leukemia-initiating cell activity via P2X7 in leukemic models. *J Clin Invest* 131:<https://doi.org/10.1172/JCI140242>
  121. Gargett CE, Cornish JE, Wiley JS (1997) ATP, a partial agonist for the P2Z receptor of human lymphocytes. *Br J Pharmacol* 122:911–917. <https://doi.org/10.1038/sj.bjp.0701447>
  122. Baricordi O, Ferrari D, Melchiorri L et al (1996) An ATP-activated channel is involved in mitogenic stimulation of human T lymphocytes. *Blood* 87:682–690. <https://doi.org/10.1182/blood.V87.2.682.bloodjournal872682>
  123. Li X-Y, Moesta AK, Xiao C et al (2019) Targeting CD39 in cancer reveals an extracellular ATP- and inflammasome-driven tumor immunity. *Cancer Discov* 9:1754–1773. <https://doi.org/10.1158/2159-8290.CD-19-0541>
  124. Borges da Silva H, Beura LK, Wang H et al (2018) The purinergic receptor P2RX7 directs metabolic fitness of long-lived memory CD8+ T cells. *Nature* 559:264–268. <https://doi.org/10.1038/s41586-018-0282-0>
  125. Park SL, Buzzai A, Rautela J et al (2019) Tissue-resident memory CD8+ T cells promote melanoma-immune equilibrium in skin. *Nature* 565:366–371. <https://doi.org/10.1038/s41586-018-0812-9>
  126. Vacchelli E, Semeraro M, Enot DP, et al (2015) Negative prognostic impact of regulatory T cell infiltration in surgically resected esophageal cancer post-radiochemotherapy. *Oncotarget* 6:20840–20850. <https://doi.org/10.18632/oncotarget.4428>
  127. De Marchi E, Orioli E, Pegoraro A et al (2019) The P2X7 receptor modulates immune cells infiltration, ectonucleotidases expression and extracellular ATP levels in the tumor microenvironment. *Oncogene* 38:3636–3650. <https://doi.org/10.1038/s41388-019-0684-y>
  128. Hubert S, Rissiek B, Klages K et al (2010) Extracellular NAD+ shapes the Foxp3+ regulatory T cell compartment through the ART2-P2X7 pathway. *J Exp Med* 207:2561–2568. <https://doi.org/10.1084/jem.20091154>
  129. Cortés-García JD, López-López C, Cortez-Espinosa N et al (2016) Evaluation of the expression and function of the P2X7 receptor and ART1 in human regulatory T-cell subsets. *Immunobiology* 221:84–93. <https://doi.org/10.1016/j.imbio.2015.07.018>
  130. Dunn GP, Bruce AT, Ikeda H et al (2002) Cancer immunoeediting: from immunosurveillance to tumor escape. *Nat Immunol* 3:991–998. <https://doi.org/10.1038/ni1102-991>
  131. Amoroso F, Salaro E, Falzoni S, et al (2016) P2X7 targeting inhibits growth of human mesothelioma. *Oncotarget* 7:49664–49676. <https://doi.org/10.18632/oncotarget.10430>
  132. Karasawa A, Kawate T (2016) Structural basis for subtype-specific inhibition of the P2X7 receptor. *Elife* 5:<https://doi.org/10.7554/eLife.22153>

133. Gilbert SM, Gidley Baird A, Glazer S et al (2017) A phase I clinical trial demonstrates that nfp2X7-targeted antibodies provide a novel, safe and tolerable topical therapy for basal cell carcinoma. *Br J Dermatol* 177:117–124. <https://doi.org/10.1111/bjd.15364>
134. Douguet L, Janho dit Hreich S, Benzaquen J, et al (2021) A small-molecule P2RX7 activator promotes anti-tumor immune responses and sensitizes lung tumor to immunotherapy. *Nat Commun* 12:653. <https://doi.org/10.1038/s41467-021-20912-2>
135. Yan J, Li X-Y, Roman Aguilera A et al (2020) Control of metastases via myeloid CD39 and NK cell effector function. *Cancer Immunol Res* 8:356–367. <https://doi.org/10.1158/2326-6066.CIR-19-0749>
136. Romagnani A, Rottoli E, Mazza EMC et al (2020) P2X7 receptor activity limits accumulation of T cells within tumors. *Cancer Res* 80:3906–3919. <https://doi.org/10.1158/0008-5472.CAN-19-3807>
137. Di Virgilio F, Giuliani AL, Vultaggio-Poma V, et al (2018) Non-nucleotide agonists triggering P2X7 receptor activation and pore formation. *Front Pharmacol* 9:<https://doi.org/10.3389/fphar.2018.00039>
138. Bidula SM, Cromer BA, Walpole S et al (2019) Mapping a novel positive allosteric modulator binding site in the central vestibule region of human P2X7. *Sci Rep* 9:3231. <https://doi.org/10.1038/s41598-019-39771-5>
139. Falk S, Schwab SD, Frøsig-Jørgensen M et al (2015) P2X7 receptor-mediated analgesia in cancer-induced bone pain. *Neuroscience* 291:93–105. <https://doi.org/10.1016/j.neuroscience.2015.02.011>
140. Bernier L-P, Ase AR, Séguéla P (2018) P2X receptor channels in chronic pain pathways. *Br J Pharmacol* 175:2219–2230. <https://doi.org/10.1111/bph.13957>

**Publisher's note** Springer Nature remains neutral with regard to jurisdictional claims in published maps and institutional affiliations.



**Serena Janho dit Hreich** is currently a PhD student at the Institute for Cancer and Ageing of Nice (IRCAN). She obtained a Master Degree in Health Science, Genetics and Immunology from the University of Nice-Côte d'Azur in 2018. She is interested in immunology and oncology and her PhD work focuses on the role of purinergic signaling, especially the P2RX7 receptor, in antitumor immunity in lung cancer.



Review

# The Purinergic Landscape of Non-Small Cell Lung Cancer

Serena Janho dit Hreich <sup>1</sup>, Jonathan Benzaquen <sup>1</sup>, Paul Hofman <sup>2,3,4</sup> and Valérie Vouret-Craviari <sup>1,\*</sup>

<sup>1</sup> Institute of Research on Cancer and Aging (IRCAN, CNRS, INSERM), FHU OncoAge, Université Côte d'Azur, 06108 Nice, France; serena.janho-dit-hreich@etu.univ-cotedazur.fr (S.J.d.H.); benzaquen.j@chu-nice.fr (J.B.)

<sup>2</sup> CHU Nice, Laboratory of Clinical and Experimental Pathology, Pasteur Hospital, Université Côte d'Azur, 06000 Nice, France; hofman.p@chu-nice.fr

<sup>3</sup> Institute of Research on Cancer and Aging (IRCAN, CNRS, INSERM, Team 4), Université Côte d'Azur, 06100 Nice, France

<sup>4</sup> CHU Nice, FHU OncoAge, Hospital-Integrated Biobank (BB-0033-00025), Université Côte d'Azur, 06000 Nice, France

\* Correspondence: vouret@unice.fr; Tel.: +33-492-031-223

**Simple Summary:** Lung cancer is the most prevalent cancer worldwide with poor overall survival despite many new therapeutic strategies. We discuss in this review the ability of the purinergic landscape to constitute a new potent strategy in the treatment of lung cancer. After defining lung cancer and its current treatments, we present the proteins of the purinergic landscape as well as the mechanisms leading to the production of extracellular ATP, which is at the top of the purinergic signaling chain. We also review the evidence supporting the potency of this strategy through clinical trials dedicated to the proteins of the purinergic landscape.

**Abstract:** Lung cancer is the most common cancer worldwide. Despite recent therapeutic advances, including targeted therapies and immune checkpoint inhibitors, the disease progresses in almost all advanced lung cancers and in up to 50% of early-stage cancers. The purpose of this review is to discuss whether purinergic checkpoints (CD39, CD73, P2RX7, and ADORs), which shape the immune response in the tumor microenvironment, may represent novel therapeutic targets to combat progression of non-small cell lung cancer by enhancing the antitumor immune response.

**Keywords:** purinergic signaling; ectonucleotidases; antitumor immunity; P2RX7; immunotherapies; lung cancer



**Citation:** Janho dit Hreich, S.; Benzaquen, J.; Hofman, P.; Vouret-Craviari, V. The Purinergic Landscape of Non-Small Cell Lung Cancer. *Cancers* **2022**, *14*, 1926. <https://doi.org/10.3390/cancers14081926>

Academic Editor: Jeffrey A. Borgia

Received: 4 March 2022

Accepted: 6 April 2022

Published: 11 April 2022

**Publisher's Note:** MDPI stays neutral with regard to jurisdictional claims in published maps and institutional affiliations.



**Copyright:** © 2022 by the authors. Licensee MDPI, Basel, Switzerland. This article is an open access article distributed under the terms and conditions of the Creative Commons Attribution (CC BY) license (<https://creativecommons.org/licenses/by/4.0/>).

## 1. Introduction

Lung cancer (LC) is the most prevalent cancer worldwide, with an estimated 2.1 million new cases and 1.8 million related deaths annually. More than 70% of LC patients are diagnosed at an advanced stage, with a 5-year survival rate of less than 10%, whereas the survival rate for patients with early-stage disease ranges from 50 to 70%. Furthermore, regardless of treatment options depending on the tumor stage (e.g., surgery, chemotherapy, radio therapy, or targeted therapies), the disease progresses in almost all advanced lung cancers and in up to 50% of early-stage cancers. New and effective strategies to improve the outcome of LC include immunotherapies based on immune checkpoint inhibitors (ICIs), which are now used in routine clinical practice.

ICIs have revolutionized the treatment of non-small cell lung cancer (NSCLC). PD-L1 expression is presently the only approved biomarker used in routine diagnostics for stratification of ICI therapies [1]. The ICIs exploit the ability of lung cancer cells to evade recognition by the PD-1 axis by restoring tumor surveillance by the immune system. ICIs approved for antitumor treatment are mainly monoclonal antibodies against PD-1 (nivolumab, pembrolizumab, cemiplimab), PD-L1 (atezolizumab, durvalumab, avelumab), and CTLA-4 (ipilimumab and tremelimumab). These treatments were initially used alone and are now combined with other immunotherapies or chemotherapies [1]. In recent years,



this new era of treatments has led to significant improvement in the survival and quality of life of patients with LC. Unfortunately, almost all patients with advanced LC experience progression of the disease regardless of treatment options, underscoring the need for new approaches to treat these patients.

Adenosine triphosphate (ATP) and adenosine are components of the tumor microenvironment (TME). Extracellular ATP (eATP) promotes tumor growth but also immune-mediated tumor eradication, mainly via the well-documented purinergic P2RX7 receptor. Adenosine, on the other hand, is generated from eATP via the ectonucleotidases CD39 and CD73 and is an immunosuppressant that acts at the A2A receptor (A2AR) level [2]. Thus, the purinergic landscape consisting of the P2X and P2Y purine receptors, CD39, CD73, and adenosine receptors (P1 purine receptors) shapes TME immune responses and likely acts “in concert” with immunotherapies. In this review, we focus on LC and discuss recent discoveries about the so-called purinergic landscape and its potential as a therapeutic target for treating patients.

## 2. Source of Extracellular ATP

ATP, often referred to as the main energy source of the cell, is released by mitochondria into the cytoplasm and used by all cellular compartments as fuel. ATP is also present outside the cell and is then referred to as extracellular ATP (eATP). eATP is a damage-associated molecular pattern (DAMP) molecule that is recognized by purinergic receptors and degraded by ectonucleotidases.

The source of eATP is generally associated with various types of injury, including trauma, oxidants, and pathogens [3]. eATP in the tumor microenvironment is present at concentrations of hundreds of micromolar [4]. It is released by activated immune cells and dying cells from the immune system, stroma, and tumor compartments.

The composition of immune cells of human non-small cell lung cancer (NSCLC) was characterized by flow cytometry. This showed that adenocarcinoma have a higher percentage of CD45+ leukocytes than the distal lung [5]. Thirteen different types of immune cells were identified. They included different subpopulations of T cells, B cells, macrophages, natural killer (NK) cells, dendritic cells (DC), and granulocytes, mainly neutrophils. Each of these cells can release ATP via specific mechanisms, including channel-mediated export, vesicular exocytosis, and cell death (Figure 1).

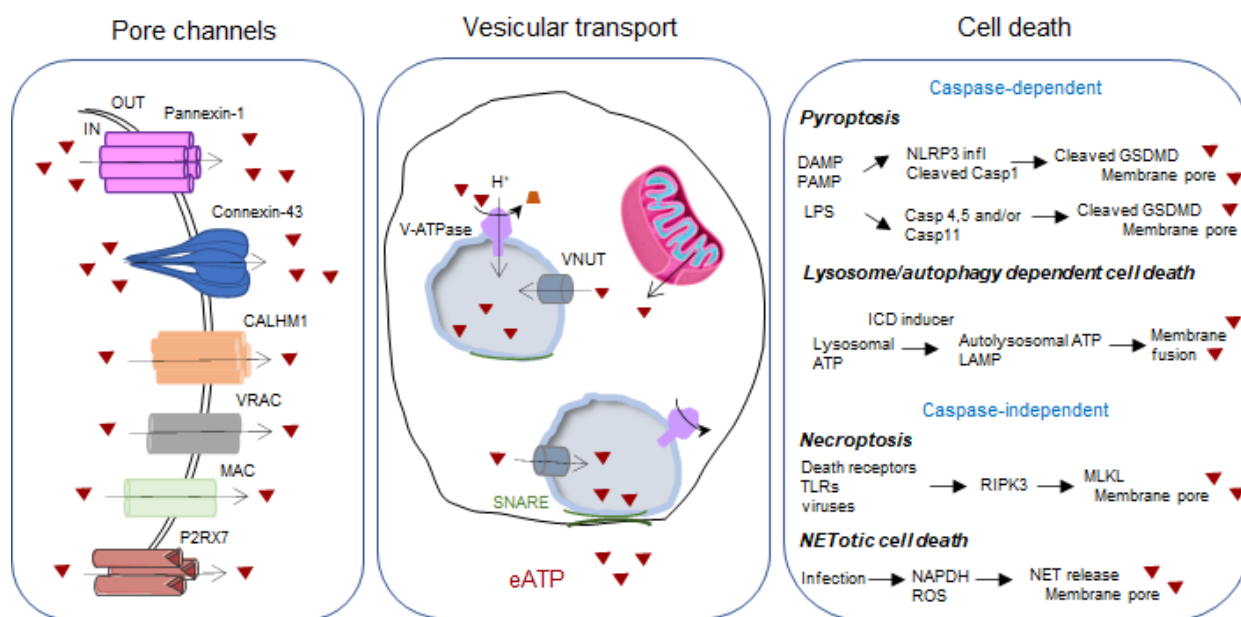


Figure 1. Schematic illustration of the mechanisms involved in the release of eATP.

Pore channels comprise the well described pannexin-1 and connexin-43 proteins assemble to form hexameric membrane structures, but also calcium homeostasis modulator 1 (CALHM1) channels, volume regulated ion channels (VRACs), maxi-anion channels (MACs), and P2RX7 itself. Whereas pore channels allow passive leakage of ATP, vesicular transport is an active mechanism under the control of the vesicular nucleotide transporter (VNUT). VNUT acts in concert with vacuolar proton ATPase (V-ATPase) to accumulate the ATP released from mitochondria within vesicles. The fusion of the vesicles with the membrane is regulated by intracellular  $\text{Ca}^{2+}$  levels and the soluble N-ethylmaleimide-sensitive factor attachment protein receptor (SNARE) and depends on actin cytoskeleton rearrangement and hypoxia. Regulated cell death represents the 3rd source of eATP which can be caspase-dependent and caspase-independent.

Neutrophils do not represent the most abundant immune cell population, accounting for 8.6% of all CD45+ cells in the TME of NSCLC [5]; nevertheless, their role in eATP production is well documented in the literature. What is the upstream activation of neutrophils? What are the signals and mechanisms that trigger ATP release? In 1998, Colgan's team showed that activated neutrophils (with fMLP) release 5'-adenosine monophosphate (AMP), which is then converted to adenosine and further promotes endothelial barrier function [6]. At that time, it was hypothesized that the release of adenine nucleotides occurs by direct transport or diffusion across the cell membrane. Today, we know that in addition to pathogenic agents, hypoxia and inflammation are pathophysiological responses that activate ATP release from neutrophils [7,8]. In particular, connexin-43 and pannexin-1 are proteins that form hemichannels involved in the release of ATP. It is worth noting that other anion channels are also involved in ATP export, as shown in Figure 1 and described elsewhere [9–11]. A substantial fraction of intracellular ATP is also located in cytoplasmic vesicles, and in addition to pore-forming proteins, vesicular exocytosis represents an independent mechanism responsible for ATP release. This mechanism relies on specialized cytosolic granules that store ATP and fuse with the plasma membrane in response to cell signals to secrete their contents. The vesicular nucleotide transporter (VNUT), encoded by the human SLC17A9 gene, is responsible for the vesicular accumulation of ATP [12]. Once accumulated in the secretory granules, ATP secretion has been shown to depend on intracellular  $\text{Ca}^{2+}$  levels and SNARE proteins that mediate membrane fusion upon stimulation [13]. The third mechanism responsible for ATP release is based on cell death, which may be random, the result of a biologically uncontrolled process, or regulated, e.g., involving tightly structured signaling cascades and defined molecular effector mechanisms. Under regulated cell death, necroptosis, pyroptosis, NETotic cell death, and lysosome-dependent cell death (which can be associated with autophagic cell death when the lysosome is fused to the autophagosome) trigger rupture of the plasma membrane and subsequent release of intracellular ATP, as described in detail elsewhere [14,15].

In addition to neutrophils, macrophages, which make up 4.7% of the immune cell infiltrate [5], can also release ATP. They undergo apoptosis, but also necroptosis, pyroptosis, and parthanatosis, a regulated cell death activated by DNA damage triggered by oxidative stress, eventually leading to necroptosis [16]. Moreover, ATP has been shown to stimulate permeabilization of the lysosomal membrane, which in turn causes the release of cathepsin and subsequent activation of pyroptosis. This cellular mechanism, which depends on the P2RX7 receptor and the  $\text{Ca}^{2+}$  influx induced by pannexin-1, highlights the existence of a positive feedback loop in macrophages in which eATP promotes the release of ATP [17].

T cells represent 47% of CD45+ immune cells and therefore dominate the LC landscape. They are sensitive to eATP that enhances their activation via P2RX4 and P2RX7 stimulation [18]. They also release ATP, being subject to death in damaged tissues and tumors [19]. However, we believe that their chronic activation within the TME likely leads to their exhaustion, and it would not be surprising if this lack of effector function correlates with the prevention of cell death in this particular context.

In addition to these mechanisms, treatments used to combat tumor growth also promote the release of ATP. For example, conventional chemotherapies used to treat NSCLC

(platinum derivatives, paclitaxel, and gemcitabine) or radiotherapies (photochemotherapy and irradiation) increase the release of ATP within the TME [20,21]. Moreover, the ATP, as well as the UTP, released after radiation-induced cell damage and cell death, have been shown to act as pro-metastatic factors in human lung cancer cells [22]. Moreover, human A549 lung cells were reported to release ATP after  $\gamma$ -irradiation, and the released ATP contributed to the DNA damage response (DDR) via the P2RX7, P2RY6, and P2RY12 receptors. Remarkably, radiation sensitization was restored when the activity of these receptors was inhibited, resulting in inhibition of the DDR [23,24]. It is important to note that under chemotherapy and radiotherapy, not only ATP but also many DAMPs are released and induce immunogenic cell death (ICD), which corresponds to cell death that causes an immune response. These DAMPs include calreticulin and heat shock proteins released at the cell surface, the chromatin-binding non-histone protein high-mobility group box 1 and the cytoplasmic protein annexin A1 released from dying cells into the TME, and type I interferons (IFNs) released during de novo synthesis [20]. Once bound to their specific pattern recognition receptors expressed by antigen-presenting cells, they trigger both the innate and adaptive immune systems, resulting in cross-presentation of tumor antigens to CD8<sup>+</sup> cytotoxic T lymphocytes, providing critical adjuvant for dying cancer cells [25,26].

Overall, several factors lead to the release of ATP into the extracellular space, resulting in the accumulation of eATP and thus its high concentration in the TME, as mentioned earlier, where its action depends on many factors, including the expression of purinergic receptors and the presence of extracellular ATP-degrading enzymes, which collectively constitute the purinergic landscape (Figure 2).

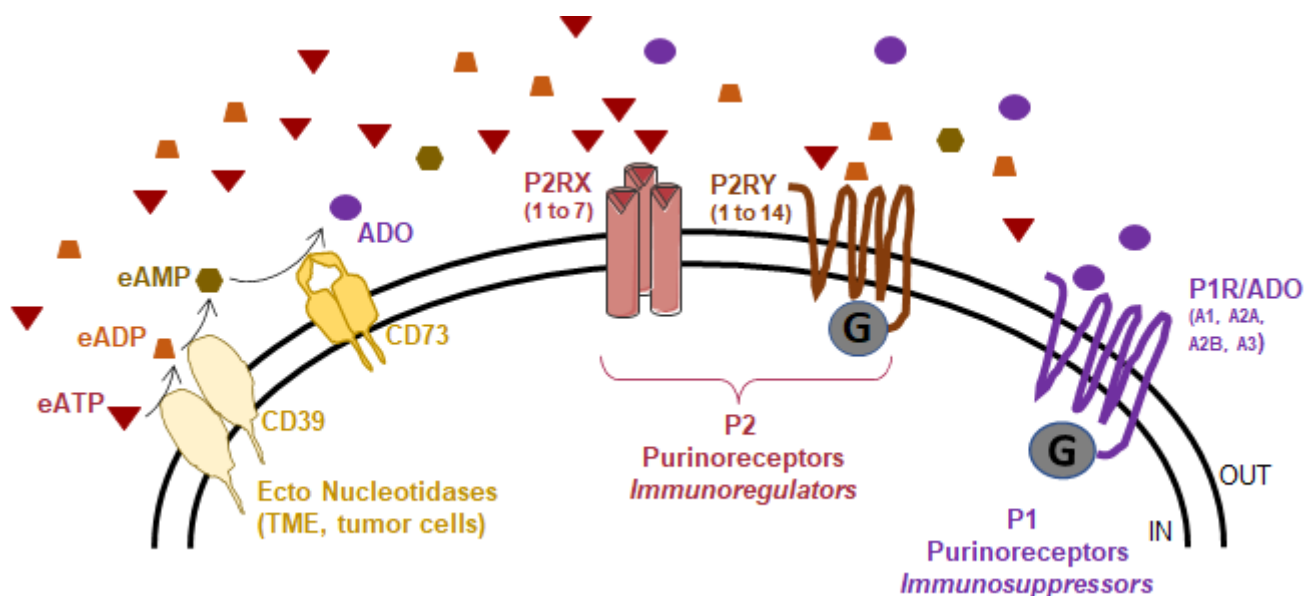


Figure 2. The purinergic landscape.

Three main protein families compose the so-called purinergic landscape: ectonucleotidases, P2 and P1 purinoreceptors. Ectonucleotidases are involved in eATP hydrolysis to produce adenosine (ADO). The P2 purinoreceptors are activated by eATP, and eADP. This family is subdivided into the P2X (homo-/heterotrimeric receptor channel) and P2Y (G-protein coupled) receptors. The P1 purinoreceptors are G-protein coupled receptors activated by adenosine. This family is composed of 4 members: ADORA1, ADORA2A, ADORA2B, and ADORA3.

### 3. The Purinergic Landscape in NSCLC

#### 3.1. Expression of Ectonucleotidases

Once released into the extracellular space, the fate of eATP depends on ectonucleotidases. Four enzyme families have been discovered, cloned, and characterized: ectonucleoside triphosphate diphosphohydrolase (NTPDases), alkaline phosphatases, ectonucleotide pyrophosphatase/phosphodiesterases of NPP type (NPP-type), and ecto-5'-nucleotidase [27]. In combination with the intracellular NAD-degrading enzyme CD38, enzymes for the nucleotide hydrolysis are particularly important in cancer, but also in aging [28]. CD39 (NTPD-1) and CD73 (NT5E) play an important role in calibrating the specificity, duration, and strength of purinergic signals by converting ATP/ADP to AMP, and AMP to adenosine, respectively.

CD39, encoded by NTPDase-1, is the rate-limiting enzyme that hydrolyzes ATP to ADP and ADP to AMP [27]. CD39 is expressed by B cells, innate cells, regulatory T cells, and activated CD4 and CD8 T cells, and has been identified as a marker of exhausted T cells in patients with chronic viral infections [29,30]. In addition to immune cells, CD39 is also expressed on the tumor-associated endothelium and tumor cells [31]. The expression of CD39 was examined in 12 patients after lung surgery, and CD39 expression was found to be increased in the immune infiltrate of the tumor compared with the adjacent non-tumor tissue [32]. Specifically, TCD4+, TCD8+, FoxP3+ regulatory T cells, CD16+ NK cells, B cells, and macrophages expressed CD39 at higher levels. Remarkably, these cells also expressed higher levels of PD-1. The limited number of patients in this study did not allow for the formal conclusion that expression of CD39 and PD-1 is a marker of poor prognosis, but the three out of five patients who relapsed had a high frequency of double-positive CD39+/PD-1+ CD8+ and CD4+ TILs, suggesting that expression of CD39 in cytotoxic T cells may be an important mechanism for tumor-induced immunosuppression in NSCLC. Interestingly, quantification of the proportion of total CD8+ and CD39+ lymphocytes by immunohistochemistry (IHC) of patients with NSCLC was not predictive of response to ICIs. However, the double positive CD39+ CD8+ fraction appears to be a strong predictive biomarker [33]. If confirmed, this finding will be of great importance as there is an urgent need to identify patients with LC who will benefit from ICIs alone or in combination with other treatments, including anti-CD39 antibodies.

CD73, encoded by NT5E, is essential for the generation of extracellular adenosine from AMP. Adenosine could also be formed via the non-canonical pathway of CD38-CD203a-CD73, which is independent of CD39 [34]. CD73 is expressed on the surface of endothelial, stromal, and immune cells, as well as on tumor cells of various origin [35]. In patients with NSCLC, CD73 is expressed on cancer cells, cancer-associated fibroblasts (CAFs), and tumor-infiltrating lymphocytes (TILs), and its expression correlates with the expression of hypoxia-inducible factor-1, a trend confirmed in *in vitro* studies using the lung cancer cell lines H1299 and A549 [36]. In this study, the authors also characterized the expression of CD39 and showed that it is predominantly expressed by CAFs and TILs, in contrast to CD73, which is expressed by both cancer cells and CAFs. Overall, their results suggest that expression of CD73 and CD39 in the tumor stroma regulates immunosuppressive pathways by promoting the prevalence of FoxP3+ and PD-1+ lymphocytes as well as PD-L1 expression by cancer cells, all suggestive of an immunosuppressive microenvironment. However, no association was found between expression of ectonucleotidase and histopathological variables or survival analysis, in contrast to a previous study showing that high CD73 expression was an independent indicator of poor prognosis for overall survival and recurrence-free survival [37].

While it is widely accepted that lung cancer immune escape, tumorigenesis, and tumor progression are associated with high levels of adenosine, PD-1, and PD-L1 within the TME, it is clear that additional work is needed to fully unravel the relationship between all of these players and to fully understand whether their expression can be considered as powerful biomarkers that could guide the choice of treatments.

Another level of complexity lies with patients whose cancer has oncogenic mutations, as highlighted in a recent study that pooled three cohorts of NSCLC patients ( $n = 4189$  total) with oncogenic alterations, including KRAS, MET, RET, BRAF-V600E and non BRAF-V600E, ROS1, ALK, EGFR exon 20, HER2, and classical EGFR (exon 19 deletion and exon 21 L858R) [38]. With regard to KRAS mutations, corresponding to the largest subgroup of oncogenic lung adenocarcinoma, it has been shown that the co-occurrence of genomic alterations in the STK11 and KEAP1 genes leads to a worse outcome in KRAS-mutated patients treated with immunotherapy [39]. In addition, the impact of the tumor mutation burden (TMB) and PD-L1 expression on the clinical outcome of ICI therapies has been demonstrated for NSCLC with BRAF mutations, while EGFR and HER2 mutations and ALK, ROS1, RET and MET fusions define NSCLC subgroups with minimal benefit from ICI, despite a high level of expression of PD-L1 in NSCLC with oncogene fusions. The mechanisms underlying the lack of efficacy of ICI in EGFR-mutated NSCLC patients appear to be related to an immune-influenced phenotype characterized by a low level of expression of PD-L1, low TMB, lower cytotoxic T cell numbers, and low T cell receptor clonality. The analysis of 75 immune checkpoint genes, NTE5 (CD73), and adenosine A1 receptor (A1R) were the most upregulated genes in EGFR-mutated tumors. A single-cell analysis revealed that the tumor cell population expressed CD73, in both treatment-naïve and resistant tumors [40]. Therefore, the CD73/adenosine pathway was identified as a potential therapeutic target for EGFR-mutated NSCLC, and there is no doubt that the information from profiling the TME and antitumor immune response can be used to tailor immunotherapy in selected patients with LC.

### 3.2. Expression of the Purinergic Receptors

The purinergic receptor family is composed of two subfamilies; the G-protein-coupled adenosine receptors (A1R, A2RA1, A2RA2, A3R), which belong to the P1 family, and the ATP receptors, which form the P2 family. The P2 family includes the ligand-gated ion channel family receptors (P2RX1–7) and the G protein-coupled receptor (GPCR) family (P2RY1–2, P2RY4, P2RY6, and P2RY11–14) [41]. A decade ago, Geoffrey Burnstock, who was one of the first to substantiate the importance of purinergic signaling in tumor progression, hypothesized that purinergic signaling might contribute to respiratory diseases [42].

#### 3.2.1. The Adenosine Receptors

Adenosine (ADO) receptors (A1, A2A, A2B, and A3) are expressed in various cells and tissues throughout the body and are activated by ADO in the nanomolar range, with the exception of A2B, which is a low-affinity receptor (micromolar range) and therefore activated mainly under pathophysiological conditions [43]. Activation of ADO receptors on cancer cells affects proliferation, apoptosis, cytoprotection, and migration [44]. Moreover, by inhibiting the antitumor function of both lymphocytes and antigen-presenting cells, ADO promotes tumor growth [45,46]. In addition, ADO can suppress T cell priming by acting directly on DC and macrophages [47]. A2AR signaling has also been shown to block the formation of Th1 and Th17 cells and induce the development of Treg cells [48,49].

The involvement of ADO receptors in progression of LC has been poorly described. A1, A2A, A2B, and A3 receptors are expressed by type I and II alveolar epithelial cells, smooth muscle cells, endothelial cells, and immune cells [42]. Particular attention has been paid to A2AR, which is expressed by T cells in hypoxia and was initially described as a nonredundant immunosuppressive mechanism to protect normal tissues from inflammatory damage and autoimmunity. However, it quickly became clear that tumor cells exploit this immunosuppressive mechanism to their own advantage [50].

#### 3.2.2. The Purinergic Receptors

The P2Y receptor family in NSCLC. The subtypes P2RY1, P2RY2, P2RY4, P2RY6, and P2RY11–14 are expressed in mammals. These G protein-coupled receptors, that stimulate Gq- or Gi-dependent cell signaling, are activated by ligands such as extracellular ATP,

ADP, UTP, UDP, UDP-glucose, and also NAD. All these ligands have different affinities for each subtype [51]. In lung cancer cells, especially in the most studied A549 cell line, the expression of P2RY-2, -6, -12 and -14 has been described. A mitogenic effect through ATP/UTP-mediated activation of P2RY2 and the UDP-activated P2RY6 was reported first [52]. Two years later, P2RY14 expression was detected in primary human type II alveolar epithelial cells, in normal bronchial epithelial cells (Beas-2b cell line), and in A549 cells.

The P2X receptor family in NSCLC. This family consists of seven members (P2RX1–7). These ATP-gated ion channel receptors are formed by three homomeric or heteromeric P2RX subunits. Their activation directly leads to Na<sup>+</sup> and Ca<sup>2+</sup> influx and K<sup>+</sup> efflux across the plasma membrane of the cell, which in turn activates downstream signaling pathways and triggers action potential in excitable cells (e.g., neurons), but also cell proliferation, differentiation, and apoptosis in non-excitable cells (e.g., epithelial cells) [53]. The expression of P2RX receptors mRNA in normal (Beas-2b) and tumor cell lines (H23 and A549) was analyzed by RT-qPCR. The results showed that P2RX-3 to 7 were expressed. P2RX3, 4 and 5 are overexpressed in cancer cells compared to normal cell lines, while P2RX6 and 7 are downregulated [54]. The observation that P2RX7 expression is downregulated in cancer cells is in contradiction with other studies reporting its expression. For example, TGF-β1-induced A549 migration, but not proliferation, is dependent on vesicular exocytosis of ATP, which in turn causes P2RX7 activation through actin fiber formation [55]. This result was confirmed in an independent report using 2 other lung cancer cell lines (lung adenocarcinoma PC-9 cells and mucoepidermoid carcinoma H292 cells), in which the authors also showed that P2RX7 was overexpressed in cancer cells compared with normal bronchial epithelial Beas-2B cells. Furthermore, the authors showed that in PC-9 cells, which have the highest expression of P2RX7, ATP is constitutively released and induced cell proliferation in an autocrine manner. Of note, the expression of P2RX7 in PC-9 cells is dependent on EGFR signaling, which is constitutively activated in this cell line [56]. It has been also shown that increased RNA expression of P2RX4 and P2RX7 correlated with the presence of distant metastases in NSCLC patients, although the status of EGFR mutations was not reported in this study [57]. In addition to migration, eATP has been shown to promote epithelial-to-mesenchymal transition following P2RX7 activation in A549 cells [58]. As mentioned previously, P2RX4 is also expressed by lung tumor cell lines, but its precise role in cancer progression is still unknown.

Despite many conflicting findings in the literature, it seems clear that extracellular nucleotides are actively involved in tumorigenesis by stimulating purinergic receptors expressed directly on tumor cells or on their neighboring stromal and immune cells. The published discrepancies regarding P2RX7 expression may be related to the tools used to characterize its expression. Indeed, there are several oligonucleotides on the market, some of which recognize both the full-length and truncated mRNA of P2RX7, whereas others are specific for one or the other form. The same conclusion can be drawn for antibodies. Some of them recognize the extracellular loop present in both the full-length protein and the truncated form, while others are specific for the C-terminal domain lost in the truncated P2RX7B isoform. For example, we were unable to detect P2RX7 expression on A549 cells when using the monoclonal antibody characterized by Buell [59], whereas the use of a commercial polyclonal antibody by other authors detected its expression on various NSCLC (including A549) and SCLC cancer cell lines [22]. In the same way, tumor cells from NSCLC patients were not stained with the conformational antibody, while immune cells from the same patients showed strong staining [60]. To add complexity, some tools can also detect the truncated isoform of P2RX7 encoded by the splice variant P2RX7B, which has been shown to behave like a protumor factor [60,61].

#### 4. The Purinergic Landscape: A Therapeutically Targetable Circuitry to Treat NSCLC

It is now generally accepted that ectonucleotidases and purinoreceptors, with respect to the purinergic landscape, jointly control tumor growth and metastatic spread. Indeed,

exciting preclinical studies have been conducted in recent years in which players of the purinergic landscape have become novel targets in the fight against LC. For example, blocking antibodies against human CD39 and CD73 promote antitumor immunity by stimulating DC and macrophages, which in turn restore effector T cell activation [62]. In addition, an independent anti-CD39 antibody was developed and tested in various mouse tumor models. This antibody alone attenuates tumor growth, and when combined with the PD-1 antibody, it further slows tumor progression; 50% of mice show complete tumor rejection via a mechanism associated with P2RX7/NLRP3/IL-18 activation in myeloid cells [63]. As for ADO receptors, the use of PBF-509, an A2AR antagonist, in combination with ICI restores the immune response (interferon  $\gamma$  production) of infiltrating lymphocytes from patients with lung tumors [64]. Moreover, the interference with P2RX7 may be particularly relevant, as shown by the numerous preclinical studies described in detail by Lara and coworkers [65]. Only a few studies were dedicated to the lungs. The first showed that the P2RX7 antagonist, AZ10606120, efficiently inhibited the growth of malignant pleural mesothelioma cell lines of patients, when the tumor cell lines were implanted in immunodeficient mice [66]. This finding was attenuated by results showing accelerated tumor growth in *p2rx7<sup>-/-</sup>* mice [67,68], highlighting the importance of P2RX7 expression in host cells. Consistent with this later finding, we recently published results showing that a positive allosteric modulator of P2RX7, in combination with immunotherapy, efficiently inhibited tumor growth in transplantable and oncogene-driven lung tumor models [69,70]. Moreover, purinergic receptors have been shown to play an important role in metastatic spread. Indeed, the migration of cancer cells to a secondary site in the host body is supported by activated platelets that express the P2RY12 receptor. Ticagrelor, a specific inhibitor of P2YR12 commonly used as an anti-platelet agent, inhibits metastasis of B16-F10 melanoma and 4T1 breast cancer in mouse lungs. This result was the first demonstration of the potential of pharmacological blockade of P2RY12 to prevent lung metastasis [71,72]. To our knowledge, there is no study reporting the use of ticagrelor in NSCLC patients. This may change, as there are reports showing that P2Y12-mediated nucleotide signaling plays a key role in the inflammatory response and that the administration of P2RY12 inhibitors to patients with arterial disease does not increase the risk of cancer [73,74]. In addition, there is evidence that the P2RY6 receptor acts as a negative regulator of NK cell function and inhibits their maturation and antitumor activities, which may favor the use of specific inhibitors to enhance the antitumor activity of NK cells [75].

The results of these preclinical studies have attracted great interest from pharmaceutical companies, as evidenced by the number of clinical trials registered on the [clinicaltrials.gov](https://clinicaltrials.gov) website since 2009. Of the 63 clinical trials dedicated to LC and immunotherapies, 25 used inhibitors of proteins from the purinergic landscape (Table 1). Ten trials were dedicated to the blockade of CD39 or CD73, using drugs or monoclonal antibodies alone or in combination with ICIs (anti PD-1 or anti PD-L1), anti A2AR, or chemotherapies. All of these studies are either ongoing in phase 1, or in the first phase of recruitment, and no results have been published yet. Twelve clinical trials, using antagonists of the A2A receptor, are ongoing. Most of these trials are in the recruitment phase and aim to test the efficacy of A2A receptor antagonists in combination with other therapies. For example, the NCT03337698 study is a Phase Ib/II multicenter, randomized, large cohort study of 435 stage IV NSCLC patients, designed to evaluate the efficacy and safety of multiple immunotherapy-based treatment combinations, testing atezolizumab with 14 different molecules, including the A2AR antagonist CPI-444. This is an ongoing study that is expected to be completed by the end of 2023. Two studies have already been completed. The NCT02080078 trial combines erlotinib, a tyrosine kinase inhibitor, with theophylline, a drug with a narrow therapeutic margin that acts as an antagonist of A2AR. The main goal is to see if blocking A2AR activity can reduce the side effect of diarrhea. The study is now complete, but no results have been published yet. In the NCT02403193 trial, the authors used the A2AR antagonist NIR-178 (PBF-509) alone or in combination with anti PD-1 antibodies for NSCLC patients with advanced cancer who had failed standard therapies,

including checkpoint inhibitors and TKI therapies. Promising results were observed, with good tolerability and clinical benefit of the molecule administered alone or in combination with anti PD-1/PD-L1 therapy, regardless of the PD-L1 status [76,77]. In parallel with A2AR inhibition, A3 receptor activation appears to be an alternative therapeutic option as it stimulates apoptosis in A549 human lung cancer cells [78]. Of note, stimulation of A3R by ADO also induces apoptosis in the Lu-65 giant cell carcinoma line and SBC-3 human small cell lung cancer [79,80] and CI-IB-MECA, a selective agonist of A3R, inhibits Lewis lung adenocarcinoma growth in vivo [81]. To our knowledge, A3R agonists have not yet been tested in NSCLC patients.

**Table 1.** Small molecule inhibitors and biologics used against players of the purinergic landscape in clinical trials dedicated to NSCLC.

Clinical Trial NCT	Targeted Protein	Name of Compound	Treatment	Phase	Results
04306900	CD39	TTX-30	±ICI, chemo	1	Active
04336098	CD39	SRF-617	±ICI, chemo	1	Recruiting
05143970	CD73	IPH-5301 (Ab)	±ICI, chemo	1	Recruiting
05001347	CD73	TJ004309 (Ab)	±ICI	2	Recruiting
04148937	CD73	LY3475070	±osinertinib	1	Active
03381274	CD73	MEDI-9447 (Ab)	±ICI	1	Recruiting
04672434	CD73	Syn-024 (Ab)	±ICI	1	Recruiting
03549000	CD73	NZV-930 (Ab)	±ICI	1/1b	Recruiting
03454451	CD73/A2AR	CPI-006 (Ab)	±ICI	1/1b	Recruiting
03549000	CD73/A2AR	NZV-930/NIR178	±ICI	1/1b	Recruiting
02403193	A2AR	PDF-509 (NIR178)	±ICI	1/1b	Completed with Clinical benefit [76,77]
03207867	A2AR	PDF-509 (NIR178)	±ICI	2	Recruiting
05060432	A2AR	EOS-448	±ICI	1/1b	Recruiting
04969315	A2AR	TT-10	±ICI	1/2	Not yet recruiting
03629756	A2AR	AB-298 (Etrumadenant)	±ICI	1	Completed, no results
03381274	A2AR	AZD-4635	±ICI, targeted therapy	1/2	Active
04262856	A2AR/A2BR	AB-298 (Etrumadenant)	±ICI	2	Recruiting
03846310	A2AR/A2BR	AB-298 (Etrumadenant)	±ICI	1/1b	Active
03274479	A2AR	PDF-1129	±ICI	1	Recruiting
05234307	A2AR	PDF-1129	±ICI	1	Not yet recruiting
03337698	A2AR	CPI-444	±ICI, targeted therapy, chemo, radio	1b/2	Recruiting
02080078	A2AR/A2BR	Theophylline	±TKI	1	Completed, no results
01038752	P2Rs	suramin	±chemo	2	Completed
00006929	P2Rs	suramin	±chemo	2	Completed
00066768	P2Rs	suramin	±chemo	1	Completed
01671332	P2Rs	suramin	±chemo	2	Completed

There are numerous small molecules and biologics targeting P2RX7, mainly developed to inhibit the receptor, that have been previously tested in humans to combat inflammatory and mood diseases [65]. We only identified 4 studies when we entered “lung cancer” and “suramin” as keywords across the 24 nonselective and selective inhibitors targeting P2RX7. Suramin is a competitive inhibitor that interacts with the ATP-binding site and potentiates the activity of chemotherapeutic agents. In 2010, suramin was tested in combination with docetaxel and gemcitabine in previously chemotherapy-treated patients with advanced NSCLC. The results of this phase 1 trial showed a manageable toxicity profile and preliminary evidence of antitumor activity [82,83]. In addition, promising results were described



with an antibody that specifically recognizes the E200 epitope of non-functional P2RX7 for the local treatment of primary basal cell carcinoma lesions [84].

Undoubtedly, all these results attest to the interest in targeting players of the purinergic landscape to combat NSCLC. Nevertheless, the search for biomarkers of response will be crucial, and we believe that further combinatorial schemes need to be tested in the future. Indeed, thanks to in silico analyses, we have shown that the molecular pattern of the “purinergic genes”, namely *P2RX7*, *NT5E* (CD73), *ENTPD1* (CD39), *ADORA2A*, *ADORA2B*, and *ADORA3*, is very heterogeneous in both the 135 NSCLC cell lines and the 995 NSCLC patients available in the cBio Cancer Genomic Portal [85,86] (unpublished results).

## 5. Conclusions

We have provided evidence for the potential of the purinergic landscape to shape anti-tumor responses. There are numerous molecules that modulate the activity of purinergic players, and it is likely that many of them are still under development. More importantly, some of them are already being tested in the clinic and the results of these clinical trials will undoubtedly provide new treatment options in the near future. However, given the number of players, their pattern of expression, their expression level, and their mode of action, we believe that studying their expression, distribution, and function will be helpful in determining the most efficient treatment for cancer patients, and this treatment will certainly combine multiple molecules administered together or sequentially. In this context, multiplex IHC analyses, artificial intelligence, and bioinformatics will undoubtedly be very helpful.

**Author Contributions:** Writing—original draft preparation, V.V.-C.; Writing—review and editing, S.J.d.H. and J.B.; Validation, P.H.; Funding acquisition, V.V.-C. All authors have read and agreed to the published version of the manuscript.

**Funding:** This research was funded by Canceropole PACA, Bristol-Myers Squibb Foundation for Research in Immuno-Oncology, the French Government (National Research Agency, ANR through the “Investments for the Future”: program reference #ANR-11-LABX-0028-01), SJH is funded by the “Ligue Nationale Contre le Cancer” and the “Fondation pour la recherche medicale” grant number #FDT202106013099 and ARC (grant number ARCTHEM2021020003478).

**Conflicts of Interest:** The authors declare no conflict of interest.

## References

1. Shields, M.D.; Marin-Acevedo, J.A.; Pellini, B. Immunotherapy for Advanced Non-Small Cell Lung Cancer: A Decade of Progress. *Am. Soc. Clin. Oncol. Educ. B* **2021**, *41*, e105–e127. [[CrossRef](#)] [[PubMed](#)]
2. Kepp, O.; Bezu, L.; Yamazaki, T.; Di Virgilio, F.; Smyth, M.J.; Kroemer, G.; Galluzzi, L. ATP and cancer immunosurveillance. *EMBO J.* **2021**, *40*, e108130. [[CrossRef](#)]
3. Divirgilio, F. Liaisons dangereuses: P2X7 and the inflammasome. *Trends Pharmacol. Sci.* **2007**, *28*, 465–472. [[CrossRef](#)] [[PubMed](#)]
4. Pellegatti, P.; Raffaghello, L.; Bianchi, G.; Piccardi, F.; Pistoia, V.; Di Virgilio, F. Increased level of extracellular ATP at tumor sites: In vivo imaging with plasma membrane luciferase. *PLoS ONE* **2008**, *3*, e2599. [[CrossRef](#)] [[PubMed](#)]
5. Stankovic, B.; Bjørhovde, H.A.K.; Skarshaug, R.; Aamodt, H.; Frafjord, A.; Müller, E.; Hammarström, C.; Beraki, K.; Bækkevold, E.S.; Woldbæk, P.R.; et al. Immune Cell Composition in Human Non-small Cell Lung Cancer. *Front. Immunol.* **2019**, *9*, 1–21. [[CrossRef](#)] [[PubMed](#)]
6. Lennon, P.F.; Taylor, C.T.; Stahl, G.L.; Colgan, S.P. Neutrophil-derived 5'-Adenosine Monophosphate Promotes Endothelial Barrier Function via CD73-mediated Conversion to Adenosine and Endothelial A2B Receptor Activation. *J. Exp. Med.* **1998**, *188*, 1433–1443. [[CrossRef](#)]
7. Eltzschig, H.K.; Ibla, J.C.; Furuta, G.T.; Leonard, M.O.; Jacobson, K.A.; Enyoloji, K.; Robson, S.C.; Colgan, S.P. Coordinated Adenine Nucleotide Phosphohydrolysis and Nucleoside Signaling in Posthypoxic Endothelium. *J. Exp. Med.* **2003**, *198*, 783–796. [[CrossRef](#)]
8. Thompson, L.F.; Eltzschig, H.K.; Ibla, J.C.; Van De Wiele, C.J.; Resta, R.; Morote-Garcia, J.C.; Colgan, S.P. Crucial Role for Ecto-5'-Nucleotidase (CD73) in Vascular Leakage during Hypoxia. *J. Exp. Med.* **2004**, *200*, 1395–1405. [[CrossRef](#)]
9. Eltzschig, H.K.; Eckle, T.; Mager, A.; Küper, N.; Karcher, C.; Weissmüller, T.; Boengler, K.; Schulz, R.; Robson, S.C.; Colgan, S.P. ATP Release From Activated Neutrophils Occurs via Connexin 43 and Modulates Adenosine-Dependent Endothelial Cell Function. *Circ. Res.* **2006**, *99*, 1100–1108. [[CrossRef](#)]

10. Bao, Y.; Chen, Y.; Ledderose, C.; Li, L.; Junger, W.G. Pannexin 1 Channels Link Chemoattractant Receptor Signaling to Local Excitation and Global Inhibition Responses at the Front and Back of Polarized Neutrophils. *J. Biol. Chem.* **2013**, *288*, 22650–22657. [[CrossRef](#)]
11. Dosch, M.; Gerber, J.; Jebbawi, F.; Beldi, G. Mechanisms of ATP Release by Inflammatory Cells. *Int. J. Mol. Sci.* **2018**, *19*, 1222. [[CrossRef](#)] [[PubMed](#)]
12. Sawada, K.; Echigo, N.; Juge, N.; Miyaji, T.; Otsuka, M.; Omote, H.; Yamamoto, A.; Moriyama, Y. Identification of a vesicular nucleotide transporter. *Proc. Natl. Acad. Sci. USA* **2008**, *105*, 5683–5686. [[CrossRef](#)] [[PubMed](#)]
13. Südhof, T.C.; Rothman, J.E. Membrane Fusion: Grappling with SNARE and SM Proteins. *Science* **2009**, *323*, 474–477. [[CrossRef](#)] [[PubMed](#)]
14. Tang, D.; Kang, R.; Berghe, T.V.; Vandenabeele, P.; Kroemer, G. The molecular machinery of regulated cell death. *Cell Res.* **2019**, *29*, 347–364. [[CrossRef](#)]
15. Martins, I.; Wang, Y.; Michaud, M.; Ma, Y.; Sukkurwala, A.Q.; Shen, S.; Kepp, O.; Métivier, D.; Galluzzi, L.; Perfettini, J.-L.; et al. Molecular mechanisms of ATP secretion during immunogenic cell death. *Cell Death Differ.* **2014**, *21*, 79–91. [[CrossRef](#)]
16. Robinson, N.; Ganesan, R.; Hegedűs, C.; Kovács, K.; Kufer, T.A.; Virág, L. Programmed necrotic cell death of macrophages: Focus on pyroptosis, necroptosis, and parthanatos. *Redox Biol.* **2019**, *26*, 101239. [[CrossRef](#)]
17. Santos, S.A.C.S.; Persechini, P.M.; Henriques-Santos, B.M.; Bello-Santos, V.G.; Castro, N.G.; Costa de Sousa, J.; Genta, F.A.; Santiago, M.F.; Coutinho-Silva, R.; Savio, L.E.B.; et al. P2X7 Receptor Triggers Lysosomal Leakage Through Calcium Mobilization in a Mechanism Dependent on Pannexin-1 Hemichannels. *Front. Immunol.* **2022**, *13*, 75105. [[CrossRef](#)]
18. Brock, V.J.; Wolf, I.M.A.; Er-Lukowiak, M.; Lory, N.; Stähler, T.; Woelk, L.-M.; Mittrücker, H.-W.; Müller, C.E.; Koch-Nolte, F.; Rissiek, B.; et al. P2X4 and P2X7 are essential players in basal T cell activity and Ca<sup>2+</sup> signaling milliseconds after T cell activation. *Sci. Adv.* **2022**, *8*, abl9770. [[CrossRef](#)]
19. Grassi, F. The P2X7 Receptor as Regulator of T Cell Development and Function. *Front. Immunol.* **2020**, *11*, 1179. [[CrossRef](#)]
20. Fucikova, J.; Kepp, O.; Kasikova, L.; Petroni, G.; Yamazaki, T.; Liu, P.; Zhao, L.; Spisek, R.; Kroemer, G.; Galluzzi, L. Detection of immunogenic cell death and its relevance for cancer therapy. *Cell Death Dis.* **2020**, *11*, 1013. [[CrossRef](#)]
21. Golden, E.B.; Apetoh, L. Radiotherapy and Immunogenic Cell Death. *Semin. Radiat. Oncol.* **2015**, *25*, 11–17. [[CrossRef](#)] [[PubMed](#)]
22. Schneider, G.; Glaser, T.; Lameu, C.; Abdelbaset-Ismail, A.; Sellers, Z.P.; Moniuszko, M.; Ulrich, H.; Ratajczak, M.Z. Extracellular nucleotides as novel, underappreciated pro-metastatic factors that stimulate purinergic signaling in human lung cancer cells. *Mol. Cancer* **2015**, *14*, 201. [[CrossRef](#)] [[PubMed](#)]
23. Ide, S.; Nishimaki, N.; Tsukimoto, M.; Kojima, S. Purine receptor P2Y6 mediates cellular response to  $\gamma$ -ray-induced DNA damage. *J. Toxicol. Sci.* **2014**, *39*, 15–23. [[CrossRef](#)] [[PubMed](#)]
24. Nishimaki, N.; Tsukimoto, M.; Kitami, A.; Kojima, S. Autocrine regulation of  $\gamma$ -irradiation-induced DNA damage response via extracellular nucleotides-mediated activation of P2Y6 and P2Y12 receptors. *DNA Repair (Amst.)* **2012**, *11*, 657–665. [[CrossRef](#)] [[PubMed](#)]
25. Ma, Y.; Adjemian, S.; Yang, H.; Catani, J.P.P.; Hannani, D.; Martins, I.; Michaud, M.; Kepp, O.; Sukkurwala, A.Q.; Vacchelli, E.; et al. ATP-dependent recruitment, survival and differentiation of dendritic cell precursors in the tumor bed after anticancer chemotherapy. *Oncoimmunology* **2013**, *2*, e24568. [[CrossRef](#)] [[PubMed](#)]
26. Ma, Y.; Adjemian, S.; Mattarollo, S.R.; Yamazaki, T.; Aymeric, L.; Yang, H.; Portela Catani, J.P.; Hannani, D.; Duret, H.; Steegh, K.; et al. Anticancer chemotherapy-induced intratumoral recruitment and differentiation of antigen-presenting cells. *Immunity* **2013**, *38*, 729–741. [[CrossRef](#)]
27. Schetinger, M.R.C.; Morsch, V.M.; Bonan, C.D.; Wyse, A.T.S. NTPDase and 5'-nucleotidase activities in physiological and disease conditions: New perspectives for human health. *BioFactors* **2007**, *31*, 77–98. [[CrossRef](#)]
28. Chini, E.N.; Chini, C.C.S.; Espindola Netto, J.M.; de Oliveira, G.C.; van Schooten, W. The Pharmacology of CD38/NADase: An Emerging Target in Cancer and Diseases of Aging. *Trends Pharmacol. Sci.* **2018**, *39*, 424–436. [[CrossRef](#)]
29. Gupta, P.K.; Godec, J.; Wolski, D.; Adland, E.; Yates, K.; Pauken, K.E.; Cosgrove, C.; Ledderose, C.; Junger, W.G.; Robson, S.C.; et al. CD39 Expression Identifies Terminally Exhausted CD8<sup>+</sup> T Cells. *PLoS Pathog.* **2015**, *11*, e1005177. [[CrossRef](#)]
30. Zhao, H.; Bo, C.; Kang, Y.; Li, H. What Else Can CD39 Tell Us? *Front. Immunol.* **2017**, *8*, 727. [[CrossRef](#)]
31. Bastid, J.; Regairaz, A.; Bonnefoy, N.; Déjou, C.; Giustiniani, J.; Laheurte, C.; Cochaud, S.; Laprevotte, E.; Funck-Brentano, E.; Hemon, P.; et al. Inhibition of CD39 Enzymatic Function at the Surface of Tumor Cells Alleviates Their Immunosuppressive Activity. *Cancer Immunol. Res.* **2015**, *3*, 254–265. [[CrossRef](#)] [[PubMed](#)]
32. Tøndell, A.; Wahl, S.G.F.; Sponaas, A.-M.; Sørhaug, S.; Børset, M.; Haug, M. Ectonucleotidase CD39 and Checkpoint Signalling Receptor Programmed Death 1 are Highly Elevated in Intratumoral Immune Cells in Non-small-cell Lung Cancer. *Transl. Oncol.* **2020**, *13*, 17–24. [[CrossRef](#)]
33. Yeong, J.; Suteja, L.; Simoni, Y.; Lau, K.W.; Tan, A.C.; Li, H.H.; Lim, S.; Loh, J.H.; Wee, F.Y.T.; Nerurkar, S.N.; et al. Intratumoral CD39<sup>+</sup>CD8<sup>+</sup> T Cells Predict Response to Programmed Cell Death Protein-1 or Programmed Death Ligand-1 Blockade in Patients With NSCLC. *J. Thorac. Oncol.* **2021**, *16*, 1349–1358. [[CrossRef](#)] [[PubMed](#)]
34. Horenstein, A.L.; Chillemi, A.; Zaccarello, G.; Bruzzone, S.; Quarona, V.; Zito, A.; Serra, S.; Malavasi, F. A CD38/CD203a/CD73 ectoenzymatic pathway independent of CD39 drives a novel adenosinergic loop in human T lymphocytes. *Oncoimmunology* **2013**, *2*, e26246. [[CrossRef](#)]

35. Chen, S.; Wainwright, D.A.; Wu, J.D.; Wan, Y.; Matei, D.E.; Zhang, Y.; Zhang, B. CD73: An emerging checkpoint for cancer immunotherapy. *Immunotherapy* **2019**, *11*, 983–997. [[CrossRef](#)]
36. Giatromanolaki, A.; Kouroupi, M.; Pouliliou, S.; Mitrakas, A.; Hasan, F.; Pappa, A.; Koukourakis, M.I. Ectonucleotidase CD73 and CD39 expression in non-small cell lung cancer relates to hypoxia and immunosuppressive pathways. *Life Sci.* **2020**, *259*, 118389. [[CrossRef](#)] [[PubMed](#)]
37. Inoue, Y.; Yoshimura, K.; Kurabe, N.; Kahyo, T.; Kawase, A.; Tanahashi, M.; Ogawa, H.; Inui, N.; Funai, K.; Shinmura, K.; et al. Prognostic impact of CD73 and A2A adenosine receptor expression in non-small-cell lung cancer. *Oncotarget* **2017**, *8*, 8738–8751. [[CrossRef](#)]
38. Negrao, M.V.; Skoulidis, F.; Montesion, M.; Schulze, K.; Bara, I.; Shen, V.; Xu, H.; Hu, S.; Sui, D.; Elamin, Y.Y.; et al. Oncogene-specific differences in tumor mutational burden, PD-L1 expression, and outcomes from immunotherapy in non-small cell lung cancer. *J. Immunother. Cancer* **2021**, *9*, e002891. [[CrossRef](#)]
39. Ricciuti, B.; Arbour, K.C.; Lin, J.J.; Vajdi, A.; Vokes, N.; Hong, L.; Zhang, J.; Tolstorukov, M.Y.; Li, Y.Y.; Spurr, L.F.; et al. Diminished Efficacy of Programmed Death-(Ligand)1 Inhibition in STK11- and KEAP1-Mutant Lung Adenocarcinoma Is Affected by KRAS Mutation Status. *J. Thorac. Oncol.* **2022**, *17*, 399–410. [[CrossRef](#)]
40. Le, X.; Negrao, M.V.; Reuben, A.; Federico, L.; Diao, L.; McGrail, D.; Nilsson, M.; Robichaux, J.; Munoz, I.G.; Patel, S.; et al. Characterization of the Immune Landscape of EGFR-Mutant NSCLC Identifies CD73/Adenosine Pathway as a Potential Therapeutic Target. *J. Thorac. Oncol.* **2021**, *16*, 583–600. [[CrossRef](#)]
41. Burnstock, G.; Di Virgilio, F. Purinergic signalling and cancer. *Purinergic Signal.* **2013**, *9*, 491–540. [[CrossRef](#)] [[PubMed](#)]
42. Burnstock, G.; Brouns, I.; Adriaensen, D.; Timmermans, J.-P. Purinergic Signaling in the Airways. *Pharmacol. Rev.* **2012**, *64*, 834–868. [[CrossRef](#)] [[PubMed](#)]
43. Sek, K.; Mølck, C.; Stewart, G.; Kats, L.; Darcy, P.; Beavis, P. Targeting Adenosine Receptor Signaling in Cancer Immunotherapy. *Int. J. Mol. Sci.* **2018**, *19*, 3837. [[CrossRef](#)] [[PubMed](#)]
44. Kazemi, M.H.; Raofi Mohseni, S.; Hojjat-Farsangi, M.; Anvari, E.; Ghalamfarsa, G.; Mohammadi, H.; Jadidi-Niaragh, F. Adenosine and adenosine receptors in the immunopathogenesis and treatment of cancer. *J. Cell. Physiol.* **2018**, *233*, 2032–2057. [[CrossRef](#)]
45. MacKenzie, W.M.; Hoskin, D.W.; Blay, J. Adenosine Suppresses  $\alpha4\beta7$  Integrin-Mediated Adhesion of T Lymphocytes to Colon Adenocarcinoma Cells. *Exp. Cell Res.* **2002**, *276*, 90–100. [[CrossRef](#)]
46. Williams, B.A.; Manzer, A.; Blay, J.; Hoskin, D.W. Adenosine Acts through a Novel Extracellular Receptor to Inhibit Granule Exocytosis by Natural Killer Cells. *Biochem. Biophys. Res. Commun.* **1997**, *231*, 264–269. [[CrossRef](#)]
47. Panther, E.; Idzko, M.; Herouy, Y.; Rheinen, H.; Gebicke-Haerter, P.J.; Mrowietz, U.; Dichmann, S.; Norgauer, J. Expression and function of adenosine receptors in human dendritic cells. *FASEB J.* **2001**, *15*, 1963–1970. [[CrossRef](#)]
48. Zarek, P.E.; Huang, C.-T.; Lutz, E.R.; Kowalski, J.; Horton, M.R.; Linden, J.; Drake, C.G.; Powell, J.D. A2A receptor signaling promotes peripheral tolerance by inducing T-cell anergy and the generation of adaptive regulatory T cells. *Blood* **2008**, *111*, 251–259. [[CrossRef](#)]
49. Sitkovsky, M.V.; Hatfield, S.; Abbott, R.; Belikoff, B.; Lukashev, D.; Ohta, A. Hostile, Hypoxia–A2-Adenosinergic Tumor Biology as the Next Barrier to Overcome for Tumor Immunologists. *Cancer Immunol. Res.* **2014**, *2*, 598–605. [[CrossRef](#)]
50. Lukashev, D.; Ohta, A.; Sitkovsky, M. Hypoxia-dependent anti-inflammatory pathways in protection of cancerous tissues. *Cancer Metastasis Rev.* **2007**, *26*, 273–279. [[CrossRef](#)]
51. Burnstock, G. Purinergic signalling. *Br. J. Pharmacol.* **2006**, *147*, S172–S181. [[CrossRef](#)] [[PubMed](#)]
52. Schäfer, R.; Sedehizade, F.; Welte, T.; Reiser, G. ATP- and UTP-activated P2Y receptors differently regulate proliferation of human lung epithelial tumor cells. *Am. J. Physiol. Cell. Mol. Physiol.* **2003**, *285*, L376–L385. [[CrossRef](#)] [[PubMed](#)]
53. Burnstock, G.; Knight, G.E. Cellular Distribution and Functions of P2 Receptor Subtypes in Different Systems. *Int. Rev. Cytol.* **2004**, *240*, 31–304. [[PubMed](#)]
54. Song, S.; Jacobson, K.N.; McDermott, K.M.; Reddy, S.P.; Cress, A.E.; Tang, H.; Dudek, S.M.; Black, S.M.; Garcia, J.G.N.; Makino, A.; et al. ATP promotes cell survival via regulation of cytosolic  $[Ca^{2+}]$  and Bcl-2/Bax ratio in lung cancer cells. *Am. J. Physiol. Physiol.* **2016**, *310*, C99–C114. [[CrossRef](#)] [[PubMed](#)]
55. Takai, E.; Tsukimoto, M.; Harada, H.; Sawada, K.; Moriyama, Y.; Kojima, S. Autocrine regulation of TGF- $\beta$ 1-induced cell migration by exocytosis of ATP and activation of P2 receptors in human lung cancer cells. *J. Cell Sci.* **2012**, *125*, 5051–5060. [[CrossRef](#)] [[PubMed](#)]
56. Takai, E.; Tsukimoto, M.; Harada, H.; Kojima, S. Autocrine signaling via release of ATP and activation of P2X7 receptor influences motile activity of human lung cancer cells. *Purinergic Signal.* **2014**, *10*, 487–497. [[CrossRef](#)]
57. Schmid, S.; Kübler, M.; Korcan Ayata, C.; Lazar, Z.; Haager, B.; Hoßfeld, M.; Meyer, A.; Cicko, S.; Elze, M.; Wiesemann, S.; et al. Altered purinergic signaling in the tumor associated immunologic microenvironment in metastasized non-small-cell lung cancer. *Lung Cancer* **2015**, *90*, 516–521. [[CrossRef](#)]
58. Cao, Y.; Wang, X.; Li, Y.; Evers, M.; Zhang, H.; Chen, X. Extracellular and macropinocytosis internalized ATP work together to induce epithelial–mesenchymal transition and other early metastatic activities in lung cancer. *Cancer Cell Int.* **2019**, *19*, 254. [[CrossRef](#)]
59. Buell, G.; Chessell, I.P.; Michel, A.D.; Collo, G.; Salazzo, M.; Herren, S.; Gretener, D.; Grahames, C.; Kaur, R.; Kosco-Vilbois, M.H.; et al. Blockade of human P2X7 receptor function with a monoclonal antibody. *Blood* **1998**, *92*, 3521–3528. [[CrossRef](#)]

60. Benzaquen, J.; Dit Hreich, S.J.; Heeke, S.; Juhel, T.; Lalvee, S.; Bauwens, S.; Saccani, S.; Lenormand, P.; Hofman, V.; Butori, M.; et al. P2RX7B is a new theranostic marker for lung adenocarcinoma patients. *Theranostics* **2020**, *10*, 10849–10860. [[CrossRef](#)]
61. Adinolfi, E.; Raffaghello, L.; Giuliani, A.L.; Cavazzini, L.; Capece, M.; Chiozzi, P.; Bianchi, G.; Kroemer, G.; Pistoia, V.; Di Virgilio, F. Expression of P2X7 receptor increases in vivo tumor growth. *Cancer Res.* **2012**, *72*, 2957–2969. [[CrossRef](#)] [[PubMed](#)]
62. Perrot, I.; Michaud, H.-A.; Giraudon-Paoli, M.; Augier, S.; Docquier, A.; Gros, L.; Courtois, R.; Déjou, C.; Jecko, D.; Becquart, O.; et al. Blocking Antibodies Targeting the CD39/CD73 Immunosuppressive Pathway Unleash Immune Responses in Combination Cancer Therapies. *Cell Rep.* **2019**, *27*, 2411–2425.e9. [[CrossRef](#)] [[PubMed](#)]
63. Li, X.-Y.; Moesta, A.K.; Xiao, C.; Nakamura, K.; Casey, M.; Zhang, H.; Madore, J.; Lepletier, A.; Aguilera, A.R.; Sundarraj, A.; et al. Targeting CD39 in Cancer Reveals an Extracellular ATP- and Inflammasome-Driven Tumor Immunity. *Cancer Discov.* **2019**, *9*, 1754–1773. [[CrossRef](#)]
64. Mediavilla-Varela, M.; Castro, J.; Chiappori, A.; Noyes, D.; Hernandez, D.C.; Allard, B.; Stagg, J.; Antonia, S.J. A Novel Antagonist of the Immune Checkpoint Protein Adenosine A2a Receptor Restores Tumor-Infiltrating Lymphocyte Activity in the Context of the Tumor Microenvironment. *Neoplasia* **2017**, *19*, 530–536. [[CrossRef](#)] [[PubMed](#)]
65. Lara, R.; Adinolfi, E.; Harwood, C.A.; Philpott, M.; Barden, J.A.; Di Virgilio, F.; McNulty, S. P2X7 in Cancer: From Molecular Mechanisms to Therapeutics. *Front. Pharmacol.* **2020**, *11*, 793. [[CrossRef](#)] [[PubMed](#)]
66. Amoroso, F.; Salaro, E.; Falzoni, S.; Chiozzi, P.; Giuliani, A.L.; Cavallesco, G.; Maniscalco, P.; Puozzo, A.; Bononi, I.; Martini, F.; et al. P2X7 targeting inhibits growth of human mesothelioma. *Oncotarget* **2016**, *7*, 49664–49676. [[CrossRef](#)] [[PubMed](#)]
67. Adinolfi, E.; Capece, M.; Franceschini, A.; Falzoni, S.; Giuliani, A.L.; Rotondo, A.; Sarti, A.C.; Bonora, M.; Syberg, S.; Corigliano, D.; et al. Accelerated tumor progression in mice lacking the ATP receptor P2X7. *Cancer Res.* **2015**, *75*, 635–644. [[CrossRef](#)] [[PubMed](#)]
68. Hofman, P.; Cherfils-Vicini, J.; Bazin, M.; Ilie, M.; Juhel, T.; Hébuterne, X.; Gilson, E.; Schmid-Alliana, A.; Boyer, O.; Adriouch, S.; et al. Genetic and pharmacological inactivation of the purinergic P2RX7 receptor dampens inflammation but increases tumor incidence in a mouse model of colitis-associated cancer. *Cancer Res.* **2015**, *75*, 835–845. [[CrossRef](#)]
69. Douguet, L.; Janho dit Hreich, S.; Benzaquen, J.; Seguin, L.; Juhel, T.; Dezitter, X.; Durant, C.; Ryffel, B.; Kanellopoulos, J.; Delarasse, C.; et al. A small-molecule P2RX7 activator promotes anti-tumor immune responses and sensitizes lung tumor to immunotherapy. *Nat. Commun.* **2021**, *12*, 653. [[CrossRef](#)]
70. Janho dit Hreich, S.; Benzaquen, J.; Hofman, P.; Vouret-Craviari, V. To inhibit or to boost the ATP/P2RX7 pathway to fight cancer—that is the question. *Purinergic Signal.* **2021**, *17*, 619–631. [[CrossRef](#)]
71. Gebremeskel, S.; LeVatte, T.; Liwski, R.S.; Johnston, B.; Bezuhly, M. The reversible P2Y12 inhibitor ticagrelor inhibits metastasis and improves survival in mouse models of cancer. *Int. J. Cancer* **2015**, *136*, 234–240. [[CrossRef](#)] [[PubMed](#)]
72. Gareau, A.J.; Brien, C.; Gebremeskel, S.; Liwski, R.S.; Johnston, B.; Bezuhly, M. Ticagrelor inhibits platelet–tumor cell interactions and metastasis in human and murine breast cancer. *Clin. Exp. Metastasis* **2018**, *35*, 25–35. [[CrossRef](#)] [[PubMed](#)]
73. Kaufmann, C.C.; Lyon, A.R.; Wojta, J.; Huber, K. Is P2Y12 inhibitor therapy associated with an increased risk of cancer? *Eur. Heart J. Cardiovasc. Pharmacother.* **2019**, *5*, 100–104. [[CrossRef](#)] [[PubMed](#)]
74. Mansour, A.; Bachelot-Loza, C.; Nessler, N.; Gaussem, P.; Gouin-Thibault, I. P2Y12 Inhibition beyond Thrombosis: Effects on Inflammation. *Int. J. Mol. Sci.* **2020**, *21*, 1391. [[CrossRef](#)] [[PubMed](#)]
75. Li, Z.; Gao, Y.; He, C.; Wei, H.; Zhang, J.; Zhang, H.; Hu, L.; Jiang, W. Purinergic Receptor P2Y 6 Is a Negative Regulator of NK Cell Maturation and Function. *J. Immunol.* **2021**, *207*, 1555–1565. [[CrossRef](#)]
76. Chiappori, A.; Williams, C.C.; Creelan, B.C.; Tanvetyanon, T.; Gray, J.E.; Haura, E.B.; Thapa, R.; Chen, D.-T.; Beg, A.A.; Boyle, T.A.; et al. Phase I/II study of the A2AR antagonist NIR178 (PBF-509), an oral immunotherapy, in patients (pts) with advanced NSCLC. *J. Clin. Oncol.* **2018**, *36*, 9089. [[CrossRef](#)]
77. Fong, L.; Forde, P.M.; Powderly, J.D.; Goldman, J.W.; Nemunaitis, J.J.; Luke, J.J.; Hellmann, M.D.; Kummar, S.; Doebele, R.C.; Mahadevan, D.; et al. Safety and clinical activity of adenosine A2a receptor (A2aR) antagonist, CPI-444, in anti-PD1/PDL1 treatment-refractory renal cell (RCC) and non-small cell lung cancer (NSCLC) patients. *J. Clin. Oncol.* **2017**, *35*, 3004. [[CrossRef](#)]
78. Kamiya, H.; Kanno, T.; Fujita, Y.; Gotoh, A.; Nakano, T.; Nishizaki, T. Apoptosis-Related Gene Transcription in Human A549 Lung Cancer Cells via A 3 Adenosine Receptor. *Cell. Physiol. Biochem.* **2012**, *29*, 687–696. [[CrossRef](#)]
79. Kanno, T.; Nakano, T.; Fujita, Y.; Gotoh, A.; Nishizaki, T. Adenosine Induces Apoptosis in SBC-3 Human Lung Cancer Cells through A 3 Adenosine Receptor-Dependent AMID Upregulation. *Cell. Physiol. Biochem.* **2012**, *30*, 666–676. [[CrossRef](#)]
80. Otsuki, T.; Kanno, T.; Fujita, Y.; Tabata, C.; Fukuoka, K.; Nakano, T.; Gotoh, A.; Nishizaki, T. A 3 Adenosine Receptor-Mediated p53-Dependent Apoptosis in Lu-65 Human Lung Cancer Cells. *Cell. Physiol. Biochem.* **2012**, *30*, 210–220. [[CrossRef](#)]
81. Nakamura, K.; Yoshikawa, N.; Yamaguchi, Y.; Kagota, S.; Shinozuka, K.; Kunitomo, M. Antitumor effect of cordycepin (3'-deoxyadenosine) on mouse melanoma and lung carcinoma cells involves adenosine A3 receptor stimulation. *Anticancer Res.* **2006**, *26*, 43–47. [[PubMed](#)]
82. Lam, E.T.; Au, J.L.-S.; Otterson, G.A.; Guillaume Wientjes, M.; Chen, L.; Shen, T.; Wei, Y.; Li, X.; Bekaii-Saab, T.; Murgo, A.J.; et al. Phase I trial of non-cytotoxic suramin as a modulator of docetaxel and gemcitabine therapy in previously treated patients with non-small cell lung cancer. *Cancer Chemother. Pharmacol.* **2010**, *66*, 1019–1029. [[CrossRef](#)] [[PubMed](#)]
83. Villalona-Calero, M.A.; Otterson, G.A.; Wientjes, M.G.; Weber, F.; Bekaii-Saab, T.; Young, D.; Murgo, A.J.; Jensen, R.; Yeh, T.-K.; Wei, Y.; et al. Noncytotoxic suramin as a chemosensitizer in patients with advanced non-small-cell lung cancer: A phase II study. *Ann. Oncol.* **2008**, *19*, 1903–1909. [[CrossRef](#)] [[PubMed](#)]

84. Gilbert, S.M.; Gidley Baird, A.; Glazer, S.; Barden, J.A.; Glazer, A.; Teh, L.C.; King, J. A phase I clinical trial demonstrates that nfP2X 7 -targeted antibodies provide a novel, safe and tolerable topical therapy for basal cell carcinoma. *Br. J. Dermatol.* **2017**, *177*, 117–124. [[CrossRef](#)] [[PubMed](#)]
85. Cerami, E.; Gao, J.; Dogrusoz, U.; Gross, B.E.; Sumer, S.O.; Aksoy, B.A.; Jacobsen, A.; Byrne, C.J.; Heuer, M.L.; Larsson, E.; et al. The cBio Cancer Genomics Portal: An Open Platform for Exploring Multidimensional Cancer Genomics Data: Figure 1. *Cancer Discov.* **2012**, *2*, 401–404. [[CrossRef](#)]
86. Gao, J.; Aksoy, B.A.; Dogrusoz, U.; Dresdner, G.; Gross, B.; Sumer, S.O.; Sun, Y.; Jacobsen, A.; Sinha, R.; Larsson, E.; et al. Integrative Analysis of Complex Cancer Genomics and Clinical Profiles Using the cBioPortal. *Sci. Signal.* **2013**, *6*, pl1. [[CrossRef](#)]





Available online at [www.sciencedirect.com](http://www.sciencedirect.com)

ScienceDirect

Biomedical Journal

journal homepage: [www.elsevier.com/locate/bj](http://www.elsevier.com/locate/bj)

## Review Article

# Alternative splicing of P2RX7 pre-messenger RNA in health and diseases: Myth or reality?

Jonathan Benzaquen<sup>a,d</sup>, Simon Heeke<sup>a,b,d</sup>, S  r  na Janho dit Hreich<sup>a</sup>,  
Laetitia Douquet<sup>a</sup>, Charles Hugo Marquette<sup>a,d,e</sup>, Paul Hofman<sup>a,b,c,d</sup>,  
Val  rie Vouret-Craviari<sup>a,d,\*</sup>

<sup>a</sup> University of Cote d'Azur, CNRS, INSERM, IRCAN, Nice, France

<sup>b</sup> Laboratory of Clinical and Experimental Pathology and Biobank, Pasteur Hospital, Nice, France

<sup>c</sup> Hospital-Related Biobank (BB-0033-00025), Pasteur Hospital, Nice, France

<sup>d</sup> FHU OncoAge, Nice, France

<sup>e</sup> University of Cote d'Azur, CHU de Nice, Department of Pulmonary Medicine, FHU OncoAge, Nice, France



Dr. Valerie Vouret-Craviari

## ARTICLE INFO

## Article history:

Received 2 April 2019

Accepted 24 May 2019

Available online 15 July 2019

## Keywords:

Purinergetic signaling

P2X7

ATP

Onco-immunology

## ABSTRACT

Alternative splicing (AS) tremendously increases the use of genetic information by generating protein isoforms that differ in protein–protein interactions, catalytic activity and/or subcellular localization. This review is not dedicated to AS in general, but rather we focus our attention on AS of P2RX7 pre-mRNA. Whereas P2RX7 mRNA is expressed by virtually all eukaryotic mammalian cells, the expression of this channel receptor is restrained to certain cells. When expressed at the cell membrane, P2RX7 controls downstream events including release of inflammatory molecules, phagocytosis, cell proliferation and death and metabolic events. Therefore, P2RX7 is an important actor of health and diseases. In this review, we summarize the general mechanisms leading to AS. Further, we recapitulate our current knowledge concerning the functional regions in P2RX7, identified at the genetic or exonic levels, and how AS may affect the expression of these regions. Finally, the potential of P2RX7 splice variants to control the fate of cancer cells is discussed.

## Splicing and alternative splicing

The first description of alternative splicing (AS) was reported by Chow and colleagues in 1977 who described a new mechanism for the biosynthesis of mRNA in mammalian cells [1]. For this discovery, Richard Roberts and Philips Sharp were awarded the Nobel Prize in 1993. Since then, more than 32,000 articles can be found on Pubmed using “alternative splicing” as key word. Of

importance, AS is linked to diseases and cancer, with 6269 and 7553 publications found at the beginning of 2019.

### General mechanisms leading to splicing

The regulation of splicing is a complex mechanism that requires several factors involved in the precise selection of splicing sites and subsequent splicing processes [2]. As illustrated in [Fig. 1A], the splicing consists of six sequential steps

\* Corresponding author. University of Cote d'Azur, CNRS, INSERM, IRCAN, 33 avenue de Valombrose, 06108 Nice, France.

E-mail address: [vouret@univ-cotedazur.fr](mailto:vouret@univ-cotedazur.fr) (V. Vouret-Craviari).

Peer review under responsibility of Chang Gung University.

<https://doi.org/10.1016/j.bj.2019.05.007>

2319-4170/   2019 Chang Gung University. Publishing services by Elsevier B.V. This is an open access article under the CC BY-NC-ND license (<http://creativecommons.org/licenses/by-nc-nd/4.0/>).



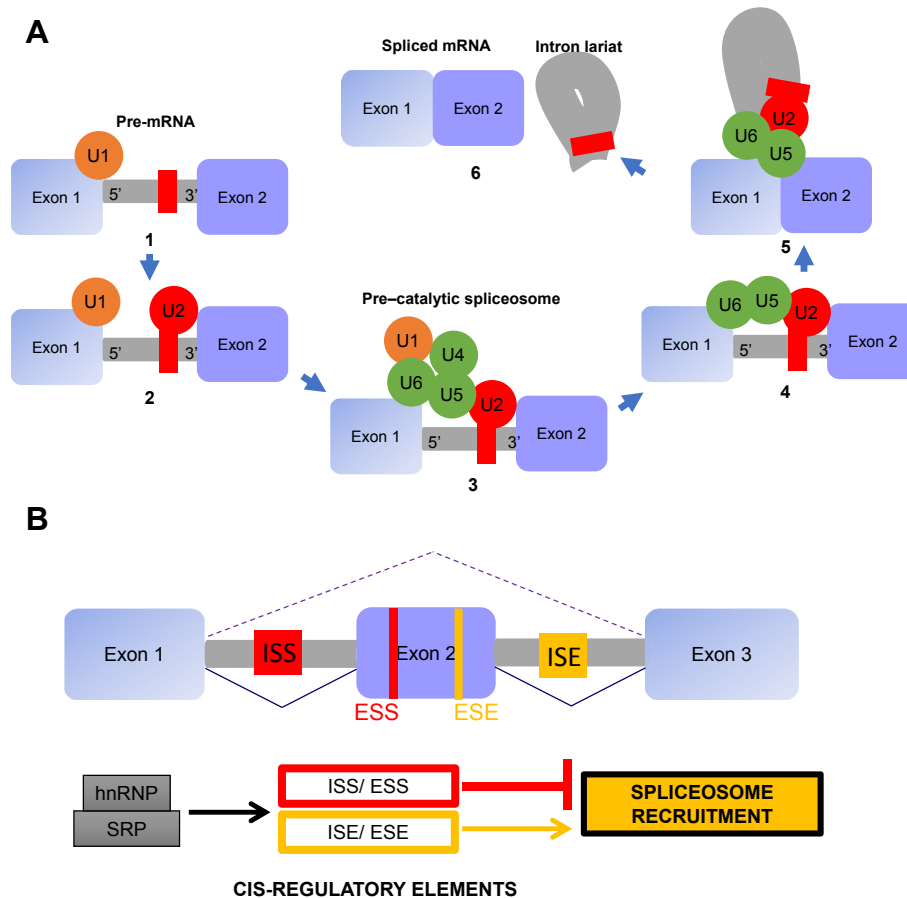


Fig. 1 Alternative Splicing requires two levels of regulation. (A) *Pre-mRNA splicing* require 6 sequential steps: 1: Pre-mRNA splicing starts with U1 snRNP (yellow circle) binding to the 5'-splice site; 2: U2 snRNP binds to the branch point (red rectangle) of the intronic sequence (gray bar); 3: Pre-assembled U4/U5/U6 snRNP (green circles) bind to U1 and U2 forming the pre-catalytic complex, and U1 snRNA 5' site is transferred to U6; 4: Spliceosome activation starts with U1 and U4 snRNP exclusion; 5: Intramolecular stem-loop between U2 and U6 allows transesterifications steps which lead to exons linking and 6: Spliced mRNA is released as a ribonucleoprotein particle; intronic sequence is released as a « lariat » (gray loop). Note: The protein composition of each spliceosomal complex is not shown in this figure for the purpose of simplification. (B) *pre-mRNA splicing regulation*. Cis-regulatory elements are sequences localized in exonic or intronic pre-mRNA which regulate alternative splicing and spliceosome recruitment. ESS (in red letters) and ISS (highlighted in red), exonic splicing silencer and intronic splicing silencer inhibit the splicing of pre-mRNA. ESE (in yellow letters) and ISE (highlighted in yellow), exonic splicing enhancer and intronic splicing enhancer are sequences which promote the splicing of pre-mRNA and will conduct in the present illustration to Exon 2 skipping (broken line). This splicing mechanism involves the recruitment of regulation proteins such as hnRNPs (Heterogeneous nuclear ribonucleoproteins), and SRP (Serine-Arginine rich proteins), which can bind on cis-regulatory elements and regulate splicing.

leading to the removal of specific sequences in a vast genomic sequence background. This "scissor mechanism" relies on five small nuclear ribonucleoproteins (snRNP U1, U2, U4, U5 and U6) which together form the core of the spliceosome. In brief, pre-mRNAs splicing is initiated by the binding of U1 on the 5'-splice site (step 1) and U2 on the branch point (step 2). Then, U4, U5 and U6 associate with U1 and U2 to form the pre-catalytic spliceosome complex (step 3). Further, U1 5' snRNA site is transferred to U6, leading to the activation of the spliceosome and to the removal of U1 and U4 from the complex (step 4). Consequently, U6 replaces U1 location and the interaction between U6 and U2 gathers the 5'-splice site and the branch point allowing the 5th transesterification step. The

two exons are then brought to close proximity by U5 and finally joint ending the splicing procedure (step 6). The splicing regulation does not only depend on the composition of splice sites, indeed, ribonuclear–protein complexes, referred as RNPs in [Fig. 1B], associate with pre-mRNA to facilitate exon recognition [3]. These regulatory proteins are classified in two major classes: heterogeneous nuclear ribonucleoproteins (hnRNPs) which bind to RNA, and SR proteins which contain serine and arginine rich protein regions involved in protein recognition. Both families regulate splicing via binding of intronic or exonic splicing silencers or enhancers as illustrated in [Fig. 1B] [2,4–6]. Finally, additional levels of regulation are sustained by the secondary structure

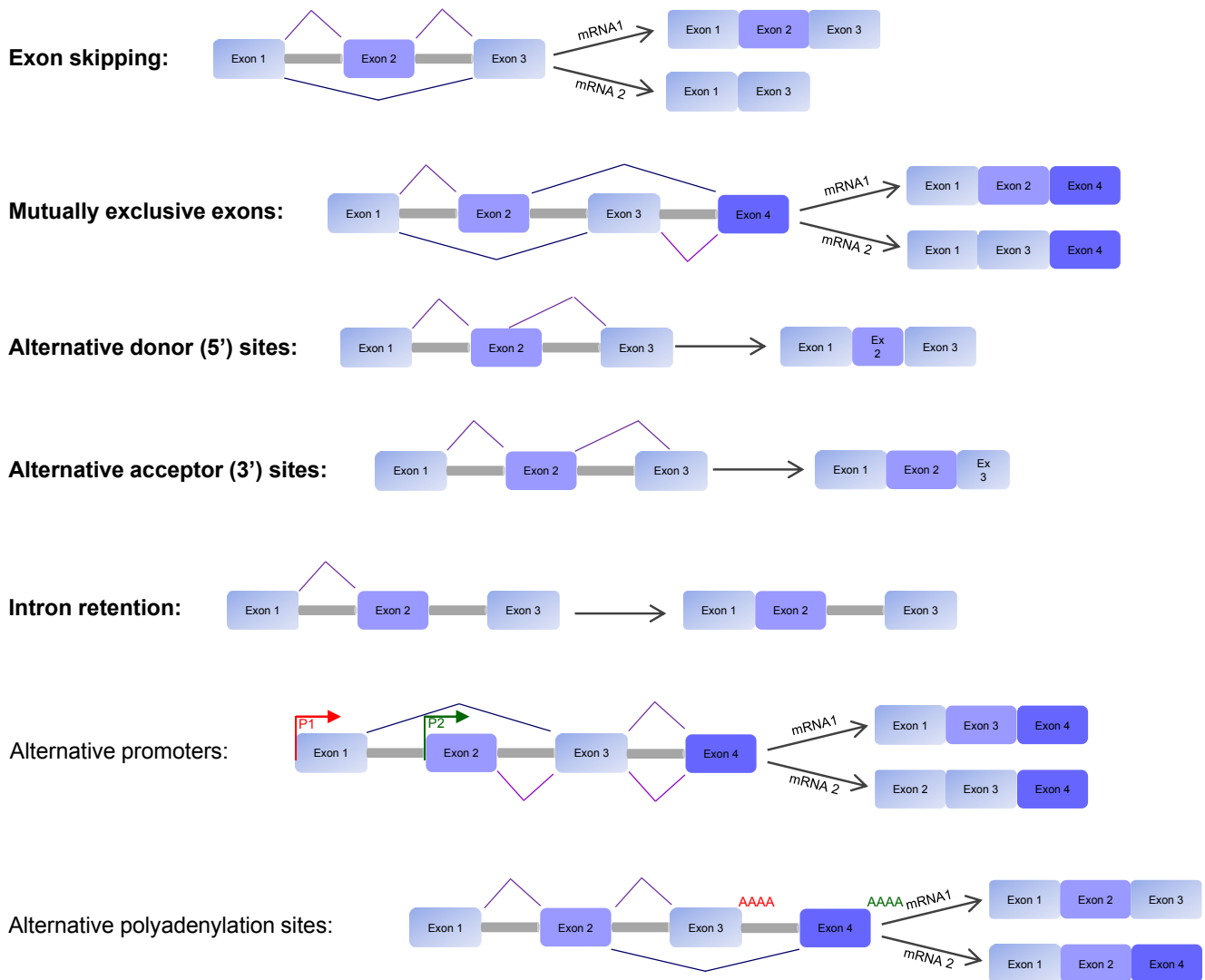


Fig. 2 From one pre-mRNA to various mRNAs. The seven described modes of alternative splicing increase the mRNA diversity. Bold characters are for the most common AS modes. Exon skipping, also named cassette exons, allows the exclusion of a full exon. Mutually exclusive exons lead to the egress of one exon out of two. Alternative donor 5' site uses an alternative 5' splice donor site to generate mRNA. Alternative acceptor 3' site uses an alternative 3' splice acceptor site. Intron retention corresponds to the addition of an intronic sequence within mRNA. Alternative promoter mode describes the use of different promoters resulting in a different start site of the mRNA transcript. An alternative promoter can be located at the 5' exon location or within an exon. Alternative polyadenylation sites refer to a splicing based on the presence and recognition of different polyadenylation sites.

of the pre-mRNA that can influence the recognition of splice sites [6], but also by cellular signal transduction pathways inducing phosphorylation events as reviewed by Stamm [7].

### Alternative splicing

Most of protein-encoding genes have multiple exons that are alternatively combined to form distinct mRNAs [8,9]. As illustrated in [Fig. 2], several patterns of alternative splicing (AS) with varying complexity exist and participate in the expansion of genetic diversity. These alternative combinations can be organ-specific, tissue-specific or cell-type specific [2,10].

It is usually accepted that events conferring biological gain of functions are conserved throughout evolution. To address whether specific AS are conserved within evolution, Merkin and collaborators performed a transcriptome sequencing (RNA Seq) analysis using paired-end short or long read sequencing of poly-A-selected RNA on nine tissues from five vertebrates [11]. Doing so, they identified almost 500 exons with conserved AS that are highly conserved in mammals. Interestingly, these exons often encode phosphorylation sites, and their tissue specific splicing may have important effect on signaling pathways. Unexpectedly, the authors described an extensive variation in the splicing of these exons between species, at a level that even exceeds intraspecies differences

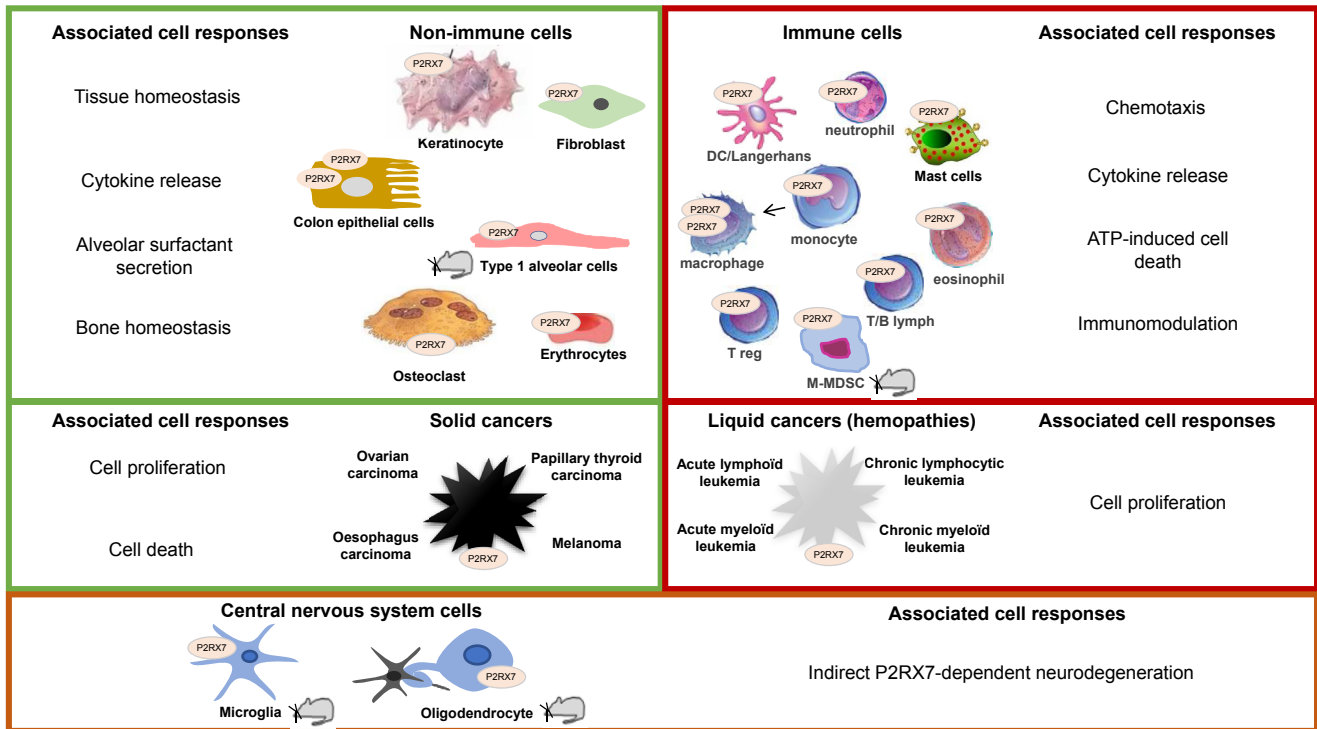


Fig. 3 P2RX7 expression in eukaryotic cells. The best way to sense cell stress is to express a receptor that is activated by molecules, like nucleotides, that are normally sequestered in the cells. Release of nucleotides, in response to mechanical injury, necrosis, apoptosis or inflammatory cell activation, depends on several molecular pathways, such as vesicular ADP release from platelets, pannexin-mediated ATP release during apoptosis, connexin- or pannexin-mediated ATP and autophagy. By sensing extracellular ATP, P2RX7 which is expressed by a large variety of cells plays such a role. In non-immune cells, functional P2RX7, (i.e. characterized by its expression at cell membrane, channel activity and/or macropore opening) has been found in colon [12] and lung epithelial cells [13], keratinocytes [14], osteoclasts [15], fibroblasts [16], and erythrocytes [17], where its activation has been shown to support tissue homeostasis, proliferation, survival and metabolism. In immune cells, expression of P2RX7 was documented in dendritic cells [18–20], neutrophils [21], mast cells [22], monocytes/macrophages [23,24], lymphocytes [25], eosinophils [26] and M-MDSC [27]. In these cells, P2RX7 expression is involved in chemotaxis, cytokine release, ATP-induced cell death and immunomodulation. In addition, P2RX7 expression was found in both solid [28–32] and liquid cancers [33–35], where it was described to sustain cell proliferation or cell death. Other publications claimed that P2RX7 was overexpressed in cancer from various origins [35,36]. Yet, these conclusions were obtained from immunohistochemistry analyses, where the identification of P2RX7 expressing cells is somehow difficult to characterize. Finally, P2RX7 was described to be expressed in microglia and oligodendrocytes [37]. Note: Here we showed P2RX7 expression reported to be functional in human cells, or in mouse cells when no data were available for human (a mouse drawing is then symbolized in this case).

between tissues [11]. In a complementary study, Barbosa-Morais and collaborators showed that in the mammalian lineage, organs of primate species have higher AS frequencies than organs of other vertebrates. They concluded that organs' AS profiles are more closely correlated to the identity of a species than to the organ, in contrast to the well conserved organ-dependent differences in mRNA expression during vertebrate evolution [38]. Together, these studies reveal that AS and transcription regulation are not subjected to the same evolutionary constraints; apparition of new mRNA variants is dominated by species-specific differences that accumulate more rapidly than transcriptional regulation even during a short period of evolution.

Whereas transcriptional regulation and constitutive splicing maintain normal cell physiology, AS can result in

various human diseases by modifying, or even abrogating, some functional regions of proteins that are involved in cell homeostasis [39]. In fact, the hundreds of factors allowing the precise regulation of AS are themselves subjected to modifications, which in turn can cause deregulation of each of the signaling pathways across virtually all biological processes. For instance and as recently reviewed by Czubay and Piekielek-Witkowska, phosphorylation of splicing factors results in changed AS of tumor suppressors, regulators of cell signaling or apoptosis resulting in an impact on cancer development and progression [40]. Modification of AS is also the result of sequence variation. Indeed, it was reported that 22% of missense disease alleles alter splicing and it was predicted that one third of all mutations affect splicing [41]. To fully appreciate the relationship between missense mutation,

AS and diseases, computational approaches [42] and animal models [43] have been developed.

Altogether, deregulation of AS has been described to play a role in diseases as diverse as diabetes, neurological diseases, cardiovascular diseases, immunological and infectious diseases as well as cancer. As this topic is far beyond the scope of this review, we invite interested readers to refer to an excellent review published by Kim and collaborators [10].

## Alternative splicing of P2RX7

### The purinergic P2RX7 receptor

Half a century was necessary to link purine nucleotides and nucleosides as extracellular ligands [44] to the existence of two families of purinergic receptors [45]. It is now well described that the P1 [46] and the P2 receptors comprise numerous members and that the P2 family is divided in two subgroups P2Y and P2X receptors [47]. The purinergic P2X receptors are activated by extracellular adenosine 5'-triphosphate (eATP) [47,48]. This family includes seven members which all share a common structure based on two transmembrane spanning regions, a large extracellular loop and intracellular N- and C-termini [48]. Within this family, sequence identity from the N terminus to the second transmembrane domain is relatively high. By contrast, their C-termini are specific to the individual P2X receptors and contain consensus binding motifs for protein kinases and other regions that may be involved in cell-signaling. This is particularly true for the seventh member of the P2X family, previously described as P2Z receptor [49], which is characterized by the presence of a long intracytoplasmic C-terminal sequence [48] and now referenced as P2RX7.

In the presence of eATP, P2RX7 trimeric receptors form a poorly-selective channel leading to membrane depolarization, potassium efflux and calcium and sodium influx [48]. Whereas P2RX7 mRNA is expressed by virtually all mammalian cells, the expression of the protein was described in immune but also in non-immune cells [Fig. 3]. In cells expressing P2RX7 at the membrane, its expression was thought to induce various downstream events including cell proliferation and cell death, metabolic events, phagocytosis and release of inflammatory molecules [50–53]. As discussed later in this manuscript, P2RX7 could be expressed but maintained within the cytoplasm. In this condition protein expression is dissociated from protein activation. In addition, it was shown in mouse CD8 T cells that the sensitivity to eATP depends more on the stage of cell differentiation than on the level of P2RX7 expression [54]. Within the P2RX family, P2RX7 is unique. First, it is activated by relatively unusual high concentration of eATP (1 mM under physiological concentration), second it allows the permeation of large molecules up to 900 Da and third it is responsible for eATP-dependent cell lysis, a response that depends on the presence of the C-terminal sequence [49]. The recently described crystal structure of mammalian P2RX7 (from panda) gave new insights on the architecture of this receptor [55]. Importantly, the trimeric association of P2RX7 was confirmed by this study; the same conclusion was drawn by Kasuya and

collaborators studying the crystal structure of the chicken P2RX7 [56]. As previously described for P2RX4 and P2RX3, the single subunit of a C-terminal truncated P2RX7 resembles a “dolphin-like” shape [57–59]. In the absence of eATP, the transmembrane helices constrict the channel gate at residues G338, S339 and S342. Hence, this conformation may represent the closed state. Unfortunately, the crystal structure in the presence of eATP was not sufficiently stable to be studied and the proposed mechanism is yet to be confirmed. By contrast, the crystal structure of P2RX7 in the presence of five different antagonists highlighted the existence of a drug binding pocket in the upper body domain which is close to the eATP binding pocket. Therefore, available antagonists act as non-competitive inhibitors. Combining different analyses, the following mechanism for P2RX7 activation and inhibition was proposed: In the presence of eATP, both the drug binding pocket and the inter-subunit cavity in the upper body domain (also called turret) of P2RX7 undergo conformational rearrangements. This leads to the narrowing of these domains, which consequently allows the enlargement of the lower body domain resulting in the opening of the channel. When allosteric antagonists are bound to P2RX7, turret closure is restrained and the channel remains closed [55]. This mechanism implies that when eATP is within its binding pocket, the drug binding pockets are inaccessible, preventing the binding of allosteric inhibitors.

Noteworthy, the crystal structure has been obtained using a C-terminally truncated version of P2RX7 which may represent a caveat in the understanding of P2RX7 biology. Indeed, the long C-terminal tail of P2RX7 has been described to be essential to sustain permeation of large molecules and cytolysis [49]. Here again, the group of Kawate improved understanding on the role of the C-termini of P2RX7 by investigating the effect of the membrane's lipid composition on P2RX7 functionality [60]. Using purified panda P2RX7 reconstituted into liposomes, it was elegantly demonstrated that the dye-permeant pore opens independently of the long C-terminal tail. Further, the authors highlighted the capacity of phosphatidylglycerol and sphingomyelin to facilitate channel activity by modifying the lipid composition of the liposomes, whereas cholesterol drastically attenuated dye-uptake by directly acting on P2RX7 transmembrane domains. So, if the dye-permeant pore of P2RX7 is independent of the N- and C-terminal extremity, do these intracytoplasmic sequences have a biological function? Part of the answer was brought by Robinson and collaborators who linked cholesterol sensitivity of P2RX7 channel activity to the presence of multiple cholesterol recognition amino acid consensus motifs within both N-terminal and proximal C-terminal regions of P2RX7 [61,62]. Additionally, it was shown that the juxta-transmembrane amino and carboxyl termini are involved in the regulation of P2RX7 gating [63]. And finally, it was demonstrated that the C-terminal Cysteine-rich region of P2RX7 counteracts the inhibitory effect of cholesterol [60]. All these evidences, combined with new technologies to analyze dilatation of P2RX7 eATP-induced pore opening [64,65], push aside the old dogma postulating that the formation of the large pore is a consequence of P2RX7 cation-selective channel dilatation and rather

highlight the importance of lipid composition to modulate the size of the pore. In agreement with this, it was shown that P2RX7 is associated with lipid rafts, which are dependent of palmitoylation of Cys residues located in the C-terminal region [61]. Yet, as nicely discussed by Di Virgilio and collaborators, we cannot exclude that consequently to P2RX7 stimulation, other permeability pathways are activated [66].

### P2RX7: one gene, many proteins

P2RX7 gene was investigated in mammalian and non-mammalian species, the more studied species being human, rat and mouse, as detailed in the well documented review published elsewhere [53]. We will focus here on human and mouse, with an emphasis on P2RX7 splice variants.

#### Human splice variants

The P2RX7 gene, which is localized on chromosome 12q24, consists of 13 exons. Constitutive splicing leads to the common P2RX7-A mRNA, but 12 additional transcripts have been described due to alternative splicing [67]. Among those splice variants, nine were studied in more detail [Fig. 4A]. Three of them, the variants -C, -E and -G, code for very short proteins and are assumed to be unable to form a channel receptor. By contrast, the variants -B and -J have been described to be expressed under normal and/or pathological conditions and to interfere with P2RX7-induced biological responses [67]. The P2RX7-B variant, which is expressed in almost all eukaryotic cells and appears to be regulated in immune cells, is characterized by the deletion of the last 249 amino acids from the C-terminal extremity that have been replaced by 18 different amino acids [67]. The homotrimer was described to retain ion-channel activity when expressed in a heterologous cell system. However, the EC<sub>50</sub> for BzATP reaches 500 μM, which questions its ability to really channel Ca<sup>2+</sup>. In addition, P2RX7-B homotrimers were described to be non-permeant to dyes, such as Yo-pro-1. On the contrary, the heterotrimer P2RX7-A/P2RX7-B was described to be more efficient than P2RX7-A, in particular by supporting cell growth [68]. With the C-terminal extremity of P2RX7 being involved in trafficking and cell surface expression, it could be that the increased efficiency of the heterotrimer is correlated with an improved expression at the plasma membrane [69–71]. Alternative splicing of exon 8 which is leading to a frameshift mutation with a new stop codon produces the P2RX7-J variant. The resulting protein is composed of the N-terminal extremity, the first transmembrane domain and 2/3 of the extracellular loop. The P2RX7-J receptor is inactive alone, but when co expressed with P2RX7-A, the association of -A and -J isoforms has a dominant negative effect over the P2RX7-A homotrimer which may protect certain cell types from eATP-induced cell death [72,73]. P2RX7-H, -D and -F result from alternative splicing leading to the insertion of an extra exon, or deletion of exons 5 and 8, respectively. The corresponding proteins are missing the N-terminal sequence, the first transmembrane domain and part of the cytoplasmic loop [Fig. 4B]. Given the fact that normal trafficking toward the cell surface requires the N-terminal sequence, it is likely that these isoforms are not correctly inserted in cell membrane. However, if expressed, these

isoforms can be localized in the cytoplasm or in intracellular vesicles. Yet, only few P2RX7-H mRNA are expressed in tissues from different origins [67]. It is important to keep in mind that all these results were obtained after overexpression of splice variants in the HEK293 heterologous cell system. Undeniably, additional studies are required to examine the endogenous expression of P2RX7 isoforms, and their functional consequences, in human cells.

#### Mouse splice variants

The murine gene of *P2rx7*, which is located on chromosome 5, maintains the same genomic organization as human P2RX7. The common *P2rx7-a* mRNA is made of 13 exons. Four alternative splice variants have been described in mice so far, *P2rx7-b*, -c, -d and -k [Fig. 4A]. Two of them, *P2rx7-b*, -c, correspond to deletions within exon 13 and give rise to shorten proteins which are characterized by lower channel activity [53]. The P2RX7-d isoform corresponds to the shortest form of the protein with a large truncation in the extra-cytoplasmic loop, loss of both the second transmembrane domain and the intracytoplasmic C-terminal tail [74]. Interestingly, this largely truncated protein retains the ability to be correctly inserted within the membrane when co-transfected with P2RX7-a. It is likely that the heterotrimer is formed during vesicle trafficking towards the cell membrane, and once inserted in the membrane, P2RX7-d downregulates eATP-induced macropore formation. On the contrary, P2RX7-k protein, which results from an alternative splicing of exon 1, differs from P2RX7-a in the N-terminal cytoplasmic extremity and most of the first transmembrane domain [75]. *P2rx7-k* mRNA is expressed in all tissues but more expressed than *P2rx7-a* in spleen and liver. P2RX7-k homotrimer is more sensitive than P2RX7-a to ATP and is more potent to permeate ions and large cations. In addition, it was shown that P2RX7-k could be activated by ADP-ribosylation, which correspond to a second mode of activation [76]. P2RX7-k seems to be exclusively expressed by T cells and no co-expression of *P2rx7-k* and *P2rx7-a* was described. This mutually exclusive expression suggests a regulation at the level of the promoter. Whether this regulation is due to epigenetic modifications (such as methylation), specific expression of transcription enhancers/inhibitors or both remains to be determined. *P2rx7-k* mRNA escapes gene deletion in the Glaxo *P2rx7*<sup>-/-</sup> mice, where *LacZ* gene was inserted after ATG at the 5' end [75]. The existence of these splice variants led to a careful re-evaluation of the expression of P2RX7 receptor isoforms in the Pfizer transgenic *P2rx7* KO mice, where region encoding Cys<sup>506</sup> to Pro<sup>532</sup> was replaced with the neomycin resistant gene [76,77]. While P2RX7-k protein is expressed in T cells from the “Glaxo mice”, Pfizer KO mice express ΔC isoforms (namely P2RX7-b, -c, -d). However, these proteins were inefficiently trafficked to the cell surface and consequently not responsive to agonistic stimulation [78]. Together, these results indicate that the Pfizer model is the preferential one to evaluate the functional role of P2RX7 in homeostasis and pathological conditions. In the same line, the third *P2rx7* KO model, in which the beta galactosidase/Neomycin genes were inserted within the exon 2 [79], is expected to be a good model, with none of the variant being expressed. In addition, two additional knock-in

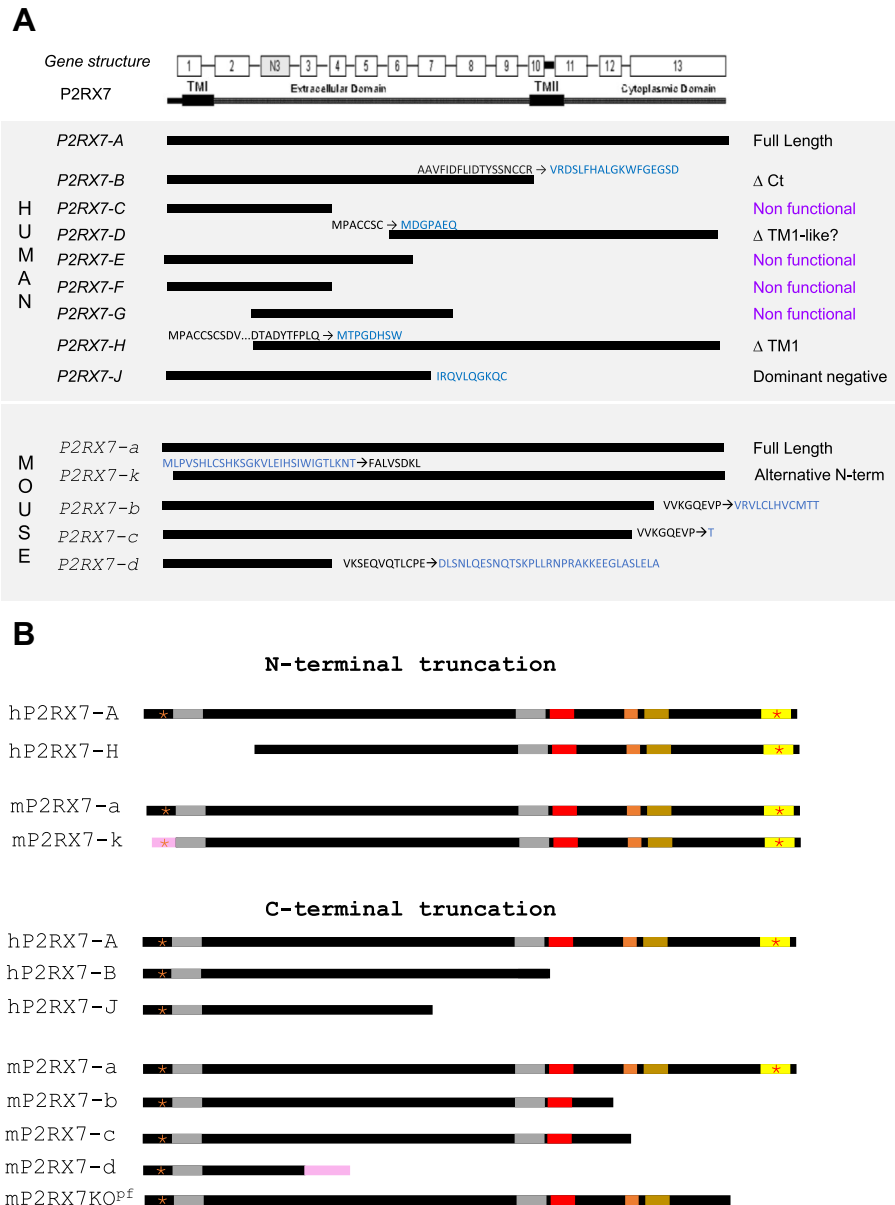


Fig. 4 Human and mouse P2RX7 splice variants. (A) Genomic organization. New sequences resulting from AS are shown in blue. Protein isoforms corresponding to P2RX7-C, -E, -F and -G were described to be nonfunctional. Yet, P2RX7-E and -F isoforms are structurally closed to the mouse P2RX7-d protein, which has been described to down regulate P2RX7 activity when co-expressed with P2RX7-A [Table 2]. By the same way, P2RX7-D corresponds to a shorter version of P2RX7-H, which has been described to be a non-functional receptor. (B) Schematic illustration showing the overall organization and the functional regions in isoforms identified at the genetic or exonic levels. Grey box: transmembrane domain 1 and 2; red box: Cys rich regions (including C371,373, 374- C477, 479, 482-C498,499, 506 and C572, 573); orange box: A actinin binding sequences; brown box: SH3 binding domain and TNF death receptor; yellow box: LPS binding domain; orange star: cholesterol sensitizing; red star: amino acids involved in trafficking and cholesterol sensitizing. The pink boxes highlighted the presence of new sequences due to splicing.

transgenic mice were generated. The first one corresponds to humanized P2RX7 mice in which the mouse exon 2 was substituted by the human cDNA covering exons 2 to 13 [80]. The second one relies on the introduction of an EGFP sequence in the 5' of exon 13 [37]. Both models were useful to characterize the expression of P2RX7 in the central nervous system (see [Fig. 3]).

*Expression of splice variants: a way to regulate P2RX7 activity?*  
As a receptor, P2RX7 has to be correctly inserted into the cell membrane to be functional. Indeed, assembly and trafficking to the plasma membrane has been described as a regulatory mechanism, at least in some immune cells [23,81]. In addition to membrane receptor density, the concentration of extracellular ions was demonstrated to be crucial for the regulation of IL-1β

**Table 1** Description of Single Nucleotide Polymorphisms of the Human P2RX7 gene that could affect alternative splicing of variant B, H and J.

dbSNP ID	Localization	"Affected" variant	Major allele	Minor allele Frequency
rs1397153443	-3, exon 11	Variant B	C	T = 0.0000
rs778937864	-4, exon 11	Variant B	C	T = 0.0000
rs756931719	-10, exon11	Variant B	T	G = 0.00001
rs190080059	-20/-40, exon 11	Variant B	G	A/T = 0.00002
rs373584182	-20/-40, exon 11	Variant B	G	T = 0.00004
rs1352183219	-20/-40, exon 11	Variant B	G	A = 0.0000
rs760740502	-20/-40, exon 11	Variant B	G	A = 0.00002
rs916695614	-20/-40, exon 11	Variant B	C	C none
rs201650139	-20/-40, exon 11	Variant B	A	G none
rs368885357	-20/-40, exon 11	Variant B	G	T = 0.0000
rs1376166550	+2, exon 2	Variant H	T	C none
rs754634787	+3, exon 2	Variant H	G	A/T = 0.0000
rs965276754	-10, exon 3	Variant H	T	A none
rs201960043	-20/-40, exon 3	Variant H	T	Insc = 0.0537 (InsDel)
rs200429438	-20/-40, exon 3	Variant H	C	A nd
rs1373724698	-20/-40, exon 3	Variant H	T	G = 0.0001
rs186332279	-20/-40, exon 3	Variant H	G	C = 0.00002
rs757343268	-20/-40, exon 3	Variant H	TTCAAA	Del, 0.00001
rs1475267143	+2, exon 7	Variant J	T	C = 0.0000
rs764748109	-8, exon 8	Variant J	T	C = 0.00001
rs1239860541	-20/-40, exon 8	Variant J	A	G = 0.0000
rs28360455	-20/-40, exon 8	Variant J	T	C = 0.0021
rs774175036	-20/-40, exon 8	Variant J	C	G/T = 0.00002
rs771002311	-20/-40, exon 8	Variant J	A	G = 0.0000
rs1210563466	-20/-40, exon 8	Variant J	C	T = 0.0000
rs1488167709	-20/-40, exon 8	Variant J	C	T = 0.00001
rs1239860541	-20/-40, exon 8	Variant J	A	G = 0.0000

secretion [82]. As discussed above, a third mode of regulation could result from the expression of homotrimer isoforms but also from the formation and expression of heterotrimeric isoforms, where the full-length form is associated with truncated splice variants.

To evaluate the role of AS in P2RX7 regulation, we focused on human and mouse P2RX7 isoforms. As shown in [Fig. 4B], two groups can be distinguished. In the first one, splicing events modify the N-terminal part of the protein, a sequence that contains amino acids critical for the localization of P2RX7 at the cell membrane. Currently, there is no evidence for a functional role of the P2RX7H isoform, which is unlikely to be trafficked to the cell membrane and does not respond to Bz-ATP [67]. However, considering the trimeric organization of P2RX7, one may speculate that a chimeric P2RX7-A/-H receptor could be assembled during ER trafficking and once correctly inserted in cell membrane, tune the amplitude of eATP-induced cell responses. However, further in-depth characterization is needed to confirm this hypothesis. On the contrary, AS in the first exon of the mouse *P2rx7* pre-mRNA produces a highly sensitive P2RX7 isoform, which is involved in immune T cells homeostasis [83]. This variant has not been described in human, even though the sequence of human intron 1-2 predicted the existence of a possible alternative splice site in exon 1 [75]. In the second group, splicing events affect exons that are crucial in mediating large cation permeation. As mentioned above, heterologous expression of human and mouse homotrimer isoforms lead to the

expression of receptors characterized by functional  $\text{Ca}^{2+}$  flux and blocked permeation of large cations. Expression of these new receptors could be considered as the first level of regulation. More interestingly, the co-expression of two isoforms bring additional levels of regulation. The heterotrimer -A/-J is dominant negative in human for instance, while in mouse the co-expression of -a/-b, -a/-c, and -a/-d downregulated, or even inhibited P2RX7 function. Strikingly, co-expression of P2RX7-A/-B in HEK293 cells seems to increase the overall activity of P2RX7 as discussed earlier [68,84]. This result was unexpected considering the contrary effect observed with the mouse heterotrimeric receptors. However, one could speculate that the overall effect on heterotrimer P2RX7 activity depends on the ratio of A versus B. For instance, 2A and 1B could be more active than 3A whereas 1A and 2B could be less active. Undoubtedly, additional experiments are needed to fully document in which cells and at which levels P2RX7 isoforms are expressed and what the functional consequences of heterotrimeric P2RX7 expression are? Another important question that remains to be solved is whether the non-functional P2RX7, that is expressed on cancer cells [85], is a consequence of AS leading to the formation of heterotrimeric P2RX7 that would not be recognized by the conformational antibody generated by Buell and co-workers [86], and that would alter P2RX7 activity [85]. This may be particularly relevant considering that the C-terminal truncation of P2RX7 leads to the deletion of several binding motifs involved in P2RX7-induced cell signaling pathways [50,87].

**Table 2 Biological activities of human and mouse P2RX7 isoforms.**

P2RX7 isoforms	Cells	Localization at the membrane	Membrane depolarization	Ca <sup>2+</sup> influx	Macropore formation	IL1B release	Refs
P2RX7-A	HEK293,	IF	++	++	++		[49,67,68,79]
P2RX7-B	HEK293	IF	+/-	Low & transient	no	Casp1	[67,68]
P2RX7-H	HEK293		no	no	no	No casp 1	[67]
P2RX7-J	Cervical cancer cells, MDCK	IF		low	no		[72]
P2RX7-A/-B	HEK293	IF	>-A	>-A	>-A		[67,83]
P2RX7-A/-J	HEK293	wb		<-A	<-A		[72]
P2RX7-a	Macrophages				++	++	[75]
	Brain, spleen, salivary gland, HEK293	wb	++	++	++		[76,77]
	Astrocytes	wb			++		[73,77]
	Pancreatic stellate cells	wb		++			[77]
P2RX7-b	Brain, spleen, salivary gland, HEK293	wb, ↓↓ vs P2RX7-a	↓↓ vs P2RX7-a				[77,78]
P2RX7-d	HEK293				no		[74]
P2RX7-k	T Lymphocytes				no		[74]
	HEK293	wb	++ (sustained vs -a)		++		[75]
P2RX7-a/-b	HEK 293	wb, b = dominant negative	b = dominant negative		↓↓ vs P2RX7-a alone		[74,78]
	Astrocytes (overexpression)				↓↓ vs P2RX7-a alone		[74]
P2RX7-a/-d	HEK293, astrocytes (overexpression)				↓↓ vs P2RX7-a alone		[74]

## P2RX7 splice variants and diseases

### SNPs and splice variants

On the beginning of 2019, 13,252 single nucleotide polymorphism (SNP) have been described in the P2RX7 gene (<https://www.ncbi.nlm.nih.gov/snp>). While non-synonymous SNPs have been linked to pathologies as diverse as infectious diseases, bone, psychiatric, inflammatory and cardiovascular disorders or cancers, as reviewed by Sluyter [88], SNPs located within intronic regions have been poorly studied. Splicing regulatory elements can be located within intronic sequences, therefore one could assume that intronic SNPs may affect splicing and in turn cause diseases [89]. Splicing regulatory sequences include the 5' and 3' splice sites defining the boundary of an intron with its upstream and downstream exon, but also the branch site upstream of the 3' splice site. Examination of the human P2RX7 sequence indicates that the major U2 class splice site consensus sequence, including GT at the 5' end and AG at the 3' end, is present on the boundary of each of the P2RX7's introns.

We speculated that SNPs might lead to alternative splicing of P2RX7 pre-mRNA. To test this hypothesis, we first listed SNPs located at the introns' boundaries. As shown in [Table 1], only one SNP, rs1475267143, changes a T to C at +2 of the 7th intron. This change, that corresponds to the most common class of non-consensus splice sites [90], may affect the splicing

of exon 7, even though this hypothesis has not been tested experimentally. However, the minor allele frequency is close to zero, and therefore it is not expected that such a frequency could significantly impact the expression of P2RX7-J. We further extended our analysis to minus 10 to cover branch-points of each boundaries' intron. As shown in [Table 1], we found several SNPs that can affect the splicing of P2RX7-B, -H and -J. Once again, all these SNPs are too sparsely expressed to envisage that they could regulate splicing events and are involved in diseases. Finally, because branchpoints within U2-type constitutive introns were located in between the position -40 to -20 from the 3' splice site, we extended our analysis to -40 nucleotides [36]. Doing so, we identified two SNPs rs28360455 and rs201960043 that could contribute to the alternative splicing of P2RX7-J and P2RX7-H, respectively. Today, no studies demonstrated that these two SNPs are linked to the expression of spliced P2RX7 mRNA but given their relative high frequency it is tempting to speculate on the existence of such a regulation. By contrast, we were unable to identify SNPs that could modulate splicing of P2RX7-B. Yet, we cannot exclude that such SNPs exist, but are located within an unstudied intronic region. Alternatively, one could hypothesize that P2RX7-B is indeed constitutively expressed in some tissues. This idea is sustained by studies showing that P2RX7-B is expressed in various organs and resting immune cells [67], and when co expressed with P2RX7-A, may affect the binding/gating properties of P2RX7 [84]. Undoubtedly, new progresses



will be made with the implementation of novel tools to specifically assess the level of expression but also the biological activity of P2RX7 splice variants.

### *P2RX7 splice variants and cancer*

One of the most intriguing questions considering P2RX7 is to explain how a receptor that induces cell death in the presence of its endogenous ligand, namely eATP, could be overexpressed in some cancers [91]. Indeed, knowing that the tumor microenvironment, like the inflammatory tissue, contain hundreds of micromolar eATP [92], it is counterintuitive to imagine that a protein leading to cell death is overexpressed by cancer cells. The best way to harmonize these two observations is to hypothesize that the receptor expressed at the surface of cancer cells is unable to trigger cell death. This idea is sustained by several studies showing that P2RX7 expressed at the surface of diseased cells is a non-functional conformation [85]. The first description of the expression of a non-functional P2RX7 (nfpP2RX7) was made in cancerous breast lesions where the group of Julian Barden used an antibody designed against an epitope located in the extracellular loop close to the eATP binding pocket and which is inaccessible in cells expressing normal functional P2RX7 [93,94]. Furthermore, the expression of non-functional P2RX7 on the surface of cancer cells was shown in organs as diverse as gut, ovary, cervix, lung, liver, and bladder [85]. Intriguingly, nfpP2RX7 electrophoretic feature is indistinguishable from P2RX7 and today, the exact nature of this receptor channel remains a mystery. Gilbert and collaborators characterized the expression of nfpP2RX7 from a panel of tumor cell lines using a new humanized antibody (BIL03) that is specific to the extracellular domain of nfpP2RX7 [95]. As suggested by previous reports, they confirmed that nfpP2RX7 is expressed in many cancer cell lines. They showed that nfpP2RX7 is molecularly distinct from P2RX7 using specific antibodies and biological assays (EtBr uptake). Finally, the authors reported that nfpP2RX7 is stored intracellularly and localized to the cell membrane upon eATP stimulation, an event that requires protein synthesis. Strikingly, it seems that expression of nfpP2RX7 is mutually exclusive since its localization to the cell membrane correlates with the loss of P2RX7. As this non-functional receptor lacks apoptotic activity but retains residual non-selective cations channel, it was proposed that it promotes tumor growth. The mechanisms leading to the expression of nfpP2RX7 is not fully understood nowadays, but at least two main hypotheses could be drawn. The first one, as discussed previously, relies on the formation of a heterotrimer, composed of P2RX7-A and P2RX7-B, which may lack the potential to induce cell death. In their study, Gilbert and collaborators did not check if expression of nfpP2RX7 requires mRNA translation, however they hypothesized that intracellular nfpP2RX7 may correspond to a misfolded protein and it is known that P2RX7-B lack C-terminal region that participates to the trafficking to the cell surface. The second one relies on the ability of cholesterol to control P2RX7-dependent large cation influx, as elegantly demonstrated by Karasawa and collaborators [60] and

discussed earlier in this review. Considering that cancer cell membranes contain more saturated lipids, it is tempting to speculate that this change in lipid composition affects P2RX7 biology [96]. This hypothesis is supported by the discovery that, in a human prostate cancer cell line (LNCaP), oxidative stress-induced cell death is reversed when cells were pre-treated with Soraphen A, an inhibitor of acetyl CoA carboxylase which modulates the synthesis of very long chain saturated, mono- and polyunsaturated fatty acids [97]. While this paper highlighted a direct relation between lipid composition and stress-induced cell death, no link was made with the eATP/P2RX7 signaling. By contrast, it is well established that P2RX7 activates phospholipid signaling pathways in epithelial cells through the modulation of phospholipases and sphingomyelinase [98]. Additionally, activation of P2RX7 drives the production of phosphatidic acid in RAW 264.7 macrophages which in turn delays eATP-induced pore opening and cytolysis. Therefore, a direct link between P2RX7 activation, membrane lipid composition and cell death was described at least in some immune cells [99,100]. Additional research is required to establish the relationship between eATP, expression of cell surface nfpP2RX7, lipid metabolism and lack of pore opening-induced cell death. Undoubtedly, if this holds true it will reconcile the fact that cancer cells are positively stained by antibodies directed against ubiquitously expressed P2RX7 epitopes.

Recently, a new P2RX7 splice variant was described, namely P2RX7-V3 which contains an extra exon N3 and corresponds to a long non-coding RNA [101]. Long non-coding RNAs do not code for proteins but have been involved in diverse cellular processes by interfering with chromatin-modifying complexes and transcription factors [102]. P2RX7-V3 is expressed at high levels in cell lines derived from uveal melanoma where it works as an oncogene. Even though the mode of action of this splice variant and its expression in other cancer tissues need to be investigated, the authors proposed that P2RX7-V3 may be an informative biomarker of cancer. Beyond, this report suggests that at least one P2RX7 splice variant might by itself, regulate cellular processes relevant for cancer, a field that has not yet been explored.

---

## **Conclusion**

Here, we discussed the role of alternative splicing in the field of P2RX7 signaling. Our attempts were to discuss if expression of P2RX7A and its splice variants in a same cell could impact the functionality of P2RX7 and to bring new thoughts on the nature of nfpP2RX7 that is expressed at the membrane of cancer cells. Despite the quantity of data published over the last two decades, there are still unresolved questions regarding the role of P2RX7 in health and diseases. Undoubtedly, development of new specific tools to unravel the expression of P2RX7 splice variants and the functionality of P2RX7 will bring new insights in biology and medicine. This is particularly relevant in the light of the recent discovery that

tumor-specific splicing produces numerous splicing associated potential neoantigens that may affect the immune response and could be exploited in the field of onco-immunology [103].

### Conflicts of interest

The authors declare they have no conflicts of interest.

### Acknowledgments

We also would like to thank Patrick Brest and Lionel Arnaud for stimulating discussions and Jean Kanellopoulos for critical reading of the manuscript. The funding sources for this work were Institut National du Cancer (INCa), Canceropole PACA, INSERM, CNRS, Bristol-Myers Squibb Foundation for Research in Immuno-Oncology, La Ligue contre le Cancer and the French Government (National Research Agency, ANR through the “Investments for the Future” LABEX SIGNALIFE: program reference #ANR-11-LABX-0028-01).

### Appendix A. Supplementary data

Supplementary data to this article can be found online at <https://doi.org/10.1016/j.bj.2019.05.007>.

### REFERENCES

- [1] Chow LT, Gelinas RE, Broker TR, Roberts RJ. An amazing sequence arrangement at the 5' ends of adenovirus 2 messenger RNA. *Cell* 1977;12:1–8.
- [2] Tazi J, Bakkour N, Stamm S. Alternative splicing and disease. *Biochim Biophys Acta – Mol Basis Dis* 2009;1792:14–26.
- [3] Bessonov S, Anokhina M, Krasauskas A, Golas MM, Sander B, Will CL, et al. Characterization of purified human Bact spliceosomal complexes reveals compositional and morphological changes during spliceosome activation and first step catalysis. *RNA* 2010;16:2384–403.
- [4] Chabot B, Shkreta L. Defective control of pre-messenger RNA splicing in human disease. *J Cell Biol* 2016;212:13–27.
- [5] Keren H, Lev-Maor G, Ast G. Alternative splicing and evolution: diversification, exon definition and function. *Nat Rev Genet* 2010;11:345–55.
- [6] Buratti E, Baralle M, Baralle FE. Defective splicing, disease and therapy: searching for master checkpoints in exon definition. *Nucleic Acids Res* 2006;34:3494–510.
- [7] Stamm S. Regulation of alternative splicing by reversible protein phosphorylation. *J Biol Chem* 2008;283:1223–7.
- [8] Pan Q, Shai O, Lee LJ, Frey BJ, Blencowe BJ. Deep surveying of alternative splicing complexity in the human transcriptome by high-throughput sequencing. *Nat Genet* 2008;40:1413–5.
- [9] Wang ET, Sandberg R, Luo S, Khrebtkova I, Zhang L, Mayr C, et al. Alternative isoform regulation in human tissue transcriptomes. *Nature* 2008;456:470–6.
- [10] Kim HK, Pham MHC, Ko KS, Rhee BD, Han J. Alternative splicing isoforms in health and disease. *Pflugers Arch Eur J Physiol* 2018;470:995–1016.
- [11] Merkin J, Russell C, Chen P, Burge CB. Evolutionary dynamics of gene and isoform regulation in mammalian tissues. *Science* (80) 2012;338:1593–9.
- [12] Cesaro A, Brest P, Hofman V, Hébuterne X, Wildman S, Ferrua B, et al. Amplification loop of the inflammatory process is induced by P2X 7 R activation in intestinal epithelial cells in response to neutrophil transepithelial migration. *Am J Physiol Cell Physiol* 2010;299:32–42.
- [13] Mishra A, Chintagari NR, Guo Y, Weng T, Su L, Liu L. Purinergic P2X 7 receptor regulates lung surfactant secretion in a paracrine manner. *J Cell Sci* 2011;124:657–68.
- [14] Ruzsnavszky O, Telek A, Gönczi M, Balogh A, Remenyik É, Csernoch L. Journal of Photochemistry and Photobiology B: biology UV-B induced alteration in purinergic receptors and signaling on HaCaT keratinocytes. *J Photochem Photobiol B Biol* 2011;105:113–8.
- [15] Jørgensen NR, Henriksen Z, Sørensen OH, Eriksen EF, Civitelli R, Steinberg TH. Intercellular calcium signaling occurs between human osteoblasts and osteoclasts and requires activation of osteoclast P2X7 receptors \*. *J Biol Chem* 2002;277:7574–80.
- [16] Solini A, Chiozzi P, Morelli A, Fellin R, Di Virgilio F. Human primary fibroblasts in vitro express a purinergic P2X 7 receptor coupled to ion fluxes, microvesicle formation and IL-6 release. *J Cell Sci* 1999;305:297–305.
- [17] Sluyter R, Shemon AN, Barden JA, Wiley JS. Extracellular ATP increases cation fluxes in human erythrocytes by activation of the P2X 7 receptor \*. *J Biol Chem* 2004;279:44749–55.
- [18] Georgiou JG, Skarratt ÁKK, Fuller ÁSJ, Martin ÁCJ, Richard I, Wiley JS, et al. Human epidermal and monocyte-derived langerhans cells express functional P2X 7 receptors. *J Investig Dermatol* 2005;125:482–90.
- [19] Baroni M, Pizzirani C, Pinotti M, Ferrari D, Adinolfi E, Calzavarini S, et al. Stimulation of P2 ( P2X 7 ) receptors in human dendritic cells induces the release of tissue factor-bearing microparticles. *FASEB J* 2007;21:1926–33.
- [20] Idzko M, Dichmann S, Ferrari D, Di Virgilio F, La Sala A, Girolomoni G, et al. Nucleotides induce chemotaxis and actin polymerization in immature but not mature human dendritic cells via activation of pertussis toxin-sensitive P2y receptors. *Blood* 2002;100:925–32.
- [21] Christenson K, Bjo L, Ta C, Bylund J. Serum amyloid A inhibits apoptosis of human neutrophils via a P2X7-sensitive pathway independent of formyl peptide receptor like 1. *J Leukoc Biol* 2008;83:139–48.
- [22] Wareham K, Vial C, Wykes RCE, Bradding P, Seward EP. Functional evidence for the expression of P2X1, P2X4 and P2X7 receptors in human lung mast cells abbreviations. *Br J Pharmacol* 2009;157:1215–24.
- [23] Gu BJ, Zhang WY, Bendall LJ, Chessell IP, Buell GN, Wiley JS. Expression of P2X7 purinoceptors on human lymphocytes and monocytes: evidence for nonfunctional P2X7 receptors. *Am J Physiol Cell Physiol* 2000;279:1189–97.
- [24] Chiozzi P, Sanz JM, Ferrari D, Falzoni S, Aleotti A, Buell GN, et al. Spontaneous cell fusion in macrophage cultures expressing high levels of the P2Z/P2X 7 receptor. *J Cell Biol* 1997;138:697–707.

- [25] Borges H, Beura LK, Wang H, Hanse EA, Gore R, Scott MC, et al. Fitness of long-lived memory CD8 + T cells. *Nature* 2018;559:264.
- [26] Idzko M, Dichmann S, Panther E, Ferrari D, Herouy Y, Virchow C, et al. Functional characterization of P2Y and P2X receptors in human eosinophils. *J Cell Physiol* 2001;188:329–36.
- [27] Bianchi G, Vuerich M, Pellegatti P, Marimpetri D, Emionite L, Marigo I, et al. ATP/P2X7 axis modulates myeloid-derived suppressor cell functions in neuroblastoma microenvironment. *Cell Death Dis* 2014;5:e1135–12.
- [28] Deli T, Varga N, Adam A, Kenessey I, Raso E, Puskas L, et al. Functional genomics of calcium channels in human melanoma cells. *Int J Cancer* 2007;121:55–65.
- [29] Solini A, Cuccato S, Ferrari D, Santini E, Gulinelli S, Callegari MG, et al. Increased P2X 7 receptor expression and function in thyroid papillary cancer: a new potential marker of the disease? *Endocrinology* 2008;149:389–96.
- [30] Vázquez-cuevas FG, Martínez-ramírez AS, Robles-martínez L, Garay E, García-carrancá A, Pérez-montiel D, et al. Paracrine stimulation of P2X7 receptor by ATP activates a proliferative pathway in ovarian carcinoma cells. *J Cell Biochem* 2014;1966:1955–66.
- [31] Santos AAJ, Cappellari AR, De Marchi FO, Gehring MP, Zaparte A, Brandão CA, et al. Potential role of P2X7R in esophageal squamous cell carcinoma proliferation. *Purine Pyrimidine Recept Pharmacol* (Jacobson KA, Linden J, Eds) 2017;13:279–92.
- [32] Li X, Qi X, Zhou L, Fu W, Gorodeski GI. P2X 7 receptor expression is decreased in epithelial cancer cells of ectodermal, uro-genital sinus, and distal paramesonephric duct origin. *Purinergic Signal* 2009;5:351–68.
- [33] Adinolfi E, Melchiorri L, Falzoni S, Chiozzi P, Morelli A, Tieghi A, et al. Brief report P2X 7 receptor expression in evolutive and indolent forms of chronic B lymphocytic leukemia. *Blood* 2002;99:706–9.
- [34] Zhang X, Zheng G, Ma X, Yang Y, Li G, Rao Q, et al. Expression of P2X7 in human hematopoietic cell lines and leukemia patients. *Leuk Res* 2004;28:1313–22.
- [35] Chong J, Zheng G, Zhu X, Guo Y, Wang L, Ma C, et al. Abnormal expression of P2X family receptors in Chinese pediatric acute leukemias. *Biochem Biophys Res Commun* 2010;391:498–504.
- [36] Pineda JMB, Bradley RK. Most human introns are recognized via multiple and tissue-specific branchpoints. *Genes Dev* 2018;32:577–91.
- [37] Kaczmarek-Hajek K, Zhang J, Kopp R, Grosche A, Rissiek B, Saul A, et al. Re-evaluation of neuronal P2X7 expression using novel mouse models and a P2X7-specific nanobody. *Elife* 2018;7:1–29.
- [38] Barbosa-Morais NL, Irimia M, Pan Q, Xiong HY, Gueroussov S, Lee LJ, et al. The evolutionary landscape of alternative splicing in vertebrate species. *Science* (80) 2012;338:1587–93.
- [39] Graveley BR. Alternative splicing: increasing diversity in the proteomic world. *Trends Genet* 2001;17:100–7.
- [40] Czubyat A, Piekietko-Witkowska A. Protein kinases that phosphorylate splicing factors: roles in cancer development, progression and possible therapeutic options. *Int J Biochem Cell Biol* 2017;91:102–15.
- [41] Lim KH, Ferraris L, Filloux ME, Raphael BJ, Fairbrother WG. Using positional distribution to identify splicing elements and predict pre-mRNA processing defects in human genes. *Proc Natl Acad Sci Unit States Am* 2011;108:11093–8.
- [42] Carazo F, Romero JP, Rubio A. Upstream analysis of alternative splicing: a review of computational approaches to predict context-dependent splicing factors. *Briefings Bioinf* 2018:1–18.
- [43] Montes M, Sanford BL, Comiskey DF, Chandler DS. RNA splicing and disease: animal models to therapies. *Trends Genet* 2019;35:68–87.
- [44] Drury AN, Szent-Györgyi A. The physiological activity of adenine compounds with especial reference to their action upon the mammalian heart. *J Physiol* 1929;68:213–37.
- [45] Burnstock G. Is there a basis for distinguishing two types of purinergic receptor. *Gen Pharmacol* 1985;16:141–54.
- [46] Jacobson KA. Introduction to adenosine receptors as therapeutic targets. *Handb Exp Pharmacol* 2009;193:1–24.
- [47] Burnstock G, Williams M. P2 purinergic receptors: modulation of cell function and therapeutic potential. *J Pharmacol Exp Ther* 2000;23:862–9.
- [48] North RA. Molecular physiology of P2X receptors. *Physiol Rev* 2002;82:1013–67.
- [49] Surprenant A, Rassendren F, Kawashima E, North RA, Buell G. The cytolytic P2Z receptor for extracellular ATP identified as a P2X receptor (P2X7). *Science* (80-) 1996;272:735–8.
- [50] Denlinger LC, Fiset PL, Sommer JA, Watters JJ, Prabhu U, DUBYAK GR, et al. Cutting edge: the nucleotide receptor P2X7 contains multiple protein- and lipid-interaction motifs including a potential binding site for bacterial lipopolysaccharide. *J Immunol* 2001;167:1871–6.
- [51] Burnstock G, Kennedy C. P2X receptors in health and disease. In: Jacobson KA, Linden J, editors. *Purine Pyrimidine Recept. Pharmacol*, vol. 61; 2011. p. 333–72.
- [52] Darmellah A, Rayah A, Auger R, Cuif MH, Prigent M, Arpin M, et al. Ezrin/radixin/moesin are required for the purinergic P2X7 receptor (P2X7R)-dependent processing of the amyloid precursor protein. *J Biol Chem* 2012;287:34583–95.
- [53] Sluyter R. The P2X7 receptor. *Adv Exp Med Biol* 2017;1051:17–53.
- [54] Mellouk A, Bobé P. CD8 + , but not CD4 + effector/memory T cells, express the CD44 high CD45RB high phenotype with aging, which displays reduced expression levels of P2X 7 receptor and ATP-induced cellular responses. *FASEB J* 2019;33:3225–36.
- [55] Karasawa A, Kawate T. Structural basis for subtype-specific inhibition of the P2X7 receptor. *Elife* 2016;5:e22153.
- [56] Kasuya G, Fujiwara Y, Tsukamoto H, Morinaga S, Ryu S, Touhara K, et al. Structural insights into the nucleotide base specificity of P2X receptors. *Sci Rep* 2017;7:45208.
- [57] Kawate T, Michel JC, Birdsong WT, Gouaux E. Crystal structure of the ATP-gated P2X4ion channel in the closed state. *Nature* 2009;460:592–8.
- [58] Hattori M, Hibbs RE, Gouaux E. A fluorescence-detection size-exclusion chromatography-based thermostability assay to identify membrane protein expression and crystallization conditions. *Structure* 2012;20:1293–9.
- [59] Mansoor SE, Lü W, Oosterheert W, Shekhar M, Tajkhorshid E, Gouaux E. X-ray structures define human P2X 3 receptor gating cycle and antagonist action. *Nature* 2016;538:66–71.
- [60] Karasawa A, Michalski K, Mikhelzon P, Kawate T. The P2X7 receptor forms a dye-permeable pore independent of its intracellular domain but dependent on membrane lipid composition. *Elife* 2017;6:e31186.
- [61] Gonnord P, Delarasse C, Auger R, Benihoud K, Prigent M, Cuif MH, et al. Palmitoylation of the P2X7 receptor, an ATP-

- gated channel, controls its expression and association with lipid rafts. *FASEB J* 2009;23:795–805.
- [62] Robinson LE, Shridar M, Smith P, Murrell-Lagnado RD. Plasma membrane cholesterol as a regulator of human and rodent P2X7 receptor activation and sensitization. *J Biol Chem* 2014;289:31983–4.
- [63] Allsopp RC, Evans RJ. Contribution of the juxtatransmembrane intracellular regions to the time course and permeation of ATP-gated P2X7 receptor ion channels. *J Biol Chem* 2015;290:14556–66.
- [64] Pippel A, Stolz M, Woltersdorf R, Kless A, Schmalzing G, Markwardt F. Localization of the gate and selectivity filter of the full-length P2X7 receptor. *Proc Natl Acad Sci USA* 2017;114:2156–65.
- [65] Harkat M, Peverini L, Cerdan AH, Dunning K, Beudez J, Martz A, et al. On the permeation of large organic cations through the pore of ATP-gated P2X receptors. *Proc Natl Acad Sci USA* 2017;114:3786–95.
- [66] Di Virgilio F, Schmalzing G, Markwardt F. The elusive P2X7 macropore. *Trends Cell Biol* 2018;28:392–404.
- [67] Cheewatrakoolpong B, Gilchrest H, Anthes JC, Greenfeder S. Identification and characterization of splice variants of the human P2X7ATP channel. *Biochem Biophys Res Commun* 2005;332:17–27.
- [68] Adinolfi E, Cirillo M, Woltersdorf R, Falzoni S, Chiozzi P, Pellegatti P, et al. Trophic activity of a naturally occurring truncated isoform of the P2X7 receptor. *FASEB J* 2010;24:3393–404.
- [69] Smart ML, Gu B, Panchal RG, Wiley J, Cromer B, Williams DA, et al. P2X7 receptor cell surface expression and cytolytic pore formation are regulated by a distal C-terminal region. *J Biol Chem* 2003;278:8853–60.
- [70] Denlinger LC, Sommer JA, Parker K, Gudipaty L, Fisette PL, Watters JW, et al. Mutation of a dibasic amino acid motif within the C terminus of the P2X7 nucleotide receptor results in trafficking defects and impaired function. *J Immunol* 2003;171:1304–11.
- [71] Murrell-Lagnado RD, Qureshi OS. Assembly and trafficking of P2X purinergic receptors (Review). *Mol Membr Biol* 2008;25:321–31.
- [72] Feng YH, Li X, Wang L, Zhou L, Gorodeski GI. A truncated P2X7 receptor variant (P2X7-j) endogenously expressed in cervical cancer cells antagonizes the full-length P2X7 receptor through hetero-oligomerization. *J Biol Chem* 2006;281:17228–37.
- [73] Guzman-Aranguez A, Pérez de Lara MJ, Pintor J. Hyperosmotic stress induces ATP release and changes in P2X7 receptor levels in human corneal and conjunctival epithelial cells. *Purinergic Signal* 2017;13:249–58.
- [74] Kido Y, Kawahara C, Terai Y, Ohishi A, Kobayashi S, Hayakawa M, et al. Regulation of activity of P2X7 receptor by its splice variants in cultured mouse astrocytes. *Glia* 2014;62:440–51.
- [75] Nicke A, Kuan YH, Masin M, Rettinger J, Marquez-Klaka B, Bender O, et al. A functional P2X7 splice variant with an alternative transmembrane domain 1 escapes gene inactivation in P2X7 knock-out mice. *J Biol Chem* 2009;284:25813–22.
- [76] Schwarz N, Drouot L, Nicke A, Fliegert R, Boyer O, Guse AH, et al. Alternative splicing of the N-terminal cytosolic and transmembrane domains of P2X7 controls gating of the ion channel by ADP-ribosylation. *PLoS One* 2012;7:e41269.
- [77] Haanes KA, Schwab A, Novak I. The P2X7 receptor supports both life and death in fibrogenic pancreatic stellate cells. *PLoS One* 2012;7:e51164.
- [78] Masin M, Young C, Lim K, Barnes SJ, Xu XJ, Marschall V, et al. Expression, assembly and function of novel C-terminal truncated variants of the mouse P2X7 receptor: Re-evaluation of P2X7 knockouts. *Br J Pharmacol* 2012;165:978–93.
- [79] Csóka B, Németh ZH, Tőro G, Idzko M, Zech A, Koscsó B, et al. Extracellular ATP protects against sepsis through macrophage P2X7 purinergic receptors by enhancing intracellular bacterial killing. *FASEB J* 2015;29:3626–37.
- [80] Metzger M, Walser S, Aprile-Garcia F, Dedic N, Chen A, Holsboer F, et al. Genetically dissecting P2rx7 expression within the central nervous system using conditional humanized mice 2016;13:153–70.
- [81] Gudipaty L, Humphreys BD, Buell G, Dubyak GR. Regulation of P2X7 nucleotide receptor function in human monocytes by extracellular ions and receptor density. *Am J Physiol Cell Physiol* 2001;280:C943–53.
- [82] Gudipaty L, Munetz J, Verhoef PA, Dubyak GR. Essential role for Ca<sup>2+</sup> in regulation of IL-1 $\beta$  secretion by P2X<sub>7</sub> nucleotide receptor in monocytes, macrophages, and HEK-293 cells. *Am J Physiol Physiol* 2003;285:C286–99.
- [83] Rissiek B, Haag F, Boyer O, Koch-Nolte F, Adriouch S. P2X7 on mouse T cells: one channel, many functions. *Front Immunol* 2015;6:1–9.
- [84] Liang X, Samways DSK, Bowles EA, Richards JP, Wolf K, Egan TM, et al. Quantifying Ca<sup>2+</sup> current and permeability in ATP-gated P2X7 receptors. *J Biol Chem* 2015;290:7930–42.
- [85] Barden JA. Non-functional P2X7: a novel and ubiquitous target in human cancer. *J Clin Cell Immunol* 2014;05:237–41.
- [86] Buell G, Chessell IP, Michel A, Collo G, Salazzo M, Herren S, et al. Blockade of human P2X7 receptor function with a monoclonal antibody. *Blood* 1998;92:3521–8.
- [87] Kim M, Jiang LH, Wilson HL, North RA, Surprenant A. Proteomic and functional evidence for a P2X7 receptor signalling complex. *EMBO J* 2001;20:6347–58.
- [88] Sluyter R, Stokes L. Significance of P2X7 receptor variants to human health and disease. *Recent Pat DNA Gene Sequences* 2011;5:41–54.
- [89] Zhang J, Manley JL. Misregulation of pre-mRNA alternative splicing in cancer. *Cancer Discov* 2013;3:1228–37.
- [90] Wu Q, Krainer AR. AT-AC pre-mRNA splicing mechanisms and conservation of minor introns in voltage-gated ion channel genes. *Mol Cell Biol* 2015;19:3225–36.
- [91] Adinolfi E, Raffaghello L, Giuliani AL, Cavazzini L, Capece M, Chiozzi P, et al. Expression of P2X7 receptor increases in vivo tumor growth. *Cancer Res* 2012;72:2957–69.
- [92] Pellegatti P, Raffaghello L, Bianchi G, Piccardi F, Pistoia V, Di Virgilio F. Increased level of extracellular ATP at tumor sites: in vivo imaging with plasma membrane luciferase. *PLoS One* 2008;3:1–9.
- [93] Barden JA, Sluyter R, Gu BJ, Wiley JS. Specific detection of non-functional human P2X7 receptors in HEK293 cells and B-lymphocytes. *FEBS Lett* 2003;538:159–62.
- [94] Slater M, Danieleto S, Pooley M, Gidley-Baird A, Cheng Teh L, Barden JA, et al. Differentiation between cancerous and normal hyperplastic lobules in breast lesions. *Breast Cancer Res Treat* 2004;83:1–10.
- [95] Gilbert S, Oliphant C, Hassan S, Peille A, Bronsert P, Falzoni S, et al. ATP in the tumour microenvironment drives expression of nP2X7, a key mediator of cancer cell survival. *Oncogene* 2018;38:194–208.
- [96] Zaidi N, Lupien L, Kuemmerle NB, Kinlaw WB, Swinnen JV, Smans K. Lipogenesis and lipolysis: the pathways exploited by the cancer cells to acquire fatty acids. *Prog Lipid Res* 2013;52:585–9.
- [97] Rysman E, Brusselmans K, Scheys K, Timmermans L, Derua R, Munck S, et al. De novo lipogenesis protects cancer cells from free radicals and chemotherapeutics by

- promoting membrane lipid saturation. *Cancer Res* 2010;70:8117–26.
- [98] Garcia-Marcos M, Pochet S, Marino A, Dehaye J. P2X7 and phospholipid signalling: the search of the “missing link” in epithelial cells. *Cell Signal* 2006;18:2098–104.
- [99] Le Stunff H, Raymond MN. P2X7 receptor-mediated phosphatidic acid production delays ATP-induced pore opening and cytolysis of RAW 264.7 macrophages. *Cell Signal* 2007;19:1909–18.
- [100] Costa-Junior HM, Marques-da-Silva C, Vieira FS, Vieira FS, Monção-Ribeiro LC, Coutinho-Silva R. Lipid metabolism modulation by the P2X7 receptor in the immune system and during the course of infection: new insights into the old view. *Purinergic Signal* 2011;7:381–92.
- [101] Pan H, Ni H, Zhang LL, Xing Y, Fan J, Li P, et al. P2RX7-V3 is a novel oncogene that promotes tumorigenesis in uveal melanoma. *Tumor Biol* 2016;37:13533–43.
- [102] Fernandes J, Acuna S, Floeter-Winter L, Muxel S. Long non-coding RNAs in the regulation of gene expression: physiology and disease. *Non-Coding RNA* 2019;5:E17.
- [103] Kahles A, Lehmann K, Toussaint N, Huser M, Stark S, Sachsenberg T, et al. Comprehensive analysis of alternative splicing across tumor form 8705 patients. *Cancer Cell* 2019;34:211–24.





## Research Paper

# P2RX7B is a new theranostic marker for lung adenocarcinoma patients

Jonathan Benzaquen<sup>1,4,5,6</sup>, Serena Janho Dit Hreich<sup>1,5</sup>, Simon Heeke<sup>1,2</sup>, Thierry Juhel<sup>1,5</sup>, Salomé Lalvee<sup>2,3</sup>, Serge Bauwens<sup>1</sup>, Simona Sacconi<sup>1</sup>, Philippe Lenormand<sup>1</sup>, Véronique Hofman<sup>1,2,3,4</sup>, Mathilde Butori<sup>1</sup>, Sylvie Leroy<sup>4,6,7</sup>, Jean-Philippe Berthet<sup>8</sup>, Charles-Hugo Marquette<sup>1,4,6</sup>, Paul Hofman<sup>1,2,3,4</sup> and Valérie Vouret-Craviari<sup>1,4,5</sup>✉

1. Université Côte d'Azur, CNRS, INSERM, IRCAN UMR 7284, 06108 Nice, France.
2. Laboratory of Clinical and Experimental Pathology and Biobank, Pasteur Hospital, Nice, France.
3. Hospital-Related Biobank (BB-0033-00025), Pasteur Hospital, Nice, France.
4. FHU OncoAge, Nice, France.
5. Centre Antoine Lacassagne, 06107 Nice, France.
6. Department of Pulmonary Medicine and Oncology, Pasteur Hospital, Nice, France.
7. Université Côte d'Azur, CNRS UMR 7275 - IPMC, Sophia Antipolis, France.
8. Department of Thoracic surgery, Pasteur Hospital, Nice, France.

✉ Corresponding author: Valérie VOURET-CRAVIARI, IRCAN, 33 avenue de Valombrose, 06108 Nice, France. Telephone number: 00 33 492031223; E-mail: vouret@unice.fr.

© The author(s). This is an open access article distributed under the terms of the Creative Commons Attribution License (<https://creativecommons.org/licenses/by/4.0/>). See <http://ivyspring.com/terms> for full terms and conditions.

Received: 2020.05.15; Accepted: 2020.06.21; Published: 2020.08.29

## Abstract

**Rationale:** The characterization of new theranostic biomarkers is crucial to improving the clinical outcome of patients with advanced lung cancer. Here, we aimed at characterizing the P2RX7 receptor, a positive modulator of the anti-tumor immune response, in patients with lung adenocarcinoma.

**Methods:** The expression of P2RX7 and its splice variants was analyzed by RT-qPCR using areas of tumor and non-tumor lung adenocarcinoma (LUAD) tissues on both immune and non-immune cells. The biological activity of P2RX7 was studied by flow cytometry using fluorescent dyes. Bi-molecular fluorescence complementation and confocal microscopy were used to assess the oligomerization of P2RX7. Tumor immune infiltrates were characterized by immunohistochemistry.

**Results:** Fifty-three patients with LUAD were evaluated. P2RX7A, and 3 alternative splice variants were expressed in LUAD tissues and expression was down regulated in tumor versus adjacent non-tumor tissues. The protein retained biological activity only in immune cells. The P2RX7B splice variant was differentially upregulated in immune cells ( $P < 0.001$ ) of the tumor and strong evidence of oligomerization of P2RX7A and B was observed in the HEK expression model, which correlated with a default in the activity of P2RX7. Finally, LUAD patients with a high level of P2RX7B had non-inflamed tumors ( $P = 0.001$ ).

**Conclusion:** Our findings identified P2RX7B as a new theranostic tool to restore functional P2RX7 activity and open alternative therapeutic opportunities to improve LUAD patient outcome.

Key words: lung cancer, P2X7R, purinergic signaling, ATP, splice variant

## Introduction

Lung cancer is the leading cause of cancer-related deaths in the world. More than two thirds of lung cancers are diagnosed at an advanced stage [1] and need medical treatment including chemotherapy, targeted therapies and immunotherapies. Despite these new approaches, the 5-year survival rate of

patients with any type of lung cancer remains at around 20%, all stages combined and ranges from 57% in localized lung cancers to 5% in metastatic lung cancers [1]. Therefore, deciphering new theranostic tools and understanding processes involved in the development of pro- or anti-tumor micro-



environments are of crucial importance to improve patient outcome.

Purinergic receptors for extracellular nucleotides (ATP, ADP, UTP, UDP) and the nucleoside adenosine have attracted growing interest since the discovery that inflammatory and cancer tissues contain high levels of extracellular ATP (eATP) [2] and adenosine (its degradation product), which has been described as an immunosuppressor [3]. The purinergic receptor family is divided into two major families, P2X and P2Y [4]. Depending on the receptor involved, extracellular purines orchestrate either immunostimulation or immunosuppression of host cells, as well as proliferation or cytotoxicity of tumor cells [5]. We focused on P2RX7, an ubiquitous receptor [6] described to be expressed at a particularly high level in white blood cells from the immune system, especially in monocytes/macrophages, lymphocytes and dendritic cells [7–10].

The full length P2RX7 receptor is an ATP-gated ion channel composed of three protein subunits encoded by *P2RX7A* mRNA. Activation of P2RX7 by high doses of eATP leads to Na<sup>+</sup> and Ca<sup>2+</sup> influx and, after prolonged activation, to the opening of a larger conductance membrane pore, also defined as macropore activity or macropore opening [11]. One consequence of this macropore opening, a unique characteristic of P2RX7, is to induce cell death in eATP rich micro-environments. This feature is linked principally to the presence of a long C-terminal domain [12].

The use of transplantable murine tumor models has demonstrated that P2RX7 expressed by host immune cells coordinates anti-tumor immune responses [13,14]. The expression of a functional P2RX7 receptor on human white blood cells and in human hemopathies has been largely documented in the literature [15–17]. However, whereas numerous publications claimed that P2RX7 is over-expressed in solid tumors, on the basis of P2RX7 immunostaining using mostly antibodies directed against either the extracellular loop [18,19] or the C-terminal domain [20–26], only a little data are available regarding functional P2RX7 in *ex vivo* human solid cancer cells. This is of particular importance considering that P2RX7 functionality can be affected by single nucleotide polymorphisms (SNP). Over the 13252 SNPs described within *P2RX7* gene in 2020, the phenotype of 16 non-synonymous SNPs has been studied, some of which leading to numerous pathologies including infectious, bone, neuropsychiatric, inflammatory, cardiovascular and cancerous diseases, but also poorer survival of cancer patients [27,28]. In addition, we found 27 SNPs located to the boundary of mRNA splicing sites

within intronic regions which may affect splicing events. However, these SNPs are too sparsely expressed to envisage that they could be involved in diseases [29].

The function of P2RX7 can also be affected by alternative splicing. Nine alternative splice variants were identified [30,31]. The function of only three of them, P2RX7H with a deletion in the first transmembrane domain ( $\Delta$ TM1) leading to a loss of ion channel function, P2RX7B with a deletion in the C-terminal domain ( $\Delta$ Ct) leading to a loss of large pore forming function, and P2RX7J with a deletion in the second transmembrane domain leading to a negative dominant isoform, have been studied in more detail [18,19,30–33].

P2RX7 protein expression in lung adenocarcinoma (LUAD) was reported by Boldrini et al. [34], but it is currently unknown whether functional P2RX7 is expressed in LUAD. In this study we aimed at deciphering the expression of P2RX7 and its splice variants, and the implication of such variants on the biological function of the receptor and on inflammatory infiltration of tumors.

## Materials and Methods

### Patients

Twenty-four bronchopulmonary samples were obtained from the middle of the tumor and from non-tumor tissue for each patient operated on for early stage (I–IIIA) LUAD. The diagnosis and the margin of the samples were confirmed as tumoral by two lung cancer pathologists. The median age was 68 years-old and 79% of the patients were smokers or former smokers. In the retrospective study, twenty-nine LUAD samples were obtained from the biobank of the Nice University Hospital (Clinical and Experimental Pathology Laboratory) and were taken from patients operated on at the thoracic surgery department of the Nice University Hospital for early stage (I–IIIA) LUAD. The median age was 67 years-old and 100% of the patients were smokers or former smokers (see **Table 1**). Free and informed consent was obtained for each patient with the agreement of the South East CPP.

### Tumor processing

After surgery, tumor tissues were kept in RPMI (Roswell Park Memorial Institute medium, Gibco®) at 4°C, for a maximum of 12 h. Sample preparation included scissor dissociation, incubation in Human Tumor Dissociation Kit (MACS®) buffer at 37°C for 40 min and washed by DPBS 10% FBS. Cells were counted and a trypan blue test was performed to ensure cell viability. Cells were magnetically sorted (mouse anti-CD45 MicroBeads, Miltenyi®) according

to the manufacturer's procedure. A sorting enrichment control experiment was performed using a humanized anti-CD45 AF488 coupled antibody (Miltenyi®) after Fc blocking (**Figure S1A**).

**Table 1.** Main epidemiological data of LUAD patients

Retrospective study (n=29)		
Age (years)	Mean (Range)	67 (41 – 85)
Sex	Female	6 (20.7%)
	Male	23 (79.3%)
Smoking history	Smokers or smoking history	29 (100%)
	Non smoker	0 (0%)
COPD #	Yes	18 (62%)
	No	11 (37.9%)
Stage at surgery	I	15 (51.7%)
	II	10 (34.4%)
	III	2 (6.9%)
	IV	0 (0%)
Adjuvant chemotherapy	Yes	3 (10.3%)
	No	26 (89.7%)
Relapse	Yes	7 (24.1%)
	No	19 (65.6%)
	Unknown	3 (10.3%)
Prospective study (n=24)		
Age (years)	Mean (Range)	68 (44 – 80)
Sex	Female	12 (50%)
	Male	12 (50%)
Smoking history	Smokers or smoking history	19 (79.2%)
	Non smoker	5 (20.8%)
COPD	Yes	6 (25%)
	No	17 (70.8%)
	Unknown	1 (4.2%)
Stage at surgery	I	12 (50%)
	II	4 (17%)
	III	8 (33%)
	IV	0 (0%)
Adjuvant chemotherapy	Yes	9 (37.5%)
	No	15 (62.5%)
Relapse	Yes	5 (20.8%)
	No	11 (45.8%)
	Unknown	8 (33.3%)

# COPD: chronic obstructive pulmonary disease.

## Immunofluorescence

After tumor processing as described in the dedicated section, the cell suspension was homogenized, 500 000 LUAD cells were plated on slide and fixed by drying at room temperature (RT) and stained. To ensure that cells came exclusively from the intratumor area of LUAD, the margins were checked on the corresponding tissue blocks and confirmed as adenocarcinomatous by two lung cancer pathologists. HEK293T cells were plated at 600 000 cells in a 6-wells culture plate containing coverslip poly-D-lysine (Gibco) coated and transfected as described below. Anti CD16/CD32 antibodies (Fc Block, BD Biosciences) were used (1 h, RT) to reduce the non-specific signal, and primary antibodies were added for 2 h at 4°C. After washing, secondary antibodies were added for an additional 1 h at RT. Anti-P2RX7 hybridoma (dil1/2) was used. This

antibody is routinely used to detect the expression of functional P2RX7 [6]. Anti-CD45-FITC (dil1/50, recombinant human IgG1, REA747 clone, MACS®) and anti-goat Alexa fluor 594, (1/200, Thermofisher) antibodies were used. The nuclei were counterstained with 4'6-Diamidino-2-phenylindole dihydrochloride (DAPI) in the mounting medium (Invitrogen Life Technologies™).

## P2RX7 functional assay

The overall cellular P2RX7 activity was evaluated by flow cytometry. This assay allows simultaneous study of live cells stimulated with BzATP (a stable analogue of ATP), for variations in calcium levels (FLUO-4-AM dye) and macropore opening (TO-PRO-3 dye) (**Figure S3**). In practice, cells were incubated in functional assay buffer (sucrose 300 mM, KCl 5 mM, MgCl<sub>2</sub> 1 mM CaCl<sub>2</sub> 1 mM, glucose 10 mM, HEPES pH 7.4 20 mM) and loaded with Fluo-4-AM (500 nM), for 30 min at RT. Propidium iodide was added for the last 5 min to stain both dying cells and P2RX7's independent permeabilization events, which will be excluded from the final analysis. FLUO-4-AM and propidium iodide were removed by 2 washes with DPBS containing FBS 5%, and 400 000 cells were incubated in the functional buffer and stimulated with BzATP in the presence of TO-PRO-3 (633 nM, Invitrogen) for the indicated time. The reaction was stopped with 2 mM MgCl<sub>2</sub> and washed with DPBS containing FBS 5%. Flow cytometry analysis was performed on a propidium negative population using a FACS Canto® II (BD Bioscience®) and data were analyzed using DIVA® or FlowJo® software. The normalization of fluorescence intensity was performed by retrieving at every time-point the fluorescence intensity (I) (FLUO-4-AM and TO-PRO-3) of the first time point (I<sub>0</sub>). Normalized data were presented as violin plot.

## RT-qPCR

Total RNA extraction from purified cell subpopulations or frozen tissues was performed using the AllPrep RNA Mini Qiagen® kit and reverse transcription of 37.2 ng total RNA was performed with the Applied Biosystems® kit. The cDNA was subjected to quantitative PCR using the Fast Sybr®Green Master Mix kit (Applied biosystems) and a StepOnePlus™ thermocycler. Relative expression was determined using the log<sub>2</sub> fold change (2<sup>-ΔΔCt</sup>) method with *RPLP0* as the housekeeping gene. The oligonucleotides, designed to overlap splicing sites, are presented in **Figure S6A**. QPCR amplicons were sequenced to confirm their specificity (data not shown) and used as matrices of standard amplification curves to validate the absolute

quantification rate and the amplification efficiency of each oligonucleotides couple (**Figure S6B**).

### Cell cultures and transfection

HEK293T cell line, provided by ATCC, were cultured in DMEM medium supplemented with 10% FBS and 100 U/mL penicillin and 100 mg/mL streptomycin at 37°C in a humid atmosphere containing 5% CO<sub>2</sub>. P2RX7A and P2RX7B splice variants were synthesized by Eurofins® and sequenced. HEK293T cells were transfected with pcDNA expression vector coding for the indicated cDNA using Lipofectamine® 3000 (ThermoFisher) according to the manufacturer's instructions. "PcDNA3.1 venus 1" and "pcDNA3.1 venus 2" were provided by Dr Sacconi's team. Transient expression analyses were processed 48-h post transfection. For the establishment of stable cell lines expressing the untagged P2RX7A, P2RX7B or P2RX7AB, blasticidin 1 µg/mL and puromycin 1 µg/mL were added to the growth media. After 3 weeks, clones were selected and tested for protein expression by Western blotting.

### Western blotting

Western blot analysis was performed following the standard protocol. In brief, cells were lysed on-ice in TR3 buffer (SDS 3%, glycerol 10%, Na<sub>2</sub>PO<sub>4</sub> 10 mM + Complete™ Protease Inhibitor Cocktail, Roche), 20 to 50 µg of total proteins were subjected to 9% SDS-PAGE and transferred onto PVDF membranes (Immobilon Millipore®). Blots were then blocked for 20 minutes with 5% non-fat dried milk and incubated with primary antibodies (Rabbit anti-Human extracellular loop of P2RX7, APR-008, Alomone), overnight at 4°C, followed by three 5-min washes with Tris-Buffered Saline 0.1% Tween® 20 detergent, then incubated with species specific secondary IgG antibodies coupled to Horseradish peroxidase (HRP) (Goat anti-Rabbit, AP307P, Sigma, and Goat anti-Mouse, AP308P, Sigma) 1 h at RT, followed by 3 more washes as described before. The signal was revealed using Pxi imaging (Syngene). In a second step, αTubulin (Mouse anti-tubulin, Sigma) level was monitored as a control for protein loading.

### Immunohistochemistry

Immunohistochemical (IHC) staining for CD45, CD3, CD8, CD20 and CD33, was performed on tumor sections obtained from LUAD patients of the prospective cohort. In brief, formalin fixed paraffin embedded 4 µm thick tissue sections were stained with specific anti-human antibodies on an automated staining platform (Benchmark ULTRA; Ventana) using the appropriate concentration. An OptiView DAB IHC Detection Kit (Ventana) and an OptiView

Amplification Kit (Ventana) were used according to the manufacturer's recommendations for the visualization of the bound antibodies; sections were counter-stained with hematoxylin. Blinded quantification of the brown staining was done as follows: 5 different zones of the scanned tumor section (NanoZoomer 2.0 HT from Hamamatsu) were selected at low magnification (1×) and images of the selected fields were analyzed at 40× magnification. Scoring of the staining was as follows: 1 = 0-10% positive cells, 2 = 10-50% positive cells and 3 = ≥ 50% positive cells.

### Bioinformatic and statistical analysis

Quantitative data were described and presented graphically as medians and inter quartiles or means and standard deviations. The distribution normality was tested with the Shapiro's test and homoscedasticity with Bartlett's test. For two categories, statistical comparisons were performed using the Student's *t*-test or the Mann-Whitney test. Overall survival was defined as the interval between the date of diagnosis and the date of death from any cause. These data were estimated and presented graphically using the Kaplan–Meier method. The survival curves were compared using the log-rank test. All statistical analyses were performed using GraphPad Prism® v.8.0.2. Tests of significance were two-tailed and considered significant with an alpha level of  $P < 0.05$ . SnapGene 4.3.8 was used for plasmid construction. The results shown in **Figure 4B** and **Supplementary Figure 7** are based on data generated by the TCGA project for which we are grateful.

## Results

### P2RX7 is expressed in LUAD

To analyze the expression levels of conformational P2RX7 in LUAD, tumor tissue was dissociated, and the cells stained with the anti-P2RX7 antibody directed against the external domain of the tertiary structure of P2RX7, which has been described to antagonize its activity [6]. Whereas most of the cells were labeled, a small fraction of cells with large nuclei, a characteristic of tumor cells, were negative (**Figure 1A**). Next, an anti-CD45 antibody was used to characterize the nature of P2RX7 expressing cells and we observed that only CD45<sup>+</sup> cells were stained with the anti-P2RX7 antibody. Since cells were permeabilized, the lack of staining in CD45<sup>-</sup> cells was not due to intracellular retention of P2RX7 (**Figure S2**). To extend this observation, immune (CD45<sup>+</sup>) and non-immune (CD45<sup>-</sup>) cells were isolated from three LUAD specimens and subjected to western blot analysis using a second antibody which recognizes the extracellular domain of P2RX7A and P2RX7B

monomers (Figure 1B). A protein of 70kDa corresponding to P2RX7A was found to be expressed by CD45<sup>+</sup> immune cells in 2 of 3 LUAD patients. These patients only showed very limited (if any) expression of P2RX7 on tumor cells. By contrast, we observed P2RX7A expression on tumor cells of the third LUAD patient. We also noticed the presence of additional bands (from 80 to 56kDa). These bands are of undetermined nature, being not recognized by the antibody in the HEK cell expression system transfected with P2RX7A. In this patient, expression of P2RX7A was poorly detected on immune cells. Instead, a protein of 55kDa, which could correspond to P2RX7B, was observed.

Therefore, using two independent antibodies, our results showed that P2RX7A is preferentially expressed on immune cells of LUAD patients.

### The macropore function of P2RX7 is impaired in immune cells of LUAD

Since P2RX7 expression could not predict P2RX7 activity, we investigated the macropore function of P2RX7 in both immune and non-immune cells of LUAD specimens and paired corresponding adjacent non-cancerous tissues (Figure 2 and Figure S4). BzATP increased the uptake of TO-PRO-3 in immune cells from both non-tumor and tumor areas (Figure 2A-B). This increase was prevented in cells pre-treated with the specific P2RX7 inhibitor, GSK1370319A [35], indicating that TO-PRO-3 uptake was dependent on the expression of P2RX7. In addition, the macropore activity was delayed in the tumor compartment. In fact, 15 min post stimulation, the normalized median percentage of TO-PRO-3<sup>+</sup> cells

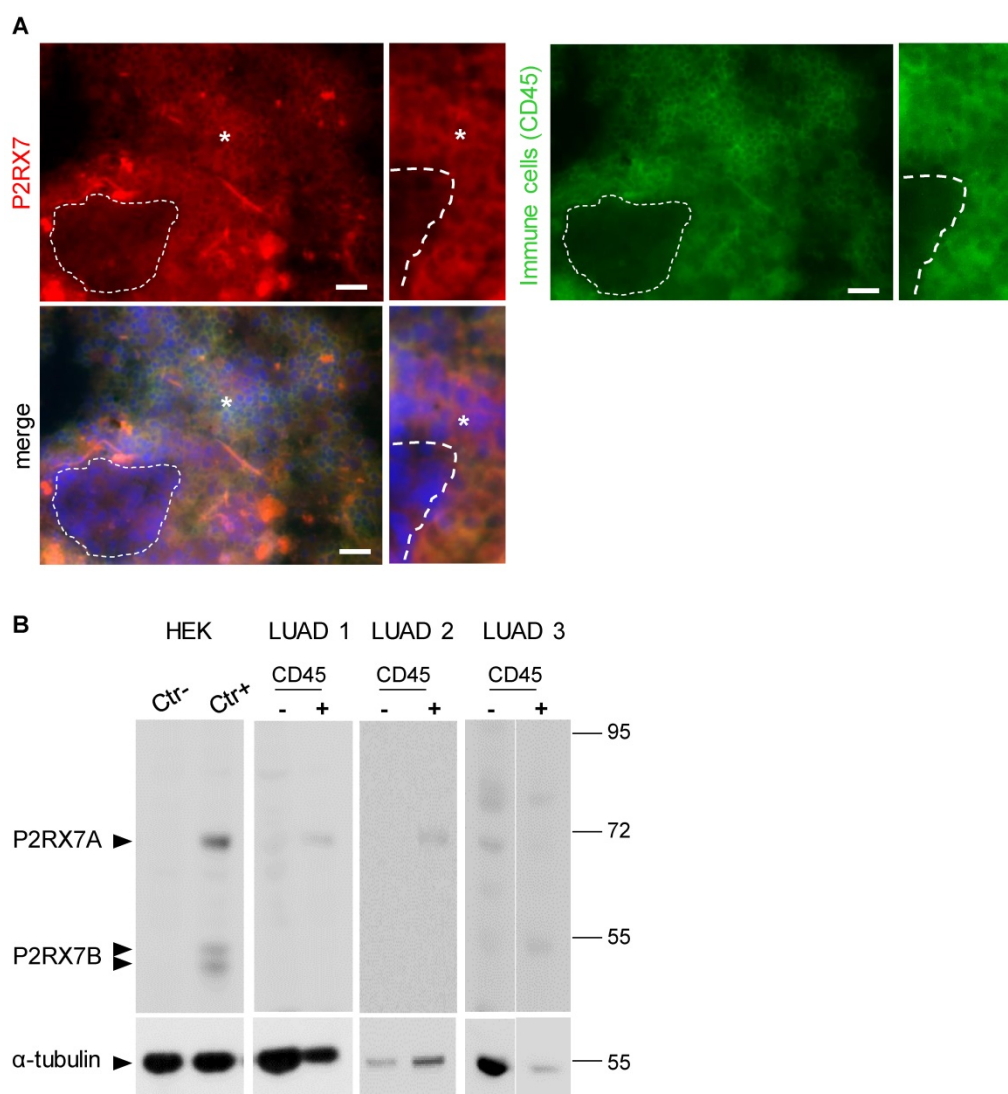
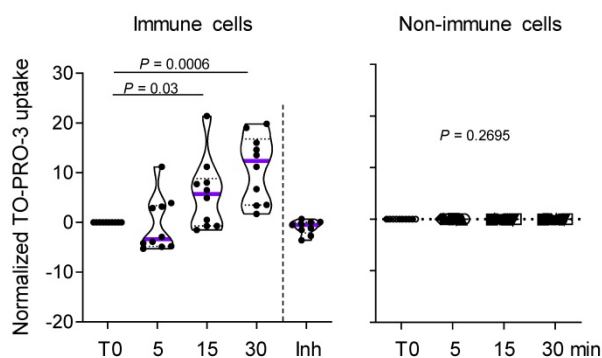


**Figure 1.** LUAD patients express P2RX7. **A.** Representative images of P2RX7 staining in LUAD tissue using the conformational anti-P2RX7 antibody, in red. CD45 staining highlighted immune cells, in green. \* showed P2RX7 expressing cells. The hatched line shows CD45<sup>-</sup> cells. DAPI staining shows nuclei. Magnification 20X, scale bar = 200  $\mu$ m. **B.** Representative Western blot showing P2RX7 expression in HEK cells transfected with empty vector (Ctrl-), cells transfected with both P2RX7A and P2RX7B expressing vectors and purified CD45<sup>+</sup> and CD45<sup>-</sup> cells isolated from tumor areas of LUAD patients using the anti P2RX7 extracellular loop antibody (Alomone, APR-008, 1/1000). The total  $\alpha$ Tubulin level was monitored as a control for protein loading.

was 1.2% in the tumor infiltrate (Figure 2B), while it reached 5.7% in the non-tumor infiltrate (Figure 2A). This difference was still observed 30 min post stimulation. These results suggest that P2RX7 expressed by immune cells within the tumor area was less functional.

Considering the differential activation status of P2RX7 in immune cells compared to non-immune cells, we hypothesized that alternative splicing of P2RX7 mRNA may generate hetero-P2RX7 trimers with altered receptor functions.

#### A Non-tumor area



#### B Tumor area

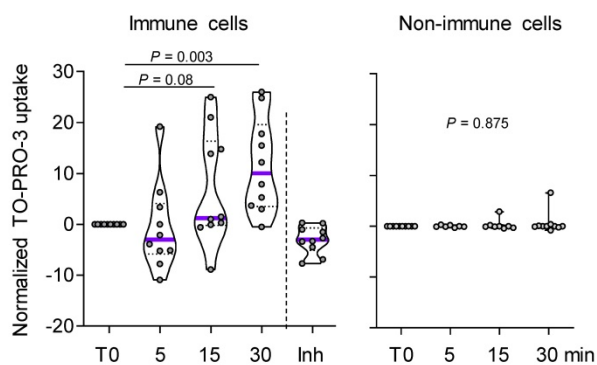


**Figure 2.** P2RX7 expressed by immune cells of LUAD patients is functional. **A.** Time course of macropore opening in purified immune and non-immune cells isolated from an adjacent non-tumor area of LUAD patients. When indicated we used a specific P2RX7 inhibitor (Inh) demonstrating that TO-PRO-3 uptake depends on P2RX7 activity. **B.** Time course of macropore opening in purified immune and non-immune cells isolated from the tumor area of LUAD tissue. The percentage of TO-PRO-3 positive cells in response to BzATP (250  $\mu$ M) is shown (paired Student's *t* test).  $n = 10$  paired LUAD specimens and corresponding adjacent non-cancerous tissues from our prospective cohort. The median value is highlighted by the violet line.

### P2RX7B is differentially upregulated in the LUAD immune infiltrate

We designed probes for the five variants described to be transcribed and translated, namely P2RX7A, B, D, H and J and analyzed their expression on human peripheral blood mononuclear cells by qualitative PCR analysis (Figure S5A). PBMCs expressed the P2RX7A, B, H and J variants (Figure

S5B). Next, using qPCR probes (Figure S6), we quantified P2RX7 expression on LUAD tissues using our two in-house cohorts (see Table 1). Using the probe which amplifies P2RX7A, B and H (further designed as P2RX7), we observed that P2RX7 was 2.5-fold less expressed in tumor versus non-tumor areas of LUAD (Figure 3A). Likewise, the specific expression of the P2RX7B, H and J splice variants was decreased 3.2-, 3.6- and 5.6-fold, respectively. These results were confirmed with TCGA RNA-seq expression data from a larger cohort of 57 LUAD (Figure S7). Further, we analyzed the expression levels of all P2RX7 mRNA in both non-tumor and tumor areas and observed that while P2RX7 was down-regulated in non-immune cells (Figure 3B), it was up-regulated in immune cells (Figure 3C). In the tumor area, P2RX7 was 15-fold up-regulated in immune cells compared to non-immune cells and the alternative splice variants P2RX7B, H and J were 7-, 6- and 15-fold up-regulated, respectively. Next, we compared the expression levels of each P2RX7 splice variant in immune cells purified from normal and tumor tissues and showed that the P2RX7B variants were differentially up-regulated in the immune infiltrates of LUAD patients (37% of the constitutive splicing), whereas the other variants were almost absent (Figure 3D). To evaluate whether up-regulation of P2RX7 may impact the fate of LUAD patients, we analyzed overall survival (OS) of the LUAD TCGA cohort, separated into two groups, stage I and stage II. A Kaplan-Meier analysis of patients with LUAD and a high expression of P2RX7 had a significantly poorer OS (38 months) than those with a low expression of P2RX7 (136 months). This tendency was present only in early-stage I LUAD and disappeared at stage II (Figure 4). At this point, no correlation with P2RX7B expression levels could be done, since neither the nature of P2RX7 splice variants nor the nature of P2RX7 expressing cells were present in TCGA database.

Collectively, these results suggest that the more P2RX7B was expressed, the more the macropore function was dysfunctional in the immune infiltrate of LUAD.

### P2RX7B expression negatively impacts the P2RX7 activity

It was previously reported that P2RX7B could heteromerize with P2RX7A [31]. Therefore, P2RX7B may be co-expressed with P2RX7A and form a chimeric receptor in the immune infiltrate of LUAD. To test this hypothesis and characterize the cellular localization of such a chimeric protein, we explored the expression and the function of P2RX7AB using a bi-molecular fluorescent complementation approach.

First, we controlled that cells transfected with individual hemi venus 1 (v1) or hemi venus 2 (v2) tagged-P2RX7 (P2RX7A and P2RX7B) did not emit a fluorescent GFP signal (**Figure S8A**). Thanks to the conformational anti-P2RX7 antibody, we demonstrated that individual v1- or v2-tagged P2RX7A formed homo trimers that are correctly localized at the cell membrane (**Figure S8A**). Next, we transiently co-transfected HEK cells with v1-P2RX7A and v2-P2RX7A. The interaction of the proteins brought the two hemi GFP within proximity, allowing GFP to reform its native structure and emit a fluorescence signal (**Figure 5A**). Confocal microscopy showed that v1+v2-P2RX7 was expressed at the cell surface. Furthermore, the tagged-P2RX7 adopted a normal conformation when stained with the conformational anti-P2RX7 antibody. Importantly, we verified that this antibody did not stain the P2RX7B protein (**Figure S9A**). We also noticed that some GFP<sup>+</sup> small dots remained within the cytoplasm. To study the impact of P2RX7B expression on P2RX7 function, HEK cells were transiently co-transfected with v1-P2RX7B and v2-P2RX7A (**Figure 5A, lower panel**). When expressed, the chimeric GFP<sup>+</sup> P2RX7AB receptor was found to be correctly inserted into the cell membrane (asterisk). The GFP chimeric proteins co-localized with P2RX7 stained with the conformational antibody (asterisk), suggesting that the chimeric receptor, like P2RX7, was inserted into the cell membrane. To confirm this finding, we quantified the percentage of tagged receptors that co-localized with P2RX7 at the membrane and observed that 35% of the chimeric protein co-localized with proteins stained with the conformational antibody (**Figure 5B and S8B**). We also observed the presence of numerous GFP<sup>+</sup> aggregates within the cytoplasm (arrowhead). We then tested whether the expression of P2RX7B modified the overall activity of P2RX7. To do so, transfected cells were stimulated with increasing doses of BzATP for 15 min, GFP<sup>+</sup> cells were sorted by FACS and the percentage of TO-PRO-3<sup>+</sup> cells within this fraction was analyzed (**Figure 5C**). BzATP dose dependency for TO-PRO-3 uptake was shifted to the right in HEK v2Av1B P2RX7 (P2RX7AB) cells compared to HEK v1Av2A P2RX7 (P2RX7A). We then calculated the EC<sub>50</sub> for macropore formation in both chimeric tagged P2RX7AB or tagged P2RX7A and P2RX7B and observed an increase of 30% (20 μM vs 14 μM) in cells co-transfected with both P2RX7A and P2RX7B (**Figure 5C**). By contrast, cells transfected with v1Bv2B P2RX7 (P2RX7B) did not show any TO-PRO-3 uptake, indicating that the homo trimer P2RX7B was unable to form a macropore, despite its expression at the cell membrane and its ability to induce Ca<sup>2+</sup> influx (**Figure**

**S9B**). To go further and given the impact of the tag on membrane localization, we decided to co-express non tagged P2RX7A and P2RX7B and reevaluate the overall activity of P2RX7. To allow a meaningful comparison, we selected clones expressing comparable protein levels of P2RX7A and P2RX7B, using an antibody specific for the extracellular loop and known to recognize both P2RX7A and P2RX7B (**Figure 5D**). We then assayed both the macropore and the Ca<sup>2+</sup> channel activities. Whereas the overall macropore activity of the cells transfected with both P2RX7A and P2RX7B proteins was inhibited by 50% compared to control cells transfected with P2RX7A only (EC<sub>50</sub> = 6.3 μM vs 13.1 μM and maximum TO-PRO-3<sup>+</sup> cells = 58% vs 84%), we did not observe any significant effect on the intracellular Ca<sup>2+</sup> concentration (**Figure 5E**). These results supported the notion that expression of the P2RX7B negatively impacted the overall macropore activity of P2RX7. At this point, we were unable to analyze the macropore activity of chimeric P2RX7AB itself. Indeed, we cannot exclude the hypothesis that the fraction of GFP<sup>+</sup> cells used to assay the macropore activity also expressed functional P2RX7A homo trimers allowing the influx of TO-PRO-3 in response to BzATP. However, based on the presence of large cytoplasmic aggregates in cells expressing both P2RX7A and P2RX7B, we can reasonably propose that P2RX7A is retained intracellularly. Such cell retention could impact the quantity of functional P2RX7 expressed at the cell membrane and consequently the macropore activity. In contrast, the absence of the effect on BzATP-induced increased Ca<sup>2+</sup> concentration might not be surprising considering that Ca<sup>2+</sup> is able to permeate more easily than a large dye, such as TO-PRO-3, across the pore formed by P2RX7.

### Expression of P2RX7B correlates with decreased T cell infiltration in LUAD

We next wondered whether *P2RX7B* expression could impact the composition of the immune infiltrate in LUAD. Analysis of the ratio of *P2RX7B* versus *P2RX7A* mRNA expression allowed us to separate two populations within the prospective cohort (**Figure 6A**). We clustered patients expressing 1 *P2RX7B* for 2 to 4 *P2RX7A* (ratio comprised between 0.2 to 0.4), which corresponded to 60% of the specimens, from patients expressing 1 *P2RX7B* for 10 or more *P2RX7A* (ratio comprised between 0.1 to 0.0003). We then performed immunohistochemistry to qualify tumor infiltrating immune cells, focusing on leukocytes (CD45<sup>+</sup> cells) (**Figure 6B**), and T lymphocytes (CD3<sup>+</sup>), CD8<sup>+</sup> T cells, B lymphocytes (CD20<sup>+</sup>) and myeloid cells (CD33<sup>+</sup>). Quantification of the staining of these cells showed that the less *P2RX7B*

is expressed the higher the number of leukocytes recruited into LUAD (Figure 6C). This was observed for the lymphoid lineage (T lymphocytes, CD8 T lymphocytes and B lymphocytes). However, we noticed an inverse correlation regarding the myeloid

lineage (monocytes/macrophages, MDSC), characterized by cells expressing the transmembrane receptor CD33.

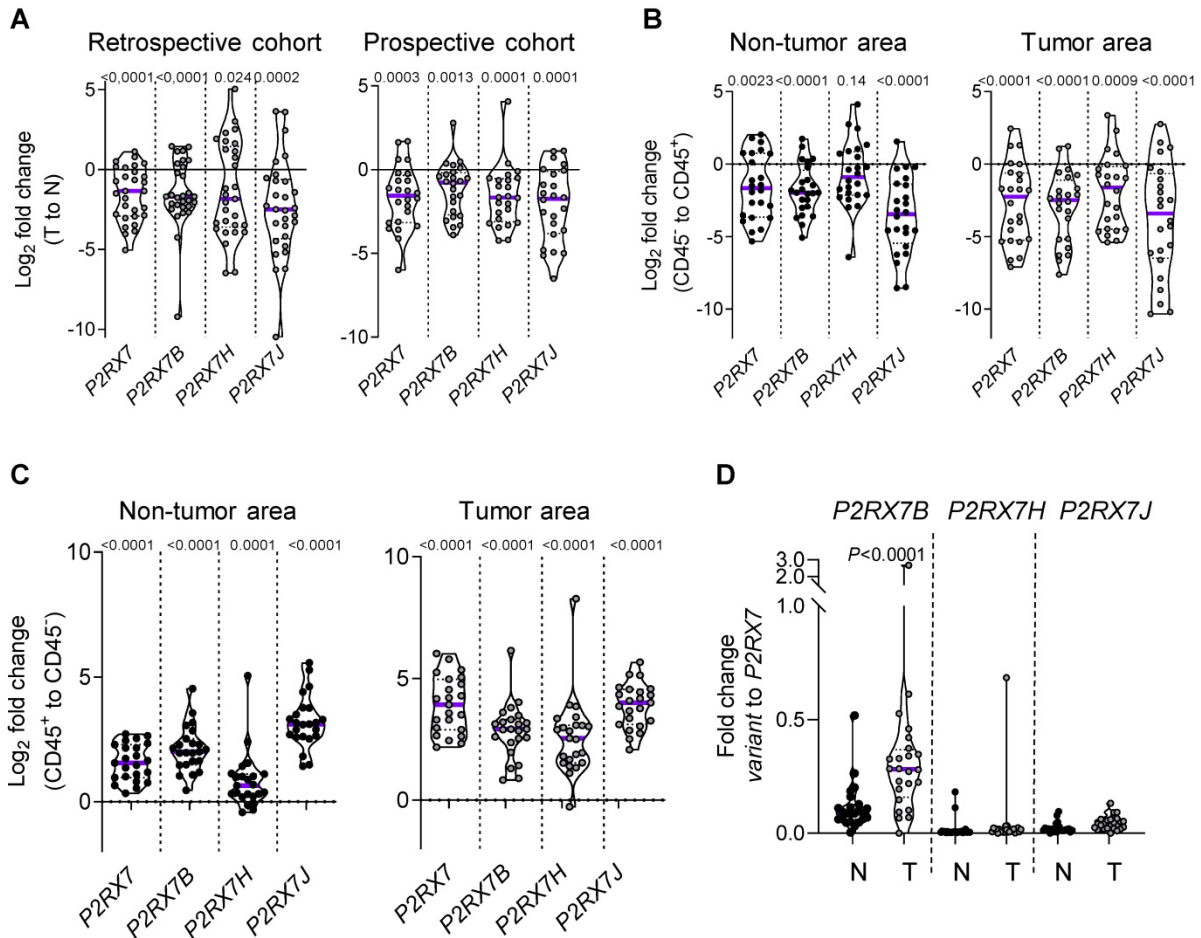


**Figure 3.** LUAD patients express *P2RX7A, B, H and J* mRNAs. **A.** *P2RX7* splice variant expression in the retrospective (n=29) and prospective cohorts (n=24) of tumor area of LUAD tissues (T) versus adjacent non-tumor lung tissues (N). **B.** *P2RX7* splice variant expression in CD45<sup>+</sup> cells isolated from adjacent non-tumor and tumor areas of LUAD patients (n=24). **C.** *P2RX7* splice variant expression in CD45<sup>+</sup> cells isolated from adjacent non-tumor and tumor areas of LUAD patients (n=24). Results are expressed in Log<sub>2</sub> fold change (meaning Log<sub>2</sub> of 1 = 2-fold and Log<sub>2</sub> of -1 = 0.5-fold). **D.** Differential up-regulation of *P2RX7B* in immune cells. n=24 (Mann-Whitney test).

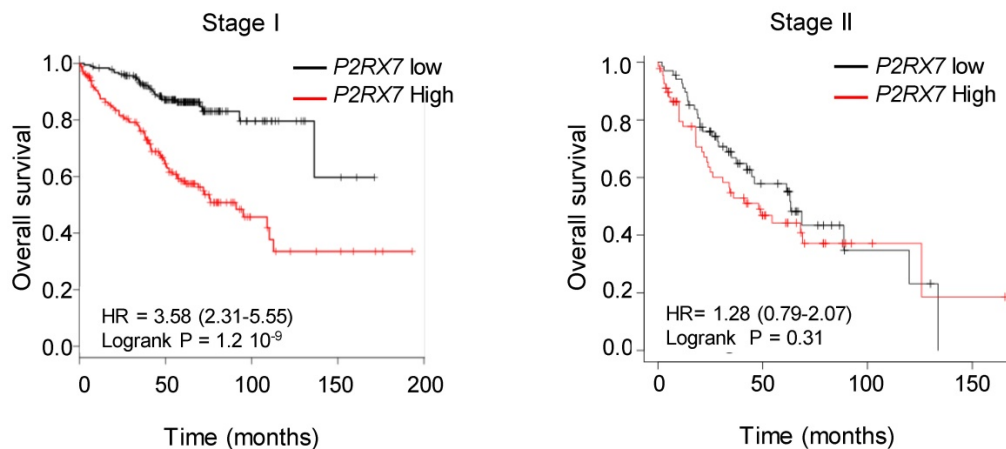


**Figure 4.** High expression of *P2RX7* is an indicator of poor survival in LUAD patients. Kaplan-Meier survival analysis (<http://kmplot.com>) [41] according to the *P2RX7* expression in patients with LUAD of indicated stage. High expression corresponds to value > *P2RX7* median expression, low expression corresponds to value < *P2RX7* median expression. Probability of survival of patients: Stage I: n=370 patients, low expression (n=187) median OS: 136 months; high expression (n=183) median OS: 38 months, HR: 3.58, 95% CI: 2.31-5.55, p=1.2 10<sup>-9</sup>. Stage II: n=136 patients, low expression (n=68) median OS: 63 months; high expression (n=68) median OS=38 months, HR: 1.28, 95% CI: 0.79-2.07, p=0.31 (log-rank test). Vertical tick-marks represent censored data.

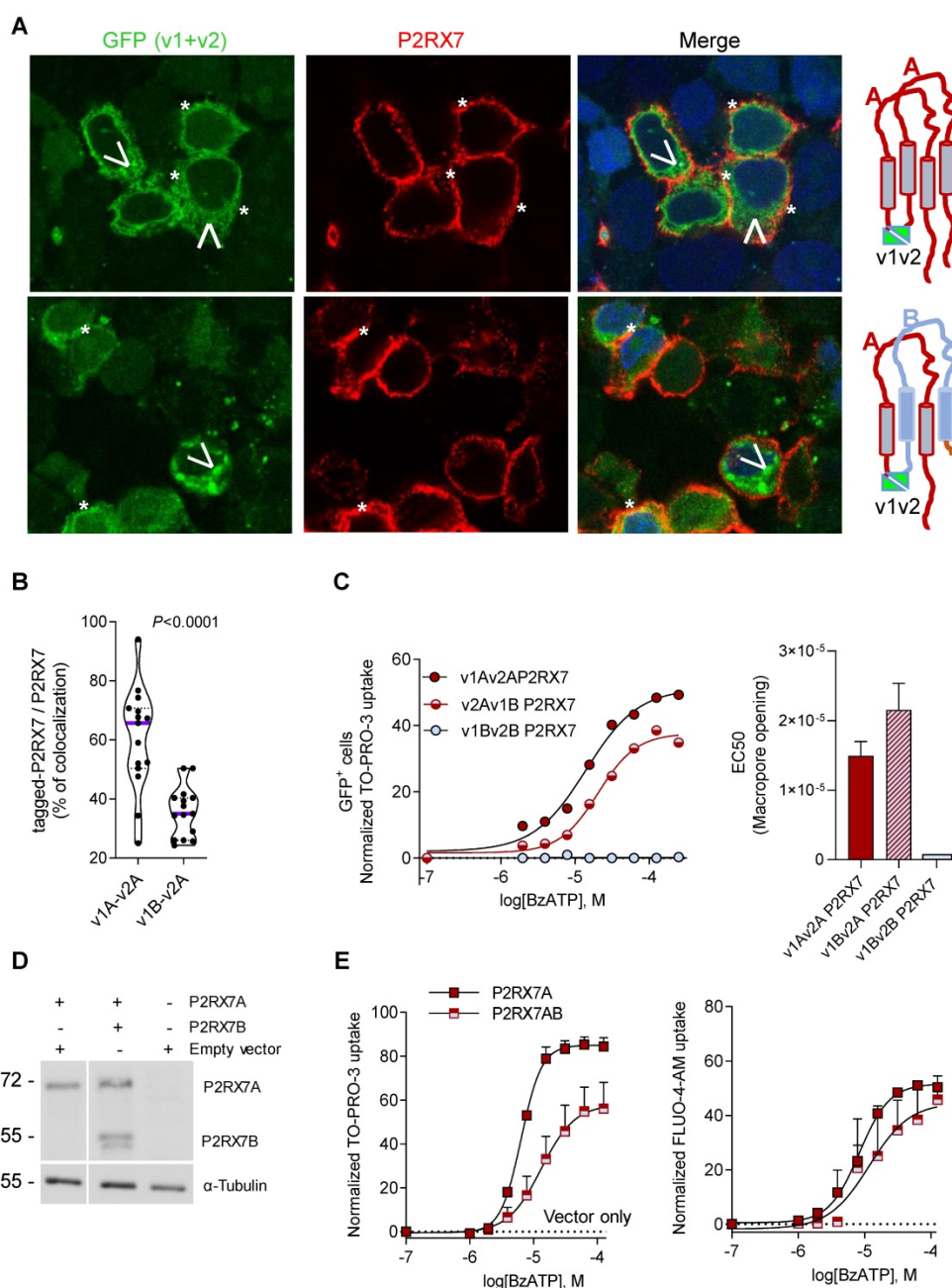


**Figure 5. Expression of P2RX7B decreases the overall activity of P2RX7.** **A.** Representative images of P2RX7 immunofluorescence in HEK cells transiently transfected with P2RX7A or with P2RX7 A + B pDNA. The tagged receptor (P2RX7A or P2RX7AB) is shown in green. The conformational receptor (P2RX7A) is shown in red. \*: P2RX7 expressed at the membrane. Arrowhead: intracellular chimeric receptor. **B.** Quantification of data presented in A.  $n = 30$  cells from 2 independent experiments. (unpaired Student's *t* test). **C.** Impact of P2RX7B expression on the P2RX7 macrophore activity. HEK cells were transiently transfected with tagged-A, -B and -A+B P2RX7 isoforms and the macrophore activity was studied on GFP<sup>+</sup> cells (right panel). The left panel shows the EC<sub>50</sub> for macrophore formation for 3 independent experiments. **D.** The expression of P2RX7A and P2RX7B was detected in stably transfected HEK clones by Western blotting using the P2RX7 anti-extracellular loop antibody. The total  $\alpha$ Tubulin level was monitored as a control for protein loading. **E.** P2RX7 activity in stably transfected HEK clones with untagged-A and -A+B P2RX7 isoforms or vector alone (hatched line). Dose response of BzATP-induced macrophore opening (left panel) and an intracellular Ca<sup>2+</sup> variation (right panel).

## Discussion

In this study we characterized the expression levels and the functionality of P2RX7 in LUAD patients and showed that whereas P2RX7 was found to be expressed in both tumor and immune cells, only immune cells expressed a functional receptor. Mechanistically, we observed differential expression of the P2RX7B splice variant in immune cells within

tumor areas. Upregulation of P2RX7B was previously described in human osteosarcoma [32]. To document P2RX7B expression, the authors used a differential screening approach, based on two antibodies, the first one recognizes both P2RX7A and P2RX7B, whereas the second is specific to P2RX7A only. Thank to this approach, specimens positively labeled with the first antibody and negatively labeled with the second were described to be positive for P2RX7B. Considering that



there is no antibody specific to P2RX7B, this technic represents a smart way to document P2RX7B expression. However, each antibody has his own affinity for its specific epitope and from this affinity depends the strength of the signal. Therefore, a subtractive strategy to qualify the expression of P2RX7B is a tricky approach to handle. To overcome this limitation, the authors further transfected Te85 osteosarcoma cell line with either P2RX7A, P2RX7B or both. Doing so, they demonstrated that cells expressing both isoforms were more proliferative and more prone to induce mineralization. More recently, expression of P2RX7B has been described to be upregulated during the osteogenic process [18]. Evidence suggesting that P2RX7A and P2RX7B might heteromerized were obtained in the *X. laevis* oocyte expressing system after co-immunoprecipitation of tagged P2RX7A and P2RX7B [31]. In addition, transfection of HEK cells with both P2RX7A and P2RX7B suggested that P2RX7B disguises P2RX7A's cytotoxic activity. If true, expression of P2RX7B will give a growth advantage and explain how P2RX7 expression (likely A and B isoforms) could have been linked to tumor growth and invasiveness in several cancer types [36–39]. Indeed, considering that P2RX7 is a pro-apoptotic receptor, it is counterintuitive to imagine that tumor cells express a receptor capable of inducing their own death. It has been proposed that tumor cells express a non-conformal receptor (nfP2RX7), which is unable to induce cell death but retains calcium channel activity and therefore could

promote tumor growth. Herein, we observed that P2RX7 expressed by tumor cells, but also normal epithelial cells, lacked the macropore function, whereas immune cells retained it. At this time, we still do not know whether the isoform of P2RX7 expressed by tumor cells corresponds to nfP2RX7, since the only way to characterize its expression relies on the use of an anti-nfP2RX7 antibody, which is not commercially available. We explored the hypothesis that the lack of macropore activity in tumor and non-tumor epithelial cells could be the consequence of expression of truncated P2RX7 isoforms, resulting from alternative splicing of P2RX7 mRNA rather than SNPs. Indeed, allele frequency of SNPs located to the boundary of mRNA splicing regulation sites within intronic regions is too low to envisage that these SNPs could explain the significant dysfunction in P2RX7 that we observed in 10 LUAD patients. Our study revealed for the first time that 3 alternative splice variants of P2RX7 are expressed in LUAD patients, namely P2RX7B, P2RX7H and P2RX7J. We also observed that all P2RX7 variants were down-regulated by at least 2.5-fold in tumor tissues versus adjacent non-tumor tissues. Since each P2RX7 variant was down-regulated to the same extent in non-immune cells, we believe that the lack of P2RX7 function is a consequence of decreased protein expression rather than the formation of hetero trimers that may be stored in intracellular vesicles, as it was proposed for nfP2RX7 [40].

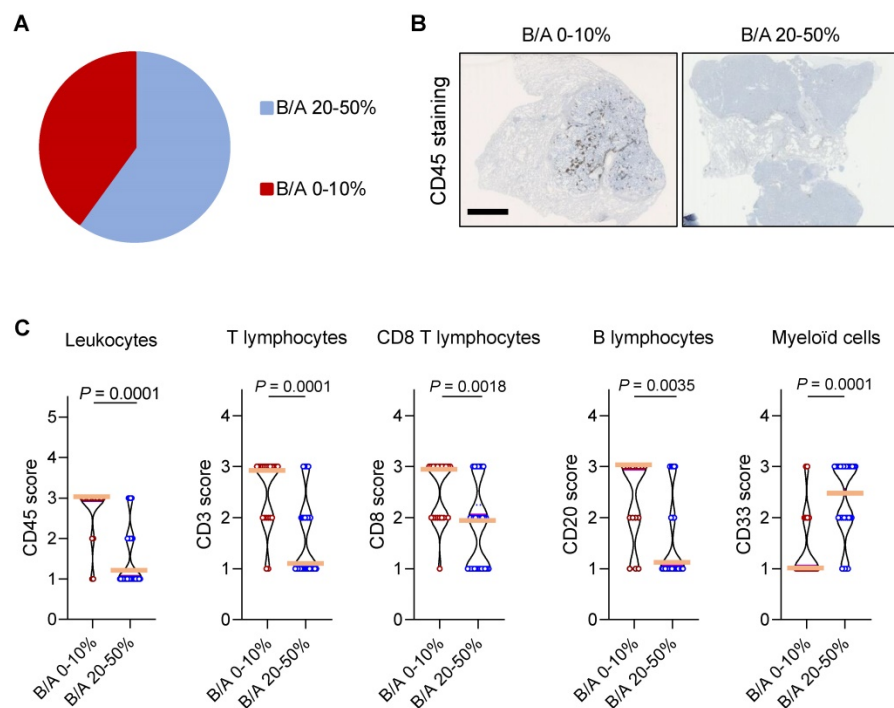


**Figure 6.** High expression of P2RX7B mRNA correlates with low leukocyte infiltration in LUAD patients. **A.** Clustering of LUAD patients expressing P2RX7B for the prospective cohort. **B.** Representative images of CD45<sup>+</sup> IHC staining of samples from LUAD patients depending on the P2RX7B expression. Bar = 5mm. **C.** Quantification of CD45, CD3, CD8, CD20 and CD33 staining. B/A 20-50%, n=6; B/A 0-10%, n=4. (CD45, CD3 and CD8: Mann-Whitney test. CD20 and CD33: unpaired Student's t test).

Whereas each *P2RX7* variant was equally down-regulated in the epithelial compartment of tumor tissues versus adjacent non-tumor tissues, we observed differential up-regulation of *P2RX7B* in the tumor immune compartment. Over expression of *P2RX7B* has already been reported in *ex vivo* mitogenic-induced immune cells, in particular in lymph nodes and lymphocytes [31], and the authors proposed that expression of *P2RX7B* correlated with lymphocyte proliferation. Our results do not support this proposition since we showed that the more *P2RX7B* is expressed the less the tumors were infiltrated by T and B lymphocytes. Besides suggesting a physiological role for the truncated *P2RX7B* isoform, this result questions how *P2RX7B* expression can impact on the immune infiltrate composition. Using the bi-molecular fluorescent approach, we confirmed that a chimeric *P2RX7AB* receptor is formed, and we showed for the first time that a large fraction (63%) was retained intracellularly. To avoid potential bias linked to the presence of the N-terminal venus tag, we co-transfected HEK cells with untagged *P2RX7A* or *P2RX7A+P2RX7B* and we selected stable clones expressing comparable protein levels of both isoforms. Doing so, we were able to demonstrate that cells expressing both *P2RX7A* and *P2RX7B* isoforms were less prone than cells expressing only *P2RX7A* to form a macropore, whereas they retained the same ion channel capability. This result does not confirm what was previously published indicating that *P2RX7B* expression positively modulates *P2RX7* function [31] but they confirm that *P2RX7B* expression could disguise *P2RX7*'s macropore activity [19,33]. Whether this alteration in macropore function observed *ex vivo* is due to the coexistence of cells expressing only homo trimeric *P2RX7B* and only homo trimeric *P2RX7A*, or to the existence of cells expressing intracellular chimeric *P2RX7AB*, or both remains to be determined. However, our results showed that tumors of LUAD patients with a high *P2RX7B* expression were less infiltrated with B and T cells and more infiltrated with myeloid cells, suggesting that differential expression of *P2RX7B* critically regulated the quality of tumor immune cell infiltration. Whether differential expression of *P2RX7B* results from tumor conditioning of the lung tissue or specific expression in immune cells before tumor conditioning is still an open question. Nevertheless, considering that expression of *P2RX7B* in LUAD correlated with both an alteration in the *P2RX7* function and the lesser infiltrated tumor phenotype (also called “cold” tumor), it is tempting to propose that *P2RX7B* participates in tumor development and may therefore represent an attractive theranostic tool.

## Supplementary Material

Supplementary figures and tables.  
<http://www.thno.org/v10p10849s1.pdf>

## Acknowledgments

The authors wish to thank Dr Laetitia Douguet for her helpful advice on flow cytometry and Dr Dominic Van Essen for his advice on the bimolecular fluorescent approach. Drs Sahil Adriouch, Pascal Lopez and Patrick Brest are thanked for their helpful discussion. The authors greatly acknowledge the IRCAN's Flow Cytometry and PICMI facilities supported by FEDER, GIS IBISA, the Ministère de l'Enseignement Supérieur, Région Provence Alpes-Côte d'Azur, Conseil Départemental 06, ITMO Cancer Aviesan (plan cancer), Cancéropole PACA, CNRS and Inserm.

## Funding

The funding sources for this work were Institut National du Cancer (INCa), Institut National de la Santé et Recherche Médicale (INSERM) Plan Cancer 2014-2019: Soutien pour la formation à la recherche fondamentale et translationnelle en cancérologie, RESPIR Foundation, the “Ligue National Contre le Cancer”, the French Government (National Research Agency, ANR through the “Investments for the Future” LABEX SIGNALIFE: program reference #ANR-11-LABX-0028-01), the Centre National de la Recherche Scientifique (CNRS).

## Competing Interests

The authors have declared that no competing interest exists.

## References

1. Siegel RL, Miller KD, Jemal A. Cancer statistics, 2020. *CA Cancer J Clin.* 2020; 70: 7-30.
2. Pellegatti P, Raffaghello L, Bianchi G, Piccardi F, Pistoia V, Di Virgilio F. Increased level of extracellular ATP at tumor sites: *In vivo* imaging with plasma membrane luciferase. *PLoS One.* 2008; 3: e2599.
3. Allard B, Beavis PA, Darcy PK, Stagg J. Immunosuppressive activities of adenosine in cancer. *Curr Opin Pharmacol.* 2016; 29: 7-16.
4. Jacob F, Novo CP, Bachert C, Van Crombruggen K. Purinergic signaling in inflammatory cells: P2 receptor expression, functional effects, and modulation of inflammatory responses. *Purinergic Signal.* 2013; 9: 285-306.
5. White N, Burnstock G. P2 receptors and cancer. *Trends Pharmacol Sci.* 2006; 27: 211-7.
6. Buell G, Chessell IP, Michel AD, Collo G, Salazzo M, Herren S, et al. Blockade of human P2X7 receptor function with a monoclonal antibody. *Blood.* 1998; 92: 3521-8.
7. Chiozzi P, Sanz JM, Ferrari D, Falzoni S, Aleotti A, Buell GN, et al. Spontaneous cell fusion in macrophage cultures expressing high levels of the P2Z/P2X7 receptor. *J Cell Biol.* 1997; 138: 697-706.
8. Baroni M, Pizzirani C, Pinotti M, Ferrari D, Adinolfi E, Calzavari S, et al. Stimulation of P2 (P2X7) receptors in human dendritic cells induces the release of tissue factor-bearing microparticles. *FASEB J.* 2007; 21: 1926-33.
9. Borges Da Silva H, Beura LK, Wang H, Hanse EA, Gore R, Scott MC, et al. The purinergic receptor P2RX7 directs metabolic fitness of long-lived memory CD8+ T cells. *Nature.* 2018; 559: 264-8.
10. Di Virgilio F, Sarti AC, Falzoni S, De Marchi E, Adinolfi E. Extracellular ATP and P2 purinergic signalling in the tumour microenvironment. *Nat Rev Cancer.* 2018; 18: 601-18.




11. Rassendren F, Buell GN, Virginio C, Collo G, North RA, Surprenant A. The permeabilizing ATP receptor, P2X7. Cloning and expression of a human cDNA. *J Biol Chem.* 1997; 272: 5482–6.
12. Smart ML, Gu B, Panchal RG, Wiley J, Cromer B, Williams DA, et al. P2X7 receptor cell surface expression and cytolytic pore formation are regulated by a distal C-terminal region. *J Biol Chem.* 2003; 278: 8853–60.
13. Hofman P, Cherfils-Vicini J, Bazin M, Ilie M, Juhel T, Hébuterne X, et al. Genetic and pharmacological inactivation of the purinergic P2RX7 receptor dampens inflammation but increases tumor incidence in a mouse model of colitis-associated cancer. *Cancer Res.* 2015; 75: 835–45.
14. Adinolfi E, Capece M, Franceschini A, Falzoni S, Giuliani AL, Rotondo A, et al. Accelerated tumor progression in mice lacking the ATP receptor P2X7. *Cancer Res.* 2015; 75: 635–44.
15. Chong J-H, Zheng G-G, Zhu X-F, Guo Y, Wang L, Ma C-H, et al. Abnormal expression of P2X family receptors in Chinese pediatric acute leukemias. *Biochem Biophys Res Commun.* 2010; 391: 498–504.
16. Zhang XJ, Zheng GG, Ma XT, Yang YH, Li G, Rao Q, et al. Expression of P2X7 in human hematopoietic cell lines and leukemia patients. *Leuk Res.* 2004; 28: 1313–22.
17. Adinolfi E, Melchiorri L, Falzoni S, Chiozzi P, Morelli A, Tieghi A, et al. P2X7 receptor expression in evolutive and indolent forms of chronic B lymphocytic leukemia. *Blood.* 2002; 99: 706–8.
18. Carluccio M, Zuccarini M, Ziberi S, Giuliani P, Morabito C, Marigliò MA, et al. Involvement of P2X7 receptors in the osteogenic differentiation of mesenchymal stromal/stem cells derived from human subcutaneous adipose tissue. *Stem Cell Rev Reports.* 2019; 15: 574–89.
19. Ziberi S, Zuccarini M, Carluccio M, Giuliani P, Ricci-Vitiani L, Pallini R, et al. Upregulation of epithelial-to-mesenchymal transition markers and P2X7 receptors is associated to increased invasiveness caused by P2X7 receptor stimulation in human glioblastoma stem cells. *Cells.* 2019; 9: 85.
20. Greig AVH, Linge C, Healy V, Lim P, Clayton E, Rustin MHA, et al. Expression of purinergic receptors in non-melanoma skin cancers and their functional roles in A431 cells. *J Invest Dermatol.* 2003; 121: 315–27.
21. White N, Butler PEM, Burnstock G. Human melanomas express functional P2X7 receptors. *Cell Tissue Res.* 2005; 321: 411–8.
22. Raffaghello L, Chiozzi P, Falzoni S, Di Virgilio F, Pistoia V. The P2X7 receptor sustains the growth of human neuroblastoma cells through a substance P-dependent mechanism. *Cancer Res.* 2006; 66: 907–14.
23. Künzli BM, Berberat PO, Giese T, Csizmadia E, Kaczmarek E, Baker C, et al. Upregulation of CD39/NTPDases and P2 receptors in human pancreatic disease. *Am J Physiol - Gastrointest Liver Physiol.* 2007; 292: G223–30.
24. Solini A, Cuccato S, Ferrari D, Santini E, Gulinelli S, Callegari MG, et al. Increased P2X7 receptor expression and function in thyroid papillary cancer: A new potential marker of the disease? *Endocrinology.* 2008; 149: 389–96.
25. Li X, Qi X, Zhou L, Fu W, Abdul-Karim FW, MacLennan G, et al. P2X7 receptor expression is decreased in epithelial cancer cells of ectodermal, uro-genital sinus, and distal paramesonephric duct origin. *Purinergic Signal.* 2009; 5: 351–68.
26. Bae JY, Lee SW, Shin YH, Lee JH, Jahng JW, Park K. P2X7 receptor and NLRP3 inflammasome activation in head and neck cancer. *Oncotarget.* 2017; 8: 48972–82.
27. Ghiringhelli F, Apetoh L, Tesniere A, Aymeric L, Ma Y, Ortiz C, et al. Activation of the NLRP3 inflammasome in dendritic cells induces IL-1B-dependent adaptive immunity against tumors. *Nat Med.* 2009; 15: 1170–8.
28. Sluyter R, Stokes L. Significance of p2x7 receptor variants to human health and disease. *Recent Patents DNA Gene Seq.* 2011; 5: 41–54.
29. Benzaquen J, Heeke S, Janho dit Hreich S, Douguet L, Marquette CH, Hofman P, et al. Alternative splicing of P2RX7 pre-messenger RNA in health and diseases: Myth or reality? *Biomed J.* 2019; 42: 141–54.
30. Feng YH, Li X, Zeng R, Gorodeski GI. Endogenously expressed truncated P2X7 receptor lacking the C-terminus is preferentially upregulated in epithelial cancer cells and fails to mediate ligand-induced pore formation and apoptosis. *Nucleosides, Nucleotides and Nucleic Acids.* 2006; 25: 1271–6.
31. Adinolfi E, Cirillo M, Woltersdorf R, Falzoni S, Chiozzi P, Pellegatti P, et al. Trophic activity of a naturally occurring truncated isoform of the P2X7 receptor. *FASEB J.* 2010; 24: 3393–404.
32. Giuliani AL, Colognesi D, Ricco T, Roncato C, Capece M, Amoroso F, et al. Trophic activity of human P2X7 receptor isoforms A and B in osteosarcoma. *PLoS One.* 2014; 9.
33. Ulrich H, Ratajczak MZ, Schneider G, Adinolfi E, Orioli E, Ferrazoli EG, et al. Kinin and purine signaling contributes to neuroblastoma metastasis. *Front Pharmacol.* 2018; 9.
34. Boldrini L, Giordano M, Ali G, Servadio A, Pelliccioni S, Niccoli C, et al. P2X7 protein expression and polymorphism in non-small cell lung cancer (NSCLC). *J Negat Results Biomed.* 2014; 13.
35. Homerin G, Jawhara S, Dezitter X, Baudelet D, Dufrenoy P, Rigo B, et al. Pyroglutamide-based P2X7 receptor antagonists targeting inflammatory bowel disease. *J Med Chem.* 2020; 63: 2074–94.
36. Adinolfi E, Raffaghello L, Giuliani AL, Cavazzini L, Capece M, Chiozzi P, et al. Expression of P2X7 receptor increases *in vivo* tumor growth. *Cancer Res.* 2012; 72: 2957–69.
37. Amoroso F, Capece M, Rotondo A, Cangelosi D, Ferracin M, Franceschini A, et al. The P2X7 receptor is a key modulator of the PI3K/GSK3β/VEGF signaling network: evidence in experimental neuroblastoma. *Oncogene.* 2015; 34: 5240–51.
38. Amoroso F, Salaro E, Falzoni S, Chiozzi P, Giuliani AL, Cavallesco G, et al. P2X7 targeting inhibits growth of human mesothelioma. *Oncotarget.* 2016; 7.
39. Qiu Y, Li WH, Zhang HQ, Liu Y, Tian XX, Fang WG. P2X7 mediates ATP-driven invasiveness in prostate cancer cells. *Kanellopoulos J, Ed. PLoS One.* 2014; 9: e114371.
40. Gilbert S, Oliphant C, Hassan S, Peille A, Bronsert P, Falzoni S, et al. ATP in the tumour microenvironment drives expression of nfp2X7, a key mediator of cancer cell survival. *Oncogene.* 2019; 38: 194–208.
41. Gyorffy B, Surowiak P, Budczies J, Láczy A. Online survival analysis software to assess the prognostic value of biomarkers using transcriptomic data in non-small-cell lung cancer. *Chellappan SP, Ed. PLoS One.* 2013; 8: e82241.





## Article

# A Novel Screen for Expression Regulators of the Telomeric Protein TRF2 Identified Small Molecules That Impair TRF2 Dependent Immunosuppression and Tumor Growth

Mounir El Maï <sup>1</sup>, Serena Janho dit Hreich <sup>1</sup>, Cedric Gaggioli <sup>1</sup>, Armelle Roisin <sup>2</sup>, Nicole Wagner <sup>3</sup>, Jing Ye <sup>4</sup>, Pierre Jalinot <sup>2</sup>, Julien Cherfils-Vicini <sup>1,\*</sup> and Eric Gilson <sup>1,4,5,\*</sup>

- <sup>1</sup> Institut National de la Santé et de la Recherche Médicale (INSERM) U1081, Université Côte d'Azur, Centre National de la Recherche Scientifique (CNRS) UMR7284, Institute for Research on Cancer and Aging, Nice (IRCAN), 06107 Nice, France; Mounir.El-Mai@unice.fr (M.E.M.); serena.janho-dit-hreich@etu.univ-cotedazur.fr (S.J.d.H.); Cedric.Gaggioli@unice.fr (C.G.)
- <sup>2</sup> Laboratory of Biology and Modelling of the Cell (LBM), ENS de Lyon, Univ Lyon, INSERM U1210, CNRS UMR 5239, Université Claude Bernard Lyon 1, 46 Allée d'Italie Site Jacques Monod, 69007 Lyon, France; armelle.roisin@ens-lyon.fr (A.R.); pierre.jalinot@ens-lyon.fr (P.J.)
- <sup>3</sup> Institut National de la Santé et de la Recherche Médicale (INSERM), Université Côte d'Azur, Centre National de la Recherche Scientifique (CNRS), Institute of Biology Valrose, 06108 Nice, France; Nicole.Wagner@unice.fr
- <sup>4</sup> International Research Project "Hematology, Cancer and Aging", Pôle Sino-Français de Recherche en Sciences du Vivant et Génomique, Shanghai Ruijin Hospital, Shanghai Jiao Tong University School of Medicine, Shanghai 200025, China; yj11254@rjh.com.cn
- <sup>5</sup> Department of Medical Genetics, Archet 2 Hospital, FHU Oncoage, CHU of Nice, 06000 Nice, France
- \* Correspondence: Julien.cherfils@unice.fr (J.C.-V.); eric.gilson@unice.fr (E.G.)



**Citation:** El Maï, M.; Janho dit Hreich, S.; Gaggioli, C.; Roisin, A.; Wagner, N.; Ye, J.; Jalinot, P.; Cherfils-Vicini, J.; Gilson, E. A Novel Screen for Expression Regulators of the Telomeric Protein TRF2 Identified Small Molecules That Impair TRF2 Dependent Immunosuppression and Tumor Growth. *Cancers* **2021**, *13*, 2998. <https://doi.org/10.3390/cancers13122998>

Academic Editor: Roman Blaheta

Received: 25 April 2021

Accepted: 8 June 2021

Published: 15 June 2021

**Publisher's Note:** MDPI stays neutral with regard to jurisdictional claims in published maps and institutional affiliations.



**Copyright:** © 2021 by the authors. Licensee MDPI, Basel, Switzerland. This article is an open access article distributed under the terms and conditions of the Creative Commons Attribution (CC BY) license (<https://creativecommons.org/licenses/by/4.0/>).

**Simple Summary:** The telomeric protein TRF2 (Telomeric repeat-binding factor 2) is upregulated in human cancers and associated with poor prognosis. TRF2 oncogenic properties rely on its intrinsic telomere protective role, but also on cell extrinsic effects through immunosuppressive and angiogenic activities. Therefore, targeting TRF2 appears as a promising therapeutic anti-cancer strategy. In this study, we developed a cell-based method to screen for TRF2 inhibitors allowing us to identify two compounds that blunt the TRF2 pro-oncogenic properties in vivo.

**Abstract:** Telomeric repeat-binding factor 2 (TRF2) is a subunit of the shelterin protein complex, which binds to and protects telomeres from unwanted DNA damage response (DDR) activation. TRF2 expression plays a pivotal role in aging and cancer, being downregulated during cellular senescence and overexpressed during oncogenesis. Cancers overexpressing TRF2 often exhibit a poor prognosis. In cancer cells, TRF2 plays multiple functions, including telomere protection and non-cell autonomous roles, promoting neo-angiogenesis and immunosuppression. We present here an original screening strategy, which enables identification of small molecules that decrease or increase TRF2 expression. By screening a small library of Food and Drug Agency (FDA)-approved drugs, we identified two molecules (AR-A014418 and alexidine·2HCl) that impaired tumor growth, neo-angiogenesis and immunosuppression by downregulating TRF2 expression in a mouse xenograft model. These results support the chemotherapeutic strategy of downregulating TRF2 expression to treat aggressive human tumors and validate this cell-based assay capable of screening for potential anti-cancer and anti-aging molecules by modulating TRF2 expression levels.

**Keywords:** TRF2; cancer; aging; cell-based screening assay; neo-angiogenesis; immune suppression

## 1. Introduction

Telomeres are specialized nucleoprotein structures found at the ends of linear chromosomes that are regulated by telomere-associated factors such as telomerase, shelterin protein complexes and non-coding telomeric repeat-containing RNA [1]. When properly regulated,

telomeres protect chromosomes against instability and senescence. Telomeric DNA shortening occurs as part of programmed physiological development and aging [2]. However, excessive telomere DNA shortening drives rare progeroid syndromes, such as dyskeratosis congenita [3]. Moreover, dysregulated telomere states are implicated in numerous diseases that are common throughout the general population, including almost all types of cancer and several degenerative diseases [4]. Thus, developing pharmacological treatments to target specific telomere components is promising to prevent and treat such diseases.

As far as telomere and cancer are concerned, vital DNA damage response (DDR) checkpoints sometimes fail; this can lead to excessive telomeric DNA shortening and aberrant chromosome rearrangements, which in turn can contribute to oncogenesis. Furthermore, upregulation of telomerase is a key event in the development of about 90% of all cancers, as this can confer unlimited growth to cancer cells [5]. For this reason, telomerase inhibition has been the target of several studies seeking to develop cancer treatments [6]. Despite recent progress, there are some limitations to the clinical use of anti-telomerase drugs. For example, to halt cancer cell proliferation, a critically short telomeric DNA length must be reached, and the anti-oncogenic effects of shortened telomeres are lost in the absence of the *p53* tumor suppressor gene [7,8]. This lag period reduces therapeutic efficacy and increases pro-aging side effects by limiting cell renewal and favoring the activation of alternative recombination-based telomere elongation mechanisms [9,10]. Therefore, anti-telomerase strategies may be better suited for targeting cancer cells that already harbor critically short telomeres [11].

In addition to telomerase, changes in the expression and activities of shelterin complex subunits (TRF1, TRF2, RAP1, TIN2, TPP1 and POT1) are involved in tumorigenesis, and in some cases independently of telomere length [12–16]. Thus, targeting shelterin for cancer treatment could be an interesting alternative to anti-telomerase interventions. The shelterin subunit TRF2 represents an interesting candidate; TRF2 is overexpressed in several human malignancies, both in cancer and vascular cells and this is typically associated with a poor prognosis [17–20]. Notably, TRF2 overexpression can promote tumorigenesis non-cell autonomously, leading to immunosuppression and neo-angiogenesis [13,18–20]. In particular, TRF2 upregulation creates a potent immunosuppressive microenvironment. By altering the expression of heparan sulfate proteoglycans, TRF2 directly recruits and activates myeloid-derived suppressive cells (MDSCs) through TLR2 pathway [21]. While TRF2 overexpression in cancer cells strongly inhibits NK cell recruitment in the tumor microenvironment by the regulation of HSPG synthesis [13], the TLR2 activation of MDSC induced by the overexpression of TRF2 leads to a powerful inhibition of the NK cell immunosurveillance with a strong decrease of NK cells degranulation, IFN $\gamma$  production and killing [21]. Thus, TRF2 overexpression strongly blunt early stage of anti-tumor immunosurveillance by directly inhibiting NK cells recruitment and indirectly the functionality of NK cells through the shaping of a MDSC dependent immunosuppressive microenvironment. Consequently, targeting TRF2 in cancers could be a valuable multi-hit strategy via cell-autonomous and non-cell-autonomous processes by promoting senescence as well as impairing neo-angiogenesis and immune escape.

To date, all identified small compounds that target TRF2 impair its ability to protect chromosome ends from DDR thus with potential pro-aging side effects [22]. Our previous work demonstrated that a partial reduction of TRF2 expression can reverse tumorigenicity in mouse models through non-cell-autonomous effects, without inducing DDR [13]. We therefore reasoned that focusing on reducing excess TRF2 in cancers resulting from its overexpression could be an interesting strategy to treat cancer without pro-aging side effects. In this study, we present an original screening platform to identify small compounds targeting TRF2 stability. We show that two top hits inhibited the tumorigenic activity of TRF2 overexpression. This study demonstrated that TRF2 expression can be pharmacologically modulated, and that our screening assay is a reliable method for the selection of drugs capable of modulating TRF2 expression levels, with potential anti-cancer and anti-aging properties.

## 2. Materials and Methods

### 2.1. Cells

Human embryonic kidney (HEK) 293-T cells (ATCC CRL-1573) and BJ-HELTRas cells [13] were grown in Dulbecco's Modified Eagle's Medium (DMEM) (Lonza, Levallois-Perret, France) supplemented with 10% fetal calf serum (FCS), 100 IU/mL penicillin and 100 µg/mL streptomycin (Invitrogen, Cergy Pontoise, France).

### 2.2. SDS-PAGE and Western Blotting

Total cell lysates were prepared, separated by electrophoresis and blotted as previously described [14]. Briefly, cells were harvested and lysed in lysis buffer (8.76 g/L NaCl, 10 mM Tris-HCl pH 7.2, 0.1% SDS, 0.1% Triton X-100, 10 g/L sodium deoxycholate, 5 mM ethylenediaminetetraacetic acid (EDTA), 10 µg/mL leupeptine, 1 mM AEBSF and 19 µg/mL aprotinin). Samples were then titrated using BCA protein assay kit (Interchim, Monluçon, France). Samples (60 µg/lane) were heated at 95 °C for 5 min in loading buffer (500 mM Tris-HCl, 100 mM DTT, 2% SDS, 0.1% bromophenol blue, 10% glycerol, pH 6.8). Then samples were loaded on 10% polyacrylamide gels and run for 45 min at 160 V. Proteins were then transferred onto Immobilon-FL membranes (Millipore, Upstate, New York, USA) using Trans-Blot SD Semi-Dry Electrophoretic Transfer Cell (Bio-Rad, Hercules, CA, USA). Membranes were blocked for 1 h in Intercept Blocking buffer (LI-COR, Lincoln, NE, USA) prior to overnight incubation at 4 °C with a mix of primary antibodies (mouse IgG1 anti-TRF2 diluted at 1:250; and rabbit IgG anti-Beta-actin diluted at 1:10,000) in Intercept Blocking buffer containing 0.5% Tween20. After being washed in PBS, 0.1% Tween20, membranes were incubated for 1 h at room temperature in Intercept blocking buffer containing 0.25% Tween20 with a mix of secondary antibodies: goat-anti-mouse IRDye 680 for anti-TRF2 antibody and goat anti-rabbit IRDye 800CW for anti-Beta-actin antibody (1:15,000 dilution). Primary and IRDye secondary antibodies that were used are listed below in the antibody table (Table 1). Finally, protein bands were visualized using LiCor Odyssey 9120 imaging system (LI-COR). TRF2 expression was measured by normalizing TRF2 band intensity to the intensities of the actin band and the background.

**Table 1.** Antibodies.

Specificity	Company	Clone	Species	Isotype	Fluorochrome	Reference
anti CD107a FITC	BD Biosciences	1D4B	Rat	IgG2a/k	FITC	553793
anti CD11b	BD Biosciences	M1/70	Rat	IgG2b	APC-H7	550993
Anti CD69 PE-Cy7	BD Biosciences	H1.2F3	Hamster	IgG1/K	PE-Cy7	552879
Anti NKp46 CD335	BD Biosciences	29A1.4	Rat	IgG2a	Alexa 647	560755
Anti-CD3e	Biolegend	145-C11	Armenin Hamster	IgG	PerCP	100302
Anti-CD45	BD Biosciences	30-F11	Rat	IgG2b, κ	AF700	560510
Anti-F4/80	Biolegend	BM8	Rat	IgG2a, κ	BV510	123135
Anti-Ly6C/Ly6G (Gr-1)	BD Biosciences	RB6-8C5	Rat	IgG2b, κ	PE	553128
anti-CD31	BD Biosciences	MEC 13.3	Rat	IgG2a, κ	BV421	562939
TRF2	Imgenex	4A794.15	Mouse	IgG1, κ	N.A.	IMG-124A
Beta-Actin	Abcam		Rabbit	IgG	N.A.	Ab8227
Anti-mouse	Licor		Goat	IgG	IRDye 680	926-32220
Anti-Rabbit	Licor		Goat	IgG	IRDye 800CW	926-32211

### 2.3. Cloning Strategy

The human TRF2 cDNA sequence was cloned between the BamHI/BclI restriction sites of a lentiviral SFFV-GPR plasmid that is a HIV-SFFV-GFP-WPRE derivative [23]. The



SFFV-GPR plasmid contains a spleen focus forming virus (SFFV) promoter controlling a GPR polycistronic gene comprising cDNA sequences for green fluorescent protein (GFP), a puromycin resistance protein and Tag-red fluorescent protein (RFP)-T (S158T mutated Tag-RFP), each separated by E2 and T2 *Picornaviridae* sequences. hTRF2 cDNA was inserted at the C-terminal region of RFP-T, to enable the expression of an RFP-TRF2 fusion protein.

#### 2.4. Lentivirus Production

For lentivirus production,  $5 \times 10^6$  HEK 293-T cells were transfected with 8.6  $\mu\text{g}$  of empty SFFV-GPR or RFP-TRF2-expressing SFFV-GPR vector, 8.6  $\mu\text{g}$  of Lenti-Delta 8.91 and 2.8  $\mu\text{g}$  of VSV-g via calcium phosphate-mediated transfection. Transfected cells were cultured in DMEM supplemented with 10% FCS at 37 °C with 5% CO<sub>2</sub> in 10-cm dishes. Supernatants containing the newly constructed viruses were collected after 48 h, then passed through a 0.45- $\mu\text{m}$  Millipore filter. After virus titration, a 1:1 (virus:cell) ratio was used to infect the BJ-HELTRas cell line, chosen for its resistance to TRF2 defects [13]. A clone that expressed GFP and the fused RFP-TRF2 protein to moderate levels was then isolated by fluorescence-activated cell sorting (FACS).

#### 2.5. Flow Cytometry Screening

BJ-HELTRas clonal line cells containing the SFFV-GPR vector and expressing the RFP-TRF2 fusion protein were cultured in 96-well plates in DMEM medium supplemented with 10% FCS and 1% penicillin/streptomycin. After 24 h of drug treatment, cells were then trypsinized and washed in phosphate buffered saline (PBS) containing 0.5 mM EDTA and 2% FCS before fixing with 0.5% formaldehyde (FA). Fixed cells were then subjected to flow cytometry using a FACS Calibur high-throughput sampler (BD Biosciences, Franklin Lakes, NJ, USA).

#### 2.6. Real-Time Quantitative Polymerase Chain Reaction (RT-qPCR)

Total RNA was isolated using RNeasy Mini Kit (Qiagen, Venlo, Netherlands). Reverse transcription was performed using Superscript II reverse transcriptase (Invitrogen) with 1  $\mu\text{g}$  of total RNA. The expression of each gene was normalized to that of GAPDH. The following primers were used: hTRF2 Fw 5'-GCTGCCTGAACTTGAAACAGT-3'; hTRF2 Rv 5'-CCGTTCTCAACCAACCCCTC-3'; hGAPDH Fw 5'-AGCCACATCGCTCAGACAC-3'; hGAPDH Rv 5'-GCCAATACGACCAAATCC-3'.

#### 2.7. AlamarBlue

In a 96-well flat-bottom plate,  $5 \times 10^3$  cells per well were seeded in 200  $\mu\text{L}$  DMEM supplemented with 10% FCS. At 24 h after drug treatment, 10  $\mu\text{L}$  of AlamarBlue (Bio-Rad) was added and absorbance was measured at 570 nm and 600 nm for 36 h in a Spectrostar Nano plate reader (BMG Labtech, Ortenberg, Germany). The oxidation–reduction percentage of AlamarBlue was determined as described by the manufacturer.

#### 2.8. Animals

Experiments were performed on 8- to 12-week-old NMRI nude female mice from Janvier Labs (France). All mouse experiments were conducted according to local and international institutional guidelines and were approved by either the Animal Care Committee of the IRCAN and the regional (CIEPAL Cote d'Azur #187 and #188) and national (French Ministry of Research #03482.01/02482.2 and # 02973.01/02973.2) authorities.

#### 2.9. Tumor Growth Experiments

Each NMRI nude mouse was injected subcutaneously in the back with  $1 \times 10^6$  BJ-HELTRas cells suspended in 100  $\mu\text{L}$  of PBS ( $n = 8$  mice per group). The mice were treated on days 16, 18, 20 and 22 with intraperitoneal injections of 100  $\mu\text{L}$  of DMSO (45%), alexidine·2HCl (1 mg/kg) or AR-A014418 (5 mg/kg), then followed up until day 26. The tumor appearance was assessed by palpation every day. Tumor size was measured ev-

ery 2–3 days using a caliper. Tumor volume was then determined using the hemi-ellipsoid formula:  $\pi \times (L \times l \times h)/6$ , where L corresponds to the length, l to the width and h to the height of the tumor, respectively.

### 2.10. Matrigel Plug Assays

BJ-HELTRas cells were treated with DMSO (1%), alexidine-2HCl (1  $\mu$ M) or AR-A014418 (10  $\mu$ M) for 2 days. Then, 100  $\mu$ L of  $1 \times 10^6$  treated cells suspended in PBS together with 400  $\mu$ L of growth-factor-reduced Matrigel (Corning, New York, USA) were inoculated subcutaneously into the back of NMRI nude mice under isoflurane anesthesia. At day 5 post-inoculation, the Matrigel plugs were harvested, and infiltrating cells were collected by enzymatic dissociation via dispase (Corning), collagenase A (Roche, Bâle, Switzerland) and DNase I (Roche) digestion for 30 min at 37 °C [13]. Cells were saturated for 15 min on ice with Fc-Block anti-CD16/CD32 antibodies (clone 2.4G2) prior to staining with coupled antibodies for 30 min at 4 °C. The conjugated antibodies used are listed in the antibody table. Cells were washed in PBS with 0.5 mM EDTA, 2% FCS and fixed with 0.5% FA. Stained cells were analyzed using an ARIA III cytometer with DIVA6 software (BD Biosciences) and FlowJo 10 (LLC).

### 2.11. Statistics

All graphs and statistical analyses were produced using GraphPad Prism software (San Diego, CA, USA). All results are represented as the mean  $\pm$  standard deviation (s.d.) or mean  $\pm$  standard error of the mean (SEM). Significant differences between the means were determined using the Mann–Whitney two-tailed test. The log-rank (Mantel–Cox) test was used to determine tumor take. For each test,  $p < 0.05$  was considered statistically significant.

## 3. Results

### 3.1. Identification of TRF2 Inhibitory Molecules

To screen for drugs capable of modulating TRF2 protein levels, we used a lentiviral system to co-transcribe the GFP gene and RFP fused to the N-terminus of TRF2. Following a general strategy described elsewhere [23], we constructed a GRT lentivirus, in which the SFFV promoter controlled the expression of a poly-cistronic gene encoding GFP, a puromycin resistance protein and either RFP-TRF2 or RFP only as a control (Figure 1A). Consequently, all transduced cells expressed both GFP and RFP-TRF2. This system was designed to identify drugs that modulate TRF2 expression, by measuring RFP intensity using flow cytometry, while GFP intensity serves as an internal control for the transcription of the reporter construct.

We transduced the GRT lentiviruses into human BJ-HELTRas fibroblasts that were immortalized by SV40 and hTERT and rendered oncogenic by Ras v12 [13]. To facilitate measurements of both up- and down-regulation of TRF2, a puromycin-resistant clone that moderately expressed both GFP and RFP-TRF2 proteins was isolated using FACS sorting and named GRT-BJ-HELTRas (Figure 1A). As a positive control, we treated GRT-BJ-HELTRas cells with 10  $\mu$ M gemcitabine, a previously described modulator of TRF2 stability [24], for 24 h. While no RFP modulation was detected in cells transduced with empty vector, a significant reduction in the RFP/GFP mean fluorescence intensity (MFI) ratio was observed in gemcitabine-treated GRT-BJ-HELTRas cells compared to the DMSO-treated control (82% of the control;  $p < 0.0001$ ) (Figure 1B). Moreover, gemcitabine specifically diminished RFP-TRF2 protein levels without affecting GFP levels (Figure S1A). Of note, we observed here that gemcitabine is reducing TRF2 level in contrast to the published work [24], a difference that may be explained by cell type differences in the DNA damage response induced by gemcitabine since TRF2 stability can be altered in a p53-dependent manner [25]. This effect was further confirmed by Western blotting analyses where we observed that endogenous TRF2 levels were affected by gemcitabine treatment on untransduced BJ-HELTRas cells (Figure S1B). Therefore, GRT-BJ-HELTRas cells enabled detection of specific variations in TRF2 protein levels induced by drug treatment.

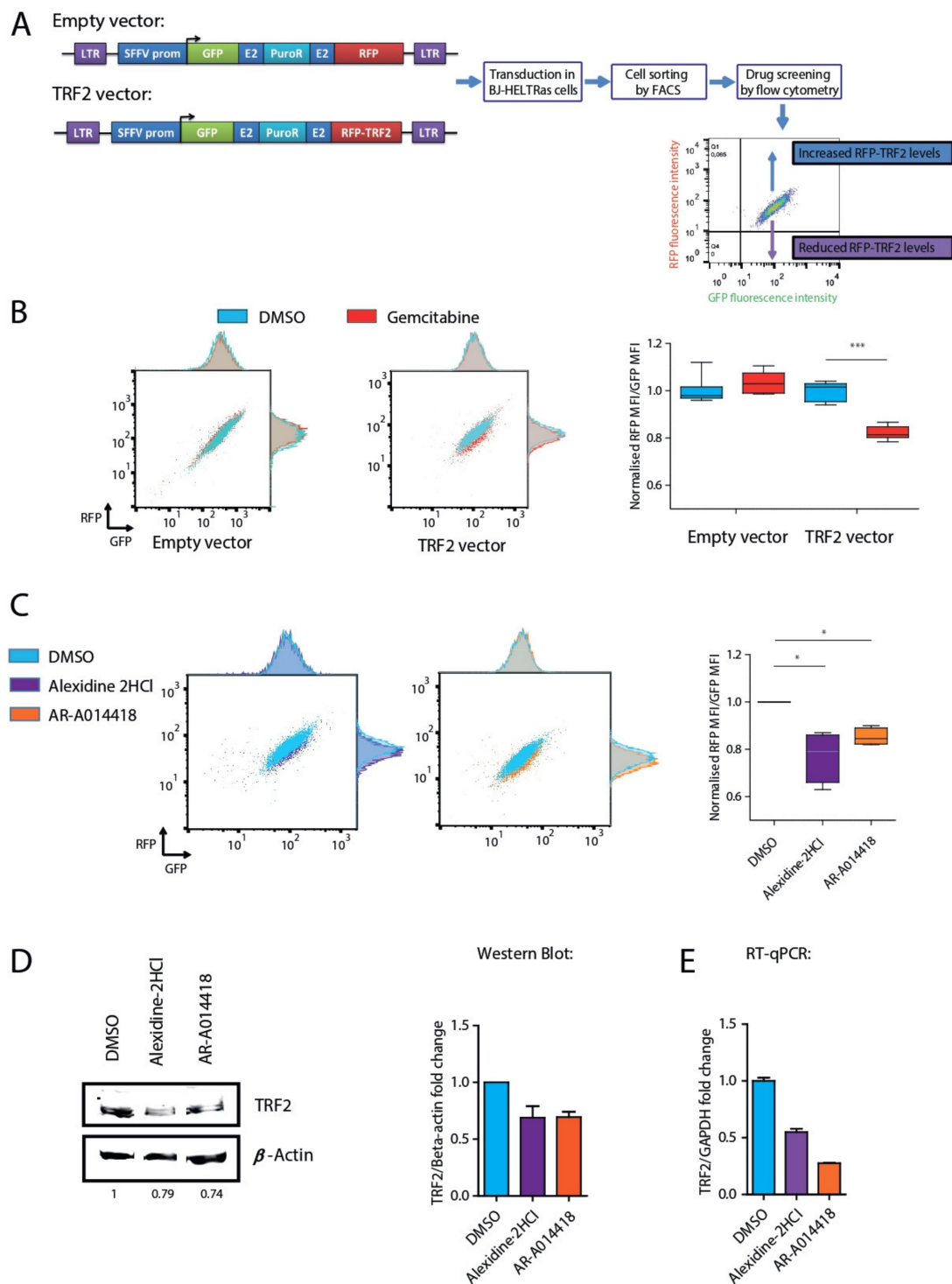


**Figure 1.** Identification of drugs that affect TRF2 expression using fluorescence-based drug screening. **(A)** Schematic representation of the drug screening experimental design. Lentiviral constructs that contained a poly-cistronic gene encoding green fluorescent protein (GFP) and either red fluorescent protein (RFP) alone (empty vector) or a fusion of RFP protein at the N-terminal region of TRF2 (TRF2 vector) were transduced into the BJ-HELTRas cell line. Clones sorted using fluorescence-activated cell sorting (FACS) were then used to screen for drugs that modified TRF2 protein levels. **(B)** Proof of concept using the TRF2-regulating drug gemcitabine as a positive control. Representative RFP/GFP flow cytometry density plots of empty vector- or TRF2 vector-transduced BJ-HELTRas cells treated with either DMSO or gemcitabine (10  $\mu$ M) (left panel). Box-plot quantification of RFP (empty vector) or RFP-TRF2 fusion (TRF2 vector) protein after treatment with DMSO

or gemcitabine (right panel) ( $n = 7$ ; \*\*\*  $p < 0.001$ ; two-tailed Student's  $t$  test). (C) Representative RFP/GFP flow cytometry plots of TRF2 vector-transduced BJ-HELTRas cells treated with 10  $\mu\text{M}$  of alexidine-2HCl, AR-A014418 or DMSO (left panel). Box-plot quantification of RFP-TRF2 fusion (TRF2 vector) protein levels following treatment with DMSO, alexidine-2HCl or AR-A014418 (right panel) ( $n = 4$ ; \*  $p < 0.05$ ; Mann-Whitney test). (D) Representative Western blotting showing reduced TRF2 protein levels following treatment with 10  $\mu\text{M}$  alexidine-2HCl or AR-A014418 compared to DMSO control treatment in untransduced BJ-HELTRas cells (left panel; full Western blotting image is presented in Figure S2A). Quantification of TRF2 protein levels after treatment with 10  $\mu\text{M}$  alexidine-2HCl or AR-A014418 compared to DMSO control treatment (right panel) ( $n = 2$ ; mean + standard error of the mean). (E) Quantification of TRF2 mRNA levels analyzed by RT-qPCR after treatment with 10  $\mu\text{M}$  alexidine-2HCl or AR-A014418 compared to DMSO control treatment.

Using flow cytometry, we then screened 396 Food and Drug Administration (FDA)-approved pharmacological compounds capable of targeting six main categories of biological processes: ion channels, phosphatases, kinases, epigenetic factors, nuclear receptor ligands and the Wnt pathway (Figure S1C). GRT-BJ-HELTRas cells were first treated with 10  $\mu\text{M}$  of each of the 396 compounds or DMSO for 24 h prior to flow cytometry analysis (Figure S1D). In this case, 84 compounds were found to modulate TRF2 protein levels (Figure S1D, right panel; Table S1), and were used for a secondary screen (Figure S1E; Table S1). In this secondary screen, in addition to treating GRT-BJ-HELTRas cells with 10  $\mu\text{M}$  of the selected compounds, non-transduced BJ-HELTRas cells or BJ-HELTRas cells transduced with an empty vector were treated similarly to discard false positives emitting red or green autofluorescence or affecting RFP or GFP proteins. The 18 best compounds were then selected to determine their ability to modulate the expression of endogenous TRF2 in non-transduced BJ-HELTRas cells, based on Western blotting (Figure S2A,B, Table S1). We defined hits as compounds modulating by at least 20% of TRF2 dosage (either up or down). Using these criteria, from the 18 drugs evaluated by Western blotting, 9 of them reduced and one increased endogenous TRF2 protein levels (Figure S2A,B, Table S1). We then decided to choose two compounds among these drugs for in vivo experiments to determine whether they could counteract the pro-oncogenic effects of TRF2 overexpression. To avoid DDR activation and side effects in non-tumorigenic cells, we selected compounds that neither reduced to the highest nor to the lowest levels TRF2 dosage. Among them, AR and AD were corresponding to those criteria. Both compounds downregulated RFP-TRF2 in GRT-BJ-HELTRas cells as analyzed by flow cytometry (Figure 1C), endogenous TRF2 protein levels as shown by Western blotting analysis (Figure 1D; Figure S2A,B) and *TERF2* mRNA levels as determined via RT-qPCR (Figure 1E). Moreover, treatment with the respective LD50 concentrations of AR and AD reduced *TERF2* mRNA expression in both BJ-HELTRas cells and in TRF2-overexpressing BJ-HELTRas cells (Figure S3A–C).

### 3.2. AR-A014418 and Alexidine-2HCl Reversed the Tumorigenicity Conferred by High TRF2 Expression Levels

We next evaluated the impact of AR and AD on tumor growth. To control for their ability to target TRF2-overexpressing cancers, we analyzed the potential anti-tumorigenic effects of AR and AD on both standard BJ-HELTRas cells and TRF2-overexpressing BJ-HELTRas cells. BJ-HELTRas cells were transduced with TRF2 lentiviral vector or empty vector, then injected subcutaneously into nude mice. The mice were then treated with DMSO, 1 mg/kg AD or 5 mg/kg AR at days 16, 18, 20 and 22 post-injection [26,27] (Figure 2A). As previously reported [13,21], TRF2 overexpression promoted tumor initiation and growth in vivo (Figure 2B–D;  $p < 0.05$ ). Treatment with neither AR nor AD impacted tumor volume in BJ-HELTRas cells transduced with the empty vector (Figure 2E, upper panels) neither tumor growth rate (Figure 2F–H). By contrast, both drugs induced a significant decrease in the tumor volume of TRF2-overexpressing xenografted tumors, leading to significantly smaller tumor sizes at day 26 (Figure 2E, middle panels;  $p < 0.0001$ ) but also of the tumor growth rate (Figure 2F–H) at each time-point. Furthermore, the volume and growth rates of TRF2-overexpressing tumors treated by the two drugs returned to levels similar to those of the control tumors, thus demonstrating the TRF2-specific

selectivity of AR and AD (Figure 2E, lower panels). These results show that AR and AD treatment reversed specifically the tumorigenicity conferred by TRF2 overexpression.

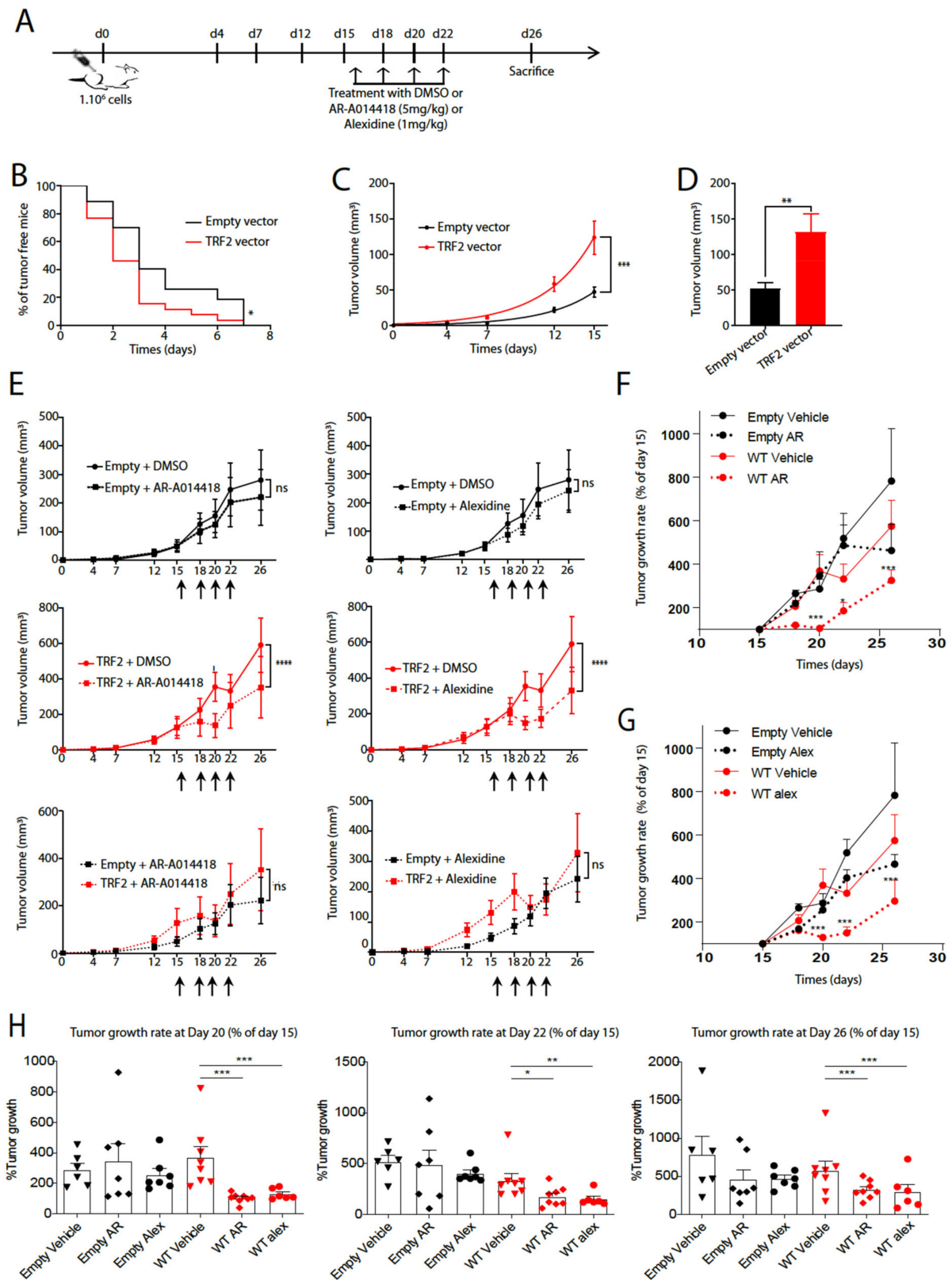


**Figure 2.** In vivo alexidine·2HCl or AR-A014418 treatment inhibited TRF2-dependent tumorigenesis. (A) Schematic representation of the experimental design. BJ-HELTRas cells either overexpressing TRF2 (TRF2 vector) or not (empty vect-

or) were injected subcutaneously ( $1 \times 10^6$  cells/100  $\mu$ L) into NMRI nude mice. The mice were then treated with DMSO, alexidine-2HCl (1 mg/kg) or AR-A014418 (5 mg/kg) at days 16, 18, 20 and 22 post-injection, then followed up until day 26 ( $n = 8$  mice per group). (B–D) The percentage of tumor-free mice (B) and tumor volumes (C) were determined at the indicated time points in mice injected with BJ-HELTRas cells overexpressing TRF2 (TRF2 vector) or empty vector. Tumor take based on palpability was determined at the indicated time-points and is represented as a percentage of tumor-free mice.  $p$  Values were determined using the log-rank Mantel-Cox test ( $* p < 0.05$ ). Tumor volumes were assessed at different time-points (mean  $\pm$  standard deviation); tumor volume at day 15 is represented in (D).  $p$  Values were determined using the Mann–Whitney test ( $* p < 0.05$ ;  $** p < 0.005$ ;  $*** p < 0.001$ ). (E) Tumor volumes were followed as in (C) after repetitive treatments with DMSO, alexidine-2HCl (1 mg/kg) or AR-A014418 (5 mg/kg).  $p$  Values were determined using the Mann–Whitney test ( $**** p < 0.0001$ ; ns: not significant). (F–H) Tumor growth rate of AR-A014418 (5 mg/kg) treated mice (F,H) or alexidine-2HCl (1 mg/kg) (G,H) treated mice were determined by considering the last day before treatment for empty vector or TRF2 vector as 100%. Variation of the growth rate in both treatment over the time are represented in (F,G) and for each time-point (H).  $p$  Values were determined using the Mann–Whitney test ( $* p < 0.05$ ;  $** p < 0.005$ ;  $*** p < 0.001$ ).

### 3.3. AR-A014418 and Alexidine-2HCl Counteracted TRF2-Dependent Immunosuppression and Neo-Angiogenesis

To determine whether the antitumor effects of AR and AD could target the non-cell autonomous oncogenic properties of TRF2, we examined immune cell infiltration and activation as well as angiogenesis in treated tumors. We treated standard and TRF2-overexpressing BJ-HELTRas cells (Figure S3A) with 1  $\mu$ M of AD, 10  $\mu$ M of AR or DMSO for 48 h before their subcutaneous injection with Matrigel into nude mice. Matrigel plugs were then collected at 5 days post-injection to analyze the tumor microenvironment by flow cytometry (Figure 3A). As expected [13,21], TRF2 overexpression did not change global immune cell (CD45+ cell) infiltration (Figure 3B; Figure S4A), but did inhibit natural killer (NK) cell recruitment (Figure 3C; Figure S4B) and NK functionality (Figure 3C–E; Figure S4C), and increase MDSC infiltration (Figure 3F). In TRF2-overexpressing BJ-HELTRas cells specifically, treatment with either drug increased global immune infiltration (Figure 3B; Figure S4A), as well as the quantity and functionality of intra-tumoral NK cells (Figure 3C–E; Figure S4B,C). Notably, both drugs fully rescued the inhibition of NK cell-mediated immune surveillance (CD107a+ and CD69+ NK cells) induced by TRF2 overexpression (Figure 3C). This was associated with a dramatic decrease in MDSC recruitment (Figure 3F; Figure S4D) and with increased recruitment of monocytes and macrophages (Figure 3G).

As previously reported [14,20], tumor angiogenesis was higher in TRF2-overexpressing tumors compared to control tumors. While TRF2 overexpression increased the quantity of CD31+ CD45– endothelial cells within the tumor bed (Figure 3H; Figure S4E), no difference was detected between empty vector or TRF2-overexpressing tumors after treatment with either drug.

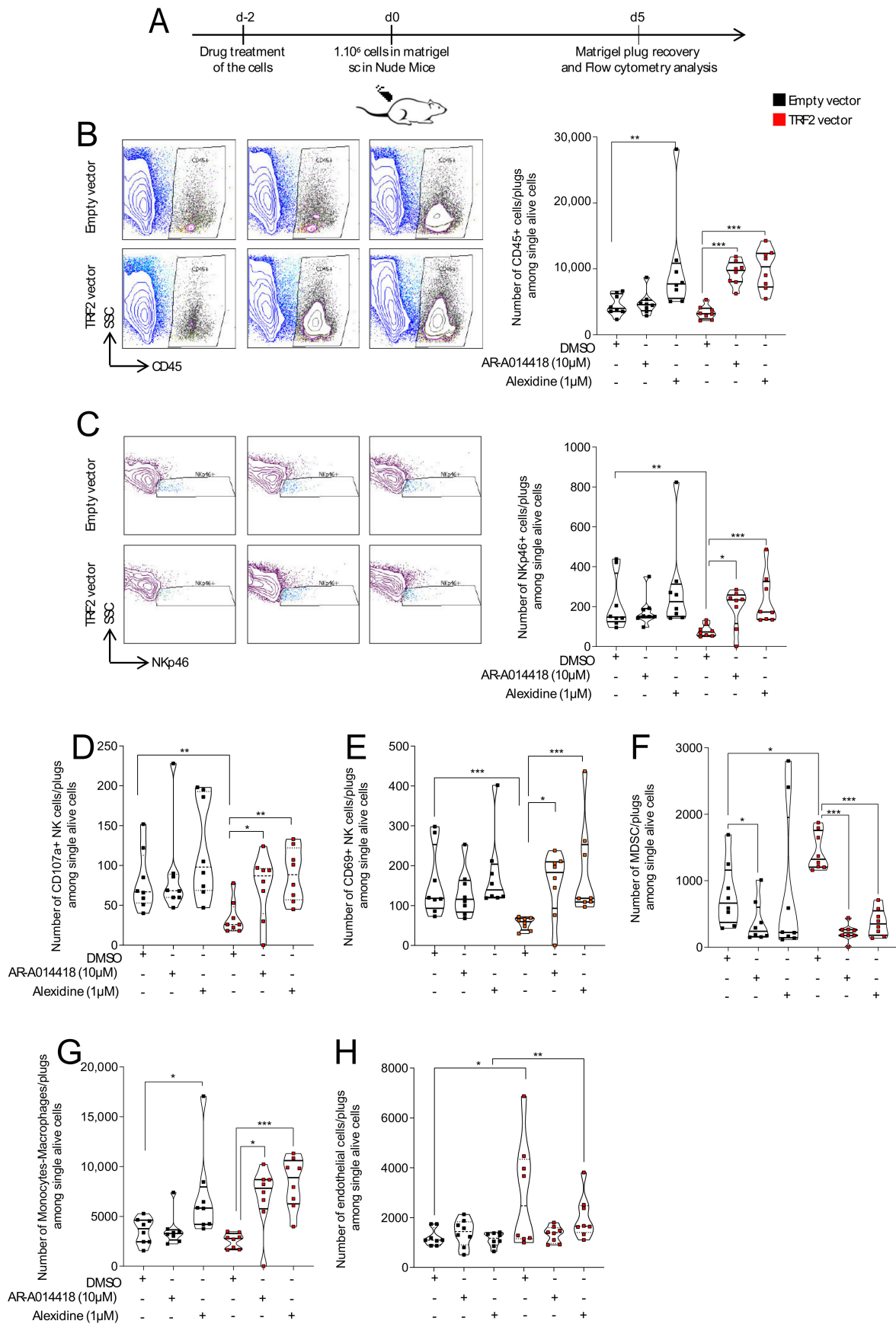


**Figure 3.** Treatment with alexidine·2HCl or AR-A014418 reverted the TRF2-mediated immunosuppressive microenvironment and restored immune cell infiltration. (A) Schematic representation of the experimental design. BJ-HELTRas cells overexpress-

ing TRF2 (TRF2 vector) or empty vector were treated with 1  $\mu$ M of alexidine-2HCl or 10  $\mu$ M of AR-A014418 or DMSO at 2 days before subcutaneous injection with Matrigel ( $1 \times 10^6$  cells) into NMRI nude mice ( $n = 8$ ). Immune and endothelial cell infiltration was then evaluated at 5 days post-injection by flow cytometry. (B–H). Flow cytometry analysis of the immune infiltration of the Matrigel plug. The numbers of immune cells infiltrating the Matrigel plugs among live cells are shown. Total immune cell infiltration (CD45+ cells) is shown in (B); natural killer (NK) cell (NKp46+ cells) infiltration is shown in (C); activated NK cell (CD107a+ and CD69+ NK cells) infiltration is shown in (D,E); myeloid-derived suppressor cell (MDSC; CD11b+ GR1+) infiltration is shown in (F); monocyte-macrophage infiltration is shown in (G) and endothelial cell infiltration is shown in (H). *p* Values were determined using the Mann-Whitney test (\*  $p < 0.05$ , \*\*  $p < 0.005$ , \*\*\*  $p < 0.001$ ;  $n = 8$  mice per group).

#### 4. Discussion

Here, we report the development of a cell-based assay to screen for compounds that modulate expression of the telomeric protein TRF2. By screening a small library of FDA-approved molecules, we identified compounds that could either increase or decrease TRF2 expression levels. We discovered that AD and AR downregulated TRF2 and exhibited anti-tumorigenic activity specific for tumor cells overexpressing TRF2. Further demonstrating their TRF2-specific activity, AR and AD treatment rescued immunosuppression and neo-angiogenesis conferred by TRF2 overexpression. Strikingly, the fact that the global immune infiltration is increased for TRF2 overexpressing tumors after AR or AD treatment suggest that those drugs are more potent to enhance immune response when TRF2 is overexpressed. Those drugs inhibit the immunosuppressive effect of TRF2 overexpression by restoring NK cell functionality (CD107a and CD69+ NK cells) and strongly decrease MDSC infiltration. This suggest that those drugs blunt the TRF2 dependent specific program that trigger immune escape and immunosuppression and may enhance the release of Danger Associated Molecules (DAMP) that enhance immune response specifically when TRF2 is overexpressed. Of note, we observe that AR and AD rescued the immunosuppressive and pro-angiogenic functions of TRF2 overexpression, two characteristics of TRF2 overexpression that we previously showed as DDR independent. Thus, we hypothesized that the AR and AD effects on tumor growth are DDR independent, a mechanism that remain to be fully described in further studies. The present proof-of-concept study provides evidence that pharmacological reduction of TRF2 expression could be a valuable anti-cancer strategy.

Even though the screening method considered TRF2 protein levels independently of transcript levels, both drugs decreased endogenous *TERF2* mRNA levels, implying that AR and AD target multiple levels of TRF2 regulation. Supporting this, AR is an inhibitor of Wnt signaling [28], which is an activator of *TERF2* transcription [29]. More generally, the drugs targeting the Wnt signaling pathway were enriched during the screening steps (Figure S1B–D). How AD, a mitochondria-targeting agent, affects TRF2 expression remains to be determined. Since cancers that exhibit high TRF2 levels have a poor prognosis and exhibit increased resistance to chemotherapy [21], AR and AD are therapeutic agents of interest for such tumors. The potential to uncouple the telomeric and pro-oncogenic activities of TRF2 [13] raises the possibility of pharmacologically downregulating TRF2, thus conferring multi-hit anti-cancer benefits without deleterious pro-aging side effects. Therefore, future studies are warranted to determine the synergistic effects of these drugs on TRF2 expression levels in clinical studies.

Even though TRF2 is upregulated in various human cancers [13,21], its expression is downregulated during both normal and pathological aging of many tissues [30,31]. Moreover, several reports involving mouse models of TRF2 dysregulation emphasize the importance of TRF2 at the crossroads between aging and cancer [31–35]. Therefore, the molecules identified by the screening procedure described here are interesting drug candidates, both as anti-cancer agents for TRF2 downregulation as confirmed in this study, and potentially as anti-aging agents by upregulating TRF2.



**Supplementary Materials:** The following are available online at <https://www.mdpi.com/article/10.3390/cancers13122998/s1>, Figure S1. Identification of drugs affecting TRF2 expression levels by flow cytometry drug screening. (A) Box plot quantification of GFP Mean of Fluorescence Intensity (MFI; left panel) or RFP MFI (right panel) in BJ-HELTRas cells infected with empty vector or BJ-HELTRas cells overexpressing TRF2 upon DMSO or 10  $\mu$ M gemcitabine treatment ( $n = 7$ ; \*\*\*  $p < 0.001$ ; compared by 2-tailed Student's  $t$  test). (B) Representative Western blotting showing reduced TRF2 protein levels following treatment with 10  $\mu$ M gemcitabine compared to DMSO control treatment in untransduced BJ-HELTRas cells (left panel). Quantification of TRF2 protein levels after treatment with 10  $\mu$ M gemcitabine compared to DMSO control treatment (right panel) ( $n = 3$ ; mean + standard error of the mean). (C) Pie chart representing the different signaling pathway targeted by the drug library and the proportion of molecules tested for each pathway. (D) Quantification (normalized RFP/GFP MFI ratio) of the primary flow cytometry drug screening assay performed on BJ-HELTRas cells overexpressing TRF2 treated with a library of molecules classified by targeted pathway compared to DMSO (10  $\mu$ M final concentration each;  $n = 2$  independent screen; mean +/– SEM) (left panel). Pie chart representing the proportion of hits selected for the secondary screening classified by targeted pathway (Right panel). (E) Quantification (normalized RFP/GFP MFI ratio) of the secondary flow cytometry drug screening assay. A subset of molecules from the library selected after the primary screen were used to treat BJ-HELTRas cells overexpressing TRF2 treated with (10  $\mu$ M final concentration;  $n = 2$  independent screen; mean +/– SEM) (left panel). In addition, and as controls, similar treatments were performed in this secondary screening on un-transduced BJ-HELTRas cells or BJ-HELTRas cells infected with empty vector. These controls allowed to exclude red or green fluorescent drugs or drugs affecting GFP or RFP protein stability. Pie chart representing the proportion of hits selected for western blot screening classified by targeted pathway (right panel). Figure S2. Western blotting analysis of TRF2 protein levels after treatment of BJ-HELTRas cells with 10  $\mu$ M of alexidine-2HCl or AR-A014418. (A) Uncropped images of the Western blotting presented in Figure 1D and representing TRF2 protein levels upon 10  $\mu$ M alexidine-2HCl or AR-A014418 treatment compared to DMSO control treatment in untransduced BJ-HELTRas cells. (B) Uncropped raw images of the three Western blots performed to measure TRF2 protein levels upon 10  $\mu$ M alexidine-2HCl or AR-A014418 treatment compared to DMSO control treatment in untransduced BJ-HELTRas cells. TRF2 recombinant proteins were used as positive controls. Quantifications of TRF2 protein levels normalized by beta-actin levels were represented in Figure 1D and Figure S3. TRF2 mRNA levels are affected by alexidine-2HCl or AR-A014418 treatment in BJ-HELTRas cells. (A) Quantification of TRF2 mRNA levels analyzed by RT-qPCR in BJ-HELTRas overexpressing or not TRF2.  $p$  Values were determined using a  $t$ -test ( $n = 3$  independent experiments; \*\*\*\*  $p < 0.0001$ ). (B) LD50 of alexidine-2HCl or AR-A014418 in BJ-HELTRas cells were determined using an AlamarBue colorimetric assay ( $n = 3$  independent experiments). (C) Quantification of TRF2 mRNA levels analyzed by RT-qPCR in BJ-HELTRas cells (with (TRF2 vector) or without (empty vector) TRF2 overexpression after alexidine-2HCl or AR-A014418 treatment at their respective LD50 concentrations.  $p$  Values were determined using the Mann–Whitney test ( $n = 3$  independent experiments; \*  $p < 0.05$ ; \*\*  $p < 0.005$ ; \*\*\*  $p < 0.001$ ; \*\*\*\*  $p < 0.0001$ ). Figure S4. Alexidine-2HCl or AR-A014418 treatment do not change global proportion of immune cells but increase the number of immune cell infiltration. Flow cytometry analysis of the immune infiltration of the Matrigel plug. The results from the Figure 3 are represented in percentage of alive cells (A) or in percentage of CD45+ cells (B–E). (A) Percentage of total immune cells (CD45+ cells) in the Matrigel plug among alive cells. (B) Percentage of NK cells (CD45+ NKp46+ cells) in the Matrigel plug among CD45+ cells. (C) Percentage of CD107a+ NK cells in the Matrigel plug among NK cells. (D) Percentage of MDSC (CD11b+ GR1+) cells in the Matrigel plug among CD45+ cells. (E) Percentage of endothelial cells (CD45– CD31+) in the Matrigel plug among alive cells. Table S1. Summary of TRF2 drug screening experiments. (A) Hits from the primary screening using flow cytometry after treatment with 10  $\mu$ M drugs as described in Figure S1D (“+”: upregulation of TRF2; “–”: downregulation of TRF2). (B) Hits from the secondary screening using flow cytometry after treatment with 10  $\mu$ M drugs as described in Figure S1E (“+”: upregulation of TRF2; “–”: downregulation of TRF2). (C) Analysis from Western blot screening after treatment with 10  $\mu$ M drugs as described in Figure S2 (“+”: upregulation of TRF2; “nc”: no changes on TRF2 levels; “–”: downregulation of TRF2).

**Author Contributions:** Conceptualization, E.G., P.J. and J.C.-V.; methodology, E.G., P.J., M.E.M., A.R. and J.C.-V.; validation, E.G., S.J.d.H., M.E.M. and J.C.-V.; formal analysis, E.G., N.W., J.Y., S.J.d.H., M.E.M. and J.C.-V.; investigation, M.E.M. and S.J.d.H.; resources, E.G., P.J. and C.G.; data curation, M.E.M. and J.C.-V.; writing—original draft preparation, E.G., M.E.M. and J.C.-V.; writing—review and editing, E.G., M.E.M. and J.C.-V.; visualization, M.E.M. and J.C.-V.; supervision, E.G. and J.C.-V.; project administration, E.G. and J.C.-V.; funding acquisition, E.G. All authors have read and agreed to the published version of the manuscript.

**Funding:** The work in EG lab was supported by the Fondation ARC (Program ARC), the ANR grants TELOPOST and TELOCHROM, the INCa grant REPLITOP and the cross-cutting Inserm program on aging (AgeMed). The work was also supported by the French Government (ANR) through the “investments for the future” LABEX SIGNALIFE program (ANR-11-LABX-002801). This work was performed using the PICMI and CYTOMED facilities of IRCAN (supported by FEDER, Ministère de l’Enseignement Supérieur, Région Provence Alpes-Côte d’Azur, Conseil Départemental 06, ITMO Cancer Aviesan (plan cancer), Cancéropole Provence Alpes-Côte d’Azur, Gis Ibis, le CNRS and l’Inserm). MEM was supported by a fellowship from the Fondation ARC pour la Recherche contre le Cancer (grant n°DOC20140601384).

**Institutional Review Board Statement:** The study was conducted according to the guidelines of the Declaration of Helsinki and approved by the Animal Care Committee of the IRCAN and the regional (CIEPAL Cote d’Azur #187 and #188) and national (French Ministry of Research #03482.01/02482.2 and # 02973.01/02973.2) authorities.

**Informed Consent Statement:** Not applicable.

**Data Availability Statement:** Further information and requests for resources and reagents should be directed to and will be fulfilled by the lead contact, E.G. (Eric.GILSON@unice.fr).

**Acknowledgments:** We thank the above-mentioned funding entities that supported the work and IRCAN core facilities for cytometry (CYTOMED) and animal house for their support.

**Conflicts of Interest:** The authors declare that they have no competing interests.

## References

1. Giraud-Panis, M.-J.; Pisano, S.; Benarroch-Popivker, D.; Pei, B.; Le Du, M.-H.; Gilson, E. One Identity or More for Telomeres? *Front. Oncol.* **2013**, *3*, 48. [[CrossRef](#)]
2. Gilson, E.; Géli, V. How telomeres are replicated. *Nat. Rev. Mol. Cell Biol.* **2007**, *8*, 825–838. [[CrossRef](#)]
3. Armanios, M.; Blackburn, E.H. The telomere syndromes. *Nat. Rev. Genet.* **2012**, *13*, 693–704. [[CrossRef](#)]
4. Kordinas, V.; Ioannidis, A.; Chatzipanagiotou, S. The Telomere/Telomerase System in Chronic Inflammatory Diseases. Cause or Effect? *Genes* **2016**, *7*, 60. [[CrossRef](#)]
5. Kim, N.; Piatyszek, M.; Prowse, K.; Harley, C.; West, M.; Ho, P.; Coviello, G.; Wright, W.; Weinrich, S.; Shay, J. Specific association of human telomerase activity with immortal cells and cancer. *Science* **1994**, *266*, 2011–2015. [[CrossRef](#)]
6. Sugarman, E.T.; Zhang, G.; Shay, J.W. In perspective: An update on telomere targeting in cancer. *Mol. Carcinog.* **2019**, *58*, 1581–1588. [[CrossRef](#)]
7. Artandi, S.E.; Chang, S.; Lee, S.-L.; Alson, S.; Gottlieb, G.J.; Chin, L.; DePinho, R.A. Telomere dysfunction promotes non-reciprocal translocations and epithelial cancers in mice. *Nat. Cell Biol.* **2000**, *406*, 641–645. [[CrossRef](#)] [[PubMed](#)]
8. Perera, S.A.; Maser, R.S.; Xia, H.; McNamara, K.; Protopopov, A.; Chen, L.; Hezel, A.F.; Kim, C.F.; Bronson, R.T.; Castrillon, D.H.; et al. Telomere dysfunction promotes genome instability and metastatic potential in a K-ras p53 mouse model of lung cancer. *Carcinogenesis* **2008**, *29*, 747–753. [[CrossRef](#)] [[PubMed](#)]
9. Bryan, T.M.; Englezou, A.; Dalla-Pozza, L.; Dunham, M.A.; Reddel, R. Evidence for an alternative mechanism for maintaining telomere length in human tumors and tumor-derived cell lines. *Nat. Med.* **1997**, *3*, 1271–1274. [[CrossRef](#)] [[PubMed](#)]
10. Hu, J.; Hwang, S.S.; Liesa, M.; Gan, B.; Sahin, E.; Jaskelioff, M.; Ding, Z.; Ying, H.; Boutin, A.T.; Zhang, H.; et al. Antitelomerase Therapy Provokes ALT and Mitochondrial Adaptive Mechanisms in Cancer. *Cell* **2012**, *148*, 651–663. [[CrossRef](#)]
11. Fernandes, S.G.; Dsouza, R.; Pandya, G.; Kirtonia, A.; Tergaonkar, V.; Lee, S.Y.; Garg, M.; Khattar, E. Role of Telomeres and Telomeric Proteins in Human Malignancies and Their Therapeutic Potential. *Cancers* **2020**, *12*, 1901. [[CrossRef](#)]
12. Augereau, A.; De Roodenbeke, C.T.; Simonet, T.; Bauwens, S.; Horard, B.; Callanan, M.; Leroux, M.; Jallades, L.; Salles, G.; Gilson, E.; et al. Telomeric damage in early stage of chronic lymphocytic leukemia correlates with shelterin dysregulation. *Blood* **2011**, *118*, 1316–1322. [[CrossRef](#)]
13. Biroccio, A.; Cherfils-Vicini, J.; Augereau, A.; Pinte, S.; Bauwens, S.; Ye, J.; Simonet, T.; Horard, B.; Jamet, K.; Cervera, L.; et al. TRF2 inhibits a cell-extrinsic pathway through which natural killer cells eliminate cancer cells. *Nat. Cell Biol.* **2013**, *15*, 818–828. [[CrossRef](#)] [[PubMed](#)]

14. El Maï, M.; Wagner, K.-D.; Michiels, J.-F.; Ambrosetti, D.; Borderie, A.; Destree, S.; Renault, V.; Djerbi, N.; Giraud-Panis, M.-J.; Gilson, E.; et al. The Telomeric Protein TRF2 Regulates Angiogenesis by Binding and Activating the PDGFR $\beta$  Promoter. *Cell Rep.* **2014**, *9*, 1047–1060. [[CrossRef](#)] [[PubMed](#)]
15. Ramsay, A.J.; Quesada, V.; Foronda, M.; Conde, L.; Martínez-Trillos, A.; Villamor, N.; Rodríguez, D.; Kwarciak, A.; Garabaya, C.; Gallardo, M.; et al. POT1 mutations cause telomere dysfunction in chronic lymphocytic leukemia. *Nat. Genet.* **2013**, *45*, 526–530. [[CrossRef](#)]
16. Bejarano, L.; Schuhmacher, A.J.; Méndez, M.; Megías, D.; Blanco-Aparicio, C.; Martínez, S.; Pastor, J.; Squatrito, M.; Blasco, M.A. Inhibition of TRF1 Telomere Protein Impairs Tumor Initiation and Progression in Glioblastoma Mouse Models and Patient-Derived Xenografts. *Cancer Cell* **2017**, *32*, 590–607. [[CrossRef](#)]
17. Benhamou, Y.; Picco, V.; Raybaud, H.; Sudaka, A.; Chamorey, E.; Brolih, S.; Monteverde, M.; Merlano, M.; Nigro, C.L.; Ambrosetti, D.; et al. Telomeric repeat-binding factor 2: A marker for survival and anti-EGFR efficacy in oral carcinoma. *Oncotarget* **2016**, *7*, 44236–44251. [[CrossRef](#)] [[PubMed](#)]
18. Cherfils-Vicini, J.; Zizza, P.; Gilson, E.; Biroccio, A. A novel pathway links telomeres to NK-cell activity. *OncolImmunology* **2014**, *3*, e27358. [[CrossRef](#)]
19. Cherfils-Vicini, J.; Gilson, E. Inhibiting TRF 1 upstream signaling pathways to target telomeres in cancer cells. *EMBO Mol. Med.* **2019**, *11*, 11. [[CrossRef](#)]
20. Zizza, P.; Dinami, R.; Porru, M.; Cingolani, C.; Salvati, E.; Rizzo, A.; D’Angelo, C.; Petti, E.; Amoreo, C.A.; Mottolese, M.; et al. TRF2 positively regulates SULF2 expression increasing VEGF-A release and activity in tumor microenvironment. *Nucleic Acids Res.* **2019**, *47*, 3365–3382. [[CrossRef](#)] [[PubMed](#)]
21. Cherfils-Vicini, J.; Iltis, C.; Cervera, L.; Pisano, S.; Croce, O.; Sadouni, N.; Györffy, B.; Collet, R.; Renault, V.M.; Rey-Millet, M.; et al. Cancer cells induce immune escape via glycoalyx changes controlled by the telomeric protein TRF 2. *EMBO J.* **2019**, *38*. [[CrossRef](#)] [[PubMed](#)]
22. Di Maro, S.; Zizza, P.; Salvati, E.; DE Luca, V.; Capasso, C.; Fotticchia, I.; Pagano, B.; Marinelli, L.; Gilson, E.; Novellino, E.; et al. Shading the TRF2 Recruiting Function: A New Horizon in Drug Development. *J. Am. Chem. Soc.* **2014**, *136*, 16708–16711. [[CrossRef](#)]
23. Roisin, A.; Buchsbaum, S.; Mocquet, V.; Jalinot, P. The fluorescent protein stability assay: An efficient method for monitoring intracellular protein stability. *Biotechniques* **2021**, *70*, btn-2021-0032. [[CrossRef](#)]
24. Su, C.-H.; Chu, W.-C.; Lan, K.-H.; Li, C.-P.; Chao, Y.; Lin, H.-C.; Lee, S.-D.; Tsai, Y.-C.; Lee, W.-P. Gemcitabine causes telomere attrition by stabilizing TRF2. *Eur. J. Cancer* **2012**, *48*, 3465–3474. [[CrossRef](#)]
25. Fujita, K.; Horikawa, I.; Mondal, A.M.; Jenkins, L.M.M.; Appella, E.; Vojtesek, B.; Bourdon, J.-C.; Lane, D.P.; Harris, C.C. Positive feedback between p53 and TRF2 during telomere-damage signalling and cellular senescence. *Nat. Cell Biol.* **2010**, *12*, 1205–1212. [[CrossRef](#)] [[PubMed](#)]
26. Shakoori, A.; Mai, W.; Miyashita, K.; Yasumoto, K.; Takahashi, Y.; Ooi, A.; Kawakami, K.; Minamoto, T. Inhibition of GSK-3 $\beta$  activity attenuates proliferation of human colon cancer cells in rodents. *Cancer Sci.* **2007**, *98*, 1388–1393. [[CrossRef](#)]
27. Kenny, H.A.; Lal-Nag, M.; White, E.A.; Shen, M.; Chiang, C.-Y.; Mitra, A.K.; Zhang, Y.; Curtis, M.W.; Schryver, E.M.; Bettis, S.; et al. Quantitative high throughput screening using a primary human three-dimensional organotypic culture predicts in vivo efficacy. *Nat. Commun.* **2015**, *6*, 1–11. [[CrossRef](#)]
28. Bhat, R.; Xue, Y.; Berg, S.; Hellberg, S.; Ormö, M.; Nilsson, Y.; Radesäter, A.-C.; Jerning, E.; Markgren, P.-O.; Borgegård, T.; et al. Structural Insights and Biological Effects of Glycogen Synthase Kinase 3-specific Inhibitor AR-A014418. *J. Biol. Chem.* **2003**, *278*, 45937–45945. [[CrossRef](#)] [[PubMed](#)]
29. Diala, I.; Wagner, N.; Magdinier, F.; Shkreli, M.; Sirakov, M.; Bauwens, S.; Schluth-Bolard, C.; Simonet, T.; Renault, V.M.; Ye, J.; et al. Telomere protection and TRF2 expression are enhanced by the canonical Wnt signalling pathway. *EMBO Rep.* **2013**, *14*, 356–363. [[CrossRef](#)] [[PubMed](#)]
30. Wagner, K.-D.; Ying, Y.; Leong, W.; Jiang, J.; Hu, X.; Chen, Y.; Michiels, J.-F.; Lu, Y.; Gilson, E.; Wagner, N.; et al. The differential spatiotemporal expression pattern of shelterin genes throughout lifespan. *Aging* **2017**, *9*, 1219–1232. [[CrossRef](#)]
31. Robin, J.D.; Burbano, M.J.; Peng, H.; Croce, O.; Thomas, J.L.; Laberthonniere, C.; Renault, V.; Lototska, L.; Pousse, M.; Tessier, F.; et al. Mitochondrial function in skeletal myofibers is controlled by a TRF2-SIRT3 axis over lifetime. *Aging Cell* **2020**, *19*, e13097. [[CrossRef](#)]
32. Muñoz, P.; Blanco, R.; Flores, J.M.; Blasco, M.A. XPF nuclease-dependent telomere loss and increased DNA damage in mice overexpressing TRF2 result in premature aging and cancer. *Nat. Genet.* **2005**, *37*, 1063–1071. [[CrossRef](#)] [[PubMed](#)]
33. Alder, J.K.; Barkauskas, C.E.; Limjunyawong, N.; Stanley, S.E.; Kembou, F.; Tuder, R.M.; Hogan, B.L.M.; Mitzner, W.; Armanios, M. Telomere dysfunction causes alveolar stem cell failure. *Proc. Natl. Acad. Sci. USA* **2015**, *112*, 5099–5104. [[CrossRef](#)] [[PubMed](#)]
34. Morgan, R.G.; Walker, A.E.; Trott, D.W.; Machin, D.R.; Henson, G.D.; Reihl, K.D.; Cawthon, R.M.; Denchi, E.L.; Liu, Y.; Bloom, S.I.; et al. Induced Trf2 deletion leads to aging vascular phenotype in mice associated with arterial telomere uncapping, senescence signaling, and oxidative stress. *J. Mol. Cell. Cardiol.* **2019**, *127*, 74–82. [[CrossRef](#)] [[PubMed](#)]
35. Wang, J.; Uryga, A.K.; Reinhold, J.; Figg, N.; Baker, L.; Finigan, A.J.; Gray, K.; Kumar, S.; Clarke, M.C.H.; Bennett, M.R. Vascular Smooth Muscle Cell Senescence Promotes Atherosclerosis and Features of Plaque Vulnerability. *Circulation* **2015**, *132*, 1909–1919. [[CrossRef](#)]





## BIBLIOGRAPHIE



- [1] A. Iwasaki, E. F. Foxman, and R. D. Molony, "Early local immune defences in the respiratory tract.," *Nat Rev Immunol*, vol. 17, no. 1, pp. 7–20, 2017, doi: 10.1038/nri.2016.117.
- [2] S. Ueha, F. H. W. Shand, and K. Matsushima, "Cellular and Molecular Mechanisms of Chronic Inflammation-Associated Organ Fibrosis," *Front Immunol*, vol. 3, 2012, doi: 10.3389/fimmu.2012.00071.
- [3] H. Zhao *et al.*, "Inflammation and tumor progression: signaling pathways and targeted intervention," *Signal Transduct Target Ther*, vol. 6, no. 1, p. 263, Dec. 2021, doi: 10.1038/s41392-021-00658-5.
- [4] N. v Serbina and E. G. Pamer, "Monocyte emigration from bone marrow during bacterial infection requires signals mediated by chemokine receptor CCR2," *Nat Immunol*, vol. 7, no. 3, pp. 311–317, Mar. 2006, doi: 10.1038/ni1309.
- [5] C. Jakubzick *et al.*, "Minimal differentiation of classical monocytes as they survey steady-state tissues and transport antigen to lymph nodes.," *Immunity*, vol. 39, no. 3, pp. 599–610, Sep. 2013, doi: 10.1016/j.immuni.2013.08.007.
- [6] S. Tamoutounour *et al.*, "Origins and functional specialization of macrophages and of conventional and monocyte-derived dendritic cells in mouse skin.," *Immunity*, vol. 39, no. 5, pp. 925–38, Nov. 2013, doi: 10.1016/j.immuni.2013.10.004.
- [7] C. Varol *et al.*, "Intestinal lamina propria dendritic cell subsets have different origin and functions.," *Immunity*, vol. 31, no. 3, pp. 502–12, Sep. 2009, doi: 10.1016/j.immuni.2009.06.025.
- [8] M. Williams *et al.*, "Alveolar macrophages develop from fetal monocytes that differentiate into long-lived cells in the first week of life via GM-CSF.," *J Exp Med*, vol. 210, no. 10, pp. 1977–92, Sep. 2013, doi: 10.1084/jem.20131199.
- [9] L. van de Laar *et al.*, "Yolk Sac Macrophages, Fetal Liver, and Adult Monocytes Can Colonize an Empty Niche and Develop into Functional Tissue-Resident Macrophages.," *Immunity*, vol. 44, no. 4, pp. 755–68, Apr. 2016, doi: 10.1016/j.immuni.2016.02.017.
- [10] E. Evren *et al.*, "CD116+ fetal precursors migrate to the perinatal lung and give rise to human alveolar macrophages," *Journal of Experimental Medicine*, vol. 219, no. 2, Feb. 2022, doi: 10.1084/jem.20210987.
- [11] B. B. Ural *et al.*, "Identification of a nerve-associated, lung-resident interstitial macrophage subset with distinct localization and immunoregulatory properties.," *Sci Immunol*, vol. 5, no. 45, 2020, doi: 10.1126/sciimmunol.aax8756.
- [12] X. Yu *et al.*, "The Cytokine TGF- $\beta$  Promotes the Development and Homeostasis of Alveolar Macrophages.," *Immunity*, vol. 47, no. 5, pp. 903–912.e4, 2017, doi: 10.1016/j.immuni.2017.10.007.
- [13] D. Hashimoto *et al.*, "Tissue-resident macrophages self-maintain locally throughout adult life with minimal contribution from circulating monocytes.," *Immunity*, vol. 38, no. 4, pp. 792–804, Apr. 2013, doi: 10.1016/j.immuni.2013.04.004.
- [14] S. L. Gibbings *et al.*, "Transcriptome analysis highlights the conserved difference between embryonic and postnatal-derived alveolar macrophages.," *Blood*, vol. 126, no. 11, pp. 1357–66, Sep. 2015, doi: 10.1182/blood-2015-01-624809.
- [15] A. Sica and A. Mantovani, "Macrophage plasticity and polarization: in vivo veritas.," *J Clin Invest*, vol. 122, no. 3, pp. 787–95, Mar. 2012, doi: 10.1172/JCI59643.



- [16] P. Italiani and D. Boraschi, "From Monocytes to M1/M2 Macrophages: Phenotypical vs. Functional Differentiation.," *Front Immunol*, vol. 5, p. 514, 2014, doi: 10.3389/fimmu.2014.00514.
- [17] S. A. Gebb *et al.*, "Sites of leukocyte sequestration in the pulmonary microcirculation.," *J Appl Physiol (1985)*, vol. 79, no. 2, pp. 493–7, Aug. 1995, doi: 10.1152/jappl.1995.79.2.493.
- [18] C. Mesnil *et al.*, "Lung-resident eosinophils represent a distinct regulatory eosinophil subset.," *J Clin Invest*, vol. 126, no. 9, pp. 3279–95, 2016, doi: 10.1172/JCI85664.
- [19] B. G. Yipp *et al.*, "The Lung is a Host Defense Niche for Immediate Neutrophil-Mediated Vascular Protection.," *Sci Immunol*, vol. 2, no. 10, Apr. 2017, doi: 10.1126/sciimmunol.aam8929.
- [20] B. Amulic, C. Cazalet, G. L. Hayes, K. D. Metzler, and A. Zychlinsky, "Neutrophil function: from mechanisms to disease.," *Annu Rev Immunol*, vol. 30, pp. 459–89, 2012, doi: 10.1146/annurev-immunol-020711-074942.
- [21] G. K. Aulakh, "Neutrophils in the lung: 'the first responders'.," *Cell Tissue Res*, vol. 371, no. 3, pp. 577–588, Mar. 2018, doi: 10.1007/s00441-017-2748-z.
- [22] M. Bhatia, R. L. Zemans, and S. Jeyaseelan, "Role of chemokines in the pathogenesis of acute lung injury.," *Am J Respir Cell Mol Biol*, vol. 46, no. 5, pp. 566–72, May 2012, doi: 10.1165/rcmb.2011-0392TR.
- [23] F. Tian *et al.*, "Pulmonary resident neutrophils regulate the production of GM-CSF and alveolar macrophages.," *FEBS J*, vol. 283, no. 8, pp. 1465–74, Apr. 2016, doi: 10.1111/febs.13684.
- [24] H. R. Hampton, J. Bailey, M. Tomura, R. Brink, and T. Chtanova, "Microbe-dependent lymphatic migration of neutrophils modulates lymphocyte proliferation in lymph nodes.," *Nat Commun*, vol. 6, p. 7139, May 2015, doi: 10.1038/ncomms8139.
- [25] J. Travers and M. E. Rothenberg, "Eosinophils in mucosal immune responses.," *Mucosal Immunol*, vol. 8, no. 3, pp. 464–75, May 2015, doi: 10.1038/mi.2015.2.
- [26] M. E. Rothenberg and S. P. Hogan, "The eosinophil.," *Annu Rev Immunol*, vol. 24, pp. 147–74, 2006, doi: 10.1146/annurev.immunol.24.021605.090720.
- [27] U. M. Padigel *et al.*, "Eosinophils Act as Antigen-Presenting Cells to Induce Immunity to *Strongyloides stercoralis* in Mice.," *J Infect Dis*, vol. 196, no. 12, pp. 1844–1851, Dec. 2007, doi: 10.1086/522968.
- [28] D. K. Chu *et al.*, "Indigenous enteric eosinophils control DCs to initiate a primary Th2 immune response in vivo.," *Journal of Experimental Medicine*, vol. 211, no. 8, pp. 1657–1672, Jul. 2014, doi: 10.1084/jem.20131800.
- [29] G. Gasteiger, X. Fan, S. Dikiy, S. Y. Lee, and A. Y. Rudensky, "Tissue residency of innate lymphoid cells in lymphoid and nonlymphoid organs.," *Science (1979)*, vol. 350, no. 6263, pp. 981–985, Nov. 2015, doi: 10.1126/science.aac9593.
- [30] B. Hervier, J. Russick, I. Cremer, and V. Vieillard, "NK Cells in the Human Lungs.," *Front Immunol*, vol. 10, p. 1263, 2019, doi: 10.3389/fimmu.2019.01263.
- [31] G. E. Cooper, K. Ostridge, S. I. Khakoo, T. M. A. Wilkinson, and K. J. Staples, "Human CD49a+ Lung Natural Killer Cell Cytotoxicity in Response to Influenza A Virus.," *Front Immunol*, vol. 9, p. 1671, 2018, doi: 10.3389/fimmu.2018.01671.
- [32] D. Brownlie *et al.*, "Expansions of adaptive-like NK cells with a tissue-resident phenotype in human lung and blood.," *Proc Natl Acad Sci U S A*, vol. 118, no. 11, 2021, doi: 10.1073/pnas.2016580118.

- [33] E. Vivier, E. Tomasello, M. Baratin, T. Walzer, and S. Ugolini, "Functions of natural killer cells," *Nat Immunol*, vol. 9, no. 5, pp. 503–10, May 2008, doi: 10.1038/ni1582.
- [34] C. von Garnier *et al.*, "Anatomical location determines the distribution and function of dendritic cells and other APCs in the respiratory tract.," *J Immunol*, vol. 175, no. 3, pp. 1609–18, Aug. 2005, doi: 10.4049/jimmunol.175.3.1609.
- [35] D. Hawiger *et al.*, "Dendritic Cells Induce Peripheral T Cell Unresponsiveness under Steady State Conditions in Vivo," *Journal of Experimental Medicine*, vol. 194, no. 6, pp. 769–780, Sep. 2001, doi: 10.1084/jem.194.6.769.
- [36] C. Kurts, H. Kosaka, F. R. Carbone, J. F. Miller, and W. R. Heath, "Class I-restricted cross-presentation of exogenous self-antigens leads to deletion of autoreactive CD8(+) T cells," *J Exp Med*, vol. 186, no. 2, pp. 239–45, Jul. 1997, doi: 10.1084/jem.186.2.239.
- [37] A. Tuettenberg *et al.*, "The Role of ICOS in Directing T Cell Responses: ICOS-Dependent Induction of T Cell Anergy by Tolerogenic Dendritic Cells," *The Journal of Immunology*, vol. 182, no. 6, pp. 3349–3356, Mar. 2009, doi: 10.4049/jimmunol.0802733.
- [38] M. Saito *et al.*, "Defective IL-10 signaling in hyper-IgE syndrome results in impaired generation of tolerogenic dendritic cells and induced regulatory T cells," *Journal of Experimental Medicine*, vol. 208, no. 2, pp. 235–249, Feb. 2011, doi: 10.1084/jem.20100799.
- [39] K. Mahnke, Y. Qian, J. Knop, and A. H. Enk, "Induction of CD4+/CD25+ regulatory T cells by targeting of antigens to immature dendritic cells," *Blood*, vol. 101, no. 12, pp. 4862–4869, Jun. 2003, doi: 10.1182/blood-2002-10-3229.
- [40] G. Hintzen *et al.*, "Induction of Tolerance to Innocuous Inhaled Antigen Relies on a CCR7-Dependent Dendritic Cell-Mediated Antigen Transport to the Bronchial Lymph Node," *The Journal of Immunology*, vol. 177, no. 10, pp. 7346–7354, Nov. 2006, doi: 10.4049/jimmunol.177.10.7346.
- [41] M. L. Kapsenberg, "Dendritic-cell control of pathogen-driven T-cell polarization.," *Nat Rev Immunol*, vol. 3, no. 12, pp. 984–93, Dec. 2003, doi: 10.1038/nri1246.
- [42] S. Halle *et al.*, "Induced bronchus-associated lymphoid tissue serves as a general priming site for T cells and is maintained by dendritic cells," *Journal of Experimental Medicine*, vol. 206, no. 12, pp. 2593–2601, Nov. 2009, doi: 10.1084/jem.20091472.
- [43] A. Bachem *et al.*, "Superior antigen cross-presentation and XCR1 expression define human CD11c+CD141+ cells as homologues of mouse CD8+ dendritic cells," *Journal of Experimental Medicine*, vol. 207, no. 6, pp. 1273–1281, Jun. 2010, doi: 10.1084/jem.20100348.
- [44] T. A. Patente, M. P. Pinho, A. A. Oliveira, G. C. M. Evangelista, P. C. Bergami-Santos, and J. A. M. Barbuto, "Human Dendritic Cells: Their Heterogeneity and Clinical Application Potential in Cancer Immunotherapy," *Front Immunol*, vol. 9, Jan. 2019, doi: 10.3389/fimmu.2018.03176.
- [45] E. E. Peterson and K. C. Barry, "The Natural Killer–Dendritic Cell Immune Axis in Anti-Cancer Immunity and Immunotherapy," *Front Immunol*, vol. 11, Feb. 2021, doi: 10.3389/fimmu.2020.621254.
- [46] S. Hong, S. Park, and J.-W. Yu, "Pyrin Domain (PYD)-containing Inflammasome in Innate Immunity," *Journal of Bacteriology and Virology*, vol. 41, no. 3, p. 133, 2011, doi: 10.4167/jbv.2011.41.3.133.

- [47] G. M. Barton and J. C. Kagan, "A cell biological view of Toll-like receptor function: regulation through compartmentalization," *Nat Rev Immunol*, vol. 9, no. 8, pp. 535–542, Aug. 2009, doi: 10.1038/nri2587.
- [48] J. J. C. Thome *et al.*, "Spatial Map of Human T Cell Compartmentalization and Maintenance over Decades of Life," *Cell*, vol. 159, no. 4, pp. 814–828, Nov. 2014, doi: 10.1016/j.cell.2014.10.026.
- [49] J. Zhu *et al.*, "The Transcription Factor T-bet Is Induced by Multiple Pathways and Prevents an Endogenous Th2 Cell Program during Th1 Cell Responses," *Immunity*, vol. 37, no. 4, pp. 660–673, Oct. 2012, doi: 10.1016/j.immuni.2012.09.007.
- [50] V. Lazarevic *et al.*, "T-bet represses TH17 differentiation by preventing Runx1-mediated activation of the gene encoding ROR $\gamma$ t," *Nat Immunol*, vol. 12, no. 1, pp. 96–104, Jan. 2011, doi: 10.1038/ni.1969.
- [51] T. Sekiya *et al.*, "Inducible Expression of a Th2-Type CC Chemokine Thymus- and Activation-Regulated Chemokine by Human Bronchial Epithelial Cells," *The Journal of Immunology*, vol. 165, no. 4, pp. 2205–2213, Aug. 2000, doi: 10.4049/jimmunol.165.4.2205.
- [52] V. Mariani *et al.*, "Immunomodulatory Mediators from Pollen Enhance the Migratory Capacity of Dendritic Cells and License Them for Th2 Attraction," *The Journal of Immunology*, vol. 178, no. 12, pp. 7623–7631, Jun. 2007, doi: 10.4049/jimmunol.178.12.7623.
- [53] W. R. Thomas and B. J. Hales, "T and B cell responses to HDM allergens and antigens," *Immunol Res*, vol. 37, no. 3, pp. 187–199, Mar. 2007, doi: 10.1007/BF02697369.
- [54] J. D. Milner, J. M. Ward, A. Keane-Myers, and W. E. Paul, "Lymphopenic mice reconstituted with limited repertoire T cells develop severe, multiorgan, Th2-associated inflammatory disease," *Proceedings of the National Academy of Sciences*, vol. 104, no. 2, pp. 576–581, Jan. 2007, doi: 10.1073/pnas.0610289104.
- [55] J. Zhu *et al.*, "Conditional deletion of Gata3 shows its essential function in TH1-TH2 responses," *Nat Immunol*, vol. 5, no. 11, pp. 1157–1165, Nov. 2004, doi: 10.1038/ni1128.
- [56] W. Zheng and R. A. Flavell, "The Transcription Factor GATA-3 Is Necessary and Sufficient for Th2 Cytokine Gene Expression in CD4 T Cells," *Cell*, vol. 89, no. 4, pp. 587–596, May 1997, doi: 10.1016/S0092-8674(00)80240-8.
- [57] F. Annunziato *et al.*, "Reversal of human allergen-specific CRTH2+ TH2 cells by IL-12 or the PS-DSP30 oligodeoxynucleotide," *Journal of Allergy and Clinical Immunology*, vol. 108, no. 5, pp. 815–821, Nov. 2001, doi: 10.1067/mai.2001.119156.
- [58] V. Santarlaschi *et al.*, "Rarity of Human T Helper 17 Cells Is due to Retinoic Acid Orphan Receptor-Dependent Mechanisms that Limit Their Expansion," *Immunity*, vol. 36, no. 2, pp. 201–214, Feb. 2012, doi: 10.1016/j.immuni.2011.12.013.
- [59] F. Salerno, R. A. W. van Lier, and M. C. Wolkers, "Better safe than sorry: TOB1 employs multiple parallel regulatory pathways to keep Th17 cells quiet," *Eur J Immunol*, vol. 44, no. 3, pp. 646–649, Mar. 2014, doi: 10.1002/eji.201444465.
- [60] L. Maggi *et al.*, "Distinctive features of classic and nonclassic (Th17 derived) human Th1 cells," *Eur J Immunol*, vol. 42, no. 12, pp. 3180–3188, Dec. 2012, doi: 10.1002/eji.201242648.
- [61] Y. Wang *et al.*, "The transcription factors T-bet and Runx are required for the ontogeny of pathogenic interferon- $\gamma$ -producing T helper 17 cells.," *Immunity*, vol. 40, no. 3, pp. 355–66, Mar. 2014, doi: 10.1016/j.immuni.2014.01.002.

- [62] T. Satoh, M. Tajima, D. Wakita, H. Kitamura, and T. Nishimura, "The development of IL-17/IFN- $\gamma$ -double producing CTLs from Tc17 cells is driven by epigenetic suppression of Socs3 gene promoter," *Eur J Immunol*, vol. 42, no. 9, pp. 2329–2342, Sep. 2012, doi: 10.1002/eji.201142240.
- [63] Y. Yu *et al.*, "Adoptive Transfer of Tc1 or Tc17 Cells Elicits Antitumor Immunity against Established Melanoma through Distinct Mechanisms," *The Journal of Immunology*, vol. 190, no. 4, pp. 1873–1881, Feb. 2013, doi: 10.4049/jimmunol.1201989.
- [64] M. Huber *et al.*, "A Th17-like developmental process leads to CD8<sup>+</sup> Tc17 cells with reduced cytotoxic activity," *Eur J Immunol*, vol. 39, no. 7, pp. 1716–1725, Jul. 2009, doi: 10.1002/eji.200939412.
- [65] H. Park *et al.*, "A distinct lineage of CD4 T cells regulates tissue inflammation by producing interleukin 17," *Nat Immunol*, vol. 6, no. 11, pp. 1133–1141, Nov. 2005, doi: 10.1038/ni1261.
- [66] M. Veldhoen, R. J. Hocking, C. J. Atkins, R. M. Locksley, and B. Stockinger, "TGF $\beta$  in the Context of an Inflammatory Cytokine Milieu Supports De Novo Differentiation of IL-17-Producing T Cells," *Immunity*, vol. 24, no. 2, pp. 179–189, Feb. 2006, doi: 10.1016/j.immuni.2006.01.001.
- [67] S. Sakaguchi, M. Miyara, C. M. Costantino, and D. A. Hafler, "FOXP3<sup>+</sup> regulatory T cells in the human immune system," *Nat Rev Immunol*, vol. 10, no. 7, pp. 490–500, Jul. 2010, doi: 10.1038/nri2785.
- [68] S. Sakaguchi, N. Sakaguchi, M. Asano, M. Itoh, and M. Toda, "Immunologic self-tolerance maintained by activated T cells expressing IL-2 receptor alpha-chains (CD25). Breakdown of a single mechanism of self-tolerance causes various autoimmune diseases.," *J Immunol*, vol. 155, no. 3, pp. 1151–64, Aug. 1995.
- [69] Y. Onishi, Z. Fehervari, T. Yamaguchi, and S. Sakaguchi, "Foxp3<sup>+</sup> natural regulatory T cells preferentially form aggregates on dendritic cells *in vitro* and actively inhibit their maturation," *Proceedings of the National Academy of Sciences*, vol. 105, no. 29, pp. 10113–10118, Jul. 2008, doi: 10.1073/pnas.0711106105.
- [70] J. J. Kobie, P. R. Shah, L. Yang, J. A. Rebhahn, D. J. Fowell, and T. R. Mosmann, "T Regulatory and Primed Uncommitted CD4 T Cells Express CD73, Which Suppresses Effector CD4 T Cells by Converting 5'-Adenosine Monophosphate to Adenosine," *The Journal of Immunology*, vol. 177, no. 10, pp. 6780–6786, Nov. 2006, doi: 10.4049/jimmunol.177.10.6780.
- [71] W. J. Grossman, J. W. Verbsky, W. Barchet, M. Colonna, J. P. Atkinson, and T. J. Ley, "Human T Regulatory Cells Can Use the Perforin Pathway to Cause Autologous Target Cell Death," *Immunity*, vol. 21, no. 4, pp. 589–601, Oct. 2004, doi: 10.1016/j.immuni.2004.09.002.
- [72] O. S. Qureshi *et al.*, "Trans-Endocytosis of CD80 and CD86: A Molecular Basis for the Cell-Extrinsic Function of CTLA-4," *Science (1979)*, vol. 332, no. 6029, pp. 600–603, Apr. 2011, doi: 10.1126/science.1202947.
- [73] H. Nishikawa and S. Sakaguchi, "Regulatory T cells in tumor immunity," *Int J Cancer*, p. n/a-n/a, Jun. 2010, doi: 10.1002/ijc.25429.
- [74] E. Montecino-Rodriguez, H. Leathers, and K. Dorshkind, "Identification of a B-1 B cell-specified progenitor.," *Nat Immunol*, vol. 7, no. 3, pp. 293–301, Mar. 2006, doi: 10.1038/ni1301.

- [75] N. Baumgarth, "The double life of a B-1 cell: self-reactivity selects for protective effector functions," *Nat Rev Immunol*, vol. 11, no. 1, pp. 34–46, Jan. 2011, doi: 10.1038/nri2901.
- [76] K. Hayakawa, R. R. Hardy, D. R. Parks, and L. A. Herzenberg, "The 'Ly-1 B' cell subpopulation in normal immunodeficient, and autoimmune mice.," *Journal of Experimental Medicine*, vol. 157, no. 1, pp. 202–218, Jan. 1983, doi: 10.1084/jem.157.1.202.
- [77] T. Okada *et al.*, "Antigen-Engaged B Cells Undergo Chemotaxis toward the T Zone and Form Motile Conjugates with Helper T Cells," *PLoS Biol*, vol. 3, no. 6, p. e150, May 2005, doi: 10.1371/journal.pbio.0030150.
- [78] A. Kato, K. E. Hulse, B. K. Tan, and R. P. Schleimer, "B-lymphocyte lineage cells and the respiratory system," *Journal of Allergy and Clinical Immunology*, vol. 131, no. 4, pp. 933–957, Apr. 2013, doi: 10.1016/j.jaci.2013.02.023.
- [79] A. Bergtold, D. D. Desai, A. Gavhane, and R. Clynes, "Cell Surface Recycling of Internalized Antigen Permits Dendritic Cell Priming of B Cells," *Immunity*, vol. 23, no. 5, pp. 503–514, Nov. 2005, doi: 10.1016/j.immuni.2005.09.013.
- [80] F. Annunziato, C. Romagnani, and S. Romagnani, "The 3 major types of innate and adaptive cell-mediated effector immunity," *Journal of Allergy and Clinical Immunology*, vol. 135, no. 3, pp. 626–635, Mar. 2015, doi: 10.1016/j.jaci.2014.11.001.
- [81] D. Hanahan and R. A. Weinberg, "The Hallmarks of Cancer," *Cell*, vol. 100, no. 1, pp. 57–70, Jan. 2000, doi: 10.1016/S0092-8674(00)81683-9.
- [82] D. Hanahan, "Hallmarks of Cancer: New Dimensions," *Cancer Discov*, vol. 12, no. 1, pp. 31–46, Jan. 2022, doi: 10.1158/2159-8290.CD-21-1059.
- [83] D. Hanahan and R. A. Weinberg, "Hallmarks of Cancer: The Next Generation," *Cell*, vol. 144, no. 5, pp. 646–674, Mar. 2011, doi: 10.1016/j.cell.2011.02.013.
- [84] T. Boon, J.-C. Cerottini, B. van den Eynde, P. van der Bruggen, and A. van Pel, "Tumor Antigens Recognized by T Lymphocytes," *Annu Rev Immunol*, vol. 12, no. 1, pp. 337–365, Apr. 1994, doi: 10.1146/annurev.iy.12.040194.002005.
- [85] G. Kroemer, C. Galassi, L. Zitvogel, and L. Galluzzi, "Immunogenic cell stress and death," *Nat Immunol*, vol. 23, no. 4, pp. 487–500, Apr. 2022, doi: 10.1038/s41590-022-01132-2.
- [86] J. P. Böttcher *et al.*, "NK Cells Stimulate Recruitment of cDC1 into the Tumor Microenvironment Promoting Cancer Immune Control," *Cell*, vol. 172, no. 5, pp. 1022–1037.e14, Feb. 2018, doi: 10.1016/j.cell.2018.01.004.
- [87] L. Galluzzi *et al.*, "Consensus guidelines for the definition, detection and interpretation of immunogenic cell death.," *J Immunother Cancer*, vol. 8, no. 1, 2020, doi: 10.1136/jitc-2019-000337.
- [88] C. Sautès-Fridman, F. Petitprez, J. Calderaro, and W. H. Fridman, "Tertiary lymphoid structures in the era of cancer immunotherapy," *Nat Rev Cancer*, vol. 19, no. 6, pp. 307–325, Jun. 2019, doi: 10.1038/s41568-019-0144-6.
- [89] M.-C. Dieu-Nosjean, N. A. Giraldo, H. Kaplon, C. Germain, W. H. Fridman, and C. Sautès-Fridman, "Tertiary lymphoid structures, drivers of the anti-tumor responses in human cancers," *Immunol Rev*, vol. 271, no. 1, pp. 260–275, May 2016, doi: 10.1111/imr.12405.
- [90] L. Shen, L. J. Sigal, M. Boes, and K. L. Rock, "Important Role of Cathepsin S in Generating Peptides for TAP-Independent MHC Class I Crosspresentation In Vivo," *Immunity*, vol. 21, no. 2, pp. 155–165, Aug. 2004, doi: 10.1016/j.immuni.2004.07.004.

- [91] M. J. Palmowski *et al.*, "Role of Immunoproteasomes in Cross-Presentation," *The Journal of Immunology*, vol. 177, no. 2, pp. 983–990, Jul. 2006, doi: 10.4049/jimmunol.177.2.983.
- [92] P. A. Roche and K. Furuta, "The ins and outs of MHC class II-mediated antigen processing and presentation.," *Nat Rev Immunol*, vol. 15, no. 4, pp. 203–16, Apr. 2015, doi: 10.1038/nri3818.
- [93] M. H. Kershaw, J. A. Westwood, and P. K. Darcy, "Gene-engineered T cells for cancer therapy," *Nat Rev Cancer*, vol. 13, no. 8, pp. 525–541, Aug. 2013, doi: 10.1038/nrc3565.
- [94] B. P. Harvey *et al.*, "Transfer of antigen from human B cells to dendritic cells," *Mol Immunol*, vol. 58, no. 1, pp. 56–65, Mar. 2014, doi: 10.1016/j.molimm.2013.10.013.
- [95] W. H. Fridman *et al.*, "B cells and cancer: To B or not to B?," *Journal of Experimental Medicine*, vol. 218, no. 1, Jan. 2021, doi: 10.1084/jem.20200851.
- [96] C. Germain *et al.*, "Presence of B Cells in Tertiary Lymphoid Structures Is Associated with a Protective Immunity in Patients with Lung Cancer," *Am J Respir Crit Care Med*, vol. 189, no. 7, pp. 832–844, Apr. 2014, doi: 10.1164/rccm.201309-1611OC.
- [97] D. Y. Ma and E. A. Clark, "The role of CD40 and CD154/CD40L in dendritic cells," *Semin Immunol*, vol. 21, no. 5, pp. 265–272, Oct. 2009, doi: 10.1016/j.smim.2009.05.010.
- [98] M. A. Cooper *et al.*, "In vivo evidence for a dependence on interleukin 15 for survival of natural killer cells," *Blood*, vol. 100, no. 10, pp. 3633–3638, Nov. 2002, doi: 10.1182/blood-2001-12-0293.
- [99] M. D. Jyothi and A. Khar, "Regulation of CD40L expression on natural killer cells by interleukin-12 and interferon  $\gamma$ : its role in the elicitation of an effective antitumor immune response," *Cancer Immunology, Immunotherapy*, vol. 49, no. 10, pp. 563–572, Dec. 2000, doi: 10.1007/s002620000151.
- [100] A. Martín-Fontecha *et al.*, "Induced recruitment of NK cells to lymph nodes provides IFN- $\gamma$  for TH1 priming," *Nat Immunol*, vol. 5, no. 12, pp. 1260–1265, Dec. 2004, doi: 10.1038/ni1138.
- [101] F. Gerosa, B. Baldani-Guerra, C. Nisii, V. Marchesini, G. Carra, and G. Trinchieri, "Reciprocal Activating Interaction between Natural Killer Cells and Dendritic Cells," *Journal of Experimental Medicine*, vol. 195, no. 3, pp. 327–333, Feb. 2002, doi: 10.1084/jem.20010938.
- [102] K. C. Barry *et al.*, "A natural killer–dendritic cell axis defines checkpoint therapy–responsive tumor microenvironments," *Nat Med*, vol. 24, no. 8, pp. 1178–1191, Aug. 2018, doi: 10.1038/s41591-018-0085-8.
- [103] L. Martinet *et al.*, "Human Solid Tumors Contain High Endothelial Venules: Association with T- and B-Lymphocyte Infiltration and Favorable Prognosis in Breast Cancer," *Cancer Res*, vol. 71, no. 17, pp. 5678–5687, Sep. 2011, doi: 10.1158/0008-5472.CAN-11-0431.
- [104] Å. Andersson *et al.*, "IL-7 Promotes CXCR3 Ligand-Dependent T Cell Antitumor Reactivity in Lung Cancer," *The Journal of Immunology*, vol. 182, no. 11, pp. 6951–6958, Jun. 2009, doi: 10.4049/jimmunol.0803340.
- [105] B. Mlecnik *et al.*, "Biomolecular Network Reconstruction Identifies T-Cell Homing Factors Associated With Survival in Colorectal Cancer," *Gastroenterology*, vol. 138, no. 4, pp. 1429–1440, Apr. 2010, doi: 10.1053/j.gastro.2009.10.057.

- [106] H. Harlin *et al.*, “Chemokine Expression in Melanoma Metastases Associated with CD8+ T-Cell Recruitment,” *Cancer Res*, vol. 69, no. 7, pp. 3077–3085, Apr. 2009, doi: 10.1158/0008-5472.CAN-08-2281.
- [107] S. Matsumura *et al.*, “Radiation-Induced CXCL16 Release by Breast Cancer Cells Attracts Effector T Cells,” *The Journal of Immunology*, vol. 181, no. 5, pp. 3099–3107, Sep. 2008, doi: 10.4049/jimmunol.181.5.3099.
- [108] L. Novak, O. Igoucheva, S. Cho, and V. Alexeev, “Characterization of the CCL21-mediated melanoma-specific immune responses and *in situ* melanoma eradication,” *Mol Cancer Ther*, vol. 6, no. 6, pp. 1755–1764, Jun. 2007, doi: 10.1158/1535-7163.MCT-06-0709.
- [109] A. M. Gocher, C. J. Workman, and D. A. A. Vignali, “Interferon- $\gamma$ : teammate or opponent in the tumour microenvironment?,” *Nat Rev Immunol*, vol. 22, no. 3, pp. 158–172, Mar. 2022, doi: 10.1038/s41577-021-00566-3.
- [110] F. Castro, A. P. Cardoso, R. M. Gonçalves, K. Serre, and M. J. Oliveira, “Interferon-Gamma at the Crossroads of Tumor Immune Surveillance or Evasion,” *Front Immunol*, vol. 9, May 2018, doi: 10.3389/fimmu.2018.00847.
- [111] A. R. Nicole M Clarke, “Genome-wide Identification of IRF1 Binding Sites Reveals Extensive Occupancy at Cell Death Associated Genes,” *J Carcinog Mutagen*, 2013, doi: 10.4172/2157-2518.S6-009.
- [112] C. v. Ramana *et al.*, “Regulation of c-myc expression by IFN- $\gamma$  through Stat1-dependent and -independent pathways,” *EMBO J*, vol. 19, no. 2, pp. 263–272, Jan. 2000, doi: 10.1093/emboj/19.2.263.
- [113] Y. E. Chin, M. Kitagawa, W.-C. S. Su, Z.-H. You, Y. Iwamoto, and X.-Y. Fu, “Cell Growth Arrest and Induction of Cyclin-Dependent Kinase Inhibitor p21<sup>WAF1/CIP1</sup> Mediated by STAT1,” *Science (1979)*, vol. 272, no. 5262, pp. 719–722, May 1996, doi: 10.1126/science.272.5262.719.
- [114] Y. E. Chin, M. Kitagawa, W.-C. S. Su, Z.-H. You, Y. Iwamoto, and X.-Y. Fu, “Cell Growth Arrest and Induction of Cyclin-Dependent Kinase Inhibitor p21<sup>WAF1/CIP1</sup> Mediated by STAT1,” *Science (1979)*, vol. 272, no. 5262, pp. 719–722, May 1996, doi: 10.1126/science.272.5262.719.
- [115] Y. E. Chin, M. Kitagawa, K. Kuida, R. A. Flavell, and X. Y. Fu, “Activation of the STAT signaling pathway can cause expression of caspase 1 and apoptosis,” *Mol Cell Biol*, vol. 17, no. 9, pp. 5328–5337, Sep. 1997, doi: 10.1128/MCB.17.9.5328.
- [116] S. Fulda and K.-M. Debatin, “IFN $\gamma$  sensitizes for apoptosis by upregulating caspase-8 expression through the Stat1 pathway,” *Oncogene*, vol. 21, no. 15, pp. 2295–2308, Apr. 2002, doi: 10.1038/sj.onc.1205255.
- [117] X. Xu, X. Y. Fu, J. Plate, and A. S. Chong, “IFN-gamma induces cell growth inhibition by Fas-mediated apoptosis: requirement of STAT1 protein for up-regulation of Fas and FasL expression,” *Cancer Res*, vol. 58, no. 13, pp. 2832–7, Jul. 1998.
- [118] R. J. Thapa *et al.*, “NF- $\kappa$ B Protects Cells from Gamma Interferon-Induced RIP1-Dependent Necroptosis,” *Mol Cell Biol*, vol. 31, no. 14, pp. 2934–2946, Jul. 2011, doi: 10.1128/MCB.05445-11.
- [119] G. L. Beatty and Y. Paterson, “IFN- $\gamma$ -Dependent Inhibition of Tumor Angiogenesis by Tumor-Infiltrating CD4<sup>+</sup> T Cells Requires Tumor Responsiveness to IFN- $\gamma$ ,” *The Journal of Immunology*, vol. 166, no. 4, pp. 2276–2282, Feb. 2001, doi: 10.4049/jimmunol.166.4.2276.

- [120] T. Kammertoens *et al.*, "Tumour ischaemia by interferon- $\gamma$  resembles physiological blood vessel regression," *Nature*, vol. 545, no. 7652, pp. 98–102, May 2017, doi: 10.1038/nature22311.
- [121] A. A. Lighvani *et al.*, "T-bet is rapidly induced by interferon- $\gamma$  in lymphoid and myeloid cells," *Proceedings of the National Academy of Sciences*, vol. 98, no. 26, pp. 15137–15142, Dec. 2001, doi: 10.1073/pnas.261570598.
- [122] J. Girdlestone and M. Wing, "Autocrine activation by interferon- $\gamma$  of STAT factors following T cell activation," *Eur J Immunol*, vol. 26, no. 3, pp. 704–709, Apr. 1996, doi: 10.1002/eji.1830260329.
- [123] L. M. Bradley, D. K. Dalton, and M. Croft, "A direct role for IFN-gamma in regulation of Th1 cell development.," *J Immunol*, vol. 157, no. 4, pp. 1350–8, Aug. 1996.
- [124] I. Voskoboinik, J. C. Whisstock, and J. A. Trapani, "Perforin and granzymes: function, dysfunction and human pathology," *Nat Rev Immunol*, vol. 15, no. 6, pp. 388–400, Jun. 2015, doi: 10.1038/nri3839.
- [125] I. Prager and C. Watzl, "Mechanisms of natural killer cell-mediated cellular cytotoxicity," *J Leukoc Biol*, vol. 105, no. 6, pp. 1319–1329, Jun. 2019, doi: 10.1002/JLB.MR0718-269R.
- [126] D. S. Chen and I. Mellman, "Oncology Meets Immunology: The Cancer-Immunity Cycle," *Immunity*, vol. 39, no. 1, pp. 1–10, Jul. 2013, doi: 10.1016/j.immuni.2013.07.012.
- [127] J. S. O'Donnell, M. W. L. Teng, and M. J. Smyth, "Cancer immunoediting and resistance to T cell-based immunotherapy," *Nat Rev Clin Oncol*, vol. 16, no. 3, pp. 151–167, Mar. 2019, doi: 10.1038/s41571-018-0142-8.
- [128] R. D. Schreiber, L. J. Old, and M. J. Smyth, "Cancer Immunoediting: Integrating Immunity's Roles in Cancer Suppression and Promotion," *Science (1979)*, vol. 331, no. 6024, pp. 1565–1570, Mar. 2011, doi: 10.1126/science.1203486.
- [129] D. I. Gabrilovich and S. Nagaraj, "Myeloid-derived suppressor cells as regulators of the immune system," *Nat Rev Immunol*, vol. 9, no. 3, pp. 162–174, Mar. 2009, doi: 10.1038/nri2506.
- [130] M. Pickup, S. Novitskiy, and H. L. Moses, "The roles of TGF $\beta$  in the tumour microenvironment," *Nat Rev Cancer*, vol. 13, no. 11, pp. 788–799, Nov. 2013, doi: 10.1038/nrc3603.
- [131] S. Viel *et al.*, "TGF- $\beta$  inhibits the activation and functions of NK cells by repressing the mTOR pathway," *Sci Signal*, vol. 9, no. 415, Feb. 2016, doi: 10.1126/scisignal.aad1884.
- [132] E. Cendrowicz, Z. Sas, E. Bremer, and T. P. Rygiel, "The Role of Macrophages in Cancer Development and Therapy," *Cancers (Basel)*, vol. 13, no. 8, p. 1946, Apr. 2021, doi: 10.3390/cancers13081946.
- [133] J. Yang, J. Yan, and B. Liu, "Targeting VEGF/VEGFR to Modulate Antitumor Immunity," *Front Immunol*, vol. 9, May 2018, doi: 10.3389/fimmu.2018.00978.
- [134] M. A. Lakins, E. Ghorani, H. Munir, C. P. Martins, and J. D. Shields, "Cancer-associated fibroblasts induce antigen-specific deletion of CD8 + T Cells to protect tumour cells," *Nat Commun*, vol. 9, no. 1, p. 948, Dec. 2018, doi: 10.1038/s41467-018-03347-0.
- [135] S. Mariathasan *et al.*, "TGF $\beta$  attenuates tumour response to PD-L1 blockade by contributing to exclusion of T cells," *Nature*, vol. 554, no. 7693, pp. 544–548, Feb. 2018, doi: 10.1038/nature25501.



- [136] D. V. F. Tauriello *et al.*, “TGFβ drives immune evasion in genetically reconstituted colon cancer metastasis,” *Nature*, vol. 554, no. 7693, pp. 538–543, Feb. 2018, doi: 10.1038/nature25492.
- [137] D. H. Peng *et al.*, “Collagen promotes anti-PD-1/PD-L1 resistance in cancer through LAIR1-dependent CD8+ T cell exhaustion,” *Nat Commun*, vol. 11, no. 1, p. 4520, Dec. 2020, doi: 10.1038/s41467-020-18298-8.
- [138] H. Salmon *et al.*, “Matrix architecture defines the preferential localization and migration of T cells into the stroma of human lung tumors,” *Journal of Clinical Investigation*, vol. 122, no. 3, pp. 899–910, Mar. 2012, doi: 10.1172/JCI45817.
- [139] J. A. Grout *et al.*, “Spatial positioning and matrix programs of cancer-associated fibroblasts promote T cell exclusion in human lung tumors,” *Cancer Discov*, Aug. 2022, doi: 10.1158/2159-8290.CD-21-1714.
- [140] Y.-P. Peng *et al.*, “Comprehensive analysis of the percentage of surface receptors and cytotoxic granules positive natural killer cells in patients with pancreatic cancer, gastric cancer, and colorectal cancer,” *J Transl Med*, vol. 11, no. 1, p. 262, Dec. 2013, doi: 10.1186/1479-5876-11-262.
- [141] E. Mamessier *et al.*, “Human breast cancer cells enhance self tolerance by promoting evasion from NK cell antitumor immunity,” *Journal of Clinical Investigation*, vol. 121, no. 9, pp. 3609–3622, Sep. 2011, doi: 10.1172/JCI45816.
- [142] L. Quatrini, F. R. Mariotti, E. Munari, N. Tumino, P. Vacca, and L. Moretta, “The Immune Checkpoint PD-1 in Natural Killer Cells: Expression, Function and Targeting in Tumour Immunotherapy,” *Cancers (Basel)*, vol. 12, no. 11, p. 3285, Nov. 2020, doi: 10.3390/cancers12113285.
- [143] G. J. Freeman *et al.*, “Engagement of the Pd-1 Immunoinhibitory Receptor by a Novel B7 Family Member Leads to Negative Regulation of Lymphocyte Activation,” *Journal of Experimental Medicine*, vol. 192, no. 7, pp. 1027–1034, Oct. 2000, doi: 10.1084/jem.192.7.1027.
- [144] Y. Latchman *et al.*, “PD-L2 is a second ligand for PD-1 and inhibits T cell activation,” *Nat Immunol*, vol. 2, no. 3, pp. 261–268, Mar. 2001, doi: 10.1038/85330.
- [145] E. Hui *et al.*, “T cell costimulatory receptor CD28 is a primary target for PD-1–mediated inhibition,” *Science (1979)*, vol. 355, no. 6332, pp. 1428–1433, Mar. 2017, doi: 10.1126/science.aaf1292.
- [146] F. Wei *et al.*, “Strength of PD-1 signaling differentially affects T-cell effector functions,” *Proceedings of the National Academy of Sciences*, vol. 110, no. 27, Jul. 2013, doi: 10.1073/pnas.1305394110.
- [147] M. Ahmadzadeh *et al.*, “Tumor antigen–specific CD8 T cells infiltrating the tumor express high levels of PD-1 and are functionally impaired,” *Blood*, vol. 114, no. 8, pp. 1537–1544, Aug. 2009, doi: 10.1182/blood-2008-12-195792.
- [148] T. J. Curiel *et al.*, “Blockade of B7-H1 improves myeloid dendritic cell–mediated antitumor immunity,” *Nat Med*, vol. 9, no. 5, pp. 562–567, May 2003, doi: 10.1038/nm863.
- [149] P. A. van der Merwe, D. L. Bodian, S. Daenke, P. Linsley, and S. J. Davis, “CD80 (B7-1) Binds Both CD28 and CTLA-4 with a Low Affinity and Very Fast Kinetics,” *Journal of Experimental Medicine*, vol. 185, no. 3, pp. 393–404, Feb. 1997, doi: 10.1084/jem.185.3.393.
- [150] A. Stojanovic, N. Fiegler, M. Brunner-Weinzierl, and A. Cerwenka, “CTLA-4 Is Expressed by Activated Mouse NK Cells and Inhibits NK Cell IFN-γ Production in

- Response to Mature Dendritic Cells," *The Journal of Immunology*, vol. 192, no. 9, pp. 4184–4191, May 2014, doi: 10.4049/jimmunol.1302091.
- [151] X. Tai *et al.*, "Basis of CTLA-4 function in regulatory and conventional CD4+ T cells," *Blood*, vol. 119, no. 22, pp. 5155–5163, May 2012, doi: 10.1182/blood-2011-11-388918.
- [152] T. Yokosuka *et al.*, "Spatiotemporal Basis of CTLA-4 Costimulatory Molecule-Mediated Negative Regulation of T Cell Activation," *Immunity*, vol. 33, no. 3, pp. 326–339, Sep. 2010, doi: 10.1016/j.immuni.2010.09.006.
- [153] R. Bellucci *et al.*, "Interferon- $\gamma$ -induced activation of JAK1 and JAK2 suppresses tumor cell susceptibility to NK cells through upregulation of PD-L1 expression," *Oncoimmunology*, vol. 4, no. 6, p. e1008824, Jun. 2015, doi: 10.1080/2162402X.2015.1008824.
- [154] H. Sung *et al.*, "Global Cancer Statistics 2020: GLOBOCAN Estimates of Incidence and Mortality Worldwide for 36 Cancers in 185 Countries," *CA Cancer J Clin*, vol. 71, no. 3, pp. 209–249, May 2021, doi: 10.3322/caac.21660.
- [155] M. Riudavets, M. Garcia de Herreros, B. Besse, and L. Mezquita, "Radon and Lung Cancer: Current Trends and Future Perspectives," *Cancers (Basel)*, vol. 14, no. 13, p. 3142, Jun. 2022, doi: 10.3390/cancers14133142.
- [156] Y. Li and S. S. Hecht, "Carcinogenic components of tobacco and tobacco smoke: A 2022 update," *Food and Chemical Toxicology*, vol. 165, p. 113179, Jul. 2022, doi: 10.1016/j.fct.2022.113179.
- [157] H. D. Hosgood *et al.*, "In-Home Coal and Wood Use and Lung Cancer Risk: A Pooled Analysis of the International Lung Cancer Consortium," *Environ Health Perspect*, vol. 118, no. 12, pp. 1743–1747, Dec. 2010, doi: 10.1289/ehp.1002217.
- [158] D. G. Hancock, M. E. Langley, K. L. Chia, R. J. Woodman, and E. M. Shanahan, "Wood dust exposure and lung cancer risk: a meta-analysis," *Occup Environ Med*, vol. 72, no. 12, pp. 889–898, Dec. 2015, doi: 10.1136/oemed-2014-102722.
- [159] S. B. Markowitz, "Lung Cancer Screening in Asbestos-Exposed Populations," *Int J Environ Res Public Health*, vol. 19, no. 5, p. 2688, Feb. 2022, doi: 10.3390/ijerph19052688.
- [160] C. Ge *et al.*, "Respirable Crystalline Silica Exposure, Smoking, and Lung Cancer Subtype Risks. A Pooled Analysis of Case–Control Studies," *Am J Respir Crit Care Med*, vol. 202, no. 3, pp. 412–421, Aug. 2020, doi: 10.1164/rccm.201910-1926OC.
- [161] Y. Huang *et al.*, "Air Pollution, Genetic Factors, and the Risk of Lung Cancer: A Prospective Study in the UK Biobank," *Am J Respir Crit Care Med*, vol. 204, no. 7, pp. 817–825, Oct. 2021, doi: 10.1164/rccm.202011-4063OC.
- [162] X. Liu *et al.*, "Lung Cancer Death Attributable to Long-Term Ambient Particulate Matter (PM<sub>2.5</sub>) Exposure in East Asian Countries During 1990–2019," *Front Med (Lausanne)*, vol. 8, Oct. 2021, doi: 10.3389/fmed.2021.742076.
- [163] H.-B. Kim, J.-Y. Shim, B. Park, and Y.-J. Lee, "Long-Term Exposure to Air Pollutants and Cancer Mortality: A Meta-Analysis of Cohort Studies," *Int J Environ Res Public Health*, vol. 15, no. 11, p. 2608, Nov. 2018, doi: 10.3390/ijerph15112608.
- [164] J. P. de Torres *et al.*, "Lung Cancer in Patients with Chronic Obstructive Pulmonary Disease," *Am J Respir Crit Care Med*, vol. 184, no. 8, pp. 913–919, Oct. 2011, doi: 10.1164/rccm.201103-0430OC.

- [165] H. Y. Park *et al.*, “Chronic obstructive pulmonary disease and lung cancer incidence in never smokers: a cohort study,” *Thorax*, vol. 75, no. 6, pp. 506–509, Jun. 2020, doi: 10.1136/thoraxjnl-2019-213732.
- [166] J. Cabrera-Sanchez, V. Cuba, V. Vega, P. van der Stuyft, and L. Otero, “Lung cancer occurrence after an episode of tuberculosis: a systematic review and meta-analysis,” *European Respiratory Review*, vol. 31, no. 165, p. 220025, Sep. 2022, doi: 10.1183/16000617.0025-2022.
- [167] S. Y. Hwang *et al.*, “Pulmonary Tuberculosis and Risk of Lung Cancer: A Systematic Review and Meta-Analysis,” *J Clin Med*, vol. 11, no. 3, p. 765, Jan. 2022, doi: 10.3390/jcm11030765.
- [168] S.-A. W. Brown *et al.*, “Idiopathic Pulmonary Fibrosis and Lung Cancer. A Systematic Review and Meta-analysis,” *Ann Am Thorac Soc*, vol. 16, no. 8, pp. 1041–1051, Aug. 2019, doi: 10.1513/AnnalsATS.201807-481OC.
- [169] B. Ballester, J. Milara, and J. Cortijo, “Idiopathic Pulmonary Fibrosis and Lung Cancer: Mechanisms and Molecular Targets,” *Int J Mol Sci*, vol. 20, no. 3, p. 593, Jan. 2019, doi: 10.3390/ijms20030593.
- [170] J. E. Bailey-Wilson, T. A. Sellers, R. C. Elston, C. C. Evens, and H. Rothschild, “Evidence for a major gene effect in early-onset lung cancer.,” *J La State Med Soc*, vol. 145, no. 4, pp. 157–62, Apr. 1993.
- [171] A. Matakidou, T. Eisen, and R. S. Houlston, “Systematic review of the relationship between family history and lung cancer risk,” *Br J Cancer*, vol. 93, no. 7, pp. 825–833, Oct. 2005, doi: 10.1038/sj.bjc.6602769.
- [172] A. G. Schwartz and M. L. Cote, “Epidemiology of Lung Cancer,” 2016, pp. 21–41. doi: 10.1007/978-3-319-24223-1\_2.
- [173] J. Malhotra, M. Malvezzi, E. Negri, C. la Vecchia, and P. Boffetta, “Risk factors for lung cancer worldwide,” *European Respiratory Journal*, vol. 48, no. 3, pp. 889–902, Sep. 2016, doi: 10.1183/13993003.00359-2016.
- [174] C. M. Rudin, E. Brambilla, C. Faivre-Finn, and J. Sage, “Small-cell lung cancer,” *Nat Rev Dis Primers*, vol. 7, no. 1, p. 3, Dec. 2021, doi: 10.1038/s41572-020-00235-0.
- [175] P. Perez-Moreno, E. Brambilla, R. Thomas, and J.-C. Soria, “Squamous Cell Carcinoma of the Lung: Molecular Subtypes and Therapeutic Opportunities,” *Clinical Cancer Research*, vol. 18, no. 9, pp. 2443–2451, May 2012, doi: 10.1158/1078-0432.CCR-11-2370.
- [176] M. J. Thun, C. A. Lally, E. E. Calle, C. W. Heath, J. T. Flannery, and W. D. Flanders, “Cigarette Smoking and Changes in the Histopathology of Lung Cancer,” *JNCI Journal of the National Cancer Institute*, vol. 89, no. 21, pp. 1580–1586, Nov. 1997, doi: 10.1093/jnci/89.21.1580.
- [177] M. Janssen-Heijnen, “The changing epidemiology of lung cancer in Europe,” *Lung Cancer*, vol. 41, no. 3, pp. 245–258, Sep. 2003, doi: 10.1016/S0169-5002(03)00230-7.
- [178] F. C. Detterbeck, D. J. Boffa, A. W. Kim, and L. T. Tanoue, “The Eighth Edition Lung Cancer Stage Classification,” *Chest*, vol. 151, no. 1, pp. 193–203, Jan. 2017, doi: 10.1016/j.chest.2016.10.010.
- [179] K. Yoshida *et al.*, “Tobacco smoking and somatic mutations in human bronchial epithelium,” *Nature*, vol. 578, no. 7794, pp. 266–272, Feb. 2020, doi: 10.1038/s41586-020-1961-1.

- [180] F. Skoulidis and J. v. Heymach, "Co-occurring genomic alterations in non-small-cell lung cancer biology and therapy," *Nat Rev Cancer*, vol. 19, no. 9, pp. 495–509, Sep. 2019, doi: 10.1038/s41568-019-0179-8.
- [181] C.-H. Yun *et al.*, "Structures of Lung Cancer-Derived EGFR Mutants and Inhibitor Complexes: Mechanism of Activation and Insights into Differential Inhibitor Sensitivity," *Cancer Cell*, vol. 11, no. 3, pp. 217–227, Mar. 2007, doi: 10.1016/j.ccr.2006.12.017.
- [182] D. K. Simanshu, D. v. Nissley, and F. McCormick, "RAS Proteins and Their Regulators in Human Disease," *Cell*, vol. 170, no. 1, pp. 17–33, Jun. 2017, doi: 10.1016/j.cell.2017.06.009.
- [183] S. Dogan *et al.*, "Molecular Epidemiology of EGFR and KRAS Mutations in 3,026 Lung Adenocarcinomas: Higher Susceptibility of Women to Smoking-Related KRAS -Mutant Cancers," *Clinical Cancer Research*, vol. 18, no. 22, pp. 6169–6177, Nov. 2012, doi: 10.1158/1078-0432.CCR-11-3265.
- [184] M. Takeda, K. Sakai, T. Takahama, K. Fukuoka, K. Nakagawa, and K. Nishio, "New Era for Next-Generation Sequencing in Japan," *Cancers (Basel)*, vol. 11, no. 6, p. 742, May 2019, doi: 10.3390/cancers11060742.
- [185] S. S. Ramalingam *et al.*, "Overall Survival with Osimertinib in Untreated, EGFR - Mutated Advanced NSCLC," *New England Journal of Medicine*, vol. 382, no. 1, pp. 41–50, Jan. 2020, doi: 10.1056/NEJMoa1913662.
- [186] S. Boumahdi and F. J. de Sauvage, "The great escape: tumour cell plasticity in resistance to targeted therapy," *Nat Rev Drug Discov*, vol. 19, no. 1, pp. 39–56, Jan. 2020, doi: 10.1038/s41573-019-0044-1.
- [187] S. J. Antonia *et al.*, "Four-year survival with nivolumab in patients with previously treated advanced non-small-cell lung cancer: a pooled analysis," *Lancet Oncol*, vol. 20, no. 10, pp. 1395–1408, Oct. 2019, doi: 10.1016/S1470-2045(19)30407-3.
- [188] H. West *et al.*, "Atezolizumab in combination with carboplatin plus nab-paclitaxel chemotherapy compared with chemotherapy alone as first-line treatment for metastatic non-squamous non-small-cell lung cancer (IMpower130): a multicentre, randomised, open-label, phase 3 trial," *Lancet Oncol*, vol. 20, no. 7, pp. 924–937, Jul. 2019, doi: 10.1016/S1470-2045(19)30167-6.
- [189] L. Paz-Ares *et al.*, "Pembrolizumab plus Chemotherapy for Squamous Non-Small-Cell Lung Cancer," *New England Journal of Medicine*, vol. 379, no. 21, pp. 2040–2051, Nov. 2018, doi: 10.1056/NEJMoa1810865.
- [190] O. Rodak, M. D. Peris-Díaz, M. Olbromski, M. Podhorska-Okółów, and P. Dzięgiel, "Current Landscape of Non-Small Cell Lung Cancer: Epidemiology, Histological Classification, Targeted Therapies, and Immunotherapy," *Cancers (Basel)*, vol. 13, no. 18, p. 4705, Sep. 2021, doi: 10.3390/cancers13184705.
- [191] L. Horn *et al.*, "Nivolumab Versus Docetaxel in Previously Treated Patients With Advanced Non-Small-Cell Lung Cancer: Two-Year Outcomes From Two Randomized, Open-Label, Phase III Trials (CheckMate 017 and CheckMate 057)," *Journal of Clinical Oncology*, vol. 35, no. 35, pp. 3924–3933, Dec. 2017, doi: 10.1200/JCO.2017.74.3062.
- [192] L. Gandhi *et al.*, "Pembrolizumab plus Chemotherapy in Metastatic Non-Small-Cell Lung Cancer," *New England Journal of Medicine*, vol. 378, no. 22, pp. 2078–2092, May 2018, doi: 10.1056/NEJMoa1801005.
- [193] S. L. Topalian *et al.*, "Five-Year Survival and Correlates Among Patients With Advanced Melanoma, Renal Cell Carcinoma, or Non-Small Cell Lung Cancer Treated With

- Nivolumab," *JAMA Oncol*, vol. 5, no. 10, p. 1411, Oct. 2019, doi: 10.1001/jamaoncol.2019.2187.
- [194] M. Camus *et al.*, "Coordination of Intratumoral Immune Reaction and Human Colorectal Cancer Recurrence," *Cancer Res*, vol. 69, no. 6, pp. 2685–2693, Mar. 2009, doi: 10.1158/0008-5472.CAN-08-2654.
- [195] M. Ayers *et al.*, "IFN- $\gamma$ -related mRNA profile predicts clinical response to PD-1 blockade," *Journal of Clinical Investigation*, vol. 127, no. 8, pp. 2930–2940, Jun. 2017, doi: 10.1172/JCI91190.
- [196] A. M. Goodman *et al.*, "Tumor Mutational Burden as an Independent Predictor of Response to Immunotherapy in Diverse Cancers," *Mol Cancer Ther*, vol. 16, no. 11, pp. 2598–2608, Nov. 2017, doi: 10.1158/1535-7163.MCT-17-0386.
- [197] E. J. Aguilar *et al.*, "Outcomes to first-line pembrolizumab in patients with non-small-cell lung cancer and very high PD-L1 expression," *Annals of Oncology*, vol. 30, no. 10, pp. 1653–1659, Oct. 2019, doi: 10.1093/annonc/mdz288.
- [198] J. Galon *et al.*, "Type, Density, and Location of Immune Cells Within Human Colorectal Tumors Predict Clinical Outcome," *Science (1979)*, vol. 313, no. 5795, pp. 1960–1964, Sep. 2006, doi: 10.1126/science.1129139.
- [199] F. Pagès *et al.*, "International validation of the consensus Immunoscore for the classification of colon cancer: a prognostic and accuracy study," *The Lancet*, vol. 391, no. 10135, pp. 2128–2139, May 2018, doi: 10.1016/S0140-6736(18)30789-X.
- [200] J. Galon *et al.*, "Efficacy of anti-PD1/PD-L1 immunotherapy in non-small cell lung cancer is dependent upon Immunoscore IC CD8 and PD-L1 status.," *Journal of Clinical Oncology*, vol. 40, no. 16\_suppl, pp. 2509–2509, Jun. 2022, doi: 10.1200/JCO.2022.40.16\_suppl.2509.
- [201] J.-D. Fumet *et al.*, "Prognostic and predictive role of CD8 and PD-L1 determination in lung tumor tissue of patients under anti-PD-1 therapy," *Br J Cancer*, vol. 119, no. 8, pp. 950–960, Oct. 2018, doi: 10.1038/s41416-018-0220-9.
- [202] J.-I. Youn *et al.*, "Peripheral natural killer cells and myeloid-derived suppressor cells correlate with anti-PD-1 responses in non-small cell lung cancer," *Sci Rep*, vol. 10, no. 1, p. 9050, Dec. 2020, doi: 10.1038/s41598-020-65666-x.
- [203] J. Koh *et al.*, "Regulatory (FoxP3+) T cells and TGF- $\beta$  predict the response to anti-PD-1 immunotherapy in patients with non-small cell lung cancer," *Sci Rep*, vol. 10, no. 1, p. 18994, Dec. 2020, doi: 10.1038/s41598-020-76130-1.
- [204] D. H. Kang *et al.*, "Circulating regulatory T cells predict efficacy and atypical responses in lung cancer patients treated with PD-1/PD-L1 inhibitors," *Cancer Immunology, Immunotherapy*, vol. 71, no. 3, pp. 579–588, Mar. 2022, doi: 10.1007/s00262-021-03018-y.
- [205] M. Ilie *et al.*, "Comparative study of the PD-L1 status between surgically resected specimens and matched biopsies of NSCLC patients reveal major discordances: a potential issue for anti-PD-L1 therapeutic strategies," *Annals of Oncology*, vol. 27, no. 1, pp. 147–153, Jan. 2016, doi: 10.1093/annonc/mdv489.
- [206] J. McLaughlin *et al.*, "Quantitative Assessment of the Heterogeneity of PD-L1 Expression in Non-Small-Cell Lung Cancer," *JAMA Oncol*, vol. 2, no. 1, p. 46, Jan. 2016, doi: 10.1001/jamaoncol.2015.3638.
- [207] M. Ilie *et al.*, "PD-L1 expression in basaloid squamous cell lung carcinoma: Relationship to PD-1+ and CD8+ tumor-infiltrating T cells and outcome," *Modern*

- Pathology*, vol. 29, no. 12, pp. 1552–1564, Dec. 2016, doi: 10.1038/modpathol.2016.149.
- [208] A. Ribas *et al.*, “PD-1 Blockade Expands Intratumoral Memory T Cells,” *Cancer Immunol Res*, vol. 4, no. 3, pp. 194–203, Mar. 2016, doi: 10.1158/2326-6066.CIR-15-0210.
- [209] V. Anagnostou *et al.*, “Multimodal genomic features predict outcome of immune checkpoint blockade in non-small-cell lung cancer,” *Nat Cancer*, vol. 1, no. 1, pp. 99–111, Jan. 2020, doi: 10.1038/s43018-019-0008-8.
- [210] N. McGranahan *et al.*, “Clonal neoantigens elicit T cell immunoreactivity and sensitivity to immune checkpoint blockade,” *Science (1979)*, vol. 351, no. 6280, pp. 1463–1469, Mar. 2016, doi: 10.1126/science.aaf1490.
- [211] N. A. Rizvi *et al.*, “Mutational landscape determines sensitivity to PD-1 blockade in non-small cell lung cancer,” *Science (1979)*, vol. 348, no. 6230, pp. 124–128, Apr. 2015, doi: 10.1126/science.aaa1348.
- [212] B. C. Taylor and J. M. Balko, “Mechanisms of MHC-I Downregulation and Role in Immunotherapy Response,” *Front Immunol*, vol. 13, Feb. 2022, doi: 10.3389/fimmu.2022.844866.
- [213] S. Gettinger *et al.*, “Impaired HLA Class I Antigen Processing and Presentation as a Mechanism of Acquired Resistance to Immune Checkpoint Inhibitors in Lung Cancer,” *Cancer Discov*, vol. 7, no. 12, pp. 1420–1435, Dec. 2017, doi: 10.1158/2159-8290.CD-17-0593.
- [214] C. Pereira *et al.*, “Genomic Profiling of Patient-Derived Xenografts for Lung Cancer Identifies *B2M* Inactivation Impairing Immunorecognition,” *Clinical Cancer Research*, vol. 23, no. 12, pp. 3203–3213, Jun. 2017, doi: 10.1158/1078-0432.CCR-16-1946.
- [215] S. J. Gallagher, E. Shklovskaya, and P. Hersey, “Epigenetic modulation in cancer immunotherapy,” *Curr Opin Pharmacol*, vol. 35, pp. 48–56, Aug. 2017, doi: 10.1016/j.coph.2017.05.006.
- [216] M. Kowanz *et al.*, “Differential regulation of PD-L1 expression by immune and tumor cells in NSCLC and the response to treatment with atezolizumab (anti-PD-L1),” *Proceedings of the National Academy of Sciences*, vol. 115, no. 43, Oct. 2018, doi: 10.1073/pnas.1802166115.
- [217] D. S. Thommen *et al.*, “Progression of Lung Cancer Is Associated with Increased Dysfunction of T Cells Defined by Coexpression of Multiple Inhibitory Receptors,” *Cancer Immunol Res*, vol. 3, no. 12, pp. 1344–1355, Dec. 2015, doi: 10.1158/2326-6066.CIR-15-0097.
- [218] S. Koyama *et al.*, “Adaptive resistance to therapeutic PD-1 blockade is associated with upregulation of alternative immune checkpoints,” *Nat Commun*, vol. 7, no. 1, p. 10501, Apr. 2016, doi: 10.1038/ncomms10501.
- [219] E. Limagne *et al.*, “Tim-3/galectin-9 pathway and mMDSC control primary and secondary resistances to PD-1 blockade in lung cancer patients,” *Oncoimmunology*, vol. 8, no. 4, p. e1564505, Apr. 2019, doi: 10.1080/2162402X.2018.1564505.
- [220] I. Datar *et al.*, “Expression Analysis and Significance of PD-1, LAG-3, and TIM-3 in Human Non-Small Cell Lung Cancer Using Spatially Resolved and Multiparametric Single-Cell Analysis,” *Clinical Cancer Research*, vol. 25, no. 15, pp. 4663–4673, Aug. 2019, doi: 10.1158/1078-0432.CCR-18-4142.
- [221] K. Sakuishi, L. Apetoh, J. M. Sullivan, B. R. Blazar, V. K. Kuchroo, and A. C. Anderson, “Targeting Tim-3 and PD-1 pathways to reverse T cell exhaustion and restore anti-

- tumor immunity,” *Journal of Experimental Medicine*, vol. 207, no. 10, pp. 2187–2194, Sep. 2010, doi: 10.1084/jem.20100643.
- [222] S.-R. Woo *et al.*, “Immune Inhibitory Molecules LAG-3 and PD-1 Synergistically Regulate T-cell Function to Promote Tumoral Immune Escape,” *Cancer Res*, vol. 72, no. 4, pp. 917–927, Feb. 2012, doi: 10.1158/0008-5472.CAN-11-1620.
- [223] Y. Wolf, A. C. Anderson, and V. K. Kuchroo, “TIM3 comes of age as an inhibitory receptor,” *Nat Rev Immunol*, vol. 20, no. 3, pp. 173–185, Mar. 2020, doi: 10.1038/s41577-019-0224-6.
- [224] J. Liu, Y. Luan, H. Deng, F. Wang, C. Wang, and Z. Zhang, “A bivalent Tim-3/PD-1 bispecific antibody for the treatment of PD-1 antibody resistant or refractory NSCLC,” *Journal of Clinical Oncology*, vol. 40, no. 16\_suppl, pp. e14597–e14597, Jun. 2022, doi: 10.1200/JCO.2022.40.16\_suppl.e14597.
- [225] H. C. Pühr and A. Ilhan-Mutlu, “New emerging targets in cancer immunotherapy: the role of LAG3,” *ESMO Open*, vol. 4, no. 2, p. e000482, 2019, doi: 10.1136/esmoopen-2018-000482.
- [226] J. Mazieres *et al.*, “Immune checkpoint inhibitors for patients with advanced lung cancer and oncogenic driver alterations: results from the IMMUNOTARGET registry,” *Annals of Oncology*, vol. 30, no. 8, pp. 1321–1328, Aug. 2019, doi: 10.1093/annonc/mdz167.
- [227] M. Offin *et al.*, “Immunophenotype and Response to Immunotherapy of *RET* - Rearranged Lung Cancers,” *JCO Precis Oncol*, no. 3, pp. 1–8, Dec. 2019, doi: 10.1200/PO.18.00386.
- [228] J. K. Sabari *et al.*, “PD-L1 expression, tumor mutational burden, and response to immunotherapy in patients with MET exon 14 altered lung cancers,” *Annals of Oncology*, vol. 29, no. 10, pp. 2085–2091, Oct. 2018, doi: 10.1093/annonc/mdy334.
- [229] J. Koh *et al.*, “EML4-ALK enhances programmed cell death-ligand 1 expression in pulmonary adenocarcinoma via hypoxia-inducible factor (HIF)-1 $\alpha$  and STAT3,” *Oncoimmunology*, vol. 5, no. 3, p. e1108514, Mar. 2016, doi: 10.1080/2162402X.2015.1108514.
- [230] E. A. Akbay *et al.*, “Activation of the PD-1 Pathway Contributes to Immune Escape in EGFR-Driven Lung Tumors,” *Cancer Discov*, vol. 3, no. 12, pp. 1355–1363, Dec. 2013, doi: 10.1158/2159-8290.CD-13-0310.
- [231] D. J. Lederer and F. J. Martinez, “Idiopathic Pulmonary Fibrosis,” *New England Journal of Medicine*, vol. 378, no. 19, pp. 1811–1823, May 2018, doi: 10.1056/NEJMra1705751.
- [232] T. M. Maher *et al.*, “Global incidence and prevalence of idiopathic pulmonary fibrosis,” *Respir Res*, vol. 22, no. 1, p. 197, Dec. 2021, doi: 10.1186/s12931-021-01791-z.
- [233] T. Zaman, T. Moua, E. Vittinghoff, J. H. Ryu, H. R. Collard, and J. S. Lee, “Differences in Clinical Characteristics and Outcomes Between Men and Women With Idiopathic Pulmonary Fibrosis,” *Chest*, vol. 158, no. 1, pp. 245–251, Jul. 2020, doi: 10.1016/j.chest.2020.02.009.
- [234] H. Strongman, I. Kausar, and T. M. Maher, “Incidence, Prevalence, and Survival of Patients with Idiopathic Pulmonary Fibrosis in the UK,” *Adv Ther*, vol. 35, no. 5, pp. 724–736, May 2018, doi: 10.1007/s12325-018-0693-1.

- [235] G. Raghu *et al.*, “Diagnosis of Idiopathic Pulmonary Fibrosis. An Official ATS/ERS/JRS/ALAT Clinical Practice Guideline,” *Am J Respir Crit Care Med*, vol. 198, no. 5, pp. e44–e68, Sep. 2018, doi: 10.1164/rccm.201807-1255ST.
- [236] R. Snetselaar *et al.*, “Short telomere length in IPF lung associates with fibrotic lesions and predicts survival,” *PLoS One*, vol. 12, no. 12, p. e0189467, Dec. 2017, doi: 10.1371/journal.pone.0189467.
- [237] K. Demopoulos, D. A. Arvanitis, D. A. Vassilakis, N. M. Siafakas, and D. A. Spandidos, “MYCL1, FHIT, SPARC, p16<sup>INK4</sup> and TP53 genes associated to lung cancer in idiopathic pulmonary fibrosis,” *J Cell Mol Med*, vol. 6, no. 2, pp. 215–222, Apr. 2002, doi: 10.1111/j.1582-4934.2002.tb00188.x.
- [238] C. Moore *et al.*, “Resequencing Study Confirms That Host Defense and Cell Senescence Gene Variants Contribute to the Risk of Idiopathic Pulmonary Fibrosis,” *Am J Respir Crit Care Med*, vol. 200, no. 2, pp. 199–208, Jul. 2019, doi: 10.1164/rccm.201810-1891OC.
- [239] D. N. O’Dwyer *et al.*, “The Toll-like Receptor 3 L412F Polymorphism and Disease Progression in Idiopathic Pulmonary Fibrosis,” *Am J Respir Crit Care Med*, vol. 188, no. 12, pp. 1442–1450, Dec. 2013, doi: 10.1164/rccm.201304-0760OC.
- [240] M. Whyte *et al.*, “Increased Risk of Fibrosing Alveolitis Associated with Interleukin-1 Receptor Antagonist and Tumor Necrosis Factor- $\alpha$  Gene Polymorphisms,” *Am J Respir Crit Care Med*, vol. 162, no. 2, pp. 755–758, Aug. 2000, doi: 10.1164/ajrccm.162.2.9909053.
- [241] N. M. Korthagen, C. H. M. van Moorsel, K. M. Kazemier, H. J. T. Ruven, and J. C. Grutters, “IL1RN genetic variations and risk of IPF: a meta-analysis and mRNA expression study,” *Immunogenetics*, vol. 64, no. 5, pp. 371–377, May 2012, doi: 10.1007/s00251-012-0604-6.
- [242] M. Y. Armanios *et al.*, “Telomerase Mutations in Families with Idiopathic Pulmonary Fibrosis,” *New England Journal of Medicine*, vol. 356, no. 13, pp. 1317–1326, Mar. 2007, doi: 10.1056/NEJMoa066157.
- [243] B. D. Stuart *et al.*, “Exome sequencing links mutations in PARN and RTEL1 with familial pulmonary fibrosis and telomere shortening,” *Nat Genet*, vol. 47, no. 5, pp. 512–517, May 2015, doi: 10.1038/ng.3278.
- [244] L. M. Noguee, A. E. Dunbar, S. E. Wert, F. Askin, A. Hamvas, and J. A. Whitsett, “A Mutation in the Surfactant Protein C Gene Associated with Familial Interstitial Lung Disease,” *New England Journal of Medicine*, vol. 344, no. 8, pp. 573–579, Feb. 2001, doi: 10.1056/NEJM200102223440805.
- [245] Y. Wang *et al.*, “Genetic Defects in Surfactant Protein A2 Are Associated with Pulmonary Fibrosis and Lung Cancer,” *The American Journal of Human Genetics*, vol. 84, no. 1, pp. 52–59, Jan. 2009, doi: 10.1016/j.ajhg.2008.11.010.
- [246] Y. Wang *et al.*, “MBD2 serves as a viable target against pulmonary fibrosis by inhibiting macrophage M2 program,” *Sci Adv*, vol. 7, no. 1, Jan. 2021, doi: 10.1126/sciadv.abb6075.
- [247] V. Bellou, L. Belbasis, and E. Evangelou, “Tobacco Smoking and Risk for Pulmonary Fibrosis,” *Chest*, vol. 160, no. 3, pp. 983–993, Sep. 2021, doi: 10.1016/j.chest.2021.04.035.
- [248] W. Bae, C.-H. Lee, J. Lee, Y. W. Kim, K. Han, and S. M. Choi, “Impact of smoking on the development of idiopathic pulmonary fibrosis: results from a nationwide population-



- based cohort study," *Thorax*, vol. 77, no. 5, pp. 470–476, May 2022, doi: 10.1136/thoraxjnl-2020-215386.
- [249] K. M. Antoniou *et al.*, "Idiopathic Pulmonary Fibrosis," *Am J Respir Crit Care Med*, vol. 177, no. 2, pp. 190–194, Jan. 2008, doi: 10.1164/rccm.200612-1759OC.
- [250] Y. Park, C. Ahn, and T.-H. Kim, "Occupational and environmental risk factors of idiopathic pulmonary fibrosis: a systematic review and meta-analyses," *Sci Rep*, vol. 11, no. 1, p. 4318, Dec. 2021, doi: 10.1038/s41598-021-81591-z.
- [251] N. J. Awadalla, A. Hegazy, R. A. Elmetwally, and I. Wahby, "Occupational and environmental risk factors for idiopathic pulmonary fibrosis in Egypt: a multicenter case-control study.," *Int J Occup Environ Med*, vol. 3, no. 3, pp. 107–116, Jul. 2012.
- [252] "What role for asbestos in idiopathic pulmonary fibrosis? Findings from the IPF job exposures study," *MedRxiv*, Mar. 2021, doi: <https://doi.org/10.1101/2021.03.09.21253224>.
- [253] C. J. Winterbottom *et al.*, "Exposure to Ambient Particulate Matter Is Associated With Accelerated Functional Decline in Idiopathic Pulmonary Fibrosis," *Chest*, vol. 153, no. 5, pp. 1221–1228, May 2018, doi: 10.1016/j.chest.2017.07.034.
- [254] L. Sesé *et al.*, "Role of atmospheric pollution on the natural history of idiopathic pulmonary fibrosis," *Thorax*, vol. 73, no. 2, pp. 145–150, Feb. 2018, doi: 10.1136/thoraxjnl-2017-209967.
- [255] C. Sack *et al.*, "Air pollution and subclinical interstitial lung disease: the Multi-Ethnic Study of Atherosclerosis (MESA) air–lung study," *European Respiratory Journal*, vol. 50, no. 6, p. 1700559, Dec. 2017, doi: 10.1183/13993003.00559-2017.
- [256] G. Sheng *et al.*, "Viral Infection Increases the Risk of Idiopathic Pulmonary Fibrosis," *Chest*, vol. 157, no. 5, pp. 1175–1187, May 2020, doi: 10.1016/j.chest.2019.10.032.
- [257] B. Ley *et al.*, "A Multidimensional Index and Staging System for Idiopathic Pulmonary Fibrosis," *Ann Intern Med*, vol. 156, no. 10, p. 684, May 2012, doi: 10.7326/0003-4819-156-10-201205150-00004.
- [258] M. Selman *et al.*, "Accelerated Variant of Idiopathic Pulmonary Fibrosis: Clinical Behavior and Gene Expression Pattern," *PLoS One*, vol. 2, no. 5, p. e482, May 2007, doi: 10.1371/journal.pone.0000482.
- [259] K. Boon *et al.*, "Molecular Phenotypes Distinguish Patients with Relatively Stable from Progressive Idiopathic Pulmonary Fibrosis (IPF)," *PLoS One*, vol. 4, no. 4, p. e5134, Apr. 2009, doi: 10.1371/journal.pone.0005134.
- [260] H. R. Collard *et al.*, "Acute Exacerbation of Idiopathic Pulmonary Fibrosis. An International Working Group Report," *Am J Respir Crit Care Med*, vol. 194, no. 3, pp. 265–275, Aug. 2016, doi: 10.1164/rccm.201604-0801CI.
- [261] N. I. Winters, A. Burman, J. A. Kropski, and T. S. Blackwell, "Epithelial Injury and Dysfunction in the Pathogenesis of Idiopathic Pulmonary Fibrosis," *Am J Med Sci*, vol. 357, no. 5, pp. 374–378, May 2019, doi: 10.1016/j.amjms.2019.01.010.
- [262] T. H. Sisson *et al.*, "Targeted Injury of Type II Alveolar Epithelial Cells Induces Pulmonary Fibrosis," *Am J Respir Crit Care Med*, vol. 181, no. 3, pp. 254–263, Feb. 2010, doi: 10.1164/rccm.200810-1615OC.
- [263] P.-J. Wipff, D. B. Rifkin, J.-J. Meister, and B. Hinz, "Myofibroblast contraction activates latent TGF- $\beta$ 1 from the extracellular matrix," *Journal of Cell Biology*, vol. 179, no. 6, pp. 1311–1323, Dec. 2007, doi: 10.1083/jcb.200704042.
- [264] I. E. Fernandez and O. Eickelberg, "The Impact of TGF- $\beta$  on Lung Fibrosis," *Proc Am Thorac Soc*, vol. 9, no. 3, pp. 111–116, Jul. 2012, doi: 10.1513/pats.201203-023AW.

- [265] A. Bellini and S. Mattoli, "The role of the fibrocyte, a bone marrow-derived mesenchymal progenitor, in reactive and reparative fibroses," *Laboratory Investigation*, vol. 87, no. 9, pp. 858–870, Sep. 2007, doi: 10.1038/labinvest.3700654.
- [266] F. Salton, M. Volpe, and M. Confalonieri, "Epithelial–Mesenchymal Transition in the Pathogenesis of Idiopathic Pulmonary Fibrosis," *Medicina (B Aires)*, vol. 55, no. 4, p. 83, Mar. 2019, doi: 10.3390/medicina55040083.
- [267] B. Hinz and D. Lagares, "Evasion of apoptosis by myofibroblasts: a hallmark of fibrotic diseases," *Nat Rev Rheumatol*, vol. 16, no. 1, pp. 11–31, Jan. 2020, doi: 10.1038/s41584-019-0324-5.
- [268] D. Lutz *et al.*, "Alveolar Derecruitment and Collapse Induration as Crucial Mechanisms in Lung Injury and Fibrosis," *Am J Respir Cell Mol Biol*, vol. 52, no. 2, pp. 232–243, Feb. 2015, doi: 10.1165/rcmb.2014-0078OC.
- [269] M. L. Smith, "The histologic diagnosis of usual interstitial pneumonia of idiopathic pulmonary fibrosis. Where we are and where we need to go," *Modern Pathology*, vol. 35, no. S1, pp. 8–14, Jan. 2022, doi: 10.1038/s41379-021-00889-5.
- [270] H. O. Coxson *et al.*, "Quantification of idiopathic pulmonary fibrosis using computed tomography and histology.," *Am J Respir Crit Care Med*, vol. 155, no. 5, pp. 1649–1656, May 1997, doi: 10.1164/ajrccm.155.5.9154871.
- [271] N. Tanabe *et al.*, "Pathology of Idiopathic Pulmonary Fibrosis Assessed by a Combination of Microcomputed Tomography, Histology, and Immunohistochemistry," *Am J Pathol*, vol. 190, no. 12, pp. 2427–2435, Dec. 2020, doi: 10.1016/j.ajpath.2020.09.001.
- [272] "Prednisone, Azathioprine, and N -Acetylcysteine for Pulmonary Fibrosis," *New England Journal of Medicine*, vol. 366, no. 21, pp. 1968–1977, May 2012, doi: 10.1056/NEJMoa1113354.
- [273] C. D. Ellson, R. Dunmore, C. M. Hogaboam, M. A. Sleeman, and L. A. Murray, "Danger-Associated Molecular Patterns and Danger Signals in Idiopathic Pulmonary Fibrosis," *Am J Respir Cell Mol Biol*, vol. 51, no. 2, pp. 163–168, Aug. 2014, doi: 10.1165/rcmb.2013-0366TR.
- [274] Y. Lai, X. Wei, T. Ye, L. Hang, L. Mou, and J. Su, "Interrelation Between Fibroblasts and T Cells in Fibrosing Interstitial Lung Diseases," *Front Immunol*, vol. 12, Nov. 2021, doi: 10.3389/fimmu.2021.747335.
- [275] B. B. Moore *et al.*, "Protection from Pulmonary Fibrosis in the Absence of CCR2 Signaling," *The Journal of Immunology*, vol. 167, no. 8, pp. 4368–4377, Oct. 2001, doi: 10.4049/jimmunol.167.8.4368.
- [276] M. A. Gibbons *et al.*, "Ly6Chi monocytes direct alternatively activated profibrotic macrophage regulation of lung fibrosis.," *Am J Respir Crit Care Med*, vol. 184, no. 5, pp. 569–81, Sep. 2011, doi: 10.1164/rccm.201010-1719OC.
- [277] M. Suga, K. Iyonaga, H. Ichiyasu, N. Saita, H. Yamasaki, and M. Ando, "Clinical significance of MCP-1 levels in BALF and serum in patients with interstitial lung diseases," *European Respiratory Journal*, vol. 14, no. 2, p. 376, Aug. 1999, doi: 10.1034/j.1399-3003.1999.14b23.x.
- [278] K. Iyonaga *et al.*, "Monocyte chemoattractant protein-1 in idiopathic pulmonary fibrosis and other interstitial lung diseases," *Hum Pathol*, vol. 25, no. 5, pp. 455–463, May 1994, doi: 10.1016/0046-8177(94)90117-1.
- [279] C. P. Baran *et al.*, "Important Roles for Macrophage Colony-stimulating Factor, CC Chemokine Ligand 2, and Mononuclear Phagocytes in the Pathogenesis of Pulmonary

- Fibrosis," *Am J Respir Crit Care Med*, vol. 176, no. 1, pp. 78–89, Jul. 2007, doi: 10.1164/rccm.200609-1279OC.
- [280] M. Kreuter *et al.*, "Monocyte Count as a Prognostic Biomarker in Patients with Idiopathic Pulmonary Fibrosis," *Am J Respir Crit Care Med*, vol. 204, no. 1, pp. 74–81, 2021, doi: 10.1164/rccm.202003-0669OC.
- [281] M. K. D. Scott *et al.*, "Increased monocyte count as a cellular biomarker for poor outcomes in fibrotic diseases: a retrospective, multicentre cohort study," *Lancet Respir Med*, vol. 7, no. 6, pp. 497–508, 2019, doi: 10.1016/S2213-2600(18)30508-3.
- [282] Y.-Z. Liu, S. Saito, G. F. Morris, C. A. Miller, J. Li, and J. J. Lefante, "Proportions of resting memory T cells and monocytes in blood have prognostic significance in idiopathic pulmonary fibrosis," *Genomics*, vol. 111, no. 6, pp. 1343–1350, Dec. 2019, doi: 10.1016/j.ygeno.2018.09.006.
- [283] A. v. Misharin *et al.*, "Monocyte-derived alveolar macrophages drive lung fibrosis and persist in the lung over the life span.," *J Exp Med*, vol. 214, no. 8, pp. 2387–2404, Aug. 2017, doi: 10.1084/jem.20162152.
- [284] W.-J. Ji *et al.*, "Spironolactone Attenuates Bleomycin-Induced Pulmonary Injury Partially via Modulating Mononuclear Phagocyte Phenotype Switching in Circulating and Alveolar Compartments," *PLoS One*, vol. 8, no. 11, p. e81090, Nov. 2013, doi: 10.1371/journal.pone.0081090.
- [285] L. A. Murray *et al.*, "TGF-beta driven lung fibrosis is macrophage dependent and blocked by Serum amyloid P," *Int J Biochem Cell Biol*, vol. 43, no. 1, pp. 154–162, Jan. 2011, doi: 10.1016/j.biocel.2010.10.013.
- [286] S. P. Atamas *et al.*, "Pulmonary and Activation-Regulated Chemokine Stimulates Collagen Production in Lung Fibroblasts," *Am J Respir Cell Mol Biol*, vol. 29, no. 6, pp. 743–749, Dec. 2003, doi: 10.1165/rcmb.2003-0078OC.
- [287] I. G. Luzina, N. Tsybalyuk, J. Choi, J. D. Hasday, and S. P. Atamas, "CCL18-stimulated upregulation of collagen production in lung fibroblasts requires Sp1 signaling and basal Smad3 activity," *J Cell Physiol*, vol. 206, no. 1, pp. 221–228, Jan. 2006, doi: 10.1002/jcp.20452.
- [288] I. G. Luzina, K. Highsmith, K. Pochetuhin, N. Nacu, J. N. Rao, and S. P. Atamas, "PKC $\alpha$  Mediates CCL18-Stimulated Collagen Production in Pulmonary Fibroblasts," *Am J Respir Cell Mol Biol*, vol. 35, no. 3, pp. 298–305, Sep. 2006, doi: 10.1165/rcmb.2006-0033OC.
- [289] G. Karakiulakis, E. Papakonstantinou, A. J. Aletras, M. Tamm, and M. Roth, "Cell Type-specific Effect of Hypoxia and Platelet-derived Growth Factor-BB on Extracellular Matrix Turnover and Its Consequences for Lung Remodeling," *Journal of Biological Chemistry*, vol. 282, no. 2, pp. 908–915, Jan. 2007, doi: 10.1074/jbc.M602178200.
- [290] M. Dadrich *et al.*, "Combined inhibition of TGF $\beta$  and PDGF signaling attenuates radiation-induced pulmonary fibrosis," *Oncoimmunology*, vol. 5, no. 5, p. e1123366, May 2016, doi: 10.1080/2162402X.2015.1123366.
- [291] P. A. Reyfman *et al.*, "Single-Cell Transcriptomic Analysis of Human Lung Provides Insights into the Pathobiology of Pulmonary Fibrosis," *Am J Respir Crit Care Med*, vol. 199, no. 12, pp. 1517–1536, Jun. 2019, doi: 10.1164/rccm.201712-2410OC.
- [292] J. C. Schupp *et al.*, "Macrophage Activation in Acute Exacerbation of Idiopathic Pulmonary Fibrosis," *PLoS One*, vol. 10, no. 1, p. e0116775, Jan. 2015, doi: 10.1371/journal.pone.0116775.

- [293] A. Prasse *et al.*, “A Vicious Circle of Alveolar Macrophages and Fibroblasts Perpetuates Pulmonary Fibrosis via CCL18,” *Am J Respir Crit Care Med*, vol. 173, no. 7, pp. 781–792, Apr. 2006, doi: 10.1164/rccm.200509-1518OC.
- [294] H.-Z. Yang *et al.*, “Targeting TLR2 Attenuates Pulmonary Inflammation and Fibrosis by Reversion of Suppressive Immune Microenvironment,” *The Journal of Immunology*, vol. 182, no. 1, pp. 692–702, Jan. 2009, doi: 10.4049/jimmunol.182.1.692.
- [295] D. Jiang *et al.*, “Regulation of lung injury and repair by Toll-like receptors and hyaluronan,” *Nat Med*, vol. 11, no. 11, pp. 1173–1179, Nov. 2005, doi: 10.1038/nm1315.
- [296] A. Paun, J. Fox, V. Balloy, M. Chignard, S. T. Qureshi, and C. K. Haston, “Combined Tlr2 and Tlr4 Deficiency Increases Radiation-Induced Pulmonary Fibrosis in Mice,” *International Journal of Radiation Oncology\*Biophysics*, vol. 77, no. 4, pp. 1198–1205, Jul. 2010, doi: 10.1016/j.ijrobp.2009.12.065.
- [297] A. Paun, M.-E. Bergeron, and C. K. Haston, “The Th1/Th17 balance dictates the fibrosis response in murine radiation-induced lung disease,” *Sci Rep*, vol. 7, no. 1, p. 11586, Dec. 2017, doi: 10.1038/s41598-017-11656-5.
- [298] M. Kolb, P. J. Margetts, D. C. Anthony, F. Pitossi, and J. Gauldie, “Transient expression of IL-1 $\beta$  induces acute lung injury and chronic repair leading to pulmonary fibrosis,” *Journal of Clinical Investigation*, vol. 107, no. 12, pp. 1529–1536, Jun. 2001, doi: 10.1172/JCI12568.
- [299] P. Gasse *et al.*, “IL-1R1/MyD88 signaling and the inflammasome are essential in pulmonary inflammation and fibrosis in mice,” *J Clin Invest*, vol. 117, no. 12, pp. 3786–99, Dec. 2007, doi: 10.1172/JCI32285.
- [300] M. P. Keane, J. A. Belperio, M. D. Burdick, and R. M. Strieter, “IL-12 attenuates bleomycin-induced pulmonary fibrosis,” *American Journal of Physiology-Lung Cellular and Molecular Physiology*, vol. 281, no. 1, pp. L92–L97, Jul. 2001, doi: 10.1152/ajplung.2001.281.1.L92.
- [301] F. Zhang *et al.*, “Reprogramming of profibrotic macrophages for treatment of bleomycin-induced pulmonary fibrosis,” *EMBO Mol Med*, vol. 12, no. 8, Aug. 2020, doi: 10.15252/emmm.202012034.
- [302] B. Manoury, S. Nénan, I. Guénon, V. Lagente, and E. Boichot, “Influence of early neutrophil depletion on MMPs/TIMP-1 balance in bleomycin-induced lung fibrosis,” *Int Immunopharmacol*, vol. 7, no. 7, pp. 900–911, Jul. 2007, doi: 10.1016/j.intimp.2007.02.009.
- [303] R. S. Thrall, S. H. Phan, J. R. McCormick, and P. A. Ward, “The development of bleomycin-induced pulmonary fibrosis in neutrophil-depleted and complement-depleted rats,” *Am J Pathol*, vol. 105, no. 1, pp. 76–81, Oct. 1981.
- [304] F. Chua *et al.*, “Mice Lacking Neutrophil Elastase Are Resistant to Bleomycin-Induced Pulmonary Fibrosis,” *Am J Pathol*, vol. 170, no. 1, pp. 65–74, Jan. 2007, doi: 10.2353/ajpath.2007.060352.
- [305] A. D. Gregory *et al.*, “Neutrophil elastase promotes myofibroblast differentiation in lung fibrosis,” *J Leukoc Biol*, vol. 98, no. 2, pp. 143–152, Aug. 2015, doi: 10.1189/jlb.3HI1014-493R.
- [306] A. Chrysanthopoulou *et al.*, “Neutrophil extracellular traps promote differentiation and function of fibroblasts,” *J Pathol*, vol. 233, no. 3, pp. 294–307, Jul. 2014, doi: 10.1002/path.4359.

- [307] A. Achaiah *et al.*, "Neutrophil lymphocyte ratio as an indicator for disease progression in Idiopathic Pulmonary Fibrosis," *BMJ Open Respir Res*, vol. 9, no. 1, p. e001202, Jun. 2022, doi: 10.1136/bmjresp-2022-001202.
- [308] A. Achaiah *et al.*, "Monocyte and neutrophil levels are potentially linked to progression to IPF for patients with indeterminate UIP CT pattern," *BMJ Open Respir Res*, vol. 8, no. 1, p. e000899, Nov. 2021, doi: 10.1136/bmjresp-2021-000899.
- [309] B. W. Kinder, K. K. Brown, M. I. Schwarz, J. H. Ix, A. Kervitsky, and T. E. King, "Baseline BAL Neutrophilia Predicts Early Mortality in Idiopathic Pulmonary Fibrosis," *Chest*, vol. 133, no. 1, pp. 226–232, Jan. 2008, doi: 10.1378/chest.07-1948.
- [310] Y. Obayashi, I. Yamadori, J. Fujita, T. Yoshinouchi, N. Ueda, and J. Takahara, "The Role of Neutrophils in the Pathogenesis of Idiopathic Pulmonary Fibrosis," *Chest*, vol. 112, no. 5, pp. 1338–1343, Nov. 1997, doi: 10.1378/chest.112.5.1338.
- [311] M. W. ZIEGENHAGEN, P. ZABEL, G. ZISSEL, M. SCHLAAK, and J. MÜLLER-QUERNHEIM, "Serum Level of Interleukin 8 Is Elevated in Idiopathic Pulmonary Fibrosis and Indicates Disease Activity," *Am J Respir Crit Care Med*, vol. 157, no. 3, pp. 762–768, Mar. 1998, doi: 10.1164/ajrccm.157.3.9705014.
- [312] J. -i. Ashitani *et al.*, "Granulocyte-colony stimulating factor levels in bronchoalveolar lavage fluid from patients with idiopathic pulmonary fibrosis," *Thorax*, vol. 54, no. 11, pp. 1015–1020, Nov. 1999, doi: 10.1136/thx.54.11.1015.
- [313] H. Hao, D. A. Cohen, C. D. Jennings, J. S. Bryson, and A. M. Kaplan, "Bleomycin-induced pulmonary fibrosis is independent of eosinophils," *J Leukoc Biol*, vol. 68, no. 4, pp. 515–21, Oct. 2000.
- [314] Y. Morimoto *et al.*, "Amphiregulin-Producing Pathogenic Memory T Helper 2 Cells Instruct Eosinophils to Secrete Osteopontin and Facilitate Airway Fibrosis.," *Immunity*, vol. 49, no. 1, pp. 134-150.e6, 2018, doi: 10.1016/j.immuni.2018.04.023.
- [315] P. C. Fulkerson, C. A. Fischetti, and M. E. Rothenberg, "Eosinophils and CCR3 Regulate Interleukin-13 Transgene-Induced Pulmonary Remodeling," *Am J Pathol*, vol. 169, no. 6, pp. 2117–2126, Dec. 2006, doi: 10.2353/ajpath.2006.060617.
- [316] J. Y. Cho *et al.*, "Inhibition of airway remodeling in IL-5-deficient mice," *Journal of Clinical Investigation*, vol. 113, no. 4, pp. 551–560, Feb. 2004, doi: 10.1172/JCI19133.
- [317] F. Huaux, T. Liu, B. McGarry, M. Ullenbruch, Z. Xing, and S. H. Phan, "Eosinophils and T Lymphocytes Possess Distinct Roles in Bleomycin-Induced Lung Injury and Fibrosis," *The Journal of Immunology*, vol. 171, no. 10, pp. 5470–5481, Nov. 2003, doi: 10.4049/jimmunol.171.10.5470.
- [318] D. Galati, S. Zanotta, G. E. Polistina, A. Coppola, L. Capitelli, and M. Bocchino, "Circulating dendritic cells are severely decreased in idiopathic pulmonary fibrosis with a potential value for prognosis prediction," *Clinical Immunology*, vol. 215, p. 108454, Jun. 2020, doi: 10.1016/j.clim.2020.108454.
- [319] J. Marchal-Sommé *et al.*, "Dendritic Cells Accumulate in Human Fibrotic Interstitial Lung Disease," *Am J Respir Crit Care Med*, vol. 176, no. 10, pp. 1007–1014, Nov. 2007, doi: 10.1164/rccm.200609-1347OC.
- [320] M. Tsoumakidou, K. P. Karagiannis, I. Bouloukaki, S. Zakyntinos, N. Tzanakis, and N. M. Sifakas, "Increased Bronchoalveolar Lavage Fluid CD1c Expressing Dendritic Cells in Idiopathic Pulmonary Fibrosis," *Respiration*, vol. 78, no. 4, pp. 446–452, 2009, doi: 10.1159/000226244.
- [321] J. Marchal-Sommé *et al.*, "Cutting edge: nonproliferating mature immune cells form a novel type of organized lymphoid structure in idiopathic pulmonary fibrosis.," *J*

- Immunol*, vol. 176, no. 10, pp. 5735–9, May 2006, doi: 10.4049/jimmunol.176.10.5735.
- [322] O. Freynet *et al.*, “Human lung fibroblasts may modulate dendritic cell phenotype and function: results from a pilot in vitro study,” *Respir Res*, vol. 17, no. 1, p. 36, Dec. 2016, doi: 10.1186/s12931-016-0345-4.
- [323] M. Tort Tarrés *et al.*, “The FMS-like tyrosine kinase-3 ligand/lung dendritic cell axis contributes to regulation of pulmonary fibrosis,” *Thorax*, vol. 74, no. 10, pp. 947–957, Oct. 2019, doi: 10.1136/thoraxjnl-2018-212603.
- [324] A. M. Manicone, I. Huizar, and J. K. McGuire, “Matrilysin (Matrix Metalloproteinase-7) regulates anti-inflammatory and antifibrotic pulmonary dendritic cells that express CD103 (alpha(E)beta(7)-integrin).,” *Am J Pathol*, vol. 175, no. 6, pp. 2319–31, Dec. 2009, doi: 10.2353/ajpath.2009.090101.
- [325] K. Shenderov, S. L. Collins, J. D. Powell, and M. R. Horton, “Immune dysregulation as a driver of idiopathic pulmonary fibrosis.,” *J Clin Invest*, vol. 131, no. 2, 2021, doi: 10.1172/JCI143226.
- [326] T. A. Wynn, “Fibrotic disease and the TH1/TH2 paradigm,” *Nat Rev Immunol*, vol. 4, no. 8, pp. 583–594, Aug. 2004, doi: 10.1038/nri1412.
- [327] J. A. Elias, S. A. Jimenez, and B. Freundlich, “Recombinant gamma, alpha, and beta interferon regulation of human lung fibroblast proliferation.,” *Am Rev Respir Dis*, vol. 135, no. 1, pp. 62–5, Jan. 1987, doi: 10.1164/arrd.1987.135.1.62.
- [328] L. Ulloa, J. Doody, and J. Massagué, “Inhibition of transforming growth factor-beta/SMAD signalling by the interferon-gamma/STAT pathway.,” *Nature*, vol. 397, no. 6721, pp. 710–3, Feb. 1999, doi: 10.1038/17826.
- [329] J. Varga, A. Olsen, J. Herhal, G. Constantine, J. Rosenbloom, and S. A. Jimenez, “Interferon-gamma reverses the stimulation of collagen but not fibronectin gene expression by transforming growth factor-beta in normal human fibroblasts.,” *Eur J Clin Invest*, vol. 20, no. 5, pp. 487–93, Oct. 1990, doi: 10.1111/j.1365-2362.1990.tb01890.x.
- [330] M. R. Duncan and B. Berman, “Gamma interferon is the lymphokine and beta interferon the monokine responsible for inhibition of fibroblast collagen production and late but not early fibroblast proliferation.,” *J Exp Med*, vol. 162, no. 2, pp. 516–27, Aug. 1985, doi: 10.1084/jem.162.2.516.
- [331] P. Gillery *et al.*, “Gamma-interferon inhibits extracellular matrix synthesis and remodeling in collagen lattice cultures of normal and scleroderma skin fibroblasts.,” *Eur J Cell Biol*, vol. 57, no. 2, pp. 244–53, Apr. 1992.
- [332] G. Gurujeyalakshmi and S. N. Giri, “Molecular mechanisms of antifibrotic effect of interferon gamma in bleomycin-mouse model of lung fibrosis: downregulation of TGF-beta and procollagen I and III gene expression.,” *Exp Lung Res*, vol. 21, no. 5, pp. 791–808, doi: 10.3109/01902149509050842.
- [333] W. Yuan, T. Yufit, L. Li, Y. Mori, S. J. Chen, and J. Varga, “Negative modulation of alpha1(I) procollagen gene expression in human skin fibroblasts: transcriptional inhibition by interferon-gamma.,” *J Cell Physiol*, vol. 179, no. 1, pp. 97–108, Apr. 1999, doi: 10.1002/(SICI)1097-4652(199904)179:1<97::AID-JCP12>3.0.CO;2-E.
- [334] S. L. Collins *et al.*, “Vaccinia vaccine-based immunotherapy arrests and reverses established pulmonary fibrosis,” *JCI Insight*, vol. 1, no. 4, Apr. 2016, doi: 10.1172/jci.insight.83116.

- [335] M. EMURA, S. NAGAI, M. TAKEUCHI, M. KITAICHI, and T. IZUMI, "In vitro production of B cell growth factor and B cell differentiation factor by peripheral blood mononuclear cells and bronchoalveolar lavage T lymphocytes from patients with idiopathic pulmonary fibrosis," *Clin Exp Immunol*, vol. 82, no. 1, pp. 133–139, Jun. 2008, doi: 10.1111/j.1365-2249.1990.tb05416.x.
- [336] I. G. Luzina, N. W. Todd, A. T. Iacono, and S. P. Atamas, "Roles of T lymphocytes in pulmonary fibrosis.," *J Leukoc Biol*, vol. 83, no. 2, pp. 237–44, Feb. 2008, doi: 10.1189/jlb.0707504.
- [337] K. Oh, M. W. Seo, Y. W. Kim, and D.-S. Lee, "Osteopontin Potentiates Pulmonary Inflammation and Fibrosis by Modulating IL-17/IFN- $\gamma$ -secreting T-cell Ratios in Bleomycin-treated Mice.," *Immune Netw*, vol. 15, no. 3, pp. 142–9, Jun. 2015, doi: 10.4110/in.2015.15.3.142.
- [338] C. Prior and P. L. Haslam, "In vivo levels and in vitro production of interferon-gamma in fibrosing interstitial lung diseases.," *Clin Exp Immunol*, vol. 88, no. 2, pp. 280–7, May 1992, doi: 10.1111/j.1365-2249.1992.tb03074.x.
- [339] L. J. Celada *et al.*, "PD-1 up-regulation on CD4<sup>+</sup> T cells promotes pulmonary fibrosis through STAT3-mediated IL-17A and TGF- $\beta$ 1 production," *Sci Transl Med*, vol. 10, no. 460, Sep. 2018, doi: 10.1126/scitranslmed.aar8356.
- [340] S.-W. Park *et al.*, "Interleukin-13 and Its Receptors in Idiopathic Interstitial Pneumonia: Clinical Implications for Lung Function," *J Korean Med Sci*, vol. 24, no. 4, p. 614, 2009, doi: 10.3346/jkms.2009.24.4.614.
- [341] J. A. Belperio *et al.*, "Interaction of IL-13 and C10 in the Pathogenesis of Bleomycin-Induced Pulmonary Fibrosis," *Am J Respir Cell Mol Biol*, vol. 27, no. 4, pp. 419–427, Oct. 2002, doi: 10.1165/rcmb.2002-0009OC.
- [342] Z. Zhu *et al.*, "Pulmonary expression of interleukin-13 causes inflammation, mucus hypersecretion, subepithelial fibrosis, physiologic abnormalities, and eotaxin production," *Journal of Clinical Investigation*, vol. 103, no. 6, pp. 779–788, Mar. 1999, doi: 10.1172/JCI5909.
- [343] R. M. Reiman *et al.*, "Interleukin-5 (IL-5) Augments the Progression of Liver Fibrosis by Regulating IL-13 Activity," *Infect Immun*, vol. 74, no. 3, pp. 1471–1479, Mar. 2006, doi: 10.1128/IAI.74.3.1471-1479.2006.
- [344] A. Saito, H. Okazaki, I. Sugawara, K. Yamamoto, and H. Takizawa, "Potential Action of IL-4 and IL-13 as Fibrogenic Factors on Lung Fibroblasts in vitro," *Int Arch Allergy Immunol*, vol. 132, no. 2, pp. 168–176, 2003, doi: 10.1159/000073718.
- [345] L. A. Murray *et al.*, "Hyper-responsiveness of IPF/UIP fibroblasts: Interplay between TGF $\beta$ 1, IL-13 and CCL2," *Int J Biochem Cell Biol*, vol. 40, no. 10, pp. 2174–2182, Jan. 2008, doi: 10.1016/j.biocel.2008.02.016.
- [346] C. G. Lee *et al.*, "Interleukin-13 Induces Tissue Fibrosis by Selectively Stimulating and Activating Transforming Growth Factor  $\beta$ 1," *Journal of Experimental Medicine*, vol. 194, no. 6, pp. 809–822, Sep. 2001, doi: 10.1084/jem.194.6.809.
- [347] T. E. King *et al.*, "Effect of interferon gamma-1b on survival in patients with idiopathic pulmonary fibrosis (INSPIRE): a multicentre, randomised, placebo-controlled trial.," *Lancet*, vol. 374, no. 9685, pp. 222–8, Jul. 2009, doi: 10.1016/S0140-6736(09)60551-1.
- [348] J. M. Parker *et al.*, "A Phase 2 Randomized Controlled Study of Tralokinumab in Subjects with Idiopathic Pulmonary Fibrosis," *Am J Respir Crit Care Med*, vol. 197, no. 1, pp. 94–103, Jan. 2018, doi: 10.1164/rccm.201704-0784OC.

- [349] K. T. Diaz *et al.*, "Delivery and safety of inhaled interferon- $\gamma$  in idiopathic pulmonary fibrosis," *J Aerosol Med Pulm Drug Deliv*, vol. 25, no. 2, pp. 79–87, Apr. 2012, doi: 10.1089/jamp.2011.0919.
- [350] T. Fusiak, G. C. Smaldone, and R. Condos, "Pulmonary Fibrosis Treated with Inhaled Interferon-gamma (IFN- $\gamma$ )," *J Aerosol Med Pulm Drug Deliv*, vol. 28, no. 5, pp. 406–10, Oct. 2015, doi: 10.1089/jamp.2015.1221.
- [351] S. D. Skaria, J. Yang, R. Condos, and G. C. Smaldone, "Inhaled Interferon and Diffusion Capacity in Idiopathic Pulmonary Fibrosis (IPF)," *Sarcoidosis Vasc Diffuse Lung Dis*, vol. 32, no. 1, pp. 37–42, Jun. 2015.
- [352] G. C. Smaldone, "Repurposing of gamma interferon via inhalation delivery," *Adv Drug Deliv Rev*, vol. 133, pp. 87–92, 2018, doi: 10.1016/j.addr.2018.06.004.
- [353] E. Cipolla *et al.*, "IL-17A deficiency mitigates bleomycin-induced complement activation during lung fibrosis," *The FASEB Journal*, vol. 31, no. 12, pp. 5543–5556, Dec. 2017, doi: 10.1096/fj.201700289R.
- [354] S. Mi *et al.*, "Blocking IL-17A Promotes the Resolution of Pulmonary Inflammation and Fibrosis Via TGF- $\beta$ 1-Dependent and -Independent Mechanisms," *The Journal of Immunology*, vol. 187, no. 6, pp. 3003–3014, Sep. 2011, doi: 10.4049/jimmunol.1004081.
- [355] M. S. Wilson *et al.*, "Bleomycin and IL-1 $\beta$ -mediated pulmonary fibrosis is IL-17A dependent," *J Exp Med*, vol. 207, no. 3, pp. 535–52, Mar. 2010, doi: 10.1084/jem.20092121.
- [356] T. Wang, Y. Liu, J.-F. Zou, and Z.-S. Cheng, "Interleukin-17 induces human alveolar epithelial to mesenchymal cell transition via the TGF- $\beta$ 1 mediated Smad2/3 and ERK1/2 activation," *PLoS One*, vol. 12, no. 9, p. e0183972, Sep. 2017, doi: 10.1371/journal.pone.0183972.
- [357] J. Zhang *et al.*, "Profibrotic effect of IL-17A and elevated IL-17RA in idiopathic pulmonary fibrosis and rheumatoid arthritis-associated lung disease support a direct role for IL-17A/IL-17RA in human fibrotic interstitial lung disease," *American Journal of Physiology-Lung Cellular and Molecular Physiology*, vol. 316, no. 3, pp. L487–L497, Mar. 2019, doi: 10.1152/ajplung.00301.2018.
- [358] G. J. Nuovo *et al.*, "The distribution of immunomodulatory cells in the lungs of patients with idiopathic pulmonary fibrosis," *Modern Pathology*, vol. 25, no. 3, pp. 416–433, Mar. 2012, doi: 10.1038/modpathol.2011.166.
- [359] S. Z. Birjandi *et al.*, "CD4+CD25<sup>hi</sup>Foxp3+ Cells Exacerbate Bleomycin-Induced Pulmonary Fibrosis," *Am J Pathol*, vol. 186, no. 8, pp. 2008–2020, Aug. 2016, doi: 10.1016/j.ajpath.2016.03.020.
- [360] S. Xiong *et al.*, "Treg depletion attenuates irradiation-induced pulmonary fibrosis by reducing fibrocyte accumulation, inducing Th17 response, and shifting IFN- $\gamma$ , IL-12/IL-4, IL-5 balance," *Immunobiology*, vol. 220, no. 11, pp. 1284–1291, Nov. 2015, doi: 10.1016/j.imbio.2015.07.001.
- [361] K. Chakraborty, S. Chatterjee, and A. Bhattacharyya, "Impact of Treg on other T cell subsets in progression of fibrosis in experimental lung fibrosis," *Tissue Cell*, vol. 53, pp. 87–92, Aug. 2018, doi: 10.1016/j.tice.2018.06.003.
- [362] X. Peng *et al.*, "CD4+CD25+FoxP3+ Regulatory Tregs inhibit fibrocyte recruitment and fibrosis via suppression of FGF-9 production in the TGF- $\beta$ 1 exposed murine lung," *Front Pharmacol*, vol. 5, May 2014, doi: 10.3389/fphar.2014.00080.



- [363] I. Kotsianidis *et al.*, "Global Impairment of CD4 + CD25 + FOXP3 + Regulatory T Cells in Idiopathic Pulmonary Fibrosis," *Am J Respir Crit Care Med*, vol. 179, no. 12, pp. 1121–1130, Jun. 2009, doi: 10.1164/rccm.200812-1936OC.
- [364] Z. Hou, Q. Ye, M. Qiu, Y. Hao, J. Han, and H. Zeng, "Increased activated regulatory T cells proportion correlate with the severity of idiopathic pulmonary fibrosis," *Respir Res*, vol. 18, no. 1, p. 170, Dec. 2017, doi: 10.1186/s12931-017-0653-3.
- [365] Z. Daniil *et al.*, "CD8+ T lymphocytes in lung tissue from patients with idiopathic pulmonary fibrosis," *Respir Res*, vol. 6, no. 1, p. 81, Dec. 2005, doi: 10.1186/1465-9921-6-81.
- [366] S. A. Papiris *et al.*, "CD8+ T lymphocytes in bronchoalveolar lavage in idiopathic pulmonary fibrosis," *J Inflamm*, vol. 4, no. 1, p. 14, 2007, doi: 10.1186/1476-9255-4-14.
- [367] E. Fireman *et al.*, "Predictive value of response to treatment of T-lymphocyte subpopulations in idiopathic pulmonary fibrosis," *Eur Respir J*, vol. 11, no. 3, pp. 706–711, Mar. 1998.
- [368] I. Yamadori *et al.*, "Lymphocyte Subsets in Lung Tissues of Non-specific Interstitial Pneumonia and Pulmonary Fibrosis Associated with Collagen Vascular Disorders: Correlation with CD4/CD8 Ratio in Bronchoalveolar Lavage," *Lung*, vol. 178, no. 6, pp. 361–370, Nov. 2000, doi: 10.1007/s004080000037.
- [369] S. A. Papiris *et al.*, "Relationship of BAL and Lung Tissue CD4+ and CD8+ T Lymphocytes, and Their Ratio in Idiopathic Pulmonary Fibrosis," *Chest*, vol. 128, no. 4, pp. 2971–2977, Oct. 2005, doi: 10.1016/S0012-3692(15)52722-0.
- [370] T. Y. Brodeur, T. E. Robidoux, J. S. Weinstein, J. Craft, S. L. Swain, and A. Marshak-Rothstein, "IL-21 Promotes Pulmonary Fibrosis through the Induction of Profibrotic CD8+ T Cells," *The Journal of Immunology*, vol. 195, no. 11, pp. 5251–5260, Dec. 2015, doi: 10.4049/jimmunol.1500777.
- [371] D. M. Habel *et al.*, "Characterization of CD28null T cells in idiopathic pulmonary fibrosis," *Mucosal Immunol*, vol. 12, no. 1, pp. 212–222, Jan. 2019, doi: 10.1038/s41385-018-0082-8.
- [372] E. Conte, E. Gili, E. Fagone, M. Fruciano, M. Iemmolo, and C. Vancheri, "Effect of pirfenidone on proliferation, TGF- $\beta$ -induced myofibroblast differentiation and fibrogenic activity of primary human lung fibroblasts," *European Journal of Pharmaceutical Sciences*, vol. 58, pp. 13–19, Jul. 2014, doi: 10.1016/j.ejps.2014.02.014.
- [373] S. Nakayama *et al.*, "Pirfenidone inhibits the expression of HSP47 in TGF- $\beta$ 1-stimulated human lung fibroblasts," *Life Sci*, vol. 82, no. 3–4, pp. 210–217, Jan. 2008, doi: 10.1016/j.lfs.2007.11.003.
- [374] S. T. Lehtonen *et al.*, "Pirfenidone and nintedanib modulate properties of fibroblasts and myofibroblasts in idiopathic pulmonary fibrosis," *Respir Res*, vol. 17, no. 1, p. 14, Dec. 2016, doi: 10.1186/s12931-016-0328-5.
- [375] L. Knüppel *et al.*, "A Novel Antifibrotic Mechanism of Nintedanib and Pirfenidone. Inhibition of Collagen Fibril Assembly," *Am J Respir Cell Mol Biol*, vol. 57, no. 1, pp. 77–90, Jul. 2017, doi: 10.1165/rcmb.2016-0217OC.
- [376] H. Oku *et al.*, "Antifibrotic action of pirfenidone and prednisolone: different effects on pulmonary cytokines and growth factors in bleomycin-induced murine pulmonary fibrosis," *Eur J Pharmacol*, vol. 590, no. 1–3, pp. 400–8, Aug. 2008, doi: 10.1016/j.ejphar.2008.06.046.

- [377] S. N. Iyer, G. Gurujeyalakshmi, and S. N. Giri, "Effects of pirfenidone on transforming growth factor-beta gene expression at the transcriptional level in bleomycin hamster model of lung fibrosis.," *J Pharmacol Exp Ther*, vol. 291, no. 1, pp. 367–73, Oct. 1999.
- [378] M. Inomata *et al.*, "Pirfenidone inhibits fibrocyte accumulation in the lungs in bleomycin-induced murine pulmonary fibrosis," *Respir Res*, vol. 15, no. 1, p. 16, Dec. 2014, doi: 10.1186/1465-9921-15-16.
- [379] F. Hilberg *et al.*, "BIBF 1120: Triple Angiokinase Inhibitor with Sustained Receptor Blockade and Good Antitumor Efficacy," *Cancer Res*, vol. 68, no. 12, pp. 4774–4782, Jun. 2008, doi: 10.1158/0008-5472.CAN-07-6307.
- [380] K. E. Hostettler *et al.*, "Anti-fibrotic effects of nintedanib in lung fibroblasts derived from patients with idiopathic pulmonary fibrosis," *Respir Res*, vol. 15, no. 1, p. 157, Dec. 2014, doi: 10.1186/s12931-014-0157-3.
- [381] L. Wollin, I. Maillet, V. Quesniaux, A. Holweg, and B. Ryffel, "Antifibrotic and anti-inflammatory activity of the tyrosine kinase inhibitor nintedanib in experimental models of lung fibrosis.," *J Pharmacol Exp Ther*, vol. 349, no. 2, pp. 209–20, May 2014, doi: 10.1124/jpet.113.208223.
- [382] J. Huang *et al.*, "Nintedanib inhibits macrophage activation and ameliorates vascular and fibrotic manifestations in the Fra2 mouse model of systemic sclerosis," *Ann Rheum Dis*, vol. 76, no. 11, pp. 1941–1948, Nov. 2017, doi: 10.1136/annrheumdis-2016-210823.
- [383] N. Bellamri *et al.*, "Alteration of human macrophage phenotypes by the anti-fibrotic drug nintedanib," *Int Immunopharmacol*, vol. 72, pp. 112–123, Jul. 2019, doi: 10.1016/j.intimp.2019.03.061.
- [384] T. E. King *et al.*, "A Phase 3 Trial of Pirfenidone in Patients with Idiopathic Pulmonary Fibrosis," *New England Journal of Medicine*, vol. 370, no. 22, pp. 2083–2092, May 2014, doi: 10.1056/NEJMoa1402582.
- [385] P. W. Noble *et al.*, "Pirfenidone in patients with idiopathic pulmonary fibrosis (CAPACITY): two randomised trials," *The Lancet*, vol. 377, no. 9779, pp. 1760–1769, May 2011, doi: 10.1016/S0140-6736(11)60405-4.
- [386] L. Richeldi *et al.*, "Efficacy and Safety of Nintedanib in Idiopathic Pulmonary Fibrosis," *New England Journal of Medicine*, vol. 370, no. 22, pp. 2071–2082, May 2014, doi: 10.1056/NEJMoa1402584.
- [387] L. Richeldi *et al.*, "Efficacy of a Tyrosine Kinase Inhibitor in Idiopathic Pulmonary Fibrosis," *New England Journal of Medicine*, vol. 365, no. 12, pp. 1079–1087, Sep. 2011, doi: 10.1056/NEJMoa1103690.
- [388] S. Saito, A. Alkhatib, J. K. Kolls, Y. Kondoh, and J. A. Lasky, "Pharmacotherapy and adjunctive treatment for idiopathic pulmonary fibrosis (IPF)," *J Thorac Dis*, vol. 11, no. S14, pp. S1740–S1754, Sep. 2019, doi: 10.21037/jtd.2019.04.62.
- [389] Y. N. Lamb, "Nintedanib: A Review in Fibrotic Interstitial Lung Diseases," *Drugs*, vol. 81, no. 5, pp. 575–586, Apr. 2021, doi: 10.1007/s40265-021-01487-0.
- [390] P. Pellegatti, L. Raffaghello, G. Bianchi, F. Piccardi, V. Pistoia, and F. di Virgilio, "Increased level of extracellular ATP at tumor sites: in vivo imaging with plasma membrane luciferase.," *PLoS One*, vol. 3, no. 7, p. e2599, Jul. 2008, doi: 10.1371/journal.pone.0002599.
- [391] N. Riteau *et al.*, "Extracellular ATP is a danger signal activating P2X7 receptor in lung inflammation and fibrosis.," *Am J Respir Crit Care Med*, vol. 182, no. 6, pp. 774–83, Sep. 2010, doi: 10.1164/rccm.201003-0359OC.

- [392] S. Janho dit Hreich, J. Benzaquen, P. Hofman, and V. Vouret-Craviari, "The Purinergic Landscape of Non-Small Cell Lung Cancer," *Cancers (Basel)*, vol. 14, no. 8, p. 1926, Apr. 2022, doi: 10.3390/cancers14081926.
- [393] V. Ralevic and G. Burnstock, "Receptors for purines and pyrimidines.," *Pharmacol Rev*, vol. 50, no. 3, pp. 413–92, Sep. 1998.
- [394] E. Adinolfi, A. L. Giuliani, E. de Marchi, A. Pegoraro, E. Orioli, and F. di Virgilio, "The P2X7 receptor: A main player in inflammation," *Biochem Pharmacol*, vol. 151, pp. 234–244, May 2018, doi: 10.1016/j.bcp.2017.12.021.
- [395] G. Burnstock and C. Kennedy, "P2X Receptors in Health and Disease," 2011, pp. 333–372. doi: 10.1016/B978-0-12-385526-8.00011-4.
- [396] G. E. Torres, T. M. Egan, and M. M. Voigt, "Hetero-oligomeric Assembly of P2X Receptor Subunits," *Journal of Biological Chemistry*, vol. 274, no. 10, pp. 6653–6659, Mar. 1999, doi: 10.1074/jbc.274.10.6653.
- [397] C. Guo, M. Masin, O. S. Qureshi, and R. D. Murrell-Lagnado, "Evidence for Functional P2X<sub>4</sub>/P2X<sub>7</sub> Heteromeric Receptors," *Mol Pharmacol*, vol. 72, no. 6, pp. 1447–1456, Dec. 2007, doi: 10.1124/mol.107.035980.
- [398] E. Craigie, R. E. Birch, R. J. Unwin, and S. S. Wildman, "The relationship between P2X<sub>4</sub> and P2X<sub>7</sub>: a physiologically important interaction?," *Front Physiol*, vol. 4, 2013, doi: 10.3389/fphys.2013.00216.
- [399] A. Nicke, "Homotrimeric complexes are the dominant assembly state of native P2X<sub>7</sub> subunits," *Biochem Biophys Res Commun*, vol. 377, no. 3, pp. 803–808, Dec. 2008, doi: 10.1016/j.bbrc.2008.10.042.
- [400] L. Antonio, A. Stewart, X. Xu, W. Varanda, R. Murrell-Lagnado, and J. Edwardson, "P2X<sub>4</sub> receptors interact with both P2X<sub>2</sub> and P2X<sub>7</sub> receptors in the form of homotrimers," *Br J Pharmacol*, vol. 163, no. 5, pp. 1069–1077, Jul. 2011, doi: 10.1111/j.1476-5381.2011.01303.x.
- [401] F. di Virgilio, D. Dal Ben, A. C. Sarti, A. L. Giuliani, and S. Falzoni, "The P2X<sub>7</sub> Receptor in Infection and Inflammation," *Immunity*, vol. 47, no. 1, pp. 15–31, Jul. 2017, doi: 10.1016/j.immuni.2017.06.020.
- [402] P. Illes *et al.*, "Update of P2X receptor properties and their pharmacology: IUPHAR Review 30," *Br J Pharmacol*, vol. 178, no. 3, pp. 489–514, Feb. 2021, doi: 10.1111/bph.15299.
- [403] A. P. Ford, "In pursuit of P2X<sub>3</sub> antagonists: novel therapeutics for chronic pain and afferent sensitization," *Purinergic Signal*, vol. 8, no. S1, pp. 3–26, Feb. 2012, doi: 10.1007/s11302-011-9271-6.
- [404] L. Yip *et al.*, "Autocrine regulation of T-cell activation by ATP release and P2X<sub>7</sub> receptors," *The FASEB Journal*, vol. 23, no. 6, pp. 1685–1693, Jun. 2009, doi: 10.1096/fj.08-126458.
- [405] V. Budagian *et al.*, "Signaling through P2X<sub>7</sub> Receptor in Human T Cells Involves p56 , MAP Kinases, and Transcription Factors AP-1 and NF-κB," *Journal of Biological Chemistry*, vol. 278, no. 3, pp. 1549–1560, Jan. 2003, doi: 10.1074/jbc.M206383200.
- [406] Y. Liu, Y. Xiao, and Z. Li, "P2X<sub>7</sub> receptor positively regulates MyD88-dependent NF-κB activation," *Cytokine*, vol. 55, no. 2, pp. 229–236, Aug. 2011, doi: 10.1016/j.cyto.2011.05.003.
- [407] D. Ferrari, C. Stroh, and K. Schulze-Osthoff, "P2X<sub>7</sub>/P2Z Purinoreceptor-mediated Activation of Transcription Factor NFAT in Microglial Cells," *Journal of Biological*

- Chemistry*, vol. 274, no. 19, pp. 13205–13210, May 1999, doi: 10.1074/jbc.274.19.13205.
- [408] M. W. Grol, A. Pereverzev, S. M. Sims, and S. J. Dixon, “P2 receptor networks regulate signaling duration over a wide dynamic range of ATP concentrations,” *J Cell Sci*, Jan. 2013, doi: 10.1242/jcs.122705.
- [409] J. Korcok, L. N. Raimundo, H. Z. Ke, S. M. Sims, and S. J. Dixon, “Extracellular Nucleotides Act Through P2X7 Receptors to Activate NF- $\kappa$ B in Osteoclasts,” *Journal of Bone and Mineral Research*, vol. 19, no. 4, pp. 642–651, Jan. 2004, doi: 10.1359/JBMR.040108.
- [410] C. Coddou, Z. Yan, T. Obsil, J. P. Huidobro-Toro, and S. S. Stojilkovic, “Activation and Regulation of Purinergic P2X Receptor Channels,” *Pharmacol Rev*, vol. 63, no. 3, pp. 641–683, Sep. 2011, doi: 10.1124/pr.110.003129.
- [411] C. Sattler *et al.*, “Relating ligand binding to activation gating in P2X2 receptors using a novel fluorescent ATP derivative,” *J Neurochem*, vol. 154, no. 3, pp. 251–262, Aug. 2020, doi: 10.1111/jnc.14948.
- [412] A. E. McCarthy, C. Yoshioka, and S. E. Mansoor, “Full-Length P2X7 Structures Reveal How Palmitoylation Prevents Channel Desensitization,” *Cell*, vol. 179, no. 3, pp. 659–670.e13, Oct. 2019, doi: 10.1016/j.cell.2019.09.017.
- [413] R. Kopp, A. Krautloher, A. Ramírez-Fernández, and A. Nicke, “P2X7 Interactions and Signaling – Making Head or Tail of It,” *Front Mol Neurosci*, vol. 12, Aug. 2019, doi: 10.3389/fnmol.2019.00183.
- [414] S. Falzoni, M. Munerati, D. Ferrari, S. Spisani, S. Moretti, and F. di Virgilio, “The purinergic P2Z receptor of human macrophage cells. Characterization and possible physiological role.,” *Journal of Clinical Investigation*, vol. 95, no. 3, pp. 1207–1216, Mar. 1995, doi: 10.1172/JCI117770.
- [415] S. Greenberg, F. di Virgilio, T. H. Steinberg, and S. C. Silverstein, “Extracellular nucleotides mediate Ca<sup>2+</sup> fluxes in J774 macrophages by two distinct mechanisms.,” *J Biol Chem*, vol. 263, no. 21, pp. 10337–43, Jul. 1988.
- [416] S. Cockcroft and B. D. Gomperts, “The ATP<sub>4</sub>- receptor of rat mast cells,” *Biochemical Journal*, vol. 188, no. 3, pp. 789–798, Jun. 1980, doi: 10.1042/bj1880789.
- [417] A. Surprenant, F. Rassendren, E. Kawashima, R. A. North, and G. Buell, “The cytolytic P2Z receptor for extracellular ATP identified as a P2X receptor (P2X<sub>7</sub>).,” *Science*, vol. 272, no. 5262, pp. 735–8, May 1996, doi: 10.1126/science.272.5262.735.
- [418] F. di Virgilio, G. Schmalzing, and F. Markwardt, “The Elusive P2X7 Macropore.,” *Trends Cell Biol*, vol. 28, no. 5, pp. 392–404, 2018, doi: 10.1016/j.tcb.2018.01.005.
- [419] E. C. Beyer and T. H. Steinberg, “Evidence that the gap junction protein connexin-43 is the ATP-induced pore of mouse macrophages.,” *J Biol Chem*, vol. 266, no. 13, pp. 7971–4, May 1991.
- [420] S. Locovei, E. Scemes, F. Qiu, D. C. Spray, and G. Dahl, “Pannexin1 is part of the pore forming unit of the P2X<sub>7</sub> receptor death complex,” *FEBS Lett*, vol. 581, no. 3, pp. 483–488, Feb. 2007, doi: 10.1016/j.febslet.2006.12.056.
- [421] P. Pelegrin and A. Surprenant, “Pannexin-1 mediates large pore formation and interleukin-1 $\beta$  release by the ATP-gated P2X<sub>7</sub> receptor,” *EMBO J*, vol. 25, no. 21, pp. 5071–5082, Nov. 2006, doi: 10.1038/sj.emboj.7601378.
- [422] A. V. P. Alberto *et al.*, “Is pannexin the pore associated with the P2X<sub>7</sub> receptor?,” *Naunyn Schmiedebergs Arch Pharmacol*, vol. 386, no. 9, pp. 775–787, Sep. 2013, doi: 10.1007/s00210-013-0868-x.

- [423] A. Karasawa, K. Michalski, P. Mikhelzon, and T. Kawate, "The P2X7 receptor forms a dye-permeable pore independent of its intracellular domain but dependent on membrane lipid composition," *Elife*, vol. 6, Sep. 2017, doi: 10.7554/eLife.31186.
- [424] M. L. Smart *et al.*, "P2X7 Receptor Cell Surface Expression and Cytolytic Pore Formation Are Regulated by a Distal C-terminal Region," *Journal of Biological Chemistry*, vol. 278, no. 10, pp. 8853–8860, Mar. 2003, doi: 10.1074/jbc.M211094200.
- [425] M. Solle *et al.*, "Altered Cytokine Production in Mice Lacking P2X7Receptors," *Journal of Biological Chemistry*, vol. 276, no. 1, pp. 125–132, Jan. 2001, doi: 10.1074/jbc.M006781200.
- [426] J. P.-Y. Ting *et al.*, "The NLR Gene Family: A Standard Nomenclature," *Immunity*, vol. 28, no. 3, pp. 285–287, Mar. 2008, doi: 10.1016/j.immuni.2008.02.005.
- [427] Y. He, M. Y. Zeng, D. Yang, B. Motro, and G. Núñez, "NEK7 is an essential mediator of NLRP3 activation downstream of potassium efflux," *Nature*, vol. 530, no. 7590, pp. 354–357, Feb. 2016, doi: 10.1038/nature16959.
- [428] F. di Virgilio, A. C. Sarti, and F. Grassi, "Modulation of innate and adaptive immunity by P2X ion channels," *Curr Opin Immunol*, vol. 52, pp. 51–59, Jun. 2018, doi: 10.1016/j.coi.2018.03.026.
- [429] R. Muñoz-Planillo, P. Kuffa, G. Martínez-Colón, B. L. Smith, T. M. Rajendiran, and G. Núñez, "K<sup>+</sup> Efflux Is the Common Trigger of NLRP3 Inflammasome Activation by Bacterial Toxins and Particulate Matter," *Immunity*, vol. 38, no. 6, pp. 1142–1153, Jun. 2013, doi: 10.1016/j.immuni.2013.05.016.
- [430] A. J. Puren, G. Fantuzzi, and C. A. Dinarello, "Gene expression, synthesis, and secretion of interleukin 18 and interleukin 1beta are differentially regulated in human blood mononuclear cells and mouse spleen cells.," *Proc Natl Acad Sci U S A*, vol. 96, no. 5, pp. 2256–61, Mar. 1999, doi: 10.1073/pnas.96.5.2256.
- [431] F. G. Bauernfeind *et al.*, "Cutting Edge: NF- $\kappa$ B Activating Pattern Recognition and Cytokine Receptors License NLRP3 Inflammasome Activation by Regulating NLRP3 Expression," *The Journal of Immunology*, vol. 183, no. 2, pp. 787–791, Jul. 2009, doi: 10.4049/jimmunol.0901363.
- [432] G. Lopez-Castejon, "Control of the inflammasome by the ubiquitin system," *FEBS J*, vol. 287, no. 1, pp. 11–26, Jan. 2020, doi: 10.1111/febs.15118.
- [433] D. G. Perregaux and C. A. Gabel, "Human monocyte stimulus-coupled IL-1 $\beta$  posttranslational processing: modulation via monovalent cations," *American Journal of Physiology-Cell Physiology*, vol. 275, no. 6, pp. C1538–C1547, Dec. 1998, doi: 10.1152/ajpcell.1998.275.6.C1538.
- [434] A. Di *et al.*, "The TWIK2 Potassium Efflux Channel in Macrophages Mediates NLRP3 Inflammasome-Induced Inflammation.," *Immunity*, vol. 49, no. 1, pp. 56-65.e4, 2018, doi: 10.1016/j.immuni.2018.04.032.
- [435] A. Franceschini *et al.*, "The P2X7 receptor directly interacts with the NLRP3 inflammasome scaffold protein," *The FASEB Journal*, vol. 29, no. 6, pp. 2450–2461, Jun. 2015, doi: 10.1096/fj.14-268714.
- [436] W. Wang *et al.*, "Paxillin mediates ATP-induced activation of P2X7 receptor and NLRP3 inflammasome," *BMC Biol*, vol. 18, no. 1, p. 182, Dec. 2020, doi: 10.1186/s12915-020-00918-w.

- [437] M. Solle *et al.*, "Altered Cytokine Production in Mice Lacking P2X7Receptors," *Journal of Biological Chemistry*, vol. 276, no. 1, pp. 125–132, Jan. 2001, doi: 10.1074/jbc.M006781200.
- [438] J. Shi *et al.*, "Cleavage of GSDMD by inflammatory caspases determines pyroptotic cell death," *Nature*, vol. 526, no. 7575, pp. 660–665, Oct. 2015, doi: 10.1038/nature15514.
- [439] L. A. Cameron *et al.*, "Airway epithelium expresses interleukin-18.," *Eur Respir J*, vol. 14, no. 3, pp. 553–9, Sep. 1999, doi: 10.1034/j.1399-3003.1999.14c12.x.
- [440] C. M. Artlett, S. Sassi-Gaha, J. L. Rieger, A. C. Boesteanu, C. A. Feghali-Bostwick, and P. D. Katsikis, "The inflammasome activating caspase 1 mediates fibrosis and myofibroblast differentiation in systemic sclerosis.," *Arthritis Rheum*, vol. 63, no. 11, pp. 3563–74, Nov. 2011, doi: 10.1002/art.30568.
- [441] C. Garlanda, C. A. Dinarello, and A. Mantovani, "The Interleukin-1 Family: Back to the Future," *Immunity*, vol. 39, no. 6, pp. 1003–1018, Dec. 2013, doi: 10.1016/j.immuni.2013.11.010.
- [442] D. Wang, S. Zhang, L. Li, X. Liu, K. Mei, and X. Wang, "Structural insights into the assembly and activation of IL-1 $\beta$  with its receptors," *Nat Immunol*, vol. 11, no. 10, pp. 905–911, Oct. 2010, doi: 10.1038/ni.1925.
- [443] D. J. Dripps, B. J. Brandhuber, R. C. Thompson, and S. P. Eisenberg, "Interleukin-1 (IL-1) receptor antagonist binds to the 80-kDa IL-1 receptor but does not initiate IL-1 signal transduction.," *J Biol Chem*, vol. 266, no. 16, pp. 10331–6, Jun. 1991.
- [444] H. Okamura *et al.*, "Cloning of a new cytokine that induces IFN-gamma production by T cells.," *Nature*, vol. 378, no. 6552, pp. 88–91, Nov. 1995, doi: 10.1038/378088a0.
- [445] C. A. Dinarello, D. Novick, S. Kim, and G. Kaplanski, "Interleukin-18 and IL-18 binding protein.," *Front Immunol*, vol. 4, p. 289, Oct. 2013, doi: 10.3389/fimmu.2013.00289.
- [446] P. Galozzi, S. Bindoli, A. Doria, and P. Sfriso, "The revisited role of interleukin-1 alpha and beta in autoimmune and inflammatory disorders and in comorbidities," *Autoimmun Rev*, vol. 20, no. 4, p. 102785, Apr. 2021, doi: 10.1016/j.autrev.2021.102785.
- [447] J. Benzaquen *et al.*, "Alternative splicing of P2RX7 pre-messenger RNA in health and diseases: Myth or reality?," *Biomed J*, vol. 42, no. 3, pp. 141–154, 2019, doi: 10.1016/j.bj.2019.05.007.
- [448] R. J. Thompson, I. Sayers, K. Kuokkanen, and I. P. Hall, "Purinergic Receptors in the Airways: Potential Therapeutic Targets for Asthma?," *Frontiers in Allergy*, vol. 2, May 2021, doi: 10.3389/falgy.2021.677677.
- [449] J. Benzaquen *et al.*, "P2RX7B is a new theranostic marker for lung adenocarcinoma patients," *Theranostics*, vol. 10, no. 24, pp. 10849–10860, 2020, doi: 10.7150/thno.48229.
- [450] E. Adinolfi *et al.*, "Trophic activity of a naturally occurring truncated isoform of the P2X7 receptor," *The FASEB Journal*, vol. 24, no. 9, pp. 3393–3404, Sep. 2010, doi: 10.1096/fj.09-153601.
- [451] M. Solle *et al.*, "Altered Cytokine Production in Mice Lacking P2X7Receptors," *Journal of Biological Chemistry*, vol. 276, no. 1, pp. 125–132, Jan. 2001, doi: 10.1074/jbc.M006781200.
- [452] R. Sluyter and L. Stokes, "Significance of P2X7 Receptor Variants to Human Health and Disease," *Recent Pat DNA Gene Seq*, vol. 5, no. 1, pp. 41–54, Apr. 2011, doi: 10.2174/187221511794839219.

- [453] R. Sluyter, A. N. Shemon, and J. S. Wiley, "Glu<sup>496</sup> to Ala Polymorphism in the P2X<sub>7</sub> Receptor Impairs ATP-Induced IL-1 $\beta$  Release from Human Monocytes," *The Journal of Immunology*, vol. 172, no. 6, pp. 3399–3405, Mar. 2004, doi: 10.4049/jimmunol.172.6.3399.
- [454] F. Ghiringhelli *et al.*, "Activation of the NLRP3 inflammasome in dendritic cells induces IL-1 $\beta$ -dependent adaptive immunity against tumors," *Nat Med*, vol. 15, no. 10, pp. 1170–1178, Oct. 2009, doi: 10.1038/nm.2028.
- [455] G. Bianchi *et al.*, "ATP/P2X<sub>7</sub> axis modulates myeloid-derived suppressor cell functions in neuroblastoma microenvironment," *Cell Death Dis*, vol. 5, no. 3, pp. e1135–e1135, Mar. 2014, doi: 10.1038/cddis.2014.109.
- [456] J. Qin *et al.*, "Blocking P2X<sub>7</sub>-Mediated Macrophage Polarization Overcomes Treatment Resistance in Lung Cancer," *Cancer Immunol Res*, vol. 8, no. 11, pp. 1426–1439, Nov. 2020, doi: 10.1158/2326-6066.CIR-20-0123.
- [457] E. Adinolfi *et al.*, "Expression of P2X<sub>7</sub> Receptor Increases *In Vivo* Tumor Growth," *Cancer Res*, vol. 72, no. 12, pp. 2957–2969, Jun. 2012, doi: 10.1158/0008-5472.CAN-11-1947.
- [458] Y. Zhang, H. Cheng, W. Li, H. Wu, and Y. Yang, "Highly-expressed P2X<sub>7</sub> receptor promotes growth and metastasis of human HOS/MNNG osteosarcoma cells *via* PI3K/Akt/GSK3 $\beta$ / $\beta$ -catenin and mTOR/HIF1 $\alpha$ /VEGF signaling," *Int J Cancer*, vol. 145, no. 4, pp. 1068–1082, Aug. 2019, doi: 10.1002/ijc.32207.
- [459] Y. Qiu, W. Li, H. Zhang, Y. Liu, X.-X. Tian, and W.-G. Fang, "P2X<sub>7</sub> Mediates ATP-Driven Invasiveness in Prostate Cancer Cells," *PLoS One*, vol. 9, no. 12, p. e114371, Dec. 2014, doi: 10.1371/journal.pone.0114371.
- [460] F. Qian, J. Xiao, B. Hu, N. Sun, W. Yin, and J. Zhu, "High expression of P2X<sub>7</sub>R is an independent postoperative indicator of poor prognosis in colorectal cancer," *Hum Pathol*, vol. 64, pp. 61–68, Jun. 2017, doi: 10.1016/j.humpath.2017.03.019.
- [461] R. Lara *et al.*, "P2X<sub>7</sub> in Cancer: From Molecular Mechanisms to Therapeutics," *Front Pharmacol*, vol. 11, Jun. 2020, doi: 10.3389/fphar.2020.00793.
- [462] A. Giannuzzo, S. F. Pedersen, and I. Novak, "The P2X<sub>7</sub> receptor regulates cell survival, migration and invasion of pancreatic ductal adenocarcinoma cells," *Mol Cancer*, vol. 14, no. 1, p. 203, Dec. 2015, doi: 10.1186/s12943-015-0472-4.
- [463] W. Zhang, C. Luo, C. Huang, F. Pu, J. Zhu, and Z. Zhu, "PI3K/Akt/GSK-3 $\beta$  signal pathway is involved in P2X<sub>7</sub> receptor-induced proliferation and EMT of colorectal cancer cells," *Eur J Pharmacol*, vol. 899, p. 174041, May 2021, doi: 10.1016/j.ejphar.2021.174041.
- [464] B. Jelassi *et al.*, "Anthraquinone emodin inhibits human cancer cell invasiveness by antagonizing P2X<sub>7</sub> receptors," *Carcinogenesis*, vol. 34, no. 7, pp. 1487–1496, Jul. 2013, doi: 10.1093/carcin/bgt099.
- [465] B. Jelassi *et al.*, "P2X<sub>7</sub> receptor activation enhances SK3 channels- and cystein cathepsin-dependent cancer cells invasiveness," *Oncogene*, vol. 30, no. 18, pp. 2108–2122, May 2011, doi: 10.1038/onc.2010.593.
- [466] Y. Zhang, J. Ding, and L. Wang, "The role of P2X<sub>7</sub> receptor in prognosis and metastasis of colorectal cancer," *Adv Med Sci*, vol. 64, no. 2, pp. 388–394, Sep. 2019, doi: 10.1016/j.advms.2019.05.002.
- [467] D. Matyśniak *et al.*, "P2X<sub>7</sub> receptor: the regulator of glioma tumor development and survival," *Purinergic Signal*, vol. 18, no. 1, pp. 135–154, Mar. 2022, doi: 10.1007/s11302-021-09834-2.

- [468] E. Takai, M. Tsukimoto, H. Harada, and S. Kojima, "Autocrine signaling via release of ATP and activation of P2X7 receptor influences motile activity of human lung cancer cells," *Purinergic Signal*, vol. 10, no. 3, pp. 487–497, Sep. 2014, doi: 10.1007/s11302-014-9411-x.
- [469] W. Wei, J. K. Ryu, H. B. Choi, and J. G. McLarnon, "Expression and function of the P2X7 receptor in rat C6 glioma cells," *Cancer Lett*, vol. 260, no. 1–2, pp. 79–87, Feb. 2008, doi: 10.1016/j.canlet.2007.10.025.
- [470] F. Amoroso *et al.*, "The P2X7 receptor is a key modulator of the PI3K/GSK3 $\beta$ /VEGF signaling network: evidence in experimental neuroblastoma," *Oncogene*, vol. 34, no. 41, pp. 5240–5251, Oct. 2015, doi: 10.1038/onc.2014.444.
- [471] A. Pegoraro *et al.*, "Differential sensitivity of acute myeloid leukemia cells to daunorubicin depends on P2X7A versus P2X7B receptor expression," *Cell Death Dis*, vol. 11, no. 10, p. 876, Oct. 2020, doi: 10.1038/s41419-020-03058-9.
- [472] L. Tattersall *et al.*, "The P2RX7B splice variant modulates osteosarcoma cell behaviour and metastatic properties," *J Bone Oncol*, vol. 31, p. 100398, Dec. 2021, doi: 10.1016/j.jbo.2021.100398.
- [473] V. F. Arnaud-Sampaio, C. A. Bento, T. Glaser, E. Adinolfi, H. Ulrich, and C. Lameu, "P2X7 receptor isoform B is a key drug resistance mediator for neuroblastoma," *Front Oncol*, vol. 12, Aug. 2022, doi: 10.3389/fonc.2022.966404.
- [474] M. Zanoni *et al.*, "Irradiation causes senescence, ATP release, and P2X7 receptor isoform switch in glioblastoma," *Cell Death Dis*, vol. 13, no. 1, p. 80, Jan. 2022, doi: 10.1038/s41419-022-04526-0.
- [475] J. A. Barden, "Non-Functional P2X7: A Novel and Ubiquitous Target in Human Cancer," *J Clin Cell Immunol*, vol. 05, no. 04, 2014, doi: 10.4172/2155-9899.1000237.
- [476] S. Gilbert *et al.*, "ATP in the tumour microenvironment drives expression of nfP2X7, a key mediator of cancer cell survival," *Oncogene*, vol. 38, no. 2, pp. 194–208, Jan. 2019, doi: 10.1038/s41388-018-0426-6.
- [477] S. Huang *et al.*, "miR-150 Promotes Human Breast Cancer Growth and Malignant Behavior by Targeting the Pro-Apoptotic Purinergic P2X7 Receptor," *PLoS One*, vol. 8, no. 12, p. e80707, Dec. 2013, doi: 10.1371/journal.pone.0080707.
- [478] A. V. H. Greig *et al.*, "Expression of Purinergic Receptors in Non-melanoma Skin Cancers and Their Functional Roles in A431 Cells," *Journal of Investigative Dermatology*, vol. 121, no. 2, pp. 315–327, Aug. 2003, doi: 10.1046/j.1523-1747.2003.12379.x.
- [479] R. Coutinho-Silva *et al.*, "P2X and P2Y purinergic receptors on human intestinal epithelial carcinoma cells: effects of extracellular nucleotides on apoptosis and cell proliferation," *American Journal of Physiology-Gastrointestinal and Liver Physiology*, vol. 288, no. 5, pp. G1024–G1035, May 2005, doi: 10.1152/ajpgi.00211.2004.
- [480] N. White, P. E. M. Butler, and G. Burnstock, "Human melanomas express functional P2X7 receptors," *Cell Tissue Res*, vol. 321, no. 3, pp. 411–418, Sep. 2005, doi: 10.1007/s00441-005-1149-x.
- [481] N. White, G. E. Knight, P. E. M. Butler, and G. Burnstock, "An in vivo model of melanoma: treatment with ATP," *Purinergic Signal*, vol. 5, no. 3, pp. 327–333, Sep. 2009, doi: 10.1007/s11302-009-9156-0.
- [482] P. Hofman *et al.*, "Genetic and Pharmacological Inactivation of the Purinergic P2RX7 Receptor Dampens Inflammation but Increases Tumor Incidence in a Mouse Model of



- Colitis-Associated Cancer,” *Cancer Res*, vol. 75, no. 5, pp. 835–845, Mar. 2015, doi: 10.1158/0008-5472.CAN-14-1778.
- [483] E. Adinolfi *et al.*, “Accelerated Tumor Progression in Mice Lacking the ATP Receptor P2X7,” *Cancer Res*, vol. 75, no. 4, pp. 635–644, Feb. 2015, doi: 10.1158/0008-5472.CAN-14-1259.
- [484] E. de Marchi *et al.*, “The P2X7 receptor modulates immune cells infiltration, ectonucleotidases expression and extracellular ATP levels in the tumor microenvironment,” *Oncogene*, vol. 38, no. 19, pp. 3636–3650, May 2019, doi: 10.1038/s41388-019-0684-y.
- [485] M. Idzko *et al.*, “Nucleotides induce chemotaxis and actin polymerization in immature but not mature human dendritic cells via activation of pertussis toxin–sensitive P2y receptors,” *Blood*, vol. 100, no. 3, pp. 925–932, Aug. 2002, doi: 10.1182/blood.V100.3.925.
- [486] Y. Ma *et al.*, “ATP-dependent recruitment, survival and differentiation of dendritic cell precursors in the tumor bed after anticancer chemotherapy,” *Oncoimmunology*, vol. 2, no. 6, p. e24568, Jun. 2013, doi: 10.4161/onci.24568.
- [487] Y. Ma *et al.*, “Anticancer Chemotherapy-Induced Intratumoral Recruitment and Differentiation of Antigen-Presenting Cells,” *Immunity*, vol. 38, no. 4, pp. 729–741, Apr. 2013, doi: 10.1016/j.immuni.2013.03.003.
- [488] P. J. Sáez, P. Vargas, K. F. Shoji, P. A. Harcha, A.-M. Lennon-Duménil, and J. C. Sáez, “ATP promotes the fast migration of dendritic cells through the activity of pannexin 1 channels and P2X7 receptors.,” *Sci Signal*, vol. 10, no. 506, Nov. 2017, doi: 10.1126/scisignal.aah7107.
- [489] K. Wilhelm *et al.*, “Graft-versus-host disease is enhanced by extracellular ATP activating P2X7R,” *Nat Med*, vol. 16, no. 12, pp. 1434–1438, Dec. 2010, doi: 10.1038/nm.2242.
- [490] H. Safya *et al.*, “Variations in Cellular Responses of Mouse T Cells to Adenosine-5'-Triphosphate Stimulation Do Not Depend on P2X7 Receptor Expression Levels but on Their Activation and Differentiation Stage,” *Front Immunol*, vol. 9, Feb. 2018, doi: 10.3389/fimmu.2018.00360.
- [491] S. Adriouch, S. Hubert, S. Pechberty, F. Koch-Nolte, F. Haag, and M. Seman, “NAD<sup>+</sup> Released during Inflammation Participates in T Cell Homeostasis by Inducing ART2-Mediated Death of Naive T Cells In Vivo,” *The Journal of Immunology*, vol. 179, no. 1, pp. 186–194, Jul. 2007, doi: 10.4049/jimmunol.179.1.186.
- [492] S. M. le Gall *et al.*, “ADAMs 10 and 17 Represent Differentially Regulated Components of a General Shedding Machinery for Membrane Proteins Such as Transforming Growth Factor  $\alpha$ , L-Selectin, and Tumor Necrosis Factor  $\alpha$ ,” *Mol Biol Cell*, vol. 20, no. 6, pp. 1785–1794, Mar. 2009, doi: 10.1091/mbc.e08-11-1135.
- [493] J. G. Foster, E. Carter, I. Kilty, A. B. MacKenzie, and S. G. Ward, “Mitochondrial Superoxide Generation Enhances P2X7R-Mediated Loss of Cell Surface CD62L on Naive Human CD4<sup>+</sup> T Lymphocytes,” *The Journal of Immunology*, vol. 190, no. 4, pp. 1551–1559, Feb. 2013, doi: 10.4049/jimmunol.1201510.
- [494] F. Aswad, H. Kawamura, and G. Dennert, “High Sensitivity of CD4<sup>+</sup> CD25<sup>+</sup> Regulatory T Cells to Extracellular Metabolites Nicotinamide Adenine Dinucleotide and ATP: A Role for P2X<sub>7</sub> Receptors,” *The Journal of Immunology*, vol. 175, no. 5, pp. 3075–3083, Sep. 2005, doi: 10.4049/jimmunol.175.5.3075.

- [495] R. Bläsche, G. Ebeling, S. Perike, K. Weinhold, M. Kasper, and K. Barth, "Activation of P2X7R and downstream effects in bleomycin treated lung epithelial cells," *Int J Biochem Cell Biol*, vol. 44, no. 3, pp. 514–524, Mar. 2012, doi: 10.1016/j.biocel.2011.12.003.
- [496] J. Heupel, R. Bläsche, K.-P. Wesslau, M. Kasper, and K. Barth, "P2X7R: independent modulation of aquaporin 5 expression in CdCl<sub>2</sub>-injured alveolar epithelial cells," *Histochem Cell Biol*, vol. 149, no. 3, pp. 197–208, Mar. 2018, doi: 10.1007/s00418-018-1637-1.
- [497] L. C. Monção-Ribeiro *et al.*, "P2X7 Receptor Modulates Inflammatory and Functional Pulmonary Changes Induced by Silica," *PLoS One*, vol. 9, no. 10, p. e110185, Oct. 2014, doi: 10.1371/journal.pone.0110185.
- [498] R. Lara *et al.*, "P2X7 in Cancer: From Molecular Mechanisms to Therapeutics," *Front Pharmacol*, vol. 11, Jun. 2020, doi: 10.3389/fphar.2020.00793.
- [499] A. Karasawa and T. Kawate, "Structural basis for subtype-specific inhibition of the P2X7 receptor," *Elife*, vol. 5, Dec. 2016, doi: 10.7554/eLife.22153.
- [500] W. Danquah *et al.*, "Nanobodies that block gating of the P2X7 ion channel ameliorate inflammation.," *Sci Transl Med*, vol. 8, no. 366, p. 366ra162, 2016, doi: 10.1126/scitranslmed.aaf8463.
- [501] X.-Y. Li *et al.*, "Targeting CD39 in Cancer Reveals an Extracellular ATP- and Inflammasome-Driven Tumor Immunity," *Cancer Discov*, vol. 9, no. 12, pp. 1754–1773, Dec. 2019, doi: 10.1158/2159-8290.CD-19-0541.
- [502] J. Yan *et al.*, "Control of Metastases via Myeloid CD39 and NK Cell Effector Function," *Cancer Immunol Res*, vol. 8, no. 3, pp. 356–367, Mar. 2020, doi: 10.1158/2326-6066.CIR-19-0749.
- [503] I. Perrot *et al.*, "Blocking Antibodies Targeting the CD39/CD73 Immunosuppressive Pathway Unleash Immune Responses in Combination Cancer Therapies," *Cell Rep*, vol. 27, no. 8, pp. 2411–2425.e9, May 2019, doi: 10.1016/j.celrep.2019.04.091.
- [504] "Activation of P2RX7 boosts antitumor immune responses and sensitizes tumors to immunotherapy," *Nature Cancer Community*, Jan. 29, 2021. <https://cancercommunity.nature.com/posts/activation-of-p2rx7-boosts-antitumor-immune-responses-and-sensitizes-tumors-to-immunotherapy>
- [505] T. Vardam-Kaur, S. van Dijk, C. Peng, K. M. Wanhainen, S. C. Jameson, and H. Borges da Silva, "The Extracellular ATP Receptor P2RX7 Imprints a Promemory Transcriptional Signature in Effector CD8<sup>+</sup> T Cells," *The Journal of Immunology*, vol. 208, no. 7, pp. 1686–1699, Apr. 2022, doi: 10.4049/jimmunol.2100555.
- [506] H. Borges da Silva *et al.*, "The purinergic receptor P2RX7 directs metabolic fitness of long-lived memory CD8<sup>+</sup> T cells," *Nature*, vol. 559, no. 7713, pp. 264–268, Jul. 2018, doi: 10.1038/s41586-018-0282-0.
- [507] K. M. Wanhainen *et al.*, "P2RX7 Enhances Tumor Control by CD8<sup>+</sup> T Cells in Adoptive Cell Therapy," *Cancer Immunol Res*, vol. 10, no. 7, pp. 871–884, Jul. 2022, doi: 10.1158/2326-6066.CIR-21-0691.
- [508] E. L. Jackson *et al.*, "Analysis of lung tumor initiation and progression using conditional expression of oncogenic *K-ras*," *Genes Dev*, vol. 15, no. 24, pp. 3243–3248, Dec. 2001, doi: 10.1101/gad.943001.
- [509] S. Zheng, A. K. El-Naggar, E. S. Kim, J. M. Kurie, and G. Lozano, "A genetic mouse model for metastatic lung cancer with gender differences in survival," *Oncogene*, vol. 26, no. 48, pp. 6896–6904, Oct. 2007, doi: 10.1038/sj.onc.1210493.

- [510] R. Mittal *et al.*, “Murine lung cancer induces generalized T-cell exhaustion,” *Journal of Surgical Research*, vol. 195, no. 2, pp. 541–549, May 2015, doi: 10.1016/j.jss.2015.02.004.
- [511] M. G. Lechner *et al.*, “Immunogenicity of Murine Solid Tumor Models as a Defining Feature of In Vivo Behavior and Response to Immunotherapy,” *Journal of Immunotherapy*, vol. 36, no. 9, pp. 477–489, Nov. 2013, doi: 10.1097/01.cji.0000436722.46675.4a.
- [512] S. I. S. Mosely *et al.*, “Rational Selection of Syngeneic Preclinical Tumor Models for Immunotherapeutic Drug Discovery,” *Cancer Immunol Res*, vol. 5, no. 1, pp. 29–41, Jan. 2017, doi: 10.1158/2326-6066.CIR-16-0114.
- [513] D. G. McFadden *et al.*, “Mutational landscape of *EGFR*-, *MYC*-, and *Kras*- driven genetically engineered mouse models of lung adenocarcinoma,” *Proceedings of the National Academy of Sciences*, vol. 113, no. 42, Oct. 2016, doi: 10.1073/pnas.1613601113.
- [514] S. Kleffel *et al.*, “Melanoma Cell-Intrinsic PD-1 Receptor Functions Promote Tumor Growth,” *Cell*, vol. 162, no. 6, pp. 1242–1256, Sep. 2015, doi: 10.1016/j.cell.2015.08.052.
- [515] T. Agaloti *et al.*, “Mutant KRAS promotes malignant pleural effusion formation,” *Nat Commun*, vol. 8, no. 1, p. 15205, Aug. 2017, doi: 10.1038/ncomms15205.
- [516] M. Shen, R. Qi, J. Ren, D. Lv, and H. Yang, “Characterization With KRAS Mutant Is a Critical Determinant in Immunotherapy and Other Multiple Therapies for Non-Small Cell Lung Cancer,” *Front Oncol*, vol. 11, Jan. 2022, doi: 10.3389/fonc.2021.780655.
- [517] L. Brisson *et al.*, “P2X7 Receptor Promotes Mouse Mammary Cancer Cell Invasiveness and Tumour Progression, and Is a Target for Anticancer Treatment,” *Cancers (Basel)*, vol. 12, no. 9, p. 2342, Aug. 2020, doi: 10.3390/cancers12092342.
- [518] R. Salcedo *et al.*, “MyD88-mediated signaling prevents development of adenocarcinomas of the colon: role of interleukin 18,” *Journal of Experimental Medicine*, vol. 207, no. 8, pp. 1625–1636, Aug. 2010, doi: 10.1084/jem.20100199.
- [519] M. H. Zaki, P. Vogel, M. Body-Malapel, M. Lamkanfi, and T.-D. Kanneganti, “IL-18 Production Downstream of the Nlrp3 Inflammasome Confers Protection against Colorectal Tumor Formation,” *The Journal of Immunology*, vol. 185, no. 8, pp. 4912–4920, Oct. 2010, doi: 10.4049/jimmunol.1002046.
- [520] T. Zhou *et al.*, “IL-18BP is a secreted immune checkpoint and barrier to IL-18 immunotherapy,” *Nature*, vol. 583, no. 7817, pp. 609–614, Jul. 2020, doi: 10.1038/s41586-020-2422-6.
- [521] S. Nishio *et al.*, “Enhanced suppression of pulmonary metastasis of malignant melanoma cells by combined administration of  $\alpha$ -galactosylceramide and interleukin-18,” *Cancer Sci*, vol. 0, no. 0, pp. 071019192917001-???, Oct. 2007, doi: 10.1111/j.1349-7006.2007.00636.x.
- [522] T. Osaki *et al.*, “IFN-gamma-inducing factor/IL-18 administration mediates IFN-gamma- and IL-12-independent antitumor effects.” *J Immunol*, vol. 160, no. 4, pp. 1742–9, Feb. 1998.
- [523] Z. Ma *et al.*, “Augmentation of Immune Checkpoint Cancer Immunotherapy with IL18,” *Clinical Cancer Research*, vol. 22, no. 12, pp. 2969–2980, Jun. 2016, doi: 10.1158/1078-0432.CCR-15-1655.

- [524] A. A. Tarhini *et al.*, “A phase 2, randomized study of SB-485232, rhIL-18, in patients with previously untreated metastatic melanoma,” *Cancer*, vol. 115, no. 4, pp. 859–868, Feb. 2009, doi: 10.1002/cncr.24100.
- [525] E. Timperi *et al.*, “IL-18 receptor marks functional CD8<sup>+</sup> T cells in non-small cell lung cancer,” *Oncoimmunology*, p. e1328337, May 2017, doi: 10.1080/2162402X.2017.1328337.
- [526] F. Pagès *et al.*, “Modulation of interleukin-18 expression in human colon carcinoma: Consequences for tumor immune surveillance,” *Int J Cancer*, vol. 84, no. 3, pp. 326–330, Jun. 1999, doi: 10.1002/(SICI)1097-0215(19990621)84:3<326::AID-IJC22>3.0.CO;2-K.
- [527] X. Feng *et al.*, “Interleukin-18 Is a Prognostic Marker and Plays a Tumor Suppressive Role in Colon Cancer,” *Dis Markers*, vol. 2020, pp. 1–9, Nov. 2020, doi: 10.1155/2020/6439614.
- [528] M. Gil and K. E. Kim, “Interleukin-18 Is a Prognostic Biomarker Correlated with CD8<sup>+</sup> T Cell and Natural Killer Cell Infiltration in Skin Cutaneous Melanoma,” *J Clin Med*, vol. 8, no. 11, p. 1993, Nov. 2019, doi: 10.3390/jcm8111993.
- [529] M. Terme *et al.*, “IL-18 Induces PD-1–Dependent Immunosuppression in Cancer,” *Cancer Res*, vol. 71, no. 16, pp. 5393–5399, Aug. 2011, doi: 10.1158/0008-5472.CAN-11-0993.
- [530] Y. Wang *et al.*, “Plasma cytokines interleukin-18 and C-X-C motif chemokine ligand 10 are indicative of the anti-programmed cell death protein-1 treatment response in lung cancer patients,” *Ann Transl Med*, vol. 9, no. 1, pp. 33–33, Jan. 2021, doi: 10.21037/atm-20-1513.
- [531] B. Chen *et al.*, “Immune-related genes and gene sets for predicting the response to anti-programmed death 1 therapy in patients with primary or metastatic non-small cell lung cancer,” *Oncol Lett*, vol. 22, no. 1, p. 540, May 2021, doi: 10.3892/ol.2021.12801.
- [532] K. O. Dixon *et al.*, “TIM-3 restrains anti-tumour immunity by regulating inflammasome activation,” *Nature*, vol. 595, no. 7865, pp. 101–106, Jul. 2021, doi: 10.1038/s41586-021-03626-9.
- [533] S. B. Wallach-Dayán *et al.*, “Cutting edge: FasL<sup>+</sup> immune cells promote resolution of fibrosis,” *J Autoimmun*, vol. 59, pp. 67–76, May 2015, doi: 10.1016/j.jaut.2015.02.006.
- [534] S. B. Wallach-Dayán, R. Golan-Gerstl, and R. Breuer, “Evasion of myofibroblasts from immune surveillance: A mechanism for tissue fibrosis,” *Proceedings of the National Academy of Sciences*, vol. 104, no. 51, pp. 20460–20465, Dec. 2007, doi: 10.1073/pnas.0705582104.
- [535] P. Gasse *et al.*, “Uric acid is a danger signal activating NALP3 inflammasome in lung injury inflammation and fibrosis,” *Am J Respir Crit Care Med*, vol. 179, no. 10, pp. 903–13, May 2009, doi: 10.1164/rccm.200808-1274OC.
- [536] Y. Nakanishi *et al.*, “IL-18 binding protein can be a prognostic biomarker for idiopathic pulmonary fibrosis,” *PLoS One*, vol. 16, no. 6, p. e0252594, 2021, doi: 10.1371/journal.pone.0252594.
- [537] L.-M. Zhang *et al.*, “Neutralization of IL-18 by IL-18 binding protein ameliorates bleomycin-induced pulmonary fibrosis via inhibition of epithelial-mesenchymal transition,” *Biochem Biophys Res Commun*, vol. 508, no. 2, pp. 660–666, 2019, doi: 10.1016/j.bbrc.2018.11.129.

- [538] A. Nakatani-Okuda *et al.*, "Protection against bleomycin-induced lung injury by IL-18 in mice," *Am J Physiol Lung Cell Mol Physiol*, vol. 289, no. 2, pp. L280-7, Aug. 2005, doi: 10.1152/ajplung.00380.2004.
- [539] J. Dupaul-Chicoine *et al.*, "Control of Intestinal Homeostasis, Colitis, and Colitis-Associated Colorectal Cancer by the Inflammatory Caspases," *Immunity*, vol. 32, no. 3, pp. 367–378, Mar. 2010, doi: 10.1016/j.immuni.2010.02.012.
- [540] Md. H. Zaki, K. L. Boyd, P. Vogel, M. B. Kastan, M. Lamkanfi, and T.-D. Kanneganti, "The NLRP3 Inflammasome Protects against Loss of Epithelial Integrity and Mortality during Experimental Colitis," *Immunity*, vol. 32, no. 3, pp. 379–391, Mar. 2010, doi: 10.1016/j.immuni.2010.03.003.
- [541] E. Elinav *et al.*, "NLRP6 Inflammasome Regulates Colonic Microbial Ecology and Risk for Colitis," *Cell*, vol. 145, no. 5, pp. 745–757, May 2011, doi: 10.1016/j.cell.2011.04.022.
- [542] L.-M. Zhang *et al.*, "Interleukin-18 promotes fibroblast senescence in pulmonary fibrosis through down-regulating Klotho expression," *Biomedicine & Pharmacotherapy*, vol. 113, p. 108756, May 2019, doi: 10.1016/j.biopha.2019.108756.
- [543] X.-H. Niu *et al.*, "IL-18/IL-18R1 promotes circulating fibrocyte differentiation in the aging population," *Inflammation Research*, vol. 69, no. 5, pp. 497–507, May 2020, doi: 10.1007/s00011-020-01330-4.
- [544] S. H. Lacy *et al.*, "Activated human T lymphocytes inhibit TGF $\beta$ -induced fibroblast to myofibroblast differentiation via prostaglandins D<sub>2</sub> and E<sub>2</sub>," *American Journal of Physiology-Lung Cellular and Molecular Physiology*, vol. 314, no. 4, pp. L569–L582, Apr. 2018, doi: 10.1152/ajplung.00565.2016.
- [545] L. Chavez-Galan *et al.*, "Fibroblasts From Idiopathic Pulmonary Fibrosis Induce Apoptosis and Reduce the Migration Capacity of T Lymphocytes," *Front Immunol*, vol. 13, Feb. 2022, doi: 10.3389/fimmu.2022.820347.
- [546] R. Golan-Gerstl, S. B. Wallach-Dayana, P. Zisman, W. v. Cardoso, R. H. Goldstein, and R. Breuer, "Cellular FLICE-like Inhibitory Protein Deviates Myofibroblast Fas-Induced Apoptosis Toward Proliferation during Lung Fibrosis," *Am J Respir Cell Mol Biol*, vol. 47, no. 3, pp. 271–279, Sep. 2012, doi: 10.1165/rcmb.2010-0284RC.
- [547] S. Nakajima *et al.*, "IL-17A as an Inducer for Th2 Immune Responses in Murine Atopic Dermatitis Models," *Journal of Investigative Dermatology*, vol. 134, no. 8, pp. 2122–2130, Aug. 2014, doi: 10.1038/jid.2014.51.
- [548] S. Kronborg-White, L. B. Madsen, E. Bendstrup, and V. Poletti, "PD-L1 Expression in Patients with Idiopathic Pulmonary Fibrosis," *J Clin Med*, vol. 10, no. 23, p. 5562, Nov. 2021, doi: 10.3390/jcm10235562.
- [549] Y. Geng *et al.*, "PD-L1 on invasive fibroblasts drives fibrosis in a humanized model of idiopathic pulmonary fibrosis," *JCI Insight*, Feb. 2019, doi: 10.1172/jci.insight.125326.
- [550] Y. Lu *et al.*, "Anti-PD-L1 antibody alleviates pulmonary fibrosis by inducing autophagy via inhibition of the PI3K/Akt/mTOR pathway," *Int Immunopharmacol*, vol. 104, p. 108504, Mar. 2022, doi: 10.1016/j.intimp.2021.108504.
- [551] R. G. Jenkins *et al.*, "An Official American Thoracic Society Workshop Report: Use of Animal Models for the Preclinical Assessment of Potential Therapies for Pulmonary Fibrosis," *Am J Respir Cell Mol Biol*, vol. 56, no. 5, pp. 667–679, May 2017, doi: 10.1165/rcmb.2017-0096ST.

- [552] J. Tashiro *et al.*, “Exploring Animal Models That Resemble Idiopathic Pulmonary Fibrosis,” *Front Med (Lausanne)*, vol. 4, Jul. 2017, doi: 10.3389/fmed.2017.00118.
- [553] R. Peng *et al.*, “Bleomycin Induces Molecular Changes Directly Relevant to Idiopathic Pulmonary Fibrosis: A Model for ‘Active’ Disease,” *PLoS One*, vol. 8, no. 4, p. e59348, Apr. 2013, doi: 10.1371/journal.pone.0059348.
- [554] B. Ballester, J. Milara, and J. Cortijo, “Idiopathic Pulmonary Fibrosis and Lung Cancer: Mechanisms and Molecular Targets,” *Int J Mol Sci*, vol. 20, no. 3, p. 593, Jan. 2019, doi: 10.3390/ijms20030593.
- [555] C. Wang and J. Yang, “Mechanical forces: The missing link between idiopathic pulmonary fibrosis and lung cancer,” *Eur J Cell Biol*, vol. 101, no. 3, p. 151234, Jun. 2022, doi: 10.1016/j.ejcb.2022.151234.
- [556] “IL-1 $\beta$  turnover by TRIP12 and ARL1 ubiquitin ligases and UBE2L3 limits inflammation,” *BioRxiv*, Sep. 2022, doi: doi: <https://doi.org/10.1101/2022.09.14.507790>.
- [557] M. J. G. Eldridge, J. Sanchez-Garrido, G. F. Hoben, P. J. Goddard, and A. R. Shenoy, “The Atypical Ubiquitin E2 Conjugase UBE2L3 Is an Indirect Caspase-1 Target and Controls IL-1 $\beta$  Secretion by Inflammasomes,” *Cell Rep*, vol. 18, no. 5, pp. 1285–1297, Jan. 2017, doi: 10.1016/j.celrep.2017.01.015.
- [558] J. S. Ainscough *et al.*, “Dendritic Cell IL-1 $\alpha$  and IL-1 $\beta$  Are Polyubiquitinated and Degraded by the Proteasome,” *Journal of Biological Chemistry*, vol. 289, no. 51, pp. 35582–35592, Dec. 2014, doi: 10.1074/jbc.M114.595686.
- [559] A. K. Giegerich *et al.*, “Autophagy-dependent PELI3 degradation inhibits proinflammatory IL1B expression,” *Autophagy*, vol. 10, no. 11, pp. 1937–1952, Nov. 2014, doi: 10.4161/auto.32178.
- [560] J. Harris *et al.*, “Autophagy Controls IL-1 $\beta$  Secretion by Targeting Pro-IL-1 $\beta$  for Degradation,” *Journal of Biological Chemistry*, vol. 286, no. 11, pp. 9587–9597, Mar. 2011, doi: 10.1074/jbc.M110.202911.
- [561] I. Couillin *et al.*, “IL-1R1/MyD88 signaling is critical for elastase-induced lung inflammation and emphysema,” *J Immunol*, vol. 183, no. 12, pp. 8195–202, Dec. 2009, doi: 10.4049/jimmunol.0803154.
- [562] A. M. Doerner and B. L. Zuraw, “TGF-beta1 induced epithelial to mesenchymal transition (EMT) in human bronchial epithelial cells is enhanced by IL-1beta but not abrogated by corticosteroids.,” *Respir Res*, vol. 10, p. 100, Oct. 2009, doi: 10.1186/1465-9921-10-100.
- [563] I. Kaplanov *et al.*, “Blocking IL-1 $\beta$  reverses the immunosuppression in mouse breast cancer and synergizes with anti-PD-1 for tumor abrogation,” *Proceedings of the National Academy of Sciences*, vol. 116, no. 4, pp. 1361–1369, Jan. 2019, doi: 10.1073/pnas.1812266115.
- [564] H. J. Kim *et al.*, “IL-18 Downregulates Collagen Production in Human Dermal Fibroblasts via the ERK Pathway,” *Journal of Investigative Dermatology*, vol. 130, no. 3, pp. 706–715, Mar. 2010, doi: 10.1038/jid.2009.302.